CARMA PROTEINS: PLAYING A HAND OF FOUR CARDS

EDITED BY: Frédéric Bornancin and Andrew L. Snow
PUBLISHED IN: Frontiers in Immunology

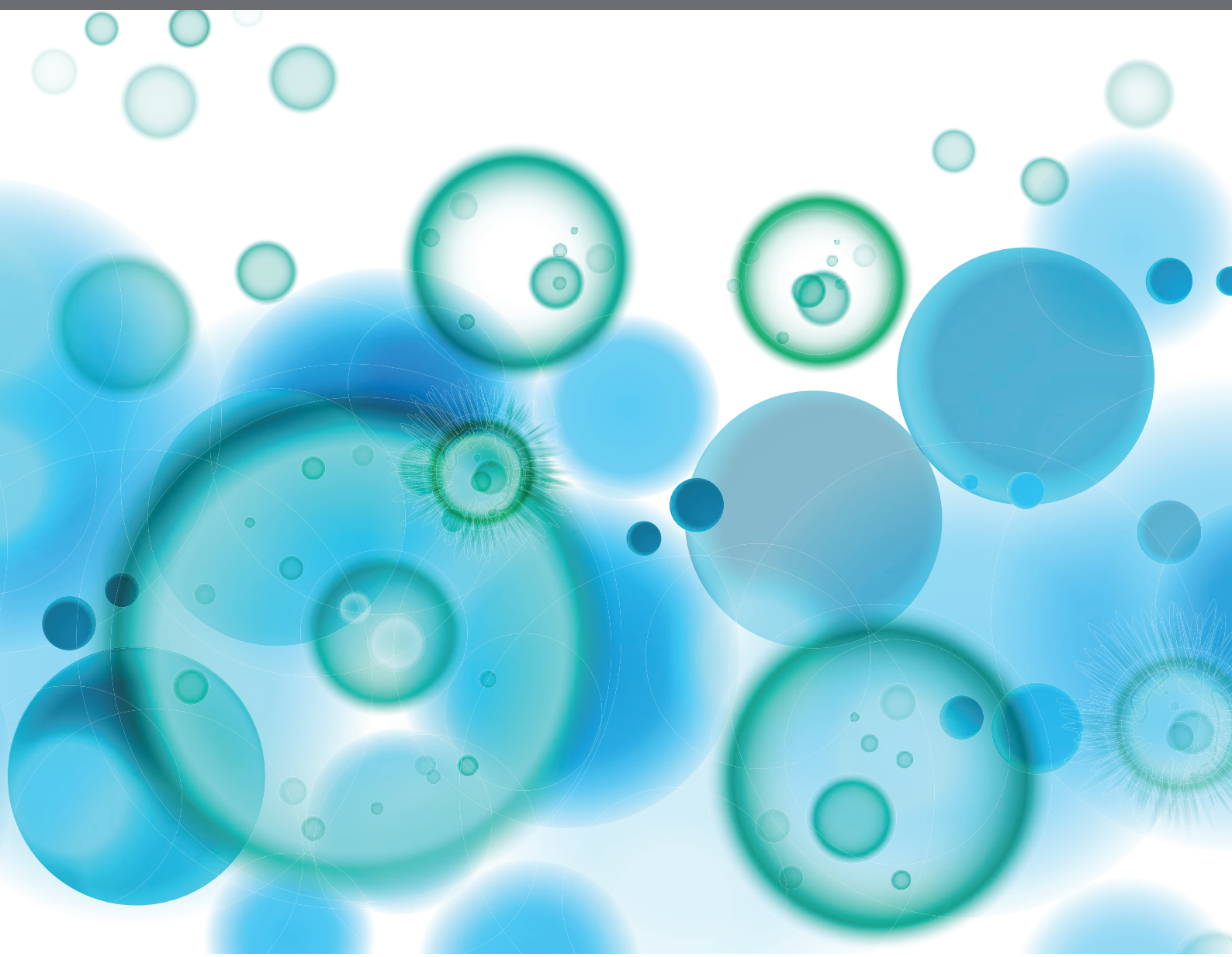

frontiers Research Topics

ISSN 1664-8714
ISBN 978-2-88963-056-1
DOI 10.3389/978-2-88963-056-1

About Frontiers

Frontiers is more than just an open-access publisher of scholarly articles: it is a pioneering approach to the world of academia, radically improving the way scholarly research is managed. The grand vision of Frontiers is a world where all people have an equal opportunity to seek, share and generate knowledge. Frontiers provides immediate and permanent online open access to all its publications, but this alone is not enough to realize our grand goals.

Frontiers Journal Series

The Frontiers Journal Series is a multi-tier and interdisciplinary set of open-access, online journals, promising a paradigm shift from the current review, selection and dissemination processes in academic publishing. All Frontiers journals are driven by researchers for researchers; therefore, they constitute a service to the scholarly community. At the same time, the Frontiers Journal Series operates on a revolutionary invention, the tiered publishing system, initially addressing specific communities of scholars, and gradually climbing up to broader public understanding, thus serving the interests of the lay society, too.

Dedication to Quality

Each Frontiers article is a landmark of the highest quality, thanks to genuinely collaborative interactions between authors and review editors, who include some of the world's best academicians. Research must be certified by peers before entering a stream of knowledge that may eventually reach the public - and shape society; therefore, Frontiers only applies the most rigorous and unbiased reviews.
Frontiers revolutionizes research publishing by freely delivering the most outstanding research, evaluated with no bias from both the academic and social point of view. By applying the most advanced information technologies, Frontiers is catapulting scholarly publishing into a new generation.

What are Frontiers Research Topics?

Frontiers Research Topics are very popular trademarks of the Frontiers Journals Series: they are collections of at least ten articles, all centered on a particular subject. With their unique mix of varied contributions from Original Research to Review Articles, Frontiers Research Topics unify the most influential researchers, the latest key findings and historical advances in a hot research area! Find out more on how to host your own Frontiers Research Topic or contribute to one as an author by contacting the Frontiers Editorial Office: researchtopics@frontiersin.org

CARMA PROTEINS: PLAYING A HAND OF FOUR CARDS

Topic Editors:
Frédéric Bornancin, Novartis Institutes for BioMedical Research, Switzerland
Andrew L. Snow, Uniformed Services University of the Health Sciences, United States

Some twenty years ago, the search began for B-cell lymphoma (BCL)-10 binding partners that connect via homophilic interaction with its N-terminal caspase recruitment domain (CARD) to induce nuclear factor-kappa B (NF-κB) activation. This effort led first to the identification of the protein CARD9. Soon afterwards, similar searches identified CARD10 (aka CARMA3), CARD11 (aka CARMA1) and CARD14 (aka CARMA2), as further BCL10 interactors. These discoveries paved the way for landmark progress in our understanding of NF-κB activation pathways downstream of several cell surface receptors on multiple cell types, focused particularly on antigen receptors on lymphocytes. An additional binding partner, called Mucosa-associated lymphoid tissue lymphoma translocation protein 1 (MALT1), was also implicated in the CARD-BCL10 pathway. Since then, the resulting "CBM" complex has been recognized as a key node in signaling cascades leading to NF-κB activation, particularly in immune cells.

Mouse models of genetic deficiencies for each CBM component provided the first evidence for their critical role in cell signaling. More recently, studies of human lymphoid malignancies and novel genetic disorders have revealed important new insights. Both gain- and loss-of-function mutations were identified, establishing these CARMA/CARD proteins as key regulators of proliferation and differentiation of immune and non-immune cells, and linking them to human disease. According to the genetic defect involved, dysregulation of CARMA/CARD pathways can lead to a broad spectrum of immune disorders, including severe immune deficiencies, lymphoproliferative disorders, psoriasis and atopy.

The aim of this Research Topic is to summarize and update our current understanding of CARMA/CARD protein biology, from initial discoveries to the most recent insights. It focuses on CARD9 and the CARMA proteins CARD10, CARD11 and CARD14, from genetic, signaling and disease perspectives. BCL10 and MALT1 are also reviewed in this context as critical nodes for CBM signal relay and regulation. This Research Topic also aims to delineate the next key questions in the field to guide future research efforts.

Citation: Bornancin, F., Snow, A. L., eds. (2019). CARMA Proteins: Playing a Hand of Four CARDs. Lausanne: Frontiers Media. doi: 10.3389/978-2-88963-056-1

Table of Contents

CARD11

CARD14

frontiers in Immunology

EDITORIAL
published: 29 May 2019
doi: 10.3389/fimmu.2019.01217

Editorial: CARMA Proteins: Playing a Hand of Four CARDs

Frédéric Bornancin[1]* *and Andrew L. Snow*[2]*

[1] Autoimmunity, Transplantation and Inflammation, Novartis Institutes for BioMedical Research, Basel, Switzerland, [2] Department of Pharmacology and Molecular Therapeutics, Uniformed Services University of the Health Sciences, Bethesda, MD, United States

Keywords: CARD9, CARD10, CARD11, CARD14, Bcl10, Malt1, CARMA, immunodeficiency

Editorial on the Research Topic

CARMA Proteins: Playing a Hand of Four CARDs

Over the past 20 years, enhanced analyses of tumor-specific genomic alterations coupled with elegant biochemical approaches have helped to map essential signaling pathways in healthy and malignant cells. For example, the B cell lymphoma/leukemia 10 (BCL10) gene was identified in 1999 from a recurrent chromosomal translocation noted in non-Hodgkin lymphomas that arise in mucosa-associated lymphoid tissue (MALT). These studies demonstrated that BCL10 could oligomerize via its caspase recruitment domain (CARD) and induce robust activation of nuclear factor of kappaB (NF-κB), a critical family of transcription factors first implicated in lymphocyte differentiation. In <3 years, multiple groups discovered that BCL10 must partner with one of four CARD-containing scaffold proteins (CARD9, CARD10, CARD11, and CARD14) and the MALT1 paracaspase (also discovered from a MALT lymphoma-derived chromosomal translocation) to drive NF-κB signaling in response to various receptor-mediated inputs. Building from murine knockout models, a growing spectrum of malignancies and human immune disorders have been genetically linked to altered signaling through this "CARD-BCL10-MALT1 (CBM) complex." As this Research Topic attests, indeed this list has expanded exponentially in just the past few years. Drawing from leading investigators in the field, including many involved in the seminal discoveries summarized above, the 10 reviews, three original research articles, and one case report compiled in this Frontiers in Immunology eBook provide a comprehensive and timely examination of CBM complex assembly and signaling. Although we now appreciate that tissue-specific expression of CARMA/CARD proteins dictates function and underlying pathology of associated diseases, this collection also underscores the ubiquity and significance of the CBM signalosome as a central governor of receptor-mediated signaling to NF-κB and additional outputs important for cell proliferation, survival, differentiation, and function.

Two reviews provide an in-depth look at the complex regulation and function of the two subunits shared by all CBM complexes: BCL10 and MALT1. Gehring et al. discuss the discovery and subsequent characterization of BCL10 as the central adaptor protein that channels various innate inflammatory and adaptive antigen receptor stimuli to NF-κB and c-Jun N-terminal kinase (JNK) activation in various immune cells. The formation of CARD-dependent cytoplasmic BCL10 filaments, "seeded" by CARD/CARMA scaffold proteins, constitute an essential platform for MALT1 protease activation and downstream signaling. Informed by studies of T and B cell receptor signaling in lymphocytes, the authors also review the complex post-translational modifications that ensure the orderly extension and degradation of putative BCL10 filaments *in vivo* that ultimately tune and regulate immune responses. Juilland and Thome provide an up-to-date overview of MALT1, which has been intensively interrogated in recent years as a potential therapeutic target for both lymphoma and autoimmune disease. MALT1 constitutively

Edited by:
Isabelle Meyts,
KU Leuven, Belgium

Reviewed by:
Vivien Béziat,
Institut National de la Santé et de la Recherche Médicale (INSERM), France

***Correspondence:**
Frédéric Bornancin
frederic.bornancin@novartis.com
Andrew L. Snow
andrew.snow@usuhs.edu

Specialty section:
This article was submitted to Primary Immunodeficiencies, a section of the journal Frontiers in Immunology

Received: *20 February 2019*
Accepted: *13 May 2019*
Published: *29 May 2019*

Citation:
Bornancin F and Snow AL (2019) Editorial: CARMA Proteins: Playing a Hand of Four CARDs. Front. Immunol. 10:1217. doi: 10.3389/fimmu.2019.01217

associates with BCL10, and functions both as a scaffold and protease activated upon CBM assembly and BCL10 filament construction. At least 10 MALT1 substrates have been described to date, with more likely to be identified in future studies. Proteolytic cleavage of many of these proteins (e.g. A20, RelB), including MALT1 itself, typically serves to prolong canonical NF-κB activation, although other MALT1 substrates are implicated in regulating cellular adhesion, mRNA stabilization, and metabolic reprogramming in lymphocytes. Both reviews discuss how loss or mutation of BCL10 or MALT1 contribute to immune deficiency and dysregulation, highlighting the need for further mechanistic studies that will better define the essential functions these proteins fulfill in propagating receptor-directed signals in immune and non-immune cells, and maintaining vigorous yet controlled immune responses.

BCL10 and MALT1 are rendered operational primarily through interactions with multi-domain scaffold proteins known as CARD-MAGUK 1-3 (CARMA1-3) and CARD9. These molecules were initially identified based on high sequence similarity shared between their CARD motifs and that of BCL10, facilitating heterotypic CARD-CARD interactions between the two. As illustrated in several salient articles collected in this eBook, these four CARD/CARMA proteins are structurally and functionally homologous in nucleating CBM complexes for downstream signaling. However, their discrete tissue-specific expression patterns dictate the upstream receptors through which these signals are conveyed in different cell types, resulting in distinct functions that help to shape immunity, inflammation, and tumorigenesis.

Two reviews examine the fundamental role of CARD9 in microbial recognition by myeloid lineage cells of the innate immune system. CARD9 is utilized by several membrane and intracellular pattern recognition receptors specific for molecules derived from both commensal and pathogenic bacteria, fungi and viruses. Based on recent studies of human patients with CARD9 deficiency, Drummond et al. discuss the indispensable function of CARD9 in human anti-fungal immunity. CARD9 facilitates CBM-dependent activation of NF-κB, activation of ERK, and production of multiple pro-inflammatory cytokines upon recognition of fungal cell wall components by SYK-coupled C-type lectin receptors such as Dectin-1. Animals and humans lacking CARD9 are particularly susceptible to pathogenic fungal infections of the oral mucosa, skin, and central nervous system, as well as certain bacterial and viral infections. The authors broadly discuss the multi-faceted role of CARD9 in innate immunity, autoimmune disease, and cancer in humans, informed by both population-based studies and rare variants in patients suffering from uncontrolled, spontaneous fungal infections. This review is complimented by original research from De Bruyne et al. describing a *CARD9* founder mutation in a cohort of 11 patients from five Turkish families suffering from various fungal infections. Consistent with a previous report, the authors demonstrate that this specific CARD9 variant (p.Arg70Trp, R70W) fails to stimulate NF-κB. Furthermore, CARD9 R70W also dominantly interferes with WT CARD9 signaling by disrupting BCL10 filament formation and attenuating NF-κB activity, although enough signaling may be preserved to explain the absence of pathology in heterozygous carriers. Remarkably, this dominant negative CARD9 mutant could also repress constitutive NF-κB signaling induced by gain-of-function variants of CARD10, CARD11, and CARD14. Although CARD9 is not co-expressed with these proteins in normal cells, this result beautifully illustrates the evolutionarily conserved requirements for scaffold multimerization and heterotypic CARD-CARD interactions in nucleating signal-competent CBM signalosomes.

In contrast, the review from Hartjes and Ruland focuses primarily on the importance of CARD9 signaling in maintaining homeostasis and a healthy microbiome in the gut. Over the past 10 years, single nucleotide polymorphisms in the human *CARD9* gene have been shown to influence susceptibility to inflammatory bowel disease (IBD) and colorectal cancer development. A detailed overview of several studies using murine colitis models reveals how loss or perturbation of Card9 signaling can alter the composition and function of resident myeloid cell populations and contribute to microbial dysbiosis, intestinal inflammation, and tumorigenesis. Future studies that delineate CARD9-dependent signaling pathways in greater molecular detail will hopefully open new therapeutic avenues for treating invasive fungal infections, IBD and colon cancer.

Four articles in this collection highlight CARD11 (a.k.a. CARMA1) as a critical regulator of adaptive immune responses. The expression of CARD11 is largely restricted to lymphocytes, where it primarily functions to bridge antigen recognition through T and B cell receptors (TCR/BCR) with downstream activation of NF-κB, JNK, and mTOR. Bedsaul et al. review the complex events surrounding TCR/BCR-induced CARD11 signaling. This process involves an elaborate intramolecular regulation of closed and open CARD11 protein conformations, which dictates recruitment and subsequent modification of BCL10, MALT1, and additional co-signaling proteins that serve to either activate the IκB kinase (IKK) complex (e.g., TRAF6, caspase 8) or terminate CARD11 signaling (e.g., GAKIN, PP2A). A brief overview of human somatic and germline *CARD11* mutations found in lymphoma and immunodeficient patients, respectively, culminates in a list of salient unanswered questions about CARD11 signaling that prompt further structure-function studies. A clever original article by Seeholzer et al. answers this call by implementing a creative approach to investigate the molecular details of CBM assembly in lymphocytes. A fusion protein joining BCL10 directly to the N-terminus of CARD11 promotes chronic MALT1 protease activation in CARD11-deficient cell lines, with differential effects on downstream NF-κB activation in B vs. T cells. Structure-guided mutagenesis of either CARD domain within the BCL10-CARD11 fusion protein helped to clarify how BCL10-MALT1 recruitment to CARD11 and formation of BCL10 CARD-dependent filaments cooperate in a highly integrated process for CBM signaling.

Lu et al. build upon this foundation by providing an exhaustive review of recently described human congenital immune disorders attributed to inherited mutations in *CARD11, BCL10,* and *MALT1*. As expected, null mutations in all three genes result in severe combined immunodeficiency, underscoring the importance of CBM signaling for mature B and T cell functions. However, various missense mutations, insertions, and/or deletions that preserve CARD11 protein

expression contribute to a surprising spectrum of disease presentations in human patients. Whereas, gain-of-function (GOF) *CARD11* mutations congruent with those found in B cell lymphoma cause a selective B cell lymphoproliferative disorder, loss-of-function (LOF)/dominant negative (DN) *CARD11* variants were recently discovered in patients with severe atopic disease. The authors compare and contrast the expanding list of phenotypic manifestations described in these patients, revealing shared features of immunodeficiency (e.g., poor humoral responses, susceptibility to certain viral infections) that relate back to dysregulated CBM-dependent signaling to NF-κB and mTOR. An intriguing case report offered by Desjardins et al. adds to this complicated picture by challenging the conventional classification of a single *CARD11* mutation as gain or loss-of-function. This study describes a four-generation family that exhibits both B cell lymphocytosis and atopy, linked to a unique inherited *CARD11* variant (p.His234_Lys238delinsLeu) that exhibits both GOF and DN activity in T cell signaling assays. Collectively, these articles describe how *CARD11* mutations can manifest in distinct and blended features of immune dysregulation, depicting the CARD11 scaffold as a critical fulcrum for balanced T and B cell responses.

Two reviews delve into CARD14/CARMA2 as the pivotal scaffold for CBM signaling in epithelial cells and keratinocytes, focusing on how dysregulation of CARD14 signaling contributes to inflammatory skin disorders such as psoriasis. CARD14/CARMA2 was perhaps the least characterized member of the CARMA/CARD protein family, but recent insights have illuminated how dysregulation of CARD14 can result in skin inflammation. Zotti et al. consider how three alternative splice variants of CARD14 affect NF-κB triggering in response to pathogen-associated molecular patterns (and stimuli yet to be identified), with a short CARMA2 isoform (CARMA2*sh*) lacking the C-terminal SH3 and guanylate kinase (GUK) domains predominating in human skin. Various GOF CARMA2*sh* variants linked to psoriasis, pityriasis and other skin disorders are also discussed in relation to an amplified pro-inflammatory NF-κB-dependent gene program in the skin. Importantly, the authors also discuss emerging roles for several proteins in enabling (e.g., TRAF2, DEPDC7) or modulating (e.g., ULK2, RNF7) CARD14 signaling, which may present novel avenues for therapeutic intervention. The article by Israel and Mellett presents a deeper dive into the molecular genetics and clinical features of inflammatory skin disorders caused by numerous human *CARD14* mutations described to date. Informed by detailed phenotyping and clinical management of patient kindreds, mouse models of psoriasis harboring synonymous *Card14* mutations, and *in vitro* molecular signaling studies, this review summarizes how different human *CARD14* variants can manifest in a heterogeneous spectrum of psoriatic skin diseases. Biologic therapies targeting TNF and the IL-12/IL-23/IL-17 cytokine axis have already proven beneficial in treating these diseases, whereas future specific inhibitors of CARD14 or MALT1 protease may prove to be attractive tools for tamping down inflammation driven by CARD14 GOF mutations.

In contrast to the other CARD/CARMA proteins, CARD10/CARMA3 is ubiquitously expressed in many non-lymphoid tissues and may play an important role in the pathogenesis of several types of cancer. Two salient reviews explore this emerging paradigm, offered from investigators that have led the characterization of CARD10 signaling since its initial discovery. Zhang and Lin provide a general overview of CARD10/CARMA3 in CBM signaling induced by multiple G-protein coupled receptors and receptor tyrosine kinases (RTKs) such as the epidermal growth factor receptor (EGFR), culminating in NF-κB activation in several cell types. The authors also discuss newly recognized partners in CARD10 signaling (e.g., TMEM43), as well as a recently uncovered role for CARD10 in the antiviral interferon response. McAuley et al. discuss knowns and unknowns about how CARD10-dependent signals downstream of a variety of GPCR/RTKs promote solid tumor pathogenesis in non-immune cells. CARD10 overexpression has been noted in many tumor types, affected in part by failed miRNA-mediated modulation. Both reviews also comment on recent reports of receptor-independent CBM signaling in response to DNA damage, and reminds readers of the many unanswered questions surrounding the mechanisms connecting CARD10-dependent CBM signaling to various receptors, and how these might be specifically targeted for anti-cancer therapy.

Finally, an original article from Staal et al. describes the ancient evolutionary origin of CBM signaling in invertebrates, revealing co-evolution of CARD-CC homologs with Bcl10, Syk-like kinases, and type I paracaspases. Careful structure/function analysis of paracaspases from invertebrates and lower vertebrates suggests that MALT1 functions for NF-κB activation evolved recently in jawed vertebrates, despite the appearance of conserved, independent scaffold and protease functions in older invertebrates. Their results highlight the utility of a comparative biology approach for studying CBM complex functions, and point to fascinating alternative CBM-independent roles for MALT1, including neuronal function in *C. elegans*.

In summary, the articles and reviews in this eBook constitute the most comprehensive, current assessment of CBM complex function in normal and pathologic settings. We hope this collection will inspire future mechanistic studies to identify novel therapeutic approaches to treating myriad diseases connected to dysregulation of this ubiquitous and critical signalosome.

AUTHOR CONTRIBUTIONS

All authors listed have made a substantial, direct and intellectual contribution to the work, and approved it for publication.

Conflict of Interest Statement: FB is an employee and shareholder of Novartis.

The remaining author declares that the research was conducted in the absence of any commercial or financial relationships that could be construed as a potential conflict of interest.

frontiers in Immunology

ORIGINAL RESEARCH
published: 24 May 2018
doi: 10.3389/fimmu.2018.01136

Ancient Origin of the CARD–Coiled Coil/Bcl10/MALT1-Like Paracaspase Signaling Complex Indicates Unknown Critical Functions

Jens Staal[1,2], Yasmine Driege[1,2], Mira Haegman[1,2], Alice Borghi[1,2], Paco Hulpiau[2,3], Laurens Lievens[1,2], Ismail Sahin Gul[2,4], Srividhya Sundararaman[2,4], Amanda Gonçalves[2,5], Ineke Dhondt[6], Jorge H. Pinzón[7], Bart P. Braeckman[6], Ulrich Technau[8], Yvan Saeys[3,9], Frans van Roy[2,4] and Rudi Beyaert[1,2]*

[1] Unit of Molecular Signal Transduction in Inflammation, VIB-UGent Center for Inflammation Research (IRC), Ghent, Belgium, [2] Department of Biomedical Molecular Biology, Ghent University, Ghent, Belgium, [3] Unit of Data Mining and Modeling for Biomedicine, VIB-UGent Center for Inflammation Research (IRC), Ghent, Belgium, [4] Unit of Molecular Cell Biology, VIB-UGent Center for Inflammation Research (IRC), Ghent, Belgium, [5] VIB Bio Imaging Core Gent, VIB-UGent Center for Inflammation Research (IRC), Ghent, Belgium, [6] Laboratory for Aging Physiology and Molecular Evolution, Biology Department, Ghent University, Ghent, Belgium, [7] Department of Biology, University of Texas Arlington, Arlington, TX, United States, [8] Department of Molecular Evolution and Development, Faculty of Life Sciences, University of Vienna, Vienna, Austria, [9] Department of Applied Mathematics, Computer Science and Statistics, Ghent University, Ghent, Belgium

OPEN ACCESS

Edited by:
Frederic Bornancin, Novartis (Switzerland), Switzerland

Reviewed by:
Liangsheng Zhang, Fujian Agriculture and Forestry University, China
Xiaocui He, La Jolla Institute for Allergy and Immunology (LJI), United States

***Correspondence:**
Jens Staal
jens.staal@irc.vib-ugent.be

Specialty section:
This article was submitted to Molecular Innate Immunity, a section of the journal Frontiers in Immunology

Received: *13 March 2018*
Accepted: *07 May 2018*
Published: *24 May 2018*

Citation:
Staal J, Driege Y, Haegman M, Borghi A, Hulpiau P, Lievens L, Gul IS, Sundararaman S, Gonçalves A, Dhondt I, Pinzón JH, Braeckman BP, Technau U, Saeys Y, van Roy F and Beyaert R (2018) Ancient Origin of the CARD–Coiled Coil/Bcl10/MALT1-Like Paracaspase Signaling Complex Indicates Unknown Critical Functions. Front. Immunol. 9:1136. doi: 10.3389/fimmu.2018.01136

The CARD–coiled coil (CC)/Bcl10/MALT1-like paracaspase (CBM) signaling complexes composed of a CARD–CC family member (CARD-9, -10, -11, or -14), Bcl10, and the type 1 paracaspase MALT1 (PCASP1) play a pivotal role in immunity, inflammation, and cancer. Targeting MALT1 proteolytic activity is of potential therapeutic interest. However, little is known about the evolutionary origin and the original functions of the CBM complex. Type 1 paracaspases originated before the last common ancestor of planulozoa (bilaterians and cnidarians). Notably in bilaterians, Ecdysozoa (e.g., nematodes and insects) lacks Bcl10, whereas other lineages have a Bcl10 homolog. A survey of invertebrate CARD–CC homologs revealed such homologs only in species with Bcl10, indicating an ancient common origin of the entire CBM complex. Furthermore, vertebrate-like Syk/Zap70 tyrosine kinase homologs with the ITAM-binding SH2 domain were only found in invertebrate organisms with CARD–CC/Bcl10, indicating that this pathway might be related to the original function of the CBM complex. Moreover, the type 1 paracaspase sequences from invertebrate organisms that have CARD–CC/Bcl10 are more similar to vertebrate paracaspases. Functional analysis of protein–protein interactions, NF-κB signaling, and CYLD cleavage for selected invertebrate type 1 paracaspase and Bcl10 homologs supports this scenario and indicates an ancient origin of the CARD–CC/Bcl10/paracaspase signaling complex. By contrast, many of the known MALT1-associated activities evolved fairly recently, indicating that unknown functions are at the basis of the protein conservation. As a proof-of-concept, we provide initial evidence for a CBM- and NF-κB-independent neuronal function of the Caenorhabditis elegans type 1 paracaspase malt-1. In conclusion, this study shows how evolutionary insights may point at alternative functions of MALT1.

Keywords: signal transduction, molecular evolution, protein–protein interaction, structure–function analysis, NF-kappaB, coral bleaching, *Nematostella vectensis*, *Caenorhabditis elegans*

INTRODUCTION

The paracaspase MALT1 (PCASP1) was originally identified in humans as an oncogenic fusion with IAP2 in low-grade antibiotic-resistant MALT lymphomas (1). Later, it was discovered that MALT1 is a critical component in T and B cell antigen receptor signaling as part of the CARD-11–Bcl10–MALT1 (CBM) signaling complex that is formed upon antigen stimulation. Antigen receptor signaling *via* the ITAM (immunoreceptor tyrosine-based activation motif)-binding SH2 domain tyrosine kinase Zap70 activates PKC, leading to CARD-11 phosphorylation and the recruitment of a preexisting Bcl10/MALT1 complex (2–4). MALT1 in the activated CBM complex recruits critical downstream proteins, such as TRAF6, for the activation of NF-κB-dependent gene expression (5) (Figure S1A in Supplementary Material). CARD-11 (also known as CARMA1) belongs to a distinct phylogenetic group of CARD domain proteins, which is characterized by a CARD and a coiled-coil (CC) domain, and this group of proteins will thus be referred to as CARD–CC proteins. Further studies made it clear that MALT1 plays a role in several different CARD–CC/Bcl10/MALT1 signaling complexes, which are composed of specific CARD–CC family proteins [CARD-9 (6), CARD-11 (4), CARD-14 (also known as CARMA2) (7–9), and CARD-10 (also known as CARMA3) (10)] and which are formed upon the stimulation of distinct receptors in several immune and non-immune cells. The use of different CARD–CC proteins in the CBM complexes has been proposed to depend on their cell-type-specific expression (11), although other mechanisms cannot be ruled out. CARD-9, CARD-10, CARD-11, and CARD-14 are the only members of this CARD–CC family in humans, which makes it unlikely that additional similar human CBM complexes will be found. MALT1 has been annotated as a "paracaspase" due to sequence similarity with the true caspases and "metacaspases" (12). A broader survey of paracaspases in the whole tree of life indicates that "paracaspases" should be considered a sub-class of "metacaspases" and that paracaspases have evolved several times independently (13). The name caspase refers to both the structure (cysteine protease) and the function (aspartic acid substrate specificity) of the protein family. The semantic association of metacaspases and paracaspases to caspases is therefore unfortunate, since these similar names inspired false assumptions of common roles and properties of the different protein families (14). Despite the identification of "paracaspase" in 2000, it was not until 2008 that the proteolytic activity of MALT1 was established (15, 16). In contrast to true caspases (but similar to metacaspases and orthocaspases), the PCASP1 cleaves substrates specifically after an arginine residue (17–19). The anti-inflammatory role of many of the known protease substrates coupled with the critical role for MALT1 in pro-inflammatory signaling has sparked an interest in targeting MALT1 protease activity as a therapeutic strategy for autoimmune diseases (20). The proteolytic activity of MALT1 was also found to be critical for certain cancers (21), which has stimulated an interest in MALT1 protease activity as a cancer therapy target as well. Although the MALT1 scaffold function for the recruitment of downstream TRAF6 has been clearly associated to NF-κB activation (22), the MALT1 proteolytic activity plays a more subtle role being required for the activation of a subset of NF-κB-dependent genes (23–26) and the stabilization of specific mRNAs (27). MALT1 belongs to the type 1 paracaspase family, which consists of an N-terminal death domain, immunoglobulin domains, and a paracaspase domain. Type 2 paracaspases only contain the paracaspase domain and are found in non-metazoans and early-branching metazoans like porifera, placozoa, and ctenophora (13). The type 1 family of paracaspases originated sometime during the Ediacaran geological period, preceding the last common ancestor of bilaterians and cnidarians (13, 28, 29). The cnidarians (e.g., jellyfish, sea anemone, hydra, and coral) and bilaterians (e.g., vertebrates, insects, nematodes, mollusks, and ringed worms) form the planulozoan clade (30). In our previous survey of paracaspases and MALT1-associated proteins, type 1 paracaspases and Bcl10 could not be found outside planulozoa (13). Cnidarians typically contain several paralogs of both type 1 and the ancient type 2 paracaspases, whereas bilaterians typically contain a single copy of a type 1 paracaspase. Notable exceptions are the jawed vertebrates, where the type 1 paracaspase got triplicated. Subsequently, two paralogs were lost in the mammalian lineage leaving MALT1 as the single paracaspase in mammals (13). Importantly, some invertebrates, such as the nematode *Caenorhabditis elegans*, contain a conserved type 1 paracaspase but lack NF-κB (31), which indicates that other roles or mechanisms might be responsible for the conservation of the general domain organization of the type 1 paracaspases (13). Mice deficient for MALT1 do not show any obvious developmental phenotypes and primarily show defects in T and B cell functions (2, 3). In addition to functional studies of MALT1 in human cells, human patients, and mouse models, investigating the evolutionary history of the type 1 paracaspases, their interacting proteins and molecular functions in alternative model systems could provide important clues to yet-unknown roles and functions of human MALT1 (13). Finding those alternative functions of MALT1 could ultimately be important in the context of future MALT1 inhibitor-based therapies (32) and could help identify yet undiscovered issues that might affect patients deficient in MALT1.

RESULTS

CBM Complex Evolution Indicates Ancient Functional Conservation

In order to unravel the evolutionary history of the CBM complex, the sequences of CARD–CC, Bcl10, and other CBM complex-associated proteins were investigated through mining of several sequence databases and through phylogenetic analyses. The CARD–CC and Bcl10 CBM complex components showed coevolution (**Figure 1A**), whereas MALT1-like paracaspases could be found also in organisms lacking the upstream signaling proteins Bcl10 and CARD–CC (**Figure 1**; Figures S1–S3 in Supplementary Material). The presence of invertebrate Syk/Zap70 homologs correlates with the presence of Bcl10 and CARD–CC (**Figure 1**; Figures S1B and S2 in Supplementary Material). Since the N-terminal SH2 domains in Syk and Zap70 are critical for interaction with upstream ITAM domain-containing receptors (33, 34), the overlapping phylogenetic distribution of the CBM complex and Syk/Zap70 indicates an

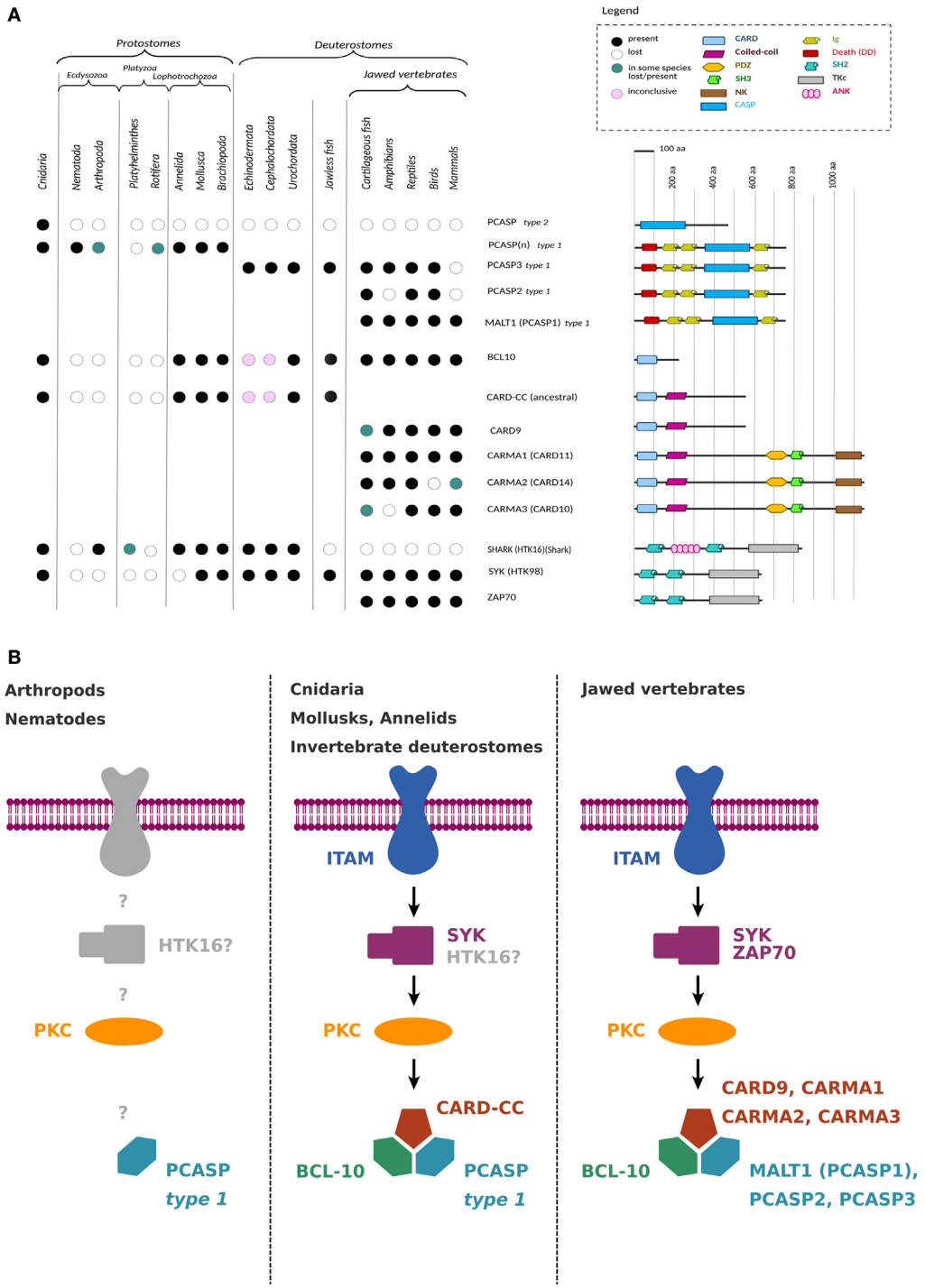

FIGURE 1 | Coevolution and proposed signaling model. **(A)** Patterns of coevolution of Syk and several CBM complex components in various organisms within the planulozoan clade. Type 1 paracaspases prior to Deuterostomes were annotated as PCASP(*n*) since currently available invertebrate genome sequences cannot determine whether a distant paracaspase is an ancient PCASP3 paralog or ortholog. One model proposes two ancient type 1 paracaspases, one Bcl10-dependent and one Bcl10-independent. The CARD–CC/Bcl10-dependent type 1 paracaspase shows MALT1-like activities. Deuterostomia (including tunicates, lancelets, vertebrates, and hemichordates), annelids, and mollusks inherited the Bcl10-dependent type 1 paracaspase, whereas most other bilaterian invertebrates kept the Bcl10-independent type 1 paracaspase. The model is based on currently available reliable sequence information and might change with additional data. Analogously, CARD–CC became duplicated and later fused with MAGUK domains in the jawed vertebrates. At this moment, we are uncertain about which of the four jawed vertebrate CARD–CC paralogs (CARD-9, -10, -11, -14) should be considered the ortholog of the ancestral CARD–CC. Also, upstream Syk became duplicated in jawed vertebrates, resulting in Zap70. **(B)** Proposed signaling model in various organism classes. Nothing is known about upstream activators of type 1 paracaspases in CARD–CC/Bcl10-independent organisms such as arthropods and nematodes.

ancient conservation of ITAM-containing upstream receptors linked to signaling *via* the CBM complex (**Figure 1B**; Figure S1A in Supplementary Material). By contrast, another invertebrate SH2 domain tyrosine kinase ("Shark"), which has been shown to also mediate ITAM-dependent immune-related signals (35), does not show a correlation with the phylogenetic distribution of the CBM complex components. Another evolutionary conserved class of receptors that can signal *via* a CBM complex-dependent pathway is the G protein-coupled receptors (GPCRs). Interestingly, a common feature for the currently known GPCR pathways that signal *via* a CBM complex is that they depend on G_{12}/G_{13}, $G_{q,}$ and RhoA (36). These components do, however, not show a pattern of CBM coevolution. In an extended analysis of homologs of human CBM-interacting proteins and comparisons to the CBM complex phylogenetic distribution, we identified proteins with phylogenetic distributions that were either not correlated (CBM-independent), correlated (CBM-coevolving), or vertebrate-specific, which might reflect on the original functions of the CBM complex: the CBM-interacting proteins AIP (37), Akt (38), CaMKII (39), caspase-8 (40), β-catenin, and its destruction complex (41), cIAP1/cIAP2 (42), CK1α (43), CRADD (44), CSN5 (45), MIB2 (46), NOTCH1 (47), p62/SQSTM1 (48), RLTPR (49), and Rubicon (50) showed a wide phylogenetic distribution with no indications of a CBM coevolution, indicating important CBM-independent roles. By contrast, A20 (15), DEPDC7 (51), HECTD3 (52), LRRK1 (53), Net1 (54), and RIG-I (55) showed a phylogenetic distribution or BLASTp ranking that correlates with the presence of the CBM complex. Other CBM-interacting proteins like ADAP (56), BINCA (57), CKIP1 (58), RIPK2 (59), and USP2a (60) were poorly conserved in invertebrates and might represent more recently evolved CBM interaction partners. Taken together, these phylogenetic patterns indicate an ancient conserved signaling pathway, possibly *via* ITAM/Syk/PKC to CBM complex activation (**Figure 1B**).

Organisms With CARD–CC and Bcl10 Have More Vertebrate-Like Type 1 Paracaspase Sequences

While searching for invertebrate homologs of type 1 paracaspases and Bcl10, it became apparent that type 1 paracaspases from species containing Syk, CARD–CC, and Bcl10 (**Figure 1**; Figures S1B and S2 in Supplementary Material) generally had higher BLASTp scores compared to species from phyla lacking these CBM complex-associated proteins. Phylogenetic analyses of several type 1 paracaspases revealed that type 1 paracaspases from species that contain *Bcl10* (cnidarians, mollusks, annelids, hemichordates) often cluster closer to the vertebrate paracaspases, either directly or indirectly by clustering with the invertebrate *Pcasp3* orthologs from tunicate and lancelet (13) (Figures S1C and S3 in Supplementary Material), indicating a conserved common Bcl10-dependent paracaspase ancestor. Since the MALT1 N-terminal death domain and immunoglobulin domain are Bcl10 binding (61), a phylogenetic analysis of the sequence N-terminal of the caspase-like domain was performed. This analysis showed a stronger association between paracaspases from *Bcl10*-containing species, but does not cluster known paralogs within the deuterostomes (Figure S1C in Supplementary Material), such as PCASP3 protein sequences from acorn worm, lancelet, or tunicate. Phylogenetic analyses of full-length paracaspases and of the highly conserved caspase-like domain indicate that the last common bilaterian ancestor had two to three different type 1 paracaspases (Figure S3 in Supplementary Material), which makes it possible that Bcl10-dependent and -independent paracaspases originated before the bilaterians. This is intriguingly similar to the early evolution of the apoptosis network, where the last planulozoan ancestor had multiple paralogs of Apaf-1, and different paralogs were kept in the different lineages (62). Because of the unclear early bilaterian evolutionary history of the type 1 paracaspases, only deuterostome paracaspases, which are clear orthologs of the vertebrate *Pcasp3* (13), were currently classified and named as *Pcasp3*. Until the invertebrate paracaspases can be more accurately classified and numbered, the three cnidarian type 1 paracaspase paralogs were annotated "A" to "C" (**Figures 1–5**; Figures S1 and S4 in Supplementary Material) in order to avoid possible future name space conflicts.

Recent Evolution of MALT1-Like Activities in Deuterostome Type 1 Paracaspases

MALT1-like protease and NF-κB-inducing scaffold activities in type 1 paracaspases were shown to be present as far back as the last common ancestor of the three jawed vertebrate paracaspase paralogs (13). All type 1 paracaspases have a conserved domain structure ever since Cnidaria (**Figure 1A**), which indicates ancient conserved functions. To further determine the evolutionary origins of these activities, we functionally analyzed the type 1 paracaspase from lamprey (*Petromyzon marinus*) (PmPCASP), which represents the paracaspase function in the last common vertebrate ancestor prior to the dramatic expansion of CBM complex-associated proteins that occurred in jawed vertebrates (**Figure 1**; Figure S2 in Supplementary Material). For the investigation of conserved substrate specificity of paracaspases within the deuterostomes, we also analyzed the paracaspase SkPCASP from the hemichordate acorn worm (*Saccoglossus kowaleski*). *MALT1*-deficient HEK293T cells were transiently transfected with constructs expressing paracaspases fused to the *ETV6* HLH domain, which is known to induce oligomerization and artificial activation (26), and analyzed for their ability to activate NF-κB-dependent luciferase reporter gene expression (reflecting paracaspase scaffold function) and CYLD cleavage (reflecting paracaspase protease substrate specificity). CYLD is chosen as a model substrate for the evaluation of MALT1-like paracaspase protease activity and specificity since it is a large protein with a single MALT1 cleavage site (R324) and many potential aspecific cleavage sites which are never cleaved by MALT1. CYLD also represents one of the oldest paracaspase substrates (13, 63). The currently most distantly related vertebrate paracaspase with conserved activity, zebrafish (*Danio rerio*) PCASP3 (DrPCASP3) (13) was used as positive control. Only the activated human MALT1 and zebrafish PCASP3 induced NF-κB-dependent luciferase reporter gene expression (**Figure 2A**), while the lamprey and hemichordate homologs failed to do so. Moreover, the latter two did not show conserved MALT1-like protease substrate specificity either, as determined by CYLD cleavage (**Figure 2B**).

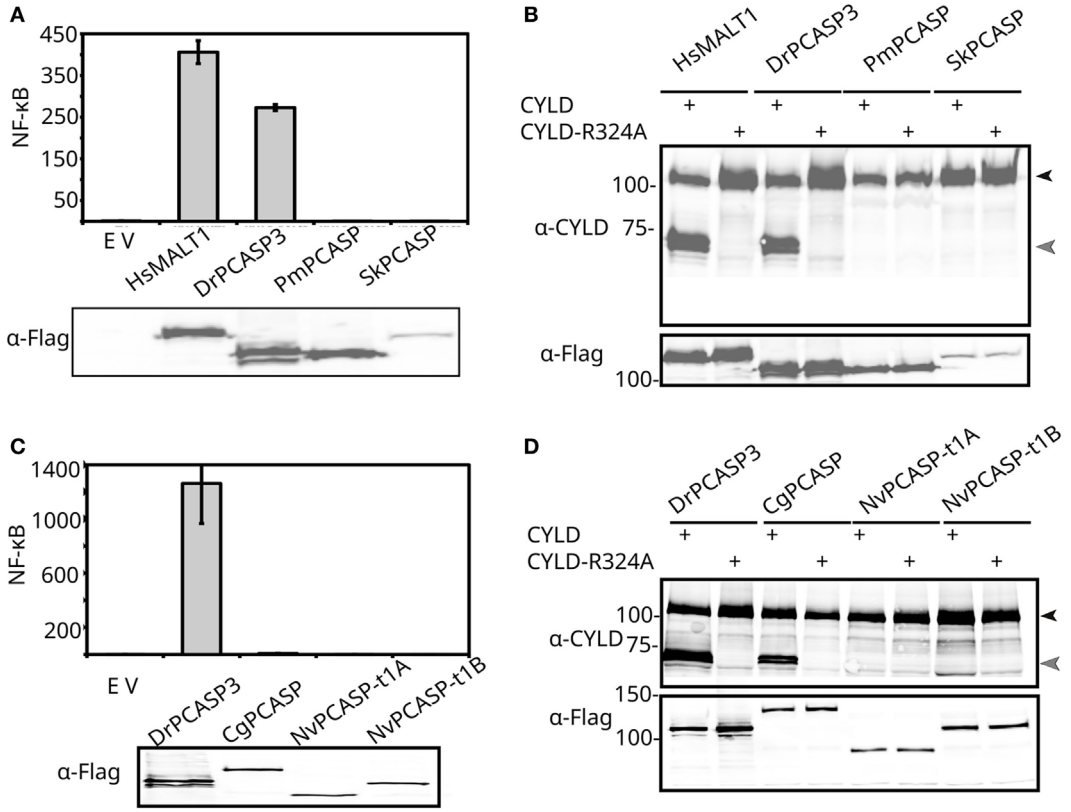

FIGURE 2 | Functional conservation of invertebrate paracaspases. **(A,C)** NF-κB-dependent luciferase reporter gene induction by HLH-paracaspase fusion proteins. The indicated Flag-tagged HLH-paracaspases were expressed in MALT1-deficient HEK293T cells together with an NF-κB-dependent luciferase reporter expression plasmid and a constituitively expressed β-galactosidase reporter gene. Luciferase values are normalized against β-galactosidase and expressed as fold induction compared to samples not expressing a HLH-paracaspase (empty vector: EV). Error bars represent 95% confidence intervals [Student's *t*-distribution (65)]. The lower part of the panel shows the expression of each HLH-paracaspase as revealed by Western blotting and development with anti-Flag antibodies. Experiments were repeated four times. **(B,D)** CYLD cleavage by HLH-paracaspase fusion proteins. MALT1-deficient HEK293T cells were transiently transfected with the indicated HLH-paracaspases together with either human WT CYLD or CYLD (R324A) in which the MALT1 cleavage site is mutated. Cell lysates were analyzed for CYLD expression and cleavage *via* Western blotting and detection with anti-CYLD antibodies. Full-length CYLD is indicated with a closed arrowhead; cleaved CYLD is indicated by an open arrowhead. To show equal expression levels of each HLH-paracaspase, the blot was also developed with anti-Flag antibodies (lower part). Experiments were repeated three times.

The very poor expression of SkPCASP, most likely related to its AT-rich nucleotide sequence (64), may hamper the detection of a weak protease activity but scaffold activity should still be visible due to the sensitive luciferase readout. These results do, however, indicate that the NF-κB-inducing MALT1-like scaffold activity and the MALT1-like protease substrate specificity evolved relatively recently, after the last common vertebrate ancestor but before the divergence of the three paracaspase paralogs in the last common jawed vertebrate ancestor (Figures S1B,C in Supplementary Material). The conservation of scaffold activity for TRAF6-mediated NF-κB activation is hard to predict by sequence analysis alone: the isoform-specific Ig2 TRAF6-binding motif (TDEAVECTE) and the C-terminal TRAF6-binding site (PVETTD) in MALT1 (22) are PCASP1-specific, but we know that jawed vertebrate PCASP2 and PCASP3 paralogs still are as efficient in NF-κB induction (13). One TRAF6-binding site (TPEETG) located in the Ig3 domain of human MALT1 is found in all three jawed vertebrate paralogs, but is absent in more distant homologs (**Figure 3**) and could represent the critical evolutionary event for NF-κB activating MALT1-like scaffold activity.

Functional Conservation or Convergent Evolution of MALT1-Like Activities in Distant Type 1 Paracaspases Reveals That MALT1 Scaffold and Proteolytic Activities Can Exist Independently

Based on BLASTp and subsequent phylogenetic analyses, the mollusk paracaspases were identified as the non-deuterostome homologs most closely resembling vertebrate type 1 paracaspases (13). The pacific sea oyster (*Crassostrea gigas*) was selected as a model and cDNA source (66) for the mollusks. Conversely, the most distantly related species where type 1 paracaspases and *Bcl10* could be found are Cnidaria (13). The cnidarian model organism starlet sea anemone [*Nematostella vectensis* (NvN)] (67) was used as a cDNA source for as distantly related homologous proteins as

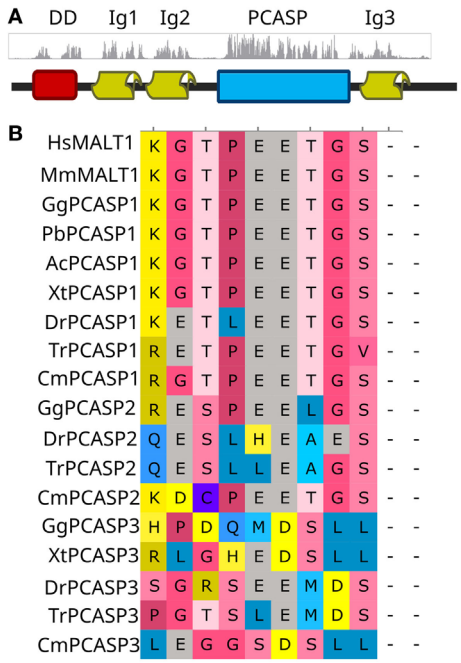

FIGURE 3 | Domain conservation and TRAF6-binding evolution. **(A)** Conservation plot of a MUSCLE alignment from a wide selection of type 1 paracaspases from Cnidaria to humans. Conserved segments correspond well to annotated domains. **(B)** MUSCLE alignment segment of the most conserved TRAF6-binding site in the Ig3 domain. The corresponding sequence is missing in type 1 paracaspase homologs from organisms that diverged before the last common ancestor of jawed vertebrates.

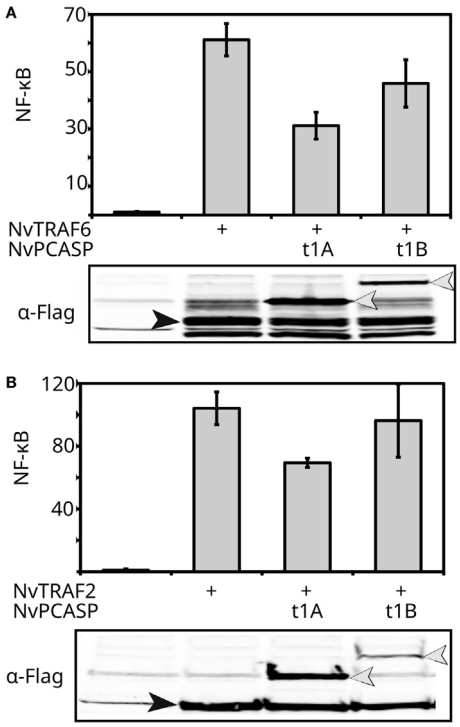

FIGURE 4 | Functional conservation of cnidarian TRAF6 and TRAF2. **(A,B)** *Nematostella vectensis* (Nvn) TRAF6 **(A)** or TRAF2 **(B)** was expressed in human HEK293T cells together with an NF-κB-dependent luciferase reporter gene and a constitutively expressed β-galactosidase reporter gene plasmids. The TRAF was transfected either alone or together with the indicated Nvn HLH-paracaspase fusion protein. Luciferase values were normalized against β-galactosidase and expressed as fold induction compared to samples not expressing the TRAF. Error bars represent 95% confidence intervals (Student's *t*-distribution). The lower part of the panel shows the expression of the TRAF (closed arrow head) and each Flag-tagged HLH-fused type 1 paracaspase (open arrow heads) as revealed by Western blotting and development with anti-Flag antibodies. Experiments were repeated at least twice.

possible. Neither mollusk (CgPCASP) nor sea anemone type 1 paracaspases (NvPCASP-t1A, NvPCASP-t1B) were able to induce NF-κB in a human cellular background (**Figure 2C**). We therefore investigated whether downstream signaling components are functionally conserved. The TRAF family of E3 ubiquitin ligases diverged before the cnidarian/bilaterian last common ancestor (68). To investigate whether the type 1 paracaspase–TRAF interaction has undergone lineage-specific divergence, we cloned the Nvn homologs of *Traf2* and *Traf6* and co-expressed them with the two Nvn type 1 paracaspase paralogs fused to the activating *ETV6* HLH domain in HEK293T cells for testing in an NF-κB luciferase reporter assay (**Figure 4**). NF-κB activation induced by the expression of cnidarian TRAF2 and TRAF6 homologs was equal in the absence or presence of paracaspases, further illustrating the lack of an NF-κB-activating scaffold function in the case of cnidarian paracaspases. Interestingly, the evaluation of MALT1-like protease activity and substrate specificity using human CYLD as a substrate revealed that mollusk paracaspase (CgPCASP) specifically cleaves human CYLD at R324, just like vertebrate paracaspases (**Figure 2D**), indicating either MALT1-like protease substrate specificity already in the last common bilaterian ancestor (Figure S1B in Supplementary Material), or a convergent evolution of MALT1-like proteolytic activity. On the other hand, the "A" and "B" type 1 paracaspase paralogs from sea anemone (NvPCASP-t1A, NvPCASP-t1B) could not cleave CYLD at all, indicating that paracaspase substrate specificity is not conserved in the cnidarians despite being an organism with a *Bcl10* homolog. In conclusion, our data show the presence of MALT1-like catalytic protease activity in organisms that predate the divergence of deuterostomian and protostomian bilaterians and reveal that the MALT1-like catalytic activity can exist independently of the MALT1-like scaffold function leading to NF-κB activation.

Functional Conservation of Bcl10-Induced MALT1 Activity Indicates Complex Molecular Interactions

Bcl10 overexpression is known to activate MALT1 activity in mammals. To further investigate the functional conservation of Bcl10/paracaspase coevolution, we transfected *H. sapiens*, *D. rerio*, *C. gigas*, and Nvn Bcl10 in MALT1-deficient HEK293T cells with or without reconstitution with human MALT1. Strikingly, not only *D. rerio* Bcl10 (DrBcl10) but also the Nvn Bcl10 (NvBcl10) could induce human MALT1-mediated NF-κB activation (**Figure 5A**). This result is highly unexpected, since a critical MALT1 Ig domain

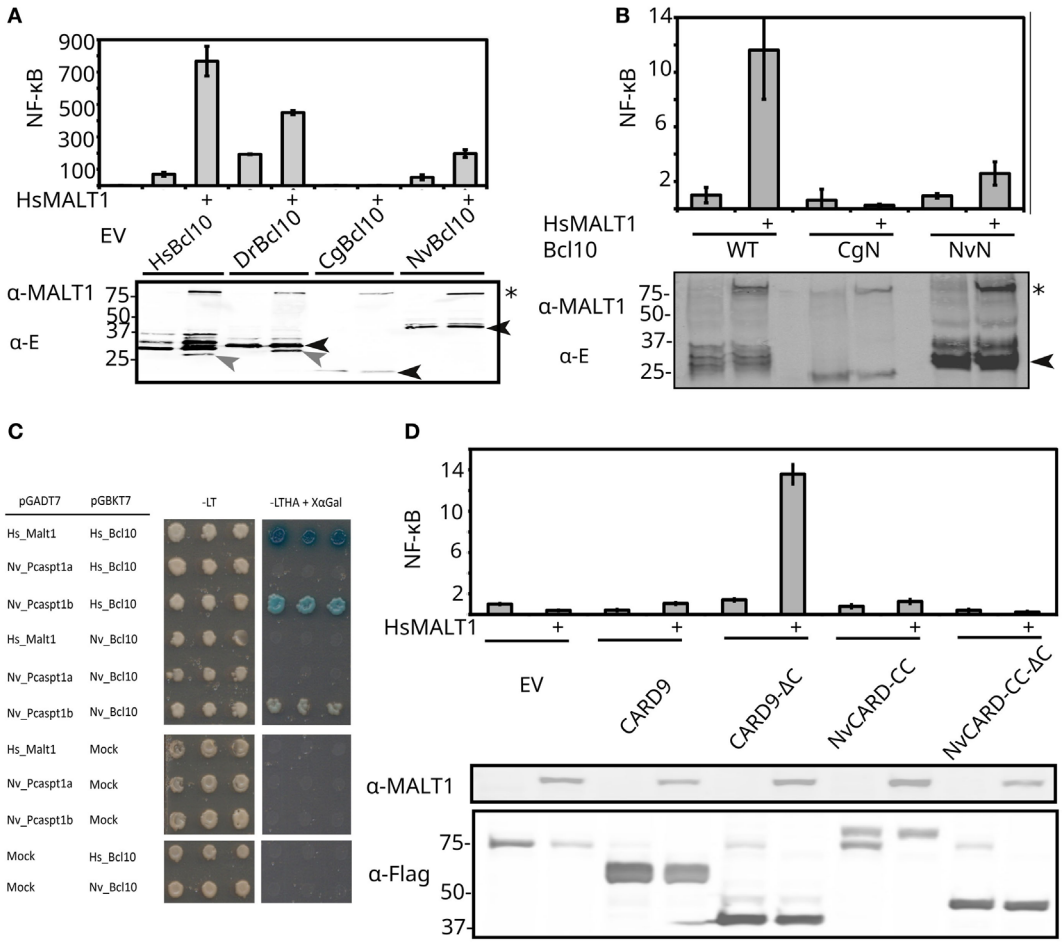

FIGURE 5 | Functional conservation of Bcl10 and CARD–CC proteins. **(A)** Human MALT1-dependent NF-κB induction by different Bcl10 homologs. The indicated E-tagged Bcl10 homologs were expressed in MALT1-deficient HEK293T cells together with an NF-κB-dependent luciferase reporter expression plasmid and a constituitively expressed β-galactosidase reporter gene. Where indicated (+), human MALT1 was also co-expressed. Luciferase values were normalized against β-galactosidase and expressed as fold induction compared to samples not expressing Bcl10 (EV). Error bars represent 95% confidence intervals (Student's *t*-distribution). The expression of E-tagged Bcl10 homologs and human MALT1 was revealed by Western blotting and detection with anti-E-tag or anti-MALT1 antibodies, respectively (lower part). Full-length Bcl10 is indicated by closed arrow heads and cleaved Bcl10 by open arrow heads. MALT1 is indicated by an asterisk. Experiments were repeated two times. **(B)** Bcl10/CARD-dependent MALT1-mediated NF-κB induction. Wild-type human Bcl10 and hybrid Bcl10 clones where residues 1–102 of human Bcl10 were replaced by the corresponding residues from *C. gigas* (CgN) or *Nematostella vectensis* (NvN) Bcl10 were expressed in MALT1-deficient HEK293T cells together with an NF-κB-dependent luciferase reporter expression plasmid and a constituitively expressed β-galactosidase reporter gene. Where indicated, (+) human MALT1 was also co-expressed. Luciferase values were normalized against β-galactosidase and expressed as fold induction compared to samples expressing human wild-type Bcl10 without MALT1. Experiments were repeated two times. **(C)** Yeast-2-hybrid assay demonstrating conserved interaction between both Nvn and human Bcl10 and type 1 paracaspases. Left panel represents growth on non-selective media and right panel selective growth (-LTHA medium), on which only a combination of bait and prey clones with interacting proteins can grow. As an independent readout, clones with strong bait–prey interactions also stain blue from X-gal. **(D)** Full-length and C-terminal deletion (ΔC) constructs of human CARD-9 and Nvn CARD–CC were expressed in MALT1-deficient HEK293T cells together with NF-κB-dependent luciferase reporter gene and constitutively expressed β-galactosidase reporter gene plasmids. Where indicated, (+) human MALT1 was also co-expressed. Luciferase values are normalized against β-galactosidase and expressed as fold induction compared to samples not expressing CARD-9 or CARD–CC (EV). Error bars represent 95% confidence intervals (Student's *t*-distribution). The lower part of the panel shows the expression of full-length and ΔC-mutant CARD-9 and Nvn CARD–CC constructs, respectively, as revealed by Western blotting and development with anti-Flag antibodies. An aspecific Flag signal at 75 kDa is sometimes visible in the MALT1-deficient HEK293T cells. Experiments were repeated two times.

interaction sequence (residues 107–119 in human Bcl10) that has been identified downstream of the CARD domain in human Bcl10 (61) can only be found in vertebrates. Importantly, the critical 107–119 residues in human Bcl10 are not conserved in *D. rerio*, demonstrating that alternative additional C-terminal paracaspase binding domains in Bcl10 exist. In contrast to human and *D. rerio* Bcl10, Nvn Bcl10 does not appear to be cleaved by human MALT1 (**Figure 5A**). The observation that cnidarian Bcl10 can activate human MALT1 indicates a highly conserved interaction surface between the two proteins. A conserved Bcl10–paracaspase interaction was confirmed with yeast-2-hybrid analysis, where the Nvn type 1 paracaspase "B" paralog readily interacted with both human and Nvn Bcl10 (**Figure 5C**). By contrast, the Nvn type 1 paracaspase "A" paralog did not show any interaction with

Bcl10. Interestingly, this difference in Bcl10 interaction is reflected by the phylogenetic analysis of the N-terminal sequence of type 1 paracaspases, where the cnidarian "B" paralog clusters closer to type 1 paracaspases from vertebrates and Bcl10-containing invertebrate bilaterian species (Figure S1C in Supplementary Material). In contrast to the functional interaction revealed in the NF-κB luciferase assays (**Figures 5A,B**), no physical interaction could be established between Nvn Bcl10 and human MALT1 by yeast-2-hybrid (**Figure 5C**) or by co-immunoprecipitation (data not shown). *C. gigas* Bcl10 failed to induce any NF-κB reporter activity (**Figure 5A**). In general, samples expressing CgBcl10 show less expression of all transfected components (e.g., MALT1 in **Figures 5A,B**). This could be due to cell death or other counter-selection in highly expressing cells, which might indicate that CgBcl10 engages in detrimental off-target protein–protein interactions in the human cell background. The invertebrate Bcl10 homologs only show a clear alignment of the CARD domain up until residue 102 of human Bcl10. This N-terminal region has been shown to be required but insufficient for NF-κB induction (61). In addition to the 102 conserved N-terminal residues, all Bcl10 homologs show a proline-rich motif close to the C-terminus. The functional importance of this proline-rich region is, however, unknown, since it is dispensable for MALT1 activation. For further proof that the Bcl10 CARD domain is functionally conserved, we generated hybrid Bcl10 clones where residues 1–102 in human Bcl10 are replaced by the corresponding residues from NvBcl10 or CgBcl10. Hybrid NvBcl10 (NvBcl10 CARD, HsBcl10 C-terminal sequence) showed the same relative level of activation as the wild-type NvBcl10 and hybrid CgBcl10 remained inactive, indicating that the suboptimal induction is due to the CARD domain and not due to lacking protein–protein interaction sequences at the C-terminal part of Bcl10 (**Figures 5A,B**). Although suboptimal Bcl10 activity (2.5- vs 10-fold MALT1-dependent NF-κB activation), we have demonstrated that the CARD domain, which is critical for paracaspase interaction, is conserved in Nvn. Functional conservation is not always directly related to primary sequence conservation. The very low sequence identity in the corresponding CARD sequence from Nvn (35% identity) is less than the closer related *C. gigas* Bcl10 CARD (40% identity), which lacks the ability to activate human MALT1. Both distant Bcl10 homologs have acidic residues that correspond to E84, a glutamine corresponding to Q92 and hydrophobic residues corresponding to residues L95, I96, and I99 in human Bcl10, which all are critical for MALT1 interaction (61). On the other hand, only NvBcl10 has an acidic residue that corresponds to the critical D80 residue in human Bcl10. From these experiments, we can conclude that the Bcl10/paracaspase interaction is likely to be ancient and that the critical Bcl10 CARD/paracaspase interaction is highly conserved. We also demonstrate that the non-CARD component of Bcl10 required for MALT1 activation is not dependent on a single highly conserved MALT1-binding peptide sequence downstream of the CARD domain.

A Conserved Intramolecular Autoinhibition Mechanism in Vertebrate CARD–CC Proteins

Bcl10 has been shown to be functionally conserved as far back as *D. rerio*, as is the upstream interaction with CARD–CC proteins (69, 70). We have now shown that Bcl10 and MALT1-like activities from type 1 paracaspases are considerably older (**Figures 2** and **5**), most likely preceding the Cambrian explosion (30). We were, however, unable to detect an interaction between full-length CARD-9 or Nvn CARD–CC and the Bcl10 clones in a yeast-2-hybrid assay (data not shown), which could be due to intramolecular CARD–CC autoinhibition. In line with this, both wild-type CARD-9 and the Nvn CARD–CC show very low MALT1-dependent activity (~2-fold, **Figure 5D**) upon overexpression in HEK293T cells, which most probably is due to an intramolecular inhibition of the CARD domain that prevents Bcl10 binding (71). In CARD-11, the linker sequence between the CC and PDZ domain acts as an intramolecular inhibitory domain (70). We hypothesized that the undefined sequence downstream of the CC domain in CARD-9 and the ancestral CARD–CC proteins could fill a similar autoinhibitory function. We therefore generated C-terminal deletion (ΔC) constructs where the sequences downstream of the CC domain of mouse or human CARD-9, -10, -11, -14, and Nvn (NvCARD–CC-ΔC) were removed. The ΔC constructs were co-expressed with human MALT1 in MALT1-deficient HEK293T cells to test their ability to induce MALT1-dependent NF-κB activation. In contrast to CARD-9 and the other vertebrate CARD–CC proteins, the C-terminal deletion was not able to activate NvCARD–CC (**Figures 5D** and **6**), indicating that the MALT1-dependent NF-κB activation downstream of this protein is due to an alternative mechanism. Taken together, we can conclude that the core CBM complex components are evolutionary linked but that functional evaluation of conservation is problematic due to lineage-specific divergence.

CBM Complex Components of the Starlet Sea Anemone (Nvn) Show an Overlapping Expression Pattern

Since the Nvn type 1 paracaspase paralog "B" was found to interact with Bcl10 of both Nvn and human (**Figure 5C**) and since Nvn CARD–CC showed a MALT1-dependent signaling activity (**Figure 5D**), it is likely that these three components together form a CBM signaling complex. Investigation of the expression patterns of the two type 1 paracaspase paralogs, Bcl10 and CARD–CC, during Nvn embryo development (11 stages, from unfertilized egg to the juvenile stage at 14 days post fertilization) using *in situ* hybridization (72) revealed overlapping temporal and spatial expression of the proposed CBM complex components (**Figure 7**). All four genes showed expression from late planula and onward in a pattern indicating neuronal expression. In addition, all four genes also showed a high expression in the tentacles at the later stages. Although we cannot show the formation of a CBM complex at the protein level in sea anemone, the overlapping temporal and spatial mRNA expression pattern of the proposed CBM complex components is indicative for the existence of such a complex.

CBM and NF-κB-Independent Functions of Type 1 Paracaspases

Our functional analyses of non-jawed vertebrate deuterostome and other invertebrate type 1 paracaspases indicate that the

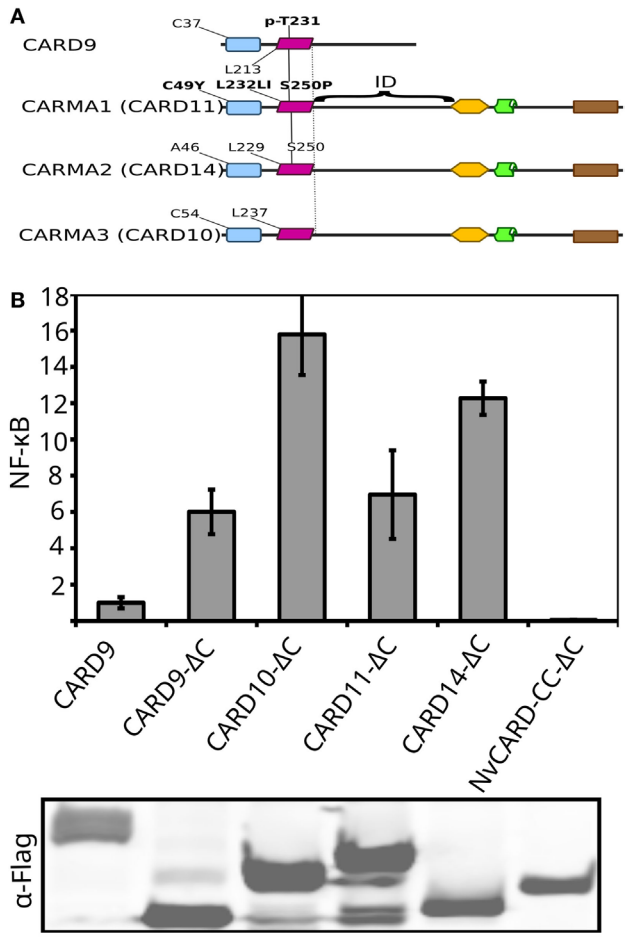

FIGURE 6 | Activation by C-terminal deletions of the CARD–Coiled Coil (CC) protein family members. **(A)** Structural features of the four mammalian CARD–CC family proteins, activating mutations/modifications in conserved residues, are highlighted in bold text. C-terminal deletion mutants in **(B)** consist of the CARD (blue) and CC (purple) domains, to the left of the dashed line. **(B)** Mutants of CARD–CC family members with C-terminal deletions were expressed in human HEK293T cells together with an NF-κB-dependent luciferase reporter gene and a constitutively expressed β-galactosidase reporter gene plasmids. Luciferase values were normalized against β-galactosidase and expressed as fold induction compared to full-length (with intramolecular repression) CARD-9.

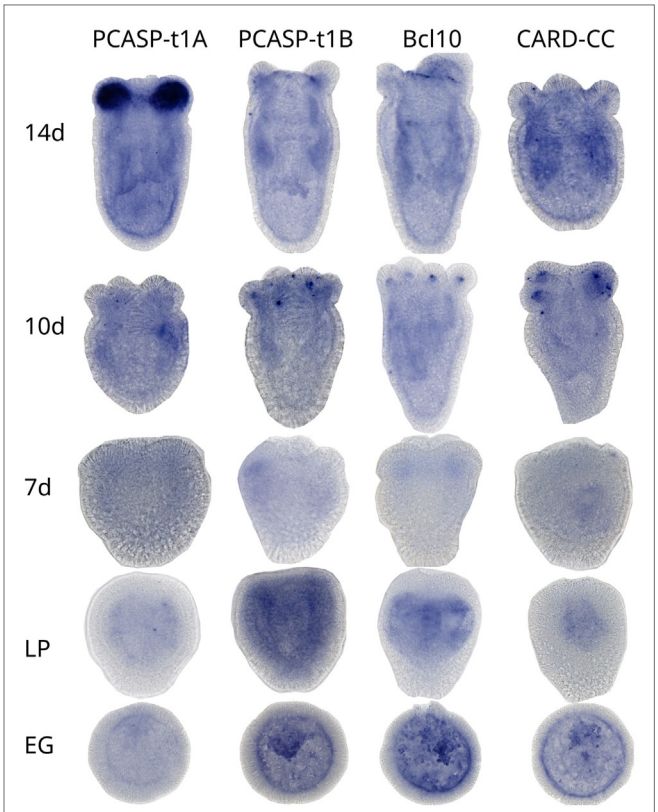

FIGURE 7 | The CBM complex components show overlapping expression in *Nematostella vectensis* (Nvn). Developing Nvn embryos were stained for the indicated genes *via in situ* hybridization at 11 different developmental stages, from the unfertilized egg stage to 14 days post fertilization. Representative pictures from 14 days (14d), 10 days (10d), 7 days (7d), late planula (LP), and early gastrula (EG) stages for all 4 CBM complex genes analyzed are shown.

remarkable domain conservation in this protein family cannot be explained by currently known mechanisms. The nematode model organism *C. elegans* is a promising system to specifically investigate unconventional functions of type 1 paracaspases because it lacks CARD–CC, Bcl10, and NF-κB. Despite the lack of upstream and downstream proteins in the known paracaspase-dependent signaling pathway, the WormBase phenotype database indicates an important role for the *C. elegans* type 1 paracaspase (*F22D3.6* or *malt1*) with a "lethal or sterile" mutant phenotype (*tm289* vs *tm321*) in nematodes (73). To investigate this further, we analyzed the life span of *C. elegans* in which the paracaspase was knocked down by RNAi. We silenced the *C. elegans* paracaspase gene systemically in the wild-type strain N2 (all tissues except the neurons) and in a strain hypersensitive to neuronal RNAi (TU3311). While systemic knockdown of *malt1* showed no effect on life span (**Figure 8A**), *malt1* silencing in the neurons caused a slight but significant reduction of life span ($p < 0.05$ in all three replicates, **Figure 8B**), hinting at a vital role of this paracaspase homolog in the *C. elegans* neurons. Remarkably, paracaspase knockdown in the neuronal RNAi hypersensitive strain also caused an increased motility (**Figure 8C**). These data indicate the existence of a previously unknown CBM- and NF-κB-independent function of paracaspases in *C. elegans* and possibly other organisms.

DISCUSSION

Extensive CBM Complex-Associated Evolutionary Events in Jawed Vertebrates

The presence of three CARMA paralogs (CARD-10, -11, and -14), the split between Syk and Zap70, the evolution of MALT1-like activities, and the divergence of three type 1 paracaspase paralogs in the vertebrate lineage all seem to have arisen in the last common ancestor of jawed vertebrates (Figure S2 in Supplementary Material), which coincides with the evolution of the vertebrate

adaptive immune system (74). Interestingly, CARD-11 shows a conserved and non-redundant function in B cell antigen receptor signaling at least as far back as the last common ancestor of mammals and dinosaurs (75). Since all jawed vertebrates have all three CARMA paralogs, a likely evolutionary scenario for the CARMA proteins is that early in the jawed vertebrate evolution, a CARD-9-like CARD–CC got fused with a ZO-1/Dlg5-like MAGUK protein upstream of the PDZ domain (76). Lampreys are in this respect more similar to invertebrates and only have a single ancestral CARD–CC (**Figure 1A**) and a single type 1 paracaspase, a PCASP3 ortholog which is related to the parent of the PCASP3 and PCASP(1/2) branches in jawed vertebrates (**Figure 1A**; Figure S1C in Supplementary Material). At this moment, we cannot determine the sequence of evolutionary events between the last common vertebrate ancestor and the last common jawed vertebrate ancestor leading to the increased complexity of the CBM-associated proteins. For example, we do not know if either the evolution of the CARMA paralogs, or the NF-κB-inducing scaffold function of paracaspases, or the expansion of the paracaspases, or the Syk/Zap70 duplication was the primary cause for the CBM-associated expansion in jawed vertebrates.

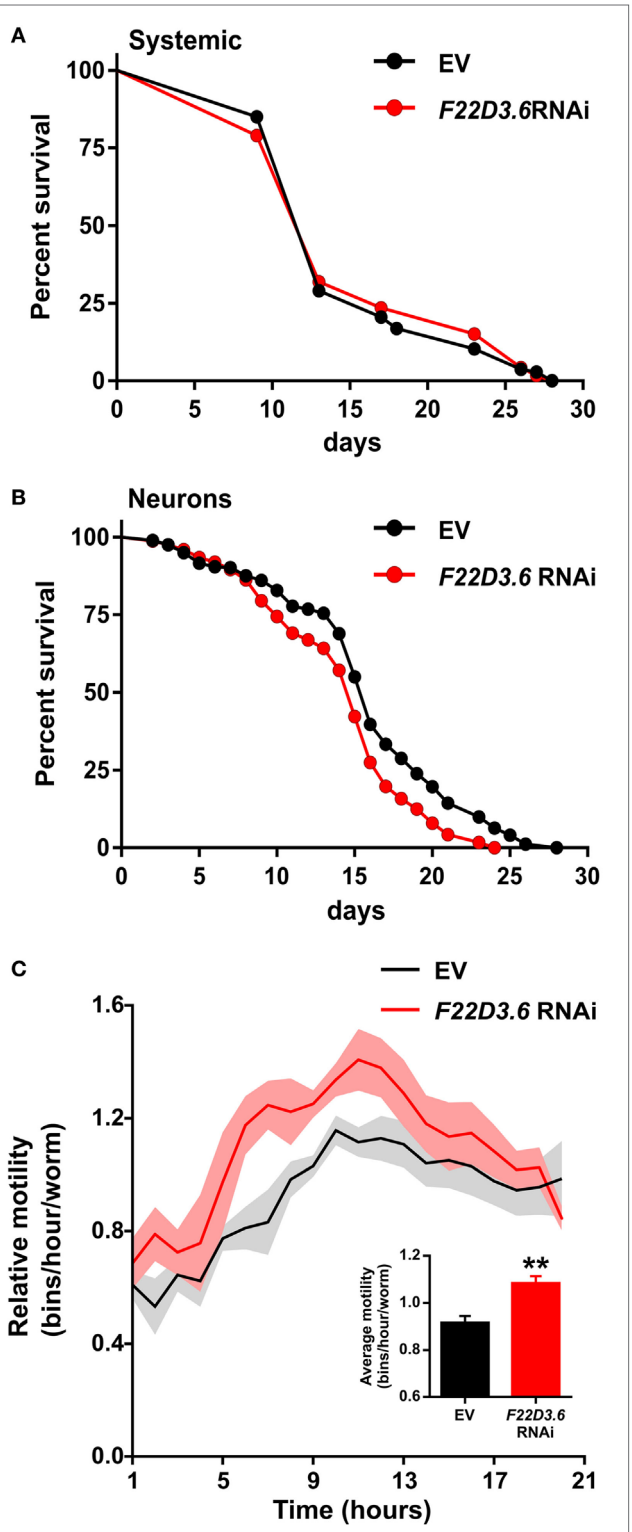

FIGURE 8 | Continued

FIGURE 8 | CBM and NF-κB-independent functions of the type 1 paracaspase *malt1* in *Caenorhabditis elegans*. **(A)** Wild-type (N2 strain) *C. elegans* worms were fed *E. coli* expressing RNAi targeting *malt1* ($N = 119$) and regularly monitored for viability compared to worms fed control RNAi ($N = 107$). No difference in life span could be detected ($p = 0.8194$). In these wild-type worms, RNAi is typically targeting every cell except neurons. Silencing in the wild-type N2 strain resulted in approximately 60% reduction of total *malt1* expression levels, indicating efficient silencing in the non-neuronal cells. **(B)** Neuronal RNAi importer transgenic (TU3311 strain; *unc-119p:sid-1* transgenic) *C. elegans* worms were fed *E. coli* expressing RNAi targeting *malt1* ($N = 399$) and regularly monitored for viability compared to worms fed control RNAi ($N = 364$). A reproducible and significant ($p = 1.4 \times 10^{-7}$) drop in survival was seen upon silencing *malt1* in the neuronal system. **(C)** Neuronal RNAi importer transgenic (TU3311 strain; *unc-119p:sid-1* transgenic) *C. elegans* worms were fed *E. coli* expressing RNAi targeting *malt1* and monitored for motility, using the Wmicrotracker device, compared to worms fed control RNAi. Panels **(A–C)** represent pooled results of three biological replicates carried out at 20°C.

Structure–Function Information From Ancient CBM Complex Molecular Interactions

There are already very good structure–function studies done on both the human Bcl10/MALT1 interaction (61) and the human CARD11/Bcl10 interaction (77). Functional characterization of evolutionary distant homologs does, however, provide complementary insights (78, 79). We could, for example, by comparative analysis between CARD–CC proteins generate activated C-terminal deletion mutants in all four jawed vertebrate CARD–CC family members (**Figure 6**). While in traditional structure–function analyses, single residues predicted to be important are mutated in order to disrupt activity, our identification of functionally conserved distant Bcl10 homologs meant that we could simultaneously "mutate" up to 65% of all residues in the critical interaction domain without completely disrupting activity. To get a better understanding of early Bcl10 structure–function evolution for interaction with CARD–CC and type 1 paracaspases, more sequences from invertebrate genomes are needed (80, 81).

Identification of CBM Complex Regulation and Function Through Comparative Biology

Investigating early-diverging biological model systems for biological function, protein–protein interactions and signal transduction mechanisms can highlight the original and most conserved functions in a native context. It is worth noting that a MALT1 homolog was recently found to be one of the most significantly upregulated genes in the coral *Orbicella faveolata* after natural bleaching stress, an environmental stress-triggered dysregulated host immune response that leads to dysbiosis (82). By re-analysis of the RNAseq sequences, we could identify the upregulated *O. faveolata* MALT1 homolog at the base of the cnidarian "B" paralog branch (Figure S4 in Supplementary Material). The other three *O. faveolata* type 1 paracaspase paralogs did not respond to the natural bleaching stress. The paralog-specific regulation indicates that the different paralogs might serve unique and specialized functions in these early-diverging organisms. This also indicates that cnidarian paracaspases can still be involved in immune-related responses despite lacking MALT1-like protease- and scaffold functions in our models. The expression patterns of Nvn Bcl10 and CARD–CC are intriguing and might indicate an ancient conserved developmental role, since it has been shown that Bcl10 and CARD-10 are involved in neural tube closure during mouse embryo development (83, 84). There are no neurodevelopmental defects in MALT1-deficient mice (3), but the expression profiles of MALT1 (EMAGE: 12681) during mouse development are strongly neuronal (85). In case there is a functional involvement of CBM complex components in the cnidarian nervous system, the reported interaction of the CBM complex with Notch1 would be a likely conserved mechanism (47, 86). The *C. elegans* phenotype also highlights an important neuronal role for CBM-independent type 1 paracaspase functions and indicates that further investigations on the role and function of *malt1* in *C. elegans* could be highly interesting. It is possible that our RNAi knockdown approach results in a less severe phenotype than the *tm289* knockout, but this mutant also disrupts another gene (*F22D3.1*). Future *C. elegans* analyses should thus focus on clean *malt1* knockout and protease-dead catalytic cysteine knockin mutant worms. Ultimately, identifying the CBM-independent type 1 paracaspase activation mechanism and function in organisms like *C. elegans* could potentially also lead to the discovery of a novel fifth (Bcl10-independent) MALT1 activation mechanism, apart from the four (CARD-9, -10, -11, and -14) currently known CBM complexes in humans.

MATERIALS AND METHODS

Sequences of Homologs of Type 1 Paracaspases, Bcl10 and CARD–CC

Protein sequences of type 1 paracaspase, Bcl10 and CARMA/CARD-9 homologs, were retrieved from NCBI,[1] Ensembl,[2] JGI,[3] OIST marine genomics[4] (87–89), ReefGenomics[5] (90), and ICMB[6] (91, 92), using BLASTp (93). Phylogenetic distribution of Bcl10, CARD–CC, and type 1 paracaspases was also confirmed with the HMMER software package[7] (94), using the highly conserved CARD and death domain sequences. All full-length sequences used in the analyses can be found in supplemental materials.

Sequence Alignment and Phylogenetic Analysis

Sequence alignments were performed on the full protein sequence, using the different alignment algorithms Clustal Omega[8] (95), MUSCLE[9] (96). Phylogenetic analyses were performed with PhyML[10] (97) and MrBayes[11] (98) methods. N-terminal paracaspase sequences were trimmed out from a MUSCLE multiple sequence alignment using Jalview (99). Trimmed N-terminal paracaspase sequences less than 190 residues long were excluded from the phylogenetic analysis. Both alignments and phylogenetic analyses were performed using UGENE[12] (100) on Arch[13] Linux (101). For the figures, one of the most representative trees (alignment and phylogenetic analysis) was selected. The final trees were re-drawn to unrooted radial cladograms using dendroscope[14] (102), and branches were colored using Inkscape.[15]

RNA Isolation and cDNA Synthesis

RNA of Nvn from various developmental stages was isolated with TRIzol (Thermo Fisher) and pooled. 1.5 µg of total RNA was subjected to 5'-RACE with a GeneRacer kit (Invitrogen) according to the manufacturer's protocol. RNA was treated with calf intestinal phosphatase to remove the 5' phosphates from truncated RNAs and non-mRNAs. After dephosphorylation of the RNA with tobacco acid pyrophosphatase, lyophilized GeneRacer RNA Oligo (provided in the kit) was added to the 5' end of the RNA with RNA ligase. The ligated RNA was reverse transcribed to cDNA using superscript III with random primers and used as templates for PCR amplifications.

DNA Constructs

Plasmids of the cloned genes were deposited in the BCCM/GeneCorner plasmid collection along with detailed descriptions of cloning strategy and plasmid sequence.[16] The starlet sea anemone (Nvn) type 1 paracaspase paralog "A" (LMBP: 9589) and zebrafish PCASP3 (LMBP: 9573) were cloned previously. Lamprey (PmPCASP; LMBP: 10451) and the hemichordate acorn worm (SkPCASP; LMBP: 10452) were generated synthetically by

[1] https://www.ncbi.nlm.nih.gov.
[2] http://metazoa.ensembl.org.
[3] http://genome.jgi.doe.gov/.
[4] http://marinegenomics.oist.jp.
[5] http://reefgenomics.org/.
[6] https://imcb.a-star.edu.sg.
[7] https://www.ebi.ac.uk/Tools/hmmer.
[8] http://www.clustal.org/omega/.
[9] http://www.drive5.com/muscle/.
[10] http://atgc_montpellier.fr/phyml/.
[11] http://mrbayes.sourceforge.net/.
[12] http://ugene.net/.
[13] http://www.archlinux.org.
[14] https://dendroscope.org.
[15] https://inkscape.org.
[16] http://www.genecorner.ugent.be/.

Gen9 (www.gen9bio.com). PmPCASP (LMBP: 10453), SkPCASP (LMBP: 10454 & 10455), the Nvn type 1 paracaspase paralogs "A" (LMBP: 9636) and "B" (LMBP: 9825), and pacific oyster (CgPCASP, LMBP: 9826 & 10456) paracaspase were cloned behind the human ETV6 HLH domain for dimerization-induced activation as described previously. Human (LMBP: 9637), zebrafish (LMBP: 9665), pacific oyster (LMBP: 9666), and Nvn (LMBP: 9822) Bcl10 were cloned in the pCAGGS vector with an N-terminal E-tag. For functional characterization of the Bcl10 CARD domain, hybrid Bcl10 clones where human residues 1–102 were replaced with the corresponding sequence from pacific oyster (CgN, LMBP: 10190) or Nvn (LMBP: 10191) were cloned. Also, minimal active Δ119–223 clones of human Bcl10 (LMBP: 10269), pacific oyster (CgN, LMBP: 10263), and Nvn (LMBP: 10264) hybrid Bcl10 were cloned for functional tests. Nvn CYLD (LMBP: 9900) was also cloned in pCAGGS with an N-terminal E-tag. The Nvn homologs of CARD–CC (LMBP: 9854) TRAF6 (LMBP: 9855) and TRAF2 (LMBP: 9856) were cloned in a pCDNA3 vector with N-terminal Flag tag. For further specific cloning purposes, human CARD-9 (LMBP: 9877), Bcl10 (LMBP: 9872), MALT1 (LMBP: 9104, 9105) and Nvn CARD–CC (LMBP: 9873), Bcl10 (LMBP: 9874), PCASP-t1A (LMBP: 9875), and PCASP-t1B (LMBP: 9876) were cloned into gateway-compatible pENTR vectors. For Y2H analysis: Human MALT1 (LMBP: 9880, 9899), Bcl10 (LMBP: 9879, 9885), CARD-9 (LMBP: 9878, 9884), and Nematostella PCASP-t1A (LMBP: 9898) PCASP-t1B (LMBP: 9883, 9888), Bcl10 (LMBP: 9882, 9887), and CARD–CC (LMBP: 9881, 9886) were cloned into the pdGADT7 or pdGBKT7 vectors by Gateway LR reaction. For Nvn ISH analysis: As RNA probe templates, pDEST12.2 clones of Nvn CARD–CC (LMBP: 9908), Bcl10 (LMBP: 9902), PCASP-t1A (LMBP: 9903), and PCASP-t1B (LMBP: 9904) were generated by Gateway LR reaction. For investigations of the CARD–CC activation mechanism through the release of an inhibitory domain downstream of the CC domain, C-terminal deletions of CARD-9 (LMBP: 10457), CARD-10 (LMBP: 10459), CARD-11 (LMBP: 10458), CARD-14 (LMBP: 10460), and NvCARD–CC (LMBP: 10461) were generated.

Cell Culture, Transfection, and Expression Analysis

TALEN-generated MALT1-deficient HEK293T cells (clone #36) (13) and WT HEK293T cells were grown under standard conditions (DMEM, 10% FCS, 5% CO_2, 37°C) and transfected with the calcium phosphate method (103). For evaluation of the conservation of cleavage activity, the HLH-fused paracaspase constructs were co-transfected with plasmids encoding wild-type CYLD (LMBP: 6613) or the uncleavable CYLD-R324A (LMBP: 6645) mutant. Cells transfected for cleavage activity evaluations were lysed directly in Laemmli buffer [0.1% 2-mercaptoethanol, 5 ppm bromophenol blue, 10% glycerol, 2% SDS, 63 mM Tris–HCl (pH 6.8)]. For evaluation of the conservation of paracaspase scaffold activity, the HLH-fused constructs were transfected in an NF-κB luciferase assay. For evaluation of NF-κB induction, candidate-inducing constructs were co-transfected with an NF-κB-dependent luciferase reporter expression plasmid (LMBP: 3249) and an actin promoter-driven β-galactosidase expression plasmid (LMBP: 4341) as transfection control. The cells used for luciferase analysis were washed with PBS and lysed in luciferase lysis buffer (25 mM Tris pH 7.8, 2 mM DTT, 2 mM CDTA, 10% glycerol, 1% Triton X-100). For the colorimetric determination (at 595 nm) of β-galactosidase activity, chlorophenol red-β-D-galactopyranoside (Roche diagnostics) was used as a substrate. Luciferase activity was measured by using beetle luciferin (Promega) as a substrate, and luminescence was measured with the GloMax® 96 Microplate Luminometer (Promega). Luciferase data processing and calculation of 95% confidence intervals (Student's *t*-distribution) (65) was done in LibreOffice (www.libreoffice.org) Calc. For evaluation of the functional conservation of Bcl10 homologs, the Bcl10 clones were co-transfected with the NF-κB luciferase reporter and β-galactosidase expression plasmids in the MALT1-deficient HEK293T cells with or without reconstitution with human MALT1 (LMBP: 5536). Human CARD-9 (LMBP: 9609) was used as control for evaluations of the functional conservation of CARD–CC proteins. Detection of cleaved CYLD was done with the E10 antibody (Santa Cruz Biotechnology) recognizing the C-terminal 70-kDa cleavage band. Expression of the fused paracaspases was determined with anti-Flag antibody (F-3165, Sigma). Human MALT1 was detected by the EP603Y monoclonal rabbit antibody (Abcam) and the E-tagged Bcl10 clones with anti-E-tag antibody (ab66152, Abcam). All Western blots were developed on an Odyssey scanner (LI-COR).

Yeast-2-Hybrid Assay

The Matchmaker Gold Yeast Two-Hybrid System (Clontech) was used with the Y2H Gold yeast strain to investigate protein–protein interactions. A pre-culture was made the day before transformation, by inoculating about 10 colonies of Y2H gold strain in 5-ml YPDA medium and growing it for about 4 h in a 30°C shaking incubator. The pre-culture was transferred to 35-ml YPDA and grown overnight in a 30°C shaking incubator. On the day of transformation, the overnight culture was diluted to an OD_{600} of 0.2 in YPDA (10-ml YPDA/transformation) and grown in a 30°C shaking incubator until an OD_{600} of 0.6–0.8. After a 5-min centrifugation step at 2,100 rpm at 23°C, the yeast pellet was resuspended in 10-ml Milli-Q water and centrifuged again for 5 min. After resuspending the pellet in 1× TE/LiAc, 100 µl of competent cells was mixed with 100 µg denatured salmon sperm DNA, 1 µg bait plasmid, 1 µg prey plasmid, and 600 µl fresh PEG400/LiAc. The yeast–DNA mixtures were incubated in a 30°C shaking incubator for 30 min. The yeast cells were transformed *via* heat shock at 42°C for 15 min. After a 1-min incubation on ice and a 30-s centrifugation step, the pellet was resuspended in 1× TE and plated on a minimal synthetic drop-out medium (SD) lacking leucine and tryptophan (SD/-Leu/-Trp). After 4 days of incubation at 30°C, colonies were picked and incubated overnight in 200-µl SD/-Leu/-Trp medium in a 96-well plate. Transformed yeast cells were grown overnight in a 30°C incubator. Cultures were then stamped on SD/-Leu/-Trp and SD/-Leu/-Trp/-His/-Ade/+ X-α-gal (40 µg/ml 5-bromo-4-chloro-3 indolyl-β-D-galactopyranoside) plates using an iron 96-well stamp and then incubated for 3–7 days at 30°C until blue colonies were visible.

In Situ Expression Analysis in Nvn

SP6 RNA polymerase (Promega) was used to generate labeled RNA probes. Fixed Nvn embryos were transferred into wells and rehydrated with 60% methanol/40% PBS with 0.1% Tween 20 (PBSTw), 40% methanol/60% PBSTw, and four times with 100% PBSTw. The samples were then digested with 10 µg/ml proteinase K (prepared in PBSTw) for 20 min. The reaction was stopped by two washes with 4 mg/ml glycine. The embryos were washed first with 1% triethanolamine (v/v in PBSTw), twice with 1% triethanolamine/3 µl acetic anhydride, and then twice with 1% triethanolamine/6 µl acetic anhydride. After two washes with PBSTw, the embryos were refixed in 3.7% paraformaldehyde (v/v in PBSTw) for 1 h and washed five times with PBSTw. Samples were prehybridized in 50% PBSTw/50% hybridization buffer (Hybe) [50% formamide, 5× SSC, 50 µg/ml heparin, 0.1% Tween 20 (v/v), 1% SDS (v/v) 100 µg/ml SS DNA and DEPC water] for 10 min, 100% Hybe buffer for 10 min, and 100% Hybe buffer overnight at 60°C. Labeled RNA probes were diluted to 0.5 ng/µl Hybe buffer and denatured at 85°C for 10 min. Hybe buffer was removed from the embryos, and for each reaction, 250- to 300-µl working stock probe was added into the *in situ* plate. The sieves with embryos were transferred to the *in situ* plate and sealed to prevent evaporation. The embryos were then incubated at 60°C for 48–72 h. The sieves were transferred to a clean rack filled with fresh preheated Hybe buffer and incubated at 60°C for 10 min. Then, the samples were washed with 100% Hybe buffer and incubated at the hybridization temperature for 40 min. The embryos were washed at the hybridization temperature for 30 min; once with 75% Hybe/25% 2× SSCT [pH 7.0, 0.3 M sodium citrate, 3 M NaCl, and 0.1% (v/v) Tween 20], once with 50% Hybe/50% 2× SSCT, once with 25% Hybe/75% 2× SSCT, once with 2× SSCT, and finally three times with 0.05× SSCT. Prior to the blocking step, the samples were washed three times with 100% PBSTw (each 10 min) at room temperature. To decrease the unspecific background, the samples were blocked in Roche blocking reagent [supplemented with 1% (w/v) 1× maleic acid] for 1 h at room temperature. The embryos were then incubated with antibody solution [Roche anti-digoxigenin-AP (alkaline phosphatase) diluted 1/2,000 in blocking buffer] at 4°C overnight. The sieves were rinsed with blocking buffer and washed 10 times with 100% PBSTw (each 15 min). The embryos were developed in AP substrate solution [5 M NaCl, 1 M $MgCl_2$, 1 M Tris pH 9.5, and 0.1% (v/v) Tween 20] at room temperature. Color development was checked every 10 min for 2 h and AP substrate solution was replaced if an extended developing period was required. Once the probe development reached the desired level, the reaction was stopped by washing with 100% PBSTw. Next, the samples were washed with 100% ethanol for 1 h and rinsed several times with 100% PBSTw. Finally, the specimens were washed with 85% glycerol (in PBSTw) at 4°C overnight and embedded to microscope slides using polyvinyl alcohol hardening mounting medium (10981-100ML, Sigma-Aldrich).

Microscopy

Images were captured with an Axio Scan.Z1 confocal microscope (Zeiss). Images were acquired with a 20× Plan-Apochromat 0.8 NA dry objective, using a Hitachi HV-F202SCL camera.

RNAi Silencing of Malt1 in *C. elegans* and Phenotypic Analysis

SID-1 is a transmembrane protein, responsible for the passive uptake of dsRNA but this protein is only present in all cells outside the nervous system. Therefore, feeding RNAi is robust in virtually all cells in *C. elegans* except neurons. To enhance neuronal RNAi, worms [TU3311 strain, uIs60 (unc-119p:yfp + unc-119p:sid-1)] were used which express wild-type sid-1 under control of the pan-neuronal promoter unc-119 (104). Synchronized L1 worms were transferred to NGM plates with RNAi-expressing bacteria (*malt1* RNAi sequences: CCTGATCCGGAACAACAAGT and TCCAGCAGATGCTCATCAAC). RNAi efficiency was evaluated by qPCR using the primers TGATGATGAAGAAGGTGTCTCAA and CATCTCAATCGTCTTCTCTGGAT. The control RNAi is the empty vector L4440. To prevent progeny, FUdR (200 µM) was added before worms became adult. Online application for survival analysis was used to perform statistical analysis of the life span assays (105). To test whether RNAi inactivation of *malt1* is accompanied by neurotoxicity, we performed a motility study with the WMicrotracker. This device is a high-throughput tracking system to record the amount of animal movement in a fixed period of time. The animal movement is detected through infrared microbeam light scattering. A 24-well plate, filled with nutrient agar, was used. Six wells were seeded with the control RNAi bacteria and six others were seeded with the RNAi bacteria against *malt1*. Neuronal RNAi-sensitive worms (TU3311 strain) were grown on RNAi bacteria until young adulthood (day 0). Around 100 adult worms were inoculated in each well. The exact number of the worms was counted afterward. Three independent biological replicates were measured over a time period of 20 h. Data acquisition and analysis was performed as described in Ref. (106). The detected signals per hour were divided by the average worm number in each well. The difference in motility was expressed relative to the control.

AUTHOR CONTRIBUTIONS

JS designed and performed experiments, cloned genes, integrated information, and wrote the paper. The paper was commented on and improved by IG, PH, AG, BB, FR, and RB. YD and MH provided technical assistance with HEK293T cell experiments. ID, BB, and AB investigated the role of the *C. elegans* paracaspase. LL and IG performed the Y2H experiments and ISH staining on *N. vectensis* embryos, which were prepared by SS in the laboratory of U. Technau. AG acquired images of the stained *N. vectensis* embryos. PH and IG assisted with phylogenetic analyses and illustrations. JP re-analyzed RNAseq data to identify the coral bleaching-associated paracaspase paralog. RB, BB, YS, and FR supervised parts of this work.

ACKNOWLEDGMENTS

Zebrafish cDNA was kindly provided by Prof. Kris Vleminckx (Ghent University). A pacific oyster (*Crassostrea gigas*) cDNA library was kindly provided by Prof. Pascal Favrel (UMR BOREA Biologie des Organismes et Ecosystèmes Aquatiques, Institut de

Biologie Fondamentale et Appliquée, Université de Caen Basse-Normandie, France).

FUNDING

Work in the Beyaert lab has been financed by the Fund for Scientific Research Flanders (FWO), the Belgian Foundation Against Cancer, Interuniversity Attraction Poles, Concerted Research Actions (GOA), and the Group-ID Multidisciplinary Research Partnership of Ghent University. AB is supported by a predoctoral fellowship from the FWO.

SUPPLEMENTARY MATERIAL

The Supplementary Material for this article can be found online at https://www.frontiersin.org/articles/10.3389/fimmu.2018.01136/full#supplementary-material.

REFERENCES

1. Dierlamm J, Baens M, Wlodarska I, Stefanova-Ouzounova M, Hernandez JM, Hossfeld DK, et al. The apoptosis inhibitor gene API2 and a novel 18q gene, MLT, are recurrently rearranged in the t(11;18)(q21;q21) associated with mucosa-associated lymphoid tissue lymphomas. *Blood* (1999) 93:3601–9.
2. Ruefli-Brasse AA, French DM, Dixit VM. Regulation of NF-kappaB-dependent lymphocyte activation and development by paracaspase. *Science* (2003) 302:1581–4. doi:10.1126/science.1090769
3. Ruland J, Duncan GS, Wakeham A, Mak TW. Differential requirement for Malt1 in T and B cell antigen receptor signaling. *Immunity* (2003) 19:749–58. doi:10.1016/S1074-7613(03)00293-0
4. Che T, You Y, Wang D, Tanner MJ, Dixit VM, Lin X. MALT1/paracaspase is a signaling component downstream of CARMA1 and mediates T cell receptor-induced NF-kappaB activation. *J Biol Chem* (2004) 279:15870–6. doi:10.1074/jbc.M310599200
5. Sun L, Deng L, Ea C-K, Xia Z-P, Chen ZJ. The TRAF6 ubiquitin ligase and TAK1 kinase mediate IKK activation by BCL10 and MALT1 in T lymphocytes. *Mol Cell* (2004) 14:289–301. doi:10.1016/S1097-2765(04)00236-9
6. Gross O, Gewies A, Finger K, Schäfer M, Sparwasser T, Peschel C, et al. CARD9 controls a non-TLR signalling pathway for innate anti-fungal immunity. *Nature* (2006) 442:651–6. doi:10.1038/nature04926
7. Afonina IS, Van Nuffel E, Baudelet G, Driege Y, Kreike M, Staal J, et al. The paracaspase MALT1 mediates CARD14-induced signaling in keratinocytes. *EMBO Rep* (2016) 17:914–27. doi:10.15252/embr.201642109
8. Howes A, O'Sullivan PA, Breyer F, Ghose A, Cao L, Krappmann D, et al. Psoriasis mutations disrupt CARD14 autoinhibition promoting BCL10-MALT1-dependent NF-κB activation. *Biochem J* (2016). doi:10.1042/BCJ20160270
9. Schmitt A, Grondona P, Maier T, Brändle M, Schönfeld C, Jäger G, et al. MALT1 protease activity controls the expression of inflammatory genes in keratinocytes upon zymosan stimulation. *J Invest Dermatol* (2016) 136: 788–97. doi:10.1016/j.jid.2015.12.027
10. McAllister-Lucas LM, Ruland J, Siu K, Jin X, Gu S, Kim DSL, et al. CARMA3/Bcl10/MALT1-dependent NF-kappaB activation mediates angiotensin II-responsive inflammatory signaling in nonimmune cells. *Proc Natl Acad Sci U S A* (2007) 104:139–44. doi:10.1073/pnas.0601947103
11. Scudiero I, Vito P, Stilo R. The three CARMA sisters: so different, so similar. A portrait of the three CARMA proteins and their involvement in human disorders. *J Cell Physiol* (2013). doi:10.1002/jcp.24543
12. Uren AG, O'Rourke K, Aravind LA, Pisabarro MT, Seshagiri S, Koonin EV, et al. Identification of paracaspases and metacaspases: two ancient families of caspase-like proteins, one of which plays a key role in MALT lymphoma. *Mol Cell* (2000) 6:961–7. doi:10.1016/S1097-2765(05)00086-9
13. Hulpiau P, Driege Y, Staal J, Beyaert R. MALT1 is not alone after all: identification of novel paracaspases. *Cell Mol Life Sci* (2016) 73:1103–16. doi:10.1007/s00018-015-2041-9
14. Salvesen GS, Hempel A, Coll NS. Protease signaling in animal and plant-regulated cell death. *FEBS J* (2015). doi:10.1111/febs.13616
15. Coornaert B, Baens M, Heyninck K, Bekaert T, Haegman M, Staal J, et al. T cell antigen receptor stimulation induces MALT1 paracaspase-mediated cleavage of the NF-kappaB inhibitor A20. *Nat Immunol* (2008) 9:263–71. doi:10.1038/ni1561
16. Rebeaud F, Hailfinger S, Posevitz-Fejfar A, Tapernoux M, Moser R, Rueda D, et al. The proteolytic activity of the paracaspase MALT1 is key in T cell activation. *Nat Immunol* (2008) 9:272–81. doi:10.1038/ni1568
17. Yu JW, Jeffrey PD, Ha JY, Yang X, Shi Y. Crystal structure of the mucosa-associated lymphoid tissue lymphoma translocation 1 (MALT1) paracaspase region. *Proc Natl Acad Sci U S A* (2011) 108:21004–9. doi:10.1073/pnas.1111708108
18. Hachmann J, Snipas SJ, van Raam BJ, Cancino EM, Houlihan EJ, Poreba M, et al. Mechanism and specificity of the human paracaspase MALT1. *Biochem J* (2012) 443:287–95. doi:10.1042/BJ20120035
19. Wiesmann C, Leder L, Blank J, Bernardi A, Melkko S, Decock A, et al. Structural determinants of MALT1 protease activity. *J Mol Biol* (2012) 419:4–21. doi:10.1016/j.jmb.2012.02.018
20. Mc Guire C, Elton L, Wieghofer P, Staal J, Voet S, Demeyer A, et al. Pharmacological inhibition of MALT1 protease activity protects mice in a mouse model of multiple sclerosis. *J Neuroinflammation* (2014) 11:124. doi:10.1186/1742-2094-11-124
21. Juilland M, Thome M. Role of the CARMA1/BCL10/MALT1 complex in lymphoid malignancies. *Curr Opin Hematol* (2016) 23:402–9. doi:10.1097/MOH.0000000000000257
22. Noels H, van Loo G, Hagens S, Broeckx V, Beyaert R, Marynen P, et al. A novel TRAF6 binding site in MALT1 defines distinct mechanisms of NF-kappaB activation by API2middle dotMALT1 fusions. *J Biol Chem* (2007) 282:10180–9. doi:10.1074/jbc.M611038200
23. Ferch U, zum Büschenfelde CM, Gewies A, Wegener E, Rauser S, Peschel C, et al. MALT1 directs B cell receptor-induced canonical nuclear factor-kappaB signaling selectively to the c-Rel subunit. *Nat Immunol* (2007) 8:984–91. doi:10.1038/ni1493
24. Gringhuis SI, Wevers BA, Kaptein TM, van Capel TMM, Theelen B, Boekhout T, et al. Selective C-Rel activation *via* Malt1 controls anti-fungal T(H)-17 immunity by dectin-1 and dectin-2. *PLoS Pathog* (2011) 7:e1001259. doi:10.1371/journal.ppat.1001259
25. Hailfinger S, Nogai H, Pelzer C, Jaworski M, Cabalzar K, Charton J-E, et al. Malt1-dependent RelB cleavage promotes canonical NF-κB activation in lymphocytes and lymphoma cell lines. *Proc Natl Acad Sci U S A* (2011) 108:14596–601. doi:10.1073/pnas.1105020108
26. Baens M, Bonsignore L, Somers R, Vanderheydt C, Weeks SD, Gunnarsson J, et al. MALT1 auto-proteolysis is essential for NF-κB-dependent gene transcription in activated lymphocytes. *PLoS One* (2014) 9:e103774. doi:10.1371/journal.pone.0103774
27. Jeltsch KM, Hu D, Brenner S, Zöller J, Heinz GA, Nagel D, et al. Cleavage of roquin and regnase-1 by the paracaspase MALT1 releases their cooperatively repressed targets to promote T(H)17 differentiation. *Nat Immunol* (2014) 15:1079–89. doi:10.1038/ni.3008
28. Peterson KJ, Lyons JB, Nowak KS, Takacs CM, Wargo MJ, McPeek MA. Estimating metazoan divergence times with a molecular clock. *Proc Natl Acad Sci U S A* (2004) 101:6536–41. doi:10.1073/pnas.0401670101
29. Knoll A, Walter M, Narbonne G, Christie-Blick N. The Ediacaran Period: a new addition to the geologic time scale. *Lethaia* (2006) 39:13–30. doi:10.1080/00241160500409223
30. Dunn CW, Giribet G, Edgecombe GD, Hejnol A. Animal phylogeny and its evolutionary implications. *Annu Rev Ecol Evol Syst* (2014) 45:371–95. doi:10.1146/annurev-ecolsys-120213-091627
31. Sullivan JC, Wolenski FS, Reitzel AM, French CE, Traylor-Knowles N, Gilmore TD, et al. Two alleles of NF-kappaB in the sea anemone *Nematostella vectensis* are widely dispersed in nature and encode proteins with distinct activities. *PLoS One* (2009) 4:e7311. doi:10.1371/journal.pone.0007311
32. Demeyer A, Staal J, Beyaert R. Targeting MALT1 proteolytic activity in immunity, inflammation and disease: good or bad? *Trends Mol Med* (2016). doi:10.1016/j.molmed.2015.12.004
33. Flaswinkel H, Barner M, Reth M. The tyrosine activation motif as a target of protein tyrosine kinases and SH2 domains. *Semin Immunol* (1995) 7:21–7. doi:10.1016/1044-5323(95)90004-7

34. Mócsai A, Ruland J, Tybulewicz VLJ. The SYK tyrosine kinase: a crucial player in diverse biological functions. *Nat Rev Immunol* (2010) 10:387–402. doi:10.1038/nri2765
35. Ziegenfuss JS, Biswas R, Avery MA, Hong K, Sheehan AE, Yeung Y-G, et al. Draper-dependent glial phagocytic activity is mediated by Src and Syk family kinase signalling. *Nature* (2008) 453:935–9. doi:10.1038/nature06901
36. Yu OM, Brown JH. G protein-coupled receptor and RhoA-stimulated transcriptional responses: links to inflammation, differentiation, and cell proliferation. *Mol Pharmacol* (2015) 88:171–80. doi:10.1124/mol.115.097857
37. Schimmack G, Eitelhuber AC, Vincendeau M, Demski K, Shinohara H, Kurosaki T, et al. AIP augments CARMA1–BCL10–MALT1 complex formation to facilitate NF-κB signaling upon T cell activation. *Cell Commun Signal* (2014) 12:49. doi:10.1186/s12964-014-0049-7
38. Narayan P, Holt B, Tosti R, Kane LP. CARMA1 is required for Akt-mediated NF-kappaB activation in T cells. *Mol Cell Biol* (2006) 26:2327–36. doi:10.1128/MCB.26.6.2327-2336.2006
39. Oruganti SR, Edin S, Grundström C, Grundström T. CaMKII targets Bcl10 in T-cell receptor induced activation of NF-κB. *Mol Immunol* (2011) 48:1448–60. doi:10.1016/j.molimm.2011.03.020
40. Kawadler H, Gantz MA, Riley JL, Yang X. The paracaspase MALT1 controls caspase-8 activation during lymphocyte proliferation. *Mol Cell* (2008) 31:415–21. doi:10.1016/j.molcel.2008.06.008
41. Bognar MK, Vincendeau M, Erdmann T, Seeholzer T, Grau M, Linnemann JR, et al. Oncogenic CARMA1 couples NF-κB and β-catenin signaling in diffuse large B-cell lymphomas. *Oncogene* (2016) 35:4269–81. doi:10.1038/onc.2015.493
42. Yang Y, Kelly P, Shaffer AL, Schmitz R, Yoo HM, Liu X, et al. Targeting non-proteolytic protein ubiquitination for the treatment of diffuse large B cell lymphoma. *Cancer Cell* (2016) 29:494–507. doi:10.1016/j.ccell.2016.03.006
43. Bidère N, Ngo VN, Lee J, Collins C, Zheng L, Wan F, et al. Casein kinase 1alpha governs antigen-receptor-induced NF-kappaB activation and human lymphoma cell survival. *Nature* (2009) 458:92–6. doi:10.1038/nature07613
44. Lin Q, Liu Y, Moore DJ, Elizer SK, Veach RA, Hawiger J, et al. Cutting edge: the "death" adaptor CRADD/RAIDD targets BCL10 and suppresses agonist-induced cytokine expression in T lymphocytes. *J Immunol* (2012) 188:2493–7. doi:10.4049/jimmunol.1101502
45. Welteke V, Eitelhuber A, Düwel M, Schweitzer K, Naumann M, Krappmann D. COP9 signalosome controls the CARMA1–Bcl10–MALT1 complex upon T-cell stimulation. *EMBO Rep* (2009) 10:642–8. doi:10.1038/embor.2009.64
46. Stempin CC, Chi L, Giraldo-Vela JP, High AA, Häcker H, Redecke V. The E3 ubiquitin ligase mind bomb-2 (MIB2) protein controls B-cell CLL/lymphoma 10 (BCL10)-dependent NF-κB activation. *J Biol Chem* (2011) 286:37147–57. doi:10.1074/jbc.M111.263384
47. Shin HM, Tilahun ME, Cho OH, Chandiran K, Kuksin CA, Keerthivasan S, et al. NOTCH1 can initiate NF-κB activation *via* cytosolic interactions with components of the T cell signalosome. *Front Immunol* (2014) 5:249. doi:10.3389/fimmu.2014.00249
48. Paul S, Traver MK, Kashyap AK, Washington MA, Latoche JR, Schaefer BC. T cell receptor signals to NF-κB are transmitted by a cytosolic p62-Bcl10-Malt1-IKK signalosome. *Sci Signal* (2014) 7:ra45. doi:10.1126/scisignal.2004882
49. Roncagalli R, Cucchetti M, Jarmuzynski N, Grégoire C, Bergot E, Audebert S, et al. The scaffolding function of the RLTPR protein explains its essential role for CD28 co-stimulation in mouse and human T cells. *J Exp Med* (2016). doi:10.1084/jem.20160579
50. Yang C-S, Rodgers M, Min C-K, Lee J-S, Kingeter L, Lee J-Y, et al. The autophagy regulator Rubicon is a feedback inhibitor of CARD9-mediated host innate immunity. *Cell Host Microbe* (2012) 11:277–89. doi:10.1016/j.chom.2012.01.019
51. D'Andrea EL, Ferravante A, Scudiero I, Zotti T, Reale C, Pizzulo M, et al. The dishevelled, EGL-10 and pleckstrin (DEP) domain-containing protein DEPDC7 binds to CARMA2 and CARMA3 proteins, and regulates NF-κB activation. *PLoS One* (2014) 9:e116062. doi:10.1371/journal.pone.0116062
52. Li Y, Chen X, Wang Z, Zhao D, Chen H, Chen W, et al. The HECTD3 E3 ubiquitin ligase suppresses cisplatin-induced apoptosis *via* stabilizing MALT1. *Neoplasia* (2013) 15:39–48. doi:10.1593/neo.121362
53. Morimoto K, Baba Y, Shinohara H, Kang S, Nojima S, Kimura T, et al. LRRK1 is critical in the regulation of B-cell responses and CARMA1-dependent NF-κB activation. *Sci Rep* (2016) 6:25738. doi:10.1038/srep25738
54. Vessichelli M, Ferravante A, Zotti T, Reale C, Scudiero I, Picariello G, et al. Neuroepithelial transforming gene 1 (Net1) binds to caspase activation and recruitment domain (CARD)- and membrane-associated guanylate kinase-like domain-containing (CARMA) proteins and regulates nuclear factor κB activation. *J Biol Chem* (2012) 287:13722–30. doi:10.1074/jbc.M111.304436
55. Poeck H, Bscheider M, Gross O, Finger K, Roth S, Rebsamen M, et al. Recognition of RNA virus by RIG-I results in activation of CARD9 and inflammasome signaling for interleukin 1 beta production. *Nat Immunol* (2010) 11:63–9. doi:10.1038/ni.1824
56. Medeiros RB, Burbach BJ, Mueller KL, Srivastava R, Moon JJ, Highfill S, et al. Regulation of NF-kappaB activation in T cells *via* association of the adapter proteins ADAP and CARMA1. *Science* (2007) 316:754–8. doi:10.1126/science.1137895
57. Woo H-N, Hong G-S, Jun J-I, Cho D-H, Choi H-W, Lee H-J, et al. Inhibition of Bcl10-mediated activation of NF-kappa B by BinCARD, a Bcl10-interacting CARD protein. *FEBS Lett* (2004) 578:239–44. doi:10.1016/j.febslet.2004.10.094
58. Sakamoto T, Kobayashi M, Tada K, Shinohara M, Io K, Nagata K, et al. CKIP-1 is an intrinsic negative regulator of T-cell activation through an interaction with CARMA1. *PLoS One* (2014) 9:e85762. doi:10.1371/journal.pone.0085762
59. Ruefli-Brasse AA, Lee WP, Hurst S, Dixit VM. Rip2 participates in Bcl10 signaling and T-cell receptor-mediated NF-kappaB activation. *J Biol Chem* (2004) 279:1570–4. doi:10.1074/jbc.C300460200
60. Li Y, He X, Wang S, Shu H-B, Liu Y. USP2a positively regulates TCR-induced NF-κB activation by bridging MALT1-TRAF6. *Protein Cell* (2013) 4:62–70. doi:10.1007/s13238-012-2120-8
61. Langel FD, Jain NA, Rossman JS, Kingeter LM, Kashyap AK, Schaefer BC. Multiple protein domains mediate interaction between Bcl10 and MALT1. *J Biol Chem* (2008) 283:32419–31. doi:10.1074/jbc.M800670200
62. Zmasek CM, Zhang Q, Ye Y, Godzik A. Surprising complexity of the ancestral apoptosis network. *Genome Biol* (2007) 8:R226. doi:10.1186/gb-2007-8-10-r226
63. Hadweh P, Chaitoglou I, Gravato-Nobre MJ, Ligoxygakis P, Mosialos G, Hatzivassiliou E. Functional analysis of the *C. elegans* cyld-1 gene reveals extensive similarity with its human homolog. *PLoS One* (2018) 13:e0191864. doi:10.1371/journal.pone.0191864
64. Gul IS, Staal J, Hulpiau P, De Keuckelaere E, Kamm K, Deroo T, et al. GC content of early metazoan genes and its impact on gene expression levels in mammalian cell lines. *Genome Biol Evol* (2018) 10:909–17. doi:10.1093/gbe/evy040
65. Student. The probable error of a mean. *Biometrika* (1908) 6:1–25. doi:10.1093/biomet/6.1.1
66. Fleury E, Huvet A, Lelong C, de Lorgeril J, Boulo V, Gueguen Y, et al. Generation and analysis of a 29,745 unique expressed sequence tags from the Pacific oyster (*Crassostrea gigas*) assembled into a publicly accessible database: the GigasDatabase. *BMC Genomics* (2009) 10:341. doi:10.1186/1471-2164-10-341
67. Putnam NH, Srivastava M, Hellsten U, Dirks B, Chapman J, Salamov A, et al. Sea anemone genome reveals ancestral eumetazoan gene repertoire and genomic organization. *Science* (2007) 317:86–94. doi:10.1126/science.1139158
68. Meyer E, Weis VM. Study of cnidarian-algal symbiosis in the "Omics" age. *Biol Bull* (2012) 223:44–65. doi:10.1086/BBLv223n1p44
69. Mazzone P, Scudiero I, Ferravante A, Paolucci M, D'Andrea LE, Varricchio E, et al. Functional characterization of zebrafish (*Danio rerio*) Bcl10. *PLoS One* (2015) 10:e0122365. doi:10.1371/journal.pone.0122365
70. Sommer K, Guo B, Pomerantz JL, Bandaranayake AD, Moreno-García ME, Ovechkina YL, et al. Phosphorylation of the CARMA1 linker controls NF-kappaB activation. *Immunity* (2005) 23:561–74. doi:10.1016/j.immuni.2005.09.014
71. Lamason RL, McCully RR, Lew SM, Pomerantz JL. Oncogenic CARD11 mutations induce hyperactive signaling by disrupting autoinhibition by the PKC-responsive inhibitory domain. *Biochemistry (Mosc)* (2010) 49:8240–50. doi:10.1021/bi101052d
72. Genikhovich G, Technau U. *In situ* hybridization of starlet sea anemone (*Nematostella vectensis*) embryos, larvae, and polyps. *Cold Spring Harb Protoc* (2009) 2009:db.rot5282. doi:10.1101/pdb.prot5282

73. C. elegans Deletion Mutant Consortium. large-scale screening for targeted knockouts in the *Caenorhabditis elegans* genome. *G3 Bethesda* (2012) 2:1415–25. doi:10.1534/g3.112.003830
74. Rast JP, Buckley KM. Lamprey immunity is far from primitive. *Proc Natl Acad Sci U S A* (2013) 110:5746–7. doi:10.1073/pnas.1303541110
75. Shinohara H, Yasuda T, Aiba Y, Sanjo H, Hamadate M, Watarai H, et al. PKC beta regulates BCR-mediated IKK activation by facilitating the interaction between TAK1 and CARMA1. *J Exp Med* (2005) 202:1423–31. doi:10.1084/jem.20051591
76. de Mendoza A, Suga H, Ruiz-Trillo I. Evolution of the MAGUK protein gene family in premetazoan lineages. *BMC Evol Biol* (2010) 10:93. doi:10.1186/1471-2148-10-93
77. Li S, Yang X, Shao J, Shen Y. Structural insights into the assembly of CARMA1 and BCL10. *PLoS One* (2012) 7:e42775. doi:10.1371/journal.pone.0042775
78. Hopf TA, Schärfe CPI, Rodrigues JPGLM, Green AG, Kohlbacher O, Sander C, et al. Sequence co-evolution gives 3D contacts and structures of protein complexes. *Elife* (2014) 3. doi:10.7554/eLife.03430
79. Oteri F, Nadalin F, Champeimont R, Carbone A. BIS2Analyzer: a server for co-evolution analysis of conserved protein families. *Nucleic Acids Res* (2017) 45:W307–14. doi:10.1093/nar/gkx336
80. GIGA community of scientists, Bracken-Grissom H, Collins AG, Collins T, Crandall K, Distel D, et al. The global invertebrate genomics alliance (GIGA): developing community resources to study diverse invertebrate genomes. *J Hered* (2014) 105:1–18. doi:10.1093/jhered/est084
81. Long KA, Nossa CW, Sewell MA, Putnam NH, Ryan JF. Low coverage sequencing of three echinoderm genomes: the brittle star *Ophionereis* fasciata, the sea star *Patiriella regularis*, and the sea cucumber *Australostichopus mollis*. *Gigascience* (2016) 5:20. doi:10.1186/s13742-016-0125-6
82. Pinzón JH, Kamel B, Burge CA, Harvell CD, Medina M, Weil E, et al. Whole transcriptome analysis reveals changes in expression of immune-related genes during and after bleaching in a reef-building coral. *R Soc Open Sci* (2015) 2:140214. doi:10.1098/rsos.140214
83. Ruland J, Duncan GS, Elia A, del Barco Barrantes I, Nguyen L, Plyte S, et al. Bcl10 is a positive regulator of antigen receptor-induced activation of NF-kappaB and neural tube closure. *Cell* (2001) 104:33–42. doi:10.1016/S0092-8674(01)00189-1
84. Grabiner BC, Blonska M, Lin P-C, You Y, Wang D, Sun J, et al. CARMA3 deficiency abrogates G protein-coupled receptor-induced NF-{kappa}B activation. *Genes Dev* (2007) 21:984–96. doi:10.1101/gad.1502507
85. Richardson L, Venkataraman S, Stevenson P, Yang Y, Moss J, Graham L, et al. EMAGE mouse embryo spatial gene expression database: 2014 update. *Nucleic Acids Res* (2013) 42:D835–44. doi:10.1093/nar/gkt1155
86. Marlow H, Roettinger E, Boekhout M, Martindale MQ. Functional roles of Notch signaling in the cnidarian *Nematostella vectensis*. *Dev Biol* (2012) 362:295–308. doi:10.1016/j.ydbio.2011.11.012
87. Shinzato C, Shoguchi E, Kawashima T, Hamada M, Hisata K, Tanaka M, et al. Using the *Acropora digitifera* genome to understand coral responses to environmental change. *Nature* (2011) 476:320–3. doi:10.1038/nature10249
88. Luo Y-J, Takeuchi T, Koyanagi R, Yamada L, Kanda M, Khalturina M, et al. The *Lingula* genome provides insights into brachiopod evolution and the origin of phosphate biomineralization. *Nat Commun* (2015) 6:8301. doi:10.1038/ncomms9301
89. Simakov O, Kawashima T, Marlétaz F, Jenkins J, Koyanagi R, Mitros T, et al. Hemichordate genomes and deuterostome origins. *Nature* (2015) 527:459–65. doi:10.1038/nature16150
90. Baumgarten S, Simakov O, Esherick LY, Liew YJ, Lehnert EM, Michell CT, et al. The genome of *Aiptasia,* a sea anemone model for coral symbiosis. *Proc Natl Acad Sci U S A* (2015) 112:11893–8. doi:10.1073/pnas.1513318112
91. Mehta TK, Ravi V, Yamasaki S, Lee AP, Lian MM, Tay B-H, et al. Evidence for at least six Hox clusters in the Japanese lamprey *(Lethenteron japonicum*). *Proc Natl Acad Sci U S A* (2013) 110:16044–9. doi:10.1073/pnas.1315760110
92. Venkatesh B, Lee AP, Ravi V, Maurya AK, Lian MM, Swann JB, et al. Elephant shark genome provides unique insights into gnathostome evolution. *Nature* (2014) 505:174–9. doi:10.1038/nature12826
93. Johnson M, Zaretskaya I, Raytselis Y, Merezhuk Y, McGinnis S, Madden TL. NCBI BLAST: a better web interface. *Nucleic Acids Res* (2008) 36:W5–9. doi:10.1093/nar/gkn201
94. Finn RD, Clements J, Arndt W, Miller BL, Wheeler TJ, Schreiber F, et al. HMMER web server: 2015 update. *Nucleic Acids Res* (2015) 43:W30–8. doi:10.1093/nar/gkv397
95. Sievers F, Higgins DG. Clustal Omega, accurate alignment of very large numbers of sequences. *Methods Mol Biol* (2014) 1079:105–16. doi:10.1007/978-1-62703-646-7_6
96. Edgar RC. MUSCLE: multiple sequence alignment with high accuracy and high throughput. *Nucleic Acids Res* (2004) 32:1792–7. doi:10.1093/nar/gkh340
97. Guindon S, Delsuc F, Dufayard J-F, Gascuel O. Estimating maximum likelihood phylogenies with PhyML. *Methods Mol Biol* (2009) 537:113–37. doi:10.1007/978-1-59745-251-9_6
98. Ronquist F, Huelsenbeck JP. MrBayes 3: Bayesian phylogenetic inference under mixed models. *Bioinformatics* (2003) 19:1572–4. doi:10.1093/bioinformatics/btg180
99. Waterhouse AM, Procter JB, Martin DMA, Clamp M, Barton GJ. Jalview Version 2-a multiple sequence alignment editor and analysis workbench. *Bioinformatics* (2009) 25:1189–91. doi:10.1093/bioinformatics/btp033
100. Okonechnikov K, Golosova O, Fursov M; UGENE Team. Unipro UGENE: a unified bioinformatics toolkit. *Bioinformatics* (2012) 28:1166–7. doi:10.1093/bioinformatics/bts091
101. Torvalds L. The linux edge. *Commun ACM* (1999) 42:38–9. doi:10.1145/299157.299165
102. Huson DH, Scornavacca C. Dendroscope 3: an interactive tool for rooted phylogenetic trees and networks. *Syst Biol* (2012) 61:1061–7. doi:10.1093/sysbio/sys062
103. Calcium phosphate-mediated transfection of eukaryotic cells. *Nat Methods* (2005) 2:319–20. doi:10.1038/nmeth0405-319
104. Calixto A, Chelur D, Topalidou I, Chen X, Chalfie M. Enhanced neuronal RNAi in *C. elegans* using SID-1. *Nat Methods* (2010) 7:554–9. doi:10.1038/nmeth.1463
105. Yang J-S, Nam H-J, Seo M, Han SK, Choi Y, Nam HG, et al. OASIS: online application for the survival analysis of lifespan assays performed in aging research. *PLoS One* (2011) 6:e23525. doi:10.1371/journal.pone.0023525
106. Simonetta SH, Migliori ML, Romanowski A, Golombek DA. Timing of locomotor activity circadian rhythms in *Caenorhabditis elegans*. *PLoS One* (2009) 4:e7571. doi:10.1371/journal.pone.0007571

Conflict of Interest Statement: The authors declare that the research was conducted in the absence of any commercial or financial relationships that could be construed as a potential conflict of interest.

frontiers in Immunology

REVIEW
published: 04 July 2018
doi: 10.3389/fimmu.2018.01539

BCL10 – Bridging CARDs to Immune Activation

*Torben Gehring, Thomas Seeholzer and Daniel Krappmann**

Research Unit Cellular Signal Integration, Institute of Molecular Toxicology and Pharmacology, Helmholtz Zentrum München – German Research Center for Environmental Health, Neuherberg, Germany

Since the B-cell lymphoma/leukemia 10 (BCL10) protein was first described in 1999, numerous studies have elucidated its key functions in channeling adaptive and innate immune signaling downstream of CARMA/caspase-recruitment domain (CARD) scaffold proteins. While T and B cell antigen receptor (TCR/BCR) signaling induces the recruitment of BCL10 bound to mucosa-associated lymphoid tissue (MALT)1 to the lymphocyte-specific CARMA1/CARD11–BCL10–MALT1 (CBM-1) signalosome, alternative CBM complexes utilize different CARMA/CARD scaffolds in distinct innate or inflammatory pathways. BCL10 constitutes the smallest subunit in all CBM signalosomes, containing a 233 amino acid coding for N-terminal CARD as well as a C-terminal Ser/Thr-rich region. BCL10 forms filaments, thereby aggregating into higher-order clusters that mediate and amplify stimulation-induced signals, ultimately leading to MALT1 protease activation and canonical NF-κB and JNK signaling. BCL10 additionally undergoes extensive post-translational regulation involving phosphorylation, ubiquitination, MALT1-catalyzed cleavage, and degradation. Through these feedback and feed-forward events, BCL10 integrates positive and negative regulatory processes that govern the function as well as the dynamic assembly, disassembly, and destruction of CBM complexes. Thus, BCL10 is a critical regulator for activation as well as termination of immune cell signaling, revealing that its role extends far beyond that of a mere linking factor in CBM complexes.

Keywords: adaptive immunity, T cell signaling, innate immunity, NF-kappa B, B-cell lymphoma/leukemia 10, CBM complex

OPEN ACCESS

Edited by:
Frederic Bornancin, Novartis, Switzerland

Reviewed by:
Lawrence Kane, University of Pittsburgh, United States
Hu Zeng, Mayo Clinic, United States

***Correspondence:**
Daniel Krappmann
daniel.krappmann@helmholtz-muenchen.de

Specialty section:
This article was submitted to T Cell Biology, a section of the journal Frontiers in Immunology

Received: *30 April 2018*
Accepted: *21 June 2018*
Published: *04 July 2018*

Citation:
Gehring T, Seeholzer T and Krappmann D (2018) BCL10 – Bridging CARDs to Immune Activation. Front. Immunol. 9:1539. doi: 10.3389/fimmu.2018.01539

DISCOVERY OF BCL10 AS AN ADAPTOR FOR CARD-DEPENDENT NF-κB ACTIVATION

The BCL10 gene has been originally cloned from the 1p22 break-point of the chromosomal translocation t(1;14)(p22;q32) associated with mucosa-associated lymphoid tissue (MALT) lymphoma (1). In parallel homology, searches and yeast-two-hybrid screens identified BCL10 (also named c-E10, CIPER, CLAP, or CARMEN) as a protein that is ubiquitously expressed in human tissues and involved in apoptosis by virtue of its N-terminal CARD (2–6). However, while demonstrating that BCL10 overexpression is poorly activating pro-apoptotic pathways, BCL10 oligomerization through the CARD was shown to strongly induce NF-κB activation (1–3). Subsequent work revealed that BCL10 connects through heterotypic CARD–CARD interaction to the CARD-containing scaffold proteins CARMA1 (CARD11), CARMA2 (CARD14), CARMA3 (CARD10), and CARD9 (**Figure 1**) (7–11). In addition, BCL10 interacts with the MALT1 paracaspase (also known as PCASP1) (12), which was initially discovered from a chromosomal translocation leading to the expression of the oncogenic API2-MALT1 fusion protein in MALT lymphoma (13, 14). Besides its proteolytically

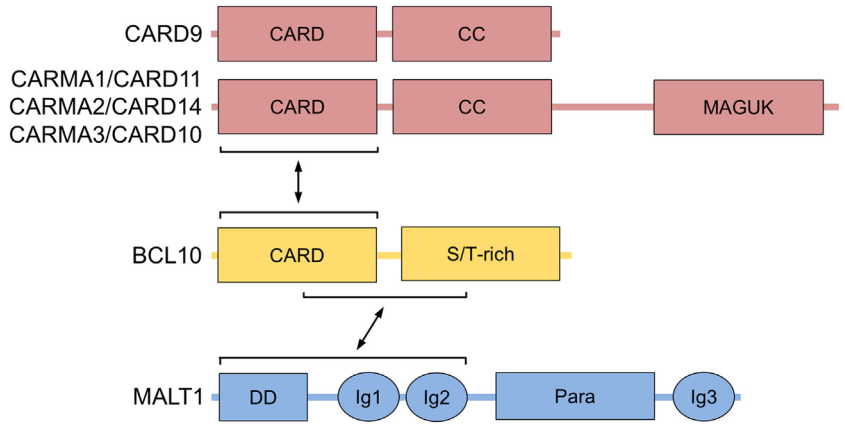

FIGURE 1 | BCL10 structure and interactors. Domain structure of BCL10 with its interacting regions that bind to CARMA/CARDs (CARMA1/CARD11, CARMA2/CARD14, CARMA3/CARD10, and CARD9) and MALT1 are shown. Abbreviations: CARD, caspase-recruitment domain; CC, coiled-coil; MAGUK, membrane-associated guanylate kinase; S/T-rich, serine/threonine-rich region; DD, death domain; Ig, immunoglobulin-like domain; Para, paracaspase domain; BCL10, B-cell lymphoma/leukemia 10; MALT, mucosa-associated lymphoid tissue.

active paracaspase domain (15, 16), MALT1 contains a death domain (DD) and two Ig domains (Ig1/2) in the N-terminus that strongly augment NF-κB activation by binding to a region C-terminal to the BCL10 CARD (17). Thus, initial studies mainly based on overexpression indicated that Bcl10 acts as an inducer of IκB kinase (IKK)/NF-κB signaling by bridging CARD-containing scaffold proteins with the MALT1 paracaspase.

BCL10 MEDIATES ADAPTIVE AND INNATE IMMUNE ACTIVATION BY VARIOUS CBM COMPLEXES

The generation of BCL10$^{-/-}$ mice gave insights into the physiological role of BCL10. As a result of defective neural tube closure, BCL10 deficiency leads to embryonal lethality in approximately one-third of the animals (18). Interestingly, even though the phenotype is not shared with other CARMA/CARD proteins or MALT1, failure of neural tube closure is seen in TRAF6 KO mice with a similar penetrance (19). In TRAF6 deficient animal, it has been attributed to a reduction in programmed cell death in the developing of the central nervous system, suggesting that deregulation in apoptotic processes may be responsible for embryonal defects in BCL10 KO mice. However, cells from BCL10-deficient mice displayed normal susceptibility to a number of apoptotic stimuli, indicating that BCL10 does not directly affect apoptosis signaling (18). Born BCL10$^{-/-}$ mice are viable and reveal no gross developmental defects. Even though BCL10 promotes survival of thymocytes, it is dispensable for overall T or B cell lineage commitment (18, 20). However, more detailed immune phenotyping showed that BCL10 is required for the proper development of regulatory T cells, natural killer (NK), and NKT cells as well as marginal zone (MZ) and B1 B cells (21, 22). T and B lymphocytes from BCL10-deficient mice are defective in NF-κB signaling, fail to upregulate cytokines like IL-2, and do not proliferate in response to TCR and BCR stimulation, which leads to blunted antigen responses and severe immune deficiency (18, 22). Similar signaling defects have been observed in mice lacking CARD11 or MALT1, indicating that BCL10 together with these two proteins orchestrates antigen signaling to mount an efficient adaptive immune response (23–28). In line, antigen stimulation induces the assembly of the higher-order CBM-1 signaling complex consisting of the core subunits CARMA1/CARD11, BCL10, and MALT1 (**Figure 2**) (29). The CBM-1 complex is lymphocyte-specific, because CARD11 expression is largely restricted to lymphoid tissues (8, 9).

As part of the CBM-1 complex, BCL10 is also required for efficient glutamine uptake by the amino acid transporter ASCT2 and an optimal activation of the protein kinase mammalian target of rapamycin (mTOR) in CD4 T cells after TCR/CD28 co-stimulation (30). In this pathway, the CBM-1 complex regulates the differentiation of naive CD4 T cells into Th1 or Th17 cells independent of its role in canonical IKK/NF-κB signaling. By utilizing shRNA or CARD11 KO Jurkat T cells, a second study confirmed the role of CARD11 and MALT1 in regulating TCR/CD28-induced mTOR activation, but BCL10 appeared to be dispensable for the pathway, which may be due to inefficient knockdown (31). Notably, the study demonstrated that MALT1 protease activity is required for mTOR activation in T cells. The exact pathway connecting CBM-1 and mTOR remains elusive, but the data point to a critical role of MALT1 substrate cleavage independent of IKK activation.

Besides its role in the lymphoid CBM-1 complex, BCL10 controls a number of other immune and pro-inflammatory pathways *via* its recruitment to various CARMA/CARD–BCL10–MALT1 complexes (**Figure 2**). In NK cells, BCL10 also in conjunction with CARD11 triggers NF-κB signaling and cytokine production upon antibody binding to FcRγ (32). By coupling Fcε receptor I (FcεRI) stimulation to NF-κB activation and secretion of the cytokines IL-6 and TNFα, BCL10 contributes to IgE-associated chronic allergic diseases, but the CARMA/CARD scaffold

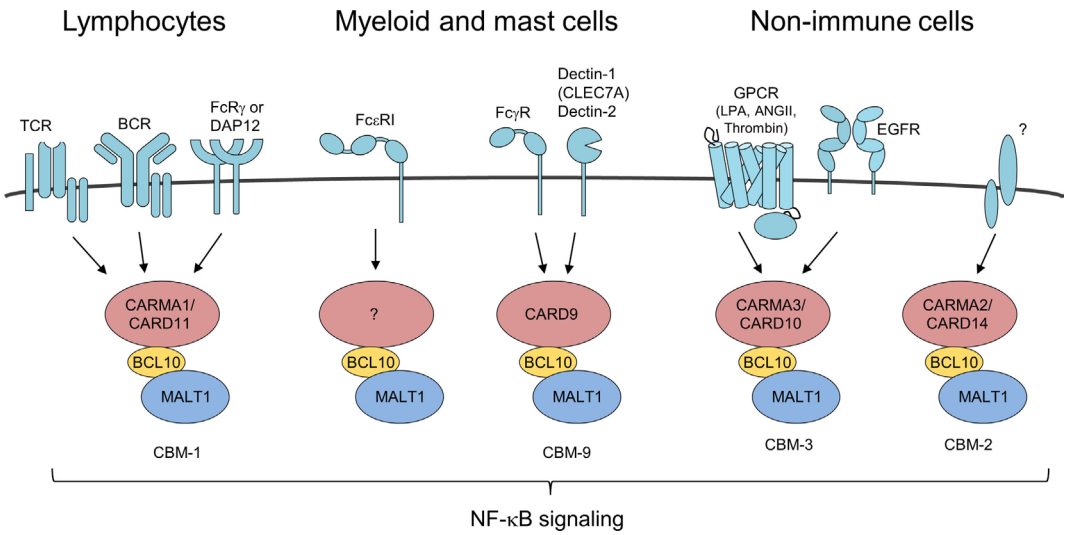

FIGURE 2 | Different CARMA/caspase-recruitment domains (CARDs) connect to B-cell lymphoma/leukemia 10 (BCL10)-mucosa-associated lymphoid tissue (MALT)1 in response to distinct upstream stimuli BCL10/MALT1 complex recruitment to different CARMA/CARD proteins is dependent on activation of various receptor types forming distinct CBM complexes. All signaling pathways converge upon formation of CBM complexes leading to IκB kinase/NF-κB and JNK activation similarly.

channeling FcεRI responses is unknown (33, 34). Chen et al. also reported on a moderate impairment of mast cell degranulation in BCL10$^{-/-}$ cells, which was not seen in the previous study and these differences may be attributed to the different markers used for detecting degranulation. In myeloid cell the alternative CARD9–BCL10–MALT1 (CBM-9) signalosome mediates FcγR stimulation as well as anti-fungal responses from C-type lectin receptors like Dectin-1 (CLEC7A) and Dectin-2 (32, 35, 36). In addition, BCL10 acts as a core component of the CARMA3/CARD10–BCL10–MALT1 (CBM-3) signaling complex that links G-protein-coupled receptor (GPCR) activated by lysophosphatidic acid, angiotensin II, or thrombin that induce pro-inflammatory gene expression also in non-immune cells (37–43). Moreover, the CBM-3 complex is crucial for NF-κB activation and tumor progression after epidermal growth factor stimulation in breast cancer cells (44). Aside from extracellular ligands, excess of intracellular free fatty acids resulting from high fat diet increases cellular diacylglycerol to promote atypical CARMA3/CARD10–BCL10-dependent, but MALT1-independent NF-κB activation in hepatocytes and thereby BCL10 deficiency contributes to insulin resistance (45). How such a CB-3 subcomplex triggers downstream signaling needs to be resolved. Finally, recent data demonstrated psoriasis associated mutations in CARMA2 (CARD14) are promoting formation of the CARMA2/CARD14–BCL10–MALT1 (CBM-2) complex to induce chronic inflammation in keratinocytes (46, 47). However, it is presently unclear what physiological stimuli and upstream signaling pathways govern CBM-2 complex activation. Taken together, BCL10 is recruited to different CARMA/CARD scaffolds to channel TCR/BCR, FcR, and GPCR signaling to induce immune and pro-inflammatory gene activation.

The crucial role of BCL10 for adaptive and innate immune activation was also observed in a human patient carrying a homozygous splice-site mutation that caused complete absence of BCL10 mRNA and protein (48). The autosomal–recessive BCL10 deficiency in humans caused combined immunodeficiency that largely mirrored the phenotype of BCL10$^{-/-}$ mice with respect to lymphocyte signaling and activation. Profound deficits in memory B and T cells were observed in the patient that were much more prominent than in BCL10$^{-/-}$ mice, most likely because the animals are housed in a largely sterile environment.

Conflicting results have been obtained regarding the requirement of BCL10 for innate toll-like receptor (TLR) pathways. Whereas MZ B cells, but not follicular (FO) B cells, fail to activate NF-κB in response to the TLR4 ligand lipopolysaccharides (22), the role of BCL10 for TLR signaling in myeloid cells is less clear. Hara et al. reported blunted TLR2, TLR4, TLR7, and TLR9 responses in CARD9 and BCL10-deficient dendritic cells (DCs), but Gross et al. failed to see any effects on TLR signaling in bone marrow-derived DCs (36, 49). Biochemical analyses showed that BCL10 can deliver full TLR4 responses in epithelial cells (50), suggesting that the effect of BCL10 may differ depending on the cell type and the exact stimulatory conditions. Interestingly, TLR and Dectin-1 signaling pathways are normal in human myeloid cells from a BCL10-deficient patient, but signaling is impaired in epithelial cells and fibroblast from the same patient, supporting the notion that the requirement for BCL10 in some of these pathways may be cell type specific (48). However, the exact mechanism how BCL10 influences MYD88-dependent innate responses and whether this is directly associated with assembly of a distinct CBM complex or results from more indirect effects is unclear.

ONCOGENIC BCR SIGNALING IN LYMPHOMAS RELIES ON BCL10

Originally, BCL10 was cloned from the chromosomal translocation t(1;14)(p22;q32) found in MALT lymphoma (1). The translocation juxtaposes the intact BCL10 gene next to the IGH enhancer, which promotes overexpression and nuclear translocation of BCL10 (1, 51). In line, heterologous expression of BCL10 in B cells of mice induces NF-κB and B cell hyperplasia (52). However, translocation and mutations in BCL10 are rare events and genetic alterations may not have a strong contribution for lymphomagenesis (53). Still, as part of the CARD11-containing CBM-1 complex, BCL10 is an essential factor for survival of the activated B cell type of diffuse large B cell lymphoma (ABC DLBCL) that are addicted to chronic BCR signaling (54). In ABC DLBCL cells, BCL10 channels oncogenic signaling driven by somatic mutations in CARD11 or the BCR adaptors CD79A/B to MALT1 protease activation and anti-apoptotic NF-κB [for review, see Ref. (55)]. Thus, even though somatic BCL10 mutations are rare, uncontrolled BCL10 activation in B cells contributes to lymphomagenesis.

BCL10 FILAMENTS—HIGHER-ORDER ASSEMBLY TO PROMOTE AND AMPLIFY TCR SIGNALING

Immunofluorescence microscopy after overexpression showed that BCL10 exhibits a clear pattern of distinct inter-connected cytoplasmic filaments (56). Mutations in the CARD of BCL10 abrogated these BCL10 assemblies and NF-κB activation, suggesting that cellular filament formation is an essential step for BCL10 activation. Subsequent work in T cells demonstrated that BCL10 is enriched in cytoplasmic structures called POLKADOTS (punctate and oligomeric killing or activating domains transducing signals) upon TCR stimulation (57, 58). The BCL10 foci are highly dynamic platforms for information exchange between BCL10 and CBM-1 signalosome binding partners such as CARD11 and TRAF6 to foster TCR-mediated signaling towards NF-κB.

The architecture and assembly of the BCL10 filaments was uncovered by cryo-electron microscopy (**Figure 3**) (59, 60). *In vitro* BCL10 assembles into helical filaments with a left-handed symmetry and three to four BCL10 subunits per helical turn. The hollow helix is formed by three types of homotypic CARD–CARD interactions

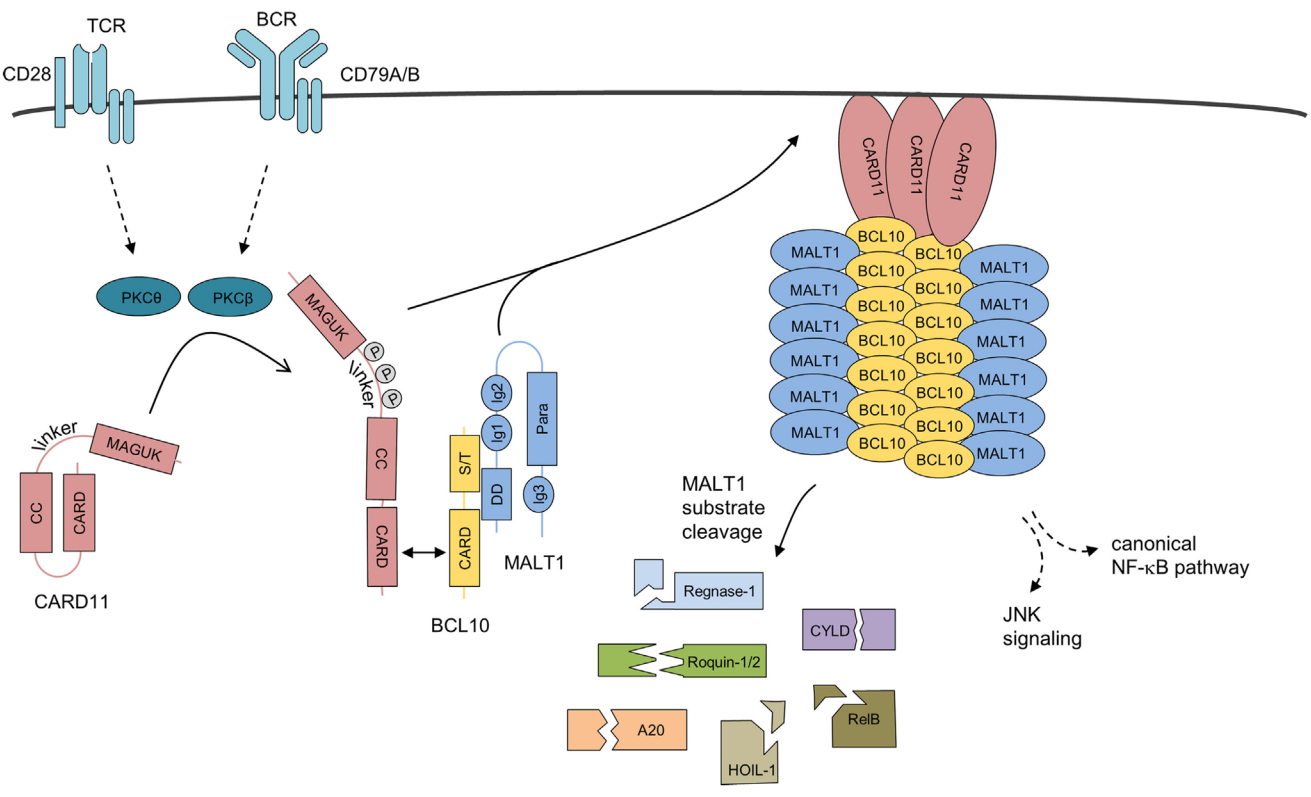

FIGURE 3 | Assembly mechanism of the higher-order CBM-1 complex. Upon antigen receptor ligation on lymphocytes, CARD11 is released from its inactive state by phosphorylation and initial homotypic CARD–CARD oligomerization. CARD11 clusters at the cell membrane, induce the recruitment of pre-assembled BCL10-MALT1 complexes, and serve as a molecular seed for the formation of BCL10 filaments. BCL10–MALT1 filaments provoke NF-κB and JNK activation. In parallel, MALT1 protease is activated, which catalyzes cleavage of various cellular substrates. Abbreviations: CARD, caspase-recruitment domain; CC, coiled-coil; MAGUK, membrane-associated guanylate kinase; S/T, Ser/Thr-rich region; DD, death domain; Ig, immunoglobulin-like domain; Para, paracaspase domain; BCL10, B-cell lymphoma/leukemia 10; MALT, mucosa-associated lymphoid tissue.

and point mutations in the interfaces abolish BCL10 filament formation as well as MALT1 and NF-κB activation in T cells, highlighting the importance for filament assembly *in vivo* (60). Indeed, heterotypic CARD–CARD contacts between CARD11 and BCL10 are selectively localizing to the tip of the BCL10 filaments, and thereby CARD11 acts as the molecular seed that nucleates BCL10 filaments (59, 60). In the first step, the positively charged CARD11 surface recruits the negatively charged BCL10 surface (60, 61). Subsequently, the CARD11-bound BCL10 exposes its basic CARD surface to engage BCL10 monomers again *via* their negatively charged surfaces ensuring a unidirectional assembly of the growing filaments. The unidirectional growth was confirmed by time-lapse confocal microscopy (59). In line with this model, CARD11 significantly decreases the lag time for BCL10 nucleation, but had no impact on the speed of the extension of the BCL10 filaments. Interestingly, the star-shaped networks indicate that multiple filaments can emanate from one seed, which may rely on the oligomeric status of CARD11 (59, 60).

To foster downstream signaling, the BCL10 core is decorated by MALT1 and TRAF6 in an all-or-none fashion, leading to filaments with a strongly enlarged diameter (59). However, the resolution of BCL10–MALT1–TRAF6 filaments is not yet sufficient to characterize the exact binding surfaces that facilitate these interactions in the context of the CBM holo-complex. Regarding the BCL10–MALT1 interface either deletions in the DD or Ig1/2 domains in MALT1 or mutations and deletions in the CARD and Ser/Thr-rich C-terminus of BCL10 are impairing the interaction (17, 62, 63). Thus, the efficient BCL10–MALT1 binding is most likely relying on the overall conformation of both proteins. The BCL10–MALT1 filaments appear to present a dynamic surface for the clustering of signaling components like the E3 ligase TRAF6 that binds to the C-terminus of MALT1 and catalyzes MALT1 poly-ubiquitination to recruit the IKK complex and induce NF-κB activation (29, 64, 65). It needs to be noted that TRAF6 deficiency does not hamper TCR/CD28-induced NF-κB signaling in murine CD4 T cells (66). Nevertheless, mutation of the TRAF6 binding motifs in MALT1 abolish NF-κB activation in Jurkat T cells as well as murine CD4 T cells (67), strongly arguing that other E3 ligase(s) can compensate for the loss of TRAF6 in primary T cells. Further work is needed to elicit the exact architecture, the assembly, and the dynamics of BCL10 filaments and the CBM holo-complex, to understand mechanistically how different players are integrated to shape activation and termination of immune signaling.

CONTROL OF CBM COMPLEX DYNAMICS BY POST-TRANSLATIONAL REGULATION OF BCL10

Initial phosphorylations of CARMA/CARD scaffolds have been demonstrated to control the recruitment of pre-assembled BCL10–MALT1 and thus CBM complex assembly after stimulation (68, 69). Subsequently, BCL10 is regulated by a variety of post-translational processes including phosphorylation, ubiquitination, complete degradation, and C-terminal cleavage (**Figure 4**).

BCL10 Phosphorylation Balances TCR Signaling

B-cell lymphoma/leukemia 10 is prone to extensive phosphorylations upon T cell activation, which initially was suggested to foster NF-κB signaling (70, 71). Calmodulin kinase II (CaMKII) was found to associate with BCL10 and promote NF-κB signaling by phosphorylating threonine 91 in the CARD domain (72).

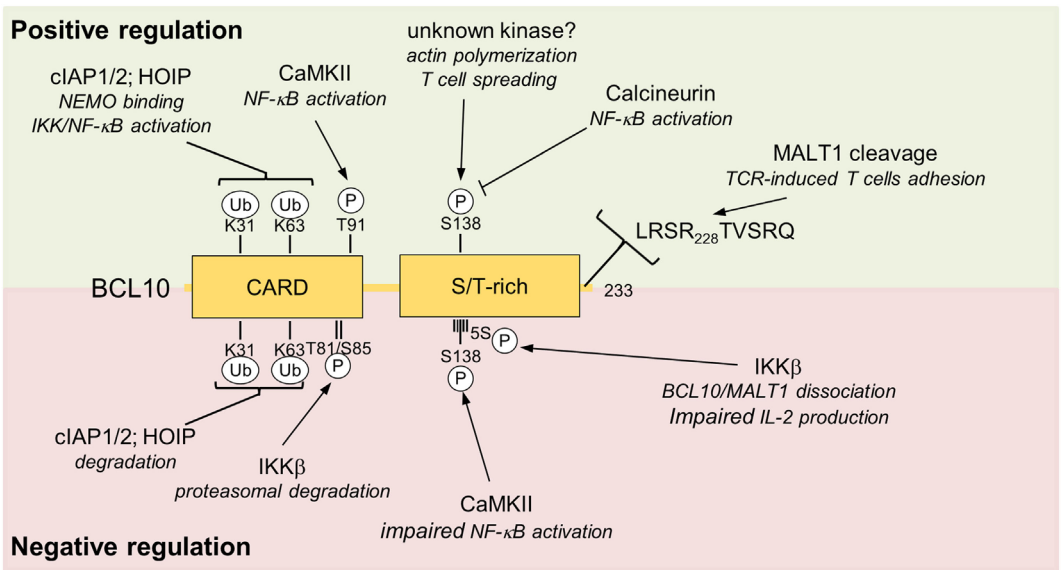

FIGURE 4 | Positive and negative regulations of BCL10. Positive and negative regulating post-translational modification sites (phosphorylation and ubiquitination) and MALT1 cleavage site are depicted. Upper box highlighted in green shows modifications of BCL10 associate with positive impact on T cell activation. The red lower box summarizes negative regulatory effects that impinge on BCL10. Abbreviations: CARD, caspase-recruitment domain; S/T-rich, serine/threonine-rich region; BCL10, B-cell lymphoma/leukemia 10; MALT, mucosa-associated lymphoid tissue.

Phospho-defective or -mimetic mutations were not interfering with CARD11 association, but it needs to be determined if threonine 91 is accessible in the context of the BCL10 filament and if phosphorylation affects filament structure and/or downstream signaling. Recently, GSK3β was also identified as a BCL10 kinase that augments CBM-1 complex formation and NF-κB activation in T cells, but the exact phosphorylation sites still need to be mapped and their functional relevance needs to be determined (73).

Other work demonstrated that BCL10 phosphorylations are largely counteracting CBM-1 signaling, and thereby exert negative regulatory roles on T cell activation (63, 74–76). The protein kinases IKKβ can catalyze BCL10 phosphorylation at multiple serines (134, 136, 138, 141, and 144) in the C-terminus and phospho-defective mutations lead to increased signaling and IL-2 production, indicating that IKKβ besides its positive role for NF-κB signaling can also put a brake on T cell activation (63). Especially phosphorylation of serine 138, which is also modified by CaMKII, is decreasing NF-κB activation (74, 76). Interestingly, C-terminal phosphorylations impair binding of BCL10 to MALT1, suggesting BCL10 phosphorylation balances signaling by structurally remodeling the CBM-1 complex (63). Phosphorylation at serine 138 was also suggested to enhance BCL10 turnover by a proteasome-independent mechanism (76), but an effect of this phosphorylation on BCL10 stability was not confirmed in other studies (77–79). The discovery of Calcineurin as a BCL10 phosphatase in T cells lends strong support to the negative control of BCL10 by protein kinases (78, 80). Inhibition by cyclosporine A or knockdown of Calcineurin augments IKKβ- or CaMKII-catalyzed BCL10 phosphorylation and persistent phosphorylation of serine 138 after TCR stimulation impedes IKK/NF-κB signaling, providing proof for the counterbalancing effect of BCL10 phosphorylation (78, 80).

Phosphorylation of BCL10 at serine 138 has also been implicated in TCR-induced actin polymerization and cell spreading of T cells (79). Furthermore, FcγR-mediated actin polymerization and phagocytosis in macrophages was impaired by BCL10 knockdown. Interestingly, this process was independent of CARD11 and MALT1, pointing to a role of BCL10 outside the CBM complex (79). Subsequent work confirmed the NF-κB-independent role of BCL10 in actin and membrane remodeling downstream of FcR in human macrophages by complexing with clathrin adaptors and recruiting the phosphatase OCRL that controls phosphatidylinositol-4,5-bisphosphate and F-actin turnover (81). The protein kinases controlling actin polymerization through serine 138 phosphorylation are unknown, but it is tempting to speculate that with IKKβ and CaMKII the same kinases that counteract NF-κB signaling by phosphorylating in this region, may also exert positive effects on actin polymerization. Certainly, further work is needed to understand the physiological relevance of BCL10-dependent actin polymerization for innate and adaptive immune responses.

Besides phosphorylation in the C-terminal Ser/Thr-rich region, IKKβ was shown to trigger phosphorylation of threonine 81 and serine 85 in the CARD of BCL10, which mediates the recruitment of Cullin1-βTRCP1 E3 ligase complex and proteasomal degradation of BCL10 (75). Since the accessibility of these residues in the BCL10 filaments is unclear and the majority of the BCL10 aggregates are removed by selective autophagy (see below) (82), IKKβ-dependent degradation may influence a distinct pool of BCL10 not attached to the CBM complex. Thus, even though the negative regulatory function of BCL10 phosphorylation on TCR activation has been confirmed in different studies, the exact regulations and mechanisms are still not completely resolved.

Balancing of BCL10 Activation and Degradation by Ubiquitination

Upon stimulation of antigen receptor signaling pathways in T and B cells, BCL10 is heavily modified by poly-ubiquitin chains, which have been associated with triggering downstream signaling pathways as well as BCL10 degradation (83–86). Indeed, BCL10 degradation and removal after T cell co-stimulation is required for post-inductive termination of CBM complex signaling (85). Mechanistically, TCR engagement promotes K63-linked ubiquitination of BCL10 leading to p62/Sequestosome-1-dependent autophagy and subsequent lysosomal degradation (82, 85). Also proteasomal BCL10 degradation was suggested to occur upon phosphorylation (75), but the efficient removal of the higher-order BCL10 filaments that form cellular clusters after lymphocyte stimulation can most likely only be achieved by selective autophagy and the delivery to lysosomal vesicles (57, 60, 82). Of note, MALT1 is spared from selective autophagy despite its constitutive association with BCL10 (82). How MALT1 is secluded from lysosomal destruction is not understood, but it may involve dissociation from hyper-phosphorylated BCL10 (63).

As mentioned earlier, ubiquitination of BCL10 is also required for T cell activation (86). Lysines 31 and 63 in the CARD domain serve as attachment sites of poly-ubiquitin chains, which promote the efficient recruitment of the IKK regulatory subunit NEMO (IKKγ) to BCL10 and IKK/NF-κB signaling (86). Thus, in conjunction with MALT1 ubiquitination, ubiquitin chains attached to BCL10 are mediating optimal IKK/NF-κB signaling after assembly of the CBM-1 complex in T cells (29, 86). Adding to the complexity, mutation of lysines 31 and 63 also leads to the stabilization of BCL10 in T cells after stimulation, suggesting that the same lysine residues are required for activation and termination of CBM-1 signaling (86).

A number of E3 ligases have been suggested to catalyze BCL10 poly-ubiquitination. Upon overexpression HECT E3 ligases NEDD4 or ITCH counteract TCR/CD28-induced NF-κB activation by promoting BCL10 poly-ubiquitination and degradation (84, 85). Indeed, ITCH deficiency is enhancing BCL10 turnover in primary T but not B cells and ITCH or NEDD4 are recruited to BCL10 *via* the protein kinase TAK1 independent of its kinase activity (77). TAK1 overexpression also decreases BCL10 amounts in ABC DLBCL cell lines that are characterized by chronic BCR signaling. In these tumor cells, kinase inactive TAK1 is responsible for BCL10 degradation and NF-κB inactivation. At the same time, TAK1 activity induces JNK signaling and both processes are required to induce cell death, and thereby counterselect BCR-addicted lymphoma cells (77).

Also cIAP2 induces BCL10 degradation, but inhibition of cIAP1/2 by antagonist did not affect BCL10 turnover in B cells

(77, 84). In fact, in ABC DLBCL tumor cells cIAP1/2 antagonists interfere with NF-κB-dependent pro-survival signaling by preventing the conjugation of K63-linked poly-ubiquitin chains on lysine 31/63 of BCL10 (87). However, since both lysine residues are also involved in degradation of BCL10, it is presently unclear how cIAP-dependent processes are balanced. In addition, most likely through K63-linked auto-ubiquitination, cIAPs recruit the linear ubiquitin chain assembly complex (LUBAC) consisting of HOIP (RNF31), HOIL-1 (RBCK1), and SHARPIN to the CBM-1 complex in ABC DLBCL cells (87, 88). Linear methionine (Met)-1 linked ubiquitination of NEMO by the LUBAC was initially found to be critical for TNFα-dependent NF-κB signaling and several studies demonstrated that LUBAC also controls NF-κB activation and survival of ABC DLBCL cells (88, 89). Furthermore, HOIP catalyzes linear ubiquitination of BCL10 in chronically activated ABC DLBCL as well as T and B cells in response to TCR and BCR stimulation, respectively (87, 90, 91). NF-κB activation is reduced after TCR/BCR cross-linking in HOIP-deficient T and B cells (89–91) and at least partially overlapping attachment sites on BCL10 have been mapped for Met1- and K63-linked ubiquitination (K14, K31, and K63 in BCL10) (91). However, neither HOIP deficiency nor mutation of BCL10 attachment completely abolished NF-κB activation, suggesting that Met-1 or K63 ubiquitination of BCL10 may not be essential but modulate CBM-1 activity. In fact, one study suggested that LUBAC may have a scaffolding function that facilitates NF-κB activation independent of HOIP catalytic activity (89).

A number of BCL10 E3 ligases have been identified, but much less is known about deubiquitinating enzymes (DUBs) counteracting BCL10 ubiquitination. *In vitro* the Met-1-selective DUB OTULIN can remove linear ubiquitin chains from BCL10 (91), but its role *in vivo* is unclear as T and B lymphocytes from conditional OTULIN KO mice are not chronically activated (92). BCL10 ubiquitination and degradation is enhanced in Jurkat T cells lacking the components of the COP9-signalosome (CSN), a multimeric complex with isopeptidase activity (93). Since the CSN is primarily influencing ubiquitin conjugation by deneddylating Cullin-RING E3 ligases complexes, the CSN may affect BCL10 stability indirectly. Finally, the ubiquitin-specific protease 9X (USP9X) interacts with BCL10 in activated T cells and silencing of USP9X augments BCL10 ubiquitination and impairs NF-κB signaling in T cells (94). Even though USP9X counteracts the assembly of K48-linked ubiquitin chains on BCL10, this does not lead to decreased BCL10 stability. At present, it is unclear how the regulation by USP9X is connected to the previously described E3 ligases and ubiquitination events, but augmented K48-ubiquitination may compete for the attachment of activating ubiquitin chains with other topologies to BCL10 and thus may promote a dysfunctional CBM-1 response.

Taken together, BCL10 acts as a platform that integrates many components of the ubiquitin system, which control BCL10 activity and stability in lymphocytes and lymphoma cells. Even further BCL10 E3 ligases, like mind bomb-2 or RNF8/RNF168 have been identified, but their role in BCL10-dependent immune signaling is unclear (95, 96). The exact order of events and the contribution of individual ubiquitin ligases and DUBs during the activation and termination phases of immune cell signaling are still to be explored.

BCL10 Cleavage by the MALT1 Protease

Upon activation, MALT1 protease cleaves a number of substrates with key functions in signaling as well as transcriptional and post-transcriptional regulation (**Figure 3**) (97). MALT1 protease also catalyzes cleavage of BCL10 at arginine 228 removing the last five amino acids from the C-terminus of BCL10 after T cell stimulation (16). C-terminal truncation of BCL10 is also visible in ABC DLBCL cells that are characterized by constitutive MALT1 activity (98, 99). Even though MALT1 protease activity enhances expression of NF-κB target genes like IL-2 in T cells, cleavage of BCL10 is not critical in this process. However, MALT1-dependent cleavage of BCL10 was required for integrin-dependent adhesion of T cells to fibronectin, which is important for the efficient contact of T cells to antigen-presenting cells (16). Interestingly, also thrombin-induced monocyte adhesion is dependent on endothelial BCL10 and thus an intact CBM-3 signalosome, but a putative involvement of the MALT1 protease and BCL10 in this process is unknown (37). Since CBM-dependent NF-κB regulation upregulates several genes controlling adhesion (e.g., ICAM-1, VCAM), it needs to be sorted out whether differences in adhesion may result from differential target gene expression after expression of cleavage defective BCL10 or MALT1 inhibition. To elucidate the physiological relevance of MALT1-catalyzed BCL10 cleavage, a mouse model expressing a cleavage resistant BCL10 R228A variant would be required.

CONCLUSION AND OUTLOOK

Since its discovery an enormous amount of data has been gathered that support the key function of BCL10 as the linker of all CBM complexes. By connecting to the scaffold proteins CARD11, CAR14, CARD10, and CARD9, BCL10 filaments channel antigenic stimulation in lymphocytes and distinct innate and inflammatory stimuli in many other cells to the NF-κB and JNK signaling pathways. BCL10 is the essential adaptor to initiate downstream signaling as well as MALT1 protease activity and substrate cleavage, which is balancing immune cell activation. Thus, BCL10 is mediating the known effects of the CARD scaffolds and acts as the bridge of all CARMA/CARDs involved in immune signaling. BCL10 is prone to numerous post-translational modifications, processing, and degradation, which control binding of interaction partners, stability and activity, highlighting that the role of BCL10 goes far beyond its function as the CBM linker. However, despite first proteomic analyses revealing BCL10 interactions and modifications in activated B cells (90), we are lacking a clear picture about the BCL10 regulation during immune cell activation. Global analyses are needed that cover the dynamics of BCL10 modifications, interactions, localization, and degradation, to elucidate the exact order of events. Moreover, we are still lacking a clear understanding how BCL10 filaments and thus the CBM holo-complexes are assembled und how this highly dynamic signalosome channels to downstream

signaling pathways. More structural and functional analyses as well as high resolution imaging are required to elucidate these processes. Several studies demonstrated functions of BCL10 in actin polymerization, phagocytosis, cell adhesion, DNA damage response, fatty acid signaling, or neural tube closure, which are presumably independent of known CARMA/CARDs and/or MALT1 (18, 45, 79, 100). It will be very interesting to explore how and to what extend BCL10 engages with other partners and functions outside the CBM complexes. Overall, in depth analyses are needed to evaluate how this important immune cell machinery can be exploited therapeutically to modulate immune responses for the treatment of autoimmune diseases, chronic or acute inflammation, and hematologic malignancies.

AUTHOR CONTRIBUTIONS

TG, TS, and DK designed and wrote the review.

ACKNOWLEDGMENTS

This work was supported by funding of the Deutsche Forschungsgemeinschaft (SFB 1054 project A04) to DK.

REFERENCES

1. Willis TG, Jadayel DM, Du MQ, Peng H, Perry AR, Abdul-Rauf M, et al. Bcl10 is involved in t(1;14)(p22;q32) of MALT B cell lymphoma and mutated in multiple tumor types. *Cell* (1999) 96:35–45. doi:10.1016/S0092-8674(00)80957-5
2. Costanzo A, Guiet C, Vito P. c-E10 is a caspase-recruiting domain-containing protein that interacts with components of death receptors signaling pathway and activates nuclear factor-kappaB. *J Biol Chem* (1999) 274:20127–32. doi:10.1074/jbc.274.29.20127
3. Koseki T, Inohara N, Chen S, Carrio R, Merino J, Hottiger MO, et al. CIPER, a novel NF kappaB-activating protein containing a caspase recruitment domain with homology to herpesvirus-2 protein E10. *J Biol Chem* (1999) 274:9955–61. doi:10.1074/jbc.274.15.9955
4. Srinivasula SM, Ahmad M, Lin JH, Poyet JL, Fernandes-Alnemri T, Tsichlis PN, et al. CLAP, a novel caspase recruitment domain-containing protein in the tumor necrosis factor receptor pathway, regulates NF-kappaB activation and apoptosis. *J Biol Chem* (1999) 274:17946–54. doi:10.1074/jbc.274.25.17946
5. Thome M, Martinon F, Hofmann K, Rubio V, Steiner V, Schneider P, et al. Equine herpesvirus-2 E10 gene product, but not its cellular homologue, activates NF-kappaB transcription factor and c-Jun N-terminal kinase. *J Biol Chem* (1999) 274:9962–8. doi:10.1074/jbc.274.15.9962
6. Yan M, Lee J, Schilbach S, Goddard A, Dixit V. mE10, a novel caspase recruitment domain-containing proapoptotic molecule. *J Biol Chem* (1999) 274:10287–92. doi:10.1074/jbc.274.15.10287
7. Bertin J, Guo Y, Wang L, Srinivasula SM, Jacobson MD, Poyet JL, et al. CARD9 is a novel caspase recruitment domain-containing protein that interacts with BCL10/CLAP and activates NF-kappa B. *J Biol Chem* (2000) 275:41082–6. doi:10.1074/jbc.C000726200
8. Bertin J, Wang L, Guo Y, Jacobson MD, Poyet JL, Srinivasula SM, et al. CARD11 and CARD14 are novel caspase recruitment domain (CARD)/membrane-associated guanylate kinase (MAGUK) family members that interact with BCL10 and activate NF-kappa B. *J Biol Chem* (2001) 276:11877–82. doi:10.1074/jbc.M010512200
9. Gaide O, Martinon F, Micheau O, Bonnet D, Thome M, Tschopp J. Carma1, a CARD-containing binding partner of Bcl10, induces Bcl10 phosphorylation and NF-kappaB activation. *FEBS Lett* (2001) 496:121–7. doi:10.1016/S0014-5793(01)02414-0
10. McAllister-Lucas LM, Inohara N, Lucas PC, Ruland J, Benito A, Li Q, et al. Bimp1, a MAGUK family member linking protein kinase C activation to Bcl10-mediated NF-kappaB induction. *J Biol Chem* (2001) 276:30589–97. doi:10.1074/jbc.M103824200
11. Wang L, Guo Y, Huang WJ, Ke X, Poyet JL, Manji GA, et al. Card10 is a novel caspase recruitment domain/membrane-associated guanylate kinase family member that interacts with BCL10 and activates NF-kappa B. *J Biol Chem* (2001) 276:21405–9. doi:10.1074/jbc.M102488200
12. Uren AG, O'Rourke K, Aravind LA, Pisabarro MT, Seshagiri S, Koonin EV, et al. Identification of paracaspases and metacaspases: two ancient families of caspase-like proteins, one of which plays a key role in MALT lymphoma. *Mol Cell* (2000) 6:961–7. doi:10.1016/S1097-2765(05)00086-9
13. Akagi T, Motegi M, Tamura A, Suzuki R, Hosokawa Y, Suzuki H, et al. A novel gene, MALT1 at 18q21, is involved in t(11;18) (q21;q21) found in low-grade B-cell lymphoma of mucosa-associated lymphoid tissue. *Oncogene* (1999) 18:5785–94. doi:10.1038/sj.onc.1203018
14. Dierlamm J, Baens M, Wlodarska I, Stefanova-Ouzounova M, Hernandez JM, Hossfeld DK, et al. The apoptosis inhibitor gene API2 and a novel 18q gene, MLT, are recurrently rearranged in the t(11;18)(q21;q21) associated with mucosa-associated lymphoid tissue lymphomas. *Blood* (1999) 93:3601–9.
15. Coornaert B, Baens M, Heyninck K, Bekaert T, Haegman M, Staal J, et al. T cell antigen receptor stimulation induces MALT1 paracaspase-mediated cleavage of the NF-kappaB inhibitor A20. *Nat Immunol* (2008) 9:263–71. doi:10.1038/ni1561
16. Rebeaud F, Hailfinger S, Posevitz-Fejfar A, Tapernoux M, Moser R, Rueda D, et al. The proteolytic activity of the paracaspase MALT1 is key in T cell activation. *Nat Immunol* (2008) 9:272–81. doi:10.1038/ni1568
17. Lucas PC, Yonezumi M, Inohara N, McAllister-Lucas LM, Abazeed ME, Chen FF, et al. Bcl10 and MALT1, independent targets of chromosomal translocation in malt lymphoma, cooperate in a novel NF-kappa B signaling pathway. *J Biol Chem* (2001) 276:19012–9. doi:10.1074/jbc.M009984200
18. Ruland J, Duncan GS, Elia A, del Barco Barrantes I, Nguyen L, Plyte S, et al. Bcl10 is a positive regulator of antigen receptor-induced activation of NF-kappaB and neural tube closure. *Cell* (2001) 104:33–42. doi:10.1016/S0092-8674(01)00189-1
19. Lomaga MA, Henderson JT, Elia AJ, Robertson J, Noyce RS, Yeh WC, et al. Tumor necrosis factor receptor-associated factor 6 (TRAF6) deficiency results in exencephaly and is required for apoptosis within the developing CNS. *J Neurosci* (2000) 20:7384–93. doi:10.1523/JNEUROSCI.20-19-07384.2000
20. Jost PJ, Weiss S, Ferch U, Gross O, Mak TW, Peschel C, et al. Bcl10/Malt1 signaling is essential for TCR-induced NF-kappaB activation in thymocytes but dispensable for positive or negative selection. *J Immunol* (2007) 178:953–60. doi:10.4049/jimmunol.178.2.953
21. Schmidt-Supprian M, Tian J, Grant EP, Pasparakis M, Maehr R, Ovaa H, et al. Differential dependence of CD4+CD25+ regulatory and natural killer-like T cells on signals leading to NF-kappaB activation. *Proc Natl Acad Sci U S A* (2004) 101:4566–71. doi:10.1073/pnas.0400885101
22. Xue L, Morris SW, Orihuela C, Tuomanen E, Cui X, Wen R, et al. Defective development and function of Bcl10-deficient follicular, marginal zone and B1 B cells. *Nat Immunol* (2003) 4:857–65. doi:10.1038/ni963
23. Brustle A, Brenner D, Knobbe-Thomsen CB, Cox M, Lang PA, Lang KS, et al. MALT1 is an intrinsic regulator of regulatory T cells. *Cell Death Differ* (2015) 24(7):1214–23. doi:10.1038/cdd.2015.104
24. Egawa T, Albrecht B, Favier B, Sunshine MJ, Mirchandani K, O'Brien W, et al. Requirement for CARMA1 in antigen receptor-induced NF-kappa B activation and lymphocyte proliferation. *Curr Biol* (2003) 13:1252–8. doi:10.1016/S0960-9822(03)00491-3
25. Hara H, Wada T, Bakal C, Kozieradzki I, Suzuki S, Suzuki N, et al. The MAGUK family protein CARD11 is essential for lymphocyte activation. *Immunity* (2003) 18:763–75. doi:10.1016/S1074-7613(03)00148-1
26. Molinero LL, Yang J, Gajewski T, Abraham C, Farrar MA, Alegre ML. CARMA1 controls an early checkpoint in the thymic development of FoxP3+ regulatory T cells. *J Immunol* (2009) 182:6736–43. doi:10.4049/jimmunol.0900498
27. Newton K, Dixit VM. Mice lacking the CARD of CARMA1 exhibit defective B lymphocyte development and impaired proliferation of their B and T lymphocytes. *Curr Biol* (2003) 13:1247–51. doi:10.1016/S0960-9822(03)00458-5

28. Ruland J, Duncan GS, Wakeham A, Mak TW. Differential requirement for Malt1 in T and B cell antigen receptor signaling. *Immunity* (2003) 19:749–58. doi:10.1016/S1074-7613(03)00293-0
29. Oeckinghaus A, Wegener E, Welteke V, Ferch U, Arslan SC, Ruland J, et al. Malt1 ubiquitination triggers NF-kappaB signaling upon T-cell activation. *EMBO J* (2007) 26:4634–45. doi:10.1038/sj.emboj.7601897
30. Nakaya M, Xiao Y, Zhou X, Chang JH, Chang M, Cheng X, et al. Inflammatory T cell responses rely on amino acid transporter ASCT2 facilitation of glutamine uptake and mTORC1 kinase activation. *Immunity* (2014) 40:692–705. doi:10.1016/j.immuni.2014.04.007
31. Hamilton KS, Phong B, Corey C, Cheng J, Gorentla B, Zhong X, et al. T cell receptor-dependent activation of mTOR signaling in T cells is mediated by Carma1 and MALT1, but not Bcl10. *Sci Signal* (2014) 7:ra55. doi:10.1126/scisignal.2005169
32. Hara H, Ishihara C, Takeuchi A, Xue L, Morris SW, Penninger JM, et al. Cell type-specific regulation of ITAM-mediated NF-kappaB activation by the adaptors, CARMA1 and CARD9. *J Immunol* (2008) 181:918–30. doi:10.4049/jimmunol.181.2.918
33. Chen Y, Pappu BP, Zeng H, Xue L, Morris SW, Lin X, et al. B cell lymphoma 10 is essential for FcepsilonR-mediated degranulation and IL-6 production in mast cells. *J Immunol* (2007) 178:49–57. doi:10.4049/jimmunol.178.1.49
34. Klemm S, Gutermuth J, Hultner L, Sparwasser T, Behrendt H, Peschel C, et al. The Bcl10-Malt1 complex segregates Fc epsilon RI-mediated nuclear factor kappa B activation and cytokine production from mast cell degranulation. *J Exp Med* (2006) 203:337–47. doi:10.1084/jem.20051982
35. Bi L, Gojestani S, Wu W, Hsu YM, Zhu J, Ariizumi K, et al. CARD9 mediates dectin-2-induced IkappaBalpha kinase ubiquitination leading to activation of NF-kappaB in response to stimulation by the hyphal form of *Candida albicans*. *J Biol Chem* (2010) 285:25969–77. doi:10.1074/jbc.M110.131300
36. Gross O, Gewies A, Finger K, Schafer M, Sparwasser T, Peschel C, et al. Card9 controls a non-TLR signalling pathway for innate anti-fungal immunity. *Nature* (2006) 442:651–6. doi:10.1038/nature04926
37. Delekta PC, Apel IJ, Gu S, Siu K, Hattori Y, McAllister-Lucas LM, et al. Thrombin-dependent NF-{kappa}B activation and monocyte/endothelial adhesion are mediated by the CARMA3.Bcl10.MALT1 signalosome. *J Biol Chem* (2010) 285:41432–42. doi:10.1074/jbc.M110.158949
38. Ekambaram P, Lee JL, Hubel NE, Hu D, Yerneni S, Campbell PG, et al. The CARMA3-Bcl10-MALT1 signalosome drives NF-kappaB activation and promotes aggressiveness in angiotensin ii receptor-positive breast cancer. *Cancer Res* (2017) 78(5):1225–40. doi:10.1158/0008-5472.CAN-17-1089
39. Grabiner BC, Blonska M, Lin PC, You Y, Wang D, Sun J, et al. CARMA3 deficiency abrogates G protein-coupled receptor-induced NF-{kappa}B activation. *Genes Dev* (2007) 21:984–96. doi:10.1101/gad.1502507
40. Klemm S, Zimmermann S, Peschel C, Mak TW, Ruland J. Bcl10 and Malt1 control lysophosphatidic acid-induced NF-kappaB activation and cytokine production. *Proc Natl Acad Sci U S A* (2007) 104:134–8. doi:10.1073/pnas.0608388103
41. Marko L, Henke N, Park JK, Spallek B, Qadri F, Balogh A, et al. Bcl10 mediates angiotensin II-induced cardiac damage and electrical remodeling. *Hypertension* (2014) 64:1032–9. doi:10.1161/HYPERTENSIONAHA.114.03900
42. McAllister-Lucas LM, Ruland J, Siu K, Jin X, Gu S, Kim DS, et al. CARMA3/Bcl10/MALT1-dependent NF-kappaB activation mediates angiotensin II-responsive inflammatory signaling in nonimmune cells. *Proc Natl Acad Sci U S A* (2007) 104:139–44. doi:10.1073/pnas.0601947103
43. Wang D, You Y, Lin PC, Xue L, Morris SW, Zeng H, et al. Bcl10 plays a critical role in NF-kappaB activation induced by G protein-coupled receptors. *Proc Natl Acad Sci U S A* (2007) 104:145–50. doi:10.1073/pnas.0601894104
44. Jiang T, Grabiner B, Zhu Y, Jiang C, Li H, You Y, et al. CARMA3 is crucial for EGFR-induced activation of NF-kappaB and tumor progression. *Cancer Res* (2011) 71:2183–92. doi:10.1158/0008-5472.CAN-10-3626
45. Van Beek M, Oravecz-Wilson KI, Delekta PC, Gu S, Li X, Jin X, et al. Bcl10 links saturated fat overnutrition with hepatocellular NF-kB activation and insulin resistance. *Cell Rep* (2012) 1:444–52. doi:10.1016/j.celrep.2012.04.006
46. Afonina IS, Van Nuffel E, Baudelet G, Driege Y, Kreike M, Staal J, et al. The paracaspase MALT1 mediates CARD14-induced signaling in keratinocytes. *EMBO Rep* (2016) 17:914–27. doi:10.15252/embr.201642109
47. Howes A, O'Sullivan PA, Breyer F, Ghose A, Cao L, Krappmann D, et al. Psoriasis mutations disrupt CARD14 autoinhibition promoting BCL10-MALT1-dependent NF-kappaB activation. *Biochem J* (2016) 473:1759–68. doi:10.1042/BCJ20160270
48. Torres JM, Martinez-Barricarte R, Garcia-Gomez S, Mazariegos MS, Itan Y, Boisson B, et al. Inherited BCL10 deficiency impairs hematopoietic and nonhematopoietic immunity. *J Clin Invest* (2014) 124:5239–48. doi:10.1172/JCI77493
49. Hara H, Ishihara C, Takeuchi A, Imanishi T, Xue L, Morris SW, et al. The adaptor protein CARD9 is essential for the activation of myeloid cells through ITAM-associated and toll-like receptors. *Nat Immunol* (2007) 8:619–29. doi:10.1038/ni1466
50. Bhattacharyya S, Borthakur A, Pant N, Dudeja PK, Tobacman JK. Bcl10 mediates LPS-induced activation of NF-kappaB and IL-8 in human intestinal epithelial cells. *Am J Physiol Gastrointest Liver Physiol* (2007) 293:G429–37. doi:10.1152/ajpgi.00149.2007
51. Ye H, Dogan A, Karran L, Willis TG, Chen L, Wlodarska I, et al. BCL10 expression in normal and neoplastic lymphoid tissue. Nuclear localization in MALT lymphoma. *Am J Pathol* (2000) 157:1147–54. doi:10.1016/S0002-9440(10)64630-5
52. Li Z, Wang H, Xue L, Shin DM, Roopenian D, Xu W, et al. Emu-BCL10 mice exhibit constitutive activation of both canonical and noncanonical NF-kappaB pathways generating marginal zone (MZ) B-cell expansion as a precursor to splenic MZ lymphoma. *Blood* (2009) 114:4158–68. doi:10.1182/blood-2008-12-192583
53. Luminari S, Intini D, Baldini L, Berti E, Bertoni F, Zucca E, et al. BCL10 gene mutations rarely occur in lymphoid malignancies. *Leukemia* (2000) 14:905–8. doi:10.1038/sj.leu.2401747
54. Ngo VN, Davis RE, Lamy L, Yu X, Zhao H, Lenz G, et al. A loss-of-function RNA interference screen for molecular targets in cancer. *Nature* (2006) 441:106–10. doi:10.1038/nature04687
55. Krappmann D, Vincendeau M. Mechanisms of NF-kappaB deregulation in lymphoid malignancies. *Semin Cancer Biol* (2016) 39:3–14. doi:10.1016/j.semcancer.2016.05.002
56. Guiet C, Vito P. Caspase recruitment domain (CARD)-dependent cytoplasmic filaments mediate bcl10-induced NF-kappaB activation. *J Cell Biol* (2000) 148:1131–40. doi:10.1083/jcb.148.6.1131
57. Rossman JS, Stoicheva NG, Langel FD, Patterson GH, Lippincott-Schwartz J, Schaefer BC. POLKADOTS are foci of functional interactions in T-cell receptor-mediated signaling to NF-kappaB. *Mol Biol Cell* (2006) 17:2166–76. doi:10.1091/mbc.e05-10-0985
58. Schaefer BC, Kappler JW, Kupfer A, Marrack P. Complex and dynamic redistribution of NF-kappaB signaling intermediates in response to T cell receptor stimulation. *Proc Natl Acad Sci U S A* (2004) 101:1004–9. doi:10.1073/pnas.0307858100
59. David L, Li Y, Ma J, Garner E, Zhang X, Wu H. Assembly mechanism of the CARMA1-BCL10-MALT1-TRAF6 signalosome. *Proc Natl Acad Sci U S A* (2018) 115(7):1499–504. doi:10.1073/pnas.1721967115
60. Qiao Q, Yang C, Zheng C, Fontan L, David L, Yu X, et al. Structural architecture of the CARMA1/Bcl10/MALT1 signalosome: nucleation-induced filamentous assembly. *Mol Cell* (2013) 51:766–79. doi:10.1016/j.molcel.2013.08.032
61. Li S, Yang X, Shao J, Shen Y. Structural insights into the assembly of CARMA1 and BCL10. *PLoS One* (2012) 7:e42775. doi:10.1371/journal.pone.0042775
62. Langel FD, Jain NA, Rossman JS, Kingeter LM, Kashyap AK, Schaefer BC. Multiple protein domains mediate interaction between Bcl10 and MALT1. *J Biol Chem* (2008) 283:32419–31. doi:10.1074/jbc.M800670200
63. Wegener E, Oeckinghaus A, Papadopoulou N, Lavitas L, Schmidt-Supprian M, Ferch U, et al. Essential role for IkappaB kinase beta in remodeling Carma1-Bcl10-Malt1 complexes upon T cell activation. *Mol Cell* (2006) 23:13–23. doi:10.1016/j.molcel.2006.05.027
64. Chiffoleau E, Kobayashi T, Walsh MC, King CG, Walsh PT, Hancock WW, et al. TNF receptor-associated factor 6 deficiency during hemopoiesis induces Th2-polarized inflammatory disease. *J Immunol* (2003) 171:5751–9. doi:10.4049/jimmunol.171.11.5751
65. Sun L, Deng L, Ea CK, Xia ZP, Chen ZJ. The TRAF6 ubiquitin ligase and TAK1 kinase mediate IKK activation by BCL10 and MALT1 in T lymphocytes. *Mol Cell* (2004) 14:289–301. doi:10.1016/S1097-2765(04)00236-9
66. King CG, Kobayashi T, Cejas PJ, Kim T, Yoon K, Kim GK, et al. TRAF6 is a T cell-intrinsic negative regulator required for the maintenance of immune homeostasis. *Nat Med* (2006) 12:1088–92. doi:10.1038/nm1449

67. Meininger I, Griesbach RA, Hu D, Gehring T, Seeholzer T, Bertossi A, et al. Alternative splicing of MALT1 controls signalling and activation of CD4(+) T cells. *Nat Commun* (2016) 7:11292. doi:10.1038/ncomms11292
68. Meininger I, Krappmann D. Lymphocyte signaling and activation by the CARMA1-BCL10-MALT1 signalosome. *Biol Chem* (2016) 397:1315–33. doi:10.1515/hsz-2016-0216
69. Roth S, Ruland J. Caspase recruitment domain-containing protein 9 signaling in innate immunity and inflammation. *Trends Immunol* (2013) 34:243–50. doi:10.1016/j.it.2013.02.006
70. Gaide O, Favier B, Legler DF, Bonnet D, Brissoni B, Valitutti S, et al. CARMA1 is a critical lipid raft-associated regulator of TCR-induced NF-kappa B activation. *Nat Immunol* (2002) 3:836–43. doi:10.1038/ni830
71. Jun JE, Wilson LE, Vinuesa CG, Lesage S, Blery M, Miosge LA, et al. Identifying the MAGUK protein Carma-1 as a central regulator of humoral immune responses and atopy by genome-wide mouse mutagenesis. *Immunity* (2003) 18:751–62. doi:10.1016/S1074-7613(03)00141-9
72. Oruganti SR, Edin S, Grundstrom C, Grundstrom T. CaMKII targets Bcl10 in T-cell receptor induced activation of NF-kappaB. *Mol Immunol* (2011) 48:1448–60. doi:10.1016/j.molimm.2011.03.020
73. Abd-Ellah A, Voogdt C, Krappmann D, Moller P, Marienfeld RB. GSK3beta modulates NF-kappaB activation and RelB degradation through site-specific phosphorylation of BCL10. *Sci Rep* (2018) 8:1352. doi:10.1038/s41598-018-19822-z
74. Ishiguro K, Ando T, Goto H, Xavier R. Bcl10 is phosphorylated on Ser138 by Ca2+/calmodulin-dependent protein kinase II. *Mol Immunol* (2007) 44:2095–100. doi:10.1016/j.molimm.2006.09.012
75. Lobry C, Lopez T, Israel A, Weil R. Negative feedback loop in T cell activation through IkappaB kinase-induced phosphorylation and degradation of Bcl10. *Proc Natl Acad Sci U S A* (2007) 104:908–13. doi:10.1073/pnas.0606982104
76. Zeng H, Di L, Fu G, Chen Y, Gao X, Xu L, et al. Phosphorylation of Bcl10 negatively regulates T-cell receptor-mediated NF-kappaB activation. *Mol Cell Biol* (2007) 27:5235–45. doi:10.1128/MCB.01645-06
77. Moreno-Garcia ME, Sommer K, Rincon-Arano H, Brault M, Ninomiya-Tsuji J, Matesic LE, et al. Kinase-independent feedback of the TAK1/TAB 1 complex on BCL10 turnover and NF-kappaB activation. *Mol Cell Biol* (2013) 33:1149–63. doi:10.1128/MCB.06407-11
78. Palkowitsch L, Marienfeld U, Brunner C, Eitelhuber A, Krappmann D, Marienfeld RB. The Ca2+-dependent phosphatase calcineurin controls the formation of the Carma1-Bcl10-Malt1 complex during T cell receptor-induced NF-kappaB activation. *J Biol Chem* (2011) 286:7522–34. doi:10.1074/jbc.M110.155895
79. Rueda D, Gaide O, Ho L, Lewkowicz E, Niedergang F, Hailfinger S, et al. Bcl10 controls TCR- and FcgammaR-induced actin polymerization. *J Immunol* (2007) 178:4373–84. doi:10.4049/jimmunol.178.7.4373
80. Frischbutter S, Gabriel C, Bendfeldt H, Radbruch A, Baumgrass R. Dephosphorylation of Bcl-10 by calcineurin is essential for canonical NF-kappaB activation in Th cells. *Eur J Immunol* (2011) 41:2349–57. doi:10.1002/eji.201041052
81. Marion S, Mazzolini J, Herit F, Bourdoncle P, Kambou-Pene N, Hailfinger S, et al. The NF-kappaB signaling protein Bcl10 regulates actin dynamics by controlling AP1 and OCRL-bearing vesicles. *Dev Cell* (2012) 23:954–67. doi:10.1016/j.devcel.2012.09.021
82. Paul S, Kashyap AK, Jia W, He YW, Schaefer BC. Selective autophagy of the adaptor protein Bcl10 modulates T cell receptor activation of NF-kappaB. *Immunity* (2012) 36:947–58. doi:10.1016/j.immuni.2012.04.008
83. Hu S, Alcivar A, Qu L, Tang J, Yang X. CIAP2 inhibits antigen receptor signaling by targeting Bcl10 for degradation. *Cell Cycle* (2006) 5:1438–42. doi:10.4161/cc.5.13.2866
84. Hu S, Du MQ, Park SM, Alcivar A, Qu L, Gupta S, et al. cIAP2 is a ubiquitin protein ligase for BCL10 and is dysregulated in mucosa-associated lymphoid tissue lymphomas. *J Clin Invest* (2006) 116:174–81. doi:10.1172/JCI25641
85. Scharschmidt E, Wegener E, Heissmeyer V, Rao A, Krappmann D. Degradation of Bcl10 induced by T-cell activation negatively regulates NF-kappa B signaling. *Mol Cell Biol* (2004) 24:3860–73. doi:10.1128/MCB.24.9.3860-3873.2004
86. Wu CJ, Ashwell JD. NEMO recognition of ubiquitinated Bcl10 is required for T cell receptor-mediated NF-kappaB activation. *Proc Natl Acad Sci U S A* (2008) 105:3023–8. doi:10.1073/pnas.0712313105
87. Yang Y, Kelly P, Shaffer AL III, Schmitz R, Yoo HM, Liu X, et al. Targeting non-proteolytic protein ubiquitination for the treatment of diffuse large B cell lymphoma. *Cancer Cell* (2016) 29:494–507. doi:10.1016/j.ccell.2016.03.006
88. Yang Y, Schmitz R, Mitala J, Whiting A, Xiao W, Ceribelli M, et al. Essential role of the linear ubiquitin chain assembly complex in lymphoma revealed by rare germline polymorphisms. *Cancer Discov* (2014) 4:480–93. doi:10.1158/2159-8290.CD-13-0915
89. Dubois SM, Alexia C, Wu Y, Leclair HM, Leveau C, Schol E, et al. A catalytic-independent role for the LUBAC in NF-kappaB activation upon antigen receptor engagement and in lymphoma cells. *Blood* (2014) 123:2199–203. doi:10.1182/blood-2013-05-504019
90. Satpathy S, Wagner SA, Beli P, Gupta R, Kristiansen TA, Malinova D, et al. Systems-wide analysis of BCR signalosomes and downstream phosphorylation and ubiquitylation. *Mol Syst Biol* (2015) 11:810. doi:10.15252/msb.20145880
91. Yang YK, Yang C, Chan W, Wang Z, Deibel KE, Pomerantz JL. Molecular determinants of scaffold-induced linear ubiquitinylation of B cell lymphoma/leukemia 10 (Bcl10) during T cell receptor and oncogenic caspase recruitment domain-containing protein 11 (CARD11) signaling. *J Biol Chem* (2016) 291(50):25921–36. doi:10.1074/jbc.M116.754028
92. Damgaard RB, Walker JA, Marco-Casanova P, Morgan NV, Titheradge HL, Elliott PR, et al. The deubiquitinase OTULIN is an essential negative regulator of inflammation and autoimmunity. *Cell* (2016) 166:1215–1230e20. doi:10.1016/j.cell.2016.07.019
93. Welteke V, Eitelhuber A, Duwel M, Schweitzer K, Naumann M, Krappmann D. COP9 signalosome controls the Carma1-Bcl10-Malt1 complex upon T-cell stimulation. *EMBO Rep* (2009) 10:642–8. doi:10.1038/embor.2009.64
94. Park Y, Jin HS, Liu YC. Regulation of T cell function by the ubiquitin-specific protease USP9X via modulating the Carma1-Bcl10-Malt1 complex. *Proc Natl Acad Sci U S A* (2013) 110:9433–8. doi:10.1073/pnas.1221925110
95. Stempin CC, Chi L, Giraldo-Vela JP, High AA, Hacker H, Redecke V. The E3 ubiquitin ligase mind bomb-2 (MIB2) protein controls B-cell CLL/lymphoma 10 (BCL10)-dependent NF-kappaB activation. *J Biol Chem* (2011) 286:37147–57. doi:10.1074/jbc.M111.263384
96. Zhao H, Zhu M, Dou G, Zhao H, Zhu B, Li J, et al. BCL10 regulates RNF8/RNF168-mediated ubiquitination in the DNA damage response. *Cell Cycle* (2014) 13:1777–87. doi:10.4161/cc.28707
97. Jaworski M, Thome M. The paracaspase MALT1: biological function and potential for therapeutic inhibition. *Cell Mol Life Sci* (2016) 73:459–73. doi:10.1007/s00018-015-2059-z
98. Ferch U, Kloo B, Gewies A, Pfander V, Duwel M, Peschel C, et al. Inhibition of MALT1 protease activity is selectively toxic for activated B cell-like diffuse large B cell lymphoma cells. *J Exp Med* (2009) 206:2313–20. doi:10.1084/jem.20091167
99. Hailfinger S, Lenz G, Ngo V, Posvitz-Fejfar A, Rebeaud F, Guzzardi M, et al. Essential role of MALT1 protease activity in activated B cell-like diffuse large B-cell lymphoma. *Proc Natl Acad Sci U S A* (2009) 106:19946–51. doi:10.1073/pnas.0907511106
100. Ismail IH, Dronyk A, Hu X, Hendzel MJ, Shaw AR. BCL10 is recruited to sites of DNA damage to facilitate DNA double-strand break repair. *Cell Cycle* (2016) 15:84–94. doi:10.1080/15384101.2015.1121322

Conflict of Interest Statement: The authors declare that the research was conducted in the absence of any commercial or financial relationships that could be construed as a potential conflict of interest.

frontiers in Immunology

REVIEW
published: 30 August 2018
doi: 10.3389/fimmu.2018.01927

Holding All the CARDs: How MALT1 Controls CARMA/CARD-Dependent Signaling

*Mélanie Juilland and Margot Thome**

Department of Biochemistry, University of Lausanne, Epalinges, Switzerland

The scaffold proteins CARMA1-3 (encoded by the genes *CARD11*, *-14* and *-10*) and CARD9 play major roles in signaling downstream of receptors with immunoreceptor tyrosine activation motifs (ITAMs), G-protein coupled receptors (GPCR) and receptor tyrosine kinases (RTK). These receptors trigger the formation of oligomeric CARMA/CARD-BCL10-MALT1 (CBM) complexes via kinases of the PKC family. The CBM in turn regulates gene expression by the activation of NF-κB and AP-1 transcription factors and controls transcript stability. The paracaspase MALT1 is the only CBM component having an enzymatic (proteolytic) activity and has therefore recently gained attention as a potential drug target. Here we review recent advances in the understanding of the molecular function of the protease MALT1 and summarize how MALT1 scaffold and protease function contribute to the transmission of CBM signals. Finally, we will highlight how dysregulation of MALT1 function can cause pathologies such as immunodeficiency, autoimmunity, psoriasis, and cancer.

Keywords: paracaspase, RNA stability, ubiquitin, Treg, BCR, TCR, GPCR, EGFR

OPEN ACCESS

Edited by:
Frederic Bornancin, Novartis, Switzerland

Reviewed by:
Jacques A. Nunes, INSERM U1068 Centre de Recherche en Cancérologie de Marseille, France
Lawrence Kane, University of Pittsburgh, United States

****Correspondence:***
Margot Thome
margot.thomemiazza@unil.ch

Specialty section:
This article was submitted to T Cell Biology, a section of the journal Frontiers in Immunology

Received: *18 June 2018*
Accepted: *06 August 2018*
Published: *30 August 2018*

Citation:
Juilland M and Thome M (2018) Holding All the CARDs: How MALT1 Controls CARMA/CARD-Dependent Signaling. Front. Immunol. 9:1927. doi: 10.3389/fimmu.2018.01927

INTRODUCTION

The past few years have seen considerable advances in our understanding of the role of MALT1 in different biological processes. It is now well accepted that MALT1 acts downstream of various receptors in a complex composed of CARMA (CARD-containing MAGUK) proteins, the adaptor protein BCL10 and MALT1 itself. These so-called CBM complexes are crucial for the regulation of the classical NF-κB pathway (also called canonical or NF-κB1 pathway) and other biological processes that will be covered in this review. We will first introduce the receptors that signal via CBM complexes and then describe the role of MALT1 in CBM-dependent signal transmission and its role in the activation of a variety of downstream signals. Finally, we will highlight how dysfunction of MALT1 can cause pathological alterations, which may be amenable to treatment with MALT1 inhibitors that are presently under development.

VARIOUS RECEPTORS SIGNAL VIA CARMA/CARD PROTEINS AND MALT1

MALT1 is a ubiquitously expressed protease that resides in the cytoplasm as a catalytically inactive BCL10-bound proenzyme. It is recruited into CBM signaling complexes upon the stimulation of specific receptors, namely those containing one or more immunoreceptor tyrosine-based activation motifs (ITAMs), G-protein-coupled receptors (GPCRs), or receptor tyrosine kinases (RTKs) **(Figure 1)** (1).

Various immunoreceptors of the innate and adaptive immune response activate MALT1. A common feature of such receptors is the presence of one or more ITAMs, which is crucial for transmembrane signal transmission (2). The ITAM can be present in the cytoplasmic tail of the immunoreceptors, as is the case for the zymosan receptor Dectin-1 present on dendritic cells (DC), or the FcεRI on mast cells. Alternatively, the ITAM can be present in a receptor-associated signaling subunit. For example, in CD3 chains associated with the T-cell receptor (TCR), the CD79 chains associated with the B-cell receptor (BCR) and the FcRγ chain associating with the myeloid cell receptor Dectin-2 or the natural killer (NK) cell receptors NK1.1/Ly49D/Ly49H/NKG2D (2, 3). Upon receptor triggering, Src family kinases phosphorylate the ITAMs, thereby providing a docking site for Syk family kinases. Once recruited, Syk kinases induce the downstream signaling events, which converge toward the activation of PKC family kinases, PKC-dependent phosphorylation of the CARMA/CARD protein and the subsequent formation of a CBM complex, for which the composition is specific for different receptor types (**Figure 1**).

A common feature of all receptors signaling via CBM complexes is the use of MALT1 as a scaffold protein for the IKK-dependent activation of the heterodimeric transcription factors of the NF-κB1 subtype, p50-RelA and p50-cRel (referred to as NF-κB). As a scaffold protein, MALT1 binds the ubiquitin ligase TRAF6, which subsequently modifies itself, BCL10, and the IKK subunit NEMO by K63-linked polyubiquitin chains (4–7). These modifications are required for the downstream activation of the IKK complex (4, 6), which phosphorylates the NF-κB inhibitor, IκBα, to trigger its proteasomal degradation (8, 9). The protease activity of MALT1 makes an additional contribution to the intensity and persistence of the NF-κB response by cleaving the proteins A20 and RelB, which act as negative regulators of NF-κB activation (10, 11). However, whether all CBM-dependent signaling pathways rely on the protease activity of MALT1, or whether some receptors only rely on the MALT1 scaffold activity remains poorly understood.

The relevance of MALT1 protease activity is strongly evidenced for ITAM-containing receptors, which promote activation of lymphoid and NK cells via CARMA1/CARD11 (11–13) and myeloid cells via CARD9 (13, 14). The protease activity of MALT1 also plays a role outside the immune system, in the activation of keratinocytes (15). Stimulation of keratinocytes with zymosan, which triggers the ITAM-containing receptor Dectin-1, leads to CBM complex activation and MALT1 protease activity via CARMA2/CARD14. This suggests that all ITAM containing receptors signal via both the scaffold and protease activity of MALT1 in immune and non-immune cells.

A variety of GPCRs (such as AT1R, Par-1, PAFR, ET_A, ET_B, CXCR2, CXCR4, LPA1-6) and RTKs (the EGFR and HER2/neu) have been shown to trigger the formation of a CBM complex comprising CARMA3/CARD10 **(Figure 1)** [see (1) and references therein]. Whether the protease function of MALT1 is involved or not in the transmission of the signaling pathway of these receptors is not well understood. For one GPCR (the thrombin receptor PAR1), the protease activity of MALT1 was found to be crucial for the regulation of the integrity of epithelial barriers, whereby stimulation of epithelial cells with thrombin lead to MALT1 proteolytic activity and CYLD cleavage (16), in addition to the previously described formation of a CBM complex comprising CARMA3 (17). These findings suggest the possibility of a broader involvement of the protease activity of MALT1 in CBM-dependent GPCR signaling. In contrast, signaling via the human EGFR2 (HER2), a receptor tyrosine kinase (RTK), has been proposed to depend mainly on the scaffold activity of MALT1 (18). It is possible that MALT1 cleaves a distinct subset of substrates in epithelial cells, or that MALT1 activation requires co-stimulation of the EGFR and another, yet to be identified co-receptor. A need for co-stimulation is observed in T cells, where optimal CBM complex assembly and activation of MALT1 protease activity requires the synergistic stimulation of both, the TCR and the costimulatory receptor CD28 (11, 12, 19, 20). Whether MALT1 protease activity is activated downstream of RTK merits further exploration.

MULTIPLE ELEMENTS CONTROL THE ASSEMBLY AND ARCHITECTURE OF THE CBM COMPLEX

A common feature of receptors that signal via MALT1 is their capacity to induce the formation of a specific type of CBM signaling complex. In resting cells, the members of the CBM complex reside in an inactive form in the cytoplasm. The catalytically inactive proenzyme MALT1 binds constitutively to BCL10, while the CARMA/CARD scaffold proteins are kept in a monomeric inactive form due to intramolecular inhibitory interactions. The inducible assembly of the CBM complex requires specific protein domains present in each CBM component (**Figure 2**). The CARD proteins CARMA1 (CARD11), CARMA2 (CARD14), and CARMA3 (CARD10)

Abbreviations: ABC, activated B-cell; AGTR1, angiotensin II receptor; ATLL, adult T-cell leukemia/lymphoma; BCL10, B-cell lymphoma-10; BCR, B-cell receptor; BENTA, B-cell expansion with NF-κB and T-cell anergy; CARD, caspase recruitment domain; CARMA, CARD-containing membrane-associated guanylate kinase; CBM, CARMA/CARD-BCL10-MALT1; CC, coil-coiled; CDE, constitutive decay element; CLL, chronic lymphocytic leukemia; CTCL, cutaneous T-cell lymphoma; DD death domain; DC, dentritic cells; DLBCL, diffuse large B-cell lymphoma; DUB, deubiquitinating enzyme; EGFR, epidermal growth factor receptor; FcR, Fc receptor; FLIP, Flice-like inhibitory protein; GPCR, G protein-coupled receptor; GUK, guanylate kinase; HER2, human EGFR-2; HOIL1, heme-oxidized IRP2 ubiquitin ligase 1; HOIP, HOIL1-interacting protein; HHV8, human herpes virus-8; Ig, Immunoglobulin; IPEX, immune dysregulation, polyendocrinopathy, enteropathy, X-linked; ITAM, immunoreceptor tyrosine-based activation motif; KSHV, Kaposi's sarcoma-associated herpes virus; LMP2A, latent membrane protein 2A; LUBAC, linear ubiquitin chain assembly complex; Mφ, macrophage; MAGUK, membrane-associated guanylate kinase; MALT, mucosa-associated lymphoid tissue; MC, myeloid cell; MCL, mantle cell lymphoma; mTORc1, mammalian target of rapamycin complex 1; MZ, marginal zone; nTreg, natural Treg; JNK, c-Jun N-terminal kinase; NF-κB, nuclear factor kappa B; NK, natural killer; OSCAR, osteoclast associated receptor; PDZ, PSD95 Dlg1 ZO-1; PEL, primary effusion lymphoma; PI, protease inactive; PKC, protein kinase C; PTCL, peripheral T-cell lymphoma; RTK, receptor tyrosine kinases; TCR, T cell receptor; TREM-1, triggering expression by myeloid cells 1; PTM, posttranslational modification; RA, rheumatoid arthritis; SH3, Src homology 3; SHARPIN, SHANK-associated RH domain interacting protein; UTR, untranslated region.

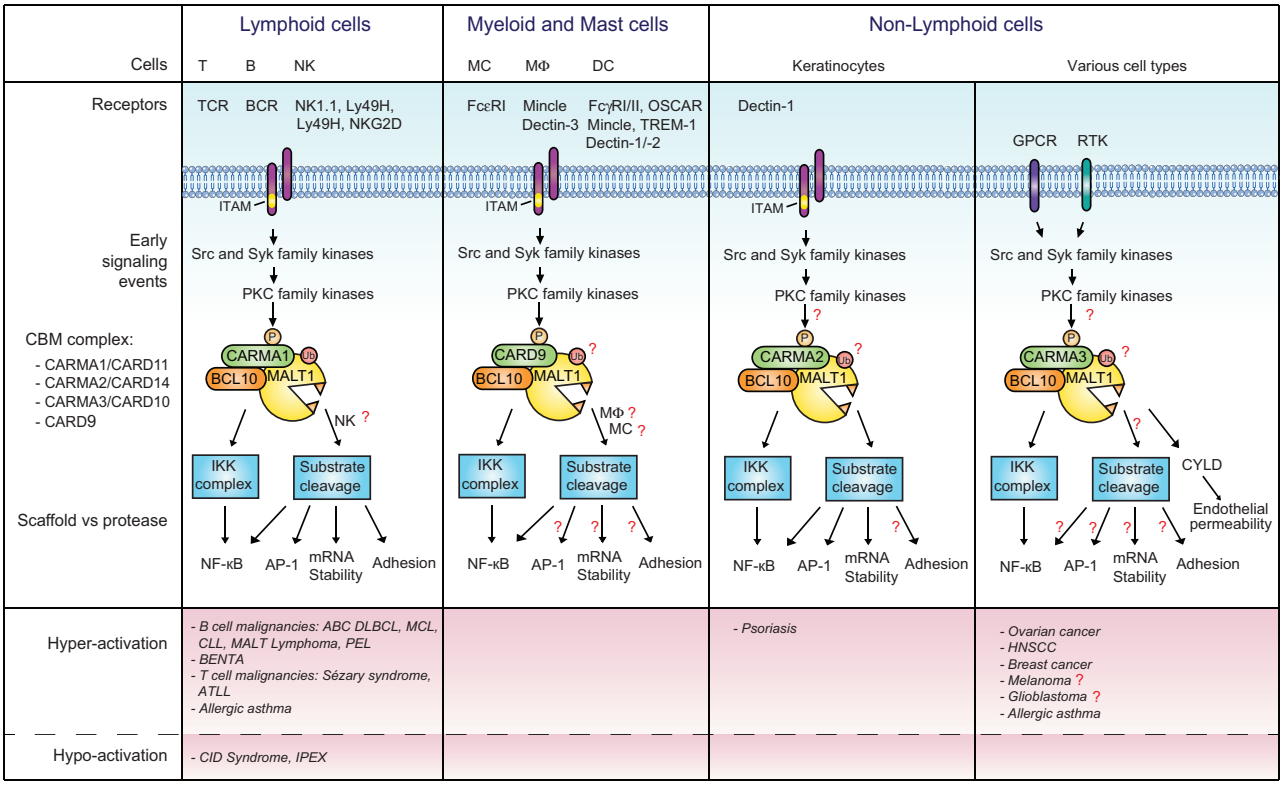

FIGURE 1 | Signaling via MALT1 downstream of various receptors and CARMA/CARD proteins. CBM complexes composed of MALT1, BCL10 and the indicated CARMA/CARD proteins are formed downstream of receptors containing immunoreceptor tyrosine-based activation motifs (ITAMs), G-protein-coupled receptors (GPCRs) or receptor tyrosine kinases (RTKs). Once formed, the CBM complex activates downstream signaling events via the scaffold and protease function of MALT1. The CBM complex of T and B cells is best characterized, while CBM complexes in other cellular contexts are less well studied. Open questions that remain to be addressed are annotated with a red question mark. Deregulated activation of the pathway results in different diseases, as summarized in the lower panel of the figure. BCR, B cell receptor; DC, dendritic cell; EGFR, epidermal growth factor receptor; FcR, Fc receptor; Mφ, macrophage; MC, myeloid cell; NK, natural killer; OSCAR, osteoclast associated receptor; PKC, protein kinase C; TCR, T cell receptor; TREM-1, triggering expression by myeloid cells 1; RA, rheumatoid arthritis.

are structurally similar. Each contains an N-terminal CARD, followed by a coil-coiled (CC) domain and a C-terminal region that shares features with proteins of the membrane-associated guanylate kinase (MAGUK) family, which contain a PDZ (PSD95, Dlg1, ZO-1), SH3 (Src homology 3), and GUK (guanylate kinase) domain. CARD9 contains a CARD and coiled-coil motif but lacks the C-terminal MAGUK features (21–25). An important structural feature of BCL10 is its N-terminal CARD that allows its inducible association with a CARMA/CARD component (21–25). Additionally, BCL10 contains a C-terminal region with a short sequence of amino acids (107-118) that is necessary for its constitutive interaction with MALT1 (21, 26). MALT1 contains an N-terminal death domain (DD) of unknown function, followed by two immunoglobulin (Ig)-like domains required for BCL10 binding, a caspase-like protease domain and a third Ig domain that plays a regulatory role for the protease function (27, 28) (**Figure 2**).

The inducible assembly of the CBM complexes seems to depend on a common, conserved mechanism that requires the receptor-induced activation of PKC family members (29, 30). These Ser/Thr kinases (and likely other kinases) phosphorylate the CARMA/CARD proteins in the linker region (**Figure 2**, illustrated here for CARMA1 (CARD11)) (29–31). This in turn is thought to weaken an inhibitory intra-molecular interaction between the CARD and linker domain, thereby promoting a CARD-mediated association with BCL10 and the formation of the CBM complex (29–31). Similar mechanisms are thought to control activation of CARMA3 (26), CARMA2 (15), and CARD9 (32), but whether PKC family members directly phosphorylate CARMA2 or CARMA3 is not known. CBM complex formation depends on homotypic CARD-CARD interactions between the CARMA/CARD proteins and BCL10 (21–23, 25, 26) and possibly on an additional interaction of the protease domain of MALT1 with the CC domain of CARD proteins as was demonstrated for CARMA1 (33). The CC region of CARMA1 has been shown to mediate oligomerization that is required for TCR-induced NF-κB activation (30, 34). Structural architecture studies and modeling suggest that the CC domain-mediated oligomerization of CARMA1 nucleates the oligomerization of BCL10 into helical filaments. BCL10 filaments are formed in a cooperative manner and stabilized through homotypic interactions formed between the CARD motifs of adjacent BCL10 monomers in the filament

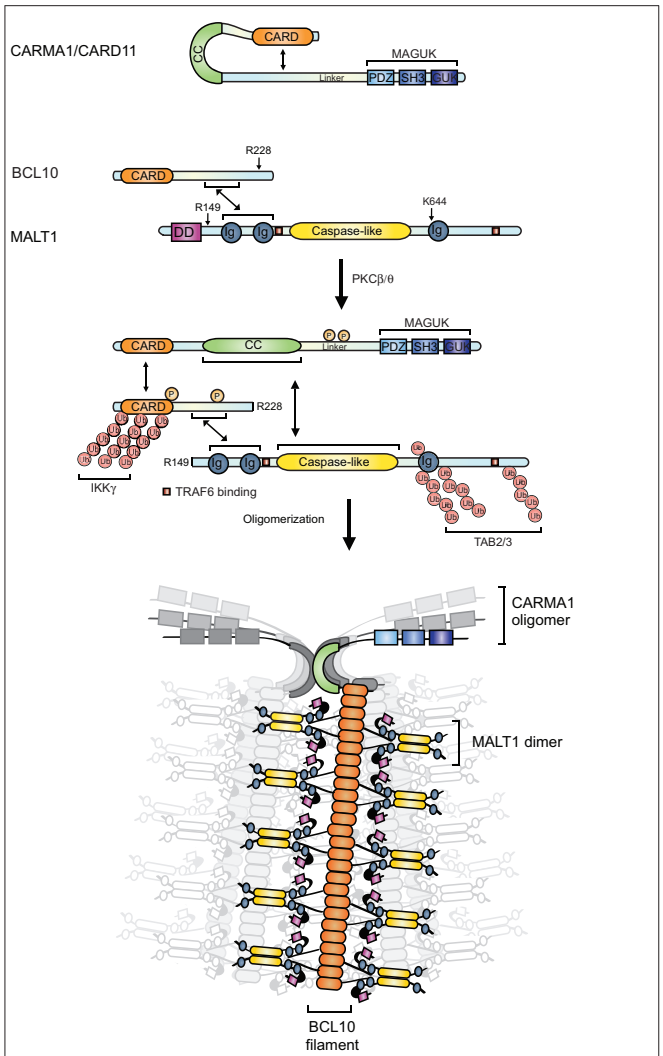

FIGURE 2 | Structure and function of the CBM complex. In resting conditions, MALT1 and BCL10 interact constitutively, while CARMA1 is dissociated from the other components of the CBM. PKC-mediated phosphorylation triggers a conformational opening and oligomerization of CARMA1, leading to the recruitment of preformed MALT1- BCL10 complexes. The E3 ligase TRAF6 is further recruited and polyubiquitinates MALT1 and BCL10. This favors the recruitment of the IKK and TAB2/3-TAK1 complexes and the downstream activation of NF-κB and AP-1. N-terminal phosphorylation of BCL10 by IKKβ enhances NF-κB activation, while a C-terminal phosphorylation disassembles MALT1 from BCL10. BCL10 can undergo both, linear polyubiquitination and K63-linked polyubiquitination, which are important for IKKγ/NEMO recruitment. Monoubiquitination activates MALT1 protease function. Once activated, MALT1 cleaves several substrates including BCL10 (after R228) and itself (after R149). The CBM signal is thought to be amplified by formation of filamentous BCL10 structures initiated by CARMA1 nucleation. BCL10 filaments are decorated with MALT1, most likely in its dimeric form. Double-headed arrows indicate interactions. Arrows indicate P, phosphorylations; Ub, ubiquitination.

(35). MALT1 is constitutively associated with BCL10, and therefore forms part of these filamentous structures (**Figures 2**,**3**) (35). Although not filamentous in nature, oligomeric signaling complexes containing proteins with CARD motifs, such as the apoptosome, inflammasome, and pyddosome, have been proposed to be key to the activation of proteases of the caspase family (36). Therefore, a prime purpose of the formation of BCL10-MALT1 filaments is likely to allow the oligomerization-dependent activation of MALT1. Crystallographic data from several groups support the idea that active MALT1 forms a dimer that is stabilized by interactions between the protease domain (37, 38). It is tempting to speculate that BCL10 filaments form a scaffold that permits additional interactions between MALT1 dimers leading to its proteolytic activation (**Figure 2**). MALT1 activation strictly requires monoubiquitination in its Ig3 domain that promotes its activation in an intra-or intermolecular manner (39). Exactly how this monoubiquitination contributes to MALT1 activation within the context of the oligomeric BCL10-MALT1 fibers remains unexplored. Although this has not yet been formally addressed, it is likely that similar oligomerization-dependent protein complexes control CBM-driven signaling for all CARMA/CARD proteins.

MALT1 FUNCTION IS DETERMINED BY ITS MULTIDOMAIN STRUCTURE

The *MALT1* gene was originally identified as the target of recurrent translocations in MALT lymphomas (40–42). Later on, *in silico* studies uncovered that MALT1 shares homology with caspases and metacaspases and therefore falls into a category of caspase-like proteases coined paracaspases (27, 43). The partial structure of the MALT1 caspase-like domain together with the third Ig domain has been recently solved and confirms the expected structural similarities between the protease domains of MALT1 and caspases (37, 38).

Apart from sharing structural homology, several other aspects of MALT1 function are shared with caspases, including cysteine-dependent protease activity (11, 12) a requirement for dimerization (38, 44), and the capacity to auto-process (45, 46). Like caspases, MALT1 contains a protease domain with a catalytic dyad comprising two amino acids that are essential for catalysis, namely C464 and H415 (27). Monomeric MALT1 is inactive and, as for caspases, requires dimerization via the caspase-like protease domain for enzymatic activity (38, 44, 47) (**Figure 3B**). Interestingly, MALT1 has been recently shown to undergo autoprocessing. However, unlike caspases, which autoprocess within the protease domain, MALT1 cleaves itself between the N-terminal death domain and the first Ig domain (45, 46). This does not seem to enhance proteolytic activity but is essential for MALT1-dependent NF-κB activation by a mechanism that is not yet understood (45, 46). In contrast to caspases, the proportion of cellular MALT1 undergoing autoprocessing is very small. It is unclear whether this reflects activation of only a very small proportion of cellular MALT1 or a subtler regulation of its activity, which needs to be investigated in more detail.

Despite the above-mentioned structural similarities between caspases and MALT1, several important differences exist. One major difference between caspases and MALT1 resides in their substrate specificity. While caspases are aspartic acid-specific proteases, MALT1 cleaves its substrates after arginine residues (11, 12, 47). The consensus cleavage site of MALT1 based on

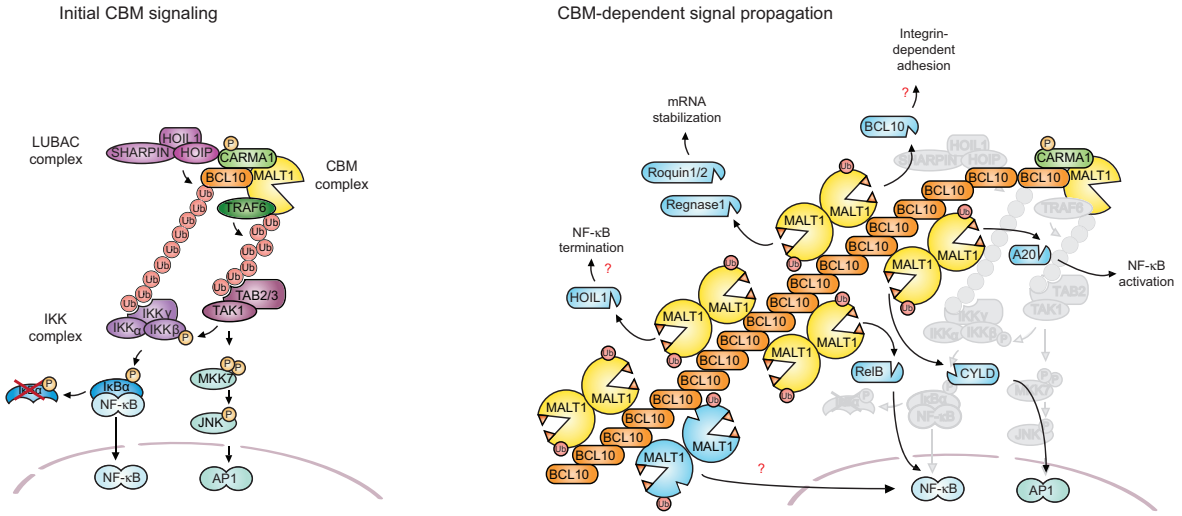

FIGURE 3 | MALT1 scaffold and protease functions. **(A)** Antigen receptor triggering leads to the formation of the CBM complex that acts as a recruiting platform for the ubiquitin ligase TRAF6 and the linear ubiquitin chain assembly complex (LUBAC). TRAF6-dependent K63-linked polyubiquitination promotes IKK complex activation by recruiting TAB2/3 together with TAK1 into proximity of the IKK complex. The TAB2/3-TAK1 complex also promotes AP-1 signaling through MKK7 and JNK activation. The CBM complex additionally recruits the LUBAC complex via a CARMA1-HOIP interaction. This is thought to support NF-κB signaling through linear ubiquitination of BCL10, which promotes the physical recruitment of IKKγ/NEMO. **(B)** Once CBM complex formation has initiated the early signaling events, the signal is most likely amplified and propagated by BCL10 oligomerization and filament formation, and through the protease function of MALT1. Filaments might support the protease function of MALT1 by promoting its dimerization and monoubiquitination. Filaments might also favor or control access of active MALT1 to cellular substrates. The protease activity of MALT1 controls NF-κB activation, AP-1 activation, mRNA stability, and cellular adhesion. This is mediated by the cleavage of the depicted substrates (depicted in blue, also for cleaved BCL10 and autoprocessed MALT1).

known substrates and screening of a tetrapeptide library, is a peptide sequence composed of an arginine at the P1 position, which is in most cases followed by a G or A residue. A hydrophobic residue is usually present at position P4, a rather variable range of amino acids is tolerated at P3 and a preference for serine or proline was found for position P2 (47). The consensus cleavage site could thus be summarized as follows: *Φ*-X-P/S-**R**'-G/A.

A second important difference between caspases and MALT1 concerns the regulation of MALT1 function, which is dependent on posttranslational modification (PTM) by ubiquitination. MALT1 is ubiquitinated, upon antigen receptor triggering, within the Ig3 domain and its C-terminal part by either K63-linked polyubiquitination or monoubquitination. MALT1 polyubiquitination mediated by TRAF6 is crucial for the activation and/or physical recruitment of the IKK complex, which phosphorylates the NF-*κ*B inhibitor I*κ*B to initiate its degradation and thus allows the nuclear translocation of NF-κB (4, 6, 7). This K63-linked polyubiquitination of MALT1 likely provides docking sites for the adaptor protein TAB2, which forms a complex with the IKK-activating kinase TAK1 (48). Additionally, the K63-linked ubiquitin chains may serve to physically recruit the IKK complex via its catalytically inactive IKKγ subunit (4, 49). MALT1 mono-ubiquitination on lysine residue 644 (K644), on the other hand, is required for the activation of MALT1 protease activity, most likely by favoring the formation of an active dimeric form of MALT (39).

A third aspect that differentiates MALT1 from caspases is the specific presence of additional protein domains that support its regulation and function. In the N-terminal part preceding the protease domain, MALT1 contains an N-terminal death domain (DD) followed by two Ig-like domains. The C-terminal part following the caspase-like domain contains a third Ig-like domain and a structurally undefined (most likely flexible) C-terminal extension (**Figure 2**). DDs can serve as protein-protein interaction domains in apoptotic signaling pathways. However, and despite its structural similarity with caspases, MALT1 does not induce apoptosis. This suggests that the MALT1 DD recruits another, yet to be identified, DD-containing protein unrelated to apoptosis. It is also possible that this domain plays an inhibitory role, since MALT1 autoprocessing, which removes the DD, is required for optimal NF-κB activation (45, 46). Additional unique features of MALT1 are the presence of three Ig domains that contribute to protein-protein interactions, and the presence of TRAF6 binding motifs. The first two Ig domains of MALT1 are necessary for the binding to BCL10 and are therefore crucial for its ability to induce CBM-mediated NF-κB activation upon engagement of the TCR (24). The region between the second Ig domain and the caspase-like domain contains a motif that is important for TRAF6 binding (4, 5), which is lacking in a recently described MALT1 splice variant (see below) (50) (**Figure 2**). Additional TRAF6 binding sites are present in the C-terminal extension, which are important for the downstream signaling event (4). The third, C-terminal Ig domain interacts physically with the protease domain and has

a particularly important role in MALT1 protease activity, which is regulated by mono-ubiquitination (**Figure 2**) (39). This and other posttranslational modifications of MALT1 and the CBM complex are important for downstream signaling events that will be discussed below.

THE CBM COMPLEX FORMS A SCAFFOLDING PLATFORM FOR PROTEIN RECRUITMENT

Once assembled, the CBM complex acts as a signaling platform for the recruitment of multiple signaling complexes, including TRAF6, the TAB1/2-TAK1 complex, the IKK complex, and the linear ubiquitin chain assembly complex (LUBAC) (51). These control various aspects of signal transmission that are essential for NF-κB and AP-1 activation.

The activation of NF-κB requires both the physical recruitment of the IKK complex and its activation by the Ser/Thr kinase TAK1. Recent data suggest an important role for both TRAF6 and the LUBAC complex in promoting IKK recruitment (4, 52). The LUBAC complex is composed of three subunits known as HOIL1 (heme-oxidized IRP2 ubiquitin ligase 1), HOIP (HOIL1-interacting protein; also known as RNF31), and SHARPIN (SHANK-associated RH domain interacting protein). The HOIP subunit has an E3 ligase activity, while HOIP and SHARPIN are important for LUBAC complex regulation, such as assuring its proper localization or stability (52, 53). The CBM complex can associate with the LUBAC complex in a transient manner in stimulated T cells, with kinetics that are similar to the association of LUBAC with the IKK complex (54). The stimulation-induced phosphorylation and conformational opening of CARMA1 is thought to lead to recruitment of both, BCL10 and HOIP (55). BCL10 thereby becomes accessible for HOIP-mediated linear ubiquitination on K17, K31, and K63 residues (55). The linear ubiquitination of BCL10 may promote NF-κB activation by providing docking sites for the physical recruitment of NEMO/IKKγ via its UBAN domain (55). However, alternative mechanisms may contribute to IKK recruitment, since another study showed a role for the LUBAC complex in optimal NF-κB activation that was independent of HOIP's ubiquitin ligase activity (54). Indeed, K31 and K63 on BCL10 can be subject to both linear or K63-linked polyubiquitination (7, 55) and the BCL10 modification by K63-linked ubiquitin chains may also contribute, although with lower affinity, to the physical recruitment of NEMO/IKKγ (7, 49, 56).

The CBM-associated E3 ubiquitin ligase responsible for synthesis of K63-linked ubiquitin chains is TRAF6, which associates with oligomeric BCL10-MALT1 complexes (4) and can be physically incorporated into the BCL10-MALT1 filaments in a cooperative manner (57). It has therefore been proposed that BCL10-MALT1 oligomers serve to activate TRAF6 to promote the ubiquitination-dependent activation of the IKK complex (4) (**Figure 3**). MALT1 is polyubiquitinated by TRAF6 on multiple sites preceding the protease domain and within the Ig3 domain (**Figure 2**). These polyubiquitination events are critical for NF-κB activation, since mutation of key amino acids important for TRAF6 binding to MALT1 impairs TCR-induced NF-κB activation (4, 5, 50). The TRAF6-mediated polyubiquitination of MALT1 and/or itself is thought to recruit the TAB2/3-TAK1 complex (4), since the adaptor proteins TAB2/3 contain ubiquitin-binding motifs that bind to K63 polyubiquitin chains (58). TAK1, which associates with TAB2/3, is thereby brought into proximity of the IKK complex to phosphorylate the IKKβ subunit. IKKβ phosphorylation activates the IKK complex, which phosphorylates the NF-κB inhibitor Iκ B, inducing its degradation to allow nuclear entry of NF-κB (4). In parallel, TAK1 contributes to AP-1 activation via the MKK7-JNK pathway (**Figure 3**) (59).

Interestingly, a recent study suggests a novel regulatory mechanism for MALT1-dependent TRAF6 recruitment by alternative splicing of MALT1 (50). In primary T cells, two MALT1 isoforms can be expressed, namely MALT1A or MALT1B, the latter of which lacks 11 amino acids encoded by exon 7 (50). These 11 amino acids encode for the first TRAF6 binding site, localized between the second Ig like domain and the paracaspase domain of MALT1 (5, 50) (**Figure 2**). Resting primary T cells express MALT1B, while MALT1A expression is induced upon TCR triggering (50). Therefore, TCR-induced expression of MALT1A likely reinforces the TRAF6-recruiting scaffolding function of the CBM complex (50).

Collectively, these findings support the notion that formation of the CBM complex has a key role in signal transmission as a protein recruitment scaffold.

THE CBM COMPLEX PROMOTES MALT1 PROTEOLYTIC ACTIVITY

The above-described steps of protein recruitment downstream of the CBM complex are most likely early signaling events that occur within the first minutes of lymphocyte stimulation, since peak Iκ B phosphorylation is detectable within a few minutes after antigen receptor engagement. The scaffolding function of MALT1 may then be amplified and propagated by its assembly with the BCL10 filamentous structures that are nucleated by CARMA1, as depicted in **Figures 2**, **3**. The activation of the MALT1 protease activity most likely depends on further amplification of the signal through filament formation, since optimal MALT1 activity is detectable later than IKK activation, and peaks roughly 30 min after antigen receptor engagement (11, 12, 19, 20). How exactly filament formation could contribute to MALT1 activation remains unknown. Interestingly, monoubiquitination on K644 within the Ig3 domain of MALT1 is required to license MALT1 protease activity (39). Indeed, a point mutation of K644 preventing monoubiquitination of MALT1 has strongly reduced protease activity and an impaired capacity to sustain IL-2 production in activated T cells (39). The incorporation of MALT1 into filaments might promote MALT1 activation in various ways, for example by allowing recruitment of the (unknown) ubiquitin ligase responsible for MALT1 monoubiquitination

and/or assuring physical proximity between MALT1 and its substrates (**Figure 3**).

MALT1 CLEAVES VARIOUS SUBSTRATES WITH DIVERSE BIOLOGICAL CONSEQUENCES

The last 10 years have witnessed impressive progress in the understanding of MALT1 protease function and its role in NF-κB- dependent and -independent aspects of lymphocyte activation. The best-explored function of MALT1 protease activity is its contribution to NF-κB activation. While MALT1 scaffold-dependent IKK activation promotes rapid but transient NF-κB activation, long-lasting NF-κB activation is assured by the MALT1-dependent cleavage of negative regulators of NF-κB, including RelB (10) and A20 (11), together with MALT1 autoprocessing (45, 46) (**Figure 3**). RelB plays a critical role as an inhibitor of the canonical NF-κB pathway in lymphocytes, by forming transcriptionally inactive complexes with RelA and c-Rel (10). MALT1-dependent RelB cleavage results in RelB proteasomal degradation, thereby favoring RelA-, and c-Rel-dependent NF-κB activation (10). MALT1-dependent cleavage of the deubiquitinating enzyme (DUB) A20, on the other hand, relieves its inhibitory role in NF-κB activation (11). How exactly A20 cleavage promotes NF-κB activation remains incompletely understood. It has been proposed that A20 negatively regulates the scaffolding function of MALT1 by removing the MALT1 polyubiquitination (60), however this function of A20 does not seem to be affected by its cleavage, since MALT1 inhibitors do not affect IKK-mediated NF-κB activation. A third cleavage event that is important for NF-κB activation is MALT1 autoprocessing (45, 46). MALT1 is autoprocessed after R149, between the N-terminal DD and the first Ig domain. This cleavage is essential for NF-κB activation downstream of its nuclear accumulation by mechanisms that are not yet elucidated (**Figure 2**) (45). Finally, NF-κB can be negatively regulated by the recently identified MALT1 substrate HOIL1, which is part of the LUBAC complex (61, 62). HOIL1 cleavage by MALT1 diminishes linear ubiquitination of cellular proteins, and has thus been proposed to provide negative feedback on the NF-κB pathway (61, 62).

Another important transcriptional pathway that is regulated by MALT1 is the JNK/AP-1 pathway. While the scaffold function of MALT1 is required for JNK activation (63), the protease activity of MALT1 provides an additional layer of control, via the cleavage of the deubiquinating enzyme (DUB) CYLD (64). CYLD cleavage is unlikely to affect JNK activation, since MALT1 knock-in mice showed no defect in inducible JNK phosphorylation (13, 14, 65, 66), Thus, CYLD cleavage regulates AP-1 through another mechanism that remains to be explored (**Figure 3**). Despite the described role of CYLD in the negative regulation of NF-κB and the fact that CYLD shares certain substrates with A20 (such as TRAF2, TRAF6, RIP1, and IKKγ) (67), CYLD cleavage is not implicated in TCR-dependent canonical NF-κB activation (64).

Several studies have identified additional NF-κB- and AP-1 independent roles for MALT1. One of these roles is the control of the stability of particular subsets of mRNA transcripts. The MALT1-dependent cleavage of the RNAse Regnase-1 (also known as MCPIP-1 or Zc3h12a) (68) and of the two RNA binding proteins Roquin-1 and Roquin-2 (69) has been shown to stabilize mRNAs by distinct mechanisms. Regnase-1 is an RNAse that cleaves stem loop structures in the 3′ untranslated region (UTR) of mRNAs, including the mRNAs of Regnase-1 itself, c-Rel, ICOS, OX40, IL-2, and IL6 (70). T cell specific Regnase-1 knockout mice developed spontaneous inflammation and premature death, demonstrating the crucial role of Regnase-1 in the regulation of mRNA stability during the adaptive immune response (68). Roquin-1 and Roquin-2 proteins bind to mRNAs via their ROQ domain, which recognizes a secondary RNA structure called constitutive decay element (CDE), and regulate gene expression at the posttranscriptional level (71). Roquin-1 and its paralog Roquin-2 are functionally interchangeable (72). To degrade mRNAs, Roquins recruit an mRNA deadenylase complex via their C-terminal part (71) and regulate the half-life of key cytokines, chemokines, and costimulatory proteins such as ICOS, OX40, and TNF (71, 73, 74). Similar to Regnase-1 deficient mice, Roquin mutant mice (expressing a Roquin mutant that cannot bind CDEs), develop autoimmunity (73). Regnase-1 and Roquins regulate mRNA decay of common and Regnase-1- or Roquin-specific mRNAs. During T cell triggering, the combined mRNAse activity of Regnase-1 and the mRNA decay activity of Roquins are overcome by their MALT1-dependent cleavage and degradation (**Figure 3**) (68, 69).

Finally, the protease activity of MALT1 also regulates transcription-independent cellular functions by the cleavage of BCL10, which promotes lymphocyte adhesion through β1 integrins (11, 12, 19, 20). MALT1-mediated BCL10 cleavage removes 5 amino acids from its C-terminus (11, 12, 19, 20). This cleavage is not required for antigen-dependent NF-κB activation but is important for integrin-mediated T-cell adhesion (11, 12, 19, 20). The molecular mechanisms controlling adhesion via BCL10 remain elusive (**Figures 2**, **3**).

Thus far, 8 different substrates of MALT1 have been functionally described in activated lymphocytes, and two additional substrates (NIK and LIMA1) have been reported as specific substrates of an oncogenic cIAP2-MALT1 fusion protein specifically expressed in MALT lymphoma (75, 76). We can therefore reasonably anticipate that MALT1 has additional substrates with functions that are much wider than anticipated. For example, MALT1 protease function has been suggested to play a key role in metabolic pathways (77). Glutamine uptake is rapidly initiated upon naive T cell activation via the amino acid transporter ASCT2 and this uptake is crucial for activation of the mammalian target of rapamycin complex 1 (mTORc1). Interestingly, both glutamine uptake and mTORc1 activation required proteins of the CBM complex and MALT1 protease activity (77). This suggests a novel role for the MALT1 protease function in the regulation of glutamine uptake via the regulation of mTORc1 and/or ASCT2 (77). Whether this regulation is mediated by one of the already described substrates of MALT1, or whether a yet unidentified MALT1 substrate can modulate the mTORc1 signaling pathway remains to be explored.

MICE LACKING MALT1 EXPRESSION OR ACTIVITY HAVE DISTINCT IMMUNOLOGICAL PHENOTYPES

The protease activity and most of the substrates of MALT1 have been initially identified and characterized in cell lines. However, recent studies using mouse models have lent strong support to the physiological relevance of MALT1 protease activity in adaptive immunity. MALT1-deficient mice show impaired B- and T-cell responses together with defects in the development of particular lymphocyte subsets such as marginal zone (MZ) and B1 B cells (63, 78). Moreover, these mice are resistant to experimental induction of experimental autoimmune encephalitis, a mouse model of multiple sclerosis (79, 80). Mice expressing a catalytically inactive mutant of MALT1 [C472A knock-in mice, subsequently called MALT1-protease inactive (PI) mice] recapitulate these aspects of the immunodeficiency phenotype of the MALT1 knockout mice to a large extent. Lymphocytes isolated from the MALT1-PI mice also revealed defects in NF-κB activation, AP-1 activation, mRNA stability and lymphocyte adhesion that are all consistent with previous studies from cell lines (13, 14, 65, 66, 81). Despite these impaired responses, the lymphocytes isolated from MALT1-PI mice showed normal antigen receptor-mediated activation of IKK or JNK (63, 78). The impaired cellular responses and the associated immunodeficiency phenotype of the MALT1-PI mice results thus principally from the inactivation of the proteolytic activity of MALT1.

In addition to defects in T- and B-cell responses, MALT1-deficient mice have impaired myeloid and mast cell responses upon Fc-receptor stimulation, reduced NK cell responses and defective innate immunity to yeast infections (63, 78, 82–84). The cellular responses of myeloid and NK cells have also been assessed in MALT1-PI mice and found to be defective.

A surprising finding of all four studies reporting MALT1-PI mice, however, is that these mice develop autoimmune symptoms, in particular a severe autoimmune gastritis of early onset, which progresses with age (13, 65, 66). The observed autoimmunity is likely the result of reduced development of natural Treg (nTreg) cells in MALT1-PI mice (13, 65, 66). Indeed, the autoimmune phenotype of MALT-PI mice can be rescued through transfer of wildtype Tregs into newborn MALT1-PI animals (13, 65). An even stronger reduction of nTregs is found in MALT1-deficient mice (13, 65, 66). However, MALT1-deficient mice show no autoimmune pathology, most likely because their lymphocyte responses are more dramatically affected (13, 14, 63, 65, 66). The reduced Treg numbers are likely caused by the absence of MALT1 function during development, since no spontaneous autoimmunity develops in adult mice treated with small molecule MALT1 inhibitors for up to 17 days (85). Indeed, young MALT1-PI mice do not show autoimmune features and are completely resistant to induction of experimental autoimmune encephalitis (13, 65). While the contribution of individual MALT1 substrate(s) to nTreg development remains largely unknown, a recent study suggests that MALT1 autoprocessing is important for nTreg development (46). Indeed, mice expressing an autoprocessing-resistant mutant of MALT1 have a partial Treg deficit that results in enhanced anti-tumor immunity without causing autoimmunity (46).

Mice deficient for the individual CARMA/CARD family members have additional phenotypic features, including a defect in innate immune responses against bacteria, fungi or viruses in CARD9 KO mice (82, 86, 87) and a specific defect in NF-κB signaling upon stimulation of GPCRs in CARMA3-deficient mice (88). Whether these phenotypes depend on MALT1 protease activity remains largely unexplored. In addition, roughly half of CARMA3- and one third of BCL10-deficient mice die prematurely due to a neuronal tube defect, suggesting a common role for CARMA3 and BCL10 in embryonic development (88, 89). This defect is neither present in MALT1-deficient nor in MALT-PI mice and therefore likely depends on MALT1-independent signaling features of CARMA3 and BCL10. CARMA2/CARD14-deficient mice have been recently generated and found to be resistant to psoriasis induction by imiquimod cream or recombinant IL-23 injection (90). The individual contributions of keratinocytes and γδ T cells to the CARMA2/CARD14 dependent-inflammation and the extent to which MALT1 protease activity contributes to inflammatory skin reactions remain to be further investigated.

MALT1 DEREGULATION IS ASSOCIATED WITH IMMUNODEFICIENCY AND LYMPHOMA

A deregulation of MALT1 function is associated with the development of various diseases. Patients with inactivating MALT1 mutations develop immunodeficiency (91–93) or immune dysregulation, polyendocrinopathy, enteropathy, and X-linked (IPEX)-like syndrome (94). Patients with an oncogenic activation of the MALT1 signaling pathway, on the other hand, develop lymphoid malignancies or lymphoproliferative disease (**Figures 1**,**4**) (95, 96). An increasing number of T and B cell malignancies are now recognized to be driven by constitutive antigen receptor signaling as a result of foreign or self-antigen recognition (97) and/or gain-of function mutations (**Figures 4A,B**) that trigger CBM complex formation and downstream signaling (95, 98–104). Such mutations can be found in the CBM component CARMA1 itself (98) or in the upstream components of the pathway, including the B-cell receptor-associated CD79 chains (103), the T-cell coreceptor CD28, PLCγ1 and PKCβ (95). Lymphomas with such mutations include the activated B-cell (ABC) subtype of diffuse large B-cell lymphoma (DLBCL) (98, 99, 103, 105, 106), in which chronic active BCR signaling is often combined with oncogenic activation of the TLR signaling component MyD88 (107). Constitutive CBM-dependent signaling is also found in mantle cell lymphomas (MCL) (104, 108, 109), chronic lymphocytic leukemia (CLL) (110), acute T-cell leukemia/lymphoma (ATLL) (102), cutaneous T-cell lymphoma (CTCL) and Sézary

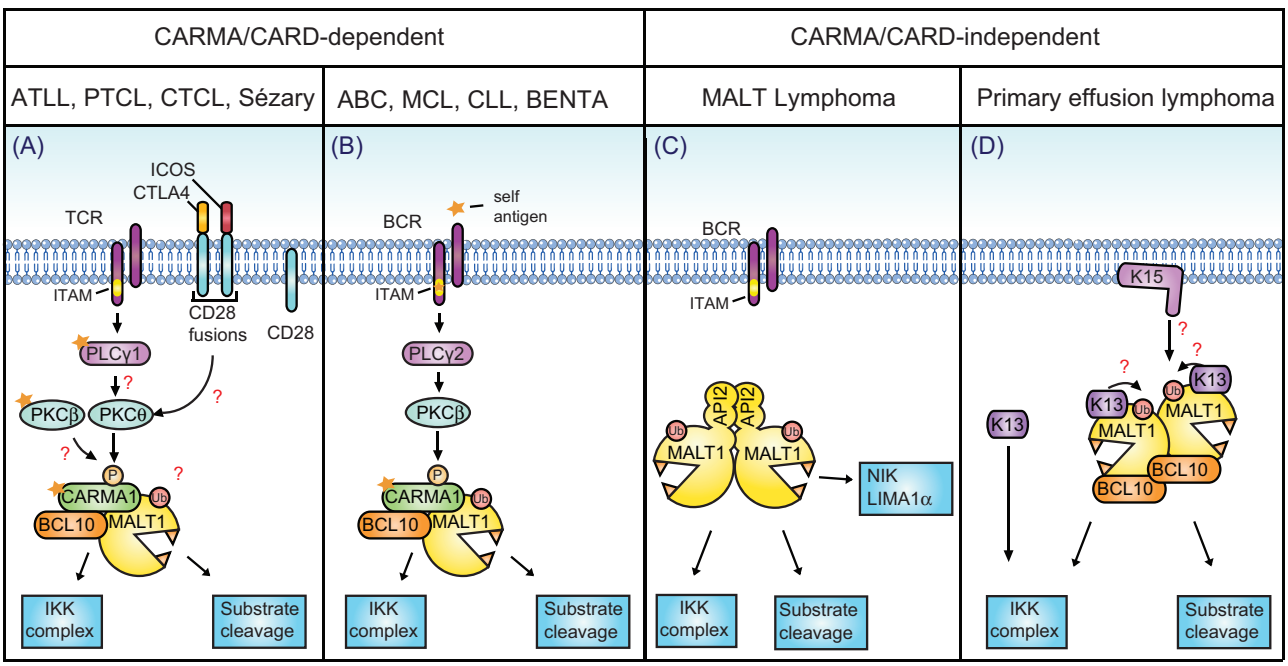

FIGURE 4 | CARMA/CARD-dependent and-independent MALT1 activation. **(A)** In the depicted T cell malignancies, gain-of-function mutations in CARMA1 or its upstream regulators or in-frame gene fusions of the T-cell co-receptor CD28 with ICOS or CTLA-4 are thought to promote MALT1 constitutive activation. **(B)** In the indicated B-cell lymphomas constitutive MALT1 protease activity can be driven by oncogenic mutations in CARMA1, CD79A or CD79B, which may be relevant in combination with self-antigen recognition. A subset of MCL and CLL are also addicted to this pathway by unknown mechanisms. **(C)** A large proportion of MALT lymphoma harbors a chromosomal translocation leading to formation of an oncogenic MALT1-API2 fusion protein. **(D)** In primary effusion lymphoma (PEL), NF-κB is activated through viral latency proteins such as K13 and K15, which activate NF-κB directly or via MALT1-BCL10. **(A,B)**, mutations and self-antigen are depicted with a yellow star. **(A,D)** Open questions are depicted with red question marks. PTCL, peripheral T-cell lymphoma; ATLL adult T-cell leukemia/lymphoma; ABC, activated B-cell subtype; DLBCL, diffuse large B-cell lymphoma; BENTA, B-cell expansion with NF-κB and T-cell anergy; MCL, mantle cell lymphoma; CLL, chronic lymphocytic/leukemia.

syndrome (100, 101), as well as peripheral T-cell lymphomas (PTCL) (111) (**Figures 4A,B**). The relevance of the CBM complex and MALT1 protease activity were formally shown by silencing of the individual CBM components in ABC DLBCL (112, 113) and MCL (104) cell lines, or by inhibition of MALT1 proteolytic function in ABC DLBCL (113, 114), MCL (104), and CLL (110) cell lines. Interestingly, gain of function mutations of CARMA1 were also reported in patients with a congenital lymphoproliferative disease known as BENTA (B-cell expansion with NF-κB and T-cell anergy) syndrome (115–117) (**Figures 4A,B**).

In some types of lymphomas, constitutive MALT1 activation is achieved by mechanisms that bypass the classical CBM signaling events. These include chromosomal translocations involving the MALT1 or BCL10 genes, which are found in MALT lymphomas (1). Such translocations can lead to overexpression of the BCL10 or MALT1 genes or, more frequently, to the generation of an oncogenic API2-MALT1 fusion protein. This fusion protein activates the classical (canonical) and alternative (non-canonical) NF-κB pathways through its scaffold and protease function thereby bypassing the BCR-dependent upstream signaling events (1). The API2-MALT1 fusion protein has constitutive protease activity and cleaves NIK (76) and LIMA1α (75), two non-canonical MALT1 substrates recruited by the cIAP2 moiety (**Figure 4C**). NIK cleavage leads to stabilization of NIK, which promotes activation of the non-canonical NF-κB pathway by phosphorylation and proteolytic maturation of the NF-κB2 precursor p100 into a mature p52 NF-κB2 subunit (76). Cleavage of LIMA1α disrupts the tumor suppressor function of this protein and promotes B cell proliferation and adhesion via the cleavage of its Lim domain, an LMO-like oncogenic protein (75) (**Figure 4C**). The cleavage of NIK and LIMA1α seems to be a specific oncogenic feature of the cIAP2-MALT1 fusion protein since it is not known to be triggered by antigen receptor-mediated MALT1 activation.

Recently, we have uncovered a role for MALT1 protease activity in the development of primary effusion lymphoma (PEL) (118). PEL is a lymphoid tumor triggered by Kaposi's sarcoma herpes virus (KSHV), an oncogenic virus also known as human herpes virus-8 (HHV8). KSHV-derived tumors derive from latently infected B cells that are characterized by constitutive NF-κB activation, which suppress the lytic program of the virus. The latency program is controlled by different viral latency genes such as K13 and K15, encoding a viral FLIP (Flice-like inhibitory protein) homolog and a membrane protein

homologous to the latent membrane protein 2A (LMP2A), respectively. K13 and K15 induce constitutive activation of NF-κB via the protease and scaffold activity of MALT1 (118) (**Figure 4D**). Pharmacological inhibition or silencing of MALT1 leads to the reactivation of the viral lytic program and induces cell death of PEL cell lines *in vitro*. MALT1 inhibitors also efficiently block the development of PELs and induce their regression *in vivo,* in a xenograft model (118). Interestingly, K13 and K15 contribute to MALT1 activation in a CARMA1-independent manner (**Figure 4D**). Whether K13 and K15 mediate MALT1 activation via other CARMA/CARD proteins, or in an entirely distinct manner, remains to be explored.

MALT1 DEREGULATION IS ASSOCIATED WITH ALLERGY, INFLAMMATORY SKIN DISEASES AND CARCINOMA

Deregulations of MALT1 function are not restricted to the above-described lymphoid pathologies but may also play wider roles in allergies, psoriasis, and various non-lymphoid cancers (**Figure 1**).

Evidence for a potential contribution of MALT1 to allergic asthma comes from two studies showing that CARMA1 is important in mouse models of allergic asthma (119, 120). CARMA3 has also been shown to play an important role in allergic airway inflammation in mice (121). The exact upstream events triggering CBM activation in these models remain undefined.

CARMA2/CARD14-mediated activation of MALT1 has been shown to play a major role in the activation of human keratinocytes upon exposure to the yeast cell wall component zymosan or *S. aureus* (15). Interestingly, activating mutations in the CARMA2-encoding gene CARD14 have been found to be associated with development of psoriasis, an inflammatory skin disease, in human patients (122, 123). Since then, an increasing number of studies have reported genetic mutations in CARD14 associated to psoriasis diseases (124). Some of the CARD14 mutations found in patients were shown to enhance NF-κB activation and promote secretion of CCL20 and IL-8, two chemokines known to be associated with psoriasis (123, 124). Similar to CARD11 mutations associated with lymphoid malignancies, CARD14 mutations were mostly found in the CC region. This suggests a similar mechanism of activation, via induction of an active CARD14 conformation and oligomerization necessary for CBM complex formation and downstream signaling events. In support of this model, a recent study showed that a single point mutation in CARD14 E138A, which renders CARD14 hyperactive, was sufficient to drive spontaneous psoriasis disease in mice (125). Inhibition of MALT1 protease activity effectively reduces cytokine and chemokine expression induced by overexpression of this hyperactive CARD14 mutant in human primary keratinocytes (126). Therefore, topical application of MALT1 inhibitors may be a future treatment option for psoriasis patients.

Finally, an increasing number of publications support a role for aberrant MALT1 signaling in the development of non-lymphoid cancers, such as glioblastoma (127), breast cancer (18, 128, 129), melanoma (130), lung cancer (18), and various other carcinomas (1, 131, 132). In these cancers, MALT1 seems to be activated by constitutive signaling from GPCRs or the EGFR via CARMA3 and/or by overexpression of MALT1 through various mechanisms.

For breast cancer, two different subtypes, which are HER2 or angiotensin II receptor (AGTR1) positive, have been described to be addicted to CBM signaling via CARMA3 (18, 128, 129). Interestingly, these two subsets show abnormal expressions of AGTR1 or HER2 in a mutually exclusive manner (128). In AGTR1 and HER2 positive breast cancer cell lines, NF-κB is activated upon stimulation with Angiotensin II or the HER2 ligand heregulin, respectively, in a CARMA3-dependent manner (18, 128, 129). Silencing of CBM components abrogates tumor cell growth, migration, and invasion (18, 128, 129) and affects the tumor microenvironment, since endothelial cell chemotaxis and angiogenesis are abolished (128). AGTR1-positive breast cancers represent 15–20% of all breast cancers (128) and HER2 positive breast cancers form 20–25% of all breast cancers (18, 128, 129, 133). It remains possible that other breast cancer subtypes depend on constitutive signaling by other GPCRs that can trigger NF-κB signaling via CARMA3 (134). In addition to its relevance in breast cancer, CARMA3 has been shown to play a role in lung cancer (18). In this context, EGFR signaling via CARMA3, BCL10, and MALT1 promotes tumorigenesis through effects on NF-κB activation, cell proliferation, migration and invasion. The relevance of the proteolytic activity of MALT1 was not formally assessed in the above-cited models of breast cancer (128) and lung cancer (18). It would thus be interesting to test the potential effectiveness of pharmacological MALT1 inhibitors in these models.

The relevance of MALT1 as a protooncogene has been recently extended to additional malignancies including melanoma (130) and glioblastoma (127), in which MALT1 can be overexpressed. Indeed, MALT1 is highly expressed in a subset of melanoma associated with poor prognosis (130). MALT1 downregulation or inhibition with the MALT1 inhibitor MI-2 (135), diminishes the growth and the dissemination of melanoma cells in the lung (130). While the proliferation of these melanoma cells is NF-κB dependent, the dissemination is JNK/c-Jun-dependent (130). In glioblastoma, it was shown that a subset of tumors with poor outcome expresses low levels of the microRNA miR181d, leading to high NF-κB activation. One of the targets of miR181d is MALT1, which is highly expressed in the miR181d-low tumors (127). Ectopic expression of miR181d and the consequent downregulation of MALT1 suppresses growth of tumor cells (127). These two studies suggest that, like in a subset of MALT lymphomas (136), MALT1 overexpression *per se* may play a role in promoting carcinogenesis, potentially by spontaneous aggregation-mediated activation of MALT1. Future studies should address how MALT1 promotes cellular transformation in various cancers, whether and how specific substrates of MALT1 contribute to tumorigenesis and if MALT1 inhibitors might be of therapeutic interest.

MALT1 INHIBITORS MAY BE OF THERAPEUTIC INTEREST FOR VARIOUS PATHOLOGIES

Several recent studies have reported the development of small molecule MALT1 inhibitors that act as active site or allosteric inhibitors (135, 137–140). These have therapeutic effects in preclinical (mouse) models of diffuse large B-cell lymphoma, (135, 137, 138) and primary effusion lymphoma (118). The idea that MALT1 inhibitors may be useful to dampen inflammatory immune responses has received support from studies using a mouse model of multiple sclerosis, in which paralysis symptoms are alleviated by treatment with a MALT1 inhibitor, or by genetic inactivation of MALT1 (13, 65, 85). The latter also protects mice from experimental induction of colitis (13). Moreover, pharmacological inhibition of MALT1 protects mice from LPS-induced inflammation and lung injury, most likely through inhibitory effects on myeloid cells (141). Nevertheless, the assumption that MALT1 inhibitors will generally dampen immune responses has been challenged by the observation that mice expressing a catalytically inactive form of MALT1 have reduced numbers of natural Treg cells and, as a consequence, progressively develop inflammatory autoimmune disease (13, 14, 65, 66). This raises the interesting possibility that, at least in the context of cancer, MALT1 inhibitors may exert their effects by a dual action on both the inhibition of the growth of cancer cells and boosting anti-tumor immune responses. Another possible field of application for MALT1 inhibitors are inflammatory skin diseases such as psoriasis, in which inhibitory effects on keratinocytes and possibly on skin T cells may benefit the patients (15, 124–126). As we progress in our knowledge about the molecular and biological function of MALT1, future applications are likely to emerge.

AUTHOR CONTRIBUTIONS

All authors listed have made a substantial, direct and intellectual contribution to the work, and approved it for publication.

FUNDING

The Thome laboratory is supported by grants from the Swiss National Science Foundation (310030_166627), the Swiss Cancer League (KFS-4095-02-2017) and the Emma Muschamp Foundation.

ACKNOWLEDGMENTS

The authors would like to acknowledge Colin Moore, Laurence Romy, and Julie Vérièpe for comments on the manuscript and Slavica Masina for proofreading.

REFERENCES

1. Rosebeck S, Rehman AO, Lucas PC, McAllister-Lucas LM. From MALT lymphoma to the CBM signalosome: three decades of discovery. *Cell Cycle* (2011) 10:2485–96. doi: 10.4161/cc.10.15.16923
2. Getahun A, Cambier JC. Of ITIMs, ITAMs, and ITAMis: revisiting immunoglobulin Fc receptor signaling. *Immunol Rev.* (2015) 268:66–73. doi: 10.1111/imr.12336
3. Brown GD, Willment JA, Whitehead L. C-type lectins in immunity and homeostasis. *Nat Rev Immunol.* (2018) 18:374–389. doi: 10.1038/s41577-018-0004-8
4. Sun L, Deng L, Ea CK, Xia ZP, Chen ZJ. The TRAF6 ubiquitin ligase and TAK1 kinase mediate IKK activation by BCL10 and MALT1 in T lymphocytes. *Mol Cell* (2004) 14:289–301. doi: 10.1016/S1097-2765(04)00236-9
5. Noels H, van Loo G, Hagens S, Broeckx V, Beyaert R, Marynen P, et al. A novel TRAF6 binding site in MALT1 defines distinct mechanisms of NF-kappaB activation by API2middle dotMALT1 fusions. *J Biol Chem*. (2007) 282:10180–9. doi: 10.1074/jbc.M611038200
6. Oeckinghaus A, Wegener E, Welteke V, Ferch U, Arslan SC, Ruland J, et al. Malt1 ubiquitination triggers NF-kappaB signaling upon T-cell activation. *EMBO J*. (2007) 26:4634–45. doi: 10.1038/sj.emboj.7601897
7. Wu CJ, Ashwell JD. NEMO recognition of ubiquitinated Bcl10 is required for T cell receptor-mediated NF-kappaB activation. *Proc Natl Acad Sci USA*. (2008) 105:3023–8. doi: 10.1073/pnas.0712313105
8. Mercurio F, Zhu H, Murray BW, Shevchenko A, Bennett BL, Li J, et al. IKK-1 and IKK-2: cytokine-activated IkappaB kinases essential for NF-kappaB activation. *Science* (1997) 278:860–6. doi: 10.1126/science.278.5339.860
9. DiDonato JA, Hayakawa M, Rothwarf DM, Zandi E, Karin M. A cytokine-responsive IkappaB kinase that activates the transcription factor NF-kappa. *Nature* (1997) 388:548–54.
10. Hailfinger S, Nogai H, Pelzer C, Jaworski M, Cabalzar K, Charton JE, et al. Malt1-dependent RelB cleavage promotes canonical NF-kappaB activation in lymphocytes and lymphoma cell lines. *Proc Natl Acad Sci USA*. (2011) 108:14596–601. doi: 10.1073/pnas.1105020108
11. Coornaert B, Baens M, Heyninck K, Bekaert T, Haegman M, Staal J, et al. T cell antigen receptor stimulation induces MALT1 paracaspase-mediated cleavage of the NF-kappaB inhibitor A20. *Nat. Immunol.* (2008) 9:263–71. doi: 10.1038/ni1561
12. Rebeaud F, Hailfinger S, Posevitz-Fejfar A, Tapernoux M, Moser R, Rueda D, et al. The proteolytic activity of the paracaspase MALT1 is key in T cell activation. *Nat Immunol.* (2008) 9:272–81. doi: 10.1038/ni1568
13. Jaworski M, Marsland BJ, Gehrig J, Held W, Favre S, Luther SA, Perroud M, et al. Malt1 protease inactivation efficiently dampens immune responses but causes spontaneous autoimmunity. *EMBO J*. (2014) 33:2765–81. doi: 10.15252/embj.201488987
14. Yu JW, Hoffman S, Beal AM, Dykon A, Ringenberg MA, Hughes AC, et al. MALT1 protease activity is required for innate and adaptive immune responses. *PLoS One* (2015) 10:e0127083. doi: 10.1371/journal.pone.0127083
15. Schmitt A, Grondona P, Maier T, Brandle M, Schonfeld C, Jager G, et al. MALT1 protease activity controls the expression of inflammatory genes in keratinocytes upon zymosan stimulation. *J Invest Dermatol.* (2016) 136:788–97. doi: 10.1016/j.jid.2015.12.027
16. Klei LR, Hu D, Panek R, Alfano DN, Bridwell RE, Bailey KM, et al. MALT1 protease activation triggers acute disruption of endothelial barrier integrity via CYLD cleavage. *Cell Rep.* (2016) 17:221–32. doi: 10.1016/j.celrep.2016.08.080
17. Delekta PC, Apel IJ, Gu S, Siu K, Hattori Y, McAllister-Lucas LM, et al. Thrombin-dependent NF-{kappa}B activation and monocyte/endothelial adhesion are mediated by the CARMA3.Bcl10.MALT1 signalosome. *J Biol Chem.* (2010) 285:41432–42. doi: 10.1074/jbc.M110.158949
18. Pan D, Jiang C, Ma Z, Blonska M, You MJ, Lin X. MALT1 is required for EGFR-induced NF-kappaB activation and contributes to EGFR-driven lung cancer progression. *Oncogene* (2016) 35:919–28. doi: 10.1038/onc.2015.146

19. Gaide O, Favier B, Legler DF, Bonnet D, Brissoni B, Valitutti S, et al. CARMA1 is a critical lipid raft-associated regulator of TCR-induced NF-kappa B activation. *Nat Immunol.* (2002) 3:836–43. doi: 10.1038/ni830
20. Wang D, You Y, Case SM, McAllister-Lucas LM, Wang L, DiStefano PS, et al. A requirement for CARMA1 in TCR-induced NF-kappa B activation. *Nat Immunol.* (2002) 3:830–5. doi: 10.1038/ni824
21. Gaide O, Martinon F, Micheau O, Bonnet D, Thome M, Tschopp J. Carma1, a CARD-containing binding partner of Bcl10, induces Bcl10 phosphorylation and NF-kappaB activation. *FEBS Lett.* (2001) 496:121–7. doi: 10.1016/S0014-5793(01)02414-0
22. Bertin J, Guo Y, Wang L, Srinivasula SM, Jacobson MD, Poyet JL, et al. CARD9 is a novel caspase recruitment domain-containing protein that interacts with BCL10/CLAP and activates NF-kappa B. *J Biol Chem.* (2000) 275:41082–6. doi: 10.1074/jbc.C000726200
23. Bertin J, Wang L, Guo Y, Jacobson MD, Poyet JL, Srinivasula SM, et al. CARD11 and CARD14 are novel caspase recruitment domain (CARD)/membrane-associated guanylate kinase (MAGUK) family members that interact with BCL10 and activate NF-kappa B. *J Biol Chem.* (2001) 276:11877–82. doi: 10.1074/jbc.M010512200
24. Lucas PC, Yonezumi M, Inohara N, McAllister-Lucas LM, Abazeed ME, Chen FF, et al. Bcl10 and MALT1, independent targets of chromosomal translocation in malt lymphoma, cooperate in a novel NF-kappa B signaling pathway. *J Biol Chem.* (2001) 276:19012–9. doi: 10.1074/jbc.M009984200
25. Wang L, Guo Y, Huang WJ, Ke X, Poyet JL, Manji GA, et al. Card10 is a novel caspase recruitment domain/membrane-associated guanylate kinase family member that interacts with BCL10 and activates NF-kappa B. *J Biol Chem.* (2001) 276:21405–9. doi: 10.1074/jbc.M102488200
26. McAllister-Lucas LM, Inohara N, Lucas PC, Ruland J, Benito A, Li Q, et al. Bimp1, a MAGUK family member linking protein kinase C activation to Bcl10-mediated NF-kappaB induction. *J Biol Chem.* (2001) 276:30589–97. doi: 10.1074/jbc.M103824200
27. Uren AG, O'Rourke K, Aravind LA, Pisabarro MT, Seshagiri S, Koonin EV, et al. Identification of paracaspases and metacaspases: two ancient families of caspase-like proteins, one of which plays a key role in MALT lymphoma. *Mol Cell* (2000) 6:961–7. doi: 10.1016/S1097-2765(00)00094-0
28. Zhou H, Du MQ, Dixit VM. Constitutive NF-kappaB activation by the t(11;18)(q21;q21) product in MALT lymphoma is linked to deregulated ubiquitin ligase activity. *Cancer Cell* (2005) 7:425–31. doi: 10.1016/j.ccr.2005.04.012
29. Sommer K, Guo B, Pomerantz JL, Bandaranayake AD, Moreno-García ME, Ovechkina YL, et al. Phosphorylation of the CARMA1 linker controls NF-kappaB activation. *Immunity* (2005) 23:561–74. doi: 10.1016/j.immuni.2005.09.014
30. Matsumoto R, Wang D, Blonska M, Li H, Kobayashi M, Pappu B, et al. Phosphorylation of CARMA1 plays a critical role in T Cell receptor-mediated NF-kappaB activation. *Immunity* (2005) 23:575–85. doi: 10.1016/j.immuni.2005.10.007
31. Rueda D, Thome M. Phosphorylation of CARMA1: the link(er) to NF-kappaB activation. *Immunity* (2005) 23:551–3. doi: 10.1016/j.immuni.2005.11.007
32. Strasser D, Neumann K, Bergmann H, Marakalala MJ, Guler R, Rojowska A, et al. Syk kinase-coupled C-type lectin receptors engage protein kinase C-sigma to elicit Card9 adaptor-mediated innate immunity. *Immunity* (2012) 36:32–42. doi: 10.1016/j.immuni.2011.11.015
33. Che T, You Y, Wang D, Tanner MJ, Dixit VM, Lin X. MALT1/paracaspase is a signaling component downstream of CARMA1 and mediates T cell receptor-induced NF-kappaB activation. *J Biol Chem.* (2004) 279:15870–6. doi: 10.1074/jbc.M310599200
34. Tanner MJ, Hanel W, Gaffen SL, Lin X. CARMA1 coiled-coil domain is involved in the oligomerization and subcellular localization of CARMA1 and is required for T cell receptor-induced NF-kappaB activation. *J Biol Chem.* (2007) 282:17141–7. doi: 10.1074/jbc.M700169200
35. Qiao Q, Yang C, Zheng C, Fontan L, David L, Yu X, et al. Structural architecture of the CARMA1/Bcl10/MALT1 signalosome: nucleation-induced filamentous assembly. *Mol Cell* (2013) 51:766–79. doi: 10.1016/j.molcel.2013.08.032
36. Festjens N, Cornelis S, Lamkanfi M, Vandenabeele P. Caspase-containing complexes in the regulation of cell death and inflammation. *Biol Chem.* (2006) 387:1005–16. doi: 10.1515/BC.2006.124
37. Yu JW, Jeffrey PD, Ha JY, Yang X, Shi Y. Crystal structure of the mucosa-associated lymphoid tissue lymphoma translocation 1 (MALT1) paracaspase region. *Proc Natl Acad Sci USA.* (2011) 108:21004–9. doi: 10.1073/pnas.1111708108
38. Wiesmann C, Leder L, Blank J, Bernardi A, Melkko S, Decock A, et al. Structural determinants of MALT1 protease activity. *J Mol Biol.* (2012) 419:4–21. doi: 10.1016/j.jmb.2012.02.018
39. Pelzer C, Cabalzar K, Wolf A, Gonzalez M, Lenz G, Thome M. The protease activity of the paracaspase MALT1 is controlled by monoubiquitination. *Nat Immunol.* (2013) 14:337–45. doi: 10.1038/ni.2540
40. Dierlamm J, Baens M, Wlodarska I, Stefanova-Ouzounova M, Hernandez JM, et al. The apoptosis inhibitor gene API2 and a novel 18q gene, MLT, are recurrently rearranged in the t(11;18)(q21;q21) associated with mucosa-associated lymphoid tissue lymphomas. *Blood* (1999) 93:3601–9.
41. Morgan JA, Yin Y, Borowsky AD, Kuo F, Nourmand N, Koontz JI, et al. Breakpoints of the t(11;18)(q21;q21) in mucosa-associated lymphoid tissue (MALT) lymphoma lie within or near the previously undescribed gene MALT1 in chromosome 18. *Cancer Res.* (1999) 59:6205–13.
42. Akagi T, Motegi M, Tamura A, Suzuki R, Hosokawa Y, Suzuki H, et al. A novel gene, MALT1 at 18q21, is involved in t(11;18) (q21;q21) found in low-grade B-cell lymphoma of mucosa-associated lymphoid tissue. *Oncogene* (1999) 18:5785–94. doi: 10.1038/sj.onc.1203018
43. Hulpiau P, Driege Y, Staal J, Beyaert R. MALT1 is not alone after all: identification of novel paracaspases. *Cell Mol Life Sci.* (2016) 73:1103–16. doi: 10.1007/s00018-015-2041-9
44. Cabalzar K, Pelzer C, Wolf A, Lenz G, Iwaszkiewicz J, Zoete V, et al. Monoubiquitination and activity of the paracaspase MALT1 requires glutamate 549 in the dimerization interface. *PLoS ONE* (2013) 8:e72051. doi: 10.1371/journal.pone.0072051
45. Baens M, Bonsignore L, Somers R, Vanderheydt C, Weeks SD, Gunnarsson J, et al. MALT1 auto-proteolysis is essential for NF-kappaB-dependent gene transcription in activated lymphocytes. *PLoS ONE* (2014) 9:e103774. doi: 10.1371/journal.pone.0103774
46. Baens M, Stirparo R, Lampi Y, Verbeke D, Vandepoel R, Cools J, et al. Malt1 self-cleavage is critical for regulatory T cell homeostasis and anti-tumor immunity in mice. *Eur J Immunol.* (2018). doi: 10.1002/eji.201847597. [Epub ahead of print].
47. Hachmann J, Snipas SJ, van Raam BJ, Cancino EM, Houlihan EJ, Poreba M, et al. Mechanism and specificity of the human paracaspase MALT1. *Biochem J.* (2012) 443:287–95. doi: 10.1042/BJ20120035
48. Chen ZJ. Ubiquitination in signaling to and activation of IK. *Immunol Rev K.* (2012) 246:95–106. doi: 10.1111/j.1600-065X.2012.01108.x
49. Lo YC, Lin SC, Rospigliosi CC, Conze DB, Wu CJ, Ashwell JD, et al. Structural basis for recognition of diubiquitins by NEM. *Mol Cell O.* (2009) 33:602–15. doi: 10.1016/j.molcel.2009.01.012
50. Meininger I, Griesbach RA, Hu D, Gehring T, Seeholzer T, Bertossi A, et al. Alternative splicing of MALT1 controls signalling and activation of CD4(+) T cells. *Nat Commun.* (2016) 7:11292. doi: 10.1038/ncomms11292
51. Meininger I, Krappmann D. Lymphocyte signaling and activation by the CARMA1-BCL10-MALT1 signalosome. *Biol Chem.* (2016) 397:1315–33. doi: 10.1515/hsz-2016-0216
52. Sasaki K, Iwai K. Roles of linear ubiquitinylation, a crucial regulator of NF-kappaB and cell death, in the immune system. *Immunol Rev.* (2015) 266:175–89. doi: 10.1111/imr.12308
53. Shimizu Y, Taraborrelli L, Walczak H. Linear ubiquitination in immunity. *Immunol Rev.* (2015) 266:190–207. doi: 10.1111/imr.12309
54. Dubois SM, Alexia C, Wu Y, Leclair HM, Leveau C, Schol E, et al. A catalytic-independent role for the LUBAC in NF-kappaB activation upon antigen receptor engagement and in lymphoma cells. *Blood* (2014) 123:2199–203. doi: 10.1182/blood-2013-05-504019
55. Yang YK, Yang C, Chan W, Wang Z, Deibel KE, Pomerantz JL. Molecular determinants of scaffold-induced linear ubiquitinylation of B cell lymphoma/leukemia 10 (Bcl10) during T cell receptor and oncogenic caspase recruitment domain-containing protein 11 (CARD11) signaling. *J Biol Chem.* (2016) 291:25921–36. doi: 10.1074/jbc.M116.754028

56. Rahighi S, Ikeda F, Kawasaki M, Akutsu M, Suzuki N, Kato R, et al. Specific recognition of linear ubiquitin chains by NEMO is important for NF-kappaB activation. *Cell* (2009) 136:1098–109. doi: 10.1016/j.cell.2009.03.007
57. David L, Li Y, Ma J, Garner E, Zhang X, Wu H. Assembly mechanism of the CARMA1-BCL10-MALT1-TRAF6 signalosome. *Proc Natl Acad Sci USA*. (2018) 115:1499–504. doi: 10.1073/pnas.1721967115
58. Komander D, Reyes-Turcu F, Licchesi JD, Odenwaelder P, Wilkinson KD, Barford D. Molecular discrimination of structurally equivalent Lys 63-linked and linear polyubiquitin chains. *EMBO Rep.* (2009) 10:466–73. doi: 10.1038/embor.2009.55
59. Blonska M, Pappu BP, Matsumoto R, Li H, Su B, Wang D, Lin X. The CARMA1-Bcl10 signaling complex selectively regulates JNK2 kinase in the T cell receptor-signaling pathway. *Immunity* (2007) 26:55–66. doi: 10.1016/j.immuni.2006.11.008
60. Duwel M, Welteke V, Oeckinghaus A, Baens M, Kloo B, Ferch U, et al. A20 negatively regulates T cell receptor signaling to NF-kappaB by cleaving Malt1 ubiquitin chains. *J Immunol.* (2009) 182:7718–28. doi: 10.4049/jimmunol.0803313
61. Klein T, Fung SY, Renner F, Blank MA, Dufour A, Kang S, et al. Overall CM. The paracaspase MALT1 cleaves HOIL1 reducing linear ubiquitination by LUBAC to dampen lymphocyte NF-kappaB signalling. *Nat Commun.* (2015) 6:8777. doi: 10.1038/ncomms9777
62. Elton L, Carpentier I, Staal J, Driege Y, Haegman M, Beyaert R. MALT1 cleaves the E3 ubiquitin ligase HOIL-1 in activated T cells, generating a dominant negative inhibitor of LUBAC-induced NF-kappaB signaling. *FEBS J.* (2016) 283:403–12. doi: 10.1111/febs.13597
63. Ruland J, Duncan GS, Wakeham A, Mak TW. Differential requirement for Malt1 in T and B cell antigen receptor signaling. *Immunity* (2003) 19:749–58. doi: 10.1016/S1074-7613(03)00293-0
64. Staal J, Driege Y, Bekaert T, Demeyer A, Muyllaert D, Van Damme P, et al. T-cell receptor-induced JNK activation requires proteolytic inactivation of CYLD by MALT1. *EMBO J.* (2011) 30:1742–52. doi: 10.1038/emboj.2011.85
65. Bornancin F, Renner F, Touil R, Sic H, Kolb Y, Touil-Allaoui I, et al. Deficiency of MALT1 paracaspase activity results in unbalanced regulatory and effector T and B cell responses leading to multiorgan inflammation. *J Immunol.* (2015) 194:3723–34. doi: 10.4049/jimmunol.1402254
66. Gewies A, Gorka O, Bergmann H, Pechloff K, Petermann F, Jeltsch KM, et al. Uncoupling Malt1 threshold function from paracaspase activity results in destructive autoimmune inflammation. *Cell Rep.* (2014) 9:1292–305. doi: 10.1016/j.celrep.2014.10.044
67. Harhaj EW, Dixit VM. Deubiquitinases in the regulation of NF-kappaB signaling. *Cell Res.* (2011) 21:22–39. doi: 10.1038/cr.2010.166
68. Uehata T, Iwasaki H, Vandenbon A, Matsushita K, Hernandez-Cuellar E, Kuniyoshi K, et al. Malt1-induced cleavage of regnase-1 in CD4(+) helper T cells regulates immune activation. *Cell* (2013) 153:1036–49. doi: 10.1016/j.cell.2013.04.034
69. Jeltsch KM, Hu D, Brenner S, Zoller J, Heinz GA, Nagel D, et al. Cleavage of roquin and regnase-1 by the paracaspase MALT1 releases their cooperatively repressed targets to promote T(H)17 differentiation. *Nat Immunol.* (2014) 15:1079–89. doi: 10.1038/ni.3008
70. Matsushita K, Takeuchi O, Standley DM, Kumagai Y, Kawagoe T, Miyake T, et al. Zc3h12a is an RNase essential for controlling immune responses by regulating mRNA decay. *Nature* (2009) 458:1185–90. doi: 10.1038/nature07924
71. Leppek K, Schott J, Reitter S, Poetz F, Hammond MC, Stoecklin G. Roquin promotes constitutive mRNA decay via a conserved class of stem-loop recognition motifs. *Cell* (2013) 153:869–81. doi: 10.1016/j.cell.2013.04.016
72. Pratama A, Ramiscal RR, Silva DG, Das SK, Athanasopoulos V, Fitch J, et al. Roquin-2 shares functions with its paralog Roquin-1 in the repression of mRNAs controlling T follicular helper cells and systemic inflammation. *Immunity* (2013) 38:669–80. doi: 10.1016/j.immuni.2013.01.011
73. Yu D, Tan AH, Hu X, Athanasopoulos V, Simpson N, Silva DG, et al. Roquin represses autoimmunity by limiting inducible T-cell co-stimulator messenger RN. *Nature A*. (2007) 450:299–303. doi: 10.1038/nature06253
74. Vogel KU, Edelmann SL, Jeltsch KM, Bertossi A, Heger K, Heinz GA, et al. Roquin paralogs 1 and 2 redundantly repress the Icos and Ox40 costimulator mRNAs and control follicular helper T cell differentiation. *Immunity* (2013) 38:655–68. doi: 10.1016/j.immuni.2012.12.004
75. Nie Z, Du MQ, McAllister-Lucas LM, Lucas PC, Bailey NG, Hogaboam CM, et al. Conversion of the LIMA1 tumour suppressor into an oncogenic LMO-like protein by API2-MALT1 in MALT lymphoma. *Nat Commun.* (2015) 6:5908. doi: 10.1038/ncomms6908
76. Rosebeck S, Madden L, Jin X, Gu S, Apel IJ, Appert A, et al. Cleavage of NIK by the API2-MALT1 fusion oncoprotein leads to noncanonical NF-kappaB activation. *Science* (2011) 331:468–72. doi: 10.1126/science.1198946
77. Nakaya M, Xiao Y, Zhou X, Chang JH, Chang M, Cheng X, et al. Inflammatory T cell responses rely on amino acid transporter ASCT2 facilitation of glutamine uptake and mTORC1 kinase activation. *Immunity* (2014) 40:692–705. doi: 10.1016/j.immuni.2014.04.007
78. Ruefli-Brasse AA, French DM, Dixit VM. Regulation of NF-kappaB-dependent lymphocyte activation and development by paracaspase. *Science* (2003) 302:1581–4. doi: 10.1126/science.1090769
79. Brustle A, Brenner D, Knobbe CB, Lang PA, Virtanen C, Hershenfield BM, et al. The NF-kappaB regulator MALT1 determines the encephalitogenic potential of Th17 cells. *J Clin Invest.* (2012) 122:4698–709. doi: 10.1172/JCI63528
80. Mc Guire C, Wieghofer P, Elton L, Muylaert D, Prinz M, Beyaert R, et al. Paracaspase MALT1 deficiency protects mice from autoimmune-mediated demyelination. *J Immunol.* (2013) 190:2896–903. doi: 10.4049/jimmunol.1201351
81. Jaworski M, Thome M. The paracaspase MALT1: biological function and potential for therapeutic inhibition. *Cell Mol Life Sci.* (2016) 73:459–73. doi: 10.1007/s00018-015-2059-z
82. Gross O, Gewies A, Finger K, Schafer M, Sparwasser T, Peschel C, et al. Card9 controls a non-TLR signalling pathway for innate anti-fungal immunity. *Nature* (2006) 442:651–6. doi: 10.1038/nature04926
83. Gross O, Grupp C, Steinberg C, Zimmermann S, Strasser D, Hannesschlager N, et al. Multiple ITAM-coupled NK-cell receptors engage the Bcl10/Malt1 complex via Carma1 for NF-kappaB and MAPK activation to selectively control cytokine production. *Blood* (2008) 112:2421–8. doi: 10.1182/blood-2007-11-123513
84. Klemm S, Gutermuth J, Hultner L, Sparwasser T, Behrendt H, Peschel C, et al. The Bcl10-Malt1 complex segregates Fc epsilon RI-mediated nuclear factor kappa B activation and cytokine production from mast cell degranulation. *J Exp Med.* (2006) 203:337–47. doi: 10.1084/jem.20051982
85. Mc Guire C, Elton L, Wieghofer P, Staal J, Voet S, Demeyer A, et al. Pharmacological inhibition of MALT1 protease activity protects mice in a mouse model of multiple sclerosis. *J Neuroinflamm.* (2014) 11:124. doi: 10.1186/1742-2094-11-124
86. Hara H, Ishihara C, Takeuchi A, Imanishi T, Xue L, Morris SW, et al. The adaptor protein CARD9 is essential for the activation of myeloid cells through ITAM-associated and Toll-like receptors. *Nat Immunol.* (2007) 8:619–29. doi: 10.1038/ni1466
87. Hsu YM, Zhang Y, You Y, Wang D, Li H, Duramad O, et al. The adaptor protein CARD9 is required for innate immune responses to intracellular pathogens. *Nat Immunol.* (2007) 8:198–205. doi: 10.1038/ni1426
88. Grabiner BC, Blonska M, Lin PC, You Y, Wang D, Sun J, et al. CARMA3 deficiency abrogates G protein-coupled receptor-induced NF-{kappa}B activation. *Genes Dev.* (2007) 21:984–96. doi: 10.1101/gad.1502507
89. Ruland J, Duncan GS, Elia A I. del Barco Barrantes, Nguyen L, Plyte S, Millar DG, et al. Bcl10 is a positive regulator of antigen receptor-induced activation of NF-kappaB and neural tube closure. *Cell* (2001) 104:33–42. doi: 10.1016/S0092-8674(01)00189-1
90. Tanaka M, Kobiyama K, Honda T, Uchio-Yamada K, Natsume-Kitatani Y, Mizuguchi K, et al. Essential role of CARD14 in murine experimental psoriasis. *J Immunol.* (2018) 200:71–81. doi: 10.4049/jimmunol.1700995
91. Jabara HH, Ohsumi T, Chou J, Massaad MJ, Benson H, Megarbane A, et al. A homozygous mucosa-associated lymphoid tissue 1 (MALT1) mutation in a family with combined immunodeficiency. *J Allergy Clin Immunol.* (2013) 132:151–8. doi: 10.1016/j.jaci.2013.04.047
92. McKinnon ML, Rozmus J, Fung SY, Hirschfeld AF, Del Bel KL, Thomas L, et al. Combined immunodeficiency associated with homozygous MALT1 mutations. *J Allergy Clin Immunol.* (2014) 133:1458–62, 1462 e1–7. doi: 10.1016/j.jaci.2013.10.045

93. Punwani D, Wang H, Chan AY, Cowan MJ, Mallott J, Sunderam U, et al. Combined immunodeficiency due to MALT1 mutations, treated by hematopoietic cell transplantation. *J Clin Immunol.* (2015) 35:135–46. doi: 10.1007/s10875-014-0125-1
94. Charbit-Henrion F, Jeverica AK, Begue B, Markelj G, Parlato M, Avcin SL, et al. Deficiency in mucosa-associated lymphoid tissue lymphoma translocation 1: a novel cause of IPEX-like syndrome. *J Pediatr Gastroenterol Nutr.* (2017) 64:378–84. doi: 10.1097/MPG.0000000000001262
95. Juilland M, Thome M. Role of the CARMA1/BCL10/MALT1 complex in lymphoid malignancies. *Curr Opin Hematol.* (2016) 23:402–9. doi: 10.1097/MOH.0000000000000257
96. Turvey SE, Durandy A, Fischer A, Fung SY, Geha RS, Gewies A, et al. The CARD11-BCL10-MALT1 (CBM) signalosome complex: stepping into the limelight of human primary immunodeficiency. *J Allergy Clin Immunol.* (2014) 134:276–84. doi: 10.1016/j.jaci.2014.06.015
97. Koehrer S, Burger JA. B-cell receptor signaling in chronic lymphocytic leukemia and other B-cell malignancies. *Clin Adv Hematol Oncol.* (2016) 14:55–65.
98. Lenz G, Davis RE, Ngo VN, Lam L, George TC, Wright GW, et al. Oncogenic CARD11 mutations in human diffuse large B cell lymphoma. *Science* (2008) 319:1676–9. doi: 10.1126/science.1153629
99. Compagno M, Lim WK, Grunn A, Nandula SV, Brahmachary M, Shen Q, et al. Mutations of multiple genes cause deregulation of NF-kappaB in diffuse large B-cell lymphoma. *Nature* (2009) 459:717–21. doi: 10.1038/nature07968
100. da Silva Almeida AC, Abate F, Khiabanian H, Martinez-Escala E, Guitart J, Tensen CP, et al. The mutational landscape of cutaneous T cell lymphoma and Sezary syndrome. *Nat Genet.* (2015) 47:1465–70. doi: 10.1038/ng.3442
101. Wang L, Ni X, Covington KR, Yang BY, Shiu J, Zhang X, et al. Genomic profiling of Sezary syndrome identifies alterations of key T cell signaling and differentiation genes. *Nat Genet.* (2015) 47:1426–34. doi: 10.1038/ng.3444
102. Kataoka K, Nagata Y, Kitanaka A, Shiraishi Y, Shimamura T, Yasunaga J, et al. Integrated molecular analysis of adult T cell leukemia/lymphoma. *Nat Genet.* (2015) 47:1304–15. doi: 10.1038/ng.3415
103. Davis RE, Ngo VN, Lenz G, Tolar P, Young RM, Romesser PB, et al. Chronic active B-cell-receptor signalling in diffuse large B-cell lymphoma. *Nature* (2010) 463:88–92. doi: 10.1038/nature08638
104. Dai B, Grau M, Juilland M, Klener P, Horing E, Molinsky J, et al. B-cell receptor-driven MALT1 activity regulates MYC signaling in mantle cell lymphoma. *Blood* (2017) 129:333–46. doi: 10.1182/blood-2016-05-718775
105. Lohr JG, Stojanov P, Lawrence MS, Auclair D, Chapuy B, Sougnez C, et al. Discovery and prioritization of somatic mutations in diffuse large B-cell lymphoma (DLBCL) by whole-exome sequencing. *Proc Natl Acad Sci USA.* (2012) 109:3879–84. doi: 10.1073/pnas.1121343109
106. Zhang J, Grubor V, Love CL, Banerjee A, Richards KL, Mieczkowski PA, et al. Genetic heterogeneity of diffuse large B-cell lymphoma. *Proc Natl Acad Sci USA.* (2013) 110:1398–403. doi: 10.1073/pnas.1205299110
107. Ngo VN, Young RM, Schmitz R, Jhavar S, Xiao W, Lim KH, et al. Oncogenically active MYD88 mutations in human lymphoma. *Nature* (2011) 470:115–9. doi: 10.1038/nature09671
108. Rahal R, Frick M, Romero R, Korn JM, Kridel R, Chan FC, et al. Pharmacological and genomic profiling identifies NF-kappaB-targeted treatment strategies for mantle cell lymphoma. *Nat Med.* (2014) 20:87–92. doi: 10.1038/nm.3435
109. Wu C, de Miranda NF, Chen L, Wasik AM, Mansouri L, Jurczak W, et al. Genetic heterogeneity in primary and relapsed mantle cell lymphomas: impact of recurrent CARD11 mutations. *Oncotarget* (2016) 7:38180–90. doi: 10.18632/oncotarget.9500
110. Saba NS, Wong DH, Tanios G, Iyer JR, Lobelle-Rich P, Dadashian EL, et al. MALT1 inhibition is efficacious in both naive and ibrutinib-resistant chronic lymphocytic leukemia. *Cancer Res.* (2017) 77:7038–48. doi: 10.1158/0008-5472.CAN-17-2485
111. Vallois D, Dobay MP, Morin RD, Lemonnier F, Missiaglia E, Juilland M, et al. Activating mutations in genes related to TCR signaling in angioimmunoblastic and other follicular helper T-cell-derived lymphomas. *Blood* (2016) 128:1490–502. doi: 10.1182/blood-2016-02-698977
112. Ngo VN, Davis RE, Lamy L, Yu X, Zhao H, Lenz G, et al. A loss-of-function RNA interference screen for molecular targets in cancer. *Nature* (2006) 441:106–10. doi: 10.1038/nature04687
113. Hailfinger S, Lenz G, Ngo V, Posvitz-Fejfar A, Rebeaud F, Guzzardi M, et al. Essential role of MALT1 protease activity in activated B cell-like diffuse large B-cell lymphoma. *Proc Natl Acad Sci USA.* (2009) 106:19946–51. doi: 10.1073/pnas.0907511106
114. Ferch U, Kloo B, Gewies A, Pfander V, Duwel M, Peschel C, et al. Inhibition of MALT1 protease activity is selectively toxic for activated B cell-like diffuse large B cell lymphoma cells. *J Exp Med.* (2009) 206:2313–20. doi: 10.1084/jem.20091167
115. Snow AL, Xiao W, Stinson JR, Lu W, Chaigne-Delalande B, Zheng L, et al. Congenital B cell lymphocytosis explained by novel germline CARD11 mutations. *J Exp Med.* (2012) 209:2247–61. doi: 10.1084/jem.20120831
116. Brohl AS, Stinson JR, Su HC, Badgett T, Jennings CD, Sukumar G, et al. Germline CARD11 mutation in a patient with severe congenital B cell lymphocytosis. *J Clin Immunol.* (2015) 35:32–46. doi: 10.1007/s10875-014-0106-4
117. Buchbinder D, Stinson JR, Nugent DJ, Heurtier L, Suarez F, Sukumar G, et al. Mild B-cell lymphocytosis in patients with a CARD11 C49Y mutation. *J Allergy Clin Immunol.* (2015) 136:819–21 e1. doi: 10.1016/j.jaci.2015.03.008
118. Bonsignore L, Passelli K, Pelzer C, Perroud M, Konrad A, Thurau M, et al. A role for MALT1 activity in Kaposi's sarcoma-associated herpes virus latency and growth of primary effusion lymphoma. *Leukemia* (2017) 31:614–24. doi: 10.1038/leu.2016.239
119. Medoff BD, Seed B, Jackobek R, Zora J, Yang Y, Luster AD, et al. CARMA1 is critical for the development of allergic airway inflammation in a murine model of asthma. *J Immunol.* (2006) 176:7272–7. doi: 10.4049/jimmunol.176.12.7272
120. Ramadas RA, Roche MI, Moon JJ, Ludwig T, Xavier RJ, Medoff BD. CARMA1 is necessary for optimal T cell responses in a murine model of allergic asthma. *J Immunol.* (2011) 187:6197–207. doi: 10.4049/jimmunol.1101348
121. Causton B, Ramadas RA, Cho JL, Jones K, Pardo-Saganta A, Rajagopal J, et al. CARMA3 is critical for the initiation of allergic airway inflammation. *J Immunol.* (2015) 195:683–94. doi: 10.4049/jimmunol.1402983
122. Jordan CT, Cao L, Roberson ED, Duan S, Helms CA, Nair RP, et al. Rare and common variants in CARD14, encoding an epidermal regulator of NF-kappaB, in psoriasis. *Am J Hum Genet.* (2012) 90:796–808. doi: 10.1016/j.ajhg.2012.03.013
123. Jordan CT, Cao L, Roberson ED, Pierson KC, Yang CF, Joyce CE, et al. PSORS2 is due to mutations in CARD14. *Am J Hum Genet.* (2012) 90:784–95. doi: 10.1016/j.ajhg.2012.03.012
124. Van Nuffel E, Schmitt A, Afonina IS, Schulze-Osthoff K, Beyaert R, Hailfinger S. CARD14-mediated activation of paracaspase MALT1 in keratinocytes: implications for psoriasis. *J Invest Dermatol.* (2017) 137:569–75. doi: 10.1016/j.jid.2016.09.031
125. Mellett M, Meier B, Mohanan D, Schairer R, Cheng P, Satoh TK, et al. CARD14 gain-of-function mutation alone is sufficient to drive IL-23/IL-17-mediated psoriasiform skin inflammation *in vivo*. *J Invest Dermatol.* (2018) 138:2010–2023. doi: 10.1016/j.jid.2018.03.1525
126. Afonina IS, Van Nuffel E, Baudelet G, Driege Y, Kreike M, Staal J, et al. The paracaspase MALT1 mediates CARD14-induced signaling in keratinocytes. *EMBO Rep.* (2016) 17:914–27. doi: 10.15252/embr.201642109
127. Yang F, Liu X, Liu Y, Liu Y, Zhang C, Wang Z, et al. miR-181d/MALT1 regulatory axis attenuates mesenchymal phenotype through NF-kappaB pathways in glioblastoma. *Cancer Lett.* (2017) 396:1–9. doi: 10.1016/j.canlet.2017.03.002
128. Ekambaram P, Lee JL, Hubel NE, Hu D, Yerneni S, Campbell PG, et al. The CARMA3-Bcl10-MALT1 signalosome drives NFkappaB activation and promotes aggressiveness in angiotensin II receptor-positive breast cancer. *Cancer Res.* (2018) 78:1225–40. doi: 10.1158/0008-5472.CAN-17-1089
129. Pan D, Zhu Y, Zhou Z, Wang T, You H, Jiang C, et al. The CBM complex underwrites NF-kappaB activation to promote HER2-associated tumor malignancy. *Mol Cancer Res.* (2016) 14:93–102. doi: 10.1158/1541-7786.MCR-15-0229-T
130. Wang Y, Zhang G, Jin J, Degan S, Tameze Y, Zhang JY. MALT1 promotes melanoma progression through JNK/c-Jun signaling. *Oncogenesis* (2017) 6:e365. doi: 10.1038/oncsis.2017.68
131. Shen W, Du R, Li J, Luo X, Zhao S, Chang A, et al. TIFA suppresses hepatocellular carcinoma progression via MALT1-dependent

and -independent signaling pathways. *Signal Transduct Target Ther.* (2016) 1:16013. doi: 10.1038/sigtrans.2016.13

132. Chiba T, Soeno Y, Shirako Y, Sudo H, Yagishita H, Taya Y, et al. MALT1 inhibition of oral carcinoma cell invasion and ERK/MAPK activation. *J Dent Res.* (2016) 95:446–52. doi: 10.1177/0022034515621740
133. Arteaga CL, Engelman JA. ERBB receptors: from oncogene discovery to basic science to mechanism-based cancer therapeutics. *Cancer Cell* (2014) 25:282–303. doi: 10.1016/j.ccr.2014.02.025
134. Rosebeck S, Lucas PC, McAllister-Lucas LM. Protease activity of the API2-MALT1 fusion oncoprotein in MALT lymphoma development and treatment. *Future Oncol.* (2011) 7:613–7. doi: 10.2217/fon.11.35
135. Fontan L, Yang C, Kabaleeswaran V, Volpon L, Osborne MJ, Beltran E, et al. MALT1 small molecule inhibitors specifically suppress ABC-DLBCL *in vitro* and *in vivo*. *Cancer Cell* (2012) 22:812–24. doi: 10.1016/j.ccr.2012.11.003
136. Streubel B, Lamprecht A, Dierlamm J, Cerroni L, Stolte M, Ott G, et al. T(14;18)(q32;q21) involving IGH and MALT1 is a frequent chromosomal aberration in MALT lymphoma. *Blood* (2003) 101:2335–9. doi: 10.1182/blood-2002-09-2963
137. Nagel D, Spranger S, Vincendeau M, Grau M, Raffegerst S, Kloo B, Hlahla D, et al. Pharmacologic inhibition of MALT1 protease by phenothiazines as a therapeutic approach for the treatment of aggressive ABC-DLBC. *Cancer Cell* (2012) 22:825–37. doi: 10.1016/j.ccr.2012.11.002
138. Lim SM, Jeong Y, Lee S, Im H, Tae HS, Kim BG, et al. Identification of beta-lapachone analogs as novel MALT1 inhibitors to treat an aggressive subtype of diffuse large B-cell lymphoma. *J Med Chem.* (2015) 58:8491–502. doi: 10.1021/acs.jmedchem.5b01415
139. Xin BT, Schimmack G, Du Y, Florea BI, van der Marel GA, Driessen C, Krappmann D, Overkleeft HS. Development of new Malt1 inhibitors and probes. *Bioorg Med Chem.* (2016) 24:3312–29. doi: 10.1016/j.bmc.2016.03.035
140. Bardet M, Unterreiner A, Malinverni C, Lafossas F, Vedrine C, Boesch D, et al. The T-cell fingerprint of MALT1 paracaspase revealed by selective inhibition. *Immunol Cell Biol.* (2018) 96:81–99. doi: 10.1111/imcb.1018
141. Li Y, Huang X, Huang S, He H, Lei T, Saaoud F, et al. Central role of myeloid MCPIP1 in protecting against LPS-induced inflammation and lung injury. *Signal Transduct Target Ther.* (2017) 2:17066. doi: 10.1038/sigtrans.2017.66

Conflict of Interest Statement: The authors declare that the research was conducted in the absence of any commercial or financial relationships that could be construed as a potential conflict of interest.

frontiers in Immunology

ORIGINAL RESEARCH
published: 20 November 2018
doi: 10.3389/fimmu.2018.02695

BCL10-CARD11 Fusion Mimics an Active CARD11 Seed That Triggers Constitutive BCL10 Oligomerization and Lymphocyte Activation

Thomas Seeholzer[1†], Susanne Kurz[1†], Florian Schlauderer[2], Simone Woods[1], Torben Gehring[1], Simon Widmann[1], Katja Lammens[2] and Daniel Krappmann[1]*

[1] Research Unit Cellular Signal Integration, Institute of Molecular Toxicology and Pharmacology, Helmholtz Zentrum München - German Research Center for Environmental Health, Neuherberg, Germany, [2] Gene Center, Ludwig-Maximilians University, Munich, Germany

OPEN ACCESS

Edited by:
Andrew L. Snow,
Uniformed Services University of the Health Sciences, United States

Reviewed by:
Lawrence Kane,
University of Pittsburgh, United States
Joel L. Pomerantz,
Johns Hopkins University, United States
Liron David,
Boston Children's Hospital, Harvard Medical School, United States

***Correspondence:**
Daniel Krappmann
daniel.krappmann@helmholtz-muenchen.de

[†]These authors have contributed equally to this work

Specialty section:
This article was submitted to T Cell Biology, a section of the journal Frontiers in Immunology

Received: 14 August 2018
Accepted: 31 October 2018
Published: 20 November 2018

Citation:
Seeholzer T, Kurz S, Schlauderer F, Woods S, Gehring T, Widmann S, Lammens K and Krappmann D (2018) BCL10-CARD11 Fusion Mimics an Active CARD11 Seed That Triggers Constitutive BCL10 Oligomerization and Lymphocyte Activation. Front. Immunol. 9:2695. doi: 10.3389/fimmu.2018.02695

Assembly of the CARD11/CARMA1-BCL10-MALT1 (CBM) signaling complex upon T or B cell antigen receptor (TCR or BCR) engagement drives lymphocyte activation. Recruitment of pre-assembled BCL10-MALT1 complexes to CARD11 fosters activation of the MALT1 protease and canonical NF-κB signaling. Structural data and *in vitro* assays have suggested that CARD11 acts as a seed that nucleates the assembly of BCL10 filaments, but the relevance of these findings for CBM complex assembly in cells remains unresolved. To uncouple cellular CARD11 recruitment of BCL10 and BCL10 filament assembly, we generated a BCL10-CARD11 fusion protein that links the C-terminus of BCL10 to the N-terminus of CARD11. When stably expressed in CARD11 KO Jurkat T cells, the BCL10-CARD11 fusion induced constitutive MALT1 activation. Furthermore, in CARD11 KO BJAB B cells, BCL10-CARD11 promoted constitutive NF-κB activation to a similar extent as CARD11 containing oncogenic driver mutations. Using structure-guided destructive mutations in the CARD11-BCL10 (CARD11 R35A) or BCL10-BCL10 (BCL10 R42E) interfaces, we demonstrate that chronic activation by the BCL10-CARD11 fusion protein was independent of the CARD11 CARD. However, activation strictly relied upon the ability of the BCL10 CARD to form oligomers. Thus, by combining distinct CARD mutations in the context of constitutively active BCL10-CARD11 fusion proteins, we provide evidence that BCL10-MALT1 recruitment to CARD11 and BCL10 oligomerization are interconnected processes, which bridge the CARD11 seed to downstream pathways in lymphocytes.

Keywords: lymphocyte signaling, CARMA1–BCL10–MALT1 (CBM) signalosome complex, CARD11, NF- kappa B, MALT1 paracaspase

INTRODUCTION

Assembly of the CARD11/CARMA1-BCL10-MALT1 (CBM) signalosome channels T and B cell antigen-receptor (TCR/BCR) ligation to MALT1 protease activation and canonical NF-κB signaling (1, 2). CARD11 phosphorylation, primarily in the central linker region, following antigenic stimulation induces conformational changes that expose the N-terminal CARD (Caspase Recruitment Domain) to recruit pre-assembled BCL10-MALT1 complexes (3, 4). Oncogenic

CARD11 variants have been identified mainly in the coiled-coil domain, and these activating mutations promote chronic CBM assembly and NF-κB-driven survival in diffuse large B cell lymphomas (DLBCL) in the absence of antigenic stimulation (5, 6).

It is well established that BCL10 associates with the CARD-containing scaffold protein CARD11 through heterotypic CARD-CARD interactions (7, 8). Overexpression studies indicate that BCL10, via its N-terminal CARD, forms filament-like clusters in cells, which are required for proper activation of canonical NF-κB signaling (9). Aggregation of BCL10 in foci was also observed following TCR ligation in T cells (10). More recent *in vitro* structural studies, combined with molecular modeling, have demonstrated that the CARD of CARD11 can function as a seed to nucleate the assembly of BCL10 CARD filaments (11–13). *In vitro* BCL10 filaments can also form in the absence of CARD11, but CARD11 decreases the lag period of BCL10 polymerization and thus appears to function as an initiator of the process (11). Impaired MALT1 activity and NF-κB signaling upon overexpression of CARD11 or BCL10 mutants, targeting either the heterotypic CARD11-BCL10 or the homotypic BCL10-BCL10 CARD interfaces, highlights the importance of the different CARD surfaces (12, 13). These experiments, however, did not address the contribution of the different interfaces to antigenic activation when expressed at endogenous levels. We have demonstrated that BCL10 oligomerization is also required for its recruitment to CARD11, indicating that both processes are highly interconnected (14). Thus, the cellular relevance of the CARD11 seeding function for BCL10 filament formation, as well as, the order of events after antigenic stimulation, have not been resolved.

Here, we used CRISPR/Cas9 technology to generate CARD11 and BCL10 KO T and B cell lines and stable lentiviral reconstitution, to investigate the cellular necessity of the CARD11 seed and BCL10 filaments in a clean genetic setup under physiological conditions. As noted earlier, we have been unable to definitively determine whether CARD11 nucleates BCL10 filaments or, if BCL10 filament formation happens prior to, or at the same time as CARD11 recruitment in stimulated T cells using missense mutations in the putative CARD11-BCL10 or BCL10-BCL10 interfaces alone (14). Thus, we uncoupled these processes by fusing BCL10 to CARD11 to bypass inducible recruitment and thereby were able to investigate the cellular necessity of CARD11 seeding and BCL10 oligomerization.

RESULTS

BCL10 Recruitment to CARD11 and BCL10 Filament Assembly Are Interconnected Processes

In order to predict mutations that would selectively interfere with CARD11 seed function or BCL10 self-assembly, we used structural modeling to fit the CARD11 seed onto the structure of BCL10 CARD filaments (**Figure 1A**). Therefore, the CARD11 CARD domain crystal structure was superimposed on to three BCL10 CARD domains at the bottom of the BCL10 filament cryo EM structure [**Figure 1A**; (13, 14)]. Since the structure of the CARD11-BCL10 interface has not been determined, the CARD11 BCL10 CARD/CARD interaction was modeled in consideration of the surface charge complementarity analysis of the BCL10-MALT1 filament cryo-EM structure and the crystal structure of the CARD11 (**Supplementary Figures 1A–C**). As noted earlier, distinct interfaces between the CARDs are required to mediate heterotypic CARD11-BCL10 interactions or homotypic BCL10-BCL10 interactions (12, 13). On the CARD11 side, R35 serves as a critical contact point to multiple residues in BCL10 including E53 and mediates recruitment of BCL10 to CARD11 [**Figure 1B**; (12)]. On BCL10, R42 contributes to the association at the BCL10-BCL10 interface I that controls BCL10 oligomerization (**Figures 1C,D**). The structure reveals that R42 is not predicted to confer CARD11-BCL10 interaction (11, 13, 14). *In vitro*, the BCL10 CARD mutation R42E prevents oligomerization of the BCL10-MALT1 complex (14). We expressed BCL10 WT and R42E in adherent U2OS cells to monitor formation of cellular clusters. Indeed, whereas overexpressed BCL10 WT forms cytosolic aggregates in U2OS cells, BCL10 R42E fails to cluster, indicating that oligomerization and filament formation is prevented by the mutation (**Figure 1E**). We performed co-immunoprecipitation (IP) of HA-BCL10 WT, together with Flag-BCL10 WT or R42E in HEK293 cells (**Figure 1F**). Despite the higher expression of BCL10 R42E, only Flag-BCL10 WT co-precipitated with HA-BCL10, validating that the mutation abolishes BCL10 self-association.

To rigorously test the function of CARD11 as a molecular seed and BCL10 as a filament forming CARD11 adaptor in B and T cells, we generated CARD11 and BCL10 KO Jurkat T cells, as well as CARD11 KO BJAB B cells, by CRISPR/Cas9 technology (**Supplementary Figure 2**). CARD11 KO Jurkat T and BJAB B cells were generated using sgRNA targeting Exon3, which induces double stranded breaks and frame shift mutations due to non-homologous end-joining (NHEJ) repair (**Supplementary Figure 2A**). An exon1-intron1 deletion strategy using two sgRNA was employed to knockout BCL10 from Jurkat T cells (**Supplementary Figure 2B**). Using these approaches, we obtained several clones that displayed loss of CARD11 or BCL10 expression as determined by Western Blot analysis (**Supplementary Figures 2C–E**). Destructive frame shift mutations in CARD11 or deletions of BCL10 in both alleles were confirmed by sequencing of the genomic loci in the respective KO cell clones (data not shown). We used PMA/Ionomycin (P/I) stimulation, which bypasses upstream TCR or BCR signaling by directly activating PKCθ or PKCβ in T and B cells and increasing cytosolic calcium levels. In line with the key role of the CBM complex, CARD11 or BCL10 deficiency abolished P/I-induced NF-κB signaling in Jurkat T or BJAB B cells as evident from lack of IκBα degradation and NF-κB DNA binding (**Supplementary Figures 2C–E**). In contrast, CBM-independent, TNFα-driven NF-κB signaling as well as ERK activation were not affected by the absence of CARD11 in Jurkat T cells, demonstrating that loss of the CBM complex selectively affects antigenic signaling. Thus, the absence of CARD11 or BCL10 in Jurkat and BJAB cells faithfully mirrors the signaling

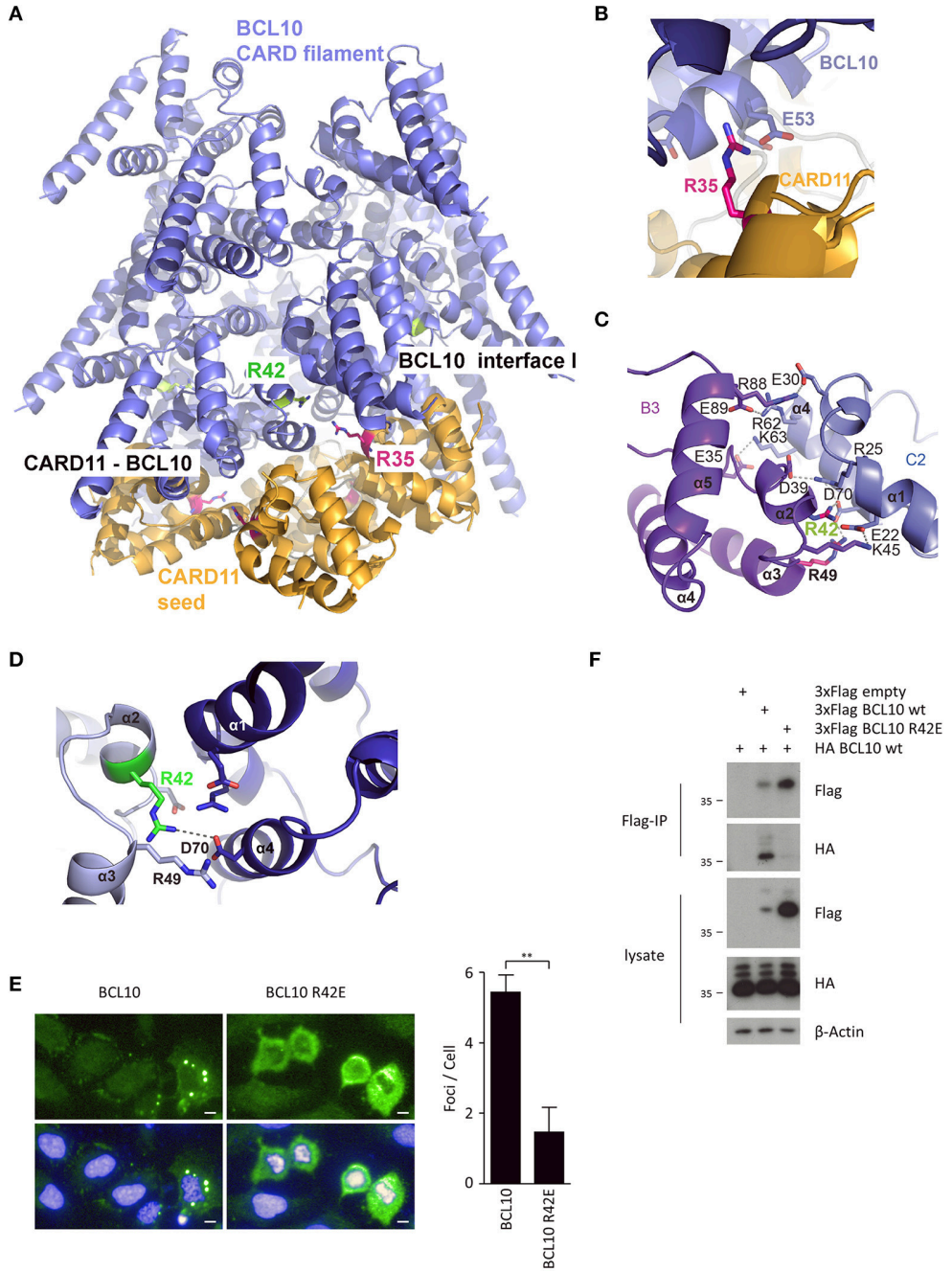

FIGURE 1 | CARD-CARD interfaces in the CARD11-BCL10 structure. **(A)** Model of the CARD11-BCL10 filament structure. The oligomeric CARD11 seed (PDB 4LWD, orange) induces BCL10 (PDB 6GK2, blue) filament assembly through the heterotypic CARD11-BCL10 interface. **(B)** Close-up view of CARD11 R35 (magenta) contacting BCL10 E53 in the modeled CARD11-BCL10 interface. **(C,D)** Close-up view of the BCL10-BCL10 interface I. Residues involved in homotypic CARD-CARD association as observed in the cryo-EM structure (EMD-0013, PDB 6GK2) (14) are shown as sticks. The mutated residue R42 is highlighted in green. **(E)** Cellular distribution of BCL10 in U2OS cells was determined after transfection of BCL10-FS or BCL10 R42E-FS and aggregate clustering was detected by indirect confocal immunofluorescence microscopy. Scale bars depict 10 μm. Average number of aggregated foci was quantified by blinded counting >30 cells per condition (mean ± s.e.m.; $^{**}p \leq 0.01$). **(F)** HEK 293 cells were transfected with Flag- and HA-tagged BCL10 constructs as indicated, and self-association of HA-BCL10 WT to Flag-BCL10 WT or R42E mutant was determined after Flag-IP.

defects observed in primary lymphocytes from CARD11$^{-/-}$ or BCL10$^{-/-}$ mice (15–17).

We then performed rescue experiments in Jurkat KO T cells to study the molecular functions of the CARD11 and BCL10 CARDs, by introducing missense mutations (CARD11 R35A and BCL10 R42E) that are both predicted to selectively interfere with heterotypic CARD11-BCL10 and homotypic BCL10-BCL10 interactions, respectively [**Figures 1**, **2A**; (12, 14)]. Jurkat

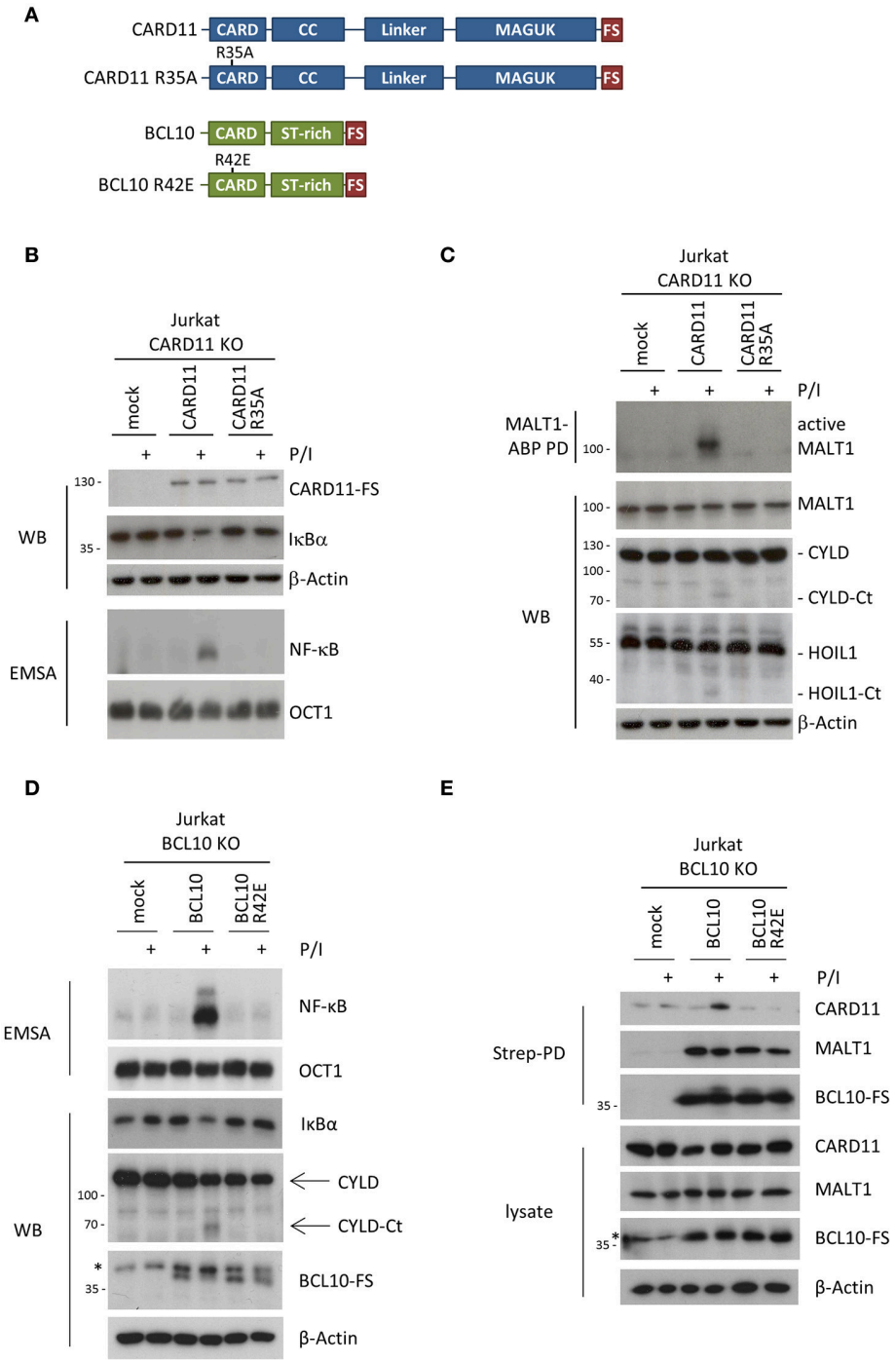

FIGURE 2 | Effects of destructive heterotypic and homotypic CARD-CARD interface mutants. **(A)** Schematic presentation of CARD11 and BCL10 WT proteins and the respective CARD mutants R35A and R42E. **(B)** CARD11 KO Jurkat T cells were reconstituted with CARD11 WT or R35A. Cells were stimulated with P/I (30 min) and effects on NF-κB signaling were determined by following IκBα degradation by WB and NF-κB activation by EMSA. **(C)** CARD11 KO Jurkat T cells were reconstituted as in **(B)**, stimulated with P/I (30 min), and MALT1 protease activity was determined via MALT1-ABP PD assay and assessment of substrate cleavage (CYLD and HOIL1) by WB. **(D)** BCL10 KO Jurkat T cells were reconstituted with BCL10 or BCL10 R42E. Cells were stimulated with P/I (30 min) and NF-κB signaling was analyzed as in **(B)**. MALT1 protease activity was determined by CYLD substrate cleavage by WB. **(E)** Recruitment of BCL10 or BCL10 R42E to CARD11 after P/I stimulation (15 min) in Jurkat T cells was monitored by ST-PD and subsequent WB. The asterisks indicate an unspecific band in the BCL10 WB.

CARD11 or BCL10 KO T cells were reconstituted by lentiviral transduction and comparable infection rates for epitope-tagged (FS: Flag-StrepTag2) CARD11 and BCL10 constructs were obtained, as determined by co-expression of the surface marker ΔCD2 (**Supplementary Figures 3A,B**). Equivalent expression of WT and mutant CARD11 or BCL10 proteins at close to endogenous levels was confirmed by Western Blotting (**Supplementary Figures 3A,B**). Functionally, lack of CARD11-dependent NF-κB activation after P/I stimulation in CARD11 KO cells was rescued upon reconstitution with CARD11 WT, but not with the CARD11 R35A mutant (**Figure 2B**). We also assessed activation of the MALT1 protease by substrate cleavage (CYLD and HOIL-1) (18) and labeling of active MALT1 by a biotinylated MALT1 activity-based probe (ABP) followed by biotin pull-down (PD) to capture active MALT1 [**Figure 2C**; (19)]. Again, CARD11 WT, but not R35A, could rescue P/I stimulated MALT1 protease activation in Jurkat T cells, revealing that this mutation abolishes all CARD11 downstream function. On the side of BCL10, we confirmed that rescue of BCL10 WT, but not BCL10 R42E, was able to trigger MALT1 activation and mediate NF-κB downstream signaling in response to P/I stimulation [**Figure 2D**; (14)]. Since the structural analyses suggested that BCL10 R42E would selectively disrupt the BCL10-BCL10 but not the CARD11-BCL10 interface (13), we asked if BCL10 R42E could still be recruited to CARD11 upon stimulation. However, no stimulation-dependent binding to CARD11 was detected with BCL10 R42E mutant [**Figure 2E**; (14)]. The data demonstrate that CARD11 recruitment and BCL10 filament formation are interconnected processes. Thus, destructive mutations in the CARD11-BCL10 or BCL10-BCL10 interfaces alone are unable to resolve whether CARD11 acts as a seed to induce BCL10 oligomerization or if an initial BCL10 filament assembly may be required for the recruitment of BCL10-MALT1 to CARD11.

BCL10-CARD11 Fusion Drives Constitutive MALT1 Activation Through BCL10 Oligomerization in Jurkat T Cells

To test the necessity for BCL10 self-association downstream of CARD11, we designed a system that bypasses inducible CARD11-BCL10 association. For this we cloned chimeric proteins that covalently fuse BCL10 through its C-terminus to the N-terminus of CARD11 (**Figure 3A**). We lentivirally transduced CARD11 KO Jurkat T cells with the SF-tagged BCL10-CARD11 construct (herein referred to as B10-C11 fusion) (**Figure 3B**). We detected a faint but distinct band corresponding to the expected size of the B10-C11 fusion using αBCL10 and αCARD11 antibodies (**Figure 3C**). Notably, expression of the B10-C11 protein triggered constitutive cleavage of CYLD and A20, as well as a reduction in endogenous BCL10, which are all MALT1 substrates (18). However, the BCL10-CARD11 fusion itself, which contains a MALT1 cleavage site at R228 in the BCL10 moiety (20), was also prone to processing, giving rise to a fragment the size of endogenous CARD11 (**Figure 3C**). Thus, the data clearly indicate that fusion of BCL10 to CARD11 is sufficient to induce MALT1 activation.

To avoid the indirect reconstitution of CARD11 from the cleaved B10-C11 fusion, we designed all further BCL10-CARD11 fusion constructs so that they contained the MALT1 cleavage resistant BCL10 R228A mutation (**Figure 3A**). The fusion constructs include the destructive mutations R42E in the BCL10 CARD, and R35A in the CARD11 CARD, both alone and in combination. All B10-C11 fusion constructs were transduced into CARD11 KO Jurkat T cells, yielding equivalent infection efficiencies as judged by ΔCD2 expression (**Figure 3D**). The chimeric proteins were expressed below the level of endogenous CARD11 and moreover, the fusions containing a functional WT BCL10 CARD were consistently expressed at lower levels compared to the BCL10 mutants R42E that prevent BCL10 oligomerization (**Figure 3E**). StrepTactin pull-downs (ST-PD) demonstrated that the BCL10-CARD11 fusion proteins retained the ability to bind endogenous MALT1, excluding that the fusion or point mutations in the CARDs interfere with MALT1 recruitment (**Figure 3E**).

Using biotin-PD after incubation with bio-MALT1-ABP, we tested MALT1 protease activity in extracts of untreated and P/I stimulated Jurkat T cells (**Figure 3F**). Expression of B10 R228A-C11, containing two functional CARDs, as well as the B10 R228A-C11 R35A fusion, with an inactivation only in the CARD11 CARD, induced strong MALT1 protease activity that was equivalent to the activation obtained in Jurkat T cells after P/I stimulation. Despite robust MALT1 activation, the R228A exchange in BCL10 prevented cleavage of the fusion constructs and thus the appearance of CARD11 (**Figure 3E**). Constitutive MALT1 activation was abrogated in the B10-C11 fusion proteins carrying the oligomerization-defective BCL10 R42E mutation, providing evidence that constitutive MALT1 activation is driven through oligomerization of endogenous BCL10 via the BCL10 CARD (**Figure 3F**). Interestingly, MALT1 activity was further enhanced after stimulation of B10 R228A-C11 expressing cells and this strictly relied on the CARD11 CARD, because the R35A mutation prevented stimulation-dependent induction. In line, even though the B10 R42E/R228A-C11 fusion containing an intact CARD11 CARD was unable to induce constitutive MALT1 activation, it was still able to mediate MALT1 activation in P/I-stimulated Jurkat T cells. Thus, stimulation dependent activation seems to rely on the recruitment of endogenous BCL10 to the CARD11 CARD in the context of the BCL10-CARD11 fusion protein. In fact, the B10 R42E/R228A-C11 fusion acted completely independently of the BCL10 CARD and exactly mirrored the rescue observed when using CARD11 WT (see **Figures 2B,C**). In agreement with these data, the triple mutant B10 R42E/R228A-C11 R35A neither promoted constitutive, nor rescued, stimulus-dependent MALT1 activation.

To confirm these findings on the level of MALT1 substrates, we assessed cleavage of CYLD, HOIL1 and A20 in B10-C11 expressing cells (**Figure 3G**). Cleavage of the three substrates was observed in Jurkat T cells expressing the fusions with an intact BCL10 CARD (B10 R228A-C11 and B10 R228A-C11 R35A), confirming that constitutive MALT1 protease activity relies on BCL10 oligomerization. The intact CARD11 CARD in B10 R42E R228A-C11 still conferred inducible substrate cleavage, which was especially evident for HOIL1 that is also most strongly

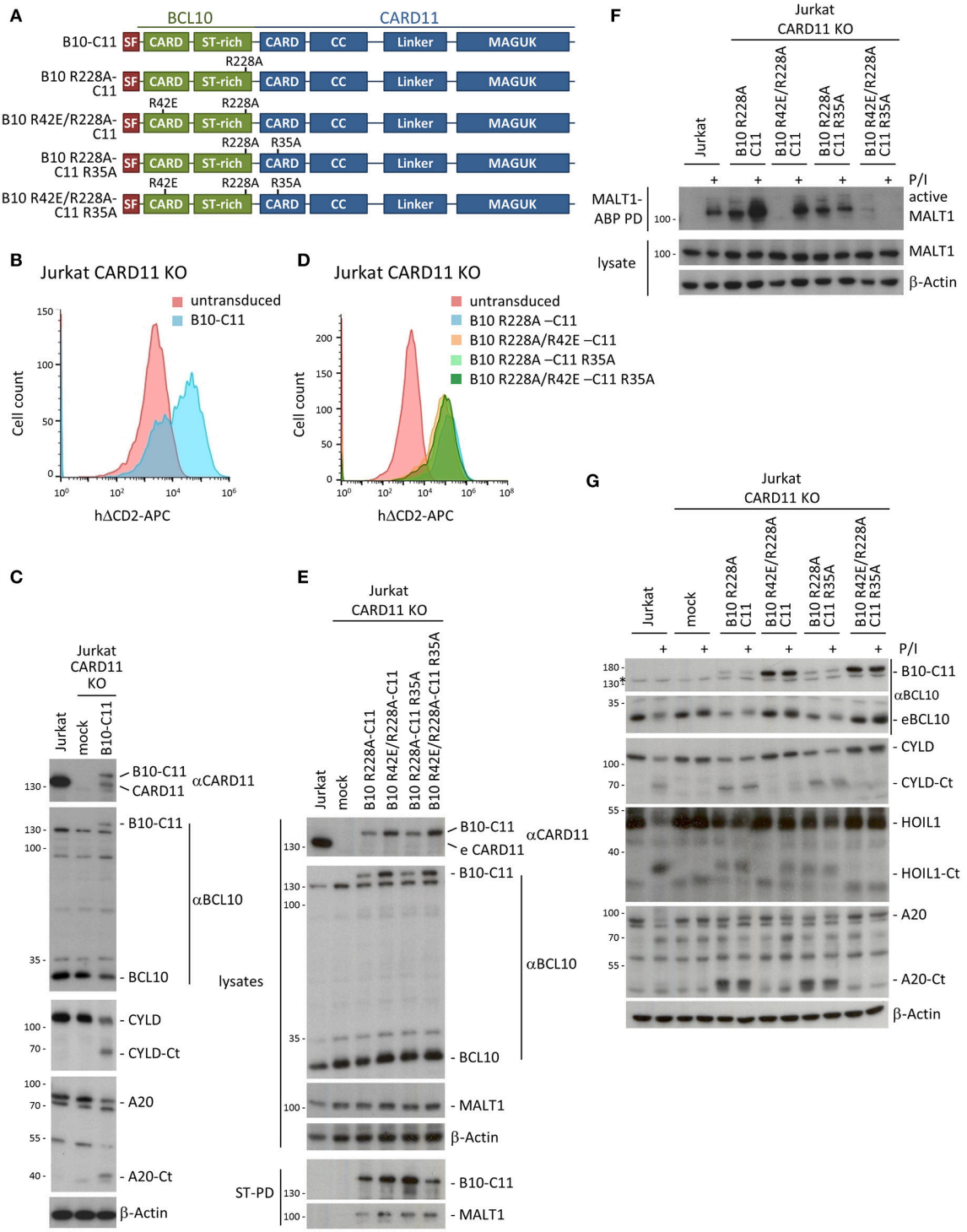

FIGURE 3 | A chimeric BCL10-CARD11 fusion protein induces constitutive MALT1 protease activity in Jurkat T cells through the BCL10 oligomerization interface. **(A)** Schematic representation of BCL10-CARD11 (B10-C11) fusion proteins with the respective CARD mutants. **(B)** Transduction efficiency of CARD11 KO Jurkat T cells with BCL10-CARD11 (B10-C11) was analyzed by FACS using the surface marker ΔCD2. **(C)** Protein expression of B10-C11 fusion construct and cleavage of MALT1 substrates compared to mock and parental Jurkat T cells was analyzed by WB. **(D)** Transduction efficiency of CARD11 KO Jurkat T cells with different B10 R228A-C11 fusion constructs as in **(B)**. **(E)** Expression of the different B10 R228A-C11 fusion proteins compared to mock and parental Jurkat T cells was analyzed by WB and binding to MALT1 assessed by Strep-PD. **(F)** CARD11 KO Jurkat T cells were reconstituted with B10 R228A-C11 fusion proteins as indicated. Active MALT1 prior or after P/I stimulation (30 min) was detected in the extracts with biotin-labeled MALT1-ABP and MALT1-ABP PD followed by WB. **(G)** CARD11 KO Jurkat T cells were reconstituted and treated as in **(F)** and cleavage of MALT1 substrates (CYLD, HOIL1, A20) was detected by WB.

cleaved after P/I stimulation of Jurkat T cells. Again, destruction of both CARDs in B10 R42E/R228A-C11 R35A led to complete loss of constitutive and inducible MALT1 activation. Thus, covalent attachment of BCL10 to the N-terminus of CARD11 is sufficient to induce MALT1 protease activation, which still relies on the oligomerization interface of the fused BCL10 moiety. These data support the concept that, in cells, CARD11 acts as a seed to induce BCL10 filament assembly.

Transient Expression of BCL10-CARD11 Induces NF-κB Activation in Jurkat T Cells

Interestingly, when we tested activation of NF-κB by B10-C11 fusion constructs in CARD11 or BCL10 KO Jurkat T cells we noticed a severely blunted response in EMSA (**Figure 4A**). There was a weak induction of constitutive NF-κB DNA binding in B10 R228A-C11, but IκBα degradation and NF-κB activation was only mildly triggered after P/I stimulation, revealing that stable expression of the active BCL10-CARD11 fusion may promote a stage of unresponsiveness in Jurkat T cells. Again, missense mutations in both CARDs completely prevented constitutive, as well as, inducible NF-κB activation in the context of the B10-C11 fusion protein. We switched to a transient transfection system and NF-κB reporter assays to investigate if BCL10-CARD11 fusion proteins can activate NF-κB. Indeed, NF-κB was strongly induced by the expression of B10 R228A-C11 fusion activated in parental Jurkat T cells or CARD11 KO Jurkat T cells (**Figures 4B,C**). However, in line with the EMSA results overall NF-κB activation was strongly diminished when the reporter assay was performed in CARD11 KO Jurkat T cells that stably express the B10-C11 fusion constructs (**Figure 4C**). Further, the oligomerization-deficient BCL10 R42E mutant severely reduced NF-κB activation by the BCL10-CARD11 fusion protein. Again, also in transient transfection we observed that BCL10-CARD11 was expressed at much lower levels compared to the B10 R42E/R228A-C11 protein, suggesting that there is a counter-selection against the expression of the active BCL10-CARD11 fusion. NF-κB induction of BCL10-CARD11 fusion protein was comparable to the induction achieved by oncogenic CARD11 L225LI or CARD11 Δlinker, especially taking into account the much weaker expression of the fusion protein [**Figure 4C**; (6, 21)]. To check if the generated BCL10-CARD11 fusion construct does not trigger unphysiological NF-κB that bypasses the necessity of known regulators, we determined the requirement for MALT1 and for TRAF6 recruitment to MALT1 (**Figure 4D**). NF-κB activation in response to antigenic stimulation is abolished MALT1 KO Jurkat T cells and signaling can be rescued by transduction of MALT1A or MALT1B, but not the respective MALT1 TRAF6 binding mutants (22). As expected, expression of B10 R228A-C11 or CARD11 Δlinker was unable to activate NF-κB in MALT1 KO Jurkat T cell (**Figure 4D**). While NF-κB activity was recovered by viral complementation with MALT1B WT, the MALT1B E795A mutant that destroys the only functional TRAF6 binding motif on MALT1B failed to rescue reporter gene expression, proving that MALT1 and TRAF6 are utilized by the BCL10-CARD11 fusion protein to activate NF-κB [**Figure 4D**; (22–24)]. Thus, while transient expression of the BCL10-CARD11 fusion protein promotes NF-κB activation, NF-κB responses are dampened in Jurkat T cells after stable expression of the fusion proteins. To corroborate whether the BCL10-CARD11 fusion protein can also compensate for BCL10 deficiency, we transduced BCL10 KO Jurkat T cells with the B10 R228A-C11 fusion protein (**Supplementary Figure 4A**). Indeed, fusion of BCL10 to CARD11 was able to trigger constitutive CYLD, A20, and HOIL1 cleavage and thus to drive MALT1 protease activation in BCL10 deficient cells (**Supplementary Figure 4B**). Again, mutation of BCL10 and CARD11 CARD (B10 R42E/R228A-C11 R35A) prevented constitutive and inducible MALT1 activation, underscoring that dimerization/oligomerization of the fusion proteins is required. Similar to the situation in CARD11 KO cells, NF-κB activation was blunted upon stable expression of B10 R228A-C11 in BCL10 KO Jurkat T cells.

BCL10-CARD11 Fusion Acts Like Oncogenic CARD11 in BJAB B Cells

To better explore the impact of stable BCL10-CARD11 fusion on NF-κB activation, we switched to GCB DLBCL derived BJAB B cells, which under basal conditions are devoid of NF-κB activity, but overexpression of oncogenic CARD11 mutants induces strong chronic NF-κB activity (5, 6, 25). We generated CARD11 KO BJAB B cells (**Supplementary Figure 2D**) and confirmed that the phenotype of the BJAB KO cells was caused by loss of CARD11. For this we reconstituted the cells with CARD11 WT, or the oncogenic CARD11 coiled-coil (CC) mutant L225LI that induces robust NF-κB and proliferation upon overexpression in B cells [**Figure 5A**; (25, 26)]. After viral transduction, BJAB B cells expressed CARD11 WT and CARD11 L225LI slightly above endogenous levels (**Figures 5B,C**). CARD11 WT was able to recover P/I-inducible NF-κB and MALT1 protease activation, but was not associated with constitutive activation (**Figures 5D,E**). In contrast, transduction of CARD11 L225LI was sufficient to promote constitutive NF-κB activation, as well as cleavage of the MALT1 substrates BCL10, CYLD, A20 and HOIL1. This effect was not further augmented by P/I stimulation (**Figures 5D,E**). Thus, CARD11 KO BJAB B cells represent a valid system to elucidate the impact of BCL10-CARD11 fusions on NF-κB signaling.

Next, we expressed B10 R228A-C11 and B10 R42E/R228A-C11 in CARD11 KO BJAB B cells (**Figure 6A**). In addition, we sought to determine whether an oncogenic mutant of CARD11 also relies on BCL10 oligomerization. We have previously shown that the activating potential of CARD11 L225LI is abolished by the R35A mutation (25). Therefore, we expressed the B10-C11 L225LI fusion constructs in the context of the CARD destructive R35A mutation so that they should rely on the BCL10 CARD (B10 R228A-C11 R35A/L225LI and B10 R42E/R228A-C11 R35A/L225LI) (**Figure 6A**). All constructs were transduced in BJAB B cells to a similar extent, as determined by the surface marker ΔCD2, but protein expression was far below endogenous CARD11 (**Figures 6B,C**). As observed in Jurkat T cells, B10 R228A-C11 constructs containing an intact BCL10 CARD were expressed at much lower levels and the variant containing

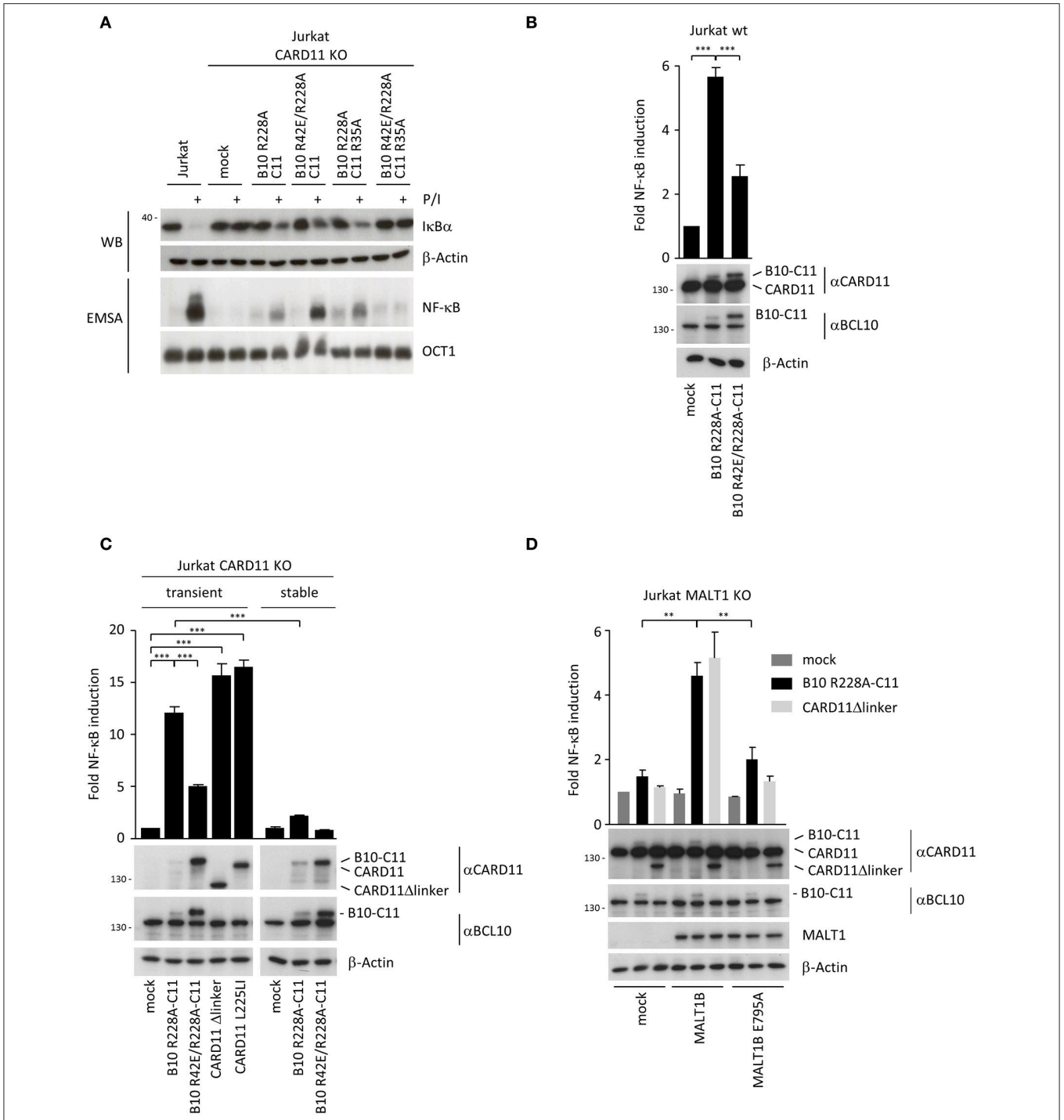

FIGURE 4 | Transient expression of chimeric BCL10-CARD11 fusion protein in Jurkat T cells triggers NF-κB activation. **(A)** NF-κB signaling was analyzed in CARD11 KO Jurkat T cells stably reconstituted with different B10 R228A-C11 fusion proteins as indicated. IκBα degradation was determined by WB and NF-κB activation was analyzed by EMSA. **(B)** B10-C11 fusion constructs were transiently expressed in Jurkat T cells together with a dual NF-κB reporter, and NF-κB induction was assessed by a dual luciferase reporter assay. Protein levels were analyzed by WB. Results are displayed relative to mock-transfected cells (mean ± s.e.m.; $n = 5$). **(C)** Jurkat CARD11 KO cells were transiently or stably reconstituted with B10-C11 fusion or CARD11 constructs and NF-κB activity determined as in **(B)**. Expression of the fusion constructs was verified by WB (mean ± s.e.m.; $n = 3$). **(D)** Transient expression of B10 R228A-C11 and CARD11 Δlinker in Jurkat MALT1 KO cells stably reconstituted with mock, MALT1 IsoB wildtype and the TRAF6 binding motif mutant E795A, respectively. NF-κB activity was determined as described in **(B)** and protein levels visualized on WB (mean ± s.e.m.; $n = 3$). $^{**}p \leq 0.01$, $^{***}p \leq 0.001$.

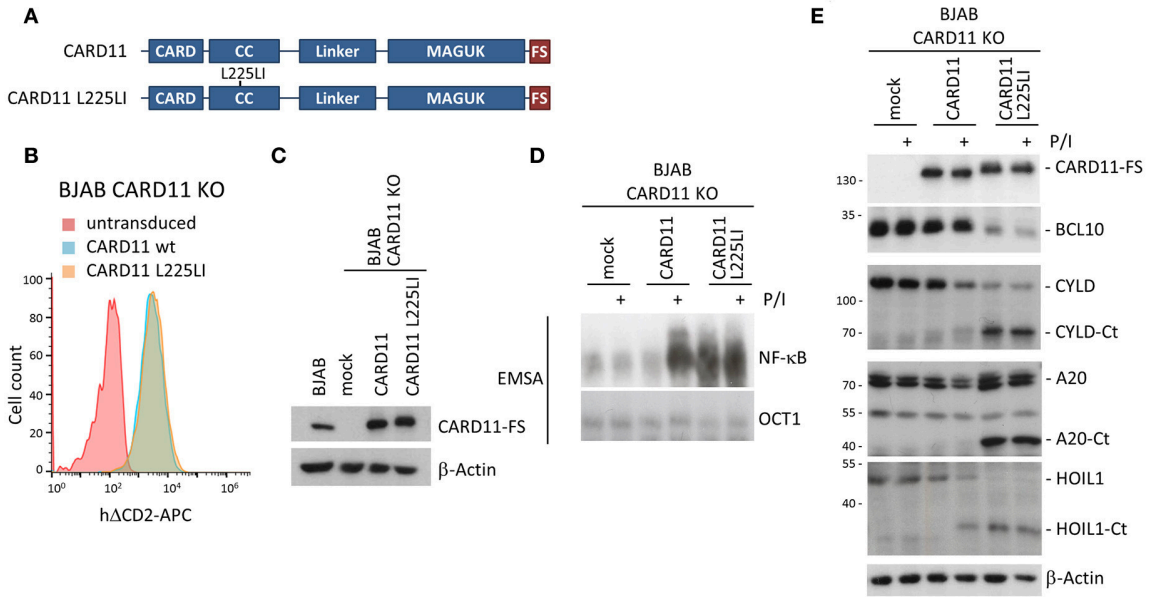

FIGURE 5 | Rescue of CARD11 KO BJAB B cells by CARD11 WT and oncogenic CARD11 L225LI. **(A)** Schematic representation of CARD11 and CARD11 L225LI proteins. **(B)** Transduction of CARD11 KO BJAB B cells with CARD11 or CARD11 L225LI expressing lentiviruses was analyzed by the surface marker ΔCD2 using FACS. **(C)** CARD11 and CARD11 L225LI protein expression, compared to parental BJAB B cells, was determined by WB. **(D)** CARD11 KO BJAB B cells after reconstitution with CARD11 WT or oncogenic CARD11 L225LI were analyzed for NF-κB activation after P/I stimulation (30 min) by EMSA. **(E)** MALT1 protease activity upon P/I stimulation (30 min) in CARD11 KO BJAB B cells reconstituted with CARD11 or CARD11 L225LI was determined by CYLD, A20, and HOIL1 cleavage on WB.

the oncogenic mutation (B10 R228A-C11 R35A/L225LI) was hardly detectable (**Figure 6C lane 5**). However, just like in Jurkat T cells, the B10 R228A-C11 fusion induced strong constitutive MALT1 activation, as evident from CYLD, HOIL1 and A20 cleavage, which strictly relied upon the BCL10 CARD interface (**Figure 6D**). Furthermore, the BCL10-CARD11 fusion combined with the oncogenic mutation L225LI (B10 R228A-C11 R35A/L225LI) induced MALT1 activation, despite its very low expression in the BJAB B cells. Again, constitutive MALT1 activation in the oncogenic BCL10-CARD11 fusion required BCL10 oligomerization, but was independent of the CARD11 CARD (**Figure 6D**).

Further, the fusion of BCL10 to CARD11 was sufficient to induce constitutive NF-κB activation in the BJAB B cells that was not further enhanced by P/I treatment (**Figure 6E**). Constitutive NF-κB activation was equivalent to that induced by the oncogenic CARD11 variant L225LI (**Figure 5D**). Despite its very weak expression, the oncogenic fusion construct B10 R228A-C11 R35A/L225LI also induced strong NF-κB activation, suggesting that the combination of fusion with the oncogenic mutant can generate a super-activator that is capable of further boosting CBM signaling. The weak expression of the B10 R228A-C11 R35A/L225LI suggests that there is a strong counter-selection against expression of the hyper-active fusion protein. Again, the constitutive activation observed with expression of the fusion constructs was solely driven by the BCL10 filament interface and was severely reduced in cells expressing the double CARD mutant B10 R42E/R228A-C11 R35A/L225LI. Finally, we confirmed that the fusion constructs also induce NF-κB-dependent gene expression by demonstrating that the prototype NF-κB target gene, NFKBIA/IκBα, is upregulated to a similar degree in the BJAB B cells expressing either CARD11 L225LI or the activating B10-C11 fusion constructs (**Figure 6F**). Thus, with respect to signaling, the fusion of BCL10 to CARD11 acts like an oncogenic CARD11 variant in B cells, through oligomerization of the BCL10 CARD interface.

DISCUSSION

BCL10 CARD filaments are formed *in vitro* and the molecular architecture of these clusters has been elucidated by cryo-electron microscopy (11, 13, 14). Although it is possible for BCL10 filaments to form in the absence of CARD11, the CARD of CARD11 appears to promote the initiation of BCL10 clustering in a cell free system. Further, CARD11 is solely located at the tip of the BCL10 filaments, lending support to the hypothesis that CARD11 functions as the molecular seed for BCL10 oligomerization (11, 13). Structure-guided missense mutations in the CARDs of CARD11 or BCL10 have been generated to show that destruction of putatively homotypic (BCL10-BCL10) or heterotypic (CARD11-BCL10) CARD-CARD interactions impedes NF-κB signaling and MALT1 protease activation after overexpression in cells (13, 14).

The functional impact of missense mutations in the CARDs of CARD11 or BCL10 on stimulus-dependent CBM complex signaling has not been thoroughly investigated. By reconstituting CARD11 or BCL10 KO Jurkat T cells, we assessed how destruction of putative CARD11-BCL10 or BCL10-BCL10 interfaces would affect signaling when expressed at endogenous levels. As expected, the CARD11 mutation R35A prevented T

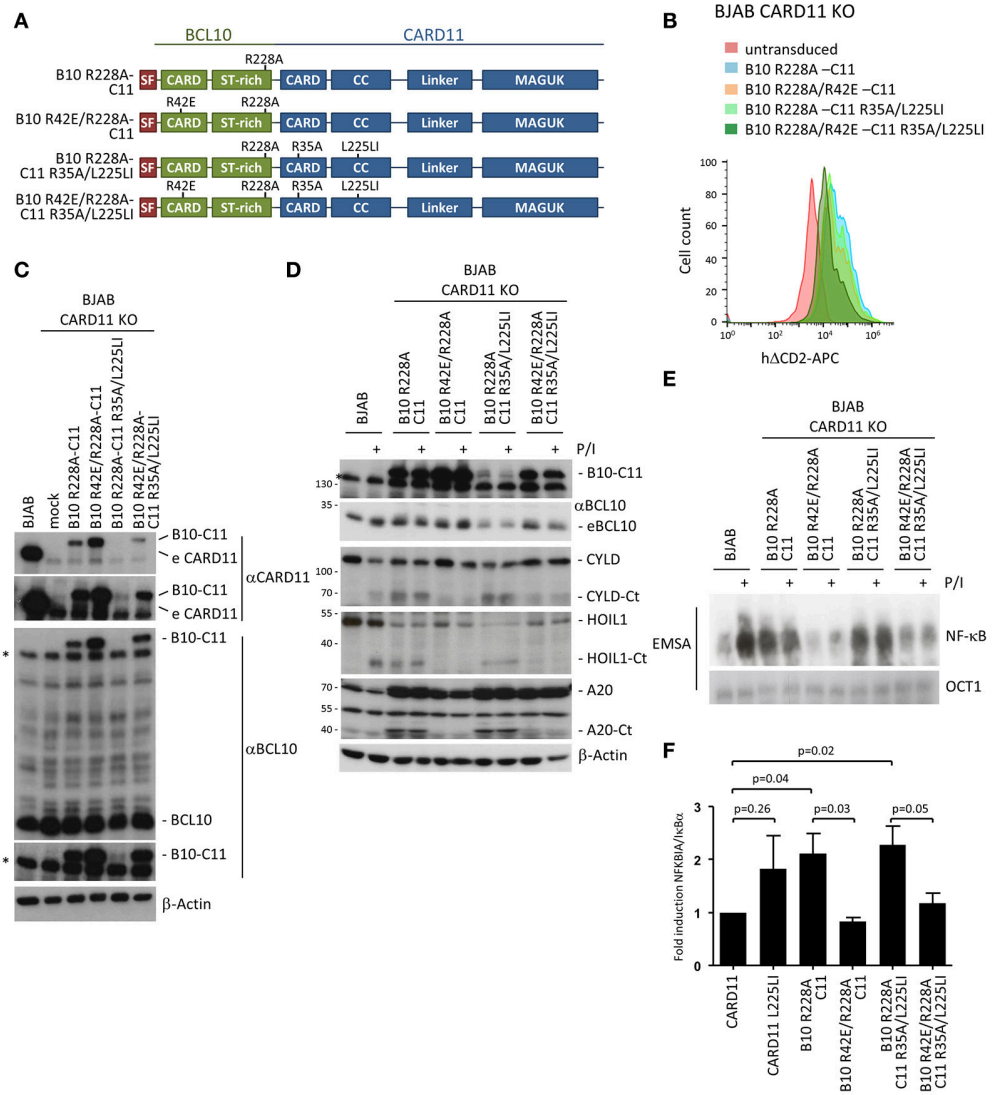

FIGURE 6 | Constitutive NF-κB and MALT1 activation by an oncogenic BCL10-CARD11 fusion protein relies on the BCL10 CARD interface in BJAB B cells. **(A)** Schematic representation of BCL10-CARD11 (B10-C11) fusion proteins containing CARD and oncogenic coiled-coil (CC) mutations. **(B)** Transduction of CARD11 KO BJAB B cells with B10 R228A-C11 fusion constructs, as depicted, was analyzed for the ΔCD2 surface marker by FACS. **(C)** Protein expression of the fusion constructs compared to parental BJAB B cells was determined by WB. **(D)** CARD11 KO BJAB B cells were reconstituted with B10 R228A-C11 fusion proteins as indicated. Constitutive and P/I-inducible (30 min) MALT1 activity was detected by CYLD, A20, and HOIL1 cleavage. **(E)** CARD11 KO BJAB B cells were reconstituted as in **(D)** and NF-κB activity was analyzed by EMSA. **(F)** Expression of the NF-κB target gene NFKBIA/IκBα in CARD11 and B10 R228A-C11 expressing BJAB B cells was determined by quantitative RT-PCR. All values were normalized to the housekeeping gene RPII and related to CARD11 (mean ± s.e.m, *p*-values as indicated).

cell stimulation due to its inability to recruit BCL10 (12, 25). In addition, the BCL10-BCL10 interface mutant R42E could not rescue NF-κB signaling in BCL10 KO cells, which confirms the critical function of BCL10-BCL10 interface I for filament assembly and signaling (13). Recently, we have been able to solve the architecture of the BCL10-MALT1 filaments using cryo-EM (14). Surprisingly, we found that different mutations in the interface I that lead to loss of BCL10 filament assembly also abolished CARD11 recruitment of BCL10 and thus CBM complex formation (14). Thus, our results question if CARD11 acts as the seed to nucleate BCL10 filaments, or whether an initial oligomerization of BCL10 is required for the recruitment to CARD11 in cells. Alternatively, our data would also be in line with a model in which CARD11-BCL10 association, but not BCL10 oligomerization, is critical to promote signaling in lymphocytes, and that filament formation is only observed with recombinant BCL10 or after high overexpression of BCL10.

To clarify the necessity of the CARD11 seed and BCL10 filaments for T and B cell activation, we fused BCL10 to CARD11 to bypass the initial step of heterotypic CARD-CARD interaction between CARD11 and BCL10. Even though this is an artificial system, it provided the first opportunity to examine

the contribution of the individual CARDs in CARD11 and BCL10. Remarkably, stable expression of the BCL10-CARD11 fusion protein promoted strong and chronic MALT1 protease activity in Jurkat T cells. While NF-κB activation was blunted in transduced Jurkat T cells, the transient transfection of BCL10-CARD11 activated NF-κB to a similar extent as an oncogenic CARD11 variant or CARD11 lacking the negative regulatory linker region (CARD11 Δlinker) (5, 6, 21). Interestingly, the BCL10-CARD11 fusion is not prone to auto-inhibition by the CARD11 linker, which acts as an inhibitory domain (27). In the fusion protein the BCL10 CARD is exposed and most likely not accessible for the CARD11 linker, especially when considering that an additional CARD cannot be bound by the linker in a 1:1 stoichiometry. Moreover, CARD11 and BCL10 CARDs are homologous, but also quite distinct and the BCL10 CARD may complex with the CARD11 linker, which would be critical for auto-inhibition (5, 27). Despite the disrupted auto-inhibition, the BCL10-CARD11 fusion protein signals to NF-κB via MALT1 and the TRAF6 binding motif on MALT1, underscoring that it utilizes the same mechanisms as a physiological CBM complex following T cell activation.

Despite the structural elucidation of BCL10-MALT1 filaments *in vitro*, the nature and relevance of cellular BCL10 oligomeric structures has not been fully resolved. BCL10 tends to aggregate via its CARD into oligomeric clusters and extended filaments after overexpression in cells (7, 9). Endogenous BCL10 forms oligomeric structures in antigen-stimulated T cells termed POLKADOTS ("punctuated and oligomeric killing or activating domains transducing signals"), which are cellular foci that serve as functional platforms for recruiting NF-κB signaling mediators following TCR stimulation (10, 28). Size exclusion chromatography demonstrated that in stimulated Jurkat T cells or ABC DLBCL tumor cells CARMA1, BCL10, and MALT1 assemble into higher order complexes with an apparent molecular weight >1 Mio. Da and the purified CBM complex displayed a filament-like structure in electron microscopy (13, 29). However, by increasing the concentration of BCL10 during the process of CBM purification, BCL10 filament formation may be initiated *in vitro* rather than taking place in living cells. Thus, there is good evidence that BCL10 can cluster via the CARD in cells, but the existence of large helical BCL10 filaments under physiological conditions in antigen-stimulated T or B cells has not been formally demonstrated. Since it may be difficult to imagine that the BCL10-CARD11 fusion itself can form long filaments in the absence of endogenous BCL10, activation by the fusion in BCL10 KO cells may indicate that BCL10-dependent dimerization or short oligomerization may be sufficient for lymphocyte activation. As for endogenous CARD11-associated BCL10, monitoring of BCL10 filament formation in the context of BCL10-CARD11 fusion is difficult with current methods, because of low expression levels. High resolution imaging techniques will be necessary to solve the extent of oligomerization and the cellular architecture of the BCL10 clusters. However, so far imaging in lymphocytes has been hampered by the unavailability of high quality antibodies as well as the small and round-shaped T and B cells that contain very little cytoplasm.

An important question that remains is the *in vivo* necessity for the formation of large, extended BCL10 filaments for signal propagation. The lack of NF-κB and MALT1 activation in BCL10 R42E in the context of the BCL10-CARD11 fusion reflects the need for BCL10 dimerization/oligomerization, but does not prove the requirement for higher order filaments. Alternatively, BCL10-MALT1 recruitment to CARD11 and BCL10 dimerization or short oligomers may be sufficient to facilitate cellular processes such as ubiquitination of CBM complex components. A number of ubiquitin ligases [e.g., TRAF6, LUBAC (linear ubiquitin chain assembly complex) and cIAP2] are recruited to the CBM complex and conjugation of mono-ubiquitin or poly-ubiquitin chains of different topology on all subunits has been implicated in triggering MALT1 activation and/or downstream signaling (1, 2). The complexity of ubiquitin-dependent regulation is exemplified by BCL10. K48-, K63-, or M1-linked ubiquitin chains are primarily conjugated on K17, K31, and/or K63 in the BCL10 CARD (30–32). Ubiquitination of these lysine residues is required for NF-κB activation in T cells and pro-survival signaling in ABC DLBCL cells (31–33). Deficiency in HOIP/RNF31, the catalytic subunit of LUBAC, suppresses NF-κB signaling in Jurkat T cells whereas HOIP activating mutations enhance NF-κB-dependent pro-survival in ABC DLBCL cells, supporting that M1-linked ubiquitin chains on BCL10 are enhancing CBM complex signaling (32, 34). However, at the same time BCL10 is degraded by lysosomal or proteasomal pathways and these processes are controlled by at least partially overlapping ubiquitination sites (31, 35–37). In addition, K48-linked poly-ubiquitination of CARD11 induces its degradation (38). Thus, the BCL10-CARD11 fusion protein is most likely strongly affected by regulatory ubiquitination and ubiquitin conjugation in each moiety may be responsible for activation, as well as the high turnover of the active BCL10-CARD11 fusions. Due to the multi-layered ubiquitin regulation and the uneven expression levels of active vs. inactive BCL10-CARD11 fusions, this system is not an ideal tool to study the relevance of BCL10 ubiquitination. However, it will be important to clarify in how far BCL10 oligomerization and potential filament formation cooperate with ubiquitination processes to induce downstream signaling or alternatively, if BCL10 ubiquitination may also facilitate CBM complex assembly.

In BJAB B cells stable BCL10-CARD11 expression activates MALT1 and NF-κB as strong as oncogenic variants of CARD11 derived from DLBCL tumor patients (5, 6, 25, 26), clearly showing that the proximity of BCL10 and CARD11 alone is sufficient to activate downstream signaling pathways. Thus, the BCL10-CARD11 fusion already provides compelling evidence that CARD11 acts as a seed in cells to boost lymphocyte activation. By introducing point mutations we were also now able to unravel the contribution of the two different CARD interfaces. Constitutive activity of the BCL10-CARD11 fusion no longer required the presence of an intact CARD11 CARD, but was solely driven by the BCL10 oligomerization interface. In contrast, stimulus-dependent MALT1 activation of the BCL10-CARD11 fusion protein relied on an intact CARD11 CARD, which most likely as in CARD11 WT serves as a platform for recruitment and oligomerization of endogenous BCL10.

Interestingly, introduction of the active oncogenic mutation L225LI into the CARD11 coiled-coil (CC) region in the context of the BCL10-CARD11 resulted in a fusion protein that was hyper-active, despite the very low expression level in the BJAB B cells. Indeed, all active BCL10-CARD11 fusion proteins were expressed at a lower level compared to their inactive counterparts. However, the very low expression of the hyper-active fusion constructs indicates that there is a strong counter-selection against the expression of these constitutively active variants in T and B cells. Since all fusions constitutively activate the MALT1 paracaspase in the two cell types, it is possible that the sustained MALT1 cleavage of mRNA processing factors Regnase-1 and Roquin1/2 may exert toxic effects that impair T and B cell survival (39, 40). More work is needed to understand under which circumstances chronic activation induces cell survival or toxicity.

While expression of BCL10-CARD11 fusion drives NF-κB activation in BJAB B cells, constitutive and inducible NF-κB signaling is severely impaired in Jurkat T cells expressing the fusion protein. Even though NF-κB activation is impaired in Jurkat T cells, MALT1 protease is still strongly activated by BCL10-CARD11 fusions, demonstrating that not all CBM downstream effects are affected. Further, the reduced responsiveness relies on the stable expression of the BCL10-CARD11 fusion protein and it needs to be explored what cell-intrinsic mechanisms operate in Jurkat T cells that counteract constitutive activation of the canonical NF-κB pathway downstream of the CBM complex. Of note, T lymphocytes from patients with germline activating CARD11 mutations are anergic, while the B cells are activated and expanding, causing a phenotype called BENTA (B cell expansion with NF-κB and T cell anergy) (41, 42). It will be interesting to see whether similar negative regulatory mechanisms observed in Jurkat T cells driven by an active BCL10-CARD11 fusion could also operate in primary T cells.

Our data suggest that upon the initial BCL10 recruitment to CARD11, the weak heterotypic interaction of the monomeric CARDs needs to be stabilized by further interactions arising from the oligomerized CARD11 seed and the helical BCL10 filaments. The additional contact points within this multimeric complex are essential for a high affinity binding and the formation of a stable CBM complex that is competent to trigger downstream signaling. Furthermore, the structural rigidity in the core BCL10-MALT1 filament may stabilize the binding, which is in line with the observation that CARD11 binding is also reduced when BCL10 is not complexed with MALT1 (14). In conclusion, we demonstrate that the recruitment of BCL10-MALT1 to CARD11 and BCL10-MALT1 filament formation are highly interconnected processes that cooperate to drive CBM downstream effects in response to physiological or pathological activation of T and B cells.

MATERIALS AND METHODS

Cell Lines and Treatments

Cell lines were maintained at 37°C in a humidified atmosphere at 5% CO_2. Jurkat T cells and BJAB B cells were cultured in RPMI 1640 Medium, and U2OS and HEK293T cells in DMEM. Media were supplemented with 10% (Jurkat T cells, U2OS, HEK293T) or 15% (BJAB B cells) fetal calf serum, 100 U/ml penicillin and 100 μg/ml streptomycin. U2OS, HEK293T and BJAB B cells were obtained from the DSMZ, Jurkat T cells were authenticated by the Authentication Service of the Leibniz Institute DSMZ. Jurkat T cells were stimulated with Phorbol 12-Myristate 13-Acetate (PMA: 200 ng/ml; Merck) and Ionomycin (300 ng/ml; Calbiochem) for 30 min, except if otherwise stated.

DNA Constructs and Antibodies

DNA constructs and antibodies used in this study are listed in **Tables 1, 2**, respectively.

Generation and Reconstitution of Knock-Out Cells

Bicistronic expression vector px458 expressing Cas9 and sgRNA (45, 46) was digested with *BbsI* and the linearized vector

TABLE 1 | DNA constructs.

pHAGE-ΔCD2-T2A	Lentiviral transfer vector used (43)
pMD2.G	Lentiviral packaging construct (Addgene: Plasmid #12259)
psPAX2	Lentiviral packaging construct (Addgene: Plasmid #12260)
pHAGE-ΔCD2-T2A-SF	Lentiviral transfer vector (mock)
CARD11-FS constructs	CARD11, CARD11 R35A, and CARD11 L225LI in pHAGE-ΔCD2-T2A (25)
BCL10-FS constructs	BCL10 and BCL10 R42E in pHAGE-ΔCD2-T2A
SF-BCL10-CARD11 (B10-C11) constructs	CARD11 and CARD11 mutants (R35A, R35A/L225LI) in SF-BCL10, SF-BCL10 R42E, SF-BCL10 R228A, or SF-BCL10 R42E/R228A containing pHAGE-ΔCD2-T2A
pGL3-6xNF-κB luc	NF-κB reporter firefly luciferase (44)
pRL-TKluc	TK reporter renilla luciferase (Promega)

TABLE 2 | Antibodies.

Primary antibodies	**Source**
A20/TNFAIP3 (D13H3)	Cell Signaling
BCL10 (C-17)	Santa Cruz
BCL10 (H-197)	Santa Cruz
CARMA1/CARD11 (1D12)	Cell Signaling
CYLD (E-10)	Santa Cruz
HOIL-1 (S150D)	MRC
IκBα (L35A5)	Cell Signaling
IκBα (phospho-Ser32/36) (5A5)	Cell Signaling
MALT1 (B-12)	Santa Cruz
StrepTagII	IBA
β-Actin (I-19)	Santa Cruz
anti-CD2-APC (RPA-2.10)	eBioscience
Secondary antibodies	**Source**
HRP-conjugated anti-goat	Jackson ImmunoResearch
HRP-conjugated anti-mouse	Jackson ImmunoResearch
HRP-conjugated anti-rabbit	Jackson ImmunoResearch
HRP-conjugated anti-sheep	Jackson ImmunoResearch
Alexa Fluor488-donkey anti-mouse	Invitrogen

was gel purified. Targeting oligos (CARD11: 5′CTCATCA ATGACCTTACACTGACGCAGGTAGG 3′BCL10: 5′AGT GAGGTCCTCCTCGGTGA 3′and 5′TTCCGCTTTCGTCTC CCGCT 3′) for each targeting site positioned as depicted in **Supplementary Figures 2A,B,** were annealed and ligated to the linearized vector. Jurkat T cells or BJAB B cells (4–8 × 10^6) were electroporated (220 V and 1,000 μF) using a Gene pulser X (Biorad) with px458 plasmids expressing sgRNA targeting CARD11 or BCL10, as well as a EGFP expression cassette. Twenty-four to forty-eight hours after electroporation, GFP positive cells were sorted using a MoFlow sorting system. Isolation of clonal cell lines was achieved by serial dilutions and was followed by an appropriate expansion period. KO cell clones were initially identified by detecting CARD11 or BCL10, respectively, by Western Blot. Clones lacking protein expression were genotyped by genomic PCR using intronic primers flanking targeting sides.

For reconstitution, lentivirus was produced in HEK293T cells. 1 × 10^6 HEK293T cells were seeded in 8 ml DMEM medium (10% FCS, 1% Pen/Strep) in 10 cm^2 dishes and grown overnight at 37°C. The next day, the cells were transfected with 1.5 μg of the packaging vector psPAX2, 1.0 μg of the lentiviral envelope plasmid pMD2.G and 2 μg pHAGE transfer vector using X-tremeGENE HP DNA Transfection Reagent (Roche) according to the manufacturer's protocol. After 3 days the supernatant of the HEK293T cells containing the virus was sterile filtered (0.45 μm). For transduction, virus supernatant was transferred to 5 × 10^5 Jurkat T cells or BJAB B cells. For BJAB B cells, supernatant was concentrated with Amicon centrifugal filter units (100 K) prior to transduction. The solution was filled up with RPMI medium (10% FCS, 1% Pen/Strep) to a final volume of 2–2.5 ml and mixed with Polybrene (8 μg/ml). To enhance transduction efficiency, BJABs were centrifuged for 1 h at 500 × g. Forty to seventy-two hours later, cells were washed with PBS (without calcium and magnesium) and re-suspended in 1–2 ml RPMI medium (10% FCS, 1% Pen/Strep). Seven to ten days after transduction infection was analyzed by determining ΔCD2 surface expression by FACS and CARD11 or BCL10 protein expression by Western Blot. Only cells yielding a transduction efficiency of >90% as determined by FACS analysis, were used for further analyses.

Generation and reconstitution of MALT1-deficient Jurkat T cells has been described (22).

Flow Cytometry (FACS)

Surface expression of ΔCD2 after lentiviral transduction of BJAB B cells or Jurkat T cells was assessed by incubating 200 μl of the cell culture for 15 min at room temperature with 2 μl anti-CD2-APC (RPA-2.10) antibody. Cells were centrifuged (1,100 rpm, 5 min) and re-suspended in 250 μl PBS before FACS using Attune Acoustic Focusing Flow Cytometer.

Cell Lysis and Precipitations

For analysis of expression via Western Blot or EMSA, cells (1–3 × 10^6) were harvested (300 × g, 5 min, 4°C) and washed once with ice cold PBS. The pellet was resuspended in 80–100 μl high salt buffer (20 mM HEPES pH 7.9, 350 mM NaCl, 20% glycerol, 1 mM $MgCl_2$, 0.5 mM EDTA, 0.1 mM EGTA, 1% NP-40, 1 mM DTT, 10 mM sodium fluoride, 8 mM β-glycerophosphate, 300 μM sodium vanadate and Roche protease inhibitor cocktail). For binding studies, cells (1–5 × 10^7) were lysed in co-IP buffer (25 mM HEPES pH 7.5, 150 mM NaCl, 0.2% NP-40, 10% glycerol, 1 mM DTT, 10 mM sodium fluoride, 8 mM β-glycerophosphate, 300 μM sodium vanadate and protease inhibitor cocktail). Lysate controls were mixed with 4xSDS loading dye and boiled. For StrepTactin pull-downs (ST-PD), 20–40 μl Strep-Tactin Sepharose (1:1 suspension) was used for binding of Strep-tagged BCL10 or BCL10-CARD11 fusion overnight at 4°C rotating. Sepharose beads were pelleted after incubation (100 × g, 4 min, 4°C), washed 3x with co-IP buffer, and boiled after the addition of 20 μl 2xSDS loading dye (Roti-load). Lysates and ST-PDs were separated by SDS-PAGE and analyzed by Western Blot.

Western Blot

Proteins were transferred onto PVDF-membranes for immunodetection using an electrophoretic semi-dry transfer system. After transfer, membranes were blocked with 5% BSA for 1 h at RT and incubated with specific primary antibodies (indicated above, diluted 1:1,000 in 2.5% BSA/PBS-T) overnight at 4°C. Membranes were washed in PBS-T before the addition of HRP-coupled secondary antibodies (indicated above, 1:7,000 in 1.25% BSA in PBS-T; 1 h, RT). HRP was detected by enhanced chemiluminescence (ECL) using the LumiGlo reagent (Cell Signaling) according to manufacturer's instructions.

Electrophoretic Mobility Shift Assay (EMSA)

For EMSAs, double-stranded NF-κB (H2K: fw: 5′-GATCCA GGGCTGGGGATTCCCCATCTCCACAGG-3′, rev: 5′- GAT CCCTGTGGAGATGGGGAATCCCCAGCCCTG-3′), and OCT1 binding sequences (fw: 5′- GATCTGTCGAATGCA AATCACTAGAA-3′, rev: 5′-GATCTTCTAGTGATTTGCATT CGACA-3′) were labeled with [α-^{32}P] dATP using Klenow Fragment (NEB). To monitor DNA binding, whole cell lysates (3–6 μg) were incubated for 30 min at RT with shift-buffer [20 mM HEPES pH 7.9, 120 mM KCl, 4% Ficoll, 5 mM DTT, 10 μg BSA and 2 μg poly-dI-dC (Roche)] and radioactive double stranded NF-κB or OCT1 probes (10,000–20,000 cpm). Samples were separated on a 5% polyacrylamide gel in TBE buffer, vacuum-dried and exposed to autoradiography.

Confocal Immunofluorescence Microscopy

The localization and distribution of BCL10 was analyzed by seeding U2OS cells in 96-well plates. Cells were transfected using Lipofectamine 3000 Transfection Reagent (Invitrogene) according to the manufacturer's instructions. To optimize cell attachment, CellCarrier-96 black plates (PerkinElmer) were coated with 100 μl poly-D-lysine at a concentration of 50 μg/ml. Twenty-four hours after transfection, cells were washed with PBS and fixed with 60 μl Methanol (−20°C) for 5–10 min at room temperature and then washed 3x with PBS. For immunostaining, cells were blocked in 2% BSA in PBS. Cells were incubated with primary antibody (anti-StrepTagII) in blocking buffer for 2 h at RT. Cells were washed 3x for

10 min at RT, before incubation with secondary antibody (Alexa Fluor488-donkey anti-mouse) in blocking buffer for 1 h at RT. Cell nuclei were visualized by incubation with Hoechst 33342 dye (Life Technologies) in PBS at a concentration of 0.5 μg/ml for 30 min at RT. Afterwards the cells were washed and covered with PBS, sealed with foil and kept at 4°C in the dark until microscopy. Confocal microscopy was performed with an Operetta high-content imaging system (Perkin-Elmer).

Labeling and Biotin Pull-Down (PD) of Active MALT1

The biotin-labeled MALT1 activity based probe (MALT1-ABP) has been described previously (19). To investigate MALT1 protease activity, Jurkat T cells (3 x 10^7) were washed with PBS, and lysed in 600 μl co-IP buffer without protease inhibitors for 30 min at 4°C. After clearing the lysates by centrifugation (20,000 × g, 4°C, 15 min), 30 μl were collected as lysate control, mixed with 4x SDS loading buffer and boiled for 5 min at 95°C. To 550 μl of the supernatant 12 μl High Capacity Streptavidin Beads (Thermo Fisher) was added and incubated for 1 h at 4°C for pre-clearing. The beads were pelleted (4,000 rpm, 2 min, 4°C) and 450 μl of supernatant was mixed with MALT1-ABP probe (0.1 μM final concentration). After 1 h rotating at room temperature, 15 μl High Capacity Streptavidin Beads was added before 1–2 h incubation at 4°C (rotating). Beads were collected and washed 3x with co-IP buffer without protease inhibitors. Beads were re-suspended in 22 μl 2x SDS loading buffer and boiled at 95°C for 7 min before SDS-PAGE and Western Blot analysis.

NF-κB Reporter Assay

For NF-κB luciferase reporter assays, 8 × 10^6 Jurkat cells were transfected by electroporation with 2 μg NF-κB firefly luciferase reporter plasmid, 1 μg renilla luciferase and 6 μg of CARD11 and BCL10-CARD11 fusion constructs using 220 V and 1,000 μF (Gene Pulser X, BioRad). After cultivation for 72 h cells were lysed in passive lysis buffer and luciferase activity measured using a dual luciferase reporter kit according to the manufacturer's protocol (Promega). All luciferase values were calculated in relation to the Renilla control.

Quantitative Reverse-Transcriptase Polymerase Chain Reaction (qRT-PCR)

RNA was isolated (QIAGEN RNeasy Kit) and equal amounts of RNA (InviTrap Spin Universal RNA Mini Kit, 1060100200, Stratec) were transcribed into cDNA using the Verso cDNA synthesis Kit (AB1453B, Thermo Fisher Scientific). Quantitative real-time (qRT) PCR was performed using KAPA SYBR FAST qPCR Master Mix (KAPA Biosystems) and standard LightCycler protocol on a Roche LightCycler 480. RNA Polymerase II (PolII) served as internal standard. The following primers were used: fw: 5′-CCGCACCTCCACTCCATCC-3′ rev: 5′-ACATCAGCACCC AAGGACACC-3′; RPII fw: 5′-GCACCACGTCCAATGACA-3′ rev: 5′-GTGCGGCTGCTTCCATAA-3′. Results represent the mean and standard error of the mean of three independent experiments.

Structural Model of CARD11-BCL10 and BCL10-BCL10 Interaction Surfaces

The CARD11-BCL10 CARD/CARD interaction model was prepared under consideration of the surface charge complementarity analysis of the BCL10-MALT1 filament cryo EM structure (EMD-0013, PDB 6GK2) and the crystal structure of the CARD11 domain (PDB 4LWD) (**Supplementary Figure 1**). The CARD11 CARD structure has been superimposed on the BCL10 CARD within the BCL10-MALT1 filament using the align command in PyMOL (The PyMOL Molecular Graphics System, Version 2.0 Schrödinger, LLC). Under consideration that the mutation of residue R35 in CARD11 abolishes the interaction to BCL10 (12), we propose that the mainly positively charged top of the CARD11 CARD interacts with the negatively charged bottom of the Bcl10 filament (**Supplementary Figures 1B,C**). The electrostatic surface was calculated with the program APBS Tool 2.1 implemented in PyMOL (47).

Statistical Analysis

Data for luciferase reporter assay, quantitative RT-PCR and fluorescence microscopy was analyzed for statistical significance using the unpaired Student's *t*-test ($^{**}p \leq 0.01$, $^{***}p \leq 0.001$). Sample size (n) is specified for each experiment and data are shown as mean ± s.e.m.

AUTHOR CONTRIBUTIONS

TS and SK conceived and performed most experiments, analyzed, and interpreted the data. FS and KL conceived and performed biophysical experiments and provided structural expertise. SW, TG, and SWi generated, verified and analyzed KO cells. DK conceived the study, experiments, wrote the manuscript, and secured funding. All authors read, acknowledged, and helped with the final version of the manuscript.

FUNDING

Deutsche Krebshilfe (grant no. 70112622) to DK supported work on oncogenic CARD11 signaling. Deutsche Forschungsgemeinschaft SFB 1054 TP A04 to DK and TP B02 to KL supported structural and mechanistic work on CBM complex signaling in T cells.

ACKNOWLEDGMENTS

We thank Katrin Demski and Kerstin Kutzner for excellent technical assistance.

SUPPLEMENTARY MATERIAL

The Supplementary Material for this article can be found online at: https://www.frontiersin.org/articles/10.3389/fimmu.2018.02695/full#supplementary-material

REFERENCES

1. Juilland M, Thome M. Role of the CARMA1/BCL10/MALT1 complex in lymphoid malignancies. *Curr Opin Hematol.* (2016) 23:402–9. doi: 10.1097/MOH.0000000000000257
2. Meininger I, Krappmann D. Lymphocyte signaling and activation by the CARMA1-BCL10-MALT1 signalosome. *Biol Chem.* (2016) 397:1315–33. doi: 10.1515/hsz-2016-0216
3. Matsumoto R, Wang D, Blonska M, Li H, Kobayashi M, Pappu B, et al. Phosphorylation of CARMA1 plays a critical role in T Cell receptor-mediated NF-kappaB activation. *Immunity* (2005) 23:575–85. doi: 10.1016/j.immuni.2005.10.007
4. Sommer K, Guo B, Pomerantz JL, Bandaranayake AD, Moreno-Garcia ME, Ovechkina YL, et al. Phosphorylation of the CARMA1 linker controls NF-kappaB activation. *Immunity* (2005) 23:561–74. doi: 10.1016/j.immuni.2005.09.014
5. Lamason RL, McCully RR, Lew SM, Pomerantz JL. Oncogenic CARD11 mutations induce hyperactive signaling by disrupting autoinhibition by the PKC-responsive inhibitory domain. *Biochemistry* (2010) 49:8240–50. doi: 10.1021/bi101052d
6. Lenz G, Davis RE, Ngo VN, Lam L, George TC, Wright GW, et al. Oncogenic CARD11 mutations in human diffuse large B cell lymphoma. *Science* (2008) 319:1676–9. doi: 10.1126/science.1153629
7. Bertin J, Wang L, Guo Y, Jacobson MD, Poyet JL, Srinivasula SM, et al. CARD11 and CARD14 are novel caspase recruitment domain (CARD)/membrane-associated guanylate kinase (MAGUK) family members that interact with BCL10 and activate NF-kappa B. *J Biol Chem.* (2001) 276:11877–82. doi: 10.1074/jbc.M010512200
8. Gaide O, Martinon F, Micheau O, Bonnet D, Thome M, Tschopp J. Carma1, a CARD-containing binding partner of Bcl10, induces Bcl10 phosphorylation and NF-kappaB activation. *FEBS Lett.* (2001) 496:121–7. doi: 10.1016/S0014-5793(01)02414-0
9. Guiet C, Vito P. Caspase recruitment domain (CARD)-dependent cytoplasmic filaments mediate bcl10-induced NF-kappaB activation. *J Cell Biol.* (2000) 148:1131–40. doi: 10.1083/jcb.148.6.1131
10. Schaefer BC, Kappler JW, Kupfer A, Marrack P. Complex and dynamic redistribution of NF-kappaB signaling intermediates in response to T cell receptor stimulation. *Proc Natl Acad Sci USA.* (2004) 101:1004–9. doi: 10.1073/pnas.0307858100
11. David L, Li Y, Ma J, Garner E, Zhang X, Wu H. Assembly mechanism of the CARMA1-BCL10-MALT1-TRAF6 signalosome. *Proc Natl Acad Sci USA.* (2018) 115:1499–504. doi: 10.1073/pnas.1721967115
12. Li S, Yang X, Shao J, Shen Y. Structural insights into the assembly of CARMA1 and BCL10. *PLoS One* (2012) 7:e42775. doi: 10.1371/journal.pone.0042775
13. Qiao Q, Yang C, Zheng C, Fontan L, David L, Yu X, et al. Structural architecture of the CARMA1/Bcl10/MALT1 signalosome: nucleation-induced filamentous assembly. *Mol Cell* (2013) 51:766–79. doi: 10.1016/j.molcel.2013.08.032
14. Schlauderer F, Seeholzer T, Desfosses A, Gehring T, Strauss M, Hopfner K-P, et al. Molecular architecture and regulation of BCL10-MALT1 filaments. *Nat Commun.* (2018) 9:4041. doi: 10.1038/s41467-018-06573-8
15. Egawa T, Albrecht B, Favier B, Sunshine MJ, Mirchandani K, O'Brien W, et al. Requirement for CARMA1 in antigen receptor-induced NF-kappa B activation and lymphocyte proliferation. *Curr Biol.* (2003) 13:1252–8. doi: 10.1016/S0960-9822(03)00491-3
16. Hara H, Wada T, Bakal C, Kozieradzki I, Suzuki S, Suzuki N, et al. The MAGUK family protein CARD11 is essential for lymphocyte activation. *Immunity* (2003) 18:763–75. doi: 10.1016/S1074-7613(03)00148-1
17. Ruland J, Duncan GS, Elia A, del Barco Barrantes I, Nguyen L, Plyte S, et al. Bcl10 is a positive regulator of antigen receptor-induced activation of NF-kappaB and neural tube closure. *Cell* (2001) 104:33–42. doi: 10.1016/S0092-8674(01)00189-1
18. Jaworski M, Thome M. The paracaspase MALT1: biological function and potential for therapeutic inhibition. *Cell Mol Life Sci.* (2016) 73:459–73. doi: 10.1007/s00018-015-2059-z
19. Eitelhuber AC, Vosyka O, Nagel D, Bognar M, Lenze D, Lammens K, et al. Activity-based probes for detection of active MALT1 paracaspase in immune cells and lymphomas. *Chem Biol.* (2015) 22:129–38. doi: 10.1016/j.chembiol.2014.10.021
20. Rebeaud F, Hailfinger S, Posevitz-Fejfar A, Tapernoux M, Moser R, Rueda D, et al. The proteolytic activity of the paracaspase MALT1 is key in T cell activation. *Nat Immunol.* (2008) 9:272–81. doi: 10.1038/ni1568
21. McCully RR, Pomerantz JL. The protein kinase C-responsive inhibitory domain of CARD11 functions in NF-kappaB activation to regulate the association of multiple signaling cofactors that differentially depend on Bcl10 and MALT1 for association. *Mol Cell Biol.* (2008) 28:5668–86. doi: 10.1128/MCB.00418-08
22. Meininger I, Griesbach RA, Hu D, Gehring T, Seeholzer T, Bertossi A, et al. Alternative splicing of MALT1 controls signalling and activation of CD4(+) T cells. *Nat Commun.* (2016) 7:11292. doi: 10.1038/ncomms11292
23. Chan W, Schaffer TB, Pomerantz JL. A quantitative signaling screen identifies CARD11 mutations in the CARD and LATCH domains that induce Bcl10 ubiquitination and human lymphoma cell survival. *Mol Cell Biol.* (2013) 33:429–43. doi: 10.1128/MCB.00850-12
24. Noels H, van Loo G, Hagens S, Broeckx V, Beyaert R, Marynen P, et al. A Novel TRAF6 binding site in MALT1 defines distinct mechanisms of NF-kappaB activation by API2middle dotMALT1 fusions. *J Biol Chem.* (2007) 282:10180–9. doi: 10.1074/jbc.M611038200
25. Bognar MK, Vincendeau M, Erdmann T, Seeholzer T, Grau M, Linnemann JR, et al. Oncogenic CARMA1 couples NF-kappaB and beta-catenin signaling in diffuse large B-cell lymphomas. *Oncogene* (2016) 35:4269–81. doi: 10.1038/onc.2015.493
26. Knies N, Alankus B, Weilemann A, Tzankov A, Brunner K, Ruff T, et al. Lymphomagenic CARD11/BCL10/MALT1 signaling drives malignant B-cell proliferation via cooperative NF-kappaB and JNK activation. *Proc Natl Acad Sci USA.* (2015) 112:E7230–8. doi: 10.1073/pnas.1507459112
27. Jattani RP, Tritapoe JM, Pomerantz JL. Intramolecular interactions and regulation of cofactor binding by the four repressive elements in the Caspase Recruitment Domain-containing Protein 11 (CARD11) inhibitory domain. *J Biol Chem.* (2016) 291:8338–48. doi: 10.1074/jbc.M116.717322
28. Rossman JS, Stoicheva NG, Langel FD, Patterson GH, Lippincott-Schwartz J, Schaefer BC. POLKADOTS are foci of functional interactions in T-cell receptor-mediated signaling to NF-kappaB. *Mol Biol Cell* (2006) 17:2166–76. doi: 10.1091/mbc.e05-10-0985
29. Oeckinghaus A, Wegener E, Welteke V, Ferch U, Arslan SC, Ruland J, et al. Malt1 ubiquitination triggers NF-kappaB signaling upon T-cell activation. *EMBO J.* (2007) 26:4634–45. doi: 10.1038/sj.emboj.7601897
30. Satpathy S, Wagner SA, Beli P, Gupta R, Kristiansen TA, Malinova D, et al. Systems-wide analysis of BCR signalosomes and downstream phosphorylation and ubiquitylation. *Mol Syst Biol.* (2015) 11:810. doi: 10.15252/msb.20145880
31. Wu CJ, Ashwell JD. NEMO recognition of ubiquitinated Bcl10 is required for T cell receptor-mediated NF-kappaB activation. *Proc Natl Acad Sci USA.* (2008) 105:3023–8. doi: 10.1073/pnas.0712313105
32. Yang YK, Yang C, Chan W, Wang Z, Deibel KE, Pomerantz JL. Molecular determinants of scaffold-induced linear ubiquitinylation of B cell lymphoma/leukemia 10 (Bcl10) during T cell receptor and oncogenic Caspase Recruitment Domain-Containing Protein 11 (CARD11) signaling. *J Biol Chem.* (2016) 291:25921–36. doi: 10.1074/jbc.M116.754028
33. Yang Y, Kelly P, Shaffer ALIII, Schmitz R, Yoo HM, Liu X, et al. Targeting non-proteolytic protein ubiquitination for the treatment of diffuse large B cell lymphoma. *Cancer Cell* (2016) 29:494–507. doi: 10.1016/j.ccell.2016.03.006
34. Yang Y, Schmitz R, Mitala J, Whiting A, Xiao W, Ceribelli M, et al. Essential role of the linear ubiquitin chain assembly complex in lymphoma revealed by rare germline polymorphisms. *Cancer Disc.* (2014) 4:480–93. doi: 10.1158/2159-8290.CD-13-0915
35. Lobry C, Lopez T, Israel A, Weil R. Negative feedback loop in T cell activation through IkappaB kinase-induced phosphorylation and degradation of Bcl10. *Proc Natl Acad Sci USA.* (2007) 104:908–13. doi: 10.1073/pnas.0606982104
36. Paul S, Kashyap AK, Jia W, He YW, Schaefer BC. Selective autophagy of the adaptor protein Bcl10 modulates T cell receptor activation of NF-kappaB. *Immunity* (2012) 36:947–58. doi: 10.1016/j.immuni.2012.04.008
37. Scharschmidt E, Wegener E, Heissmeyer V, Rao A, Krappmann D. Degradation of Bcl10 induced by T-cell activation negatively

regulates NF-kappa B signaling. *Mol Cell Biol.* (2004) 24:3860–73. doi: 10.1128/MCB.24.9.3860-3873.2004
38. Moreno-Garcia ME, Sommer K, Rincon-Arano H, Brault M, Ninomiya-Tsuji J, Matesic LE, et al. Kinase-independent feedback of the TAK1/TAB1 complex on BCL10 turnover and NF-kappaB activation. *Mol Cell Biol.* (2013) 33:1149–63. doi: 10.1128/MCB.06407-11
39. Jeltsch KM, Hu D, Brenner S, Zoller J, Heinz GA, Nagel D, et al. Cleavage of roquin and regnase-1 by the paracaspase MALT1 releases their cooperatively repressed targets to promote T(H)17 differentiation. *Nat Immunol.* (2014) 15:1079–89. doi: 10.1038/ni.3008
40. Uehata T, Iwasaki H, Vandenbon A, Matsushita K, Hernandez-Cuellar E, Kuniyoshi K, et al. Malt1-induced cleavage of regnase-1 in CD4(+) helper T cells regulates immune activation. *Cell* (2013) 153:1036–49. doi: 10.1016/j.cell.2013.04.034
41. Arjunaraja S, Nose BD, Sukumar G, Lott NM, Dalgard CL, Snow AL. Intrinsic plasma cell differentiation defects in B cell expansion with NF-kappaB and T cell anergy patient B cells. *Front Immunol.* (2017) 8:913. doi: 10.3389/fimmu.2017.00913
42. Snow AL, Xiao W, Stinson JR, Lu W, Chaigne-Delalande B, Zheng L, et al. Congenital B cell lymphocytosis explained by novel germline CARD11 mutations. *J Exp Med.* (2012) 209:2247–61. doi: 10.1084/jem.20120831
43. Hadian K, Griesbach RA, Dornauer S, Wanger TM, Nagel D, Metlitzky M, et al. NF-kappaB essential modulator (NEMO) interaction with linear and lys-63 ubiquitin chains contributes to NF-kappaB activation. *J Biol Chem.* (2011) 286:26107–17. doi: 10.1074/jbc.M111.233163
44. Bergmann M, Hart L, Lindsay M, Barnes PJ, Newton R. IkappaBalpha degradation and nuclear factor-kappaB DNA binding are insufficient for interleukin-1beta and tumor necrosis factor-alpha-induced kappaB-dependent transcription. Requirement for an additional activation pathway *J Biol Chem.* (1998) 273:6607–10. doi: 10.1074/jbc.273.12.6607
45. Cong L, Ran FA, Cox D, Lin S, Barretto R, Habib N, et al. Multiplex genome engineering using CRISPR/Cas systems. *Science* (2013) 339:819–23. doi: 10.1126/science.1231143
46. Ran FA, Hsu PD, Wright J, Agarwala V, Scott DA, Zhang F. Genome engineering using the CRISPR-Cas9 system. *Nature protocols* (2013) 8:2281–308. doi: 10.1038/nprot.2013.143
47. Baker NA, Sept D, Joseph S, Holst MJ, McCammon JA. Electrostatics of nanosystems: application to microtubules and the ribosome. *Proc Natl Acad Sci USA.* (2001) 98:10037–41. doi: 10.1073/pnas.181342398

Conflict of Interest Statement: The authors declare that the research was conducted in the absence of any commercial or financial relationships that could be construed as a potential conflict of interest.

frontiers in Immunology

MINI REVIEW
published: 06 August 2018
doi: 10.3389/fimmu.2018.01836

Human CARD9: A Critical Molecule of Fungal Immune Surveillance

Rebecca A. Drummond[1†], Luis M. Franco[2] and Michail S. Lionakis[1]*

[1] *Fungal Pathogenesis Section, Laboratory of Clinical Immunology and Microbiology (LCIM), National Institute of Allergy and Infectious Diseases (NIAID), National Institutes of Health (NIH), Bethesda, MD, United States,* [2] *Laboratory of Immune System Biology (LISB), National Institute of Allergy and Infectious Diseases (NIAID), National Institutes of Health (NIH), Bethesda, MD, United States*

CARD9 is a signaling adaptor protein that is involved in the transduction of signals from a variety of innate pattern recognition receptors, including the C-type lectin receptors and intracellular NOD receptors and nucleic acid sensors. As a result, CARD9 has been shown in animal models to be an important regulator of immunity to bacteria, fungi, and viruses. Studies in humans with autosomal recessive CARD9 deficiency have indicated a highly specific role for this molecule in the activation of antifungal immune responses in the central nervous system, the oral mucosa, and the skin. Moreover, CARD9-dependent functions have recently been indicated to modulate the development of autoimmunity, inflammatory bowel diseases, and cancer. In this mini-review, we highlight the recent studies that have identified several novel functions of CARD9 in various disease contexts, and we summarize the contemporary understanding of the genetics and immunology of human CARD9 deficiency.

Keywords: CARD9, fungi, primary immunodeficiency, C-type lectin receptors, candidiasis, neutrophils

OPEN ACCESS

Edited by:
Frederic Bornancin, Novartis (Switzerland), Switzerland

Reviewed by:
Yuval Itan, Icahn School of Medicine at Mount Sinai, United States
Ruben Martinez-Barricarte, Rockefeller University, United States

****Correspondence:***
Michail S. Lionakis
lionakism@niaid.nih.gov

†Present address:
Rebecca A. Drummond, Institute of Immunology and Immunotherapy, Institute of Microbiology and Infection, University of Birmingham, Birmingham, United Kingdom

Specialty section:
This article was submitted to Primary Immunodeficiencies, a section of the journal Frontiers in Immunology

Received: *01 May 2018*
Accepted: *25 July 2018*
Published: *06 August 2018*

Citation:
Drummond RA, Franco LM and Lionakis MS (2018) Human CARD9: A Critical Molecule of Fungal Immune Surveillance. Front. Immunol. 9:1836. doi: 10.3389/fimmu.2018.01836

INTRODUCTION

Innate recognition of microbes by pattern recognition receptors (PRRs) is a critical first step in the defense against infection. To activate antimicrobial immunity, PRRs must initiate intracellular signaling cascades which control cellular responses, such as cytokine production, phagocytosis, and assembly of microbial killing complexes. Many PRRs use signaling molecules and adaptor proteins that are shared with other members of the same PRR family. As a result, deficiency of a shared signaling or adaptor protein often results in immune dysfunctions that are more severe than a deficiency in a single receptor and can have profound consequences for the control of infections (1).

Pathogenic fungi are predominantly recognized by the C-type lectin receptor (CLR) and toll-like receptor (TLR) families, of which many members couple to the signaling adaptor proteins CARD9 and MyD88, respectively, in order to activate their functions and initiate defense against fungal invasion (2). Although both CLRs and TLRs bind to and activate antifungal immune responses, the phenotypic consequences of human deficiencies in either of the two shared signaling adaptors have demonstrated that CARD9 plays a specific, superior role in the control of fungal diseases in humans compared to that of MyD88. Indeed, patients with genetic deficiency in CARD9 exhibit a primary immunodeficiency disorder (PID) which manifests as an extreme susceptibility to fungal infections, but not bacterial, viral, or parasitic infections, and is the only PID described to date that specifically predisposes to fungal diseases without other infectious or non-infectious sequelae (3). In contrast, MyD88 deficiency results in the development of life-threatening pyogenic bacterial infections without the spontaneous development of fungal disease (4). The highly specific susceptibility to fungi in CARD9-deficient patients further extends to

the fungal species and organs affected, indicating that CARD9 is required for organ-specific antifungal immune responses of which we are only now beginning to define. Furthermore, animal models and genome-wide analyses of human single-nucleotide polymorphisms (SNPs) have indicated that CARD9 may also function to promote immunity to other pathogens and contribute toward autoimmune and hyperinflammatory disorders. Thus, CARD9 is a multi-functional signaling protein involved in many aspects of the immune system.

In this review, we discuss recent research that has unveiled the many possible functional roles of CARD9, predominantly defined using animal models. Finally, we discuss the genetics of human CARD9 deficiency and highlight the critical role for this molecule in antifungal immune surveillance in humans.

THE MULTI-FUNCTIONAL ROLES OF CARD9

CARD9 Is a Critical Activator of Antifungal Immune Responses

Many of the prototypical PRRs that recognize common components of fungal cell walls are members of the CLR family, and include Dectin-1, Dectin-2, Dectin-3, Mincle, and the Mannose Receptor (CD206). Many of these receptors initiate intracellular signaling cascades that are CARD9-dependent, the best studied of which is the Syk-dependent pathway downstream of Dectin-1 (**Figure 1A**). In brief, ligation of Dectin-1 by β-glucan (the fungal ligand for this receptor) results in recruitment of Syk kinase and the formation of the CBM signalosome, composed of CARD9, BCL10, and MALT1 (5). Activation of CARD9 function requires Vav proteins, of which there are three isoforms (Vav1, Vav2, and Vav3). Deletion of Vav1-3 in mice results in a phenocopy of CARD9-deficiency, indicating that Vav-mediated activation of CARD9 is a critical step in the induction of protective antifungal immunity. In line with this, human *VAV3* SNPs are enriched in patient cohorts with candidemia (6). Activated CARD9 then leads to the production of inflammatory mediators, such as IL-6, IL-12, GM-CSF, TNF, and IL-1β *via* the activation of NFκB and ERK, the latter of which occurs *via* a RASGRF1–H-Ras pathway (7). These CARD9-dependent signaling pathways are regulated by Rubicon, a protein best known for its functions in autophagy (8). Rubicon competitively binds to CARD9 which results in the disassembly of the CBM complex, thus switching off signaling and preventing excessive inflammatory responses. However, modulation of Rubicon expression levels using lentiviral vectors in mice demonstrated that a reduction in Rubicon expression could help promote fungal clearance and survival by enhancing

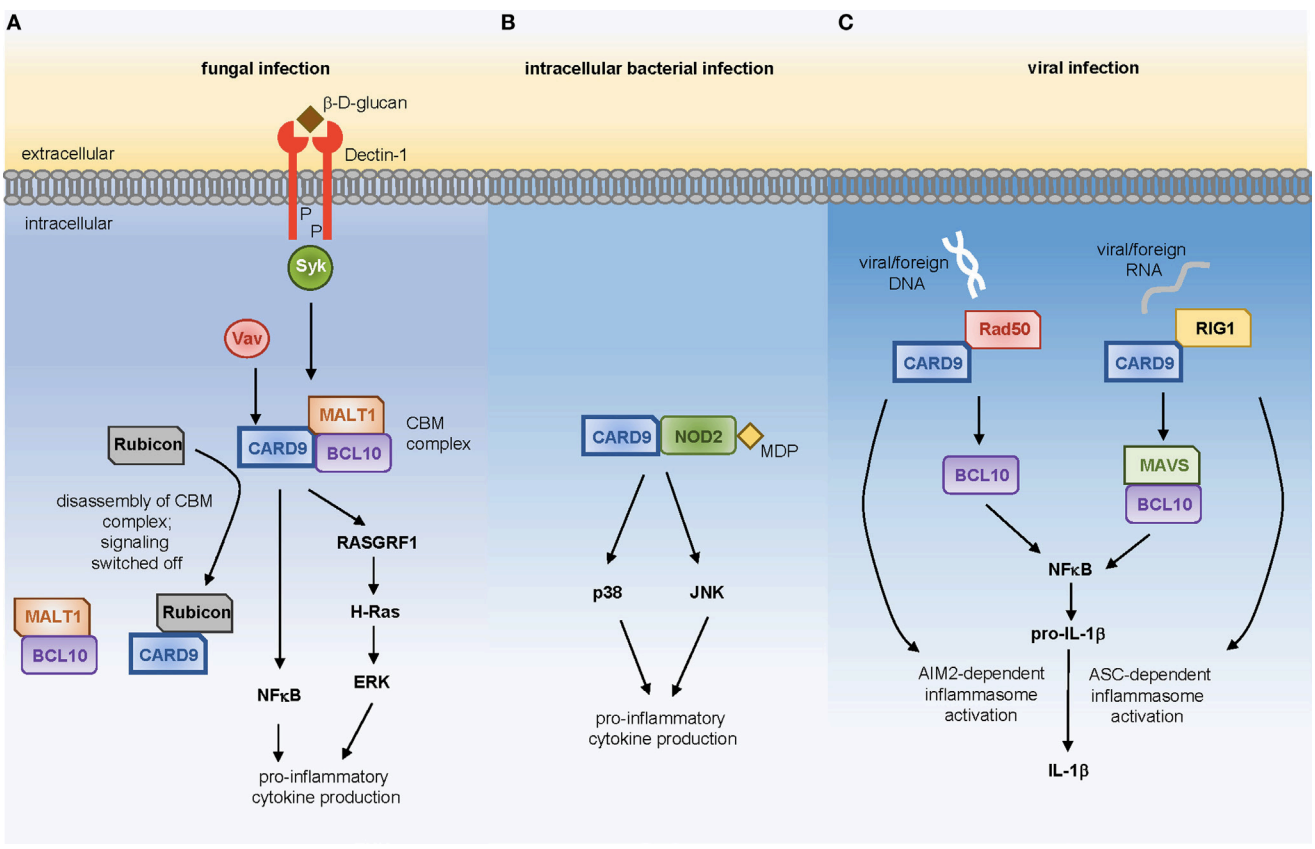

FIGURE 1 | CARD9-dependent signaling in response to **(A)** fungal ligands *via* Dectin-1, **(B)** muramyl-dipeptide derived from intracellular bacterial pathogens, or **(C)** viral DNA or RNA.

CARD9-dependent antifungal immune responses, at least in acute infection models (8). Compared to other PRR families, the molecular signaling events that occur upon CLR ligation are poorly defined. Yet, understanding these pathways will be critical to determine how iatrogenic interventions that manipulate these pathways affect vulnerable patients. For example, the recently introduced Syk inhibitors for hematological malignancies and graft-versus-host disease (9, 10), may predispose to the development of dangerous invasive fungal infections in patient cohorts already at risk for these diseases.

Animals with a genetic deletion of Card9 are susceptible to challenge with a variety of fungal species, including *Candida albicans*, *Aspergillus fumigatus, Cryptococcus neoformans*, and some rarer dematiaceous fungi (11–14). In each of these models, *Card9*$^{-/-}$ mice generally exhibit reduced inflammatory cytokine production, which contributes to the inability to control fungal growth within infected organs. Protective antifungal cytokines that appear critically dependent on CARD9 function include IL-6, TNF, and IL-1β. In humans, CARD9 deficiency predisposes to a smaller range of pathogenic fungi (discussed below) indicating that CARD9-dependent functions in humans may be more context-dependent than in the mouse.

Despite the central position of CARD9 in the CLR signaling pathway, ablation of CARD9 function does not result in complete abrogation of antifungal immune responses (in either mice or human), indicating that CARD9-dependent mechanisms are required only for certain protective processes that may be specific to the cell type in question. Indeed, the dependency on CARD9 for NFκB activation has been shown to vary among different types of myeloid cells (7), including neutrophils, macrophages, and dendritic cells (DCs) (13). Neutrophils are the most important effector cell in the defense against systemic *C. albicans* infections, since neutropenia is a significant independent risk factor for the development of and suffering worse outcome from these infections in humans, and neutrophil depletion significantly reduces survival to *C. albicans* challenge in mice (2, 15). Many intrinsic neutrophil functions, including phagocytosis, production of reactive oxygen species (ROS), and chemotaxis appear largely independent of CARD9 for a variety of fungal species, shown with *ex vivo* studies using human neutrophils (16–19). In contrast, for ROS-independent fungal killing, CARD9 is required for the killing of unopsonized yeast cells as part of a PI3Kγ-dependent pathway, whereas killing of opsonized *C. albicans* yeast largely requires FcRγ and PKC and is independent of CARD9 (20). These two distinct fungal killing pathways utilized by neutrophils helps to explain the observation that neutrophils isolated from CARD9-deficient patients exhibit a selective killing defect toward unopsonized yeast (18, 19). This defect may partly contribute toward the fungal central nervous system (CNS)-tropism observed in CARD9-deficient patients (see below), since opsonization is naturally low in the CNS and thus CARD9-dependent killing of unopsonized cells would be particularly critical at this site. However, human neutrophil killing against the invasive filamentous *Candida* forms observed in tissue appears intact, whether opsonized or unopsonized (19). In addition, we and others have shown that a critical function of CARD9 in antifungal defense is promoting neutrophil recruitment specifically into fungal-infected organs *via* CXC chemokine production in both mice and humans (19, 21), which appears to largely contribute toward the organ-specific manifestation of fungal diseases observed in CARD9-deficient humans.

In experimental *C. albicans* CNS infections in mice, CARD9 promotes neutrophil recruitment in a fungal- and brain-specific manner (19). In this situation, CARD9 is required for the appropriate induction of CXC chemokines in the CNS by resident macrophages (i.e., microglia) and glia cells, as well as recruited neutrophils. Therefore, CARD9 controls local inflammatory chemokine production in addition to a neutrophil-intrinsic positive feedback chemotaxis loop in the brain (19). CARD9-dependent production of neutrophil-attracting chemokines is also evident during pulmonary infection with *A. fumigatus* in mice (14), and we recently reported CARD9-deficient patients who developed extrapulmonary *A. fumigatus* infection that was associated with a lack of neutrophil accumulation at the infected site (21). Moreover, reduced production of CXC chemokines resulting in a lack of neutrophil recruitment has been described in chronically fungal-infected subcutaneous tissue in experimental phaeohyphomycosis models (22). Therefore, CARD9 appears to be a central regulator of neutrophil recruitment to specific organs during invasive fungal infection.

CARD9 and Anti-Bacterial Immunity

Stimulation of *Card9*$^{-/-}$ myeloid cells with purified bacterial products has revealed that CARD9 is required for inflammatory cytokine production in response to specific bacterial stimuli. IL-6 production following stimulation with peptidoglycan or muramyl-dipeptide (MDP), predominant components of Gram-positive bacterial cell walls, is highly dependent on CARD9 whereas responses to LPS are CARD9-independent (23). Recognition of MDP is largely controlled by the intracellular NOD2 receptor, to which CARD9 couples in order to drive activation of p38 and JNK kinases (**Figure 1B**), thus promoting immunity to intracellular bacterial pathogens including *Listeria monocytogenes* (23) and *Mycobacterium tuberculosis* (24).

In addition to activating innate immune responses to intracellular bacteria, other studies have indicated that CARD9 may be involved in the induction of adaptive immunity to these pathogens. Mouse T-cells specific for flagellin were shown to require Syk-CARD9 signaling for their activation, which was mechanistically linked to TLR5-dependent antigen presentation by CARD9-expressing DCs (25). Polarization to the Th17 lineage also depends on CARD9 in the context of gastrointestinal (GI) bacterial infection (26), similar to what has been described for the generation of Th17 responses in the fungal-infected oral mucosa (27). Moreover, humoral immunity mediated by B-cells has also been shown to be affected by deletion of Card9, since bacterial-specific IgG production during GI infection is significantly reduced in *Card9*$^{-/-}$ animals (28). Thus, animal models have demonstrated that Card9 can play distinct protective roles in immunity to intracellular bacterial pathogens, however, the relevance of these functions in humans remains to be determined given that CARD9-deficient patients do not appear susceptible to bacterial infections.

CARD9 and Antiviral Immunity

Studies delineating the molecular pathways controlling IL-1β activation and secretion by myeloid cells in response to viral infection have identified CARD9 as a key regulator of these responses (**Figure 1C**). Following viral infection or transfection with foreign DNA, CARD9 directly interacts with Rad50, a cytosolic DNA sensor, and these CARD9-Rad50 complexes subsequently recruit BCL10 to promote IL-1β secretion. Using a vaccinia virus infection model, *Card9*$^{-/-}$ animals were shown to produce reduced levels of IL-1β following infection which negatively impacted the ability of these animals to generate an appropriate antiviral CD8^{+} T-cell response (29). CARD9 is also required for immunity to retroviruses by transducing RIG-1-dependent signals *via* MAVS and BCL10 to activate NFκB and transcription of pro-IL-1β, which in turn is processed into active IL-1β by ASC-dependent activation of the inflammasome (30). As shown for antifungal immunity, Rubicon can also regulate these CARD9-dependent antiviral functions, since enhancing Rubicon expression levels was found to significantly skew host immunity in favor of pathogen resistance (8).

CARD9 and Autoimmunity

Recent studies have demonstrated potential novel roles of CARD9 in autoimmune diseases using animal models, providing interesting new insights into how this protein functions in organ-specific inflammation. During experimental uveitis, Mincle-mediated activation of CARD9 is required for the recruitment of pathogenic Th1 and Th17 cells (31), and it was later shown that fungal antigens could exacerbate the development of this disease and this occurred *via* Dectin-2-CARD9 signaling (32). In line with the critical role for CARD9 in neutrophil recruitment, *Card9*$^{-/-}$ animals showed reduced production of neutrophil-targeted chemokines, such as CXCL1, CXCL2, and CCL3, resulting in decreased accumulation of neutrophils to the arthritic joint (33). As a result, *Card9*$^{-/-}$ animals are protected from autoantibody-induced arthritis, and this protection was mapped to neutrophils using neutrophil-specific Card9-deficient mice (33). Population-based human studies have indicated that *CARD9* genetic variation may modulate the risk of development of inflammatory bowel diseases (IBD; discussed below), ankylosing spondylitis (34), IgA nephropathy (35), and primary sclerosing cholangitis (36), and more studies are required to determine the role of the CLR/CARD9 axis in organ-specific autoimmune disease development.

CARD9 and Cancer

CARD9-dependent signaling in tumor development and metastasis has been revealed in several recent studies using animal models and cell lines. Patients with IBD are at risk for the development of colonic cancers. Human SNPs in *CARD9* have been identified as risk factors for IBD by several GWAS-based studies (discussed below), and animal models have shown that CARD9 promotes the production of pro-inflammatory cytokines IL-1β and IL-22 in the gut during active colitis, which in turn drives colonic tumor growth (37). Other work has additionally shown that metastasis of colonic tumor cells to the liver depends on CARD9 signaling. CARD9 is highly expressed by tumor-infiltrating macrophages and has been shown to be a critical modulator of the polarization of these cells toward a highly inflammatory metastatic-inducing phenotype (38).

In addition to colonic cancer, CARD9 signaling has also been implicated in the inappropriate activation of renal cell carcinoma (RCC) cells. Mutation affecting the tumor suppressor gene *VHL* (most often somatic, but occasionally involving germline cells) is a major hallmark of RCC, which in turn causes inappropriate activation of NFκB and c-Jun. CARD9 is a mechanistic link between VHL inactivation and the activation of these inflammatory transcription factors (39, 40). Direct interaction between CARD9 and VHL is required for C-terminal phosphorylation of CARD9 by the kinase CK2, which limits CARD9 activity and NFκB activation. Reducing CARD9 expression with a silencing RNA approach in *VHL*$^{-/-}$ cells lowered NFκB activity to wild-type levels, and significantly reduced the tumorigenic potential of these cells (40). Similarly, the loss of VHL promotes an additional pro-inflammatory CARD9-dependent pathway that results in the activation of JNK signaling and c-Jun activity (39). Collectively, these studies provide the intriguing possibility that inappropriate CARD9 activation contributes to the development of certain cancers and may be a novel target of future therapies for these diseases.

THE GENETICS AND CLINICAL SPECTRUM OF HUMAN *CARD9* MUTATIONS

Despite the wide range of CARD9-dependent functions identified in animal models and the potential influence of this protein in several disease scenarios, loss-of-function mutations in human *CARD9* have unequivocally demonstrated the importance of CARD9 in antifungal immunity. Human CARD9 deficiency is characterized by the spontaneous development of fungal infections that predominantly localize to the oral mucosa, CNS, bone, and subcutaneous tissues, and often involves specific families of pathogenic fungi including *Candida* species (CNS, bone, and mucosal disease) and dark-walled molds and yeast-like fungi (e.g., *Aspergillus*, *Exophiala*, and *Phialophora*) that localize to the CNS, skin, bone, and abdominal organs (3, 21, 41–43). The underlying mechanisms that cause susceptibility to fungal diseases in CARD9-deficient patients is not well understood, and could be related to the poor production of inflammatory cytokines and chemokines in response to fungal agonists (13, 18, 19). Indeed, a cohort of French-Canadian CARD9-deficient patients were successfully treated with recombinant GM-CSF therapy, which the authors show corrected defective GM-CSF responses and ERK signaling in CARD9-deficient myeloid cells (43), while another study used G-CSF therapy to correct defective IL-17 responses in a CARD9-deficient patient (44). These studies indicate that replacing cytokines that are classically associated with antifungal defense may be an appropriate therapy option for human CARD9 deficiency. However, we recently showed that these approaches may not be effective

for all patients which are potentially related to the variety of *CARD9* mutations observed (see below). Our data indicated that although different *CARD9* mutations disrupt GM-CSF production by myeloid cells, the impact of these mutations on ERK activation varied with mutation and appeared to correlate with the efficacy of GM-CSF therapy in these patients (45). Thus, treatment options for human CARD9-deficiency are still limited, and further investigation into the mechanisms that cause fungal susceptibility in these patients is warranted. In addition, the organ- and fungal species-specific nature of CARD9-deficiency disease is also poorly understood. As discussed above, we and others have shown that defects in neutrophil recruitment are likely the major contributing factor toward the organ-specific nature of the disease, however, other contributing roles of tissue-resident macrophages, stromal cells, and/or additional functional deficits in recruited inflammatory cells remain to be fully explored.

Although many CARD9-deficient patients have similar clinical presentations, there is diversity in the genetic mutations underlying the condition [see Ref. (3) for a table of all reported human *CARD9* mutations]. More than 15 missense and nonsense mutations in *CARD9* have now been described in the coiled-coil and CARD domains, as well as the promoter region (3). Inactivation of both alleles appears to be necessary for the occurrence of disease, so the condition follows an autosomal recessive mode of inheritance. *De novo* variants in *CARD9* have also been reported in patients with debilitating fungal infections of the eyes, bone, and skin (46, 47). Interestingly, although some of the reported *CARD9* mutations have been identified in unrelated patients, there are instances where the same mutation does not give rise to a similar clinical phenotype (3). For example, homozygosity for the Q298X mutation has been reported to give rise to *Candida* meningoencephalitis and deep dermatophytosis in different patients (41, 48), while patients with very similar clinical presentations can have mutations in different parts of the *CARD9* gene (47). Therefore, it is currently unclear which mutations predispose to which clinical phenotypes and whether there is any overlap, and this will require more clinical descriptions of CARD9-deficient patients and further investigations into CARD9-dependent immune signaling and functions, especially in humans.

Like many other genes that are associated with Mendelian traits, human *CARD9* is intolerant to sequence variation. To quantify gene-level intolerance to functional genetic variation, Petrovski et al. proposed a Residual Variation Intolerance Score (49). Of the nine CARD genes for which a score was calculated in that study, only three (*CARD9*, *CARD10*, and *CARD11*) had negative scores, suggesting low tolerance to functional genetic variation. In fact, *CARD9* had lower tolerance to variation than 82% of the 16,956 genes for which a score was calculated in the study.

In addition to deleterious mutations which predispose to fungal infection, there have been reports of genetic variants of *CARD9* in humans that associate with autoimmune disease. The CARD9 single-nucleotide polymorphism S12N (rs4077515) was recently shown to be highly enriched in patients with allergic bronchopulmonary aspergillosis, which the authors linked to RelB activation by this CARD9 variant that subsequently activated IL-5 production by alveolar macrophages and drove pathogenic eosinophil recruitment and Th2 responses within the lung (50). Another example is the CARD9 variant in which the C-terminal region is truncated (51, 52). One of these truncated variants of CARD9 (S12NΔ11 or *CARD9*Δ11) is strongly associated with protection against IBD, which is mechanistically linked to the inability of these variants to be activated by TRIM62, a ubiquitin ligase that is required for CARD9 activation and subsequent pro-inflammatory cytokine production. While the lack of TRIM62-mediated activation is protective in the context of inappropriate intestinal inflammation and may represent a target for therapeutic intervention in IBD (53), these mutations would be predicted to negatively affect antifungal immunity, since *Trim62*$^{-/-}$ animals are unable to control fungal growth and succumb to infection significantly faster compared to their wild-type counterparts (52). Intriguingly, in human cell lines, *CARD9*Δ11 variants act in a dominant-negative fashion (52), raising the possibility of the existence of humans who may be heterozygous for dominant-negative *CARD9* mutations in the C-terminal region and yet may present with functional CARD9-deficiency. This possibility should be considered by clinicians looking for the underlying cause of an extreme fungal infection in an otherwise immunocompetent patient.

While the *CARD9*Δ11 variant is protective in IBD, other lines of evidence suggest a role for *CARD9* in the pathogenesis of the disease. Specifically, there are other *CARD9* variants that are enriched in patient cohorts with IBD (51) indicating that dysregulated CARD9 function can have profound consequences for immune homeostasis in the gut. The *CARD9* human SNP, S12N, is associated with increased *CARD9* mRNA expression and IBD development (51, 54), but not fungemia (55), thus supporting the notion that CARD9-dependent functions in the immune system are context-dependent. However, many studies analyzing the functions of CARD9 in the context of GI inflammation have discovered links between the development of GI disorders and fungal commensals, indicating that CARD9-dependent functions in innate fungal defense may also be important in gut-related diseases. For example, CARD9 deficiency has been associated with an over-representation of fungi within the microbiota (56), and there have been reports of CARD9-deficient patients developing colitis caused by invasive intestinal infection with *Candida glabrata* (48), and most recently by the β-glucan-containing microalgae *Prototheca zopfii* (57). These studies suggest that, at least partially, CARD9 may function to control fungal microbes in the gut and prevent infection-related disease in these tissues, which might explain the strong association between human *CARD9* genetic variants and the development of IBD-related disorders.

CONCLUDING REMARKS

The significance of CARD9 and its signaling partners in antifungal defense has been an important realization for the field in the past two decades. A comprehensive understanding of the CARD9-dependent signaling pathways and their relevance for

disease processes will be required to (1) utilize CARD9 as a future therapeutic target and (2) prevent and treat possible side-effects of immune-based therapies for cancer and autoimmunity. In particular, the non-fungal-related functions of CARD9 warrant further study, especially to understand the relevance of these functions in humans who carry genetic variants of *CARD9*, which are currently only partially defined yet have the potential to significantly influence CARD9-dependent functions. The study of human CARD9 deficiency has yielded novel insights into how this adaptor signaling molecule functions to protect against invasive fungal diseases and, importantly, these findings point to potential new avenues for the development of immune-based treatments for invasive fungal infections, which represent a global clinical challenge.

AUTHOR CONTRIBUTIONS

All authors contributed in writing the mini-review.

FUNDING

This work was supported by the Intramural Research Program of the National Institute of Allergy and Infectious Disease, National Institutes of Health.

REFERENCES

1. Lionakis MS, Netea MG, Holland SM. Mendelian genetics of human susceptibility to fungal infection. *Cold Spring Harb Perspect Med* (2014) 4:1–21. doi:10.1101/cshperspect.a019638
2. Lionakis MS, Iliev ID, Hohl TM. Immunity against fungi. *JCI Insight* (2017) 2(11):e93156. doi:10.1172/jci.insight.93156
3. Drummond RA, Lionakis MS. Mechanistic insights into the role of C-type lectin receptor/CARD9 signaling in human antifungal immunity. *Front Cell Infect Microbiol* (2016) 6:39. doi:10.3389/fcimb.2016.00039
4. von Bernuth H, Picard C, Jin Z, Pankla R, Xiao H, Ku CL, et al. Pyogenic bacterial infections in humans with MyD88 deficiency. *Science* (2008) 321: 691–6. doi:10.1126/science.1158298
5. Drummond RA, Saijo S, Iwakura Y, Brown GD. The role of Syk/CARD9 coupled C-type lectins in antifungal immunity. *Eur J Immunol* (2011) 41: 276–81. doi:10.1002/eji.201041252
6. Roth S, Bergmann H, Jaeger M, Yeroslaviz A, Neumann K, Koenig P-A, et al. Vav proteins are key regulators of Card9 signaling for innate antifungal immunity. *Cell Rep* (2016) 17:2572–83. doi:10.1016/j.celrep.2016.11.018
7. Jia X-M, Tang B, Zhu L-L, Liu Y-H, Zhao X-Q, Gorjestani S, et al. CARD9 mediates Dectin-1-induced ERK activation by linking Ras-GRF1 to H-Ras for antifungal immunity. *J Exp Med* (2014) 211:2307–21. doi:10.1084/jem.20132349
8. Yang C-S, Rodgers M, Min C-K, Lee J-S, Kingeter L, Lee J-Y, et al. The autophagy regulator rubicon is a feedback inhibitor of CARD9-mediated host innate immunity. *Cell Host Microbe* (2012) 11:277–89. doi:10.1016/j.chom.2012.01.019
9. Liu D, Mamorska-Dyga A. Syk inhibitors in clinical development for hematological malignancies. *J Hematol Oncol* (2017) 10:145. doi:10.1186/s13045-017-0512-1
10. Flynn R, Allen JL, Luznik L, MacDonald KP, Paz K, Alexander KA, et al. Targeting Syk-activated B cells in murine and human chronic graft-versus-host disease. *Blood* (2015) 125:4085–94. doi:10.1182/blood-2014-08-595470
11. Yamamoto H, Nakamura Y, Sato K, Takahashi Y, Nomura T, Miyasaka T, et al. Defect of CARD9 leads to impaired accumulation of gamma interferon-producing memory phenotype T cells in lungs and increased susceptibility to pulmonary infection with *Cryptococcus neoformans*. *Infect Immun* (2014) 82:1606–15. doi:10.1128/IAI.01089-13
12. Wu W, Zhang R, Wang X, Song Y, Liu Z, Han W, et al. Impairment of immune response against dematiaceous fungi in Card9 knockout mice. *Mycopathologia* (2016) 181(9–10):631–42. doi:10.1007/s11046-016-0029-0
13. Gross O, Gewies A, Finger K, Schafer M, Sparwasser T, Peschel C, et al. Card9 controls a non-TLR signalling pathway for innate anti-fungal immunity. *Nature* (2006) 442:651–6. doi:10.1038/nature04926
14. Jhingran A, Kasahara S, Shepardson KM, Junecko BAF, Heung LJ, Kumasaka DK, et al. Compartment-specific and sequential role of MyD88 and CARD9 in chemokine induction and innate defense during respiratory fungal infection. *PLoS Pathog* (2015) 11:e1004589. doi:10.1371/journal.ppat.1004589
15. Lionakis MS, Levitz SM. Host control of fungal infections: lessons from basic studies and human cohorts. *Annu Rev Immunol* (2018) 36:157–91. doi:10.1146/annurev-immunol-042617-053318
16. Li X, Cullere X, Nishi H, Saggu G, Durand E, Mansour MK, et al. PKC-δ activation in neutrophils promotes fungal clearance. *J Leukoc Biol* (2016) 100(3):581–8. doi:10.1189/jlb.4A0915-405R
17. Liang P, Wang X, Wang R, Wan Z, Han W, Li R. CARD9 deficiencies linked to impaired neutrophil functions against *Phialophora verrucosa*. *Mycopathologia* (2015) 179(5–6):347–57. doi:10.1007/s11046-015-9877-2
18. Drewniak A, Gazendam RP, Tool ATJ, van Houdt M, Jansen MH, van Hamme JL, et al. Invasive fungal infection and impaired neutrophil killing in human CARD9 deficiency. *Blood* (2013) 121:2385–92. doi:10.1182/blood-2012-08-450551
19. Drummond RA, Collar AL, Swamydas M, Rodriguez CA, Lim JK, Mendez LM, et al. CARD9-dependent neutrophil recruitment protects against fungal invasion of the central nervous system. *PLoS Pathog* (2015) 11:e1005293. doi:10.1371/journal.ppat.1005293
20. Gazendam RP, van Hamme JL, Tool ATJ, van Houdt M, Verkuijlen PJJH, Herbst M, et al. Two independent killing mechanisms of *Candida albicans* by human neutrophils: evidence from innate immunity defects. *Blood* (2014) 124:590–7. doi:10.1182/blood-2014-01-551473
21. Rieber N, Gazendam RP, Freeman AF, Hsu AP, Collar AL, Sugui JA, et al. Extrapulmonary *Aspergillus* infection in patients with CARD9 deficiency. *JCI Insight* (2016) 1(17):e89890. doi:10.1172/jci.insight.89890
22. Wang X, Zhang R, Wu W, Song Y, Wan Z, Han W, et al. Impaired specific antifungal immunity in CARD9-deficient patients with Phaeohyphomycosis. *J Invest Dermatol* (2018) 138:607–17. doi:10.1016/j.jid.2017.10.009
23. Hsu Y-MS, Zhang Y, You Y, Wang D, Li H, Duramad O, et al. The adaptor protein CARD9 is required for innate immune responses to intracellular pathogens. *Nat Immunol* (2007) 8:198–205. doi:10.1038/ni1426
24. Dorhoi A, Desel C, Yeremeev V, Pradl L, Brinkmann V, Mollenkopf HJ, et al. The adaptor molecule CARD9 is essential for tuberculosis control. *J Exp Med* (2010) 207:777–92. doi:10.1084/jem.20090067
25. Atif SM, Lee S-J, Li L-X, Uematsu S, Akira S, Gorjestani S, et al. Rapid CD4(+) T-cell responses to bacterial flagellin require dendritic cell expression of Syk and CARD9. *Eur J Immunol* (2015) 45:513–24. doi:10.1002/eji.201444744
26. Sokol H, Conway KL, Zhang M, Choi M, Morin B, Cao Z, et al. Card9 mediates intestinal epithelial cell restitution, T-helper 17 responses, and control of bacterial infection in mice. *Gastroenterology* (2013) 145:591–601. doi:10.1053/j.gastro.2013.05.047
27. Bishu S, Hernández-Santos N, Simpson-Abelson MR, Huppler AR, Conti HR, Ghilardi N, et al. The adaptor CARD9 is required for adaptive but not innate immunity to oral mucosal *Candida albicans* infections. *Infect Immun* (2014) 82:1173–80. doi:10.1128/IAI.01335-13
28. Lamas B, Michel M-L, Waldschmitt N, Pham H-P, Zacharioudaki V, Dupraz L, et al. Card9 mediates susceptibility to intestinal pathogens through microbiota modulation and control of bacterial virulence. *Gut* (2017) 1–9. doi:10.1136/gutjnl-2017-314195
29. Roth S, Rottach A, Lotz-Havla AS, Laux V, Muschaweckh A, Gersting SW, et al. Rad50-CARD9 interactions link cytosolic DNA sensing to IL-1[beta] production. *Nat Immunol* (2014) 15:538–45. doi:10.1038/ni.2888
30. Poeck H, Bscheider M, Gross O, Finger K, Roth S, Rebsamen M, et al. Recognition of RNA virus by RIG-I results in activation of CARD9 and inflammasome signaling for interleukin 1β production. *Nat Immunol* (2009) 11:63. doi:10.1038/ni.1824

31. Lee EJ, Brown BR, Vance EE, Snow PE, Silver PB, Heinrichs D, et al. Mincle activation and the Syk/Card9 signaling axis are central to the development of autoimmune disease of the eye. *J Immunol* (2016) 196(7):3148–58. doi:10.4049/jimmunol.1502355
32. Brown BR, Lee EJ, Snow PE, Vance EE, Iwakura Y, Ohno N, et al. Fungal-derived cues promote ocular autoimmunity through a Dectin-2/Card9-mediated mechanism. *Clin Exp Immunol* (2017) 190:293–303. doi:10.1111/cei.13021
33. Nemeth T, Futosi K, Sitaru C, Ruland J, Mocsai A. Neutrophil-specific deletion of the CARD9 gene expression regulator suppresses autoantibody-induced inflammation in vivo. *Nat Commun* (2016) 7:11004. doi:10.1038/ncomms11004
34. Pointon JJ, Harvey D, Karaderi T, Appleton LH, Farrar C, Stone MA, et al. Elucidating the chromosome 9 association with AS; CARD9 is a candidate gene. *Genes Immun* (2010) 11:490–6. doi:10.1038/gene.2010.17
35. Kiryluk K, Li Y, Scolari F, Sanna-Cherchi S, Choi M, Verbitsky M, et al. Discovery of new risk loci for IgA nephropathy implicates genes involved in immunity against intestinal pathogens. *Nat Genet* (2014) 46:1187–96. doi:10.1038/ng.3118
36. Janse M, Lamberts LE, Franke L, Raychaudhuri S, Ellinghaus E, MuriBoberg K, et al. Three ulcerative colitis susceptibility loci are associated with primary sclerosing cholangitis and indicate a role for IL2, REL and CARD9. *Hepatology* (2011) 53:1977–85. doi:10.1002/hep.24307
37. Bergmann H, Roth S, Pechloff K, Kiss EA, Kuhn S, Heikenwalder M, et al. Card9-dependent IL-beta regulates IL-22 production from group 3 innate lymphoid cells and promotes colitis-associated cancer. *Eur J Immunol* (2017) 47:1342–53. doi:10.1002/eji.201646765
38. Yang M, Shao JH, Miao YJ, Cui W, Qi YF, Han JH, et al. Tumor cell-activated CARD9 signaling contributes to metastasis-associated macrophage polarization. *Cell Death Differ* (2014) 21:1290–302. doi:10.1038/cdd.2014.45
39. An JB, Liu HR, Magyar CE, Guo YC, Veena MS, Srivatsan ES, et al. Hyper-activated JNK is a therapeutic target in pVHL-deficient renal cell carcinoma. *Cancer Res* (2013) 73:1374–85. doi:10.1158/0008-5472.CAN-12-2362
40. Yang H, Minamishima YA, Yan Q, Schlisio S, Ebert BL, Zhang X, et al. pVHL acts as an adaptor to promote the inhibitory phosphorylation of the NF-kappa B agonist Card9 by CK2. *Mol Cell* (2007) 28:15–27. doi:10.1016/j.molcel.2007.09.010
41. Lanternier F, Pathan S, Vincent QB, Liu L, Cypowyj S, Prando C, et al. Deep dermatophytosis and inherited CARD9 deficiency. *N Engl J Med* (2013) 369:1704–14. doi:10.1056/NEJMoa1208487
42. Glocker EO, Hennigs A, Nabavi M, Schaffer AA, Woellner C, Salzer U. A homozygous CARD9 mutation in a family with susceptibility to fungal infections. *N Engl J Med* (2009) 361:1727–35. doi:10.1056/NEJMoa0810719
43. Gavino C, Hamel N, Zeng JB, Legault C, Guiot M-C, Chankowsky J, et al. Impaired RASGRF1/ERK-mediated GM-CSF response characterizes CARD9 deficiency in French-Canadians. *J Allergy Clin Immunol* (2015) 137(4):1178.e–88.e. doi:10.1016/j.jaci.2015.09.016
44. Celmeli F, Oztoprak N, Turkkahraman D, Seyman D, Mutlu E, Frede N, et al. Successful granulocyte colony stimulating factor treatment of relapsing *Candida albicans* meningoencephalitis caused by CARD9 deficiency. *Pediatr Infect Dis J* (2015) 35(4):428–31. doi:10.1097/inf.0000000000001028
45. Drummond RA, Zahra FT, Natarajan M, Swamydas M, Hsu AP, Wheat LJ, et al. GM-CSF therapy in human CARD9 deficiency. *J Allergy ClinImmunol* (2018). doi:10.1016/j.jaci.2018.05.025
46. Jones N, Garcez T, Newman W, Denning D. Endogenous *Candida* endophthalmitis and osteomyelitis associated with CARD9 deficiency. *BMJ Case Rep* (2016) 2016:1–3. doi:10.1136/bcr-2015-214117
47. Wang X, Wang W, Lin Z, Wang X, Li T, Yu J, et al. CARD9 mutations linked to subcutaneous phaeohyphomycosis and TH17 cell deficiencies. *J Allergy Clin Immunol* (2014) 133:905.e–8.e. doi:10.1016/j.jaci.2013.09.033
48. Lanternier F, Mahdaviani SA, Barbati E, Chaussade H, Koumar Y, Levy R, et al. Inherited CARD9 deficiency in otherwise healthy children and adults with *Candida* species-induced meningoencephalitis, colitis, or both. *J Allergy Clin Immunol* (2015) 135:1558–68. doi:10.1016/j.jaci.2014.12.1930
49. Petrovski S, Wang Q, Heinzen EL, Allen AS, Goldstein DB. Genic intolerance to functional variation and the interpretation of personal genomes. *PLoS Genet* (2013) 9:e1003709. doi:10.1371/journal.pgen.1003709
50. Xu X, Xu J-F, Zheng G, Lu H-W, Duan J-L, Rui W, et al. CARD9S12N facilitates the production of IL-5 by alveolar macrophages for the induction of type 2 immune responses. *Nat Immunol* (2018) 19:547–60. doi:10.1038/s41590-018-0112-4
51. Rivas MA, Beaudoin M, Gardet A, Stevens C, Sharma Y, Zhang CK, et al. Deep resequencing of GWAS loci identifies independent rare variants associated with inflammatory bowel disease. *Nat Genet* (2011) 43:1066–U50. doi:10.1038/ng.952
52. Cao Z, Conway KL, Heath RJ, Rush JS, Leshchiner ES, Ramirez-Ortiz ZG, et al. Ubiquitin ligase TRIM62 regulates CARD9-mediated anti-fungal immunity and intestinal inflammation. *Immunity* (2015) 43:715–26. doi:10.1016/j.immuni.2015.10.005
53. Leshchiner ES, Rush JS, Durney MA, Cao Z, Dančík V, Chittick B, et al. Small-molecule inhibitors directly target CARD9 and mimic its protective variant in inflammatory bowel disease. *Proc Natl Acad Sci U S A* (2017) 114:11392–7. doi:10.1073/pnas.1705748114
54. Beaudoin M, Goyette P, Boucher G, Lo KS, Rivas MA, Stevens C, et al. Deep resequencing of GWAS loci identifies rare variants in CARD9, IL23R and RNF186 that are associated with ulcerative colitis. *PLoS Genet* (2013) 9(9):e1003723. doi:10.1371/journal.pgen.1003723
55. Rosentul DC, Plantinga TS, Oosting M, Scott WK, Edwards DRV, Smith PB, et al. Genetic variation in the Dectin-1/CARD9 recognition pathway and susceptibility to candidemia. *J Infect Dis* (2011) 204:1138–45. doi:10.1093/infdis/jir458
56. Lamas B, Richard ML, Leducq V, Pham H-P, Michel M-L, Da Costa G, et al. CARD9 impacts colitis by altering gut microbiota metabolism of tryptophan into aryl hydrocarbon receptor ligands. *Nat Med* (2016) 22(6):598–605. doi:10.1038/nm.4102
57. Sari S, Dalgic B, Muehlenbachs A, DeLeon-Carnes M, Goldsmith CS, Ekinci O, et al. *Prototheca zopfii* colitis in inherited CARD9 deficiency. *J Infect Dis* (2018) 218(3):485–9. doi:10.1093/infdis/jiy198

Conflict of Interest Statement: The authors declare that the research was conducted in the absence of any commercial or financial relationships that could be construed as a potential conflict of interest.

frontiers in Immunology

ORIGINAL RESEARCH
published: 31 October 2018
doi: 10.3389/fimmu.2018.02366

A *CARD9* Founder Mutation Disrupts NF-κB Signaling by Inhibiting BCL10 and MALT1 Recruitment and Signalosome Formation

Marieke De Bruyne[1,2,3], Levi Hoste[1,3], Delfien J. Bogaert[1,2,3,4], Lien Van den Bossche[5,6], Simon J. Tavernier[1,4], Eef Parthoens[6,7], Mélanie Migaud[8], Deborah Konopnicki[9], Jean Cyr Yombi[10], Bart N. Lambrecht[4,11], Sabine van Daele[3], Ana Karina Alves de Medeiros[12], Lieve Brochez[12], Rudi Beyaert[13], Elfride De Baere[2], Anne Puel[8], Jean-Laurent Casanova[8,14], Jean-Christophe Goffard[15], Savvas N. Savvides[5,6], Filomeen Haerynck[1,3†], Jens Staal[13†] and Melissa Dullaers[1,4†]*

[1] Primary Immunodeficiency Research Lab, Department of Pulmonary Medicine, Centre for Primary Immunodeficiencies, Jeffrey Modell Diagnosis and Research Centre, Ghent University Hospital, Ghent, Belgium, [2] Center for Medical Genetics, Ghent University and Ghent University Hospital, Ghent, Belgium, [3] Department of Pediatric Immunology and Pulmonology, Centre for Primary Immunodeficiencies, Jeffrey Modell Diagnosis and Research Centre, Ghent University Hospital, Ghent, Belgium, [4] Laboratory of Immunoregulation, VIB-UGent Center for Inflammation Research, Ghent, Belgium, [5] Laboratory for Protein Biochemistry and Biomolecular Engineering, Department of Biochemistry and Microbiology, Ghent University, Ghent, Belgium, [6] VIB-UGent Center for Inflammation Research, Ghent, Belgium, [7] VIB Bioimaging Core, VIB, Ghent, Belgium, [8] Laboratory of Human Genetics of Infectious Diseases, INSERM UMR1163, Necker Medical School, Imagine Institute, Paris Descartes University, Paris, France, [9] Infectious Diseases Department, Saint-Pierre University Hospital, Université Libre de Bruxelles, Brussels, Belgium, [10] Department of Internal Medicine and Infectious Diseases, Cliniques Universitaires Saint Luc, Université Catholique de Louvain, Brussels, Belgium, [11] Department of Internal Medicine, Ghent University, Ghent, Belgium, [12] Department of Dermatology, Ghent University Hospital, Ghent, Belgium, [13] Unit of Molecular Signal Transduction in Inflammation, Department of Biomedical Molecular Biology, VIB-UGent Center for Inflammation Research, Ghent University, Ghent, Belgium, [14] St Giles Laboratory of Human Genetics of Infectious Diseases, Rockefeller University, New York, NY, United States; Pediatric Hematology-Immunology Unit, Necker Hospital, AP-HP, Paris, France; Howard Hughes Medical Institute, New York, NY, United States, [15] Immunodeficiency Unit, University Hospital ULB Erasme, Brussels, Belgium

Background: Inherited CARD9 deficiency constitutes a primary immunodeficiency predisposing uniquely to chronic and invasive fungal infections. Certain mutations are shown to negatively impact CARD9 protein expression and/or NF-κB activation, but the underlying biochemical mechanism remains to be fully understood.

Objectives: To investigate a possible founder origin of a known CARD9 R70W mutation in five families of Turkish origin. To explore the biochemical mechanism of immunodeficiency by R70W CARD9.

Methods: We performed haplotype analysis using microsatellite markers and SNPs. We designed a model system exploiting a gain-of-function (GOF) CARD9 L213LI mutant that triggers constitutive NF-κB activation, analogous to an oncogenic CARD11 mutant, to study NF-κB signaling and signalosome formation. We performed reporter assays, immunoprecipitation and confocal imaging on HEK cells overexpressing different CARD9 variants.

Results: We identified a common haplotype, thus providing evidence for a common Turkish founder. CARD9 R70W failed to activate NF-κB and abrogated NF-κB activation

OPEN ACCESS

Edited by:
Frederic Bornancin, Novartis, Switzerland

Reviewed by:
Lisa Renee Forbes, Baylor College of Medicine, United States
Jose R. Regueiro, Complutense University of Madrid, Spain

***Correspondence:**
Filomeen Haerynck
filomeen.haerynck@uzgent.be

[†]These senior authors contributed equally

Specialty section:
This article was submitted to Primary Immunodeficiencies, a section of the journal Frontiers in Immunology

Received: *28 May 2018*
Accepted: *24 September 2018*
Published: *31 October 2018*

Citation:
De Bruyne M, Hoste L, Bogaert DJ, Van den Bossche L, Tavernier SJ, Parthoens E, Migaud M, Konopnicki D, Yombi JC, Lambrecht BN, van Daele S, Alves de Medeiros AK, Brochez L, Beyaert R, De Baere E, Puel A, Casanova J-L, Goffard J-C, Savvides SN, Haerynck F, Staal J and Dullaers M (2018) A CARD9 Founder Mutation Disrupts NF-κB Signaling by Inhibiting BCL10 and MALT1 Recruitment and Signalosome Formation. Front. Immunol. 9:2366. doi: 10.3389/fimmu.2018.02366

by WT CARD9 and by GOF CARD9. Notably, R70W CARD9 also exerted negative effects on NF-κB activation by CARD10, CARD11, and CARD14. Consistent with the NF-κB results, the R70W mutation prevented GOF CARD9 to pull down the signalosome partner proteins BCL10 and MALT1. This reflected into drastic reduction of BCL10 filamentous assemblies in a cellular context. Indeed, structural analysis revealed that position R70 in CARD9 maps at the putative interface between successive CARD domains in CARD9 filaments.

Conclusions: The R70W mutation in CARD9 prevents NF-κB activation by inhibiting productive interactions with downstream BCL10 and MALT1, necessary for assembly of the filamentous CARD9-BCL10-MALT1 signalosome.

Keywords: CARD9 deficiency, founder mutation, BCL10, MALT1, CBM complex, NF-κB, filament, signalosome

INTRODUCTION

In the past decade, the importance of IL-17-mediated immunity in host defense against fungal infections has become clear, in large part by studies of patients with inborn errors of IL-17 immunity and relentless chronic mucocutaneous candidiasis (CMC) as a common theme. Mutations in key components of the IL-17A/IL-17F pathway were shown to compromise cellular responses to these cytokines, thus predisposing to CMC (1–3). Furthermore, patients with inherited disorders affecting IL-17A/IL-17F production (low Th17 cells) often present CMC in combination with other infections/clinical features (1–3). Caspase recruitment domain family member 9 (CARD9) is an adaptor molecule connecting dectin-1 fungal sensing to nuclear factor κB (NF-κB) signaling and thus important in host defense against fungal infections. It was first shown that Card9-deficient (Card9$^{-/-}$) mice are highly susceptible to fungal infection (*Candida albicans*) due to their inability to produce proinflammatory cytokines in response to dectin-1 stimulation e.g. by zymosan or *C. albicans* (4). Subsequently in 2009, autosomal recessive (AR) *CARD9* deficiency was identified to be responsible for recurrent superficial fungal infections and central invasion with *Candida* spp. (5).

To date, 63 patients of 38 kindreds originating from at least 14 countries with *CARD9* mutations have been reported (see **Supplemental Table 1**, including references). Even though clinical presentation is highly variable, CARD9 deficiency predisposes uniquely to chronic and invasive fungal infections in otherwise healthy individuals (6). As proposed in a recent review (7), clinical presentation can be classified as (1) isolated CMC, (2) infections of skin and subcutaneous tissues with fungal species including *Trichopython* spp, *Phialophora verrucosa* and *Corynespora cassiicola,* and (3) systemic fungal disease manifesting primarily as meningoencephalitis, osteomyelitis and intra-abdominal infections with *Candida* spp, *Trichophyton* spp, *Exophiala spp,* and rarely *Aspergillus* (5–10). All patients are homozygous or compound heterozygous for 21 different mutations in the CARD9 CARD and coiled-coil (CC) domains (**Figure 2A**, **Supplemental Table 1**). Most of these mutations are missense and nonsense mutations, but also frameshifts, synonymous substitutions and an in-frame deletion have been described.

CARD9 is an intracellular adaptor molecule that mediates signaling downstream of C-type lectin receptors, including Dectin-1 and Dectin-2, upon fungal recognition by myeloid or epithelial cells. CARD9 forms signaling complexes with B-cell CLL/lymphoma 10 (BCL10) and mucosa-associated lymphoid tissue lymphoma translocation protein 1 (MALT1), termed CARD-CC/BCL10/MALT1 (CBM) complexes. Such CBM signalosomes mediate NF-κB activation resulting in induction of pro-inflammatory cytokines, such as IL-1, IL-6, and IL-23. These promote the differentiation of T lymphocytes into IL-17 producing T cells, further mediating anti-fungal immunity (7).

Caspase recruitment domains (CARD) are the common motif in the CARD subfamily of death domain proteins containing 33 human CARD-containing proteins. Homotypic CARD-CARD domain interactions between CARD-proteins regulate the assembly of many signaling complexes, including the CBM signalosome and many others such as the apoptosome and the inflammasome (11). CARD9 belongs to a phylogenetically distinct family of CARD-proteins along with CARD10 (CARMA3), CARD11 (CARMA1), and CARD14 (CARMA2) which are defined by their CARD and coiled-coil (CC) domains (11, 12). The four different CARD-CC proteins all form CBM signaling complexes, mediated mainly by CARD-domain hetero-multimerization. CBM complexes form a critical link between cell-surface receptors that associate with extracellular molecular antigens and downstream activation of NF-κB. Active CBM signalosomes are formed when pre-existing filamentous BCL10 structures are nucleated by activation of CARD-CC proteins (13–15). Genetic defects in several components of the CBM complex have been linked to human immunopathology.

Abbreviations: AR, autosomal recessive; BCL10, B-cell CLL/lymphoma 10; CARD9, caspase recruitment domain family member 9; CBM, CARD-CC/BCL10/MALT1; CC, coiled-coil; CMC, chronic mucocutaneous candidiasis; Co-IP, co-immunoprecipitation; GOF, gain-of-function; IBD, Identity-by-descent; LOF, loss-of-function; LTT, lymphocyte transformation test; MALT1, mucosa-associated lymphoid tissue lymphoma translocation protein 1; NF-κB, nuclear factor kappa-light-chain-enhancer of activated B cells; PMA, phorbol 12-myristate 13-acetate; PWM, pokeweed mitogen; SNP, single-nucleotide polymorphism; WT, wild-type.

Somatic and germline gain-of-function (GOF) mutations in *CARD11*, *MALT1,* and *BCL10* cause B cell lymphomas and lymphoproliferative disorders (16). Biallelic loss-of-function (LOF) mutations in *CARD11*, *MALT1,* and *BCL10* lead to combined immunodeficiencies (16–18) whereas the here-discussed CARD9 deficiency predisposes exclusively to fungal infections.

The R70W (c.208C>T) *CARD9* mutation was previously reported in four patients of three unrelated families of consanguineous Turkish decent, living in Belgium or France (10, 19). We here expand the R70W CARD9 cohort to 11 patients of five unrelated families all from Turkish descent and we provide evidence supporting a common founder origin of this mutation. The R70W *CARD9* variant was shown to affect CARD9 protein expression and is associated with impaired NF-κB activation (10). In this study, we interrogated the biochemical mechanism of the R70W mutation in CARD9 and found that it disrupts NF-κB activation by abrogating recruitment of BCL10 and subsequent filamentous signalosome formation.

MATERIALS AND METHODS

Patients

Patients were recruited in Ghent University Hospital, Ghent, Belgium (19); University Hospital ULB Erasme, Brussels, Belgium; Saint Pierre University hospital, ULB, Brussels, Belgium; University Hospital Saint Luc, UCL, Brussels, Belgium; the Infectious Diseases Unit in Bretonneau Hospital, Tours, France and Necker Hospital, Paris, France (10). This study was conducted in accordance with the Helsinki Declaration and was approved by the ethical committee of Ghent University Hospital (2012/593). All patients and their relatives provided written informed consent for participation in the study.

Extended case reports are provided in the online supplement.

T-Cell Proliferation

T-cell proliferation assay was a standard lymphocyte proliferation test (LTT) performed in routine immunology laboratories. Responses to *C. albicans* and the mitogens phytohemaglutinin (PHA), Concanavalin A (ConA), or Pokeweed mitogen (PWM) were assessed.

Immunologic Assessment of Th17 Function and Fungal Recognition

For intracellular cytokine staining, $1*10^6$ PBMC were cultured in complete medium with phorbol 12-myristate 13-acetate (PMA) (200 ng/mL) and Ionomycin (1 μg/mL) in the presence of Brefeldin A (20 μg/mL) (all from Sigma). Cells were stained with CD4 T cell surface markers (CD3, CD4, CD45RO), fixed and then stained intracellularly for IL-17A (eBio64dec17) and IFNg (4s.B3, eBioscience). IL-17+ cells were scored within CD3+CD4+CD45RO+ cells. In addition, IL-17 production upon stimulation with SEB or PMA/ionomycin was measured by ELISA.

To test fungal recognition, $2*10^5$ PBMC were cultured for 2 days in complete medium without or with heat-killed *Candida albicans* (Invivogen, 10 μg/mL). ELISA for IL-6 was performed on supernatants (eBioscience Ready-Set-Go).

Haplotype Analysis

Genomic DNA was isolated from whole blood cells according to standard procedures. Identity-by-descent (IBD) mapping was carried out in two affected individuals (F2 III:2, III:3) from family 2 by genome-wide single-nucleotide polymorphism (SNP) arrays using the HumanCytoSNP-12 BeadChip platform (Illumina, San Diego, CA). Ten IBD regions (>1 Mb) were identified using PLINK software (20). Starting from the IBD region (3.3 Mb) encompassing CARD9, four microsatellite markers were selected using NCBI Map Viewer (including genetic maps deCODE, Généthon, Marshfield and Rutgers Map v.3). In addition, five tagging SNP markers (UCSC Table Browser) were genotyped to further delineate the common haplotype. Primers were designed with Primer3Plus. Fragment analysis and sequencing were performed on the ABI 3730XL DNA Analyzer (Applied Biosystems). Data analysis of the microsatellite markers was performed with the GeneMapper v5 software (Applied Biosystems) and SNP markers were analyzed with SeqScape v2.5 (Life Technologies). Microsatellite and SNP markers were genotyped for haplotype analysis in ten affected patients and eleven healthy family members of the five families.

Cloning and Mutagenesis

Plasmids of the cloned genes were deposited in the LMBP/GeneCorner plasmid collection for public access along with detailed descriptions of cloning strategy and plasmid sequence (http://www.genecorner.ugent.be). Identification of the conserved site corresponding to the oncogenic CARMA1 L225LI (L232LI in long splice form) mutation was done in a MUSCLE multiple sequence alignment of a wide selection of CARD-CC proteins from Cnidaria to humans using UGENE (21). A pcDNA3-Flag (LMBP: 9609) or pENTR3C (LMBP: 9877) clone of human CARD9 was used as a template to generate the R70W (LMBP: 10266), L213LI (LMBP: 10178) and the R70W/L213LI (LMBP: 10265) mutants by PCR with Universe High-Fidelity Hot Start Taq (Bimake).

Two truncated CARD9 variants were generated. One downstream of the first CC domain CARD9-Q295X (LMBP: 10532) found in 11 patients and one downstream of the second CC domain CARD9-E419X (LMBP: 10457) constructed based on the last residue of the CC domain.

To test the effect of R70W CARD9 on the other CARD-CC proteins, analogously auto-actived mutants were generated by introducing a premature stop codon in between the CC-domain and the downstream C terminal inhibitory domain: CARD9-E419X (LMBP: 10457), CARD10-ΔC (LMBP: 10459), CARD11-ΔC (LMBP: 10458), and CARD14-ΔC (LMBP: 10460).

Cell Culture, Transfection, and Expression Analysis

MALT1 deficient HEK293T cells (generated in house, clone #36) (22) were grown under standard conditions (DMEM, 10% FCS, 5% CO_2, 37°C) and transfected with the calcium

phosphate method (23). For NF-κB reporter assays, the indicated CARD9 construct was co-transfected with an NF-κB-dependent luciferase reporter expression plasmid (LMBP: 3249) and an actin promoter-driven β-galactosidase expression plasmid (LMBP: 4341) as transfection control. The cells were washed with PBS and lysed in luciferase lysis buffer (25 mM Tris pH7.8, 2 mM DTT, 2 mM CDTA, 10% glycerol, 1% Triton X-100). For the colorimetric determination (at 595 nm) of β-galactosidase activity, chlorophenol red-β-D-galactopyranoside (CPRG) (Roche diagnostics) was used as a substrate. Luciferase activity was measured by using beetle luciferin (Promega) as a substrate and luminescence was measured with the GloMax® 96 Microplate Luminometer (Promega). Luciferase data processing was done in LibreOffice (www.libreoffice.org) Calc. For evaluation of the MALT1-dependent signaling effects, the CARD9 clones were co-transfected with the NF-κB luciferase reporter and β-galactosidase expression plasmids in the MALT1 deficient HEK293T cells with or without reconstitution with human MALT1 (LMBP: 5536). For immunoprecipitation experiments, E-tagged human BCL10 (LMBP: 9637) and human MALT1 were co-transfected with the different CARD9 clones. Cells expressing BCL10 and MALT1 but no Flag-tagged CARD9 construct were used as background control for the immunoprecipitation. Immunoprecipitation was performed with anti-Flag antibody (F-3165, Sigma) in IP buffer (25 mM HEPES pH 7.5, 150 mM NaCl, 0.2% NP-40, 10% glycerol) with protein G magnetic Dynabeads (Invitrogen). For immunoblot detection, MALT1 was detected by a rabbit monoclonal antibody (EP603Y, Abcam), BCL10 with rabbit anti-E-tag antibody (ab66152, Abcam) and CARD9 with mouse anti-Flag antibody (F-3165, Sigma) or anti-Flag-HRP (A-8592, Sigma). All western blots were developed on an Odyssey scanner (LI-COR) except for HRP, which was developed with an Amersham Imager 600 (GE). For studies of inducible interactions of WT CARD9 with BCL10 and MALT1, transfected HEK293T cells were treated with 200 ng/ml PMA for 30 minutes before lysis and immunoprecipitation.

Structural Analysis of CARD9 and Structural Context of R70W CARD9

A structural model for human CARD9 was initially created from structure-based sequence alignments of the sequence encoding the CARD domain of human CARD9 (uniprot Q9H257) and was further improved via models computed via I-TASSER and QUARK (24). The homology model of the CARD domain of CARD9 was docked into a three-dimensional model representing the human BCL10 filament (Electron Microscopy Data Base code EMD-5729; (15) using the segment fitting algorithms implemented in Chimera (25).

Confocal Imaging

HEK293T cells were seeded in 8-well chamber slides (Ibidi). Ninety percent confluent cells were transfected using polyethylenimine [PEI, 25kDa branched (26)] with Flag-CARD9 and E-BCL10 (150 ng plasmid DNA each per well). The next day, cells were fixed with 4% PFA and were stained with mouse anti-Flag-tag (Sigma F3165) and rabbit anti-E-tag (Abcam ab66152) in triton containing staining buffer. Primary antibodies were detected using donkey anti-mouse-AF594 and donkey anti-rabbit 650.

Confocal images were captured with a Zeiss LSM880 confocal microscope (Zeiss, Zaventem, Belgium). Images were taken using a 63 × Pln Apo/1.4 oil objective. The pinhole was set at 1Airy Unit and scans ware made with a pixel dwell time of 2.62 μs. The scan area covered 800 by 800 pixels. Combined with a zoom of 2.2 this resulted in a pixel size of 0.077 μm. A Z-stack of 40–50 slices was recorded with a z-interval of 0.6 μm. 3D reconstructions were made in the 3D opacity mode of Volocity 6.3 (Perkin Elmer).

Statistical Analysis

Graphpad Prism was used to perform one-way ANOVA analysis followed by Tukey's *post-hoc* testing to assess statistical significance of the reporter assay data.

RESULTS

Clinical Presentation Is Highly Variable in the R70W CARD9 Patient Cohort

We studied a cohort of 11 patients all harboring a known missense mutation in *CARD9*: R70W (c.208C>T). Family trees are provided in **Figure 1**. Because all patients originated from the Turkish provinces Afyonkarahisar and Eskişehir, we suspected a founder effect. Indeed, haplotype analysis provided evidence for a common Turkish founder (**Figure 2B**, **Supplemental Figure 1**).

Despite all bearing the R70W CARD9 mutation, the 11 patients present various fungal infections, including isolated CMC, chronic and invasive dermatophytosis, *Candida* meningoencephalitis and osteomyelitis, and intra-abdominal infections with *C. albicans* and *Aspergillus* spp (**Table 1**). Extra-pulmonary aspergillosis was only recently associated with AR CARD9 deficiency in 2 children (9). We here present an additional patient, F2 I.2, who reported to be healthy until she presented with retro-peritoneal aspergillosis at age 48. Consistent with previous reports (7, 10), the severity of the phenotype increases with age in the R70W CARD9 cohort, with childhood CMC often pre-dating invasive infections. This was also the case for patient F3 II.2, who developed CMC at age 36 and *C. albicans* encephalitis at age 39.

Routine immunological work up revealed generally normal T and B cell subsets in all patients (**Table 1**). Lymphocyte proliferation upon stimulation with *C. albicans* was decreased in 5 out of 8 patients tested. Five patients displayed elevated serum IgE levels and 4 had eosinophilia. Th17 function was significantly decreased in 7 out of 10 patients tested. Pro-inflammatory cytokine production upon *Candida* stimulation was decreased in 6 out of 8 patients available for testing. Neither of the parameters reflecting anti-fungal immunity (Th17, anti-*candida* response) correlated with disease severity. Detailed case reports can be found in the online supplement.

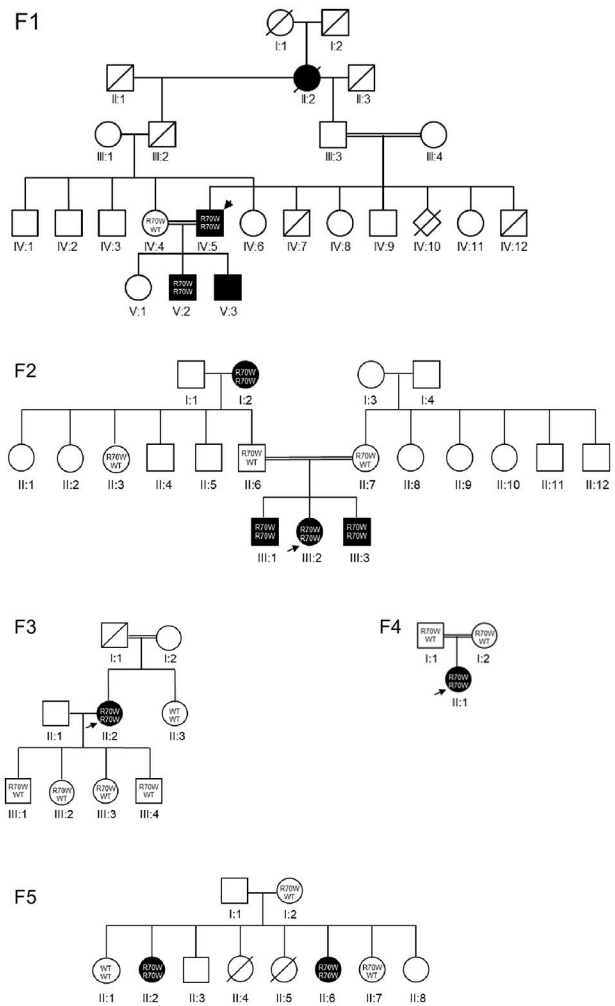

FIGURE 1 | Pedigrees. *CARD9* R70W mutations were identified in five families. Each kindred is identified by a number (F1–F5), each generation by a Roman numeral (I–V), and each subject by an Arabic numeral (1–12). Square, circle and diamond shapes indicate male, female, and sex unknown, respectively. A double line represents reported consanguinity. Diagonal lines indicate deceased individuals. Filled symbols represent affected individuals, clear symbols represent unaffected individuals. The index patients are indicated with arrows. Where available, the genotype is mentioned. WT, wild-type allele.

R70W CARD9 Does Not Activate NF-κB and Inhibits NF-κB Activation by WT CARD9 and a Gain-of-Function CARD9 Mutant

Upon overexpression, wild-type (WT) CARD9 only moderately induced NF-κB activity in MALT-1-deficient HEK293T cells, but this was promoted by MALT-1 co-expression (27). Indeed, overexpression of WT CARD9 induced a 2- to 4-fold increase of MALT-1-dependent NF-κB reporter activity (**Figures 3A,B,D**). The R70W mutant, however, did not exhibit MALT-1-dependent NF-κB activation. More importantly, upon co-transfection of WT and R70W, the R70W mutant exerted an inhibitory effect on MALT-1-dependent NF-κB activation induced by WT CARD9 (**Figures 3A,B**). Off note, protein expression of the R70W allele was often weaker than the WT CARD9 allele, as had been reported before (10). We here report only data from those experiments where protein expression of R70W CARD9 was comparable to WT.

In that earlier report studying R70W CARD9 (10), co-expression of upstream (Dectin-1, Syk) and downstream (BCL10) signaling proteins together with fungal stimulation was used to determine the effects of CARD9 mutations on NF-κB activation. In that system of upstream activation, the R70W mutant also exhibited impaired NF-κB signaling. This strategy may also activate endogenous CARD10 present in HEK293T cells due to the high sequence conservation of the CARD-domain, which could mask effects of CARD9 mutations. To avoid this potential confounding factor and to specifically study signaling events downstream of CARD9, we generated a gain-of-function (GOF) mutant analogous to an oncogenic constitutively active CARD11 L225LI mutant. Like other oncogenic mutations in CARD11, this mutation is situated in the CC-domain and triggers constitutive NF-κB activation (17). The isoleucine insertion site is highly conserved ever since the single ancestral CARD-CC protein in the last common vertebrate ancestor (**Supplemental Figure 2**) and allowed us to generate an analogous isoleucine insertion mutant in CARD9 (L213LI). This CARD9 GOF mutant shows dramatically higher induction of NF-κB activity compared to WT, which we used as a model system for CARD9 activation, to test the effect of the R70W mutation. The L213LI CARD9 constitutive NF-κB activation was completely suppressed by the R70W mutation both in co-transfection of single mutants and in a double mutant setup (L213LI/R70W) (**Figures 3C,D**). Upon co-transfection, the double mutant also substantially reduced NF-κB activation by the GOF mutant but not as dramatically as the R70W single mutant. Since the protein expression of the R70W/L213LI double mutant was significantly lower than the other CARD9 alleles despite equal DNA dosage, this indicated a dose-dependency of the R70W inhibiting effect. Indeed, a cross-over dose-titration of the GOF L213LI mutant and the R70W/L213LI double mutant, confirmed such dose-dependency (**Figure 3E**). Importantly, at a 1:1 DNA ratio (reminiscent of heterozygosity) there was still 22% residual NF-κB activation.

Considering the known structural homology and the potential for functional redundancy between CARD-CC proteins, we also assessed the effect of R70W CARD9 on auto-active mutants of CARD10, CARD11, and CARD14, all lacking the C-terminal inhibitory domain (**Figure 4A**). Surprisingly, upon co-transfection R70W CARD9 repressed NF-κB activity by all 4 auto-active CARD-CC proteins.

The proposed mechanism of the L225LI mutation in CARD11 is that it blocks intramolecular auto-inhibition from an inhibitory domain in the linker between the CC and the C-terminal domain (17). To investigate whether the sequence downstream of the CC domain(s) in CARD9 acts as an inhibitory domain in an analogous manner, we generated CARD9 constructs harboring a premature stop after the first CC (295*) and the second CC (419*). As expected, the two truncated forms show elevated activity compared to WT CARD9, indicating a common activation mechanism among CARD-CC proteins (**Figure 4B**).

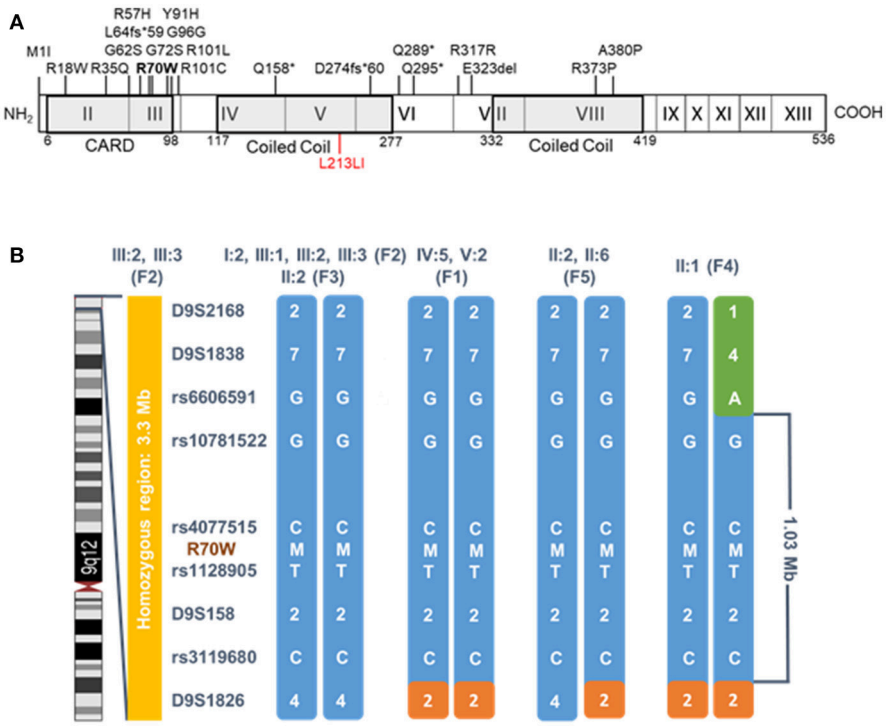

FIGURE 2 | *CARD9* structure and haplotype analysis of the R70W (c.208C>T) mutation. **(A)** Schematic *CARD9* gene structure and reported disease-associated mutations. Roman numbered boxes represent exons. Gray boxes situate the CARD and Coiled Coil domains at protein level. The R70W mutation is shown in bold, the gain-of-function L213LI mutation in red. **(B)** Segregation analysis of flanking microsatellites and single nucleotide polymorphisms revealed a common haplotype of 1.03 Mb. Patients codes refer to the pedigrees in **Figure 1**. Segregation of the haplotype in all available family members is shown in **Supplemental Figure 1**. M, mutant allele; F, family.

The Q295* mutation and similar Q289* are the two most common mutations occurring in patients with CARD9 deficiency (11 and 15 patients, respectively) (**Supplemental Table 1**). Auto-activation had already been shown for the Q295* mutant (10) but we here propose the mechanism behind that observation.

R70W CARD9 Disrupts Downstream NF-κB Signaling by Inhibiting BCL10 Recruitment and Filamentous Network Formation

To elucidate the underlying mechanism prohibiting R70W CARD9 from activating NF-κB, we studied its interactions with BCL10 and MALT1, which together with CARD9 form filamentous CBM complexes. As previously shown (28), without upstream activation, WT CARD9 failed to pull down BCL10 and MALT1, despite its activation of NF-κB in the reporter assays, presumably because that latter assay is more sensitive. To verify WT CARD9 could be activated by upstream stimuli, we used a setup similar to **Figure 3A**, but with upstream activation by PMA that activates protein kinase C upstream of CARD9. The results show that WT CARD9 is able to pull-down BCL10 and MALT1 upon activation (**Supplemental Figure 3**). Despite a decreased protein expression for the CARD9 mutants (**Supplemental Figure 4**), but in line with the reporter assay results, the GOF CARD9 mutant was exclusively able to pull-down BCL10 and MALT1. The R70W mutant did not pull down BCL10 and MALT1 and inhibited the GOF mutant to do so in the double mutant setup (**Figure 5A**), thus revealing that BCL10 recruitment is impaired by the R70W mutation. To rationalize the functional impact of the R70W mutation in CARD9 and to obtain complementary mechanistic insights, we leveraged structural information regarding the assembly principles of filamentous BCL10 and the CARD11-BCL10-MALT1 signalosome (15). N-terminal CARD domains sharing strong conservation in sequence and structure, constitute a hallmark of signalosome proteins, and are responsible for the ability of such proteins to oligomerize into intracellular filamentous structures (13–15). Given the paucity of structural information for the CARD domain of CARD9, we took advantage of the high sequence and structural homology shared by CARD domains to create a homology model for the CARD domain of CARD9 (**Supplemental Figure 5** and main **Figure 5B**). In the first instance, this revealed that position R70 maps to the end of helix 4 (α4) at the surface of the helical CARD9 scaffold (**Figure 5B**). Therefore, we reasoned that radical mutation of R70 to a tryptophan (grantham score = 101), as is the case in the identified R70W CARD, could be deleterious for the ability of CARD9 to interact either with itself to form filaments, or to annex to BCL10 filaments to nucleate signaling-competent CBM

TABLE 1 | Clinical and immunological details of the patients.

Kindred	**F1**			**F2**				**F3**	**F4**	**F5**		**Summary**
Patient	**IV:5 (index)**	**V:2**	**V:3**	**I:2**	**III:1**	**III:2 (index)**	**III:3**	**II:2 (index)**	**II:1 (index)**	**II:2 (index)**	**II:6**	
Age of onset (y)	8	8	5	48	18	7	2.5	39	5	8	35	2.5–48
Age at last follow-up (y)	57	34	NA	59	18	16	10	42	8	43	37	8–59
Current age	57	35	32	65	20	17	11	46	15	NA	NA	11–65
Region of origin (Turkey)	Eskişehir	Eskişehir	Eskişehir	Emirdag	Emirdag	Emirdag	Emirdag	Afyon	NA	Emirdag	Emirdag	Afyon + Eskişehir + Emirdag
Country of living	Belgium	Belgium	Belgium	Belgium	Belgium	Belgium	Belgium	France	Belgium	Belgium	Belgium	Belgium + France
Associated fungal disease(s)	*Mucosal;* CMC, *systemic;* lymphadenitis, chronic + invasive dermatophytosis	*Mucosal;* CMC	*Mucosal;* CMC, *systemic;* encephalitis	*Systemic;* Retroperitoneal aspergillosis	*Mucosal;* Pityriasis versicolor	*Mucosal;* CMC	*Mucosal;* CMC	*Mucosal;* CMC, *systemic;* meningo-encephalitis	*Mucosal;* CMC, *systemic;* meningo-encephalitis	*Mucosal;* CMC, *systemic;* osteomyelitis	*Mucosal;* CMC, *systemic;* abdominal candidiasis, lymphadenitis	range
Non infectious disease(s)	nasal obstruction, allergic asthma, dyspepsia, gonarthrosis, caries	substance abuse, psychosis	hypopara-thyroidism	hypothyroidism, diabetes, osteoporosis		reccurent warts on foot soles	reccurent warts on foot soles, visual problems, headaches					auto-immune endocrinopathy, various
Fungus cultured	*Trichophyton violaceum*, *T. verrucosum*, *T. rubrum*, *Malassezia furfur*	NA	*C. albicans*	*Aspergillus fumigatus*	*T. rubrum*	*C. albicans*	*C. albicans*	*C. albicans*	*C. albicans*	*C. albicans*	*C. albicans*	*C. albicans*, *Trychophyton* spp, *Aspergillus*
CD4T	Normal	High	Normal	Normal	NA	Normal	Normal	Normal	NA	Normal	Normal	8/9 normal
CD8T	Normal	Normal	Normal	Normal	NA	Normal	Normal	Normal	NA	Normal	Normal	9/9 normal
LTT[$]	Mitogens[a,c,d]: normal[f] Candida[a]: defect[h]	Mitogens[a,c,d]: normal[f] Candida[a]: defect[h]	Mitogens[a,c,d]: normal[f] Candida[a]: defect[h]	Mitogens[a,c,d]: normal[f] Candida[a]: NA	NA	Mitogens[a,c,d]: strong[i] Candida[a]: weak[g]	Mitogens[a,c,d]: strong[i] Candida[a]: weak[g]	Mitogens[a,c,d]: normal[f] Candida[a]: normal[f]	NA	Mitogens[b,c,e]: strong[i] Candida: NA	Mitogens[b,c,f]: normal[a] Candida: NA	5/8 decreased to *Candida*
Bc	Normal	Normal	Normal	NA	NA	Normal	Normal	Low	NA	Normal	Normal	7/8 normal
NKc	Normal	Normal	Normal	Normal	NA	Normal	Normal	Normal	NA	Normal	Normal	9/9 normal
IgE[£]	High[l] (18,200 kU/L) Ref: 0-100 kU/L	High[l] (843 kU/L) Ref: 0-100 kU/L	Increased[k] (161 kU/L) Ref: 0-100 kU/L	Increased[k] (276.7 kU/L) Ref: 0-100 kU/L	NA	Normal[j] (20.5 kU/L) Ref: 0-200 kU/L	Normal[j] (20.6 kU/L) Ref: 0-90 kU/L	NA	NA	Normal[j] (114 kU/L) Ref: 0-200 kU/L	High[l] (1,137 kU/L) Ref: 0-200 kU/L	5/8 hyper IgE

(Continued)

TABLE 1 | Continued

Kindred	F1			F2				F3	F4	F5		Summary
Patient	**IV:5 (index)**	**V:2**	**V:3**	**I:2**	**III:1**	**III:2 (index)**	**III:3**	**II:2 (index)**	**II:1 (index)**	**II:2 (index)**	**II:6**	
IgA	Normal (3.3 g/L) Ref: 0.83-4.07 g/L	Normal (4.1 g/L) Ref: 0.83-4.07 g/L	Normal (1.99 g/L) Ref: 0.83-4.07 g/L	Normal	NA	Normal (1.4 g/L) Ref:0.71-3.65 g/L	Normal (1.1 g/L) Ref:0.5-1.66 g/L	Normal	NA	Normal	Normal	8/8 normal
IgM	Normal (0.7 g/L) Ref: 0.34-2.14 g/L	Normal (0.7 g/L) Ref: 0.34-2.14 g/L	Normal (1.75 g/L) Ref: 0.34-2.14 g/L	Normal	NA	Normal (2.0 g/L) Ref: 0.40-2.48 g/L	Normal (0.9 g/L) Ref: 0.27-0.74 g/L	Normal	NA	Normal	Normal	9/9 normal
IgG	Normal (13.5 g/L) Ref: 7.0-16.0 g/L	Normal (13.9 g/L) Ref: 7.0-16.0 g/L	Normal (16.63 g/L) Ref: 7.0-16.0 g/L	Normal	NA	Normal (15.5 g/L) Ref: 7.0-16.0 g/L	Normal (11.9 g/L) Ref: 4.7-11.9 g/L	Normal	NA	Normal	Normal	9/9 normal
Eosinophilia	Yes	No	Yes	No	NA	No	No	Yes	Yes	No	No	4/10 eosinophilia
Th17 function[#]	ICS: Low[p] ELISA[m]: Low[p]	ICS: Low[p] ELISA[m]: Low[p]	NA	ICS: Low[p] ELISA[m]: Low[p]	ICS: Normal[°] ELISA[m]: Normal[°]	ICS: Low[p] ELISA[m]: Low[p]	ICS: Low[p] ELISA[m]: Low[p]	ICS: Normal[°] ELISA[n]: Normal[°]	ICS: Normal[°] ELISA[n]: Normal[°]	ICS: Low[p] ELISA[m,n]: Low[p]	ICS: Low[p] ELISA[m,n]: Low[p]	7/10 decreased
Fungal recognition[§] (IL-6 upon candida)	Low[s]	Low[s]	NA	Low-normal[r]	Normal[q]	Low[s]	Low[s]	Low-normal[r]	Low-normal[r]	NA	NA	6/8 decreased

CMC, chronic mucocutaneous candidiasis; LTT, lymphocyte transformation test; NA, not available.

If available, reference values are mentioned for tests performed in a routine diagnostic setting. For research assays, no reference values are available. Results were scored compared to internal assay healthy controls (HC). [$] For LTT the reference ranges depends on the lab where tests were run. The response on different stimuli was determined for 3 reference HCs to define internal criteria that can be used as cutoff. In addition the reference range was developed for fresh and frozen samples to take into account biological variability. To correct for interrun variability, the 3 reference HCs together with one variable HC were run together with the patient samples[(a)]. In another center a standard reference range was used[(b)]. Responses to C. albicans and the mitogens PHA[(c)], ConA[(d)] or PWM[(e)] were assessed. LTT was scored normal[(f)] if response comparable to HC, weak[(g)] for values below reference range, defect[(h)] for absent response and strong[(i)] for stronger response compared to HC. [£] IgE was scored normal[(i)] for values within the normal reference range, increased[(k)] for values above the reference range and high[(l)] for strong increased values. [#] Th17 function was assessed by intracellular cytokine staining (ICS) (proportion IL-17+ cells after stimulation with PMA/ionomycin measured by flow cytometry) and measurement of IL-17 production upon stimulation with SEB[(m)] and/or PMA/ionomycin[(n)] by ELISA. Th17 function was scored normal[(o)] for values within the HC range and low[(p)] if strongly impaired in comparison with the HCs. [§] Fungal recognition (IL-6 secretion upon Candida) was scored normal[(q)] for values within the HC range, low-normal[(r)] for values below the HC range and low[(s)] if secretion was strongly impaired.

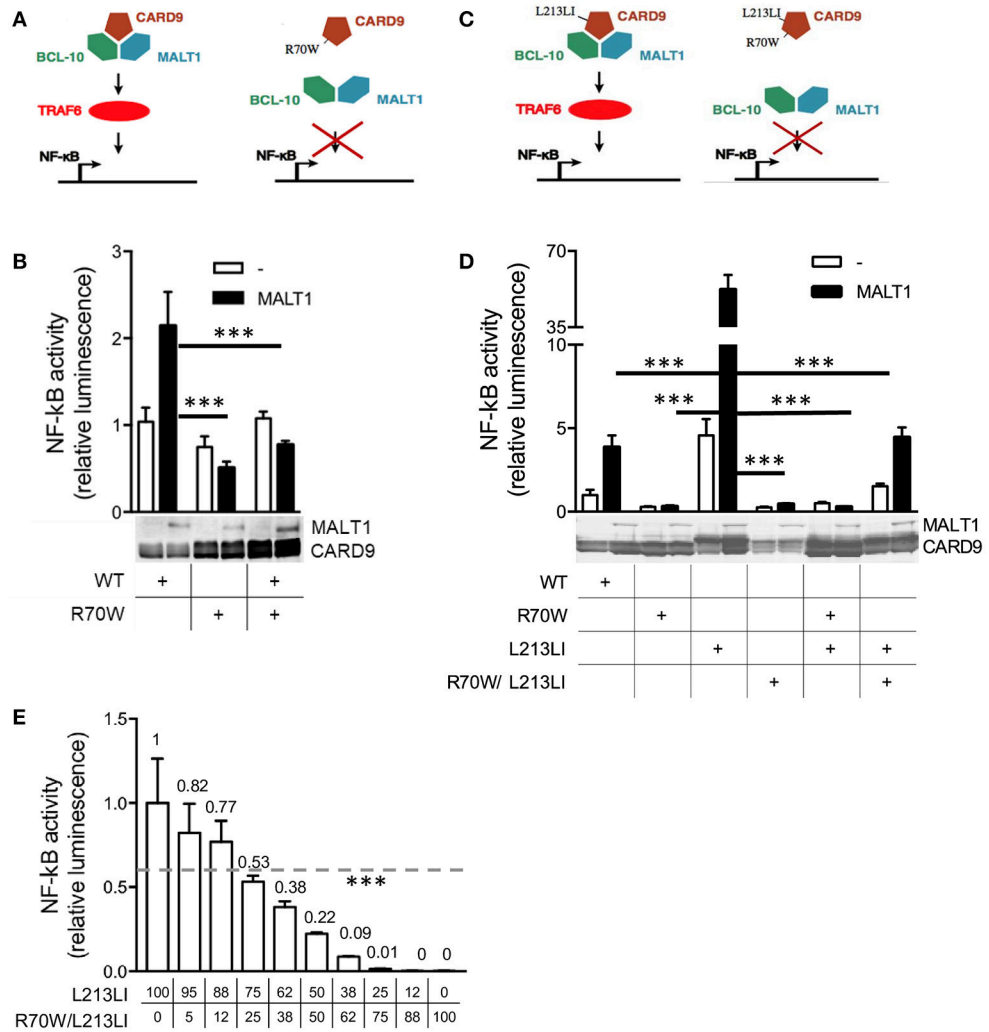

FIGURE 3 | R70W CARD9 inhibits NF-κB transcriptional activity. **(A, C)** Schematic summaries of the experimental conditions in **(B,D)** respectively, adjusted from (13). **(B, D)** MALT1-deficient HEK293T cells were transfected with WT, R70W, L213LI and R70W/L213LI CARD9 as indicated, with fixed total DNA quantities, with or without MALT1 as indicated, together with an NF-κB-dependent luciferase reporter expression plasmid and a constitutively expressed β-galactosidase reporter gene. Luciferase values were normalized against β-galactosidase and expressed as fold induction compared to WT CARD9 without MALT1. Expression of MALT1 and CARD9 protein measured by western blot are shown below the graphs. **(E)** WT HEK293T cells were co-transfected with decreasing doses of L213LI DNA and increasing doses of R70W/L213LI CARD9 DNA (ng/well, doses specified under graph). The total DNA amount was kept constant at 400ng/well. Luciferase values were expressed as fold induction compared to L213LI CARD9 alone. All values under the dotted line are significant.Results shown in **(B,D,E)** are mean +/- standard deviation of 4 replicates. One out of 2–3 representative experiments is shown. Statistical analysis was performed on reporter assay data with one-way ANOVA and Tukey's multiple comparison's **(B, D, E)** post-testing. The most relevant statistical differences are shown, a list of all p-values is provided in **Supplemental Tables 2–4**. $p < 0.001$ (***) in all panels, in **(B,D)** only for reporter assays with MALT1 reconstitution.

signalosomes, or to interact with other partner proteins. Indeed, modeling of CARD9-CARD structures into the BCL10-CARD filament as revealed by electron microscopy (15), indicates that position R70 localizes at the heart of the interfaces of consecutive CARD9-CARD modules within the helical filament (**Figure 5C**). Thus, mutation of this position to any amino acid residue, and in particular to a radically different amino acid in terms of structural and chemical properties such as tryptophan, will be expected to abrogate the ability of CARD9-CARD to mediate filamentous forms of the protein.

Looking for evidence to substantiate our *in silico* predictions, we performed confocal imaging on HEK293T cells transfected with Flag-CARD9 and E-BCL10. Wild-type CARD9 was found as a diffuse signal neighboring BCL10 filaments, which were polarized at one side of the nucleus (**Figure 5D** left panel). Compared to WT, the GOF L213LI CARD9 mutant induced a clustering of CARD9 in dense spheroid structures ornamenting an intricate network of branched BCL10 filaments that stretched all over the cellular body (**Figure 5D** middle panel). In contrast, the GOF/LOF double mutant CARD9

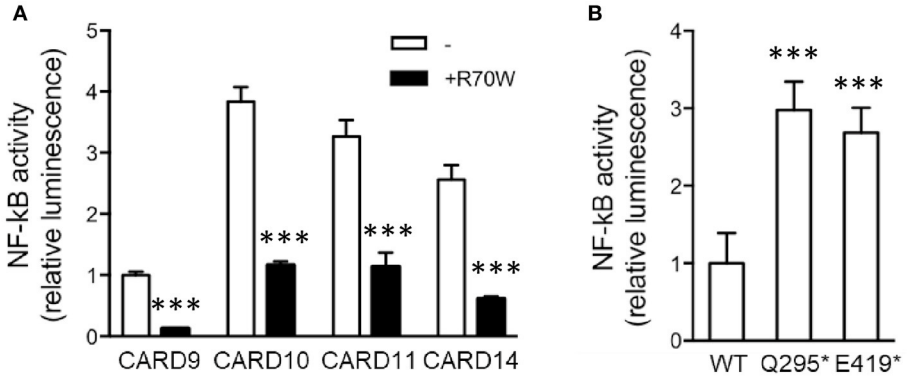

FIGURE 4 | CARD9 premature stop mutants reveal the presence of an N-terminal auto-inhibition domain **(A)**. NF-κB luciferase reporter assay of R70W CARD9 co-transfected with auto-active mutants of CARD9, CARD10, CARD11, and CARD14, all lacking the C-terminal inhibitory domain. Luciferase values were expressed as fold induction compared to WT CARD9 alone. **(B)** NF-κB luciferase reporter assay of CARD9 constructs, harboring a premature stop after the first CC (Q295*) and the second CC (E419*) domain. Results shown in both panels are mean +/- standard deviation of 4 replicates. Statistical analysis was performed on reporter assay data with one-way ANOVA and Tukey's multiple comparison's post-testing. The most relevant statistical differences are shown: each CARD protein compared with and without CARD9 R70W in **(A)** and each mutant compared to WT CARD9 in **(B)**. A list of all *p*-values is provided in **Supplemental Tables 5, 6**. ***$p < 0.001$.

failed to form a BCL10 network. Despite concentration of CARD9 in spheroid structures, suggesting that CARD9 itself was activated, the BCL10 filaments remained polarized at one side of the nucleus and failed to form a branched network all over the cell (**Figure 5D** right panel). This demonstrates that the R70W mutation indeed abrogates filamentous signalosome formation.

DISCUSSION

The adaptor protein CARD9 connects C-type lectin-receptor signals to the CBM signalosome to activate NF-κB upon fungal recognition by myeloid cells. Biallelic *CARD9* LOF mutations are associated with a wide range of fungal infections (**Supplemental Table 1**) and the here described R70W CARD9 patient cohort displays the same heterogeneity. This demonstrates that the nature of fungal infections a patient suffers from, is not determined by the type of *CARD9* mutation. The degree and severity of the presenting phenotype vary considerably between affected individuals and seem to aggravate with age with CMC always preceding invasive fungal disease (except in the case of F2 I:2 for whom this is unknown). Hence, an early diagnosis and accurate prophylaxis and follow-up are imperative to prevent CARD9 deficient patients from developing invasive infections.

The presence of a *CARD9* R70W founder mutation in the Turkish population from Afyonkarahisar/Eskişehir might simplify the laboratory diagnosis of CARD9 deficiency by targeted sequencing of the third exon. However, other mutations could be prevalent in that same population, since at least three patients of Turkish origin (though not precisely defined from which region) have been described with a Q295* nonsense mutation (exon 6) and a clinical presentation similar to the patients described in this manuscript (29, 30). Targeted resequencing of the R70W mutation in 68 healthy Turkish individuals from the Istanbul region (results not shown) showed that the allele was absent there, suggesting that it may be geographically confined to the rural provinces of Afyonkarahisar and Eskişehir, where a tradition of consanguineous marriages promotes passing on of recessive disease (31). At this moment, we have no evidence that the R70W *CARD9* mutation would provide any beneficial traits to the population, and its presence could thus be a direct consequence of endogamy within a small and genetically homogenous population, where a detrimental recessive allele became common through the founder effect (32, 33). Earlier research has already shown a common founder origin for another *CARD9* mutation [Q289*; (7)] of middle-eastern origin, which raises the idea that CARD9 heterozygosity may offer a certain protective effect in populations from the greater Mediterranean basin. Larger genetic studies looking at carriership of rare *CARD9* variants in this and other populations may provide more substance to this hypothesis.

We confirmed earlier observations that R70W CARD9 fails to activate NF-κB (10). In addition, we uncovered that this is because the R70W mutation disrupts the interaction with the critical downstream signaling proteins, BCL10 and MALT1, thus preventing the formation of CBM signalosomes.

Remarkable was the inhibitory effect of the R70W allele seen *in vitro* upon co-transfection with WT and GOF CARD9, which stands in sharp contrast to the absence of symptoms in heterozygous R70W carriers. The lack of phenotype in heterozygous carriers can be explained by a dose-dependent activation of NF-κB. This is supported by previous observations (10) and our own that the R70W allele has a tendency to produce less protein compared to WT. From our dose-response curves, we know that the R70W mutation, when expressed in the double mutant with the GOF allele, at a 1:1 DNA ratio with the GOF single mutant, leaves about 22% residual NF-κB activity. Translated to heterozygotes, such residual NF-κB activity could explain the absence of disease. Based on the low expression levels of the R70W allele that we (**Supplemental Figure 4**) and others (10) observed, heterozygotes would have a relative expression of

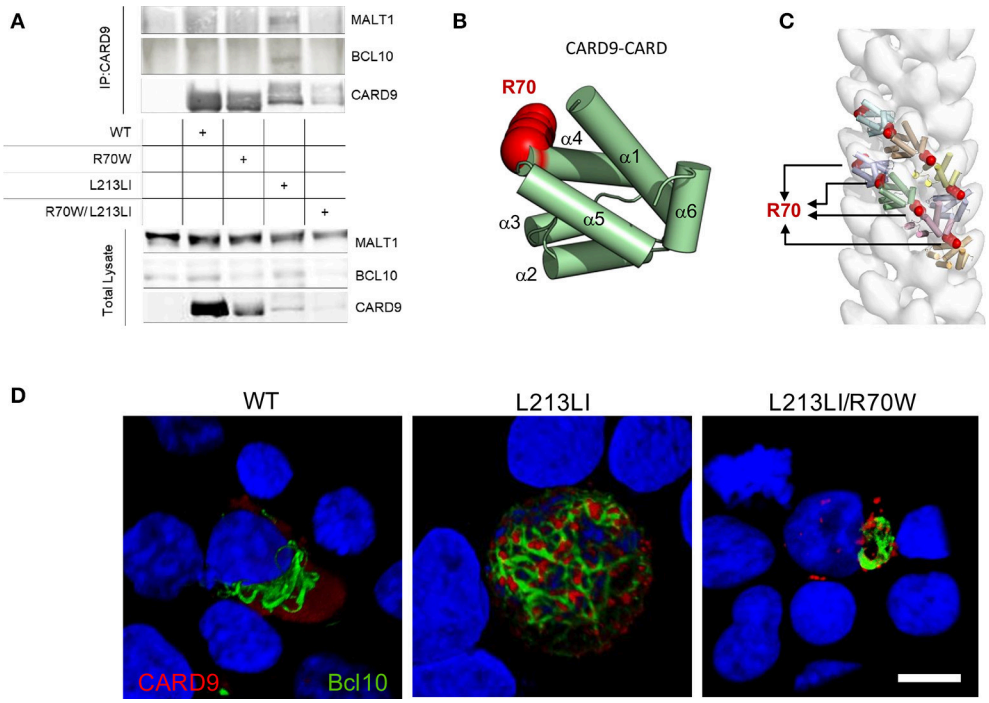

FIGURE 5 | R70W CARD9 fails to pull down BCL10 and MALT1 and inhibits BCL10 filamentous network formation. **(A)** WT HEK293T cells were co-transfected with MALT1 and E-tagged BCL10 with indicated Flag-tagged CARD9 constructs. The CARD9 variants were immunoprecipitated with anti-Flag antibody and co-immunoprecipitation of BCL10 and MALT1 was detected ("IP", upper panel) by anti-E-tag (BCL10) and anti-MALT1 antibody. CARD9 was detected with anti-Flag-HRP antibody. Input controls as immunoblotted on total lysate are shown in the lower panel. Density quantification of CARD9 on the total lysates is shown in **Supplemental Figure 4**. **(B)** A structural model for human CARD9 was created from structure-based sequence alignments of the sequence encoding the CARD domain of human CARD9 (uniprot Q9H257) and further improved computed via I-TASSER and QUARK. The R70 residue is depicted in red. **(C)** The homology model of the CARD domain of CARD9 was docked into a three-dimensional model representing the human BCL10 filament using the segment fitting algorithms implemented in Chimera. **(D)** E-tagged BCL10 was co-transfected with indicated Flag-tagged CARD9 constructs in un-stimulated HEK293T cells. Confocal imaging was performed with anti-E (BCL10, Green) and anti-Flag (CARD9, Red). 3D reconstructions of 50 Z-stacks are shown. Scale bar = 10μm.

WT/mutant CARD9 somewhere in the range of 70/30 or higher, hence even more residual NF-kB activity could be suspected.

The key to the profound inhibiting effect of R70W CARD9 lies in the structural data, which revealed that position R70 in CARD9-CARD maps at the interface between successive CARD domains in CARD9 filaments. We have illustrated the dramatic impact of R70W CARD9 that is intrinsically unable to participate in CARD9 and BCL10 filaments to seed signalosome assembly in a cellular context. This is in line with previous observations that many of the BCL10-CARD and CARD11-CARD interfacial residues are crucial for BCL10 polymerization as well as CARD11-CBM complex formation-induced NF-κB activation (15). The same study further demonstrates how CARD11 nucleates BCL10 filaments in order to form an active CBM signalosome (15). They propose a scenario in which CARD11 forms short helical segments to nucleate BCL10 segments using its coiled-coil domain. Our high resolution confocal data corroborate that scenario of short spheroid-like segments. Most missense disease-causing mutations, like R70W, are situated in the CARD9 CARD- and CC-domains. Along the scenario proposed by Qiao et al., these mutations are highly likely to abolish BCL10 filamentous network formation. Such profound inhibition against WT proteins is a characteristic of mutants of highly oligomeric assemblies (15, 34), such as the inflammasome adaptor Apoptosis-associated speck-like protein (ASC), where ASC mutants with a non-functional CARD only assemble filaments but not specks, thus inhibiting formation of functional inflammasomes (35).

Our structural insights rationalize the use of the L213LI GOF mutant. Like many lymphoma-related mutations (17), it maps to the coiled-coil. Along the Qiao scenario, its gain-of-function action thus derives likely both from overcoming auto-inhibition and by enhancing oligomerization (18). The use of this GOF mutant as a model for the *in vitro* activation of CARD9 in HEK293T cells, allowed us to observe a much stronger inhibitory effect of the R70W mutant allele in comparison to an upstream activation model (10). The GOF CARD9 model system focuses on CARD9-CBM NF-κB activation, whereas upstream stimuli, be it Dectin1-ligation or PMA, would also activate endogenous other CARD-CC proteins (CARD10 in case of HEK293T cells) or alternative pathways, thereby possibly masking the full effect of the R70W allele.

The different CARD-CC proteins are to some extent functionally redundant: CARD10 was shown to be able to

complement CARD11 deficiency in T cells (36), and there is evidence for CARD14-mediated zymosan signaling in keratinocytes (27). The R70W CARD9 allele also inhibited NF-κB activation by the three other CARD-CC proteins, CARD10, CARD11, and CARD14. This confirms the profound negative behavior of R70W CARD9 and demonstrates that hetero-multimerization can occur in the formation of a signaling-competent CBM signalosome. *In vivo*, however, CARD9 expression is confined to myeloid cells whereas CARD11 is expressed in lymphocytes and CARD10 and CARD14 mainly in different non-immune cells (www.biogps.org). These cell-type-specific expression profiles of the different CARD-CC proteins make it unlikely that a LOF CARD9 mutant would be able to influence the other CARD-CC signaling pathways *in vivo*. This is supported by the absence of symptoms others than fungal infections in CARD9 deficient patients.

The GOF CARD9 model system can be useful for future functional characterization of other disease-associated CARD9 mutations, as we illustrated for the Q295* allele. The method is however not without limitations, since disease-causing mutations that influence the response of CARD9 to upstream activating signals would be expected to leave a GOF CARD9 mutant unaffected. In that case, co-expression of CARD9 mutants with upstream signaling components would still be the best option.

In conclusion, we here expand the R70W CARD9 cohort to 11 patients of five unrelated families from Turkish descent and provide evidence supporting a common founder origin of this mutation. We demonstrate that the R70W mutation disrupts the interaction with the critical downstream signaling partners BCL10 and MALT1, thus prohibiting the formation of CBM signalosomes and NF-κB signaling.

AUTHOR CONTRIBUTIONS

MaD performed genetic analyses, analyzed genetic, and molecular analyses and wrote the manuscript. LH and DB assisted in genetic analyses. LV, EP, and MeD performed confocal analyses. ST assisted in molecular analyses. MM performed genetic analyses and provided patients samples. DK, BL, AA, LB, SvD, JY, and J-CG managed patients and provided clinical data. RB supervised molecular analyses. ED supervised genetic analyses. AP and J-LC provided patients samples and critically reviewed the data. SS performed structural analysis and critically reviewed the data. FH conceptualized the study, managed patients, provided clinical data and critically reviewed the data. JS conceptualized the study, supervised molecular analyses, performed data analysis and wrote the manuscript. MeD conceptualized the study, supervised experiments, performed data analysis and wrote the manuscript. All authors provided critical input and approved the final manuscript as submitted.

ACKNOWLEDGMENTS

This work was supported by the Jeffrey Modell Foundation, the Research Foundation Flanders (FWO), the University Hospital Ghent Spearhead Initiative for Immunology Research and by the Agence National pour la Recherche ANR HGDIFD (ANR-14-CE15-0006-01). DB is a PhD fellow and ED a senior clinical investigator of the FWO.

The authors gratefully acknowledge the patients and their family who participated in this study. We thank Fanny Lanternier, Veronique Debacker, Nancy De Cabooter, Mira Haegman, Yasmine Driege and Marja Kreike for excellent technical assistance and Debby Laukens and Sarah Gerlo for constructive feedback on the manuscript.

SUPPLEMENTARY MATERIAL

The Supplementary Material for this article can be found online at: https://www.frontiersin.org/articles/10.3389/fimmu.2018.02366/full#supplementary-material

REFERENCES

1. Puel A, Cypowyj S, Bustamante J, Wright JF, Liu L, Lim HK, et al. Chronic mucocutaneous candidiasis in humans with inborn errors of interleukin-17 immunity. *Science* (2011) 332:65–8. doi: 10.1126/science.1200439
2. Okada S, Puel A, Casanova J-L, Kobayashi M. Chronic mucocutaneous candidiasis disease associated with inborn errors of IL-17 immunity. *Clin Trans Immunol.* (2016) 5:e114–9. doi: 10.1038/cti.2016.71
3. Li J, Vinh DC, Casanova J-L, Puel A. Inborn errors of immunity underlying fungal diseases in otherwise healthy individuals. *Curr Opin Microbiol.* (2017) 40:46–57. doi: 10.1016/j.mib.2017.10.016
4. Gross O, Gewies A, Finger K, Schäfer M, Sparwasser T, Peschel C, et al. Card9 controls a non-TLR signalling pathway for innate anti-fungal immunity. *Nature* (2006) 442:651–6. doi: 10.1038/nature04926
5. Glocker EO, Hennigs A, Nabavi M, Schäffer AA, Woellner C, Salzer U, et al. A homozygous CARD9 mutation in a family with susceptibility to fungal infections. *N Engl J Med.* (2009) 361:1727–35. doi: 10.1056/NEJMoa0810719
6. Corvilain E, Casanova JL, Puel A. Inherited CARD9 Deficiency: invasive disease caused by ascomycete fungi in previously healthy children and adults. *J Clin Immunol.* (2018) 38:656–93. doi: 10.1007/s10875-018-0539-2
7. Drummond RA, Lionakis MS. Mechanistic insights into the role of C-Type lectin receptor/CARD9 signaling in human antifungal immunity. *Front Cell Inf Microbio.* (2016) 6:39. doi: 10.3389/fcimb.2016.00039
8. Lanternier F, Pathan S, Vincent QB, Liu L, Cypowyj S, Prando C, et al. Deep dermatophytosis and inherited CARD9 deficiency. *N Engl J Med.* (2013) 369:1704–14. doi: 10.1056/NEJMoa1208487
9. Rieber N, Gazendam RP, Freeman AF, Hsu AP, Collar AL, Sugui JA, et al. Extrapulmonary Aspergillus infection in patients with CARD9 deficiency. *JCI Insight* (2016) 1:e89890. doi: 10.1172/jci.insight.89890
10. Lanternier F, Mahdaviani SA, Barbati E, Chaussade H, Koumar Y, Levy R, et al. Inherited CARD9 deficiency in otherwise healthy children and adults with Candida species-induced meningoencephalitis, colitis, or both. *J. Allergy Clin Immunol.* (2015) 135:1558–68.e2. doi: 10.1016/j.jaci.2014.12.1930
11. Kao WP, Yang CY, Su TW, Wang YT, Lo YC, Lin SC. The versatile roles of CARDs in regulating apoptosis, inflammation, and NF-κB signaling. *Apoptosis* (2015) 20:174–95. doi: 10.1007/s10495-014-1062-4
12. Staal J, Driege Y, Haegman M, Borghi A, Hulpiau P, Lievens L, et al. Ancient origin of the CARD–Coiled Coil/Bcl10/MALT1-Like paracaspase signaling complex indicates unknown critical functions. *Front Immunol.* (2018) 9:1–16. doi: 10.3389/fimmu.2018.01136

13. Guiet C, Vito P. Caspase recruitment domain (CARD)-dependent cytoplasmic filaments mediate bcl10-induced NF-kappaB activation. *J. Cell Biol.* (2000) 148:1131–40. doi: 10.1083/jcb.148.6.1131
14. Bertin J, Guo Y, Wang L, Srinivasula SM, Jacobson MD, Poyet JL, et al. CARD9 Is a novel caspase recruitment domain-containing protein that interacts with BCL10/CLAP and Activates NF-κB. *J Biol Chem*. (2000) 275:41082–6. doi: 10.1074/jbc.C000726200
15. Qiao Q, Yang C, Zheng C, Fontán L, David L, Yu X, et al. Structural architecture of the CARMA1/Bcl10/MALT1 signalosome: nucleation-induced filamentous assembly. *Mol Cell* (2013) 51:766–79. doi: 10.1016/j.molcel.2013.08.032
16. Pérez de Diego R, Sánchez-Ramón S, López-Collazo E, Martínez-Barricarte R, Cubillos-Zapata C, Ferreira Cerdán A, et al. Genetic errors of the human caspase recruitment domain-B-cell lymphoma 10-mucosa-associated lymphoid tissue lymphoma-translocation gene 1 (CBM) complex: Molecular, immunologic, and clinical heterogeneity. *J Allergy Clin Immunol.* (2015) 136:1139–49. doi: 10.1016/j.jaci.2015.06.031
17. Lenz G, Davis RE, Ngo VN, Lam L, George TC, Wright GW, et al. Oncogenic CARD11 mutations in human diffuse large B cell lymphoma. *Science* (2008) 319:1676–9. doi: 10.1126/science.1153629
18. Turvey SE, Durandy A, Fischer A, Fung SY, Geha RS, Gewies A, et al. The CARD11-BCL10-MALT1 (CBM) signalosome complex: Stepping into the limelight of human primary immunodeficiency. *J Allergy Clin Immunol.* (2014) 134:276–84. doi: 10.1016/j.jaci.2014.06.015
19. de Medeiros AK, Lodewick E, Bogaert DJ, Haerynck F, Van Daele S, Lambrecht B, et al. Chronic and Invasive Fungal Infections in a Family with CARD9 Deficiency. *J Clin Immunol*. (2016) 36:204–9. doi: 10.1007/s10875-016-0283-4
20. Purcell S, Neale B, Todd-Brown K, Thomas L, Ferreira MA, Bender D, et al. PLINK: a tool set for whole-genome association and population-based linkage analyses. *Am J Human Genet*. (2007) 81:559–75. doi: 10.1086/519795
21. Okonechnikov K, Golosova O, Fursov M, UGENE team. Unipro UGENE: a unified bioinformatics toolkit. *Bioinformatics* (2012) 28:1166–7. doi: 10.1093/bioinformatics/bts091
22. Hulpiau P, Driege Y, Staal J, Beyaert R. MALT1 is not alone after all: identification of novel paracaspases. *Cell Mol Life Sci.* (2016) 73:1103–16. doi: 10.1007/s00018-015-2041-9
23. Calcium phosphate–mediated transfection of eukaryotic cells. *Nat Methods* (2005) 2:319–20. doi: 10.1038/nmeth0405-319
24. Zhang C, Mortuza SM, He B, Wang Y, Zhang Y. Template-based and free modeling of I-TASSER and QUARK pipelines using predicted contact maps in CASP12. *Proteins* (2017) 79:37. doi: 10.1002/prot.25414
25. Pettersen EF, Goddard TD, Huang CC, Couch GS, Greenblatt DM, Meng EC, et al. UCSF Chimera–a visualization system for exploratory research and analysis. *J Comput Chem*. (2004) 25:1605–12. doi: 10.1002/jcc.20084
26. Aricescu AR, Lu W, Jones EY. A time- and cost-efficient system for high-level protein production in mammalian cells. *Acta Crystallogr.* (2006) 62:1243–50. doi: 10.1107/S0907444906029799
27. Afonina IS, Van Nuffel E, Baudelet G, Driege Y, Kreike M, Staal J, et al. The paracaspase MALT1 mediates CARD14-induced signaling in keratinocytes. *EMBO Rep*. (2016) 17:914–27. doi: 10.15252/embr.201642109
28. Strasser D, Neumann K, Bergmann H, Marakalala MJ, Guler R, Rojowska A, et al. Syk kinase-coupled C-type lectin receptors engage protein kinase C-σ to elicit Card9 adaptor-mediated innate immunity. *Immunity* (2012) 36:32–42. doi: 10.1016/j.immuni.2011.11.015
29. Herbst M, Gazendam R, Reimnitz D, Sawalle-Belohradsky J, Groll A, Schlegel PG, et al. Chronic candida albicans meningitis in a 4-Year-Old girl with a homozygous mutation in the CARD9 gene (Q295X). *Pediatr Infect Dis J.* (2015) 34:999–1002. doi: 10.1097/INF.0000000000000736
30. Celmeli F, Oztoprak N, Turkkahraman D, Seyman D, Mutlu E, Frede N, et al. Successful granulocyte colony-stimulating factor treatment of relapsing candida albicans meningoencephalitis caused by CARD9 deficiency. *Pediatr Infect Dis J.* (2016) 35:428–31. doi: 10.1097/INF.0000000000001028
31. Kaplan S, Pinar G, Kaplan B, Aslantekin F, Karabulut E, Ayar B, et al. The prevalence of consanguineous marriages and affecting factors in Turkey: a national survey. *J Biosoc Sci.* (2016) 48:616–30. doi: 10.1017/S0021932016000055
32. Reniers G. The post-migration survival of traditional marriage patterns: consanguineous marriages among Turks and Moroccans in Belgium. *J Comp Fam Stud*. (2001) 32:21–45.
33. Staal J. Applied cultural and social studies are needed for a sustainable reduction of genetic disease incidence. *Eur J Sociol Anthropol.* (2017) 2:1–10. doi: 10.20897/ejsa.201701
34. Wu H, Fuxreiter M. The structure and dynamics of higher-order assemblies: amyloids, signalosomes, and granules. *Cell* (2016) 165:1055–66. doi: 10.1016/j.cell.2016.05.004
35. Dick MS, Sborgi L, Rühl S, Hiller S, Broz P. ASC filament formation serves as a signal amplification mechanism for inflammasomes. *Nat Commun*. (2016) 7:11929. doi: 10.1038/ncomms11929
36. Matsumoto R, Wang D, Blonska M, Li H, Kobayashi M, Pappu B, et al. Phosphorylation of CARMA1 plays a critical role in T Cell receptor-mediated NF-kappaB activation. *Immunity* (2005) 23:575–85. doi: 10.1016/j.immuni.2005.10.007

Conflict of Interest Statement: The authors declare that the research was conducted in the absence of any commercial or financial relationships that could be construed as a potential conflict of interest.

frontiers in Immunology

MINI REVIEW
published: 11 March 2019
doi: 10.3389/fimmu.2019.00419

CARD9 Signaling in Intestinal Immune Homeostasis and Oncogenesis

Lara Hartjes[1] *and Jürgen Ruland*[1,2,3]*

[1] *Institute of Clinical Chemistry and Pathobiochemistry, School of Medicine, Technical University of Munich, Munich, Germany,* [2] *German Cancer Consortium (DKTK), Heidelberg, Germany,* [3] *German Center for Infection Research (DZIF), Munich, Germany*

Intestinal homeostasis requires a balanced interaction between the host innate immune system and the gut microbiota. A dysregulation of this interdependency can result in inflammatory bowel diseases (IBDs), and this dysregulation is a key pathogenic factor during the development of colorectal cancer. CARD9 is a central signaling molecule in the innate immune system, which is essential for host defense against infection. Moreover, polymorphisms in *CARD9* are key risk factors for IBD development, indicating that CARD9 signaling is critical for intestinal immune homeostasis. This review summarizes recent insights into the regulation of CARD9 signaling, its pathophysiological role during IBD development via effects on the microbiota and epithelial regeneration and the pro- and antitumor immune functions of CARD9 during intestinal carcinogenesis.

Keywords: CARD9, intestinal immune homeostasis, inflammatory bowel disease, intestinal inflammation, intestinal carcinogenesis, gut microbiome

OPEN ACCESS

Edited by:
Frederic Bornancin, Novartis, Switzerland

Reviewed by:
Harry Sokol, Saint Antoine Hospital, APHP, France
Suryasarathi Dasgupta, University of California, San Diego, United States

***Correspondence:**
Jürgen Ruland
j.ruland@tum.de
orcid.org/0000-0002-8381-3597

Specialty section:
This article was submitted to Molecular Innate Immunity, a section of the journal Frontiers in Immunology

Received: *04 December 2018*
Accepted: *18 February 2019*
Published: *11 March 2019*

Citation:
Hartjes L and Ruland J (2019) CARD9 Signaling in Intestinal Immune Homeostasis and Oncogenesis. Front. Immunol. 10:419. doi: 10.3389/fimmu.2019.00419

INTRODUCTION

Homeostasis in the gastrointestinal tract depends on balanced interactions between the host immune system and the gut microbiome. The microbiome encompasses bacteria, fungi, and other microorganisms, and its composition is dynamically shaped by the host immune system, which continuously senses microbes and their metabolites and reacts with tolerogenic or stimulatory signals (1). Dysregulation of the immune-microbial balance due to the host's genetic composition, microbial dysbiosis, or environmental factors can cause inflammatory bowel diseases (IBDs), such as ulcerative colitis and Crohn's disease (2). Moreover, both overt chronic inflammation and smoldering inflammation are key risk factors for the development of gastrointestinal cancers (3). Therefore, understanding the reciprocal interaction between the host immune system and the intestinal microbiome is of great biomedical importance.

To sense microbial structures in the gut, innate immune cells are located in the lamina propria underneath the intestinal epithelium and in organized lymphoid structures. These cells are equipped with germline-encoded pattern recognition receptors (PRRs) that survey the intestinal environment and engage intracellular signaling pathways to induce the production of effector molecules that orchestrate local immunity. Importantly, a majority of genetic susceptibility loci that modulate the risk of developing IBD lie within genes involved in immune responses (4), which underscores the importance of immune signaling in IBD development. One very prominent IBD susceptibility gene whose key function in intestinal pathophysiology is being increasingly understood is *CARD9,* which encodes the innate immune signaling adapter protein CARD9 (4–8). This review will summarize recent insights into the molecular functions of CARD9 signaling and its role in intestinal inflammation and oncogenesis.

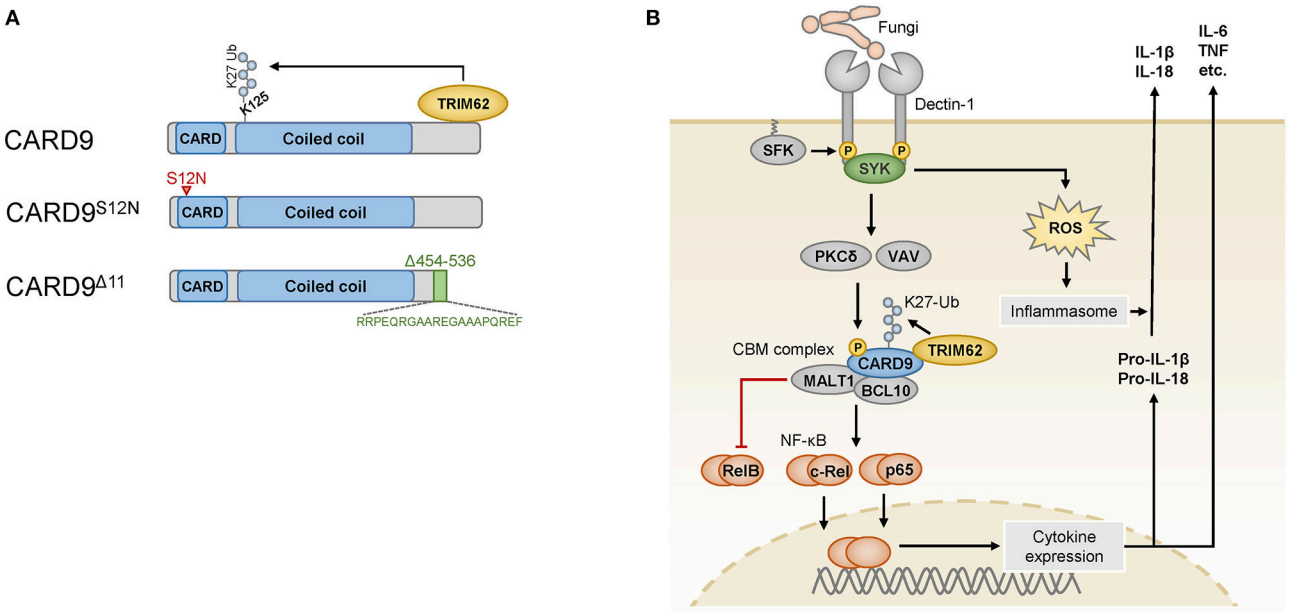

FIGURE 1 | (A) The wild-type CARD9 protein consists of an N-terminal caspase activation and recruitment domain (CARD) followed by a coiled-coil domain and a C-terminal tail. The C-terminus mediates binding to the ubiquitin ligase TRIM62, which ubiquitinates CARD9 at K125. The CARD9^{S12N} variant encoded by an IBD risk-associated SNP carries an amino acid substitution in the N-terminal portion of the CARD domain (indicated by the red arrowhead). The rare variant CARD9$^{\Delta 11}$ results from the skipping of exon 11, and instead of the amino acids 454–536, it bears a shortened and altered C-terminus (indicated in green) that is unable to bind to TRIM62. **(B)** Fungi are sensed by myeloid cells through Dectin-1, which is phosphorylated by SRC-family kinases (SFK) in its cytoplasmic portion upon ligand binding. The spleen tyrosine kinase (SYK) can recognize these phosphosites and activate the protein kinase C (PKC) δ and VAV proteins, which cooperate to phosphorylate CARD9, enabling it to assemble the CARD9-BCL10-MALT1 (CBM) complex. K27 ubiquitination of CARD9 by TRIM62 enables the activation of NF-κB, which consists of the transcriptionally active subunits c-Rel, p65 and RelB. RelB is counterregulated by the proteolytic activity of MALT1. Cytokines produced after stimulation of this pathway include IL-6, TNF and pro-IL-1β, which is further processed and released by inflammasomes that are triggered in a SYK- and reactive oxygen species (ROS)-dependent manner. Pro-IL-18 is similarly processed and released by the inflammasome.

MOLECULAR MECHANISMS OF CARD9 SIGNALING

CARD9 is selectively expressed in myeloid immune cells, including dendritic cells, macrophages, and neutrophils, and it is composed of an N-terminal caspase-activating and recruitment domain (CARD), a coiled-coil domain and a C-terminal tail with no specific domain structure (9) (**Figure 1A**). CARD9 can be activated by several plasma membrane-associated and intracellular PRRs (10, 11), and it is critical for the function of SYK-coupled C-type lectin receptors (CLRs). These CLRs, including Dectin-1 (12), Dectin-2 (13), and Mincle (14, 15), are key PRRs for the detection of commensal and pathogenic fungi but can also sense certain bacteria or danger signals released from dying host cells (16). The CLR-mediated activation of SYK leads to the activation of PKCδ via intermediate steps (**Figure 1B**), and PKCδ then directly phosphorylates CARD9 at T231 in the coiled-coil domain (17) in cooperation with VAV proteins (18). These molecular events enable CARD9 activation and the assembly of a BCL10- and MALT1-containing signaling platform, termed the CARD9-BCL10-MALT1 (CBM) complex, which serves as a scaffold to place ubiquitin modifiers and protein kinases in proximity to activate downstream effector pathways (9).

One major effector pathway of the CBM complex is the canonical IκB kinase (IKK)-mediated NF-κB pathway, which controls the expression of a variety of immune-regulatory factors. The NF-κB family consists of several subunits, of which p65, c-Rel, and RelB are transcriptionally active and form homodimers and heterodimers with other NF-κB proteins to initiate gene expression (19). To mediate NF-κB signaling, CARD9 recruits the ubiquitin ligase TRIM62, which binds to the C-terminal tail of CARD9 and mediates K27-linked ubiquitination of CARD9 on K125 in the coiled-coil domain (20) (**Figure 1A**). This modification is dispensable for the formation of the CBM complex but critical for the downstream activation of NF-κB (20). The CBM complex activates NF-κB dimers containing the subunits p65 or c-Rel (18), while MALT1 also functions as a protease that can inactivate the subunit RelB (21) to control distinct NF-κB subprograms. RelB is a subunit that is primarily activated by the noncanonical NF-κB pathway, and it can bind to the *IL5* promoter to activate *IL5* transcription in myeloid cells (22). Factors regulated by the canonical NF-κB pathway include pro-inflammatory cytokines, including TNF, IL-6 and the pro-inflammatory cytokine precursor pro-IL-1β, which is processed by inflammasomes into mature IL-1β. Inflammasomes are activated in response to fungal recognition in a SYK- and reactive oxygen species-dependent manner (23), and they can process additional cytokines of the IL-1 family, e.g., IL-18.

CARD9 signaling can also be activated by intracellular PRRs, such as the nucleotide-binding oligomerization domain-containing protein 2 (NOD2) (11), which is encoded by another important IBD risk gene, *NOD2* (4). In this pathway, NF-κB is activated independently of CARD9 by the interaction of NOD2 with RIPK2, whereas the interaction of NOD2 with CARD9 promotes the activation of the MAP kinases p38 and JNK, supporting pro-inflammatory cytokine production in response to stimulation with the bacterial cell wall component peptidoglycan or *Listeria monocytogenes* infection (11). Moreover, CARD9 is activated in response to the ligation of the nucleic acid receptors RIG-I (24) and RAD50 (25) after recognition of bacterial or viral nucleic acids, which also trigger the activation of the NF-κB pathway and the subsequent production of pro-inflammatory cytokines.

These CARD9-mediated signaling pathways are critical for host defense, particularly for protection against fungi, as CARD9-deficient mice and humans with *CARD9* loss-of-function mutations exhibit severe susceptibility to fungal infections caused by species such as *Candida albicans* (26) or dermatophytes (27), with invasive fungal growth into tissues (28). These protective functions are in part mediated by the critical role of CARD9 in inducing adaptive T_H17 cell responses (26, 29), which exert defense mechanisms against fungi and other extracellular pathogens. Moreover, during fungal infection, CARD9 controls the induction of neutrophilic myeloid-derived suppressor cells (MDSCs) (30), which prevent damaging hyperinflammation by counterbalancing T and NK cell responses.

CARD9 GENETIC VARIANTS IN INTESTINAL INFLAMMATION

While a complete loss of CARD9 results in immunodeficiency, several single-nucleotide polymorphisms (SNPs) in the human *CARD9* gene are associated with inflammatory diseases, particularly with IBD (rs10781499 (4), rs10870077 (5), and rs4077515 (6, 7)). Non-coding or synonymous variants presumably influence the level of CARD9 expression (31, 32) and thereby modulate the strength of CARD9 signaling. In addition, the IBD-associated SNP rs4077515 encodes a missense CARD9 variant that carries an asparagine instead of a serine residue in the CARD domain in position 12 ($CARD9^{S12N}$) (**Figure 1A**). Experiments with knock-in mice that carry the $CARD9^{S12N}$-encoding allele have demonstrated that $CARD9^{S12N}$ leads to aberrant activation of RelB and subsequent excessive production of IL-5 by myeloid cells in response to *A. fumigatus*, which skews T cell responses toward T_H2 differentiation (22). These findings indicate that $CARD9^{S12N}$ deviates physiological CARD9 signaling and suggest that the respective SNP in human IBD could potentially contribute to intestinal inflammation through related mechanisms, although this possibility remains to be investigated.

While the above-mentioned *CARD9* risk SNPs are relatively frequent and only moderately increase IBD risk (odds ratio (OR) $\approx$ 1.2), a rare splice site variant of CARD9 confers strong protection from IBD (OR $\approx$ 0.3–0.4) (8, 33). This specific variant, IVS11+1C>G, results in the skipping of exon 11, which leads to a CARD9 protein with a shortened C-terminal tail ($CARD9^{\Delta 11}$) (**Figure 1A**). $CARD9^{\Delta 11}$ is unable to bind TRIM62 and consequently fails to induce pro-inflammatory cytokines in myeloid cells after stimulation with fungal particles (20), which is thought to be responsible for the protective activity of $CARD9^{\Delta 11}$ during IBD pathogenesis.

CARD9 SIGNALING IN MURINE MODELS OF INTESTINAL INFLAMMATION

Based on the association of *CARD9* SNPs with IBD susceptibility, several research groups have started to investigate the role of CARD9 in murine models of experimental colitis (34, 35). In these studies, colitis was triggered by the administration of the chemical compound dextran sodium sulfate (DSS) via the drinking water (34, 35) or by oral inoculation with *Citrobacter rodentium* (34, 36). Both regimens damage the colonic epithelium and enable the entry of intestinal contents including bacteria and fungi into submucosal layers, triggering intestinal inflammation that leads to weight loss in the animals, followed by a recovery phase after DSS discontinuance in the DSS model (37, 38) or upon bacterial clearance in the *C. rodentium* model (34, 36).

CARD9-deficient mice exhibited a defect in epithelial regeneration and a significant delay in weight gain during the recovery phase after acute colitis (34, 35). The deficiency of CARD9 affects primarily myeloid cells and cytokines produced by these cells, which secondarily act on other cell types in the intestinal environment. Based on this interplay, CARD9 deficiency results in reduced production of pro-inflammatory cytokines (IL-6, TNFα, and IFNγ) and T_H17- and innate lymphoid cell (ILC)-related cytokines (IL-17A, IL-17F, and importantly IL-22) by leukocytes in the lamina propria and mesenteric lymph nodes (34, 35). This phenotype is in part caused by defective production of the chemokine CCL20, which is required to recruit T_H17 cells and ILCs to sites of epithelial damage (34), and by the failure of CARD9-deficient myeloid cells to secrete optimal amounts of IL-1β, which is necessary to stimulate IL-22 production by ILCs (**Figure 2**) (35). IL-22 is a key cytokine that promotes recovery from DSS-induced or *C. rodentium*-induced inflammation. IL-22 binds to its receptor on intestinal epithelial cells (IECs), which drives their regenerative proliferation (39) and stimulates the expression of antimicrobial peptides for innate defense against intruding microbes. As a consequence of impaired IL-22 and IL-17 signals, the IECs in CARD9-deficient mice do not receive the proper pro-proliferative signals for recovery (35), and they fail to produce sufficient amounts of antimicrobial peptides (34). Apart from controlling gut microbes through the epithelial compartment, CARD9-expressing myeloid cells also provide signals that support humoral responses to *C. rodentium* (36), although the exact mechanisms of this interaction remain to be investigated.

Additional work demonstrated that CARD9 also shapes the composition of the gut microbiome and affects both fungal

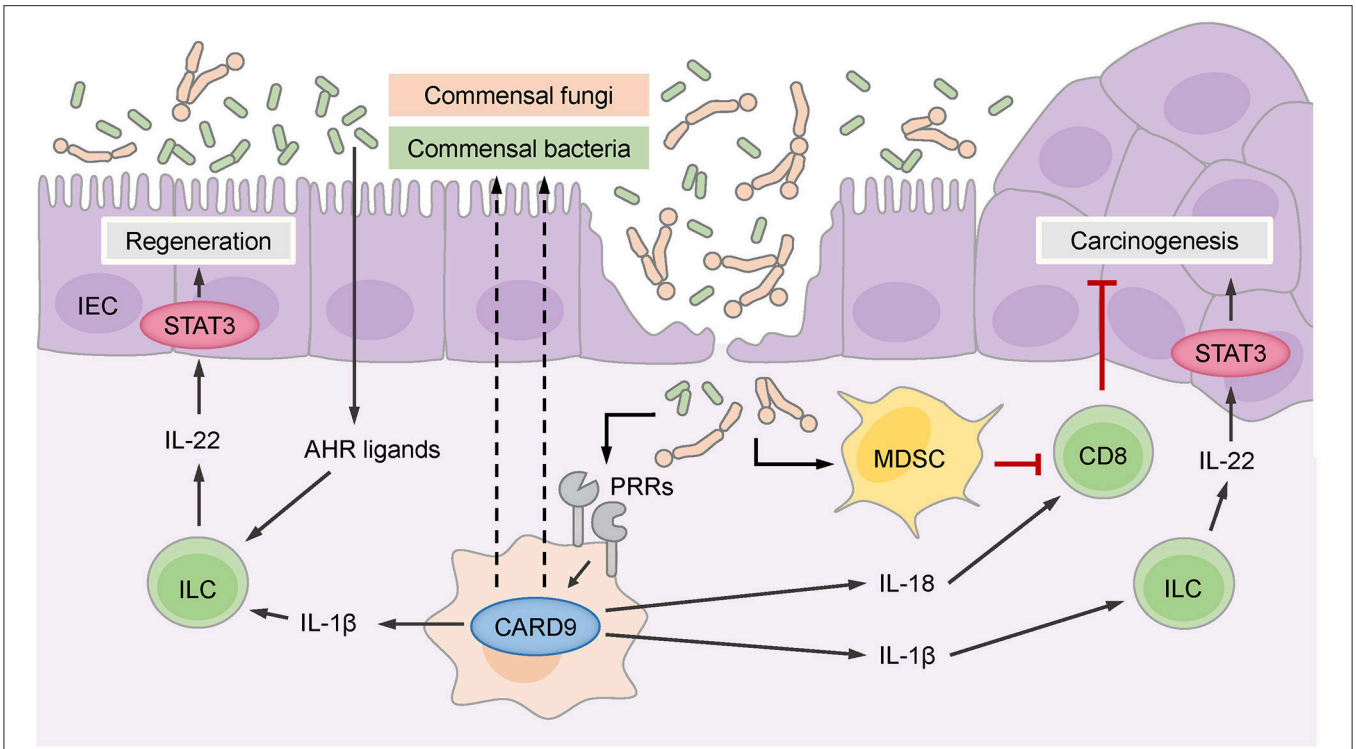

FIGURE 2 | CARD9 controls the intestinal microbiome, which consists of commensal bacteria and fungi. Commensal gut bacteria supported by CARD9 provide aryl hydrocarbon receptor (AHR) ligands for the stimulation of innate lymphoid cells (ILCs) that secrete IL-22 to promote the regeneration of intestinal epithelial cells (IECs) through signal transducer and activator of transcription 3 (STAT3). ILCs are also stimulated by IL-1β, which is produced in a CARD9-dependent manner. CARD9 activated by pattern recognition receptors (PRRs) regulates commensal gut fungi that enter the damaged epithelium and promotes the accumulation of myeloid-derived suppressor cells (MDSCs). MDSCs inhibit $CD8^+$ cytotoxic T cells that keep malignant IECs in check and thereby prevent carcinogenesis. $CD8^+$ T cells are also stimulated by IL-18, which is secreted in response to commensal fungi in a CARD9-dependent manner. The CARD9-dependent IL-1β-IL-22 axis can support carcinogenesis through the stimulation of STAT3 in malignant IECs.

and bacterial communities (40). Under steady-state conditions, the fungal burden is increased in CARD9-deficient mice, and during colitis, the fungal microbiome changes more substantially in CARD9-deficient mice than in wild-type mice. Similarly, at baseline, the composition of the bacterial microbiome is disturbed in CARD9-deficient mice and exhibits decreased stability during DSS colitis. Underrepresented bacteria in CARD9-deficient mice include, for example, species from the *Adlercreutzia* genus and *Lactobacillus reuteri*. Under steady-state conditions, this dysbiotic microbiota of CARD9-deficient mice exhibits a striking failure to metabolize tryptophan into ligands of the aryl hydrocarbon receptor (AHR) transcription factor (**Figure 2**), which is crucial for the expression of IL-22 by T_H17 cells (39). This failure to produce AHR ligands has also been linked to impaired IL-22 production and delayed epithelial restitution in CARD9-deficient mice (40). Together, these experimental studies revealed that CARD9 signaling within the myeloid compartment affects epithelial regeneration during the recovery from colitis by triggering ILC and T_H17 responses, in part by directing the microbiota toward AHR ligand-producing species. These pathways are presumably also important for the pathogenesis of IBD in patients with CARD9 risk variants, as a deficiency in AHR ligands is observed in the microbiota of IBD patients with the *CARD9* risk SNP rs10781499 (40).

CARD9 IN IMMUNE ENVIRONMENTS IN COLORECTAL CANCER

The inflammatory pathways that stimulate the regenerative expansion of normal IECs are also frequent drivers of malignant proliferation and survival in transformed epithelial cells during colorectal cancer pathogenesis (3). However, in addition to providing pro-inflammatory, tumor-promoting effects, immune cells also play a protective role in colorectal cancer, which is largely executed via the antitumor activity of cytotoxic $CD8^+$ T cells, whose presence within the tumor tissue is one of the strongest prognostic markers for a positive clinical outcome in colorectal cancer patients (41). Recent studies revealed that CARD9 signaling can contribute to both tumor-promoting and tumor-suppressive immunity in the intestine, and these distinct effects are strongly influenced by the composition of the microbiota (35, 42, 43).

To explore the role of CARD9 in colitis-associated cancer (CAC) independent groups used CARD9-deficient mice in the

AOM/DSS model (35, 42–44). In this model, the administration of the carcinogen azoxymethane (AOM) initiates mutations in IECs, and subsequent cycles of DSS administration trigger inflammation that promotes epithelial dysplasia through a variety of immune cell-derived mediators, growth factors and cytokines. In wild-type mice, this treatment protocol provokes the formation of multiple polyploid lesions in the colon and rectum, with histological scores from low to high grade, but invasive dysplasia rarely occurs in this context.

To minimize the effects of the microbiota on tumor development, Bergmann et al. co-housed CARD9-deficient mice and littermate controls from birth on and during the AOM/DSS treatment protocol (35). Under these conditions, CARD9-deficient mice displayed smaller polyps in the distal colon than wild-type mice, although the total number of polyps did not differ between CARD9-deficient and wild-type mice. Moreover, the rate of tumor cell proliferation was decreased in CARD9-deficient mice, and the tumor cell-intrinsic activation of STAT3 was substantially reduced. STAT3 is a key transcription factor that drives the proliferation and survival of malignant cells during CAC pathogenesis (45) and is activated by several cytokines and growth factors, including IL-22 (39). These experiments indicate that CARD9 signaling in the immune environment of developing colorectal cancers can trigger the tumor-promoting STAT3 pathway within tumor cells, presumably via ILC-mediated IL-22 production, comparable to its role during epithelial regeneration after acute colitis (34, 35).

Two subsequent studies single-housed CARD9-deficient and wild-type animals to dissect the microbiota-dependent influences on CAC development using the AOM/DSS model (42, 43). Under these conditions, CARD9-deficient mice develop more and larger tumors than wild-type mice, and these effects were attributed to an aberrant fungal microbiome and secondary effects of fungi on antitumor T cells (42, 43). Wang et al. found that several fungal species, particularly *Candida tropicalis,* were enriched in the intestinal flora of CARD9-deficient mice (43) and interestingly also in the feces of colorectal cancer patients (43). Moreover, monocolonizing germ-free mice with *C. tropicalis*, but not with the irrelevant fungal species *Saccharomycopsis fibuligera,* increased their susceptibility to CAC in the AOM/DSS model, indicating that this species can support cancer development (43). Mechanistically, Wang et al. proposed that specific fungi promote the accumulation and activation of granulocytic MDSCs in the colonic lamina propria, which suppress the proliferation and effector functions of T cells and thereby negatively interfere with T cell-mediated antitumor immunity and enable enhanced colorectal cancer growth (**Figure 2**). Since the fungal load in the feces of colorectal cancer patients positively correlates with MDSC frequencies in the tumor, this pathway could also play an important role in clinical settings (43).

Similarly, Malik et al. observed an increased tumor burden in CARD9-deficient mice using the AOM/DSS model under single-housing conditions (42), but they propose an additional mechanism. While this group also demonstrates that CARD9 signaling shapes the composition of fungal communities and T cell immunity in the colon, they show that CARD9 controls the IL-1 family cytokine IL-18 through a canonical SYK-dependent pathway in myeloid cells in the early phase of the AOM/DSS treatment protocol (42) (**Figure 2**). IL-18 can maintain intestinal epithelial integrity during inflammation and stimulate IFNγ and FASL expression by T cells (42, 46), supporting antitumor immunity during CAC development. Consistent with this model, supplementation with exogenous IL-18 restored T cell function in CARD9-deficient mice during CAC, ameliorated the exacerbated intestinal inflammation and reduced tumor development (42).

Together, these two studies reveal previously unknown functions of CARD9 in the control of fungal communities that initiate MDSCs and stimulate IL-18 secretion, both of which regulate the function of antitumor $CD8^+$ T cells during CAC development (**Figure 2**). Nevertheless, it remains unclear to what extent the overall fungal load determines CAC outcome, as the pharmacological depletion of fungi can on one hand reduce MDSC frequencies and thus enhance antitumor T cell responses in CARD9-deficient mice (43) but on the other hand result in a lack of IL-18 signals for stimulation of antitumor T cells (42).

CONCLUSION AND PERSPECTIVE

The human *CARD9* locus has been a known IBD susceptibility factor for more than 10 years, and during that time, the basic mechanisms of CARD9 signaling have been elucidated (9). In IBD, both risk-promoting and protective CARD9 variants have been identified, and based on an understanding of the protective CARD9 variant, which is defective in the CARD9-TRIM62 interaction, small-molecule inhibitors that block the CARD9-TRIM62 interaction have been developed that might be useful for IBD treatment (47). Additional pathomechanisms of CARD9 signaling during IBD are alterations in regenerative IL-22 signaling via the effects of CARD9-expressing myeloid cells on ILCs (34, 35) or via the effects of CARD9 on the control of the microbiota (40, 42, 43), which could also provide new strategies for IBD treatment. The key role of CARD9 in intestinal immune homeostasis is also underscored by the influence of CARD9 signaling on colorectal cancer development. Here, depending on the composition of the microbiota, particularly the fungal communities, CARD9 can play a pro-tumorigenic role by triggering inflammation-induced oncogenic STAT3 activation within malignant cells or a tumor-suppressive function by promoting antitumor T cell responses through various mechanisms. How the balance between these CARD9-mediated pro- and antitumor immune functions is precisely tuned requires further investigation. Such studies are expected to provide further insights into the complex interplay among the immune system, the microbiota, tissue homeostasis and cancer development, as well as potential rational targets for therapeutic interventions.

AUTHOR CONTRIBUTIONS

All authors listed have made a substantial, direct and intellectual contribution to the work, and approved it for publication.

FUNDING

Work in the authors' laboratory is supported by research grants from the Deutsche Forschungsgemeinschaft (SFB 1054/B01, SFB 1335/P01 and P08, TRR 237/A10, and RU 695/9-1) and the European Research Council (FP7, Grant Agreement No. 322865) to JR and the international doctoral programme i-Target: Immunotargeting of Cancer, funded by the Elite Network of Bavaria.

REFERENCES

1. Thaiss CA, Zmora N, Levy M, Elinav E. The microbiome and innate immunity. *Nature.* (2016) 535:65–74. doi: 10.1038/nature18847
2. Ananthakrishnan AN, Bernstein CN, Iliopoulos D, Macpherson A, Neurath MF, Ali RAR, et al. Environmental triggers in IBD: a review of progress and evidence. *Nat Rev Gastroenterol Hepatol.* (2017) 15:39–49. doi: 10.1038/nrgastro.2017.136
3. Terzic J, Grivennikov S, Karin E, Karin M. Inflammation and colon cancer. *Gastroenterology.* (2010) 138:2101–14.e2105. doi: 10.1053/j.gastro.2010.01.058
4. Jostins L, Ripke S, Weersma RK, Duerr RH, McGovern DP, Hui KY, et al. Host-microbe interactions have shaped the genetic architecture of inflammatory bowel disease. *Nature.* (2012) 491:119–24. doi: 10.1038/nature11582
5. Zhernakova A, Festen EM, Franke L, Trynka G, van Diemen CC, Monsuur AJ, et al. Genetic analysis of innate immunity in Crohn's disease and ulcerative colitis identifies two susceptibility loci harboring CARD9 and IL18RAP. *Am J Hum Genet.* (2008) 82:1202–10. doi: 10.1016/j.ajhg.2008.03.016
6. Franke A, McGovern DP, Barrett JC, Wang K, Radford-Smith GL, Ahmad T, et al. Meta-analysis increases to 71 the tally of confirmed Crohn's disease susceptibility loci. *Nat Genet.* (2010) 42:1118–25. doi: 10.1038/ng.717
7. McGovern DP, Gardet A, Törkvist L, Goyette P, Essers J, Taylor KD, et al. Genome-wide association identifies multiple ulcerative colitis susceptibility loci. *Nat Genet.* (2010) 42:332–7. doi: 10.1038/ng.549
8. Rivas MA, Beaudoin M, Gardet A, Stevens C, Sharma Y, Zhang CK, et al. Deep resequencing of GWAS loci identifies independent rare variants associated with inflammatory bowel disease. *Nat Genet.* (2011) 43:1066–73. doi: 10.1038/ng.952
9. Ruland J, Hartjes L. CARD–BCL-10–MALT1 signalling in protective and pathological immunity. *Nat Rev Immunol.* (2018) 19:118–34. doi: 10.1038/s41577-018-0087-2
10. Hara H, Ishihara C, Takeuchi A, Imanishi T, Xue L, Morris SW, et al. The adaptor protein CARD9 is essential for the activation of myeloid cells through ITAM-associated and Toll-like receptors. *Nat Immunol.* (2007) 8:619–29. doi: 10.1038/ni1466
11. Hsu YM, Zhang Y, You Y, Wang D, Li H, Duramad O, et al. The adaptor protein CARD9 is required for innate immune responses to intracellular pathogens. *Nat Immunol.* (2007) 8:198–205. doi: 10.1038/ni1426
12. Gross O, Gewies A, Finger K, Schäfer M, Sparwasser T, Peschel C, et al. Card9 controls a non-TLR signalling pathway for innate anti-fungal immunity. *Nature.* (2006) 442:651–6. doi: 10.1038/nature04926
13. Robinson MJ, Osorio F, Rosas M, Freitas RP, Schweighoffer E, Gross O, et al. Dectin-2 is a Syk-coupled pattern recognition receptor crucial for Th17 responses to fungal infection. *J Exp Med.* (2009) 206:2037–51. doi: 10.1084/jem.20082818
14. Dorhoi A, Desel C, Yeremeev V, Pradl L, Brinkmann V, Mollenkopf HJ, et al. The adaptor molecule CARD9 is essential for tuberculosis control. *J Exp Med.* (2010) 207:777–92. doi: 10.1084/jem.20090067
15. Shenderov K, Barber DL, Mayer-Barber KD, Gurcha SS, Jankovic D, Feng CG, et al. Cord factor and peptidoglycan recapitulate the Th17-promoting adjuvant activity of mycobacteria through mincle/CARD9 signaling and the inflammasome. *J Immunol.* (2013) 190:5722–30. doi: 10.4049/jimmunol.1203343
16. Brown GD, Willment JA, Whitehead L. C-type lectins in immunity and homeostasis. *Nat Rev Immunol.* (2018) 18:374–89. doi: 10.1038/s41577-018-0004-8
17. Strasser D, Neumann K, Bergmann H, Marakalala MJ, Guler R, Rojowska A, et al. Syk kinase-coupled C-type lectin receptors engage protein kinase C-sigma to elicit Card9 adaptor-mediated innate immunity. *Immunity.* (2012) 36:32–42. doi: 10.1016/j.immuni.2011.11.015
18. Roth S, Bergmann H, Jaeger M, Yeroslaviz A, Neumann K, Koenig PA, et al. Vav proteins are key regulators of card9 signaling for innate antifungal immunity. *Cell Rep.* (2016) 17:2572–83. doi: 10.1016/j.celrep.2016.11.018
19. Hayden MS, Ghosh S. NF-kappaB, the first quarter-century: remarkable progress and outstanding questions. *Genes Dev.* (2012) 26:203–34. doi: 10.1101/gad.183434.111
20. Cao Z, Conway KL, Heath RJ, Rush JS, Leshchiner ES, Ramirez-Ortiz ZG, et al. Ubiquitin ligase TRIM62 regulates CARD9-mediated anti-fungal immunity and intestinal inflammation. *Immunity.* (2015) 43:715–26. doi: 10.1016/j.immuni.2015.10.005
21. Hailfinger S, Nogai H, Pelzer C, Jaworski M, Cabalzar K, Charton JE, et al. Malt1-dependent RelB cleavage promotes canonical NF-kappaB activation in lymphocytes and lymphoma cell lines. *Proc Natl Acad Sci USA.* (2011) 108:14596–601. doi: 10.1073/pnas.1105020108
22. Xu X, Xu J-F, Zheng G, Lu H-W, Duan J-L, Rui W. CARD9(S12N) facilitates the production of IL-5 by alveolar macrophages for the induction of type 2 immune responses. *Nat Immunol.* (2018) 19:547–60. doi: 10.1038/s41590-018-0112-4
23. Gross O, Poeck H, Bscheider M, Dostert C, Hannesschläger N, Endres S, et al. Syk kinase signalling couples to the Nlrp3 inflammasome for anti-fungal host defence. *Nature.* (2009) 459:433–6. doi: 10.1038/nature07965
24. Poeck H, Bscheider M, Gross O, Finger K, Roth S, Rebsamen M, et al. Recognition of RNA virus by RIG-I results in activation of CARD9 and inflammasome signaling for interleukin 1 beta production. *Nat Immunol.* (2010) 11:63–9. doi: 10.1038/ni.1824
25. Roth S, Rottach A, Lotz-Havla AS, Laux V, Muschaweckh A, Gersting SW, et al. Rad50-CARD9 interactions link cytosolic DNA sensing to IL-1beta production. *Nat Immunol.* (2014) 15:538–45. doi: 10.1038/ni.2888
26. Glocker EO, Hennigs A, Nabavi M, Schäffer AA, Woellner C, Salzer U, et al. A homozygous CARD9 mutation in a family with susceptibility to fungal infections. *N Engl J Med.* (2009) 361:1727–35. doi: 10.1056/NEJMoa0810719
27. Lanternier F, Mahdaviani SA, Barbati E, Chaussade H, Koumar Y, Levy R, et al. Inherited CARD9 deficiency in otherwise healthy children and adults with Candida species-induced meningoencephalitis, colitis, or both. *J Allergy Clin Immunol.* (2015) 135:1558–68 e1552. doi: 10.1016/j.jaci.2014.12.1930
28. Lanternier F, Pathan S, Vincent QB, Liu L, Cypowyj S, Prando C, et al. Deep dermatophytosis and inherited CARD9 deficiency. *N Engl J Med.* (2013) 369:1704–14. doi: 10.1056/NEJMoa1208487
29. LeibundGut-Landmann S, Gross O, Robinson MJ, Osorio F, Slack EC, Tsoni SV, et al. Syk- and CARD9-dependent coupling of innate immunity to the induction of T helper cells that produce interleukin 17. *Nat Immunol.* (2007) 8:630–8. doi: 10.1038/ni1460
30. Rieber N, Singh A, Öz H, Carevic M, Bouzani M, Amich J, et al. Pathogenic fungi regulate immunity by inducing neutrophilic myeloid-derived suppressor cells. *Cell Host Microbe.* (2015) 17:507–14. doi: 10.1016/j.chom.2015.02.007
31. Pointon JJ, Harvey D, Karaderi T, Appleton LH, Farrar C, Stone MA, et al. Elucidating the chromosome 9 association with AS; CARD9 is a candidate gene. *Genes Immun.* (2010) 11:490–6. doi: 10.1038/gene.2010.17
32. Fairfax BP, Humburg P, Makino S, Naranbhai V, Wong D, Lau E, et al. Innate immune activity conditions the effect of regulatory variants upon monocyte gene expression. *Science.* (2014) 343:1246949. doi: 10.1126/science.1246949
33. Beaudoin M, Goyette P, Boucher G, Lo KS, Rivas MA, Stevens C, et al. Deep resequencing of GWAS loci identifies rare variants in CARD9, IL23R and RNF186 that are associated with ulcerative colitis. *PLoS Genet.* (2013) 9:e1003723. doi: 10.1371/journal.pgen.1003723
34. Sokol H, Conway KL, Zhang M, Choi M, Morin B, Cao Z, et al. Card9 mediates intestinal epithelial cell restitution, T-helper 17 responses, and control of bacterial infection in mice. *Gastroenterology.* (2013) 145:591–601 e593. doi: 10.1053/j.gastro.2013.05.047

35. Bergmann H, Roth S, Pechloff K, Kiss EA, Kuhn S, Heikenwälder M, et al. Card9-dependent IL-1β regulates IL-22 production from group 3 innate lymphoid cells and promotes colitis-associated cancer. *Eur J Immunol.* (2017) 47:1342–53. doi: 10.1002/eji.201646765
36. Lamas B, Michel ML, Waldschmitt N, Pham HP, Zacharioudaki V, Dupraz L, et al. Card9 mediates susceptibility to intestinal pathogens through microbiota modulation and control of bacterial virulence. *Gut.* (2018) 67:1836–44. doi: 10.1136/gutjnl-2017-314195
37. Mizoguchi A, Mizoguchi E. Animal models of IBD: linkage to human disease. *Curr Opin Pharm.* (2010) 10:578–87. doi: 10.1016/j.coph.2010.05.007
38. Collins JW, Keeney KM, Crepin VF, Rathinam VA, Fitzgerald KA, Finlay BB, et al. Citrobacter rodentium: infection, inflammation and the microbiota. *Nat Rev Microbiol.* (2014) 12:612–23. doi: 10.1038/nrmicro3315
39. Eyerich K, Dimartino V, Cavani A. IL-17 and IL-22 in immunity: driving protection and pathology. *Eur J Immunol.* (2017) 47:607–14. doi: 10.1002/eji.201646723
40. Lamas B, Richard ML, Leducq V, Pham HP, Michel ML, Da Costa G, et al. CARD9 impacts colitis by altering gut microbiota metabolism of tryptophan into aryl hydrocarbon receptor ligands. *Nat Med.* (2016) 22:598–605. doi: 10.1038/nm.4102
41. Fridman WH, Pagès F, Sautès-Fridman C, Galon J, Fridman WH, Pages F, Sautes-Fridman C, Galon J. The immune contexture in human tumours: impact on clinical outcome. *Nat Rev Cancer.* (2012) 12:298–306. doi: 10.1038/nrc3245
42. Malik A, Sharma D, Malireddi RKS, Guy CS, Chang TC, Olsen SR, et al. SYK-CARD9 signaling axis promotes gut fungi-mediated inflammasome activation to restrict colitis and colon cancer. *Immunity.* (2018) 49:515–30.e515. doi: 10.1016/j.immuni.2018.08.024
43. Wang T, Fan C, Yao A, Xu X, Zheng G, You Y, et al. The adaptor protein card9 protects against colon cancer by restricting mycobiota-mediated expansion of myeloid-derived suppressor cells. *Immunity.* (2018) 49:504–14.e504. doi: 10.1016/j.immuni.2018.08.018
44. Okayasu I, Ohkusa T, Kajiura K, Kanno J, Sakamoto S. Promotion of colorectal neoplasia in experimental murine ulcerative colitis. *Gut.* (1996) 39:87–92. doi: 10.1136/gut.39.1.87
45. Yu H, Pardoll D, Jove R. STATs in cancer inflammation and immunity: a leading role for STAT3. *Nat Rev Cancer.* (2009) 9:798–809. doi: 10.1038/nrc2734
46. Dinarello C, Novick D, Kim S, Kaplanski G. Interleukin-18 and IL-18 binding protein. (2013) 4:289. doi: 10.3389/fimmu.2013.00289
47. Leshchiner ES, Rush JS, Durney MA, Cao Z, Dančík V, Chittick B, et al. Small-molecule inhibitors directly target CARD9 and mimic its protective variant in inflammatory bowel disease. *Proc Natl Acad Sci USA.* (2017) 114:11392–7. doi: 10.1073/pnas.1705748114

Conflict of Interest Statement: The authors declare that the research was conducted in the absence of any commercial or financial relationships that could be construed as a potential conflict of interest.

frontiers in Immunology

REVIEW
published: 13 February 2019
doi: 10.3389/fimmu.2019.00176

CARMA3: Scaffold Protein Involved in NF-κB Signaling

*Shilei Zhang and Xin Lin**

Department of Basic Medical Sciences, Tsinghua University School of Medicine, Beijing, China

Scaffold proteins are defined as pivotal molecules that connect upstream receptors to specific effector molecules. Caspase recruitment domain protein 10 (CARD10) gene encodes a scaffold protein CARMA3, belongs to the family of CARD and membrane-associated guanylate kinase-like protein (CARMA). During the past decade, investigating the function of CARMA3 has revealed that it forms a complex with BCL10 and MALT1 to mediate different receptors-dependent signaling, including GPCR and EGFR, leading to activation of the transcription factor NF-κB. More recently, CARMA3 and its partners are also reported to be involved in antiviral innate immune response and DNA damage response. In this review, we summarize the biology of CARMA3 in multiple receptor-induced NF-κB signaling. Especially, we focus on discussing the function of CARMA3 in regulating NF-κB activation and antiviral IFN signaling in the context of recent progress in the field.

Keywords: CARMA3, CARD10, NF-κB, GPCR, EGFR, DNA damage, virus infection

OPEN ACCESS

Edited by:
Frederic Bornancin, Novartis, Switzerland

Reviewed by:
Jan Fric, International Clinical Research Center (FNUSA-ICRC), Czechia
Matthew Cook, Australian National University, Australia

***Correspondence:**
Xin Lin
linxin307@tsinghua.edu.cn

Specialty section:
This article was submitted to Molecular Innate Immunity, a section of the journal Frontiers in Immunology

Received: *07 July 2018*
Accepted: *21 January 2019*
Published: *13 February 2019*

Citation:
Zhang S and Lin X (2019) CARMA3: Scaffold Protein Involved in NF-κB Signaling. Front. Immunol. 10:176. doi: 10.3389/fimmu.2019.00176

INTRODUCTION

Caspase recruitment domain and membrane-associated guanylate kinase-like protein 3 (CARMA3), also known as CARD10, is one of CARMA family members that include CARMA1, CARMA2, and CARMA3. CARMA proteins conserved across many species which are characterized by the different functional domains shared by all members of the family: the N-terminal CARD domain, following with a coiled-coil domain, a linker region, a PDZ domain, a SH3 domain, and the C-terminal guanylate kinase-like domain (GUK) (**Figure 1**) (1, 2). Although CARMA family proteins share a high degree of sequence and structural homology, they are transcribed by different genes and expressed in different tissues. Specifically, CARMA1 is primarily expressed in the hematopoietic system, including the spleen, thymus and peripheral blood leukocytes; CARMA2 is expressed in the mucosal tissues and skin; and CARMA3 is expressed in a broad range of tissues, particularly at high levels in lung, kidney, liver and heart, but not in hematopoietic cells (3).

CARMA proteins are also known as CARD11, CARD14, and CARD10, because they were originally identified as CARD domain-containing proteins by bioinformatics approaches. In spite of distinct tissue distribution, CARMA proteins mediate different signaling pathways but utilize a similar mechanism to activate downstream effector molecules (**Figure 1**) (4, 5). Upon signaling, CARMA proteins, through their CARD domain, recruit two signaling molecules: Bcl10 (B cell lymphoma protein 10), and MALT1 (mucosa-associated lymphoid tissue lymphoma translocation gene 1) to form the CARMA-Bcl10-MALT1 (also known as CBM complex), and then activate the downstream IKK complex, leading to the activation of NF-κB (6–8). Considering that Bcl10 and MALT1 are expressed in all tissues, the different tissue distribution indicates that CARMA proteins may function upstream of Bcl10 and MALT1 to mediate the certain receptor-induced NF-κB activation in different cells.

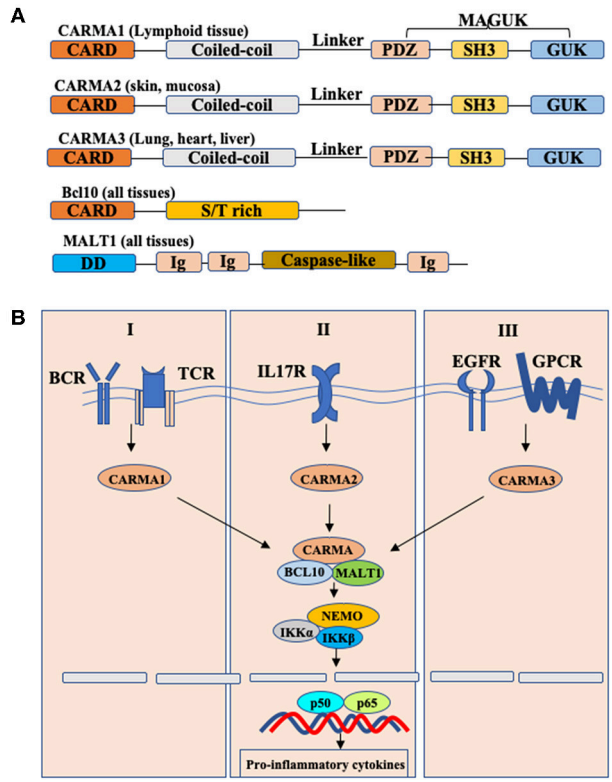

FIGURE 1 | Schematic model of CBM complex-induced NF-κB activation. **(A)** Structures of CARMA1,2,3 and their interactors. Each CARMA member shares similar structures: caspase-recruitment domain (CARD), followed by a coiled-coil domain (CC), a linker region, a PDZ domain, an SH3 domain, and a GUK-like domain. BCL10, B-cell lymphoma/leukemia 10; S/T-rich, serine/threonine-rich region; MALT, mucosa-associated lymphoid tissue; DD, death domain; Ig, immunoglobulin-like domain; **(B)** Conserved Bcl10-Malt1 complexes interact with different CARMA proteins to link various receptors to NF-κB signaling.

Early studies have showed that CARMA1 is required for antigen receptor-induced NF-κB activation in T cells and B cells, leading to lymphocyte activation and proliferation (9, 10). Recently, Wang et.al shows that CARMA2 plays a critical role mediating IL-17RA signaling in keratinocytes, and CARMA2 gain-of-function mutations result in constitutively activated IL-17RA signaling, leading to the development of skin inflammation and psoriasis (11). Previously, several studies indicate that CARMA3 functions as an indispensable adaptor protein in modulating NF-κB signaling downstream of some GPCRs (G protein-coupled receptors), including angiotensin II receptor and lysophosphatidic acid receptor, as well as receptor tyrosine kinases (RTKs), such as epidermal growth factor (EGF) receptor and insulin-like growth factor (IGF) receptor (12–14). Recent studies indicate that besides NF-κB signaling, CARMA3 also serves as a modulator in antiviral RLR signaling, providing a new understanding of CARMA3 (15). In this review, we summarize the biology of CARMA3 and discuss the roles of CARMA3 and its related proteins in different signaling pathways.

MECHANISM OF CARMA3 ACTIVATION

Upon receptor activation, CARMA proteins may be recruited to the cytoplasmic membrane by adaptor proteins and then be further phosphorylated by upstream kinases, which results in the recruitment and activation of downstream effector proteins. In particular, in response to antigen receptors activation, PKCs are activated, which phosphorylate serine at S564/649/657 and S552 on the linker region of CARMA1, and triggers CBM complex oligomerization (16–19). Similar to CARMA1, phosphorylation of CARMA3 at Ser520, an analog to Ser552 of CARMA1, might be crucial for CARMA3 activation (16). Future studies are still needed to determine if other residues in CARMA3 can be phosphorylated by PKC, as well as other kinases may also contribute to CARMA3 activation. Upon phosphorylation, CARMA3 forms a CBM complex with Bcl10 and MALT1, contributing to downstream NF-κB activation by regulating the IKK complex activity through NEMO polyubiquitination (20).

Besides Bcl10 and MALT1, some other molecules are also reported to be involved in CARMA3 mediated NF-κB activation. D'Andrea et al. utilized a two-hybrid screening to identify a DEP domain-containing protein DEPDC7 as a cellular binding partner of CARMA2 and CARMA3 but not CARMA1, which serves as a specific mediator of GPCR-induced NF-κB activation (21). Upon GPCR activation, β-arrestin 2, but not the β-arrestin 1, associates with CARMA3 and most likely recruiting CARMA3 into the receptor complex to mediate LPA-induced NF-κB activation and subsequent IL-6 expression (22, 23). More recently, Jiang et al. identified a transmembrane protein, TMEM43 (also known as LUMA) as a new CARMA3-associating protein that contributes to EGFR-induced NF-κB activation in cancer cells (24).

CARMA3 IN EGFR SIGNALING AND GPCR SIGNALING

Since receptor tyrosine kinases (RTKs), integrins, and G protein-coupled receptors (GPCRs) have been reported to activate NF-κB signaling through PKCs (14), Grabiner BC et al. found that CARMA3-deficient mouse embryonic fibroblasts (MEFs) failed to trigger NF-κB activation upon stimulation with endothelin (ET-1) (20) and lysophosphatidic acid (LPA) (20), which are ligands for two different GPCRs. Specifically, CARMA3 is mainly required for GPCR-induced NF-κB activation (**Figure 1**), because this activation induced by other cell surface receptors such as TNFR or TLR4 do not require CARMA3 (20). Similar to CARMA1 in antigen receptor-induced NF-κB activation, CARMA3 also controls NF-κB activation by forming the CBM complex. Several laboratories showed that GPCR-induced NF-κB activation is also defective in Bcl10-deficient cells (25, 26). In addition, Malt1 is also critically required for the degradation of IκBα and the subsequent NF-κB induction in response to LPA stimulation (27, 28). Moreover, Bcl10 and Malt1 are selectively for LPA-induced NF-κB activation but are dispensable for the activation of the JNK, p38, ERK MAP kinase, and Akt signaling

pathways (25). By analyzing angiotensin II (Ang II)-induced NF-κB activation, blocking the function of any components in the CARMA3-Bcl10-Malt1 signalosome, through the use of either RNAi, dominant-negative mutants, effectively impairs Ang II-induced NF-κB activation (27). In endothelial cells, the angiotensin II receptor AGTR1 induces NF-κB-dependent pro-inflammatory responses, which is relied on PKC-dependent assembly of a signaling complex comprised of CARMA3, Bcl10, and MALT1, contributing to endothelial dysfunction and vascular disease (29–32). In some breast cancers, aberrantly overexpressed AGTR1 induces both ligand-dependent and ligand-independent NF-κB activation, mediated by CARMA3, Bcl10, and MALT1, driving cancer cell-intrinsic responses that include proliferation, migration and invasion, as well as cancer cell-extrinsic effects to promote tumor angiogenesis through impacting endothelial cells of the tumor microenvironment (33). In airway epithelial cells (AECs), Causton et al. showed that CARMA3 contributed to NF-κB activation and the production of proasthmatic mediators in response to a panel of asthma-relevant GPCR ligands. Through genetically modified mice with CARMA3-deficient AECs, they demonstrated that CARMA3 in AEC is involved in allergic airway inflammation and bridges the innate and adaptive immune responses in the lung (34, 35). More studies have further indicated that the CARMA3-Bcl10-Malt1 signalosome plays a critical role in other GPCRs-induced NF-κB activation in different cellular context (27, 33, 36, 37). Together, these studies suggest that CARMA3-Bcl10-Malt1 signalosome is an essential signaling complex linking GPCRs to NF-κB activation (**Figure 2**).

Receptor tyrosine kinases (RTKs), a family of cell surface receptors, are key players in mediating multiple cellular responses upon the stimulation of growth factors, cytokines, and polypeptide hormones. Multiple growth factors, including insulin-like growth factor (38), epidermal growth factor (39), and fibroblast growth factor (40), can induce notable NF-κB signaling through their receptors that belong to the RTKs family. Since PKC is required for EGFR-induced NF-κB activation and given the importance of CBM complex in IKK activation (14), Jiang et al. explored a possibility whether EGFR-induced NF-κB activation involves the CBM complex. Consistent with this hypothesis, their data indicate that CARMA3 and Bcl10 are required for EGFR-induced NF-κB activation in both EGFR-expressing human cancer cell lines and mouse embryonic fibroblasts (41). Using biochemical and genetic approaches, Pan et al. found that CBM complex is required for HER2-induced NF-κB activation and functionally contributes to multiple properties of malignancy, including proliferation, migration and invasion, both *in vitro* and *in vivo* (42). Upon stimulation, the CBM complex recruits E3 ligase TRAF6 to provide a positive signal to activate IKK complex via Lys63-linked polyubiquitination (43). Therefore, these studies indicate that stimulation of RTKs, including EGFR and HER2, induces NF-κB activation through CARMA3-associated complex (**Figure 2**).

However, it remains to be determined the mechanism by which the CBM complex is linked to EGFR signaling pathway. To address this question, Jiang et al. performed a high-throughput and functional genomic screen (also named

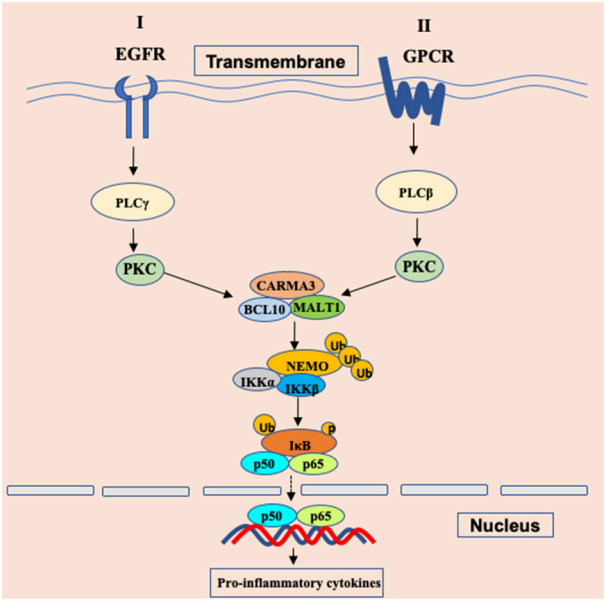

FIGURE 2 | Schematic of GPCR/EGFR-CARMA3 signaling pathway leading to NF-κB activation. In cancer cells and endothelial cells, stimulations of the surface receptor EGFR and GPCR trigger the proximal signaling, leading to activation of phospholipase C (PLC) and protein kinase C (PKC). The activated PKC further phosphorylates CARMA3 and enables CARMA3 to form the CBM complex through interaction with the downstream Bcl10 and MALT1. Formation of the CBM complex leads to activation of the IKK complex through NEMO polyubiquitination. Ub, ubiquitination; p, phosphorylation.

Bi-molecule fluorescence complementation assay, BiFC) to identify potential CARMA3-binding proteins, and found that TMEM43 (also known as ARVD5 or LUMA) might be a critical component in EGFR signaling network through interaction with CARMA3 and its associating complex to induce downstream NF-κB activation following EGF stimulation, but not on TNF-α stimulation (24). Mechanically, they revealed that TMEM43 inducibly interacted with EGFR and mediated the formation of CARMA3 and Bcl10 complex (24), which may bridge EGFR and CBM complex, leading to the activation of IKK. Regarding to the intracellular protein tyrosine kinase activity of EGFR, it still need to be investigated whether the inducible association between EGFR and TMEM43 may lead to TMEM43 or its binding proteins being phosphorylated by EGFR, which may enable TMEM43 to interact with CARMA3/Bcl10 complex.

CONTRIBUTION OF CARMA3 TO DNA DAMAGE RESPONSE

NF-κB is a family of transcription factors that induce the expression of multiple anti-apoptotic genes (44, 45). Although NF-κB is activated as part of DNA damage responses, which protects cells from DNA damage-induced program cell death (46), the molecular mechanism by which DNA damage activates NF-κB remains to be determined. Zhang et al. showed that the CBM complex not only responds to extracellular

stimuli by various receptors, but also mediates intracellular signal elicited from ATM-mediated DNA damage response (47). PKC is generally considered regulating CARMA1 or CARMA3 activation through phosphorylation of the linker region of CARMA proteins (17, 48). However, Zhang et al. found that PKC activity is dispensable for Doxorubicin-induced NF-κB activation (47), indicating that other kinases may phosphorylate CARMA proteins, or alternatively, CAMRA proteins may be activated through different mechanisms, such as ubiquitination upon DNA damage. Interestingly, this study revealed that CARMA3 could be modified by K63-linked ubiquitination upon Doxorubicin stimulation (47). In addition, CBM complex is linking TRAF6 to IKK complex in response to EGF stimulation in A431 cells (49). Consistent with the role of TRAF6 in activation of IKK, Zhang et al found that DNA damage triggered the association between CARMA3 and TRAF6, suggesting that TRAF6 may function to activate CBM complex by K63-linked polyubiquitination of CARMA3 (**Figure 3**) (47).

The anti-tumor effect of many chemotherapy drugs relies on their ability to induce cell apoptosis due to the DNA damage response (50, 51). However, cancer cells can induce NF-κB activation as a mechanism to avoid DNA damage-induced apoptosis and develop drug resistance for chemotherapy (52). Since Doxorubicin induces more cell apoptosis in CARMA3- and Bcl10-deficient cells than WT cells, this result suggests that the CBM complex might contribute to the resistance of chemotherapy-induced cell death (47). Although irradiation-induced damage can be repaired, damage to normal tissue is one of main side effects for cancer radiotherapy. In their study, Zhang et al. found that the tissue repair and cell proliferation were impaired in CARMA3-deficient mice exposed to irradiation, indicating the protective role of CARMA3 in cell survival (47). Together, this study revealed the molecular mechanism by which DNA damage activates NF-κB is mediated by CBM complex, therefore, providing a molecular basis for targeting the CBM complex to block DNA damage-induced NF-κB pathway (47).

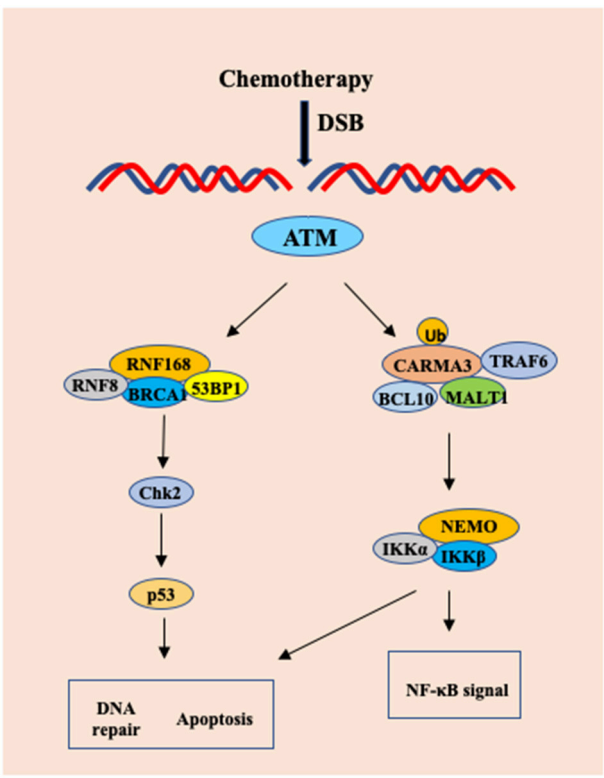

FIGURE 3 | The CARMA3-BCL1-MALT1 (CBM) complex contributes to DNA damage-induced NF-kB activation. Upon chemotherapy drug in HeLa cells and MEF cells, DNA damage-induced NF-kB activation involves the recruitment of TRAF6 to CARMA3, which leads to formation of the CARMA3/Bcl10/MALT1/TRAF6 complex, which finally results in a CARMA3-dependent, but PKC-independent polyubiquitination of IKK complex.

ROLE OF CARMA3 IN ANTIVIRAL RIG-I-MAVS SIGNALING

It has been an important question why different individual displays highly variable responses and infectious outcomes to influenza virus infection. To explore the host genetic polymorphisms contributed to this variation, Ferris et al. identified quantitative trait loci (QTL), Hrl4, contains 13 genes (53). Among of these genes, Card10 gene, which encodes CARMA3, may have a potential link to the antiviral innate response. To determine the functional role of CARMA3 in antiviral innate immune response, Jiang et al. challenged CARMA3-deficient mice with influenza virus or vesicular stomatitis virus and found that CARMA3-deficient mice showed more resistance to virus infection, which was characterized by less weight loss, lower viral yield, and greatly attenuated lung injury, suggesting that CARMA3 plays a negative role in antiviral response against virus infection (15). Transcriptional factors NF-κB and IRFs induce the expression of multiple antiviral pro-inflammatory cytokines and type I interferon expression. Interestingly, following influenza virus or vesicular stomatitis virus infection, the production of pro-inflammatory cytokines, such as IL-6, IL-1β, and TNF-α in the lung or sera of CARMA3-deficient mice was significantly reduced compared to wild-type mice, while more type I IFN was induced in CARMA3 KO mice, indicating that CARMA3 plays a negative role in regulating antiviral responses in the host, but it plays a positive role in regulating the expression of pro-inflammatory cytokines in response to viral infection (**Figure 4**) (15). Mechanically, they found that CARMA3 is a regulator of RIG-I-MAVS signaling pathway, which modulates MAVS-mediated NF-κB and TBK1-IRF3 activation in a two-phase mechanism (15). Upon RIG-I activation at the early time of viral infection, MAVS is firstly activated on mitochondrial, activating downstream IKKα/IKKβ/NEMO signaling in a CARMA3-dependent manner (**Figure 4**). However, in the early phase of post-infection, the CARMA3-BCL10 complex interacts with MAVS, therefore, preventing the formation of high-molecular weight MAVS aggregates that is required for downstream TBK1-IRF3 activation (**Figure 4**). Unlike other reported molecules including

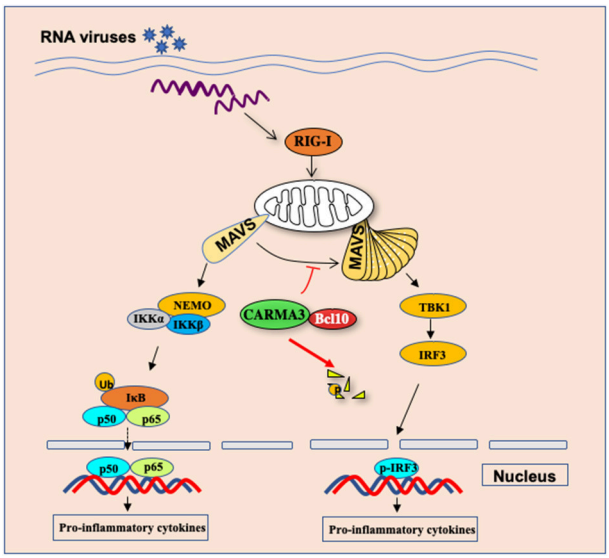

FIGURE 4 | CARMA3 Is a host factor regulating the balance of inflammatory and antiviral responses against viral infection. Upon RNA virus infection in airway epithelial cells, CARMA3 sequesters MAVS from forming high-molecular-weight aggregates, thereby suppressing TBK1/IRF3 activation. Following NF-kB activation upon virus infection, CARMA3 undergoes K48-linked ubiquitination and is targeted for proteasome-dependent degradation, which releases MAVS to activate IRF3.

A20, CYLD, and NEMO, which are either positive or negative mediators for both TBK1-IRF3 signaling and NF-κB activation (54–56), CARMA3 contributes to RNA virus infection-induced NF-κB signal but prevented TBK1/IRF3 activation through disruption of MAVS oligomerization. However, RNA virus infection also activates an unknown E3 ubiquitin ligase that induces CARMA3 polyubiquitination and degradation (**Figure 4**), leading to releasing the CARMA3-dependent inhibition on the MAVS-TBK1-IRF3 signaling in the late phase of RNA virus infection (15).

Since CARMA1, instead of CARMA3, is expressed in hematopoietic cells, it will be interesting to determine whether CARMA1 functions in mediating RIG-I/MAVS signaling in myeloid cells. However, our unpublished data revealed that CARMA1 was not involved in the regulation of neither RIG-I/MAVS in anti-RNA virus nor cGAS/STING in anti-DNA virus signaling (data was not shown here). In addition to CARMA1, CARD9, a protein structurally related to CARMA family but only expressed in myeloid cells, resulted in defects in NF-κB activation and production of pro-inflammatory cytokines, including IL-6 and IL-1β, in response to 5′ppp dsRNA treatment and DNA virus infection (57, 58). However, it did not alter the production of type I IFN. In contrast to the CARMA family that are differentially expressed in different tissues and cells, BCL10 is ubiquitously expressed. Similar to the role of CARD9 in dendritic cells, BCL10 mediated NF-κB activation and production of pro-inflammatory cytokines in response to 5′ppp dsRNA treatment or DNA virus infection (57, 58), whereas, in primary MEF cells, BCL10 functions similarly to CARMA3 upon VSV infection or poly(I:C) treatment (15), suggesting that BCL10 may regulate RIG-I/MAVS signaling in a cell-type-specific manner.

During the past decade, it has been shown that posttranslational modifications including phosphorylation, ubiquitination, and SUMOylation, play important roles in fine-tuning innate immunity by either modulating the stability of key proteins in the immune system (59). Recent studies indicate that ubiquitination may also regulate the function of CBM complex. Several laboratories showed that in lymphocytes, TCR activation induces the ubiquitination of lysine residues in the SH3 and GUK domains of CARMA1, leading to a proteasome-dependent degradation of CARMA1; while in natural killer T cells, the E3 ligase Cbl-b mediated the agonistic ligand α-galactosylceramide-induced ubiquitination and degradation of CARMA1 (60, 61). Similar processes also regulate BCL10 as shown that PKC or TCR/CD28 co-stimulation signaling in primary T cells results in ubiquitination of Bcl10 and degradation by the autophagy-dependent proteolysis machinery but not by the proteasome complex (61). Thus, these studies indicate a feedback mechanism in which E3 ubiquitin ligases mediate ubiquitination and degradation of CARMA1-BCL10 complex following the stimulation of antigen receptors. However, whether the CARMA3-BCL10 complex also undergoes ubiquitination and proteasomal degradation is still unclear. Jiang et al. revealed that the stability of BCL10 was not significantly altered following VSV infection, indicating that posttranslational modification of BCL10 is a signaling-specific manner. In contrast to BCL10, CARMA3 is gradually targeted for K48-linked ubiquitination and degradation following VSV infection (15), which may serve as a new mechanism to attenuate NF-κB signaling, and meanwhile, it releases MAVS from CARMA3-BCL10-MAVS complex to form functional aggregates to trigger TBK1-IRF3 activation (**Figure 4**) (15). Altogether, it suggests that CARMA3 is a key factor that regulates the balance of inflammatory and antiviral responses against viral infection. However, it remains to be determined how CARMA3 is targeted for K48-linked ubiquitination and degradation, which may help to design therapeutic agents for reducing inflammation but enhancing the antiviral response.

CONCLUSIONS AND OUTSTANDING QUESTIONS

During the past decade, many progress has been made in the understanding of CARMA3 functions in the NF-κB signaling pathways. These studies demonstrate that CARMA3-dependent IKK activation is involved in GPCR-, RTK-, ATM-, and RLR-induced NF-κB activation. However, further investigation is still needed to reveal the mechanism by which CARMA3 are linked to the different receptors. Therefore, it is important to determine whether CARMA3 is associated with other proteins following different stimuli. Identifications of such proteins will provide the molecular basis of how CARMA3-containing complexes are involved in mediating NF-κB activation induced by different stimuli.

Several groups have shown that CARMA3 was overexpressed in several tumor cells and correlated with tumor progression (42, 62, 63), indicating that CARMA3 may serve as a potential drug target for cancer treatment. Moreover, Zhang et al. highlights the role of CARMA3 in DNA damage-induced NF-κB activation, which may explain the resistance of some tumor cells to chemotherapy or radiation-therapy (47). Thus, more studies are required to define the regulation of CARMA3-mediated signaling transduction and the role of CARMA3 or its interacting proteins in cancers.

Given that *Card10*, CARMA3 encoding gene, might contribute to the host susceptibility to influenza virus (53), and since CARMA3 plays a positive role in RIG-I-induced NF-κB activation, leading to the induction of pro-inflammatory cytokines, but negatively regulates MAVS-induced TBK1/IRF3 signaling and production antiviral Type-I IFN (15), it will be interesting to investigate the role of CARMA3 in influenza virus pathogenesis. Considering the ubiquitination and degradation of CARMA3 upon VSV infection, it will be interesting to determine whether some virus, such as influenza virus, Ebola, SARS, and MERS, may modulate the mechanism of proteasomal degradation of CARMA3, which may regulate the expression of pro-inflammatory cytokines and type I IFN expression, and result in virus infection-associated cytokine storm, thereby contributing to the pathogenesis of virus infection.

Until now, no missense mutations of CARMA3 have been reported to contribute to the pathogenesis in human disease, besides some studies suggest that CARMA3 is overexpressed in several tumors (63), which may affect the onset and progression of tumorigenesis. Therefore, it will be interesting to investigate whether there are CARMA3 polymorphisms that affects the ubiquitination and degradation of CARMA3, resulting in variations of individuals to tumor development, chemotherapy resistance, and susceptibility to virus infection. This kind of study will provide the new molecular insight for designing the therapeutic agents for cancer and infectious diseases.

AUTHOR CONTRIBUTIONS

All authors listed have made a substantial, direct and intellectual contribution to the work, and approved it for publication.

FUNDING

This work was partially supported by a grant (81570211 to XL) from National Natural Science Foundation of China.

REFERENCES

1. Bertin J, Wang L, Guo Y, Jacobson MD, Poyet JL, Srinivasula SM, et al. DiStefano PS, Alnemri ES, CARD11 and CARD14 are novel caspase recruitment domain (CARD)/membrane-associated guanylate kinase (MAGUK) family members that interact with BCL10 and activate NF-kappa B. *J Biol Chem.* (2001) 276:11877–82. doi: 10.1074/jbc.M010512200
2. Gaide O, Martinon F, Micheau O, Bonnet D, Thome M, Tschopp J. Carma1, a CARD-containing binding partner of Bcl10, induces Bcl10 phosphorylation and NF-kappaB activation. *FEBS Lett.* (2001) 496:121–7. doi: 10.1016/S0014-5793(01)02414-0
3. Blonska M, Lin X. NF-kappaB signaling pathways regulated by CARMA family of scaffold proteins. *Cell Res.* (2011) 21:55–70. doi: 10.1038/cr.2010.182
4. McAllister-Lucas LM, Inohara N, Lucas PC, Ruland J, Benito A, Li Q, et al. Bimp1, a MAGUK family member linking protein kinase C activation to Bcl10-mediated NF-kappaB induction. *J Biol Chem.* (2001) 276:30589–97. doi: 10.1074/jbc.M103824200
5. Wang L, Guo Y, Huang WJ, Ke XL, Poyet JL, Manji GA, et al. CARD10 is a novel caspase recruitment domain/membrane-associated guanylate kinase family member that interacts with BCL10 and activates NF-kappa B. *J Biol Chem.* (2001) 276:21405–9. doi: 10.1074/jbc.M102488200
6. Willis TG, Jadayel DM, Du MQ, Peng HZ, Perry AR, Abdul-Rauf M, et al. Bcl10 is involved in t(1;14)(p22;q32) of MALT B cell lymphoma and mutated in multiple tumor types. *Cell* (1999) 96:35–45. doi: 10.1016/S0092-8674(00)80957-5
7. Akagi T, Motegi M, Tamura A, Suzuki R, Hosokawa Y, Suzuki H, et al. A novel gene, MALT1 at 18q21, is involved in t(11;18) (q21;q21) found in low-grade B-cell lymphoma of mucosa-associated lymphoid tissue. *Oncogene* (1999) 18:5785–94. doi: 10.1038/sj.onc.1203018
8. Gaide O, Favier B, Legler DF, Bonnet D, Brissoni B, Valitutti S, et al. CARMA1 is a critical lipid raft-associated regulator of TCR-induced NF-kappa B activation. *Nat Immunol.* (2002) 3:836–43. doi: 10.1038/ni830
9. Wang DH, You Y, Case SM, McAllister-Lucas LM, Wang L, DiStefano PS, et al. A requirement for CARMA1 in TCR-induced NF-kappa B activation. *Nat Immunol.* (2002) 3:830–5. doi: 10.1038/ni824
10. Pomerantz JL, Denny EM, Baltimore D. CARD11 mediates factor-specific activation of NF-kappa B by the T cell receptor complex. *Embo J.* (2002) 21:5184–94. doi: 10.1093/emboj/cdf505
11. Wang M, Zhang S, Zheng G, Huang J, Songyang Z, Zhao X, et al. Gain-of-function mutation of Card14 leads to spontaneous psoriasis-like skin inflammation through enhanced keratinocyte response to IL-17A. *Immunity* (2018) 49:66–79 e5. doi: 10.1016/j.immuni.2018.05.012
12. Shahrestanifar M, Fan XM, Manning DR. Lysophosphatidic acid activates NF-kappa B in fibroblasts - A requirement for multiple inputs. *J Biol Chem.* (1999) 274:3828–33. doi: 10.1074/jbc.274.6.3828
13. Juliano RL. Signal transduction by cell adhesion receptors and the cytoskeleton: functions of integrins, cadherins, selectins, and immunoglobulin-superfamily members. *Annu Rev Pharmacol Toxicol.* (2002) 42:283–323. doi: 10.1146/annurev.pharmtox.42.090401.151133
14. Biswas DK, Cruz AP, Gansberger E, Pardee AB. Epidermal growth factor-induced nuclear factor kappa B activation: a major pathway of cell-cycle progression in estrogen-receptor negative breast cancer cells. *Proc Natl Acad Sci USA.* (2000) 97:8542–7. doi: 10.1073/pnas.97.15.8542
15. Jiang CY, Zhou ZC, Quan YP, Zhang SL, Wang TT, Zhao XQ, et al. CARMA3 Is a host factor regulating the balance of inflammatory and antiviral responses against viral infection. *Cell Rep.* (2016) 14:2389–401. doi: 10.1016/j.celrep.2016.02.031
16. Matsumoto R, Wang D, Blonska M, Li H, Kobayashi M, Pappu B, et al. Phosphorylation of CARMA1 plays a critical role in T Cell receptor-mediated NF-kappaB activation. *Immunity* (2005) 23:575–85. doi: 10.1016/j.immuni.2005.10.007
17. Sommer K, Guo B, Pomerantz JL, Bandaranayake AD, Moreno-Garcia ME, Ovechkina YL, et al. Phosphorylation of the CARMA1 linker controls NF-kappaB activation. *Immunity* (2005) 23:561–74. doi: 10.1016/j.immuni.2005.09.014
18. Shinohara H, Maeda S, Watarai H, Kurosaki T. IkappaB kinase beta-induced phosphorylation of CARMA1 contributes to CARMA1 Bcl10 MALT1 complex formation in B cells. *J Exp Med.* (2007) 204:3285–93. doi: 10.1084/jem.20070379
19. McCully RR, Pomerantz JL. The protein kinase C-responsive inhibitory domain of CARD11 functions in NF-kappaB activation to regulate the association of multiple signaling cofactors that differentially depend on Bcl10 and MALT1 for association. *Mol Cell Biol.* (2008) 28:5668–86. doi: 10.1128/MCB.00418-08
20. Grabiner BC, Blonska M, Lin PC, You Y, Wang DH, Sun JY, et al. CARMA3 deficiency abrogates G protein-coupled receptor-induced

NF-kappa B activation. *Genes Dev.* (2007) 21:984–96. doi: 10.1101/gad.1502507
21. D'Andrea EL, Ferravante A, Scudiero I, Zotti T, Reale C, Pizzulo M, et al. The Dishevelled, EGL-10 and pleckstrin (DEP) domain-containing protein DEPDC7 binds to CARMA2 and CARMA3 proteins, and regulates NF-kappaB activation. *PLoS ONE* (2014) 9:e116062. doi: 10.1371/journal.pone.0116062
22. Sun J, Lin X. Beta-arrestin 2 is required for lysophosphatidic acid-induced NF-kappaB activation. *Proc Natl Acad Sci USA.* (2008) 105:17085–90. doi: 10.1073/pnas.0802701105
23. Lefkowitz RJ, Shenoy SK. Transduction of receptor signals by beta-arrestins. *Science* (2005) 308:512–7. doi: 10.1126/science.1109237
24. Jiang C, Zhu Y, Zhou Z, Gumin J, Bengtsson L, Wu W, et al. TMEM43/LUMA is a key signaling component mediating EGFR-induced NF-kappa B activation and tumor progression. *Oncogene* (2017) 36:2813–23. doi: 10.1038/onc.2016.430
25. Klemm S, Zimmermann S, Peschel C, Mak TW, Ruland J. Bcl10 and Malt1 control lysophosphatidic acid-induced NF-kappa B activation and cytokine production. *Proc Natl Acad Sci USA.* (2007) 104:134–8. doi: 10.1073/pnas.0608388103
26. McAllister-Lucas LM, Jin XH, Gu SF, Siu K, McDonnell S, Ruland J, et al. The CARMA3-Bcl10-MALT1 signalosome promotes angiotensin II-dependent vascular inflammation and atherogenesis. *J Biol Chem.* (2010) 285:25880–4. doi: 10.1074/jbc.C110.109421
27. McAllister-Lucas LM, Ruland J, Siu K, Jin XH, Gu SF, Kim DS, et al. CARMA3/Bcl10/MALT1-dependent NF-kappa B activation mediates angiotensin II-responsive inflammatory signaling in nonimmune cells. *Proc Natl Acad Sci USA.* (2007) 104:139–44. doi: 10.1073/pnas.0601947103
28. Rehman AO, Wang CY. CXCL12/SDF-1 alpha activates NF-kappa B and promotes oral cancer invasion through the Carma3/Bcl10/Malt1 complex. *Int J Oral Sci.* (2009) 1:105–18. doi: 10.4248/IJOS.09059
29. Juilland M, Thome M. Role of the CARMA1/BCL10/MALT1 complex in lymphoid malignancies. *Curr Opin Hematol.* (2016) 23:402–9. doi: 10.1097/MOH.0000000000000257
30. Rosebeck S, Rehman AO, Lucas PC, McAllister-Lucas LM. From MALT lymphoma to the CBM signalosome: three decades of discovery. *Cell Cycle* (2011) 10:2485–96. doi: 10.4161/cc.10.15.16923
31. Meininger I, Krappmann D. Lymphocyte signaling and activation by the CARMA1-BCL10-MALT1 signalosome. *Biol Chem.* (2016) 397:1315–33. doi: 10.1515/hsz-2016-0216
32. Wegener E, Krappmann D. CARD-Bcl10-Malt1 signalosomes: missing link to NF-kappaB. *Sci STKE* (2007) 2007:pe21. doi: 10.1126/stke.3842007pe21
33. Ekambaram P, Lee JL, Hubel NE, Hu D, Yerneni S, Campbell PG, et al. The CARMA3-Bcl10-MALT1 signalosome drives NFkappaB activation and promotes aggressiveness in angiotensin II receptor-positive breast cancer. *Cancer Res.* (2018) 78:1225–40. doi: 10.1158/0008-5472.CAN-17-1089
34. Causton B, Pardo-Saganta A, Gillis J, Discipio K, Kooistra T, Rajagopal J, et al. CARMA3 mediates allergic lung inflammation in response to alternaria alternata. *Am J Respir Cell Mol Biol.* (2018) 59:684–94. doi: 10.1165/rcmb.2017-0181OC
35. Causton B, Ramadas RA, Cho JL, Jones K, Pardo-Saganta A, Rajagopal J, et al. CARMA3 is critical for the initiation of allergic airway inflammation. *J Immunol.* (2015) 195:683–94. doi: 10.4049/jimmunol.1402983
36. Woo HN, Hong GS, Jun JI, Cho DH, Choi HW, Lee HJ, et al. Inhibition of Bcl10-mediated activation of NF-kappa B by BinCARD, a Bcl10-interacting CARD protein. *FEBS Lett.* (2004) 578:239–44. doi: 10.1016/j.febslet.2004.10.094
37. Delekta PC, Apel IJ, Gu S, Siu K, Hattori Y, McAllister-Lucas LM, et al. Thrombin-dependent NF-{kappa}B activation and monocyte/endothelial adhesion are mediated by the CARMA3.Bcl10.MALT1 signalosome. *J Biol Chem.* (2010) 285:41432–42. doi: 10.1074/jbc.M110.158949
38. Kaliman P, Canicio J, Testar X, Palacin M, Zorzano A. Insulin-like growth factor-II, phosphatidylinositol 3-kinase, nuclear factor-kappaB and inducible nitric-oxide synthase define a common myogenic signaling pathway. *J Biol Chem.* (1999) 274:17437–44. doi: 10.1074/jbc.274.25.17437
39. Sun L, Carpenter G. Epidermal growth factor activation of NF-kappaB is mediated through IkappaBalpha degradation and intracellular free calcium. *Oncogene* (1998) 16:2095–102. doi: 10.1038/sj.onc.1201731
40. Byrd VM, Ballard DW, Miller GG, Thomas JW. Fibroblast growth factor-1 (FGF-1) enhances IL-2 production and nuclear translocation of NF-kappaB in FGF receptor-bearing Jurkat T cells. *J Immunol.* (1999) 162:5853–9.
41. Jiang T, Grabiner B, Zhu YF, Jiang CY, Li HX, You Y, et al. CARMA3 is crucial for EGFR-induced activation of NF-kappa B and tumor progression. *Cancer Res.* (2011) 71:2183–92. doi: 10.1158/0008-5472.CAN-10-3626
42. Pan D, Zhu YF, Zhou ZC, Wang TT, You H, Jiang CY, et al. The CBM complex underwrites NF-kappa B activation to promote HER2-associated tumor malignancy. *Mol Cancer Res.* (2016) 14:93–102. doi: 10.1158/1541-7786.MCR-15-0229-T
43. Sun LJ, Deng L, Ea CK, Xia ZP, Chen ZJJ. The TRAF6 ubiquitin ligase and TAK1 kinase mediate IKK activation by BCL10 and MALT1 in T lymphocytes. *Mol Cell* (2004) 14:289–301. doi: 10.1016/S1097-2765(04)00236-9
44. Van Antwerp DJ, Martin SJ, Verma IM, Green DR. Inhibition of TNF-induced apoptosis by NF-kappa B. *Trends Cell Biol.* (1998) 8:107–11. doi: 10.1016/S0962-8924(97)01215-4
45. Kucharczak J, Simmons MJ, Fan Y, Gelinas C. To be, or not to be: NF-kappaB is the answer–role of Rel/NF-kappaB in the regulation of apoptosis. *Oncogene* (2003) 22:8961–82. doi: 10.1038/sj.onc.1207230
46. Wang W, Mani AM, Wu ZH. DNA damage-induced nuclear factor-kappa B activation and its roles in cancer progression. *J Cancer Metastasis Treat.* (2017) 3:45–59. doi: 10.20517/2394-4722.2017.03
47. Zhang SL, Pan D, Jia XM, Lin X, Zhao XQ. The CARMA3-BCL10-MALT1 (CBM) complex contributes to DNA damage-induced NF-kappa B activation and cell survival. *Protein Cell* (2017) 8:856–60. doi: 10.1007/s13238-017-0441-3
48. Mahanivong C, Chen HM, Yee SW, Pan ZK, Dong Z, Huang S. Protein kinase C alpha-CARMA3 signaling axis links Ras to NF-kappa B for lysophosphatidic acid-induced urokinase plasminogen activator expression in ovarian cancer cells. *Oncogene* (2008) 27:1273–80. doi: 10.1038/sj.onc.1210746
49. Pan D, Jiang C, Ma Z, Blonska M, You MJ, Lin X. MALT1 is required for EGFR-induced NF-kappaB activation and contributes to EGFR-driven lung cancer progression. *Oncogene* (2016) 35:919–28. doi: 10.1038/onc.2015.146
50. Johnstone RW, Ruefli AA, Lowe SW. Apoptosis: a link between cancer genetics and chemotherapy. *Cell* (2002) 108:153–64. doi: 10.1016/S0092-8674(02)00625-6
51. Li Y, Wang Y, Zhou Y, Li J, Chen K, Zhang L, et al. Cooperative effect of chidamide and chemotherapeutic drugs induce apoptosis by DNA damage accumulation and repair defects in acute myeloid leukemia stem and progenitor cells. *Clin Epigenetics* (2017) 9:83. doi: 10.1186/s13148-017-0377-8
52. Godwin P, Baird AM, Heavey S, Barr MP, O'Byrne KJ, Gately K. Targeting nuclear factor-kappa B to overcome resistance to chemotherapy. *Front Oncol.* (2013) 3:120. doi: 10.3389/fonc.2013.00120
53. Ferris MT, Aylor DL, Bottomly D, Whitmore AC, Aicher LD, Bell TA, et al. Modeling host genetic regulation of influenza pathogenesis in the collaborative cross. *PLoS Pathogens* (2013) 9:e1003196. doi: 10.1371/journal.ppat.1003196
54. Friedman CS, O'Donnell MA, Legarda-Addison D, Ng A, Cardenas WB, Yount JS, et al. The tumour suppressor CYLD is a negative regulator of RIG-I-mediated antiviral response. *Embo Rep.* (2008) 9:930–6. doi: 10.1038/embor.2008.136
55. Maelfait J, Roose K, Bogaert P, Sze M, Saelens X, Pasparakis M, et al. A20 (Tnfaip3) Deficiency in myeloid cells protects against influenza A virus infection. *PLoS Pathogens* (2012) 8:e1002570. doi: 10.1371/journal.ppat.1002570
56. Zhao TJ, Yang L, Sun Q, Arguello M, Ballard DW, Hiscott J, et al. The NEMO adaptor bridges the nuclear factor-kappa B and interferon regulatory factor signaling pathways. *Nat Immunol.* (2007) 8:592–600. doi: 10.1038/ni1465
57. Poeck H, Bscheider M, Gross O, Finger K, Roth S, Rebsamen M, et al. Recognition of RNA virus by RIG-I results in activation of CARD9 and inflammasome signaling for interleukin 1 beta production. *Nat Immunol.* (2010) 11:63–1824. doi: 10.1038/ni.1824
58. Roth S, Rottach A, Lotz-Havla AS, Laux V, Muschaweckh A, Gersting SW, et al. Rad50-CARD9 interactions link cytosolic DNA sensing to IL-1 beta production. *Nat Immunol.* (2014) 15:538–45. doi: 10.1038/ni.2888
59. Davis ME, Gack MU. Ubiquitination in the antiviral immune response. *Virology* (2015) 479:52–65. doi: 10.1016/j.virol.2015.02.033

60. Qiao GL, Li ZP, Molinero L, Alegre ML, Ying HY, Sun ZM, et al. T-Cell receptor-induced NF-kappa B activation is negatively regulated by E3 ubiquitin ligase Cbl-b. *Mol Cell Biol.* (2008) 28:2470–80. doi: 10.1128/MCB.01505-07
61. Scharschmidt E, Wegener E, Heissmeyer V, Rao A, Krappmann D. Degradation of Bcl10 induced by T-cell activation negatively regulates NF-kappa B signaling. *Mol Cell Biol.* (2004) 24:3860–73. doi: 10.1128/MCB.24.9.3860-3873.2004
62. Xia ZX, Li ZX, Zhang M, Sun LM, Zhang QF, Qiu XS. CARMA3 regulates the invasion, migration, and apoptosis of non-small cell lung cancer cells by activating NF-kappa B and suppressing the P38 MAPK signaling pathway. *Exp Mol Pathol.* (2016) 100:353–60. doi: 10.1016/j.yexmp.2015.10.004
63. Xie CY, Han Y, Fu L, Li QC, Qiu XS, Wang EH. Overexpression of CARMA3 is associated with advanced tumor stage, cell cycle progression, and cisplatin resistance in human epithelial ovarian cancer. *Tumor Biol.* (2014) 35:7957–64. doi: 10.1007/s13277-014-2070-2

Conflict of Interest Statement: The authors declare that the research was conducted in the absence of any commercial or financial relationships that could be construed as a potential conflict of interest.

frontiers in Immunology

REVIEW
published: 15 August 2018
doi: 10.3389/fimmu.2018.01887

CARMA3 Is a Critical Mediator of G Protein-Coupled Receptor and Receptor Tyrosine Kinase-Driven Solid Tumor Pathogenesis

*J. Randall McAuley[1,2], Tanner J. Freeman[2], Prasanna Ekambaram[1], Peter C. Lucas[1,2] and Linda M. McAllister-Lucas[1]**

[1] Department of Pediatrics, Division of Pediatric Hematology-Oncology, University of Pittsburgh School of Medicine, Pittsburgh, PA, United States, [2] Department of Pathology, University of Pittsburgh School of Medicine, Pittsburgh, PA, United States

The CARMA–Bcl10–MALT1 (CBM) signalosome is an intracellular protein complex composed of a CARMA scaffolding protein, the Bcl10 linker protein, and the MALT1 protease. This complex was first recognized because the genes encoding its components are targeted by mutation and chromosomal translocation in lymphoid malignancy. We now know that the CBM signalosome plays a critical role in normal lymphocyte function by mediating antigen receptor-dependent activation of the pro-inflammatory, pro-survival NF-κB transcription factor, and that deregulation of this signaling complex promotes B-cell lymphomagenesis. More recently, we and others have demonstrated that a CBM signalosome also operates in cells outside of the immune system, including in several solid tumors. While CARMA1 (also referred to as CARD11) is expressed primarily within lymphoid tissues, the related scaffolding protein, CARMA3 (CARD10), is more widely expressed and participates in a CARMA3-containing CBM complex in a variety of cell types. The CARMA3-containing CBM complex operates downstream of specific G protein-coupled receptors (GPCRs) and/or growth factor receptor tyrosine kinases (RTKs). Since inappropriate expression and activation of GPCRs and/or RTKs underlies the pathogenesis of several solid tumors, there is now great interest in elucidating the contribution of CARMA3-mediated cellular signaling in these malignancies. Here, we summarize the key discoveries leading to our current understanding of the role of CARMA3 in solid tumor biology and highlight the current gaps in our knowledge.

Keywords: CARMA3, Bcl10, MALT1, G protein-coupled receptor, receptor tyrosine kinases, NF-κB, cancer

OPEN ACCESS

Edited by:
Frederic Bornancin, Novartis, Switzerland

Reviewed by:
Brian C. Schaefer, Uniformed Services University of the Health Sciences, United States
Jens Staal, Ghent University, Belgium

****Correspondence:***
Linda M. McAllister-Lucas
linda.mcallister@chp.edu

Specialty section:
This article was submitted to Primary Immunodeficiencies, a section of the journal Frontiers in Immunology

Received: *27 May 2018*
Accepted: *31 July 2018*
Published: *15 August 2018*

Citation:
McAuley JR, Freeman TJ, Ekambaram P, Lucas PC and McAllister-Lucas LM (2018) CARMA3 Is a Critical Mediator of G Protein-Coupled Receptor and Receptor Tyrosine Kinase-Driven Solid Tumor Pathogenesis. Front. Immunol. 9:1887. doi: 10.3389/fimmu.2018.01887

INTRODUCTION

In the late 1990s, a large family of proteins containing a homophilic protein–protein interaction module referred to as a "caspase activation and recruitment domain" (CARD) was discovered (1). While initially associated with apoptotic signaling, several proteins in this family were eventually linked to activation of the NF-κB transcription factor. In 2000, CARD9 was identified as a protein that directly interacts with the CARD of Bcl10, a signaling protein involved in regulating NF-κB (2). Subsequently in 2001, three proteins structurally related to CARD9, namely CARMA3 (also

referred to as CARD10 and Bimp1), CARMA1 (CARD11 and Bimp3), and CARMA2 (CARD14 and Bimp2), was discovered as a unique family of proteins that contained both CARD domains and membrane-associated guanylate kinase domains (**Figure 1A**) (3–6). Each of these proteins was shown to engage in CARD–CARD interaction with Bcl10 to enact canonical, IKK complex-associated NF-κB activation. The notion of a tripartite CARMA-containing signaling complex came with the discovery that a third protein, MALT1, interacted with Bcl10 to activate NF-κB (7–9). This complex is now referred to as the CARMA–Bcl10–MALT1 (CBM) signalosome.

CARMA family members appear to be functionally similar, albeit with differing expression patterns (5, 10). CARMA1 is found primarily in hematopoetic cells. CARMA2 is present in placenta, skin, and several mucosal tissues including buccal mucosa, esophagus, and pharyngeal mucosa, while CARMA3 is widely expressed in many tissues but not in hematopoietic cells (11). The upstream signaling events that regulate formation of the CBM complex were originally elucidated in lymphocytes for the CARMA1-containing CBM. Specifically, lymphocyte antigen receptor stimulation leads to activation of protein kinase C (PKC), which subsequently phosphorylates CARMA1 (12, 13). This phosphorylation triggers a conformational change in CARMA1 that allows it to form a polymeric complex with Bcl10/MALT1 (**Figure 1B**). Different PKC isoforms phosphorylate CARMA1 in different cell subtypes: PKCβ in B cells and PKCθ in T cells (12, 13). While specific PKC-mediated signaling events upstream of the CBM complex have not been elucidated for CARMA2 and CARMA3-containing complexes, PKC agonists such as phorbol myristate acetate and ionomycin (14) have been shown to activate CBM signaling in CARMA3-containing cells, suggesting that this phosphorylation-dependent mechanism for activation of the CARMA3–CBM complex is likely similar to that of the CARMA1–CBM complex (15).

CARMA1 phosphorylation triggers CBM complex oligomerization (16–21). Phosphorylated CARMA1 nucleates a very long filament of Bcl10 which is decorated around the outside of the filament by MALT1. MALT1 serves as the effector protein of the CBM complex and possesses at least two distinct functions by which it carries out downstream signaling: First, MALT1 functions as a scaffold, capable of engaging in protein–protein interactions and second, MALT1 functions as a protease. As a

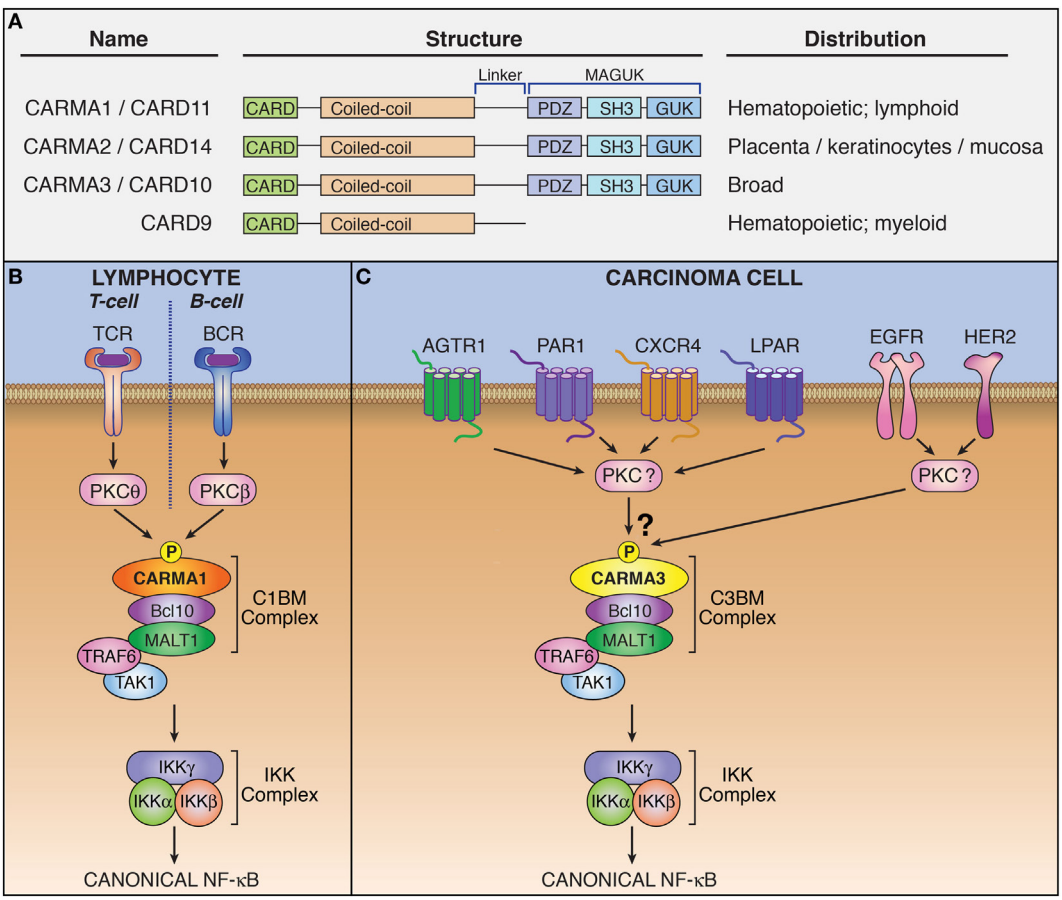

FIGURE 1 | The CARMA3-containing CARMA–Bcl10–MALT1 (CBM) complex mediates signaling downstream of specific G protein-coupled receptors (GPCRs) and receptor tyrosine kinases (RTKs). **(A)** Domain structure and tissue distribution of CARMA protein family members. **(B)** Schematic of lymphocyte antigen receptor-dependent CARMA1-containing CBM complex signaling. **(C)** Schematic of CARMA3-containing CBM complex signaling.

scaffold, activated MALT1 interacts with components of the NF-κB signaling machinery including the TRAF6 ubiquitin ligase (22–24). These interactions result in the polyubiquitination of IKKγ and the subsequent activation of the IKK complex (25, 26). The active IKK complex then induces the phosphorylation of Inhibitor of κB (IκB), targeting IκB for proteasomal degradation and freeing NF-κB transcription factor dimers to translocate into the nucleus and modulate the transcription of target genes (9). As a protease, MALT1 cleaves multiple specific substrates, including the NF-κB family transcription factor subunit RelB, and the deubiquitinases, CYLD and A20 (27–29). [For a detailed description of the multiple known MALT1 substrates, please refer to recent reviews (30, 31).] The effects of MALT1 protease activity are not yet completely understood, and many current studies suggest that one of the consequences of MALT1-dependent substrate cleavage is to maximize and sustain signaling by inactivating inhibitors of the NF-κB pathway. MALT1 proteolytic activity is transient after receptor triggering and the kinetics of MALT1 protease-dependent effects on cellular signaling has not yet been analyzed in detail.

CARMA1, Bcl10, and MALT1 are each *bona fide* proto-oncoproteins, since recurrent chromosomal translocations and gain-of-function mutations that lead to deregulation of these signaling proteins have been identified in B-cell lymphoma. Three specific recurrent chromosomal translocations were discovered in the B-cell malignancy, MALT lymphoma, and each involves components of the CBM complex: the first described was the t(11;18) resulting in expression of the API2–MALT1 fusion oncoprotein (32–34). Two other translocations were also identified, each involving the Ig heavy chain enhancer: t(1;14) and t(14;18), placing the intact Bcl10 and MALT1 genes, respectively, under control of the enhancer and leading to their overexpression (35, 36). In activated B-cell type diffuse large B-cell lymphoma (ABC-DLBCL), activating mutations in B-cell receptor subunits are present in approximately 23% of cases and result in constitutive BCR-driven CBM-dependent NF-κB activity (37–39). Gain-of-function mutations of CARMA1 occur in another 9% of cases and similarly result in constitutive CBM activity. More recent studies have suggested a role for constitutive CBM activity in driving other lymphoid cancers beyond MALT lymphoma and ABC-DLBCL. For example, activating mutations in CARMA1 have been identified in a subset of T-cell malignancies including adult T-cell leukemia/lymphoma, peripheral T cell lymphoma, and Sezary syndrome (40). Also, in the B-cell malignancy, primary effusion lymphoma, the Kaposi sarcoma herpes virus is thought to utilize the K13 viral oncoprotein to form a "KBM" complex composed of K13, Bcl10, and MALT1 to promote lymphomagenesis (41). In each of these malignancies, either viral oncogenes, oncogenic mutations, or chromosomal translocations drive deregulated inappropriate NF-κB activity (9).

With the identification of these CBM-associated genetic aberrations, the vast majority of research on the CBM complex in cancer has been focused on lymphoma. Over the last decade, a large number of studies have demonstrated a critical role for the CARMA3-containing CBM complex in solid tumors. Here, we summarize the key findings that have led to our current understanding of the role of CARMA3 in solid tumor biology.

A CARMA3-CONTAINING CBM COMPLEX OPERATES DOWNSTREAM OF G PROTEIN-COUPLED RECEPTORS (GPCRs) IN NON-IMMUNE CELLS

Early investigations showed that CARMA1 expression is predominantly restricted to lymphoid tissue, while CARMA3 is more widely expressed (3–6). Subsequent bioinformatic analysis revealed that CARMA3 is in fact expressed in almost all tissue types, including kidney, heart, brain, liver, and many other tissues of ectodermal, mesodermal, and endodermal origin, as are Bcl10 and MALT1. The only exception appears to be tissues dominated by cells of hematopeoitic origin, such as spleen, thymus, and lymph node, where CARMA1 predominates (10). CARMA1 and CARMA3 share both structural and functional similarity, and CARMA3 is able to complement CARMA1 deficiency in T-cells, rescuing the NF-κB defect (42). Given the similarities between CARMA1 and CARMA3, we and two other groups sought to investigate whether CARMA3 fulfilled a similar functional role to that of CARMA1, but in a different cellular context and downstream of receptors other than the lymphocyte antigen receptor. Indeed, we found that the CARMA3-containing CBM complex (*abbreviated henceforth as C3BM*) can promote NF-κB activation in cells outside of the immune system. These initial studies all demonstrated that the C3BM complex operates downstream of specific GPCRs that are known to stimulate PKC (**Figure 1C**) (43–45). Our own laboratory's initial studies revealed that the C3BM complex could be activated by a GPCR that serves as a receptor for the peptide hormone, angiotensin II (AGTR1), while others focused initially on the lysophosphatidic acid receptor (LPAR) family (43, 45), and the receptor for endothelin-1 (EDNRA; also known as ET_AR) (45). Since the time of these initial discoveries in 2007, the list of GPCRs that signal *via* the C3BM complex has continued to expand to include a wide array of receptors such as chemokine receptor type 2 (CXCR2) (46), CXCR4 (47), platelet-activating factor receptor (PTAFR; also known as PAF-R) (48), and protease-activated receptor 1 (F2R; also known as PAR1) (49) (**Figure 1C**; **Table 1**). Because inappropriate GPCR activation underlies the pathogenesis of many inflammatory and malignant disorders, these discoveries have led to notion that the CARMA3-containing CBM signalosome may represent a promising new target for therapeutic inhibition in GPCR-driven inflammation and cancer.

C3BM Signaling Plays a Critical Role in GPCR-Driven Solid Tumors

G protein-coupled receptor signaling has long been associated with oncogenesis and cancer progression (60). The discovery that the C3BM complex functions downstream of GPCRs to activate the pro-oncogenic NF-κB transcription factor in non-immune cells raised the possibility that the CARMA3-containing CBM complex might play a role in solid tumor pathogenesis. Indeed, C3BM complex signaling has now been demonstrated to have protumorigenic effects in several tumor types associated with dysregulated GPCR signaling. Furthermore, deficiency of C3BM complex components appear to blunt cancer growth in a range of

model systems, indicating a possible therapeutic role for targeting C3BM complex signaling in the treatment of selected solid tumors. Below, we discuss the specific GPCRs currently known to stimulate C3BM signaling in solid tumors.

LPAR

Lysophosphatidic acid (LPA) is a lipid signaling molecule that plays an important role in a diverse array of biological contexts ranging from tissue development and remodeling to pathological processes including reactive airway disease and cancer cell proliferation (54, 55, 61–63). Acting in an autocrine or paracrine manner, LPA can engage a family of GPCRs, LPARs 1–6, to stimulate various intracellular signaling pathways, including activation of NF-κB. Synthetic enzymes responsible for generating LPA, such as autotaxin and lipase member 1 (LIPI), are highly upregulated in multiple aggressive tumors including breast cancer, ovarian cancer, and metastatic Ewing's sarcoma (62, 64). In addition, deregulation of the LPAR–NF-κB signaling pathway has been implicated in driving a variety of tumors, including breast (63), colon (65), and prostate cancers (66, 67).

One of the first indications of a role for the C3BM complex in non-immune cells was the finding that LPA induction of NF-κB in mouse embryonic fibroblast (MEF) cells requires Bcl10 (43, 45). A subsequent study then demonstrated that the C3BM complex plays an important role in the pathophysiology of LPA-induced ovarian cancer cell migration and invasion (**Table 1A**) (51). These authors showed that siRNA-mediated knockdown of either CARMA3, Bcl10, or MALT1 suppressed LPA-induced NF-κB activation in ovarian cancer cell models. Furthermore, suppression of CBM signaling through the expression of a dominant-negative CARMA3 attenuated LPA-induced ovarian cancer cell invasion. Intriguingly, a dominant-negative variant of PKCα inhibited LPA-induced NF-κB activation in this system, suggesting that this PKC isoform might have a role in upstream regulation of the CARMA3-containing CBM complex in ovarian cancer cells. This study, published in 2008, marked the first demonstration of a role for a GPCR–C3BM signaling axis in cancer.

CXCR4

The chemokine receptor subfamily represents another group of GPCRs closely linked to cancer metastasis (68). Chemokine receptors respond to extracellular signaling molecules to regulate cellular processes such as chemotaxis, motility, and adhesion (69). One member of this subfamily, CXCR4, is overexpressed in a variety of malignancies and is well known to drive the metastatic spread of multiple cancers (70, 71). CXCR4 is stimulated by the ligand, stromal cell-derived factor 1α (SDF-1α; also referred to as CXCL12) (72). Interestingly, cells within the tumor microenvironment at common sites of metastasis, such as lung, liver, bone marrow, and lymph node often express high levels of SDF-1α. As a result, CXCR4 is thought to play a particularly important role in the homing of malignant cells to these metastatic sites and in promoting cell migration, growth, and survival at these distant sites (73, 74).

The fact that members of the chemokine receptor subfamily are known to promote activation of NF-κB *via* a PKC-dependent mechanism led investigators to hypothesize that a C3BM complex serves to mediate chemokine-induced NF-κB signaling. This hypothesis was first tested for CXCR4, and in 2009, CXCR4 became the second GPCR shown to utilize a C3BM signaling mechanism in cancer cells. Specifically, CXCR4 was found to activate NF-κB signaling through the C3BM complex in oral squamous cell carcinoma (OSCC) cells (**Table 1A**) (47). Stimulation of OSCCs with SDF-1α results in NF-κB activation that is suppressed by siRNA-mediated CARMA3, Bcl10, or MALT1 knockdown. Furthermore, knockdown of the C3BM components attenuates SDF-1α-induced OSCC invasion through a protein matrix. These important observations suggested that targeting the C3BM–NF-κB signaling pathway in OSCC may provide an important therapeutic opportunity for controlling metastasis of OSCC driven by SDF-1α. Moreover, since CXCR4-dependent signaling has been identified as a key regulator of cancer growth, invasion, and metastasis for a wide variety of other malignancies, including breast (75–77), ovarian (78), and prostate cancers (79–82), it will be of great interest to determine if the C3BM complex plays a key role in mediating SDF-1α dependent tumor progression or metastasis for these other tumor subtypes.

AGTR1

Our laboratory provided one of the first pieces of evidence for the existence of a C3BM signalosome by showing that each of

TABLE 1 | Receptors that signal *via* CARMA3.

(A) G protein-coupled receptors (GPCRs) in solid tumors

Receptor	Ligand	Tumor-type	Reference
AGTR1	Angiotensin II	Breast cancer	Ekambaram et al. (50)
CXCR4	CXCL12/SDF-1	Oral squamous cell carcinoma	Rehman and Wang (47)
LPAR	LPA	Ovarian cancer	Mahanivong et al. (51)

(B) GPCRs in non-malignant cells

Receptor	Ligand	Disease/cellular system	Reference
AGTR1	Angiotensin II	Vascular inflammation and atherogenesis	McAllister-Lucas et al. (52)
		Hepatocytes	McAllister-Lucas et al. (44)
CXCR2	CXCL8/IL8	Endothelial cells	Martin et al. (46)
ET_AR	Endothelin-1	Mouse embryonic fibroblasts (MEFs)	Grabiner et al. (53)
LPAR	LPA	Asthma	Medoff et al. (54) and Causton et al. (55)
		MEFs	Grabiner et al. (53)
PAR1	Thrombin	Endothelial cells	Delekta et al. (49) and Klei et al. (56)
PAF-R	PAF	Intestinal epithelial cells	Borthakur et al. (48)

(C) Receptor tyrosine kinases in solid tumors

Receptor	Ligand	Tumor-type	Reference
EGFR	EGF	Non-small cell lung carcinoma	Li et al. (57)
		Breast and other cancer cells	Jiang et al. (58)
HER2		Breast cancer	Pan et al. (59)

the three components of this complex is indispensable for NF-κB activation induced by the hormone angiotensin II in hepatocytes (44). Since angiotensin II signaling is classically known for its role in promoting vascular inflammation and dysfunction, we initially focused our subsequent work in this area on implications for the AGTR1–C3BM signaling axis in vascular biology and atherogenesis (52). Yet, we also recognized that there was a growing body of literature implicating both angiotensin II and its receptor AGTR1 as key players in the pathogenesis of a variety of cancers, including squamous cell carcinoma of the skin (83), glioblastoma (84), gastric cancer (85), ovarian cancer (86), and others (87). Furthermore, in 2009, our group participated in a multidisciplinary bioinformatic meta-analysis effort which identified AGTR1 as the second most high-scoring gene expression outlier in breast cancer cases (88). As expected, HER2 (ERBB2) was the top-scoring outlier, with HER2 overexpression occurring in approximately 25–30% of cases. Yet, we noted significant AGTR1 overexpression in nearly as many cases (approximately 20%) and demonstrated that AGTR1 and HER2 overexpression are mutually exclusive in breast cancer. In addition, our subsequent bioinformatic analyses demonstrated that AGTR1 overexpression correlates with aggressive clinical features in breast cancer, including a higher rate of lymph node metastasis, reduced responsiveness to neoadjuvant therapy, and reduced overall survival (50).

Since HER2 and AGTR1 overexpression are mutually exclusive in breast cancer, we hypothesized that these two receptors likely activate redundant signaling pathways, critical for driving pathogenesis. Thus, because HER2-dependent NF-κB activation underwrites several of the hallmarks of cancer (89), we reasoned that AGTR1 might similarly drive breast cancer progression *via* an NF-κB-dependent mechanism, and possibly through the same C3BM signaling pathway that we had clearly described as operating in endothelial cells in the context of vascular pathobiology. Indeed, we found that that AGTR1 overexpression, in both breast cancer patient samples and breast cancer cell lines, drives NF-κB activation and an associated NF-κB gene expression signature; as we expected, CARMA3, Bcl10, and MALT1 are each required for this to occur (**Table 1A**) (50). Functionally, we found that activation of the AGTR1–C3BM–NF-κB signaling axis drives multiple breast cancer cell intrinsic responses including cell proliferation, migration, and invasion. In addition, we found evidence for cancer cell extrinsic effects in that the signaling axis drives expression and secretion of several cytokines and growth factors that can act on cells of the tumor microenvironment. These include IL-6, IL-8, Activin A, and IL-1β, among others, all of which influence endothelial cells, stromal cells, and immune cells. Indeed, we were able to demonstrate that conditioned media from AGTR1 + breast cancer cells drives endothelial chemotaxis through one or more of these secreted, C3BM-dependent factors. Furthermore, using a mouse model of AGTR1 + breast cancer, we found that suppression of C3BM signaling using an shRNA directed against Bcl10 results in significantly impaired tumor angiogenesis. Taken together, our study provided the first demonstration of a role for the C3BM complex in AGTR1 + breast cancer. Since several other GPCRs implicated as oncogenic drivers in breast cancer, including the LPARs, CXCR4, and PAR1, have been shown to stimulate NF-κB *via* a CARMA3-dependent pathway, albeit in other contexts, we speculate that the C3BM signalosome may act as a central signaling node for multiple subsets of breast cancer characterized by overexpression and/or hyperactivity of these related GPCRs.

Other GPCRs Signal *via* the CARMA3-Containing CBM Complex

In addition to LPAR, CXCR4, and AGTR1 described above, several other GPCRs have been found to signal through the C3BM complex in cells outside of the immune system (**Table 1B**). In these specific cases (i.e., for ET_AR, CXCR2, PAF-R, and PAR1), the GPCR–C3BM axis has so far been linked only to inflammatory processes and not to solid tumor pathogenesis. For example, the endothelin-1 receptor, ET_AR, was one of the first GPCRs found to operate through the C3BM complex to activate NF-κB. Specifically, endothelin-1 treatment induces robust NF-κB activation in $Bcl10^{+/-}$ MEFs but not in $Bcl10^{-/-}$ MEFs (45). Intriguingly, there has been little additional work to explore the pathophysiologic consequences of C3BM signaling downstream of ET_AR since this initial observation, and to our knowledge, there have been no studies to test its potential relevance to cancer biology. Nevertheless, several reports have recently emerged implicating endothelin-1/ET_AR associated NF-κB activation in the pathogenesis of ovarian cancer (90), cervical cancer (91), prostate cancer (92), and chondrosarcoma (93). Thus, it is conceivable that the C3BM complex could play a pathogenic role downstream of ET_AR in these cancers.

As another example, the interleukin-8 (IL-8/CXCL8) receptor, CXCR2, similar to CXCR4 described above, is a CXC-family GPCR cytokine receptor that operates upstream of the C3BM complex. IL-8 is critically involved in a wide array of cellular processes and has potent pro-inflammatory and proangiogenic signaling capacity. IL-8 stimulation of endothelial cells induces the expression of VEGF, and this occurs *via* a CXCR2–C3BM–NF-κB signaling pathway (46). The VEGF produced *via* this mechanism in turn acts in autocrine fashion on endothelial cells to further stimulate angiogenesis. The establishment of this feed-forward autocrine loop could therefore play a prominent role in tumor angiogenesis and cancer promotion, but the role for the IL-8-CXCR2–C3BM signaling axis has not yet been formally studied in the context of cancer biology.

PAF-R is another example of a GPCR that signals *via* the C3BM complex (48). The levels of platelet-activating factor (PAF), the ligand for PAF-R, are elevated in patients suffering from disorders associated with intestinal inflammation such as Crohn's disease (94), ulcerative colitis (95), and neonatal necrotizing enterocolitis (96). It is thought that PAF causes intestinal injury *via* induction of NF-κB driven inflammation. In intestinal epithelial cells, PAF-R stimulation induces the interaction of Bcl10 with CARMA3, and Bcl10 deficiency abrogates PAF-R-dependent pro-inflammatory signaling (48). Currently, there is no known connection between PAF-R dependent C3BM signaling and the development of colon cancer associated with inflammatory bowel disease.

The thrombin receptor, PAR1, is one of the four members of the protease-activated receptor (PAR) family of GPCRs and is normally expressed in both platelets and endothelial cells (97,

98). In platelets, thrombin activation of PAR1 promotes platelet aggregation and coagulation, while in endothelial cells, PAR1 activation promotes an inflammatory response associated with enhanced endothelial permeability, immune cell attachment and adhesion, and the pathogenesis of diseases associated with endothelial dysfunction such as atherogenesis (99, 100). Our group found that the C3BM complex operates downstream of PAR1 in endothelial cells where it mediates thrombin-dependent NF-κB activation and expression of the cell-surface VCAM and ICAM adhesion molecules (49). As such, the C3BM complex controls thrombin-dependent adhesion of monocytes to the endothelial surface, which is an early step in the transmural migration of circulating monocytes into the vascular intimal space (49). In follow-up studies, we discovered that thrombin stimulation of endothelial cells induces MALT1 proteolytic activity and cleavage of the microtubule-binding protein, CYLD, resulting in microtubule destabilization (56). This destabilization then sets in motion a cascade of events that result in endothelial cell membrane retraction and increased vascular permeability (56). Together, these studies suggest that the C3BM complex plays a critical role in regulating both immune cell attachment to the endothelium and endothelial permeability to allow for transendothelial migration of immune cells. Thus, the C3BM complex may represent an important therapeutic target in the setting of vascular inflammatory disorders associated with endothelial dysfunction. As with the other GPCRs discussed in this section, the existing literature on the PAR1–C3BM signaling axis has not yet addressed any potential role in cancer biology.

Given the evidence of an important role for the CARMA3-containing CBM complex in mediating NF-κB signaling downstream of PAR1 and CXCR2 in endothelial cells, ET_AR in fibroblasts, and PAF-R in intestinal epithelial cells, it will be of great interest to investigate the contribution of the CARMA3 complex to mediating the protumorigenic effects of each of these GPCRs. For example, PAR1 promotes the invasiveness of several types of cancer, including melanoma (101), breast cancer (102–104), and prostate cancer (105). Similarly, the IL-8/CXCR2 axis is thought to play a key role in promoting progression of a variety of tumors (106) including prostate cancer (107, 108), breast cancer (109), and melanoma (110). Since CXCR2 may be expressed on cancer cells, endothelial cells, and even immune cells, this signaling axis has the potential to exert protumorigenic effects both within the tumor cells themselves and also within cells of the tumor microenvironment to influence angiogenesis and the immune contexture. Thus, we speculate that there are still un-realized opportunities to establish novel links between CARMA3 and several other GPCRs in the pathobiology of selected solid tumors.

RECEPTOR TYROSINE KINASES (RTKs) ALSO SIGNAL *VIA* THE CARMA3-CONTAINING CBM COMPLEX IN SOLID TUMORS

Several growth factors, including platelet-derived growth factor (111), fibroblast growth factor (112), insulin-like growth factor (113), and epidermal growth factor (EGF) (114), induce NF-κB activation through receptors that are members of the RTK family. EGF and the EGF receptor EGFR (HER1) have been extensively studied in cancer, with EGFR amplification implicated in the pathogenesis of lung cancer (115), glioblastoma (116), and breast cancer (117), among others. Indeed, EGFR itself is the target of several therapeutics: either RTK inhibitors such as gefitinib, used in lung cancer, or monoclonal antibody inhibitors such as cetuximab, employed against colon cancer (118). Because EGFR is known to activate NF-κB through a PKC-dependent mechanism, the research group led by Xin Lin sought to investigate whether a CARMA3-containing CBM signaling complex might serve to bridge EGFR stimulation and NF-κB activation in cancer cells. In 2011, the Lin group demonstrated that EGF stimulation of breast cancer and epidermoid carcinoma cells leads to CARMA3-dependent NF-κB activation (**Table 1C**) (58). CARMA3 suppression in these cells was associated with an increase in cancer cell apoptosis, a loss of EGF-induced migration, and decreased tumor growth in a mouse xenograft tumor model. Excitingly, this study was the first demonstration of a receptor class outside of GPCRs capable of signaling through the CARMA3-containing CBM complex.

Following this initial discovery, the Lin group demonstrated that the C3BM complex is also required for activation of NF-κB by HER2, an EGFR-related RTK that is overexpressed in a large fraction of breast cancers (**Table 1C**) (59). They found that CARMA3 is required for the proliferation and survival of HER2 + breast cancer cells, and also required for HER2 to induce the upregulation of metalloproteinases that contribute to tumor metastasis. Moreover, they found that while overexpression of HER2 in the mouse mammary tissue leads to spontaneous development of mammary tumors, the growth of these tumors is significantly reduced in MALT1-deficient mice, providing evidence that the C3BM complex contributes to HER2-induced breast cancer progression *in vivo*. Thus far, EGFR and HER2 are the only RTKs that have been shown to signal *via* the C3BM complex. Future studies are needed to determine if other related RTKs might also utilize a CARMA3-dependent downstream signaling mechanism.

More recently, the Lin group used a functional genomics approach to identify a transmembrane protein of unknown function, TMEM43 (also referred as LUMA) as a new CARMA3-binding partner that serves as a critical mediator of EGFR-induced NF-κB activation in cancer cells (119). Interestingly, they found that TMEM43 is highly expressed in glioblastoma multiforme and that high TMEM43 expression correlates with poor survival outcome in patients with brain tumors. Furthermore, knocking out either CARMA3 or TMEM43 results in decreased growth and survival of human glioblastoma cells, both *in vitro* and *in vivo*. Based on these findings, the authors propose that TMEM43 serves to bridge EGFR and the C3BM complex. A role for TMEM43 in bridging the related RTK, HER2, to CARMA3 has not yet been investigated.

OTHER STUDIES OF CARMA3 IN SOLID TUMORS

The role of the CARMA3-containing CBM complex in solid tumors has also been investigated outside the context of GPCR

and RTK-driven NF-κB activation. Examples of some of these key studies of CARMA3 are reviewed below.

Receptor-Independent Mechanisms for CARMA3–Bcl10–MALT1 Activation

One recent study examined the role of the C3BM complex in mediating DNA damage-induced NF-κB activation (120). While ionizing radiation and many chemotherapeutics used in the treatment of solid malignancies operate through induction of DNA damage and subsequent apoptosis, the molecular mechanism by which cancer cells upregulate DNA damage repair functions to resist these therapies has not been fully described (121). NF-κB has been known to play a pro-survival role in the context of irradiation or chemotherapeutic treatment, inducing cell cycle arrest and allowing for DNA damage repair and ultimately promoting therapeutic resistance and tumor survival. Given the involvement of the NF-κB transcription factor family in solid tumor DNA damage resistance (122), the laboratories of Xin Lin and Xuequiang Zhao asked whether the C3BM complex plays a role in this context (120). Intriguingly, they found that NF-κB induction by the chemotherapeutics etoposide or camptothecin require MALT1, suggesting a role for the C3BM complex in DNA damage-associated NF-κB activation. Furthermore, CARMA3, MALT1, and Bcl10 were each shown to be required for NF-κB induction by doxorubicin. The authors then exposed CARMA3$^{-/-}$ mice to radiation and compared their survival to irradiated heterozygous CARMA$^{+/-}$ littermate controls. Whereas all of the CARMA3$^{+/-}$ mice survived 12 Gy radiation, CARMA3$^{-/-}$ mice showed decreased radiation survival. Histological examination of tissue from irradiated mice showed decreased proliferation in CARMA3 homozygous knockouts, suggesting a role for the C3BM complex in post-radiation tissue repair. Finally, DNA damage-induced NF-κB activation appeared to be PKC-independent in cervical cancer cells, pointing to a novel upstream mechanism activating the C3BM complex and NF-κB signaling in response to DNA damage.

Overexpression of CARMA3 in Cancer

The CBM complex generally acts to transmit intracellular signals from upstream receptors to downstream targets such as NF-κB in a controlled manner; however, enforced overexpression of CARMA3, Bcl10, or MALT1 in transfected cells can result in inappropriate CBM signaling and activation of downstream targets, independent of upstream input (5, 8, 35, 36). The precise mechanisms for this activation are not clearly understood, but may stem from C3BM oligomerization driven by concentration-dependent mass action. Recently, multiple groups have examined whether CARMA3 or other CBM proteins are overexpressed in cancer cells compared with normal tissue and whether CARMA3 overexpression correlates with increased cancer progression or lower rates of patient survival. In 2012, a semi-quantitative immunohistochemical (IHC) analysis of non-small-cell lung cancer specimens demonstrated that 70% of tumor samples exhibited increased CARMA3 staining relative to normal tissue from the same patients (57). Higher CARMA3 expression levels correlated significantly with advanced TNM staging and larger primary tumor size. The authors also reported a significant correlation between CARMA3 expression and expression of EGFR as well as EGFR mutation. In addition, they showed that CBM protein knockdown in lung cancer cell lines suppressed lung cancer cell proliferation and invasion *in vitro*.

CARMA3 expression studies have been performed in a variety of other solid tumors with similar results. In colon cancer, IHC analysis showed that approximately 31% of colon cancers harbor increased CARMA3 expression (123); CARMA3 knockdown in colon cancer cells resulted in decreased NF-κB activity and led to decreased proliferation and cell cycle arrest. In another report, 42% of breast cancer samples demonstrated increased CARMA3 expression by IHC, and CARMA3 expression level positively correlated with TNM staging. Furthermore, CARMA3 knockdown in breast cancer cells with high endogenous CARMA3 resulted in increased paclitaxel-induced apoptosis, while overexpression of CARMA3 resulted in enhanced proliferation and reduced apoptosis, results which suggested a role for CARMA3 in chemotherapeutic resistance (124). In glioma patient tumor specimens, 26% of samples showed CARMA3 overexpression relative to normal astrocytes in the same specimen (125); the authors also showed that CARMA3 knockdown in a glioma cell line suppresses cell invasion *in vitro* and results in decreased expression of MMP9, a matrix metalloprotease closely linked with tissue invasion. These results suggested a possible mechanism by which C3BM signaling promotes invasion in human glioma. Strong associations between CARMA3 expression level, tumor grade, and lymph node metastasis have also been reported in pancreatic and ovarian cancers, with 36 and 52% of samples showing increased CARMA3 expression, respectively (126, 127). In ovarian cancer, the authors also noted that CARMA3 knockdown increased the cytotoxic effects of cisplatin on tumor cells, again pointing to a possible mechanism by which C3BM signaling promotes resistance to genotoxic chemotherapy. Finally, a study of CARMA3 expression performed in renal cell carcinoma samples showed a significant association between CARMA3 expression and tumor size, stage, and metastases (128). Patients with renal cell carcinomas expressing high levels of CARMA3 had a significantly worse prognosis relative to patients with tumors of lower CARMA3 expression, indicating the possible utility of CARMA3 expression as a prognostic biomarker in renal cell carcinoma.

While the above studies provide evidence for an intriguing link between CARMA3 expression levels and the pathogenesis of several solid tumors, it remains unclear as to whether the naturally occurring CARMA3 overexpression observed in some cancer cells is sufficient to drive dysregulated C3BM signaling, as it is when CARMA3 is artificially overexpressed in transfected cells. Alternatively, it is possible that the elevated levels of CARMA3 seen in these cancers acts to simply sensitize cancer cells to signaling from upstream GPCRs or RTKs. Further work is required to integrate findings from CARMA3 overexpression studies in cancer with those from studies focused on overexpression of protumorigenic receptors.

Regulation of CARMA3 by MicroRNAs (miRNAs)

While advances have been made in elucidating the role of C3BM signaling in solid tumors, the molecular mechanisms that regulate the expression of CARMA3, Bcl10, and MALT1 remain largely unknown. CARMA3 expression appears to be widely distributed in varied tissue types throughout the body, but the transcription factors and signaling networks responsible for the regulation of CARMA3 expression have not been fully investigated. Recently, two regulatory miRNAs, small single-strand noncoding RNA oligomers important in gene expression regulation through post-transcriptional mRNA silencing (129), have been reported to play a role in regulating CARMA3 levels. miR-195, previously described as a tumor suppressor in colorectal cancer, attenuates CARMA3 expression, and reduced expression of miR-195 has been associated with increased colorectal cancer metastasis to lymph nodes as well as poor prognosis (130, 131). Furthermore, the authors demonstrated that miR-195 expression suppresses colorectal cancer cell proliferation, MMP9 expression, and *in vitro* invasion. These effects of miR-195 could be reversed by CARMA3 overexpression, suggesting that miR-195-mediated downregulation of CARMA3 could be an important mechanism by which miR-195 acts as a colorectal cancer suppressor.

Recently, miR-24 was identified in bladder cancer as a second miRNA capable of targeting CARMA3 (132). miR-24 is downregulated in bladder cancer cells, supporting its role as a possible tumor suppressor (133). Furthermore, miR-24 overexpression blunts bladder cancer cell proliferation and invasion *in vitro* and appears to reduce expression of N-cadherin and vimentin, proteins important in cell adhesion and cytoskeletal structure, respectively, that are associated with the epithelial–mesenchymal transition (EMT). EMT is the process by which cancer cells undergo the substantial gene expression reprogramming necessary for the spread of cancer and formation of distant metastasis, and is reflected by a change in morphology and an increased capacity for tissue invasion (134). Overexpression of CARMA3 "rescued" bladder cancer cells with coexpressed miR-24, partially restoring proliferation and invasion *in vitro* and upregulating EMT markers.

Taken together, these two studies suggest that CARMA3 expression may be governed by miRNAs that act as tumor suppressors. Increased CARMA3 expression, in spite of these miRNAs, appears to promote tumor progression in specific cancers.

LOOKING TO THE FUTURE: UNANSWERED QUESTIONS AND CONCLUSIONS

Among the myriad of unanswered questions surrounding the role of CARMA3 in solid tumor pathophysiology, four important and related issues remain unaddressed. First, are gain-of-function mutations in CARMA3, similar to those found in CARMA1 in B-cell lymphoma, present in any solid tumors? To date, no gain-of-function mutations of CARMA3 have been reported in cancer or in any other disease. Second, what are the precise molecular mechanisms by which upstream GPCRs and/or RTKs regulate C3BM activity? Compared to antigen receptor engagement of CARMA1, much less is known about the intermediate proteins linking either GPCRs or RTKs to CARMA3. Is CARMA3, like CARMA1, subject to receptor-dependent phosphorylation and subsequent conformational change, thus allowing interaction with Bcl10, formation of a polymeric CBM complex, and subsequent downstream signaling? While inhibitor studies have implicated a role for PKCs in GPCR–C3BM signaling (43, 51, 53, 135), definitive phosphorylation of CARMA3 by PKCs, or any other kinase, has not yet been demonstrated. In addition, biophysical studies examining the detailed structural properties of the CARMA3-containing CBM complex, like those describing the CARMA1-containing complex (18, 19, 21), have not yet been reported.

Third, what is the role of MALT1 proteolytic activity, which is required for the survival of lymphoma cells harboring B-cell receptor or CARMA1 gain-of-function mutations, in tumors characterized by GPCR or RTK-driven CARMA3 activation? Our laboratory recently found that that stimulating the PAR1 receptor induces MALT1 protease activity in endothelial cells, providing the first evidence that a GPCR–CARMA3 signaling axis can trigger MALT1 proteolytic activity (56). It is important to point out that these studies were performed in endothelial cells and that MALT1 protease activity has not yet been evaluated in GPCR or RTK-driven CARMA3-dependent solid tumors. Based on our findings in endothelial cells, it seems likely that MALT1 proteolytic activity will be induced by oncogenic cell-surface receptors such as PAR1, AGTR1, CXCRs, and LPARs and will play a role in mediating the pro-tumorgenic effects of these receptors in solid tumors.

Fourth, what are the downstream molecular mechanisms by which CARMA3-dependent CBM signaling promotes tumorigenesis? Most of the existing literature has focused on NF-κB-dependent transcriptional reprogramming as the critical downstream event in GPCR/RTK-C3BM-driven tumorgenesis. Since the C1BM complex in lymphocytes is known to activate other transcription factors, such as Jun N-terminal kinase (JNK), in addition to NF-κB (136, 137), it seems possible that the C3BM complex in solid tumor cells may also activate JNK-dependent transcription, as well as other transcription factors. In addition, it will be important to consider potential transcription-independent mechanisms by which C3BM signaling could promote tumorgenesis. For example, several studies in immune cells have suggested that Bcl10/MALT1 can regulate actin and membrane remodeling *via* a transcription-independent mechanism (138, 139). It is thus possible that Bcl10/MALT1 may promote tumorigenesis in GPCR/RTK-C3BM-driven solid tumors *via* mechanisms that do not involve transcriptional reprogramming.

The answers to these questions will help to determine whether targeting specific receptors that drive CARMA3 signaling, targeting the C3BM signaling complex itself, or targeting the MALT1 protease, could represent promising therapeutic approaches for treating specific solid tumors. It will also be of interest to consider how the C3BM complex in solid tumors might be specifically targeted without impacting the C1BM complex in lymphocytes. Perhaps future structural analyses of the C3BM complex will reveal critical differences between how CARMA3 and CARMA1 interact with Bcl10/MALT1 that could be harnessed in designing novel protein–protein inhibitors specific to the C3BM?

Alternatively, it may be possible in the future to specifically inhibit C3BM by engineering tissue/cell type-specific delivery of MALT1 protease inhibitors.

The current body of knowledge of CARMA3 and C3BM signaling in solid tumors paints a picture of an intracellular signaling pathway associated with numerous steps in solid tumor pathophysiology: from tumor growth to chemotherapeutic resistance, EMT, angiogenesis, invasion, and metastasis. Furthermore, CARMA3-dependent signaling has been implicated in the pathogenesis of a striking variety of solid tumors, suggesting that targeting the C3BM pathway could have wide-ranging therapeutic application in clinical oncology. With the body of research focused on CARMA3 in solid tumors built over this last decade, we now await the next decade of C3BM research with great anticipation and hope for novel treatments for our patients.

AUTHOR CONTRIBUTIONS

JM wrote the initial draft of the manuscript text. TF and PE prepared figures and tables and reviewed/edited the text. PL and LM-L supervised all aspects of manuscript preparation and performed final editing.

FUNDING

JM is supported by funding from the NIH (NCI) 5F30CA196095. This work was supported in part by funding from the NIH (R01 HL082914, to PL and LM-L), a grant from the Cancer Research Fund of the University of Michigan Comprehensive Cancer Center (to PL), and a Hyundai Hope on Wheels Scholar Grant (to LM-L).

REFERENCES

1. Hofmann K, Bucher P, Tschopp J. The CARD domain: a new apoptotic signalling motif. *Trends Biochem Sci* (1997) 22(5):155–6. doi:10.1016/S0968-0004(97)01043-8
2. Bertin J, Guo Y, Wang L, Srinivasula SM, Jacobson MD, Poyet JL, et al. CARD9 is a novel caspase recruitment domain-containing protein that interacts with BCL10/CLAP and activates NF-kappa B. *J Biol Chem* (2000) 275(52):41082–6. doi:10.1074/jbc.C000726200
3. Bertin J, Wang L, Guo Y, Jacobson MD, Poyet JL, Srinivasula SM, et al. CARD11 and CARD14 are novel caspase recruitment domain (CARD)/membrane-associated guanylate kinase (MAGUK) family members that interact with BCL10 and activate NF-kappa B. *J Biol Chem* (2001) 276(15):11877–82. doi:10.1074/jbc.M010512200
4. Gaide O, Martinon F, Micheau O, Bonnet D, Thome M, Tschopp J. Carma1, a CARD-containing binding partner of Bcl10, induces Bcl10 phosphorylation and NF-kappaB activation. *FEBS Lett* (2001) 496(2–3):121–7. doi:10.1016/S0014-5793(01)02414-0
5. McAllister-Lucas LM, Inohara N, Lucas PC, Ruland J, Benito A, Li Q, et al. Bimp1, a MAGUK family member linking protein kinase C activation to Bcl10-mediated NF-kappaB induction. *J Biol Chem* (2001) 276(33):30589–97. doi:10.1074/jbc.M103824200
6. Wang L, Guo Y, Huang WJ, Ke X, Poyet JL, Manji GA, et al. Card10 is a novel caspase recruitment domain/membrane-associated guanylate kinase family member that interacts with BCL10 and activates NF-kappa B. *J Biol Chem* (2001) 276(24):21405–9. doi:10.1074/jbc.M102488200
7. Uren AG, O'Rourke K, Aravind LA, Pisabarro MT, Seshagiri S, Koonin EV, et al. Identification of paracaspases and metacaspases: two ancient families of caspase-like proteins, one of which plays a key role in MALT lymphoma. *Mol Cell* (2000) 6(4):961–7. doi:10.1016/S1097-2765(05)00086-9
8. Lucas PC, Yonezumi M, Inohara N, McAllister-Lucas LM, Abazeed ME, Chen FF, et al. Bcl10 and MALT1, independent targets of chromosomal translocation in malt lymphoma, cooperate in a novel NF-kappa B signaling pathway. *J Biol Chem* (2001) 276(22):19012–9. doi:10.1074/jbc.M009984200
9. Rosebeck S, Rehman AO, Lucas PC, McAllister-Lucas LM. From MALT lymphoma to the CBM signalosome: three decades of discovery. *Cell Cycle* (2011) 10(15):2485–96. doi:10.4161/cc.10.15.16923
10. Blonska M, Lin X. NF-kappaB signaling pathways regulated by CARMA family of scaffold proteins. *Cell Res* (2011) 21(1):55–70. doi:10.1038/cr.2010.182
11. Scudiero I, Vito P, Stilo R. The three CARMA sisters: so different, so similar: a portrait of the three CARMA proteins and their involvement in human disorders. *J Cell Physiol* (2014) 229(8):990–7. doi:10.1002/jcp.24543
12. Matsumoto R, Wang D, Blonska M, Li H, Kobayashi M, Pappu B, et al. Phosphorylation of CARMA1 plays a critical role in T Cell receptor-mediated NF-kappaB activation. *Immunity* (2005) 23(6):575–85. doi:10.1016/j.immuni.2005.10.007
13. Sommer K, Guo B, Pomerantz JL, Bandaranayake AD, Moreno-Garcia ME, Ovechkina YL, et al. Phosphorylation of the CARMA1 linker controls NF-kappaB activation. *Immunity* (2005) 23(6):561–74. doi:10.1016/j.immuni.2005.09.014
14. Chatila T, Silverman L, Miller R, Geha R. Mechanisms of T cell activation by the calcium ionophore ionomycin. *J Immunol* (1989) 143(4):1283–9.
15. Stilo R, Liguoro D, Di Jeso B, Formisano S, Consiglio E, Leonardi A, et al. Physical and functional interaction of CARMA1 and CARMA3 with Ikappa kinase gamma-NFkappaB essential modulator. *J Biol Chem* (2004) 279(33):34323–31. doi:10.1074/jbc.M402244200
16. Schaefer BC, Kappler JW, Kupfer A, Marrack P. Complex and dynamic redistribution of NF-kappaB signaling intermediates in response to T cell receptor stimulation. *Proc Natl Acad Sci U S A* (2004) 101(4):1004–9. doi:10.1073/pnas.0307858100
17. Rossman JS, Stoicheva NG, Langel FD, Patterson GH, Lippincott-Schwartz J, Schaefer BC. POLKADOTS are foci of functional interactions in T-Cell receptor-mediated signaling to NF-kappaB. *Mol Biol Cell* (2006) 17(5):2166–76. doi:10.1091/mbc.e05-10-0985
18. Li S, Yang X, Shao J, Shen Y. Structural insights into the assembly of CARMA1 and BCL10. *PLoS One* (2012) 7(8):e42775. doi:10.1371/journal.pone.0042775
19. Qiao Q, Yang C, Zheng C, Fontan L, David L, Yu X, et al. Structural architecture of the CARMA1/Bcl10/MALT1 signalosome: nucleation-induced filamentous assembly. *Mol Cell* (2013) 51(6):766–79. doi:10.1016/j.molcel.2013.08.032
20. Paul S, Traver MK, Kashyap AK, Washington MA, Latoche JR, Schaefer BC. T cell receptor signals to NF-kappaB are transmitted by a cytosolic p62-Bcl10-Malt1-IKK signalosome. *Sci Signal* (2014) 7(325):ra45. doi:10.1126/scisignal.2004882
21. David L, Li Y, Ma J, Garner E, Zhang X, Wu H. Assembly mechanism of the CARMA1-BCL10-MALT1-TRAF6 signalosome. *Proc Natl Acad Sci U S A* (2018) 115(7):1499–504. doi:10.1073/pnas.1721967115
22. Sun L, Deng L, Ea CK, Xia ZP, Chen ZJ. The TRAF6 ubiquitin ligase and TAK1 kinase mediate IKK activation by BCL10 and MALT1 in T lymphocytes. *Mol Cell* (2004) 14(3):289–301. doi:10.1016/S1097-2765(04)00236-9
23. Shambharkar PB, Blonska M, Pappu BP, Li H, You Y, Sakurai H, et al. Phosphorylation and ubiquitination of the IkappaB kinase complex by two distinct signaling pathways. *EMBO J* (2007) 26(7):1794–805. doi:10.1038/sj.emboj.7601622
24. Afonina IS, Elton L, Carpentier I, Beyaert R. MALT1 – a universal soldier: multiple strategies to ensure NF-kappaB activation and target gene expression. *FEBS J* (2015) 282(17):3286–97. doi:10.1111/febs.13325
25. Zhou H, Wertz I, O'Rourke K, Ultsch M, Seshagiri S, Eby M, et al. Bcl10 activates the NF-kappaB pathway through ubiquitination of NEMO. *Nature* (2004) 427(6970):167–71. doi:10.1038/nature02273
26. Oeckinghaus A, Wegener E, Welteke V, Ferch U, Arslan SC, Ruland J, et al. Malt1 ubiquitination triggers NF-kappaB signaling upon T-cell activation. *EMBO J* (2007) 26(22):4634–45. doi:10.1038/sj.emboj.7601897
27. Coornaert B, Baens M, Heyninck K, Bekaert T, Haegman M, Staal J, et al. T cell antigen receptor stimulation induces MALT1 paracaspase-mediated

cleavage of the NF-kappaB inhibitor A20. *Nat Immunol* (2008) 9(3):263–71. doi:10.1038/ni1561
28. Hailfinger S, Nogai H, Pelzer C, Jaworski M, Cabalzar K, Charton JE, et al. Malt1-dependent RelB cleavage promotes canonical NF-kappaB activation in lymphocytes and lymphoma cell lines. *Proc Natl Acad Sci U S A* (2011) 108(35):14596–601. doi:10.1073/pnas.1105020108
29. Staal J, Driege Y, Bekaert T, Demeyer A, Muyllaert D, Van Damme P, et al. T-cell receptor-induced JNK activation requires proteolytic inactivation of CYLD by MALT1. *EMBO J* (2011) 30(9):1742–52. doi:10.1038/emboj.2011.85
30. Demeyer A, Staal J, Beyaert R. Targeting MALT1 proteolytic activity in immunity, inflammation and disease: good or bad? *Trends Mol Med* (2016) 22(2):135–50. doi:10.1016/j.molmed.2015.12.004
31. Jaworski M, Thome M. The paracaspase MALT1: biological function and potential for therapeutic inhibition. *Cell Mol Life Sci* (2016) 73(3):459–73. doi:10.1007/s00018-015-2059-z
32. Akagi T, Motegi M, Tamura A, Suzuki R, Hosokawa Y, Suzuki H, et al. A novel gene, MALT1 at 18q21, is involved in t(11;18) (q21;q21) found in low-grade B-cell lymphoma of mucosa-associated lymphoid tissue. *Oncogene* (1999) 18(42):5785–94. doi:10.1038/sj.onc.1203018
33. Dierlamm J, Baens M, Wlodarska I, Stefanova-Ouzounova M, Hernandez JM, Hossfeld DK, et al. The apoptosis inhibitor gene API2 and a novel 18q gene, MLT, are recurrently rearranged in the t(11;18)(q21;q21) associated with mucosa-associated lymphoid tissue lymphomas. *Blood* (1999) 93(11):3601–9.
34. Morgan JA, Yin Y, Borowsky AD, Kuo F, Nourmand N, Koontz JI, et al. Breakpoints of the t(11;18)(q21;q21) in mucosa-associated lymphoid tissue (MALT) lymphoma lie within or near the previously undescribed gene MALT1 in chromosome 18. *Cancer Res* (1999) 59(24):6205–13.
35. Willis TG, Jadayel DM, Du MQ, Peng H, Perry AR, Abdul-Rauf M, et al. Bcl10 is involved in t(1;14)(p22;q32) of MALT B cell lymphoma and mutated in multiple tumor types. *Cell* (1999) 96(1):35–45. doi:10.1016/S0092-8674(00)80957-5
36. Streubel B, Lamprecht A, Dierlamm J, Cerroni L, Stolte M, Ott G, et al. T(14;18)(q32;q21) involving IGH and MALT1 is a frequent chromosomal aberration in MALT lymphoma. *Blood* (2003) 101(6):2335–9. doi:10.1182/blood-2002-09-2963
37. Lenz G, Davis RE, Ngo VN, Lam L, George TC, Wright GW, et al. Oncogenic CARD11 mutations in human diffuse large B cell lymphoma. *Science* (2008) 319(5870):1676–9. doi:10.1126/science.1153629
38. Bohers E, Mareschal S, Bouzelfen A, Marchand V, Ruminy P, Maingonnat C, et al. Targetable activating mutations are very frequent in GCB and ABC diffuse large B-cell lymphoma. *Genes Chromosomes Cancer* (2014) 53(2):144–53. doi:10.1002/gcc.22126
39. Bohers E, Mareschal S, Bertrand P, Viailly PJ, Dubois S, Maingonnat C, et al. Activating somatic mutations in diffuse large B-cell lymphomas: lessons from next generation sequencing and key elements in the precision medicine era. *Leuk Lymphoma* (2015) 56(5):1213–22. doi:10.3109/10428194.2014.941836
40. Juilland M, Thome M. Role of the CARMA1/BCL10/MALT1 complex in lymphoid malignancies. *Curr Opin Hematol* (2016) 23(4):402–9. doi:10.1097/MOH.0000000000000257
41. Bonsignore L, Passelli K, Pelzer C, Perroud M, Konrad A, Thurau M, et al. A role for MALT1 activity in Kaposi's sarcoma-associated herpes virus latency and growth of primary effusion lymphoma. *Leukemia* (2017) 31(3):614–24. doi:10.1038/leu.2016.239
42. Wang D, You Y, Case SM, McAllister-Lucas LM, Wang L, DiStefano PS, et al. A requirement for CARMA1 in TCR-induced NF-kappa B activation. *Nat Immunol* (2002) 3(9):830–5. doi:10.1038/ni824
43. Klemm S, Zimmermann S, Peschel C, Mak TW, Ruland J. Bcl10 and Malt1 control lysophosphatidic acid-induced NF-kappaB activation and cytokine production. *Proc Natl Acad Sci U S A* (2007) 104(1):134–8. doi:10.1073/pnas.0608388103
44. McAllister-Lucas LM, Ruland J, Siu K, Jin X, Gu S, Kim DS, et al. CARMA3/Bcl10/MALT1-dependent NF-kappaB activation mediates angiotensin II-responsive inflammatory signaling in nonimmune cells. *Proc Natl Acad Sci U S A* (2007) 104(1):139–44. doi:10.1073/pnas.0601947103
45. Wang D, You Y, Lin PC, Xue L, Morris SW, Zeng H, et al. Bcl10 plays a critical role in NF-kappaB activation induced by G protein-coupled receptors. *Proc Natl Acad Sci U S A* (2007) 104(1):145–50. doi:10.1073/pnas.0601894104
46. Martin D, Galisteo R, Gutkind JS. CXCL8/IL8 stimulates vascular endothelial growth factor (VEGF) expression and the autocrine activation of VEGFR2 in endothelial cells by activating NFkappaB through the CBM (Carma3/Bcl10/Malt1) complex. *J Biol Chem* (2009) 284(10):6038–42. doi:10.1074/jbc.C800207200
47. Rehman AO, Wang CY. CXCL12/SDF-1 alpha activates NF-kappaB and promotes oral cancer invasion through the Carma3/Bcl10/Malt1 complex. *Int J Oral Sci* (2009) 1(3):105–18. doi:10.4248/IJOS.09059
48. Borthakur A, Bhattacharyya S, Alrefai WA, Tobacman JK, Ramaswamy K, Dudeja PK. Platelet-activating factor-induced NF-kappaB activation and IL-8 production in intestinal epithelial cells are Bcl10-dependent. *Inflamm Bowel Dis* (2010) 16(4):593–603. doi:10.1002/ibd.21092
49. Delekta PC, Apel IJ, Gu S, Siu K, Hattori Y, McAllister-Lucas LM, et al. Thrombin-dependent NF-{kappa}B activation and monocyte/endothelial adhesion are mediated by the CARMA3.Bcl10.MALT1 signalosome. *J Biol Chem* (2010) 285(53):41432–42. doi:10.1074/jbc.M110.158949
50. Ekambaram P, Lee JL, Hubel NE, Hu D, Yerneni S, Campbell PG, et al. The CARMA3-Bcl10-MALT1 signalosome drives NF-kappaB activation and promotes aggressiveness in angiotensin II receptor-positive breast cancer. *Cancer Res* (2017) 78(5):1225–40. doi:10.1158/0008-5472.CAN-17-1089
51. Mahanivong C, Chen HM, Yee SW, Pan ZK, Dong Z, Huang S. Protein kinase C alpha-CARMA3 signaling axis links Ras to NF-kappa B for lysophosphatidic acid-induced urokinase plasminogen activator expression in ovarian cancer cells. *Oncogene* (2008) 27(9):1273–80. doi:10.1038/sj.onc.1210746
52. McAllister-Lucas LM, Jin X, Gu S, Siu K, McDonnell S, Ruland J, et al. The CARMA3-Bcl10-MALT1 signalosome promotes angiotensin II-dependent vascular inflammation and atherogenesis. *J Biol Chem* (2010) 285(34):25880–4. doi:10.1074/jbc.C110.109421
53. Grabiner BC, Blonska M, Lin PC, You Y, Wang D, Sun J, et al. CARMA3 deficiency abrogates G protein-coupled receptor-induced NF-{kappa}B activation. *Genes Dev* (2007) 21(8):984–96. doi:10.1101/gad.1502507
54. Medoff BD, Landry AL, Wittbold KA, Sandall BP, Derby MC, Cao Z, et al. CARMA3 mediates lysophosphatidic acid-stimulated cytokine secretion by bronchial epithelial cells. *Am J Respir Cell Mol Biol* (2009) 40(3):286–94. doi:10.1165/rcmb.2008-0129OC
55. Causton B, Ramadas RA, Cho JL, Jones K, Pardo-Saganta A, Rajagopal J, et al. CARMA3 Is Critical for the initiation of allergic airway inflammation. *J Immunol* (2015) 195(2):683–94. doi:10.4049/jimmunol.1402983
56. Klei LR, Hu D, Panek R, Alfano DN, Bridwell RE, Bailey KM, et al. MALT1 protease activation triggers acute disruption of endothelial barrier integrity via CYLD cleavage. *Cell Rep* (2016) 17(1):221–32. doi:10.1016/j.celrep.2016.08.080
57. Li Z, Qu L, Dong Q, Huang B, Li H, Tang Z, et al. Overexpression of CARMA3 in non-small-cell lung cancer is linked for tumor progression. *PLoS One* (2012) 7(5):e36903. doi:10.1371/journal.pone.0036903
58. Jiang T, Grabiner B, Zhu Y, Jiang C, Li H, You Y, et al. CARMA3 is crucial for EGFR-induced activation of NF-kappaB and tumor progression. *Cancer Res* (2011) 71(6):2183–92. doi:10.1158/0008-5472.CAN-10-3626
59. Pan D, Zhu Y, Zhou Z, Wang T, You H, Jiang C, et al. The CBM complex underwrites NF-kappaB activation to promote HER2-associated tumor malignancy. *Mol Cancer Res* (2016) 14(1):93–102. doi:10.1158/1541-7786.MCR-15-0229-T
60. O'Hayre M, Degese MS, Gutkind JS. Novel insights into G protein and G protein-coupled receptor signaling in cancer. *Curr Opin Cell Biol* (2014) 27:126–35. doi:10.1016/j.ceb.2014.01.005
61. Lin ME, Herr DR, Chun J. Lysophosphatidic acid (LPA) receptors: signaling properties and disease relevance. *Prostaglandins Other Lipid Mediat* (2010) 91(3–4):130–8. doi:10.1016/j.prostaglandins.2009.02.002
62. Willier S, Butt E, Grunewald TG. Lysophosphatidic acid (LPA) signalling in cell migration and cancer invasion: a focussed review and analysis of LPA receptor gene expression on the basis of more than 1700 cancer microarrays. *Biol Cell* (2013) 105(8):317–33. doi:10.1111/boc.201300011
63. Wang J, Sun Y, Qu J, Yan Y, Yang Y, Cai H. Roles of LPA receptor signaling in breast cancer. *Expert Rev Mol Diagn* (2016) 16(10):1103–11. doi:10.1080/14737159.2016.1238763
64. Liu S, Murph M, Panupinthu N, Mills GB. ATX-LPA receptor axis in inflammation and cancer. *Cell Cycle* (2009) 8(22):3695–701. doi:10.4161/cc.8.22.9937
65. Shida D, Kitayama J, Yamaguchi H, Okaji Y, Tsuno NH, Watanabe T, et al. Lysophosphatidic acid (LPA) enhances the metastatic potential of human colon carcinoma DLD1 cells through LPA1. *Cancer Res* (2003) 63(7):1706–11.

66. Raj GV, Sekula JA, Guo R, Madden JF, Daaka Y. Lysophosphatidic acid promotes survival of androgen-insensitive prostate cancer PC3 cells via activation of NF-kappaB. *Prostate* (2004) 61(2):105–13. doi:10.1002/pros.20083
67. Ketscher A, Jilg CA, Willmann D, Hummel B, Imhof A, Russeler V, et al. LSD1 controls metastasis of androgen-independent prostate cancer cells through PXN and LPAR6. *Oncogenesis* (2014) 3:e120. doi:10.1038/oncsis.2014.34
68. Koizumi K, Hojo S, Akashi T, Yasumoto K, Saiki I. Chemokine receptors in cancer metastasis and cancer cell-derived chemokines in host immune response. *Cancer Sci* (2007) 98(11):1652–8. doi:10.1111/j.1349-7006.2007.00606.x
69. Chow MT, Luster AD. Chemokines in cancer. *Cancer Immunol Res* (2014) 2(12):1125–31. doi:10.1158/2326-6066.CIR-14-0160
70. Domanska UM, Kruizinga RC, Nagengast WB, Timmer-Bosscha H, Huls G, de Vries EG, et al. A review on CXCR4/CXCL12 axis in oncology: no place to hide. *Eur J Cancer* (2013) 49(1):219–30. doi:10.1016/j.ejca.2012.05.005
71. Guo F, Wang Y, Liu J, Mok SC, Xue F, Zhang W. CXCL12/CXCR4: a symbiotic bridge linking cancer cells and their stromal neighbors in oncogenic communication networks. *Oncogene* (2016) 35(7):816–26. doi:10.1038/onc.2015.139
72. Sun X, Cheng G, Hao M, Zheng J, Zhou X, Zhang J, et al. CXCL12/CXCR4/CXCR7 chemokine axis and cancer progression. *Cancer Metastasis Rev* (2010) 29(4):709–22. doi:10.1007/s10555-010-9256-x
73. Liekens S, Schols D, Hatse S. CXCL12-CXCR4 axis in angiogenesis, metastasis and stem cell mobilization. *Curr Pharm Des* (2010) 16(35):3903–20. doi:10.2174/138161210794455003
74. Scala S. Molecular pathways: targeting the CXCR4-CXCL12 axis – untapped potential in the tumor microenvironment. *Clin Cancer Res* (2015) 21(19):4278–85. doi:10.1158/1078-0432.CCR-14-0914
75. Muller A, Homey B, Soto H, Ge N, Catron D, Buchanan ME, et al. Involvement of chemokine receptors in breast cancer metastasis. *Nature* (2001) 410(6824):50–6. doi:10.1038/35065016
76. Mukherjee D, Zhao J. The role of chemokine receptor CXCR4 in breast cancer metastasis. *Am J Cancer Res* (2013) 3(1):46–57.
77. Xu C, Zhao H, Chen H, Yao Q. CXCR4 in breast cancer: oncogenic role and therapeutic targeting. *Drug Des Devel Ther* (2015) 9:4953–64. doi:10.2147/DDDT.S84932
78. Mao TL, Fan KF, Liu CL. Targeting the CXCR4/CXCL12 axis in treating epithelial ovarian cancer. *Gene Ther* (2017) 24(10):621–9. doi:10.1038/gt.2017.69
79. Singh S, Singh UP, Grizzle WE, Lillard JW Jr. CXCL12-CXCR4 interactions modulate prostate cancer cell migration, metalloproteinase expression and invasion. *Lab Invest* (2004) 84(12):1666–76. doi:10.1038/labinvest.3700181
80. Gladson CL, Welch DR. New insights into the role of CXCR4 in prostate cancer metastasis. *Cancer Biol Ther* (2008) 7(11):1849–51. doi:10.4161/cbt.7.11.7218
81. Dubrovska A, Elliott J, Salamone RJ, Telegeev GD, Stakhovsky AE, Schepotin IB, et al. CXCR4 expression in prostate cancer progenitor cells. *PLoS One* (2012) 7(2):e31226. doi:10.1371/journal.pone.0031226
82. Conley-LaComb MK, Semaan L, Singareddy R, Li Y, Heath EI, Kim S, et al. Pharmacological targeting of CXCL12/CXCR4 signaling in prostate cancer bone metastasis. *Mol Cancer* (2016) 15(1):68. doi:10.1186/s12943-016-0552-0
83. Takeda H, Kondo S. Differences between squamous cell carcinoma and keratoacanthoma in angiotensin type-1 receptor expression. *Am J Pathol* (2001) 158(5):1633–7. doi:10.1016/S0002-9440(10)64119-3
84. Juillerat-Jeanneret L, Celerier J, Chapuis Bernasconi C, Nguyen G, Wostl W, Maerki HP, et al. Renin and angiotensinogen expression and functions in growth and apoptosis of human glioblastoma. *Br J Cancer* (2004) 90(5):1059–68. doi:10.1038/sj.bjc.6601646
85. Rocken C, Rohl FW, Diebler E, Lendeckel U, Pross M, Carl-McGrath S, et al. The angiotensin II/angiotensin II receptor system correlates with nodal spread in intestinal type gastric cancer. *Cancer Epidemiol Biomarkers Prev* (2007) 16(6):1206–12. doi:10.1158/1055-9965.EPI-05-0934
86. Suganuma T, Ino K, Shibata K, Kajiyama H, Nagasaka T, Mizutani S, et al. Functional expression of the angiotensin II type 1 receptor in human ovarian carcinoma cells and its blockade therapy resulting in suppression of tumor invasion, angiogenesis, and peritoneal dissemination. *Clin Cancer Res* (2005) 11(7):2686–94. doi:10.1158/1078-0432.CCR-04-1946
87. Wegman-Ostrosky T, Soto-Reyes E, Vidal-Millan S, Sanchez-Corona J. The renin-angiotensin system meets the hallmarks of cancer. *J Renin Angiotensin Aldosterone Syst* (2015) 16(2):227–33. doi:10.1177/1470320313496858
88. Rhodes DR, Ateeq B, Cao Q, Tomlins SA, Mehra R, Laxman B, et al. AGTR1 overexpression defines a subset of breast cancer and confers sensitivity to losartan, an AGTR1 antagonist. *Proc Natl Acad Sci U S A* (2009) 106(25):10284–9. doi:10.1073/pnas.0900351106
89. Hanahan D, Weinberg RA. Hallmarks of cancer: the next generation. *Cell* (2011) 144(5):646–74. doi:10.1016/j.cell.2011.02.013
90. Cianfrocca R, Tocci P, Semprucci E, Spinella F, Di Castro V, Bagnato A, et al. beta-Arrestin 1 is required for endothelin-1-induced NF-kappaB activation in ovarian cancer cells. *Life Sci* (2014) 118(2):179–84. doi:10.1016/j.lfs.2014.01.078
91. von Brandenstein MG, Ngum Abety A, Depping R, Roth T, Koehler M, Dienes HP, et al. A p38-p65 transcription complex induced by endothelin-1 mediates signal transduction in cancer cells. *Biochim Biophys Acta* (2008) 1783(9):1613–22. doi:10.1016/j.bbamcr.2008.04.003
92. Banerjee S, Hussain M, Wang Z, Saliganan A, Che M, Bonfil D, et al. In vitro and in vivo molecular evidence for better therapeutic efficacy of ABT-627 and taxotere combination in prostate cancer. *Cancer Res* (2007) 67(8):3818–26. doi:10.1158/0008-5472.CAN-06-3879
93. Wu MH, Lo JF, Kuo CH, Lin JA, Lin YM, Chen LM, et al. Endothelin-1 promotes MMP-13 production and migration in human chondrosarcoma cells through FAK/PI3K/Akt/mTOR pathways. *J Cell Physiol* (2012) 227(8):3016–26. doi:10.1002/jcp.23043
94. Kald B, Olaison G, Sjodahl R, Tagesson C. Novel aspect of Crohn's disease: increased content of platelet-activating factor in ileal and colonic mucosa. *Digestion* (1990) 46(4):199–204. doi:10.1159/000200346
95. Sobhani I, Hochlaf S, Denizot Y, Vissuzaine C, Rene E, Benveniste J, et al. Raised concentrations of platelet activating factor in colonic mucosa of Crohn's disease patients. *Gut* (1992) 33(9):1220–5. doi:10.1136/gut.33.9.1220
96. Frost BL, Jilling T, Caplan MS. The importance of pro-inflammatory signaling in neonatal necrotizing enterocolitis. *Semin Perinatol* (2008) 32(2):100–6. doi:10.1053/j.semperi.2008.01.001
97. Coughlin SR. Protease-activated receptors in hemostasis, thrombosis and vascular biology. *J Thromb Haemost* (2005) 3(8):1800–14. doi:10.1111/j.1538-7836.2005.01377.x
98. Crawley JT, Zanardelli S, Chion CK, Lane DA. The central role of thrombin in hemostasis. *J Thromb Haemost* (2007) 5(Suppl 1):95–101. doi:10.1111/j.1538-7836.2007.02500.x
99. Riewald M, Petrovan RJ, Donner A, Ruf W. Activated protein C signals through the thrombin receptor PAR1 in endothelial cells. *J Endotoxin Res* (2003) 9(5):317–21. doi:10.1177/09680519030090050801
100. Gudmundsdottir IJ, Lang NN, Boon NA, Ludlam CA, Webb DJ, Fox KA, et al. Role of the endothelium in the vascular effects of the thrombin receptor (protease-activated receptor type 1) in humans. *J Am Coll Cardiol* (2008) 51(18):1749–56. doi:10.1016/j.jacc.2007.12.047
101. Villares GJ, Zigler M, Bar-Eli M. The emerging role of the thrombin receptor (PAR-1) in melanoma metastasis – a possible therapeutic target. *Oncotarget* (2011) 2(1–2):8–17. doi:10.18632/oncotarget.211
102. Boire A, Covic L, Agarwal A, Jacques S, Sherifi S, Kuliopulos A. PAR1 is a matrix metalloprotease-1 receptor that promotes invasion and tumorigenesis of breast cancer cells. *Cell* (2005) 120(3):303–13. doi:10.1016/j.cell.2004.12.018
103. Hernandez NA, Correa E, Avila EP, Vela TA, Perez VM. PAR1 is selectively over expressed in high grade breast cancer patients: a cohort study. *J Transl Med* (2009) 7:47. doi:10.1186/1479-5876-7-47
104. Yang E, Cisowski J, Nguyen N, O'Callaghan K, Xu J, Agarwal A, et al. Dysregulated protease activated receptor 1 (PAR1) promotes metastatic phenotype in breast cancer through HMGA2. *Oncogene* (2016) 35(12):1529–40. doi:10.1038/onc.2015.217
105. Tantivejkul K, Loberg RD, Mawocha SC, Day LL, John LS, Pienta BA, et al. PAR1-mediated NFkappaB activation promotes survival of prostate cancer cells through a Bcl-xL-dependent mechanism. *J Cell Biochem* (2005) 96(3):641–52. doi:10.1002/jcb.20533
106. Waugh DJ, Wilson C. The interleukin-8 pathway in cancer. *Clin Cancer Res* (2008) 14(21):6735–41. doi:10.1158/1078-0432.CCR-07-4843
107. Lehrer S, Diamond EJ, Mamkine B, Stone NN, Stock RG. Serum interleukin-8 is elevated in men with prostate cancer and bone metastases. *Technol Cancer Res Treat* (2004) 3(5):411. doi:10.1177/153303460400300501
108. Seaton A, Scullin P, Maxwell PJ, Wilson C, Pettigrew J, Gallagher R, et al. Interleukin-8 signaling promotes androgen-independent proliferation

of prostate cancer cells via induction of androgen receptor expression and activation. *Carcinogenesis* (2008) 29(6):1148–56. doi:10.1093/carcin/bgn109
109. Todorovic-Rakovic N, Milovanovic J. Interleukin-8 in breast cancer progression. *J Interferon Cytokine Res* (2013) 33(10):563–70. doi:10.1089/jir.2013.0023
110. Singh RK, Varney ML. IL-8 expression in malignant melanoma: implications in growth and metastasis. *Histol Histopathol* (2000) 15(3):843–9. doi:10.14670/HH-15.843
111. Romashkova JA, Makarov SS. NF-kappaB is a target of AKT in anti-apoptotic PDGF signalling. *Nature* (1999) 401(6748):86–90. doi:10.1038/43474
112. Byrd VM, Ballard DW, Miller GG, Thomas JW. Fibroblast growth factor-1 (FGF-1) enhances IL-2 production and nuclear translocation of NF-kappaB in FGF receptor-bearing Jurkat T cells. *J Immunol* (1999) 162(10):5853–9.
113. Heck S, Lezoualc'h F, Engert S, Behl C. Insulin-like growth factor-1-mediated neuroprotection against oxidative stress is associated with activation of nuclear factor kappaB. *J Biol Chem* (1999) 274(14):9828–35. doi:10.1074/jbc.274.14.9828
114. Sun L, Carpenter G. Epidermal growth factor activation of NF-kappaB is mediated through IkappaBalpha degradation and intracellular free calcium. *Oncogene* (1998) 16(16):2095–102. doi:10.1038/sj.onc.1201731
115. Liu TC, Jin X, Wang Y, Wang K. Role of epidermal growth factor receptor in lung cancer and targeted therapies. *Am J Cancer Res* (2017) 7(2):187–202.
116. Xu H, Zong H, Ma C, Ming X, Shang M, Li K, et al. Epidermal growth factor receptor in glioblastoma. *Oncol Lett* (2017) 14(1):512–6. doi:10.3892/ol.2017.6221
117. Moerkens M, Zhang Y, Wester L, van de Water B, Meerman JH. Epidermal growth factor receptor signalling in human breast cancer cells operates parallel to estrogen receptor alpha signalling and results in tamoxifen insensitive proliferation. *BMC Cancer* (2014) 14:283. doi:10.1186/1471-2407-14-283
118. Yewale C, Baradia D, Vhora I, Patil S, Misra A. Epidermal growth factor receptor targeting in cancer: a review of trends and strategies. *Biomaterials* (2013) 34(34):8690–707. doi:10.1016/j.biomaterials.2013.07.100
119. Jiang C, Zhu Y, Zhou Z, Gumin J, Bengtsson L, Wu W, et al. TMEM43/LUMA is a key signaling component mediating EGFR-induced NF-kappaB activation and tumor progression. *Oncogene* (2017) 36(20):2813–23. doi:10.1038/onc.2016.430
120. Zhang S, Pan D, Jia XM, Lin X, Zhao X. The CARMA3-BCL10-MALT1 (CBM) complex contributes to DNA damage-induced NF-kappaB activation and cell survival. *Protein Cell* (2017) 8(11):856–60. doi:10.1007/s13238-017-0441-3
121. O'Connor MJ. Targeting the DNA damage response in cancer. *Mol Cell* (2015) 60(4):547–60. doi:10.1016/j.molcel.2015.10.040
122. Wang W, Mani AM, Wu ZH. DNA damage-induced nuclear factor-kappa B activation and its roles in cancer progression. *J Cancer Metastasis Treat* (2017) 3:45–59. doi:10.20517/2394-4722.2017.03
123. Miao Z, Zhao T, Wang Z, Xu Y, Song Y, Wu J, et al. CARMA3 is overexpressed in colon cancer and regulates NF-kappaB activity and cyclin D1 expression. *Biochem Biophys Res Commun* (2012) 425(4):781–7. doi:10.1016/j.bbrc.2012.07.152
124. Zhao T, Miao Z, Wang Z, Xu Y, Wu J, Liu X, et al. CARMA3 overexpression accelerates cell proliferation and inhibits paclitaxel-induced apoptosis through NF-kappaB regulation in breast cancer cells. *Tumour Biol* (2013) 34(5):3041–7. doi:10.1007/s13277-013-0869-x
125. Feng X, Miao G, Han Y, Xu Y. CARMA3 is overexpressed in human glioma and promotes cell invasion through MMP9 regulation in A172 cell line. *Tumour Biol* (2014) 35(1):149–54. doi:10.1007/s13277-013-1018-2
126. Du S, Jia L, Zhang Y, Fang L, Zhang X, Fan Y. CARMA3 is upregulated in human pancreatic carcinoma, and its depletion inhibits tumor proliferation, migration, and invasion. *Tumour Biol* (2014) 35(6):5965–70. doi:10.1007/s13277-014-1791-6
127. Xie C, Han Y, Fu L, Li Q, Qiu X, Wang E. Overexpression of CARMA3 is associated with advanced tumor stage, cell cycle progression, and cisplatin resistance in human epithelial ovarian cancer. *Tumour Biol* (2014) 35(8):7957–64. doi:10.1007/s13277-014-2070-2
128. Wu GL, Yuan JL, Huang XD, Rong JF, Zhang LX, Liu YP, et al. Evaluating the expression of CARMA3 as a prognostic tumor marker in renal cell carcinoma. *Tumour Biol* (2013) 34(6):3431–5. doi:10.1007/s13277-013-0917-6
129. Ha M, Kim VN. Regulation of microRNA biogenesis. *Nat Rev Mol Cell Biol* (2014) 15(8):509–24. doi:10.1038/nrm3838
130. Wang X, Wang J, Ma H, Zhang J, Zhou X. Downregulation of miR-195 correlates with lymph node metastasis and poor prognosis in colorectal cancer. *Med Oncol* (2012) 29(2):919–27. doi:10.1007/s12032-011-9880-5
131. Wang L, Qian L, Li X, Yan J. MicroRNA-195 inhibits colorectal cancer cell proliferation, colony-formation and invasion through targeting CARMA3. *Mol Med Rep* (2014) 10(1):473–8. doi:10.3892/mmr.2014.2178
132. Zhang S, Zhang C, Liu W, Zheng W, Zhang Y, Wang S, et al. MicroRNA-24 upregulation inhibits proliferation, metastasis and induces apoptosis in bladder cancer cells by targeting CARMA3. *Int J Oncol* (2015) 47(4):1351–60. doi:10.3892/ijo.2015.3117
133. Inoguchi S, Seki N, Chiyomaru T, Ishihara T, Matsushita R, Mataki H, et al. Tumour-suppressive microRNA-24-1 inhibits cancer cell proliferation through targeting FOXM1 in bladder cancer. *FEBS Lett* (2014) 588(17):3170–9. doi:10.1016/j.febslet.2014.06.058
134. Nieto MA, Huang RY, Jackson RA, Thiery JP. Emt: 2016. *Cell* (2016) 166(1):21–45. doi:10.1016/j.cell.2016.06.028
135. Cummings R, Zhao Y, Jacoby D, Spannhake EW, Ohba M, Garcia JG, et al. Protein kinase Cdelta mediates lysophosphatidic acid-induced NF-kappaB activation and interleukin-8 secretion in human bronchial epithelial cells. *J Biol Chem* (2004) 279(39):41085–94. doi:10.1074/jbc.M404045200
136. Blonska M, Lin X. CARMA1-mediated NF-kappaB and JNK activation in lymphocytes. *Immunol Rev* (2009) 228(1):199–211. doi:10.1111/j.1600-065X.2008.00749.x
137. Juilland M, Gonzalez M, Erdmann T, Banz Y, Jevnikar Z, Hailfinger S, et al. CARMA1- and MyD88-dependent activation of Jun/ATF-type AP-1 complexes is a hallmark of ABC diffuse large B-cell lymphomas. *Blood* (2016) 127(14):1780–9. doi:10.1182/blood-2015-07-655647
138. Rueda D, Gaide O, Ho L, Lewkowicz E, Niedergang F, Hailfinger S, et al. Bcl10 controls TCR- and FcgammaR-induced actin polymerization. *J Immunol* (2007) 178(7):4373–84. doi:10.4049/jimmunol.178.7.4373
139. Marion S, Mazzolini J, Herit F, Bourdoncle P, Kambou-Pene N, Hailfinger S, et al. The NF-kappaB signaling protein Bcl10 regulates actin dynamics by controlling AP1 and OCRL-bearing vesicles. *Dev Cell* (2012) 23(5):954–67. doi:10.1016/j.devcel.2012.09.021

Conflict of Interest Statement: The authors declare that the research was conducted in the absence of any commercial or financial relationships that could be construed as a potential conflict of interest.

frontiers in Immunology

REVIEW
published: 19 September 2018
doi: 10.3389/fimmu.2018.02105

Mechanisms of Regulated and Dysregulated CARD11 Signaling in Adaptive Immunity and Disease

*Jacquelyn R. Bedsaul, Nicole M. Carter, Katelynn E. Deibel, Shelby M. Hutcherson, Tyler A. Jones, Zhaoquan Wang, Chao Yang, Yong-Kang Yang and Joel L. Pomerantz**

Department of Biological Chemistry, Institute for Cell Engineering, The Johns Hopkins University School of Medicine, Baltimore, MD, United States

CARD11 functions as a key signaling scaffold that controls antigen-induced lymphocyte activation during the adaptive immune response. Somatic mutations in CARD11 are frequently found in Non-Hodgkin lymphoma, and at least three classes of germline CARD11 mutations have been described as the basis for primary immunodeficiency. In this review, we summarize our current understanding of how CARD11 signals, how its activity is regulated, and how mutations bypass normal regulation to cause disease.

Keywords: CARD11, Bcl10, MALT1, primary immunodeficiency, lymphoma, T cell receptor, B cell receptor

OPEN ACCESS

Edited by:
Frederic Bornancin, Novartis, Switzerland

Reviewed by:
Ruben Martinez-Barricarte, Rockefeller University, United States
Jens Staal, Ghent University, Belgium

****Correspondence:***
Joel L. Pomerantz
joel.pomerantz@jhmi.edu

Specialty section:
This article was submitted to Primary Immunodeficiencies, a section of the journal Frontiers in Immunology

Received: *05 June 2018*
Accepted: *28 August 2018*
Published: *19 September 2018*

Citation:
Bedsaul JR, Carter NM, Deibel KE, Hutcherson SM, Jones TA, Wang Z, Yang C, Yang Y-K and Pomerantz JL (2018) Mechanisms of Regulated and Dysregulated CARD11 Signaling in Adaptive Immunity and Disease. Front. Immunol. 9:2105. doi: 10.3389/fimmu.2018.02105

INTRODUCTION

Our understanding of the immune system has benefited greatly from the study of the molecular circuitry in lymphocytes that governs antigen recognition and the cellular and systemic response to pathogens. This circuitry is elaborate, highly regulated, sensitive, and specific. As the study of immune cell signal transduction has highlighted networks of molecules that translate antigen sensing into lymphocyte action, it has also revealed how the dysregulation of signaling machinery can precipitate disease, including immunodeficiencies, autoimmunity syndromes, leukemia, and lymphoma.

CARD11 is a fascinating, multi-domain scaffold protein that plays a key role as a signaling hub during the adaptive immune response. Underscoring its importance, the CARD11 gene is extremely intolerant to loss-of-function (LOF) mutation or genetic variation in the human population (1, 2). Since its discovery in 2001 (3), many studies have revealed its obligate role in antigen-mediated lymphocyte activation and its susceptibility to mutations that can cause immunodeficiency or contribute to the development of lymphoma. CARD11 is best understood at present as a signal integrator that translates B cell receptor (BCR) and T cell receptor (TCR) triggering into the activation of NF-κB, JNK, and mTOR (**Figure 1**). Several excellent reviews have summarized the biological roles of CARD11 gleaned from mice and humans deficient in CARD11 or its signaling partner proteins (4–8). Here we will review our current understanding of (1) how the structure of CARD11 allows it to function as a signal-responsive scaffold; (2) how CARD11 orchestrates downstream signaling events; (3) the mechanisms that limit or terminate CARD11 signaling activity; (4) how gain-of-function (GOF) disease-associated CARD11 mutations bypass normal regulation; and (5) how LOF disease-associated CARD11 mutations disrupt CARD11 activity.

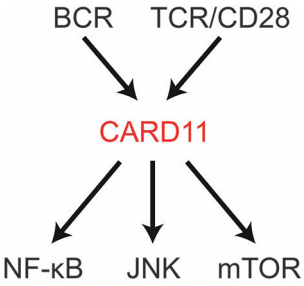

FIGURE 1 | CARD11 relays signaling from antigen receptors to NF-κB, JNK, and mTOR.

OVERVIEW

CARD11 can be thought of as a string of protein-protein interaction domains, each of which presents surfaces for the binding and regulation of interaction targets (**Figure 2A**). The protein interacts with more than 20 different proteins during signaling, and it has evolved to present its interaction surfaces dynamically in response to signaling inputs (**Figure 2B**). Prior to receptor engagement the protein exists in a closed, inactive state. Receptor engagement leads to the conversion of CARD11 to an open, active scaffold that binds signaling partners. Cofactor binding leads to the generation of downstream signaling intermediates that activate the IKK complex, a central target in the canonical NF-κB signaling pathway, as well as JNK2, and mTOR. Following activation, binding partners dissociate from CARD11 and the protein returns to the inactive state. This cycle, from closed to open and back to closed states, is thought to occur over the course of approximately 60 minutes following BCR or TCR engagement.

MAINTENANCE OF THE CLOSED INACTIVE STATE

Like many signaling proteins that promote cellular proliferation and activation and whose signaling could be dangerous if dysregulated, CARD11 contains an internal autoinhibitory domain that keeps CARD11 inactive in the absence of receptor triggering (9–11). This domain, termed the Inhibitory Domain (ID), is located in the primary sequence between the Coiled-coil and PDZ domain (**Figure 2A**). Remarkably, the autoinhibitory action of the ID is accomplished by four small Repressive Elements (REs), ranging in size from 11 to 53 amino acids, that function cooperatively with redundancy (12, 13). Other than a short 5-residue region of homology between RE2 and RE3, the four REs do not resemble each other. While the mutation of any single RE has little to no effect on basal CARD11 signaling, their combinatorial mutation cooperatively increases activity, and the simultaneous mutation of all four leads to a remarkable 640-fold enhancement of activity (12). The four REs function together to prevent cofactor binding to CARD11 prior to receptor engagement, but it is not completely clear how they do so. RE1, RE2, and RE3 interact with other CARD11 domains, including the CARD, LATCH, Coiled-coil, L3, and GUK, with somewhat overlapping intramolecular specificities, presumably to maintain CARD11 in a conformation in which protein-interaction surfaces of the CARD and Coiled-coil are inaccessible (13). However, RE4, which may be the most potent inhibitory element, does not appear to participate in intramolecular interactions and likely functions in cooperation with the other REs through an unknown mechanism, possibly via the recruitment of a repressor *in trans*.

RECEPTOR-INDUCED ACTIVATION OF CARD11 SCAFFOLD POTENTIAL AND CONVERSION TO THE OPEN ACTIVE STATE

Antigen receptor engagement by antigen in the appropriate context leads to a cascade of signaling events upstream of CARD11 that have been extensively reviewed (14). At present, it appears that the inputs that CARD11 receives from upstream signaling consist of phosphorylation events within the ID (9, 10, 15–17). Serines 564, 567, 577, and 657 all appear to be phosphorylated as a result of antigen receptor signaling. Somehow the modification of these residues leads to sufficient neutralization of RE activity to allow CARD11 signaling cofactors to bind and signaling events to ensue. Serines 564 and 657 appear to be targeted by PKCβ in B cells and PKCθ in T cells, while serine 567 appears to be phosphorylated by IKKβ. The kinase that targets serine 577 has not yet been reported. Additional phosphorylation events may also be important for maximal CARD11 activity, depending on cellular context (18–20). The phosphorylation-mediated activation of CARD11 scaffold activity may occur in a step-wise manner, with an initial step that elicits some IKKβ kinase activity and a subsequent step in which IKKβ phosphorylation of serine 577 promotes full scaffold activity (15, 21). Precisely how the phosphorylation events convert CARD11 into an active scaffold remains mysterious. It is possible that phosphorylation induces a conformational change in CARD11 that disallows RE-mediated inhibitory intramolecular interactions. Alternatively, the phosphorylated residues may be recognized by an unknown factor *in trans* that actively prevents cooperative RE action.

RECEPTOR-INDUCED RECRUITMENT OF SIGNALING COFACTORS

Upon activation, the protein interaction surfaces of CARD11 become accessible for binding to a variety of proteins (**Figure 2B**). Bcl10 was the first protein shown to bind CARD11, with MALT1 recruited indirectly through Bcl10. These observations led to the notion of a "CBM complex," which is a misleading misnomer because it ignores the binding of other critical factors to CARD11. Bcl10 requires both the CARD and Coiled-coil domain of CARD11 for its recruitment at physiological levels of expression (11). The CARD and Coiled-coil are also required for the recruitment of TRAF6, IKKγ, and Caspase-8 (11). The CARD alone is required for TAK1 binding (11), while the Coiled-coil alone is required for binding

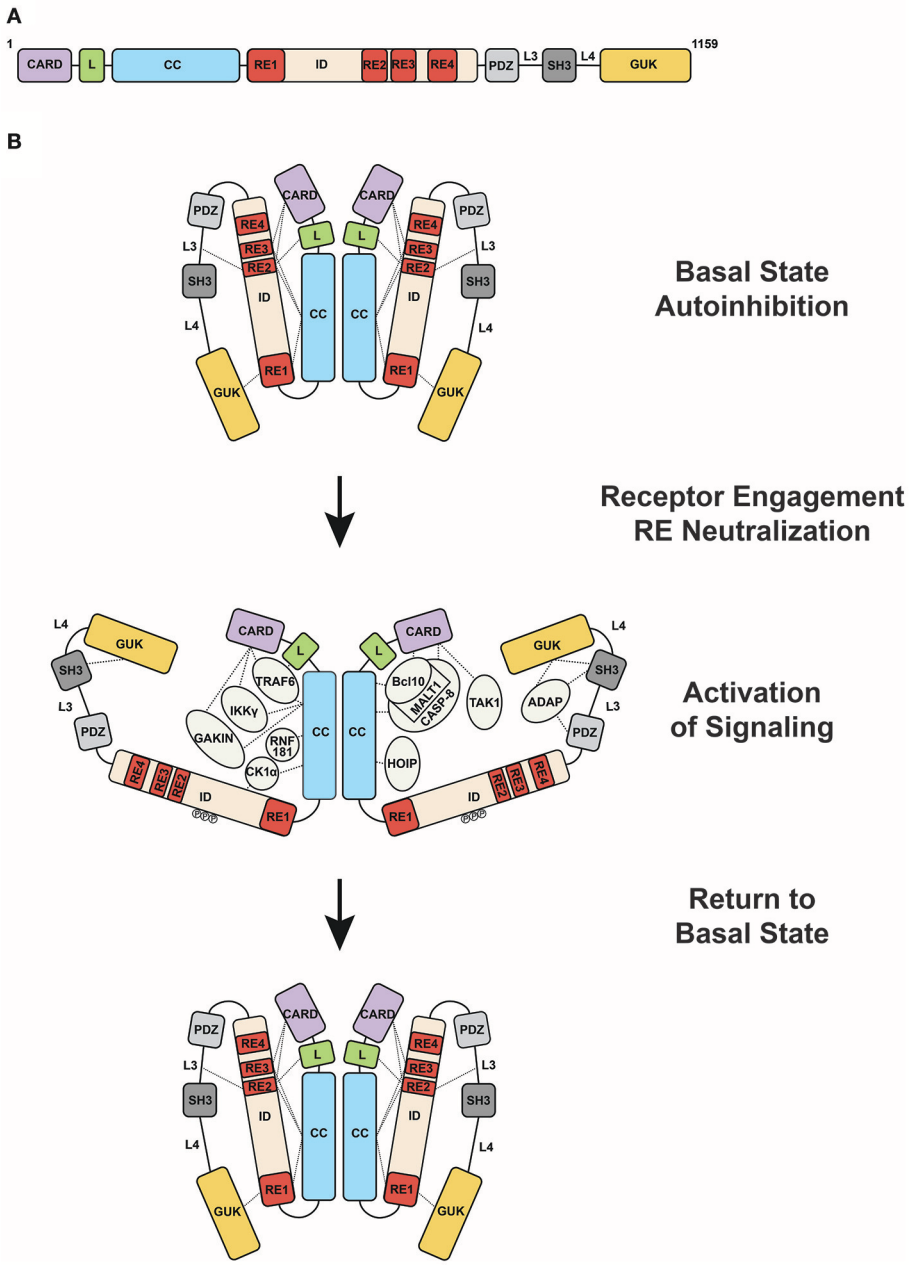

FIGURE 2 | Activation of CARD11 activity during antigen receptor signaling. **(A)** Domain structure of CARD11. **(B)** Transition of CARD11 from closed, inactive to open, active states and back again. Dashed lines indicate mapped protein-protein interactions. Abbreviations: CARD, Caspase Recruitment Domain; L, Latch; CC, coiled-coil; ID, Inhibitory Domain; PDZ, PSD-95/Discs-Large/ZO-1 domain; SH3, Src Homology 3 domain; GUK, Guanylate Kinase domain; RE1, Repressive Element 1; RE2, Repressive Element 2; RE3, Repressive Element 3; RE4, Repressive Element 4; L3, Linker 3; L4, Linker 4.

to HOIP, the catalytic subunit of the Linear Ubiquitin Chain Assembly Complex (LUBAC) (22). CK1α is recruited through the Coiled-coil and ID (23). The preponderance of protein interactions occurs through the N-terminal half of CARD11 that includes the CARD, LATCH, and Coiled-coil, although the C-terminal PDZ-SH3-MAGUK region can bind the ADAP adapter (24) and AIP (25). In T cells, the site of CARD11 complex assembly appears to be the immunological synapse (26, 27).

In addition to the intramolecular interactions mediated by the REs in the ID, two other CARD11 regions have been shown to mediate CARD11-CARD11 interactions. The Coiled-coil domain, predicted to form four discontinuous regions with coiled-coil character, mediates assembly of CARD11 into an

oligomer of undetermined stoichiometry. The SH3-GUK domain tandem has also been shown to participate in modular inter- and intramolecular binding interactions that appear to be required for higher order clustering of CARD11 visible via microscopy (28).

CARD11-DEPENDENT SIGNALING EVENTS IN ANTIGEN RECEPTOR SIGNALING

The transient recruitment of cofactors to CARD11 ultimately leads to the activation of the IKK complex in the canonical NF-κB activation pathway. As it assembles cofactors into complexes, CARD11 orchestrates ubiquitinylation and phosphorylation events that somehow work together to promote IKK kinase action on inhibitory IκB proteins that tether NF-κB in the cytoplasm. The phosphorylation of IκBs promotes their ubiquitinylation and degradation by the proteasome, which allows NF-κB to stably translocate to the nucleus to bind target genes.

BCL10 POLYUBIQUITINYLATION

The signal-induced recruitment of Bcl10 and HOIP to CARD11 allows HOIP (enzyme) to conjugate Bcl10 (substrate) with linear ubiquitin chains, to produce $LinUb_n$-Bcl10 (22). $LinUb_n$-Bcl10 then binds the IKK complex through the UBAN domain of IKKγ (22) in an interaction thought to be required for IKK complex kinase activation (29). $LinUb_n$-Bcl10 is a signaling intermediate that determines the extent of NF-κB activation downstream of CARD11 triggering. For a range of hyperactive CARD11 variants (see below), the levels of $LinUb_n$-Bcl10 produced by each variant correlates with the degree of NF-κB activation it achieves (22). Signaling through $LinUb_n$-Bcl10 accounts for 50-60% of the signaling output of CARD11 to NF-κB. In addition to CARD11, TCR-induced $LinUb_n$-Bcl10 generation also requires MALT1, but not the SHARPIN subunit of LUBAC (22).

Bcl10 is also conjugated with K63-linked ubiquitin chains during antigen receptor signaling (30, 31) to form Ub_n(K63)-Bcl10. This modification, mediated by cIAPs, has been shown to be a prerequisite for linear ubiquitinylation of Bcl10 in the context of chronic BCR signaling (32).

IKKγ POLYUBIQUITINYLATION

CARD11 facilitates the polyubiquitinylation of IKKγ with K63-linked chains in response to antigen receptor triggering (33), which is accomplished by a MALT1-associated E3 ligase activity (34). Linear ubiquitinylation of IKKγ has also been implicated in the antigen receptor pathway (35, 36). Since CARD11 recruits both HOIP and IKKγ upon activation, CARD11 likely facilitates LUBAC action on IKKγ.

MALT1 POLYUBIQUITINYLATION

MALT1 is also conjugated with K63-linked ubiquitin chains during signaling, which facilitates its interaction with IKKγ (37); however, MALT1 polyubiquitinylation has not been formally shown to require CARD11. TRAF6 has been implicated as the E3 ligase for this process, and its recruitment by CARD11 may promote its action on MALT1.

MALT1 PROTEOLYTIC ACTION

CARD11 is also required for MALT1 protease activity on several targets, including Bcl10 and MALT1 itself (7, 38–40). MALT1 cleaves the inhibitory deubiquitinase A20 (41, 42) to limit its removal of polyubiquitinylated MALT1, thereby extending the time-course of NF-κB activation. MALT1 also cleaves the NF-κB subunit RelB, limiting its potential to repress transcriptional activation by RelA and c-Rel (43). In addition, MALT1 cleaves the HOIL-1L subunit of LUBAC and in so doing limits the degree of NF-κB activation downstream of CARD11 (36, 44, 45). MALT1 has also been shown to cleave the deubiquitinase CYLD to maximize NF-κB and JNK activation (46–48). CARD11 may promote MALT1 protease activity by activating enzymatic potential, by recruiting enzyme to substrate, or both, but further studies are required to define mechanisms.

MTOR ACTIVATION

The activation of mTOR downstream of TCR engagement also requires CARD11, in a role independent of IKK complex activation (49, 50). CARD11 signaling to mTORC1 depends upon the proteolytic activity of MALT1 (49) and the rapid uptake of glutamine through the ASCT2 glutamine transporter (50). CARD11 signaling promotes ASCT2 expression and ASCT2 associates with CARD11, Bcl10, and MALT1 during signaling, suggesting an active regulation of transporter activity (50).

JNK ACTIVATION

CARD11 is also required for the activation of JNK signaling following antigen receptor triggering (51, 52), in a manner that also requires Bcl10 and MALT1. For JNK activation, CARD11 appears to promote Bcl10 oligomerization, followed by the binding of Bcl10 to TAK1, MKK7, and JNK2, which is thought to engage this MAP kinase cascade for JNK2 activation leading to increased levels of c-Jun and c-Jun phosphorylation (53, 54).

BCL10 FILAMENT FORMATION

CARD11 fragments that include the CARD, LATCH and portions of the Coiled-coil domain have been shown *in vitro* to nucleate the formation of helical filaments of Bcl10 (55, 56). These Bcl10 filaments assemble through interactions between Bcl10 CARD domains and polymerize in a unidirectional manner (56). MALT1 and TRAF6 cooperatively associate with the Bcl10 filament (56) and stimulate MALT1 proteolytic activity (55). Bcl10 mutations that affect filament formation perturb NF-κB activation by overexpressed Bcl10 in cells (55), implicating these structures in CARD11 signaling. However, further work is needed to bolster the importance of Bcl10

filaments in antigen receptor signaling through CARD11 *in vivo* at physiological levels of expression, resolve how Bcl10 and MALT1 ubiquitinylation is accommodated or promoted by Bcl10 filament formation, and explain the mechanistic relationship between Bcl10 filament formation and other steps in CARD11 signaling that require the L3, SH3, L4, and GUK domains, which are required for physiological CARD11 signaling but are not required to nucleate Bcl10 filaments.

MODULATION AND TERMINATION OF CARD11 SIGNALING

Multiple mechanisms have evolved to tune and terminate CARD11 signaling to ensure appropriate pathway output and avoid pathological immune cell activation and proliferation. First, cofactor association to CARD11 is regulated. The E3 ligase RNF181 limits the steady-state level of Bcl10 through K48-linked ubiquitinylation and degradation, thereby limiting the amount of Bcl10 that can bind CARD11 (57). Once signaling initiates, the kinesin GAKIN competes with Bcl10 for binding to CARD11 and limits the dwell time of CARD11 at the immune synapse (58). The phosphatase PP2A removes an activating phosphate from CARD11, which limits cofactor binding to CARD11 (59). Once CK1α is recruited to CARD11 in a step required for signaling, it phosphorylates CARD11 to inhibit the extent of CARD11 signaling (23).

Second, cofactors that associate with CARD11 in a signal-inducible manner rapidly dissociate from CARD11 during the initial ∼60 minutes after receptor triggering. The mechanisms of complex disassembly remain poorly defined, but disassembly limits the generation of CARD11-promoted signaling intermediates. In some contexts, cofactors disassemble from CARD11 in an obligate step in productive signaling, such as in the assembly of complexes containing p62, Bcl10, MALT1, and the IKK complex that can prolong IKK activation (60, 61).

Third, key polyubiquitinylated signaling intermediates, including $LinUb_n$-Bcl10, Ub_n(K63)-Bcl10, and Ub_n(K63)-MALT1 rapidly disappear as the result of the action of A20 (42), CYLD (46, 47), and likely other deubiquitinases. The removal of these potent intermediates attenuates the extent and duration of IKK complex activation. Fourth, CARD11 and Bcl10 are themselves degraded to limit signaling, and perhaps make cells refractory to immediate re-initiation of the CARD11-dependent pathway (15, 62–66).

SOMATIC GAIN-OF-FUNCTION CARD11 MUTATIONS IN LYMPHOMA

The dysregulated, constitutive signaling to NF-κB observed in several types of leukemia and lymphoma endows the transformed cells with a proliferative and survival advantage through the induction of pro-proliferative and anti-apoptotic NF-κB gene targets (40, 67–69). Leukemias and lymphomas exploit a variety of strategies of genomic alteration to achieve constitutive NF-κB activity. The regulation of CARD11 activity by an internal autoinhibitory domain makes CARD11 highly susceptible to mutations that can cause GOF signaling independent of upstream antigen receptor engagement. GOF CARD11 mutations occur in approximately 10% of cases of the Activated B Cell-Like (ABC) subtype of Diffuse Large B Cell Lymphoma (DLBCL) (70), but they have also been observed in other DLBCL subtypes (71–76), as well as in Acute T-cell Leukemia/Lymphoma (77), Sézary syndrome (78, 79) Mantle Cell Lymphoma (80), and Angioimmunoblastic T-cell lymphoma (81). In many cases, however, the signaling potency of CARD11 alleles found in patient biopsies has not been thoroughly characterized, or confirmed to be required for aberrant proliferation, as has been done for many CARD11 mutations found in ABC DLBCL. **Figure 3** depicts lymphoma-associated mutations that have been directly shown to potently increase CARD11 signaling.

GOF CARD11 mutations cause constitutive hyperactive CARD11 signaling by bypassing the action of the four REs in the ID that normally keep CARD11 basally inactive (13, 22, 31, 82) (**Figure 4**). Mutations in the CARD, LATCH, and Coiled-coil of CARD11 disrupt the function of multiple REs to allow partial conversion of CARD11 to an open, active state that can recruit Bcl10 (31, 82) and HOIP (22), but not other factors recruited during normal antigen receptor signaling, including TAK1, TRAF6, IKKγ, and Caspase-8 (31, 82), at least for the mutants that have been characterized. The spontaneous recruitment of Bcl10 and HOIP to GOF CARD11 variants leads to the spontaneous generation of $LinUb_n$-Bcl10, the levels of which appear to determine the quantitative output of NF-κB activation (22). Potent GOF mutations in the CARD, LATCH, and Coiled-coil can enhance basal CARD11 signaling by 80- to 160-fold (31, 82), and they appear to do so in part by interfering with inhibitory intramolecular interactions mediated by multiple REs (13). Potent GOF point mutations do not occur in the ID itself, due to the redundant action of the four REs; three or more REs would have to be disabled to achieve a comparable level of dysregulated signaling (12). For ABC DLBCL cells, the quantitative degree to which a GOF CARD11 allele activates NF-κB largely correlates with its ability to support aberrant cell proliferation (31, 70). However, the dysregulation of B cell proliferation *in vivo* by a CARD11 GOF allele requires both NF-κB and JNK activation (83). CARD11 GOF mutations in lymphoma occur in the presence of many other genomic alterations. While overexpression of an extremely potent CARD11 GOF allele is sufficient to cause lethal B cell proliferation (83), in human lymphomas it is likely that multiple genomic lesions cooperate with a GOF CARD11 mutation to maintain the proliferation and survival of the transformed cells.

GERMLINE CARD11 MUTATIONS IN PRIMARY IMMUNODEFICIENCY

One of the most exciting recent developments in the study of CARD11 has been the recognition of germline CARD11 mutations in primary immunodeficiency. Three different forms of primary immunodeficiency (PID) have been described so

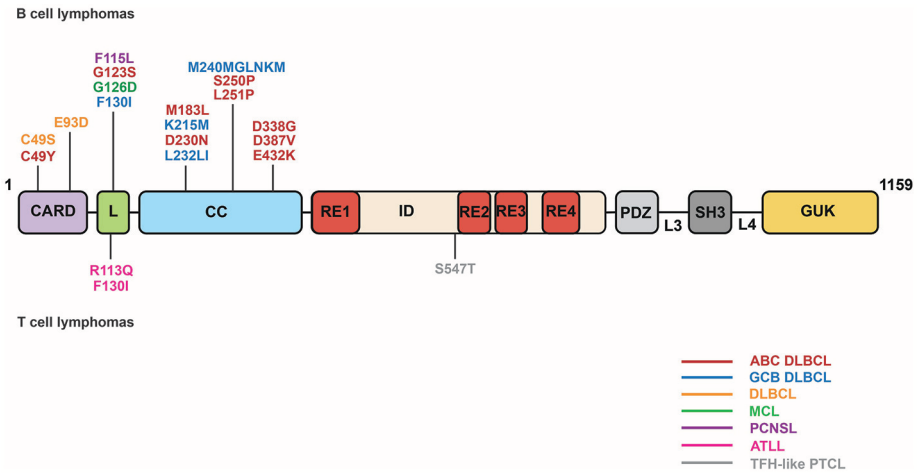

FIGURE 3 | Lymphoma-associated CARD11 mutations. Mutations are depicted that have been validated to have at least a 3-fold increase in CARD11 signaling in a quantitative signaling assay. ABC, Activated B Cell-like; DLBCL, Diffuse Large B Cell Lymphoma; GCB, Germinal Center B cell; MCL, Mantle Cell Lymphoma; PCNSL, Primary Central Nervous System Lymphoma; ATLL, Acute T cell Leukemia/Lymphoma; TFH, Follicular T helper; PTCL, Peripheral T cell Lymphoma.

far that result from germline mutations in the CARD11 gene, (1) CARD11 deficiency, (2) BENTA disease, and (3) Immunodeficiency with atopy.

CARD11 deficiency caused by homozygous LOF mutations in CARD11 was first reported in two studies in 2013 (84, 85). These patients, who presented with severe *Pneumocystis jirovecii* infections as infants, displayed normal T and B cell counts but hypogammaglobulinemia, deficits in mature or differentiated B and T cells (CD4 and CD8), reduced Treg numbers, and defective B and T cell activation *in vitro*. The homozygous mutations found in these patients include a deletion of exon 21 that results in a lack of detectable CARD11 expression (85) and a premature stop codon at glutamine 945 in the GUK domain (84) (**Figure 5**). Notably, family members that are heterozygous for these alleles do not present with immunodeficiency.

BENTA disease (B cell Expansion with NF-κB and T cell Anergy), caused by heterozygous GOF CARD11 mutations, has been described in 16 patients so far beginning in 2012 (86–90). BENTA patients experience recurrent ear, sinopulmonary, and viral infections (molluscum contagiosum, BK virus, Epstein-Barr virus), and exhibit a profound expansion in the number of B cells, a skewing of B cells toward transitional states, an unresponsiveness of T cells to antigen, and a poor antibody response to pneumococcal and meningococcal capsular polysaccharides. BENTA-associated mutations are located in the CARD (C49Y), LATCH (G116S, G123S, G123D, E127H), and Coiled-coil (E134G, H234L+Δ235-8) domains (**Figure 5**). Some (C49Y, G123S, G123D) are identical to those found in DLBCL. The alleles induce constitutive NF-κB activation in lymphocytes, presumably through the same signaling intermediates discussed above, but it remains unclear precisely how their constitutive signaling results in disparate effects in different immune cell subtypes.

Immunodeficiency with atopy, caused by heterozygous, LOF CARD11 mutations that appear to act as strong dominant negative alleles, was reported in 2017 by two studies (91, 92). In the five families described so far, affected individuals experience severe atopic dermatitis, recurrent pneumonia, and other upper respiratory tract infections, asthma, and food allergies with varying severities. While patient B cells exhibit mild defects in antigen-induced activation, patient T cells display reduced activation and proliferation *in vitro*, consistent with a poor T cell response to prior antigen exposure. Patients also display elevated serum IgE levels but low-to-normal levels of other Ig classes. CARD11 mutations that cause Immunodeficiency with atopy have been found in the CARD (R30W, E57D), Coiled-coil (L194P, dupM183-K196), and GUK (R975W) (**Figure 5**). E57D and L194P have been shown to interfere with recruitment of Bcl10 and MALT1 to CARD11 following TCR signaling (91), while R30W appears to have a milder effect on recruitment of these cofactors to CARD11 (92). This class of dominant negative mutants has also been shown to disrupt CARD11 signaling to mTOR and to the activation of MALT1 protease activity (91).

CURRENT KEY QUESTIONS AND OPPORTUNITIES

What Is the 3D Structure of CARD11?

A thorough understanding of how CARD11 is kept inactive prior to signaling, and how CARD11 converts to an open, active scaffold will require determination of the three-dimensional structure of CARD11 in "closed" and "open" states. Structural studies so far have solved the structure of the CARD domain of CARD11 and have modeled how the CARD11 CARD can nucleate the formation of Bcl10 filaments (55, 56, 93, 94).

However, the structure of 90% of the protein is unknown. Structural information will be invaluable for understanding how the multiple domains in CARD11 signal to its targets and how GOF and LOF mutations induce or disrupt CARD11 activity.

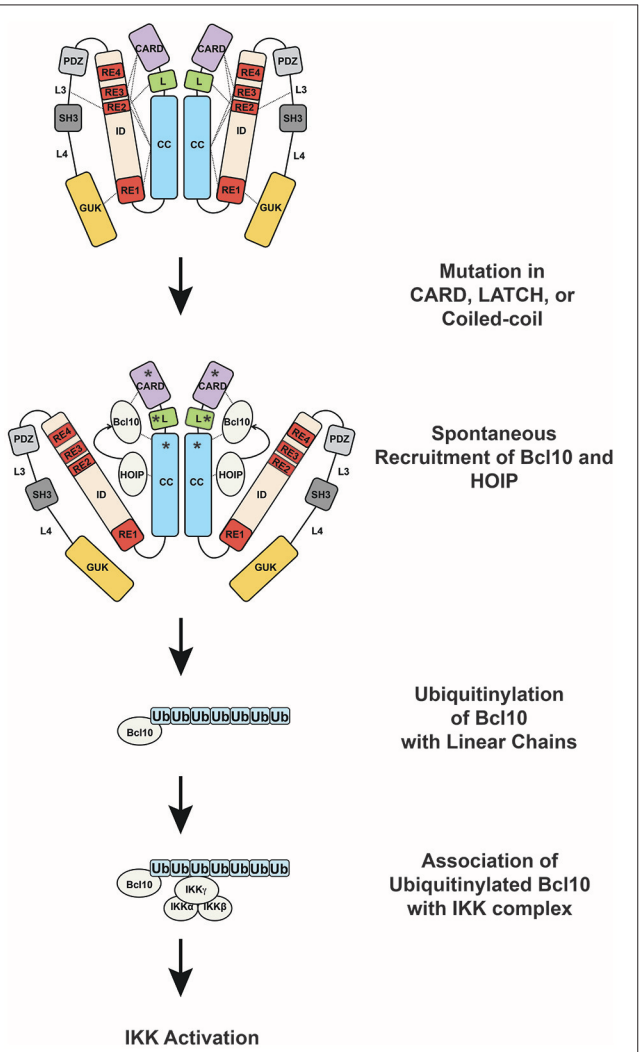

FIGURE 4 | Oncogenic CARD11 signaling. Lymphoma-associated gain-of-function mutations in the CARD, LATCH, and Coiled-coil are represented by asterisks.

How Does CARD11 Mediate IKK Complex Activation?

It remains unclear precisely how CARD11 signaling results in the activation of IKK kinase activity. The generation of ubiquitinylated Bcl10, MALT1, and IKKγ species is thought to induce a network of interacting proteins, in which ubiquitin chains are recognized by specific domains within signaling cofactors. This web of intermolecular binding can induce the proximity and clustering of IKK complexes, but how kinase activity is induced under physiological conditions, and whether other requisite components have yet to be discovered are unclear. It should also be explored whether CARD11 simply recruits enzymes (E3 ligases, kinases, protease) to their substrates or whether CARD11 binding plays a more active role in allosteric regulation of catalytic activity or substrate competency.

What Is the Physiological Function of the Four REs?

Although it is clear that the four REs within the ID function cooperatively to keep CARD11 inactive prior to signaling, it remains unclear why the protein has evolved this unique array of redundant repressive elements. RE redundancy does prevent unwanted GOF mutations from occurring in the ID, but it does not prevent their occurrence in the CARD, LATCH, and Coiled-coil. It is possible that the REs determine the kinetics of CARD11 "activation" during signaling, or the kinetics by which CARD11 returns to the basal inactive state following signaling, but further studies are needed to test these hypotheses.

How Precisely Do CARD11 GOF and LOF Alleles Cause Immunodeficiencies of Variable Phenotype?

The discovery of patients with germline CARD11 LOF and GOF mutations provides exciting opportunities for obtaining insight into the molecular mechanisms of CARD11 signaling and the cellular interplay of immune cell subtypes affected by CARD11 dysfunction. It remains unclear why some CARD11 LOF mutations are dominant negative and manifest disease when heterozygous, while other CARD11 LOF mutations manifest

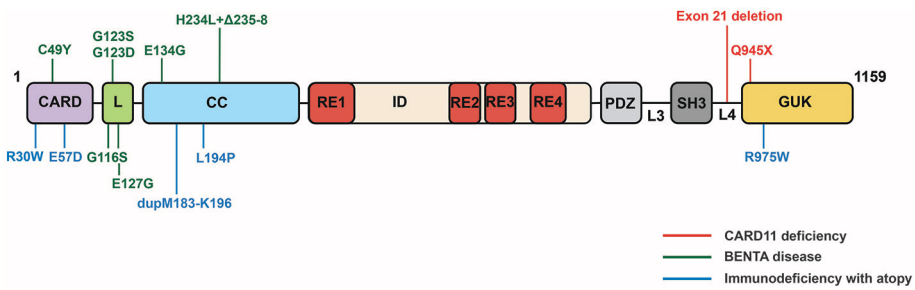

FIGURE 5 | CARD11 mutations identified in three classes of primary immunodeficiency.

disease only when homozygous. In addition, it is not firmly established whether all disease-associated CARD11 alleles affect signaling to mTOR and JNK, or which dysregulated pathways downstream of CARD11 are responsible for which disease manifestations. Also unknown is whether modifier genes in the patients studied have influenced their presentation, since only a small number of patients have been identified so far. It will be interesting to see whether additional CARD11 alleles will be discovered in the human population, leading to variable phenotypes of immunodeficiency and atopy.

What Other Signaling Pathways Depend on CARD11?

Several studies have implicated a role for CARD11 in pathways distinct from antigen receptors, including those emanating from activating NK cell receptors (95–97), OX40 (98), and the IL-2 receptor (99). The mechanistic role of CARD11 in these pathways deserves further study. It is possible that additional signaling pathways will be identified that rely on CARD11 activity, and if dysregulated, may contribute to human disease.

AUTHOR CONTRIBUTIONS

All authors listed have made substantial, direct, and intellectual contribution to the work and approved it for publication.

FUNDING

This work was supported by RO1CA177600 from the National Institutes of Health.

REFERENCES

1. Petrovski S, Wang Q, Heinzen EL, Allen AS, Goldstein DB. Genic intolerance to functional variation and the interpretation of personal genomes. *PLoS Genet.* (2013) 9:e1003709. doi: 10.1371/annotation/32c8d343-9e1d-46c6-bfd4-b0cd3fb7a97e
2. Lek M, Karczewski KJ, Minikel EV, Samocha KE, Banks E, Fennell T, et al. Analysis of protein-coding genetic variation in 60,706 humans. *Nature* (2016) 536:285–91. doi: 10.1038/nature19057
3. Bertin J, Wang L, Guo Y, Jacobson MD, Poyet JL, Srinivasula SM, et al. CARD11 and CARD14 are novel caspase recruitment domain (CARD)/membrane-associated guanylate kinase (MAGUK) family members that interact with BCL10 and activate NF-kappa B. *J Biol Chem.* (2001) 276:11877–82. doi: 10.1074/jbc.M010512200
4. Turvey SE, Durandy A, Fischer A, Fung SY, Geha RS, Gewies A, et al. The CARD11-BCL10-MALT1 (CBM) signalosome complex: stepping into the limelight of human primary immunodeficiency. *J Allergy Clin Immunol.* (2014) 134:276–84. doi: 10.1016/j.jaci.2014.06.015
5. Perez De Diego R, Sanchez-Ramon S, Lopez-Collazo E, Martinez-Barricarte R, Cubillos-Zapata C, Ferreira Cerdan A, et al. Genetic errors of the human caspase recruitment domain-B-cell lymphoma 10-mucosa-associated lymphoid tissue lymphoma-translocation gene 1 (CBM) complex: molecular, immunologic, and clinical heterogeneity. *J Allergy Clin Immunol.* (2015) 136:1139–49. doi: 10.1016/j.jaci.2015.06.031
6. Shi JH, Sun SC. TCR signaling to NF-κB and mTORC1: expanding roles of the CARMA1 complex. *Mol Immunol.* (2015) 68:546–57. doi: 10.1016/j.molimm.2015.07.024
7. Meininger I, Krappmann D. Lymphocyte signaling and activation by the CARMA1-BCL10-MALT1 signalosome. *Biol Chem.* (2016) 397:1315–33. doi: 10.1515/hsz-2016-0216
8. Zhang Q, Lenardo MJ, Baltimore D. 30 Years of NF-κB: a blossoming of relevance to human pathobiology. *Cell* (2017) 168:37–57. doi: 10.1016/j.cell.2016.12.012
9. Matsumoto R, Wang D, Blonska M, Li H, Kobayashi M, Pappu B, et al. Phosphorylation of CARMA1 plays a critical role in T cell receptor-mediated NF-κB Activation. *Immunity* (2005) 23:575–85. doi: 10.1016/j.immuni.2005.10.007
10. Sommer K, Guo B, Pomerantz JL, Bandaranayake AD, Moreno-Garcia ME, Ovechkina YL, et al. Phosphorylation of the CARMA1 linker controls NF-κB activation. *Immunity* (2005) 23:561–74. doi: 10.1016/j.immuni.2005.09.014
11. Mccully RR, Pomerantz JL. The protein kinase C-responsive inhibitory domain of CARD11 functions in NF-κB activation to regulate the association of multiple signaling cofactors that differentially depend on Bcl10 and MALT1 for association. *Mol Cell Biol.* (2008) 28:5668–86. doi: 10.1128/MCB.00418-08
12. Jattani RP, Tritapoe JM, Pomerantz JL. Cooperative control of Caspase Recruitment Domain-containing protein 11 (CARD11) signaling by an unusual array of redundant repressive elements. *J Biol Chem.* (2016) 291:8324–36. doi: 10.1074/jbc.M115.683714
13. Jattani RP, Tritapoe JM, Pomerantz JL. Intramolecular interactions and regulation of cofactor binding by the four repressive elements in the Caspase Recruitment Domain-containing protein 11 (CARD11) Inhibitory domain. *J Biol Chem.* (2016) 291:8338–48. doi: 10.1074/jbc.M116.717322
14. Paul S, Schaefer BC. A new look at T cell receptor signaling to nuclear factor-kappaB. *Trends Immunol.* (2013) 34:269–81. doi: 10.1016/j.it.2013.02.002
15. Wegener E, Oeckinghaus A, Papadopoulou N, Lavitas L, Schmidt-Supprian M, Ferch U, et al. Essential role for IkappaB kinase beta in remodeling Carma1-Bcl10-Malt1 complexes upon T cell activation. *Mol Cell* (2006) 23:13–23. doi: 10.1016/j.molcel.2006.05.027
16. Shinohara H, Maeda S, Watarai H, Kurosaki T. IkappaB kinase beta-induced phosphorylation of CARMA1 contributes to CARMA1 Bcl10 MALT1 complex formation in B cells. *J Exp Med.* (2007) 204:3285–93. doi: 10.1084/jem.20070379
17. Thome M, Charton JE, Pelzer C, Hailfinger S. Antigen receptor signaling to NF-{kappa}B via CARMA1, BCL10, and MALT1. *Cold Spring Harb Perspect Biol.* (2010) 2:a003004. doi: 10.1101/cshperspect.a003004
18. Ishiguro K, Green T, Rapley J, Wachtel H, Giallourakis C, Landry A, et al. Ca^{2+}/calmodulin-dependent protein kinase II is a modulator of CARMA1-mediated NF-κB activation. *Mol Cell Biol.* (2006) 26:5497–508. doi: 10.1128/MCB.02469-05
19. Brenner D, Brechmann M, Rohling S, Tapernoux M, Mock T, Winter D, et al. Phosphorylation of CARMA1 by HPK1 is critical for NF-κB activation in T cells. *Proc Natl Acad Sci USA.* (2009) 106:14508–13. doi: 10.1073/pnas.0900457106
20. Cheng J, Hamilton KS, Kane LP. Phosphorylation of Carma1, but not Bcl10, by Akt regulates TCR/CD28-mediated NF-κB induction and cytokine production. *Mol Immunol.* (2014) 59:110–6. doi: 10.1016/j.molimm.2014.01.011
21. Shinohara H, Behar M, Inoue K, Hiroshima M, Yasuda T, Nagashima T, et al. Positive feedback within a kinase signaling complex functions as a switch mechanism for NF-κB activation. *Science* (2014) 344:760–4. doi: 10.1126/science.1250020
22. Yang YK, Yang C, Chan W, Wang Z, Deibel KE, Pomerantz JL. Molecular determinants of scaffold-induced linear ubiquitinylation of B cell lymphoma/Leukemia 10 (Bcl10) during T cell receptor and oncogenic Caspase Recruitment Domain-containing protein 11 (CARD11) signaling. *J Biol Chem.* (2016b) 291:25921–36. doi: 10.1074/jbc.M116.754028
23. Bidere N, Ngo VN, Lee J, Collins C, Zheng L, Wan F, et al. Casein kinase 1alpha governs antigen-receptor-induced NF-κB activation and human lymphoma cell survival. *Nature* (2009) 458:92–6. doi: 10.1038/nature07613
24. Medeiros RB, Burbach BJ, Mueller KL, Srivastava R, Moon JJ, Highfill S, et al. Regulation of NF-κB activation in T cells via association of the adapter proteins ADAP and CARMA1. *Science* (2007) 316:754–8. doi: 10.1126/science.1137895

25. Schimmack G, Eitelhuber AC, Vincendeau M, Demski K, Shinohara H, Kurosaki T, et al. AIP augments CARMA1-BCL10-MALT1 complex formation to facilitate NF-κB signaling upon T cell activation. *Cell Commun Signal.* (2014) 12:49. doi: 10.1186/s12964-014-0049-7
26. Hara H, Bakal C, Wada T, Bouchard D, Rottapel R, Saito T, et al. The molecular adapter Carma1 controls entry of IkappaB kinase into the central immune synapse. *J Exp Med.* (2004) 200:1167–77. doi: 10.1084/jem.20032246
27. Wang D, Matsumoto R, You Y, Che T, Lin XY, Gaffen SL, et al. CD3/CD28 costimulation-induced NF-κB activation is mediated by recruitment of protein kinase C-theta, Bcl10, and IkappaB kinase beta to the immunological synapse through CARMA1. *Mol Cell Biol.* (2004) 24:164–71. doi: 10.1128/MCB.24.1.164-171.2003
28. Hara H, Yokosuka T, Hirakawa H, Ishihara C, Yasukawa S, Yamazaki M, et al. Clustering of CARMA1 through SH3-GUK domain interactions is required for its activation of NF-κB signalling. *Nat Commun.* (2015) 6:5555. doi: 10.1038/ncomms6555
29. Hadian K, Griesbach RA, Dornauer S, Wanger TM, Nagel D, Metlitzky M, et al. NF-κB essential modulator (NEMO) interaction with linear and lys-63 ubiquitin chains contributes to NF-κB activation. *J Biol Chem.* (2011) 286:26107–17. doi: 10.1074/jbc.M111.233163
30. Wu CJ, Ashwell JD. NEMO recognition of ubiquitinated Bcl10 is required for T cell receptor-mediated NF-κB activation. *Proc Natl Acad Sci U.S.A.* (2008) 105:3023–8. doi: 10.1073/pnas.0712313105
31. Chan W, Schaffer TB, Pomerantz JL. A quantitative signaling screen identifies CARD11 mutations in the CARD and LATCH domains that induce Bcl10 ubiquitination and human lymphoma cell survival. *Mol Cell Biol.* (2013) 33:429–43. doi: 10.1128/MCB.00850-12
32. Yang Y, Kelly P, Shaffer AL III, Schmitz R, Yoo HM, Liu X, et al. Targeting non-proteolytic protein ubiquitination for the treatment of diffuse large B cell lymphoma. *Cancer Cell* (2016) 29:494–507. doi: 10.1016/j.ccell.2016.03.006
33. Shambharkar PB, Blonska M, Pappu BP, Li H, You Y, Sakurai H, et al. Phosphorylation and ubiquitination of the IkappaB kinase complex by two distinct signaling pathways. *Embo J.* (2007) 26:1794–805. doi: 10.1038/sj.emboj.7601622
34. Zhou H, Wertz I, O'rourke K, Ultsch M, Seshagiri S, Eby M, et al. Bcl10 activates the NF-κB pathway through ubiquitination of NEMO. *Nature* (2004) 427:167–71. doi: 10.1038/nature02273
35. Tokunaga F, Sakata S, Saeki Y, Satomi Y, Kirisako T, Kamei K, et al. Involvement of linear polyubiquitylation of NEMO in NF-κB activation. *Nat Cell Biol.* (2009) 11:123–32. doi: 10.1038/ncb1821
36. Klein T, Fung SY, Renner F, Blank MA, Dufour A, Kang S, et al. The paracaspase MALT1 cleaves HOIL1 reducing linear ubiquitination by LUBAC to dampen lymphocyte NF-κB signalling. *Nat Commun.* (2015) 6:8777. doi: 10.1038/ncomms9777
37. Oeckinghaus A, Wegener E, Welteke V, Ferch U, Arslan SC, Ruland J, et al. Malt1 ubiquitination triggers NF-κB signaling upon T-cell activation. *Embo J.* (2007) 26:4634–45. doi: 10.1038/sj.emboj.7601897
38. Rebeaud F, Hailfinger S, Posevitz-Fejfar A, Tapernoux M, Moser R, Rueda D, et al. The proteolytic activity of the paracaspase MALT1 is key in T cell activation. *Nat Immunol.* (2008) 9:272–81. doi: 10.1038/ni1568
39. Baens M, Bonsignore L, Somers R, Vanderheydt C, Weeks SD, Gunnarsson J, et al. MALT1 auto-proteolysis is essential for NF-kappaB-dependent gene transcription in activated lymphocytes. *PLoS ONE* (2014) 9:e103774. doi: 10.1371/journal.pone.0103774
40. Juilland M, Thome M. Role of the CARMA1/BCL10/MALT1 complex in lymphoid malignancies. *Curr Opin Hematol.* (2016) 23:402–9. doi: 10.1097/MOH.0000000000000257
41. Coornaert B, Baens M, Heyninck K, Bekaert T, Haegman M, Staal J, et al. T cell antigen receptor stimulation induces MALT1 paracaspase-mediated cleavage of the NF-κB inhibitor A20. *Nat Immunol.* (2008) 9:263–71. doi: 10.1038/ni1561
42. Duwel M, Welteke V, Oeckinghaus A, Baens M, Kloo B, Ferch U, et al. A20 negatively regulates T cell receptor signaling to NF-κB by cleaving Malt1 ubiquitin chains. *J Immunol.* (2009) 182:7718–28. doi: 10.4049/jimmunol.0803313
43. Hailfinger S, Nogai H, Pelzer C, Jaworski M, Cabalzar K, Charton JE, et al. Malt1-dependent RelB cleavage promotes canonical NF-κB activation in lymphocytes and lymphoma cell lines. *Proc Natl Acad Sci USA.* (2011) 108:14596–601. doi: 10.1073/pnas.1105020108
44. Douanne T, Gavard J, Bidere N. The paracaspase MALT1 cleaves the LUBAC subunit HOIL1 during antigen receptor signaling. *J Cell Sci.* (2016) 129:1775–80. doi: 10.1242/jcs.185025
45. Elton L, Carpentier I, Staal J, Driege Y, Haegman M, Beyaert R. MALT1 cleaves the E3 ubiquitin ligase HOIL-1 in activated T cells, generating a dominant negative inhibitor of LUBAC-induced NF-κB signaling. *FEBS J.* (2016) 283:403–12. doi: 10.1111/febs.13597
46. Reiley WW, Jin W, Lee AJ, Wright A, Wu X, Tewalt EF, et al. Deubiquitinating enzyme CYLD negatively regulates the ubiquitin-dependent kinase Tak1 and prevents abnormal T cell responses. *J Exp Med.* (2007) 204:1475–85. doi: 10.1084/jem.20062694
47. Sun SC. CYLD: a tumor suppressor deubiquitinase regulating NF-κB activation and diverse biological processes. *Cell Death Differ.* (2010) 17:25–34. doi: 10.1038/cdd.2009.43
48. Staal J, Driege Y, Bekaert T, Demeyer A, Muyllaert D, Van Damme P, et al. T-cell receptor-induced JNK activation requires proteolytic inactivation of CYLD by MALT1. *EMBO J.* (2011) 30:1742–52. doi: 10.1038/emboj.2011.85
49. Hamilton KS, Phong B, Corey C, Cheng J, Gorentla B, Zhong X, et al. T cell receptor-dependent activation of mTOR signaling in T cells is mediated by Carma1 and MALT1, but not Bcl10. *Sci Signal.* (2014) 7:ra55. doi: 10.1126/scisignal.2005169
50. Nakaya M, Xiao Y, Zhou X, Chang JH, Chang M, Cheng X, et al. Inflammatory T cell responses rely on amino acid transporter ASCT2 facilitation of glutamine uptake and mTORC1 kinase activation. *Immunity* (2014) 40:692–705. doi: 10.1016/j.immuni.2014.04.007
51. Hara H, Wada T, Bakal C, Kozieradzki I, Suzuki S, Suzuki N, et al. The MAGUK family protein CARD11 is essential for lymphocyte activation. *Immunity* (2003) 18:763–75. doi: 10.1016/S1074-7613(03)00148-1
52. Jun JE, Wilson LE, Vinuesa CG, Lesage S, Blery M, Miosge LA, et al. Identifying the MAGUK protein Carma-1 as a central regulator of humoral immune responses and atopy by genome-wide mouse mutagenesis. *Immunity* (2003) 18:751–62. doi: 10.1016/S1074-7613(03)00141-9
53. Blonska M, Pappu BP, Matsumoto R, Li H, Su B, Wang D, et al. The CARMA1-Bcl10 signaling complex selectively regulates JNK2 kinase in the T cell receptor-signaling pathway. *Immunity* (2007) 26:55–66. doi: 10.1016/j.immuni.2006.11.008
54. Blonska M, Lin X. CARMA1-mediated NF-κB and JNK activation in lymphocytes. *Immunol Rev.* (2009) 228:199–211. doi: 10.1111/j.1600-065X.2008.00749.x
55. Qiao Q, Yang C, Zheng C, Fontan L, David L, Yu X, et al. Structural architecture of the CARMA1/Bcl10/MALT1 signalosome: nucleation-induced filamentous assembly. *Mol Cell* (2013) 51:766–79. doi: 10.1016/j.molcel.2013.08.032
56. David L, Li Y, Ma J, Garner E, Zhang X, Wu H. Assembly mechanism of the CARMA1-BCL10-MALT1-TRAF6 signalosome. *Proc Natl Acad Sci USA.* (2018) 115:1499–504. doi: 10.1073/pnas.1721967115
57. Pedersen SM, Chan W, Jattani RP, Mackie DS, Pomerantz JL. Negative Regulation of CARD11 Signaling and Lymphoma Cell Survival by the E3 Ubiquitin Ligase RNF181. *Mol Cell Biol.* (2016) 36:794–808. doi: 10.1128/MCB.00876-15
58. Lamason RL, Kupfer A, Pomerantz JL. The dynamic distribution of CARD11 at the immunological synapse is regulated by the inhibitor kinesin GAKIN. *Mol Cell* (2010) 40:798–809. doi: 10.1016/j.molcel.2010.11.007
59. Eitelhuber AC, Warth S, Schimmack G, Duwel M, Hadian K, Demski K, et al. Dephosphorylation of Carma1 by PP2A negatively regulates T-cell activation. *EMBO J.* (2011) 30:594–605. doi: 10.1038/emboj.2010.331
60. Carvalho G, Le Guelte A, Demian C, Vazquez A, Gavard J, Bidere N. Interplay between BCL10, MALT1 and IkappaBalpha during T-cell-receptor-mediated NFkappaB activation. *J Cell Sci.* (2010) 123:2375–80. doi: 10.1242/jcs.069476
61. Paul S, Traver MK, Kashyap AK, Washington MA, Latoche JR, Schaefer BC. T cell receptor signals to NF-κB are transmitted by a cytosolic p62-Bcl10-Malt1-IKK signalosome. *Sci Signal.* (2014) 7:ra45. doi: 10.1126/scisignal.2004882
62. Scharschmidt E, Wegener E, Heissmeyer V, Rao A, Krappmann D. Degradation of Bcl10 induced by T-cell activation negatively regulates NF-kappa B signaling. *Mol Cell Biol.* (2004) 24:3860–73. doi: 10.1128/MCB.24.9.3860-3873.2004
63. Lobry C, Lopez T, Israel A, Weil R. Negative feedback loop in T cell activation through IkappaB kinase-induced phosphorylation and degradation of Bcl10. *Proc Natl Acad Sci USA.* (2007) 104:908–13. doi: 10.1073/pnas.0606982104

64. Zeng H, Di L, Fu G, Chen Y, Gao X, Xu L, et al. Phosphorylation of Bcl10 negatively regulates T-cell receptor-mediated NF-κB activation. *Mol Cell Biol.* (2007) 27:5235–45. doi: 10.1128/MCB.01645-06
65. Moreno-Garcia ME, Sommer K, Shinohara H, Bandaranayake AD, Kurosaki T, Rawlings DJ. MAGUK-controlled ubiquitination of CARMA1 modulates lymphocyte NF-κB activity. *Mol Cell Biol.* (2010) 30:922–34. doi: 10.1128/MCB.01129-09
66. Paul S, Kashyap AK, Jia W, He YW, Schaefer BC. Selective autophagy of the adaptor protein Bcl10 modulates T cell receptor activation of NF-kappaB. *Immunity* (2012) 36:947–58. doi: 10.1016/j.immuni.2012.04.008
67. Jost PJ, Ruland J. Aberrant NF-κB signaling in lymphoma: mechanisms, consequences, and therapeutic implications. *Blood* (2007) 109:2700–7. doi: 10.1182/blood-2006-07-025809
68. Staudt LM. Oncogenic activation of NF-kappaB. *Cold Spring Harb Perspect Biol.* (2010) 2:a000109. doi: 10.1101/cshperspect.a000109
69. Rui L, Schmitz R, Ceribelli M, Staudt LM. Malignant pirates of the immune system. *Nat Immunol* (2011) 12:933–40. doi: 10.1038/ni.2094
70. Lenz G, Davis RE, Ngo VN, Lam L, George TC, Wright GW, et al. Oncogenic CARD11 mutations in human diffuse large B cell lymphoma. *Science* (2008) 319:1676–9. doi: 10.1126/science.1153629
71. Compagno M, Lim WK, Grunn A, Nandula SV, Brahmachary M, Shen Q, et al. Mutations of multiple genes cause deregulation of NF-κB in diffuse large B-cell lymphoma. *Nature* (2009) 459:717–21. doi: 10.1038/nature07968
72. Montesinos-Rongen M, Schmitz R, Brunn A, Gesk S, Richter J, Hong K, et al. Mutations of CARD11 but not TNFAIP3 may activate the NF-κB pathway in primary CNS lymphoma. *Acta Neuropathol.* (2010) 120:529–35. doi: 10.1007/s00401-010-0709-7
73. Pasqualucci L, Trifonov V, Fabbri G, Ma J, Rossi D, Chiarenza A, et al. Analysis of the coding genome of diffuse large B-cell lymphoma. *Nat Genet.* (2011) 43:830–7. doi: 10.1038/ng.892
74. Bu R, Bavi P, Abubaker J, Jehan Z, Al-Haqawi W, Ajarim D, et al. Role of NF-κB regulators-TNFAIP3 and CARD11 in middle eastern diffuse large B cell lymphoma. *Leuk Lymphoma* (2012) 53:1971–7. doi: 10.3109/10428194.2012.668286
75. Lohr JG, Stojanov P, Lawrence MS, Auclair D, Chapuy B, Sougnez C, et al. Discovery and prioritization of somatic mutations in diffuse large B-cell lymphoma (DLBCL) by whole-exome sequencing. *Proc Natl Acad Sci USA.* (2012) 109:3879–84. doi: 10.1073/pnas.1121343109
76. Schmitz R, Wright GW, Huang DW, Johnson CA, Phelan JD, Wang JQ, et al. Genetics and Pathogenesis of Diffuse Large B-Cell Lymphoma. *N Engl J Med.* (2018) 378:1396–407. doi: 10.1056/NEJMoa1801445
77. Kataoka K, Nagata Y, Kitanaka A, Shiraishi Y, Shimamura T, Yasunaga J, et al. Integrated molecular analysis of adult T cell leukemia/lymphoma. *Nat Genet.* (2015) 47:1304–15. doi: 10.1038/ng.3415
78. Da Silva Almeida AC, Abate F, Khiabanian H, Martinez-Escala E, Guitart J, Tensen CP, et al. The mutational landscape of cutaneous T cell lymphoma and Sezary syndrome. *Nat Genet.* (2015) 47:1465–70. doi: 10.1038/ng.3442
79. Wang L, Ni X, Covington KR, Yang BY, Shiu J, Zhang X, et al. Genomic profiling of Sezary syndrome identifies alterations of key T cell signaling and differentiation genes. *Nat Genet.* (2015) 47:1426–34. doi: 10.1038/ng.3444
80. Wu C, De Miranda NF, Chen L, Wasik AM, Mansouri L, Jurczak W, et al. Genetic heterogeneity in primary and relapsed mantle cell lymphomas: impact of recurrent CARD11 mutations. *Oncotarget* (2016) 7:38180–90. doi: 10.18632/oncotarget.9500
81. Vallois D, Dobay MP, Morin RD, Lemonnier F, Missiaglia E, Juilland M, et al. Activating mutations in genes related to TCR signaling in angioimmunoblastic and other follicular helper T-cell-derived lymphomas. *Blood* (2016) 128:1490–502. doi: 10.1182/blood-2016-02-698977
82. Lamason RL, Mccully RR, Lew SM, Pomerantz JL. Oncogenic CARD11 mutations induce hyperactive signaling by disrupting autoinhibition by the PKC-responsive inhibitory domain. *Biochemistry* (2010b) 49:8240–50. doi: 10.1021/bi101052d
83. Knies N, Alankus B, Weilemann A, Tzankov A, Brunner K, Ruff T, et al. Lymphomagenic CARD11/BCL10/MALT1 signaling drives malignant B-cell proliferation via cooperative NF-κB and JNK activation. *Proc Natl Acad Sci USA.* (2015) 112:E7230–8. doi: 10.1073/pnas.1507459112
84. Greil J, Rausch T, Giese T, Bandapalli OR, Daniel V, Bekeredjian-Ding I, et al. Whole-exome sequencing links caspase recruitment domain 11 (CARD11) inactivation to severe combined immunodeficiency. *J Allergy Clin Immunol.* (2013) 131:1376. e3–83.e3. doi: 10.1016/j.jaci.2013.02.012
85. Stepensky P, Keller B, Buchta M, Kienzler AK, Elpeleg O, Somech R, et al. Deficiency of caspase recruitment domain family, member 11 (CARD11), causes profound combined immunodeficiency in human subjects. *J Allergy Clin Immunol.* (2013) 131:477.e1–85.e1. doi: 10.1016/j.jaci.2012.11.050
86. Snow AL, Xiao W, Stinson JR, Lu W, Chaigne-Delalande B, Zheng L, et al. Congenital B cell lymphocytosis explained by novel germline CARD11 mutations. *J Exp Med.* (2012) 209:2247–61. doi: 10.1084/jem.20120831
87. Brohl AS, Stinson JR, Su HC, Badgett T, Jennings CD, Sukumar G, et al. Germline CARD11 Mutation in a Patient with Severe Congenital B Cell Lymphocytosis. *J Clin Immunol.* (2014) 35:32–46. doi: 10.1007/s10875-014-0106-4
88. Buchbinder D, Stinson JR, Nugent DJ, Heurtier L, Suarez F, Sukumar G, et al. Mild B-cell lymphocytosis in patients with a CARD11 C49Y mutation. *J Allergy Clin Immunol.* (2015) 136:819–21. doi: 10.1016/j.jaci.2015.03.008
89. Arjunaraja S, Nose BD, Sukumar G, Lott NM, Dalgard CL, Snow AL. Intrinsic plasma cell differentiation defects in B cell expansion with NF-κB and T cell anergy patient B cells. *Front Immunol.* (2017) 8:913. doi: 10.3389/fimmu.2017.00913
90. Arjunaraja S, Angelus P, Su HC, Snow AL. Impaired control of Epstein-Barr Virus infection in B-cell expansion with NF-κB and T-cell anergy disease. *Front Immunol.* (2018) 9:198. doi: 10.3389/fimmu.2018.00198
91. Ma CA, Stinson JR, Zhang Y, Abbott JK, Weinreich MA, Hauk PJ, et al. Germline hypomorphic CARD11 mutations in severe atopic disease. *Nat Genet.* (2017) 49:1192–201. doi: 10.1038/ng.3898
92. Dadi H, Jones TA, Merico D, Sharfe N, Ovadia A, Schejter Y, et al. Combined immunodeficiency and atopy caused by a dominant negative mutation in caspase activation and recruitment domain family member 11 (CARD11). *J Allergy Clin Immunol.* (2018) 141:1818.e2–30.e2. doi: 10.1016/j.jaci.2017.06.047
93. Li S, Yang X, Shao J, Shen Y. Structural insights into the assembly of CARMA1 and BCL10. *PLoS ONE* (2012) 7:e42775. doi: 10.1371/journal.pone.0042775
94. Jang TH, Park JH, Park HH. Novel disulfide bond-mediated dimerization of the CARD domain was revealed by the crystal structure of CARMA1 CARD. *PLoS ONE* (2013) 8:e79778. doi: 10.1371/journal.pone.0079778
95. Gross O, Grupp C, Steinberg C, Zimmermann S, Strasser D, Hannesschlager N, et al. Multiple ITAM-coupled NK-cell receptors engage the Bcl10/Malt1 complex via Carma1 for NF-κB and MAPK activation to selectively control cytokine production. *Blood* (2008) 112:2421–8. doi: 10.1182/blood-2007-11-123513
96. Hara H, Ishihara C, Takeuchi A, Xue L, Morris SW, Penninger JM, et al. Cell type-specific regulation of ITAM-mediated NF-κB activation by the adaptors, CARMA1 and CARD9. *J Immunol.* (2008) 181:918–30. doi: 10.4049/jimmunol.181.2.918
97. Rajasekaran K, Kumar P, Schuldt KM, Peterson EJ, Vanhaesebroeck B, Dixit V, et al. Signaling by Fyn-ADAP via the Carma1-Bcl-10-MAP3K7 signalosome exclusively regulates inflammatory cytokine production in NK cells. *Nat Immunol.* (2013) 14:1127–36. doi: 10.1038/ni.2708
98. So T, Soroosh P, Eun SY, Altman A, Croft M. Antigen-independent signalosome of CARMA1, PKCtheta, and TNF receptor-associated factor 2 (TRAF2) determines NF-κB signaling in T cells. *Proc Natl Acad Sci USA.* (2011) 108:2903–8. doi: 10.1073/pnas.1008765108
99. Lee AJ, Wu X, Cheng H, Zhou X, Cheng X, Sun SC. CARMA1 regulation of regulatory T cell development involves modulation of interleukin-2 receptor signaling. *J Biol Chem.* (2010) 285:15696–703. doi: 10.1074/jbc.M109.095190

Conflict of Interest Statement: The authors declare that the research was conducted in the absence of any commercial or financial relationships that could be construed as a potential conflict of interest.

frontiers in Immunology

REVIEW
published: 19 September 2018
doi: 10.3389/fimmu.2018.02078

The CBM-opathies—A Rapidly Expanding Spectrum of Human Inborn Errors of Immunity Caused by Mutations in the CARD11-BCL10-MALT1 Complex

Henry Y. Lu[1,2], *Bradly M. Bauman*[3], *Swadhinya Arjunaraja*[3], *Batsukh Dorjbal*[3], *Joshua D. Milner*[4], *Andrew L. Snow*[3†] *and Stuart E. Turvey*[1,2*†]

[1] Department of Pediatrics, British Columbia Children's Hospital, The University of British Columbia, Vancouver, BC, Canada, [2] Experimental Medicine Program, Faculty of Medicine, The University of British Columbia, Vancouver, BC, Canada, [3] Department of Pharmacology and Molecular Therapeutics, Uniformed Services University of the Health Sciences, Bethesda, MD, United States, [4] Laboratory of Allergic Diseases, National Institute of Allergy and Infectious Diseases, National Institutes of Health, Bethesda, MD, United States

OPEN ACCESS

Edited by:
Elissa Deenick,
Garvan Institute of Medical Research, Australia

Reviewed by:
Ruben Martinez-Barricarte, Rockefeller University, United States
Jolan Eszter Walter, University of South Florida, United States

***Correspondence:**
Stuart E. Turvey
sturvey@cw.bc.ca

[†] These authors have contributed equally to this work

Specialty section:
This article was submitted to Primary Immunodeficiencies, a section of the journal Frontiers in Immunology

Received: 21 July 2018
Accepted: 22 August 2018
Published: 19 September 2018

Citation:
Lu HY, Bauman BM, Arjunaraja S, Dorjbal B, Milner JD, Snow AL and Turvey SE (2018) The CBM-opathies—A Rapidly Expanding Spectrum of Human Inborn Errors of Immunity Caused by Mutations in the CARD11-BCL10-MALT1 Complex. Front. Immunol. 9:2078. doi: 10.3389/fimmu.2018.02078

The caspase recruitment domain family member 11 (CARD11 or CARMA1)—B cell CLL/lymphoma 10 (BCL10)—MALT1 paracaspase (MALT1) [CBM] signalosome complex serves as a molecular bridge between cell surface antigen receptor signaling and the activation of the NF-κB, JNK, and mTORC1 signaling axes. This positions the CBM complex as a critical regulator of lymphocyte activation, proliferation, survival, and metabolism. Inborn errors in each of the CBM components have now been linked to a diverse group of human primary immunodeficiency diseases termed "CBM-opathies." Clinical manifestations range from severe combined immunodeficiency to selective B cell lymphocytosis, atopic disease, and specific humoral defects. This surprisingly broad spectrum of phenotypes underscores the importance of "tuning" CBM signaling to preserve immune homeostasis. Here, we review the distinct clinical and immunological phenotypes associated with human CBM complex mutations and introduce new avenues for targeted therapeutic intervention.

Keywords: CBM complex, CARD11, MALT1, BCL10, combined immunodeficiency, severe combined immunodeficiency, primary atopic disease, BENTA

INTRODUCTION

Inborn errors of immunity or primary immunodeficiency diseases (PIDs) are a group of ∼350 genetic disorders that are characterized by defects in immune system development and/or function (1). Defining the genetic and molecular basis of these diseases has not only benefitted the affected individuals but has greatly enhanced our understanding of the fundamental factors that regulate human immunity. A powerful example of the value of studying patients with PIDs is nuclear factor kappa B (NF-κB)—a critical transcription factor that facilitates lymphocyte activation, proliferation and survival. Aberrant signaling in the NF-κB pathway is associated with inflammatory diseases (2), malignancy (3), autoimmunity (4), and immunodeficiency (5). With the description of patients with monogenic immune disorders affecting various components of this signaling cascade, we now have an improved understanding of how NF-κB is positively and negatively regulated.

In the past decade, the assembly of the caspase recruitment domain family member 11 (CARD11 or CARMA1)—B cell CLL/lymphoma 10 (BCL10)—MALT1 paracaspase (MALT1) [CBM] signalosome complex has emerged as a critical step in the antigen-dependent activation of NF-κB in B and T lymphocytes (6). Major landmarks in the understanding of CBM function first came from oncology. These advances included the characterization of mutant BCL10 and MALT1 proteins caused by chromosomal translocations leading to constitutive/aberrant NF-κB signaling in lymphoma (7), the discovery of CARD11 and its ability to interact with and regulate BCL10 (8), and the identification of mutant CARD11 isoforms affecting the coiled-coil domain that activate NF-κB, constituting ∼10% of activated B cell-like diffuse large B cell lymphomas (9, 10). These findings, along with the generation and study of *Card11*$^{-/-}$ (11–13), *Bcl10*$^{-/-}$ (14, 15), and *Malt1*$^{-/-}$ (16) mice, collectively positioned the CBM complex as a central modulator of lymphocyte signaling through the regulation of the NF-κB, c-Jun N-terminal kinase (JNK), and mechanistic target of rapamycin complex (mTORC1) pathways (**Figures 1**, **2**).

The importance of the CBM complex in adaptive immunity was experimentally established by the fact that B and T cells from mice deficient in *Card11*, *Bcl10*, or *Malt1* all displayed impaired cellular activation and proliferation, aberrant cytokine secretion, and blocks in cell differentiation, resulting in diminished serum immunoglobulin levels. These experimental observations were then validated in the intact human system by the recent discovery of individuals suffering from profound immune defects [i.e., combined immunodeficiency (CID) and severe combined immunodeficiency (SCID)] involving germline loss-of-function (LOF) mutations in *CARD11* (17–19), *BCL10* (20), and *MALT1* (21–24) (**Figure 1**). While human deficiency of each of the CBM components has some unique defining clinical features (e.g., gastrointestinal inflammation seen in MALT1 deficiency or susceptibility to *Pneumocystis jirovecii* pneumonia (PJP) typical for CARD11 deficiency), as testament to their highly synergistic activities, many phenotypic manifestations are shared across these CBM deficiencies. In particular, some unifying features of CBM PIDs include: CID/SCID occurring in the context of generally normal total B and T cell numbers, a predominantly naïve phenotype in peripheral blood lymphocytes, impaired T cell proliferation, and compromised antigen receptor-induced NF-κB activation.

Recent discoveries have now moved beyond relatively simple LOF mutations, and there is now an interesting spectrum of additional clinical phenotypes attributed to *CARD11* mutations (25), with gain-of-function mutations causing "B cell Expansion with NF-κB and T cell Anergy" (BENTA) disease (26–30), hypomorphic dominant-interfering mutations causing combined immunodeficiency with atopic disease "CARD11-associated Atopy with Dominant Interference of NF-κB Signaling" (CADINS) (31, 32), and loss-of-function mutations with somatic reversion associated with Omenn syndrome (19) (**Figure 1**).

In this review, we will illustrate the current understanding of CBM-mediated activation of the NF-κB, JNK, and mTORC1 pathways in lymphocytes, and highlight the diverse and rapidly expanding clinical and immunological phenotypes of "CBM-opathies."

THE CBM COMPLEX IN ANTIGEN RECEPTOR SIGNALING

Proximal Antigen Receptor Signaling

Upon antigen recognition, the CBM complex is primarily involved in signal transduction downstream of antigen receptors leading to the activation of NF-κB, JNK, and mTORC1 in lymphocytes (33–35) (**Figure 2**). Signaling following B cell receptor (BCR) and T cell receptor (TCR) activation is highly symmetrical and begins with the phosphorylation of immunoreceptor tyrosine-based activation motifs (ITAMs) found on the CD79A/CD79B chains of the BCR and the ζ-chains of the TCR complex by Src family tyrosine kinases LYN and lymphocyte-specific protein tyrosine kinase (LCK), respectively (33, 36). This facilitates the recruitment and phosphorylation of the spleen tyrosine kinase (Syk) family tyrosine kinases SYK (for BCR) and zeta-chain-associated protein kinase 70 (ZAP70) (for TCR) (33, 36) (**Figure 2**). From here, a collection of adaptor, phospholipase, and kinase proteins come together to form signalosomes, including B cell linker protein (BLNK) and Bruton tyrosine kinase (BTK) for the BCR and SH2 domain containing leukocyte protein of 76 kDa (SLP76), linker of activated T cells (LAT), and IL-2 inducible T cell kinase (ITK) for the TCR. This assembly ultimately culminates in the activation of phospholipase Cγ1 (PLCγ1) for the TCR, PLCγ2 for the BCR, and phosphatidylinositol-4,5-bisphosphate 3-kinase (PI3K) for both (37, 38) (**Figure 2**).

CBM Assembly

Phosphorylated PLCγ1 and PLCγ2 mediate the hydrolysis of phosphatidylinositol 4,5 biphosphate (PIP_2) to synthesize the second messengers diacylglycerol (DAG) and inositol-1,4,5-triphosphate (IP_3) (37, 38). While IP_3 induces calcium influx, DAG activates protein kinase C (PKC) θ (in T cells) and PKCβ (in B cells) (**Figure 2**). PKCθ/β act to phosphorylate a series of serine sites along the CARD11 inhibitory domain, the first of several post-translational modifications required for the assembly of the CBM complex (39, 40). CARD11 converts to an open conformation, making it accessible for BCL10-MALT1 binding. BCL10, which constitutively associates with MALT1 through serine/threonine-rich and immunoglobulin-like domain interactions, respectively (7, 41), binds to CARD11 through caspase recruitment domain (CARD)-CARD domain interactions (42) (**Figure 1**). MALT1 can also bind directly to CARD11 through the interaction of its paracaspase domain and the coiled-coil domain of CARD11 (43). These initial events nucleate the formation of higher order structures consisting of branched BCL10 filaments sheathed with MALT1, allowing for MALT1 oligomerization and activation, and the cooperative recruitment and incorporation of tumor necrosis factor receptor-associated factor 6 (TRAF6) (41, 42).

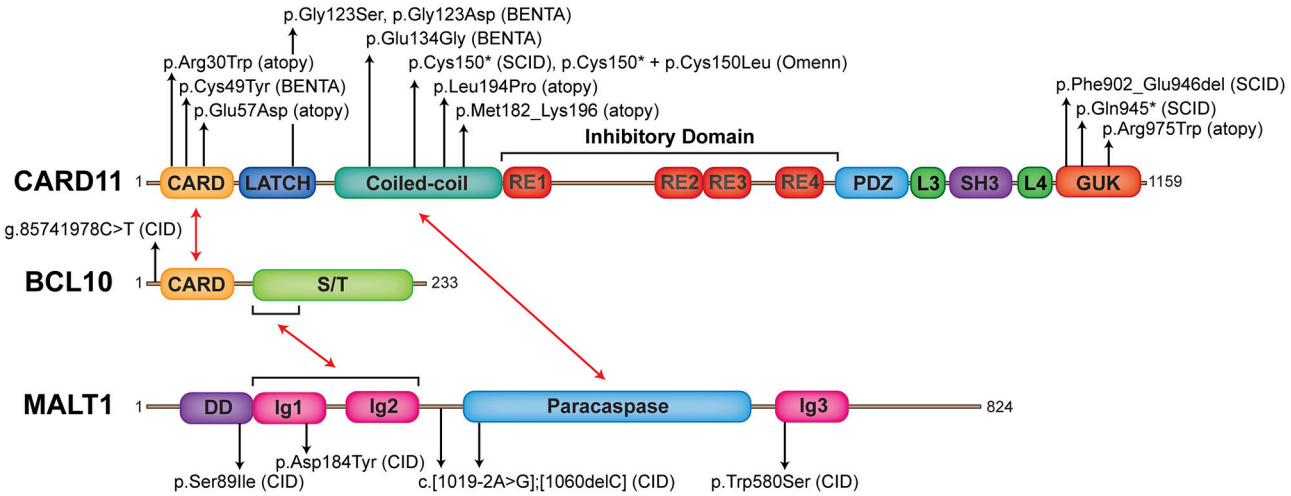

FIGURE 1 | The landscape of human germline mutations causing CBM-opathies. Schematic representation of protein domains found in CARD11, BCL10, and MALT1. Red arrows indicate interactions between domains. Annotated are confirmed mutations causing CBM-opathies and where they localize to on the protein. CARD, caspase recruitment domain; RE, repressive element; L, linker; PDZ, postsynaptic density protein (PSD95), *Drosophila* disc large tumor suppressor (Dlg1), zonula occludens-1 protein (zo-1) domain; SH3, SRC homology 3 (SH3); GUK, guanylate kinase domain; S/T, serine/threonine; DD, death domain; Ig, immunoglobulin-like domain.

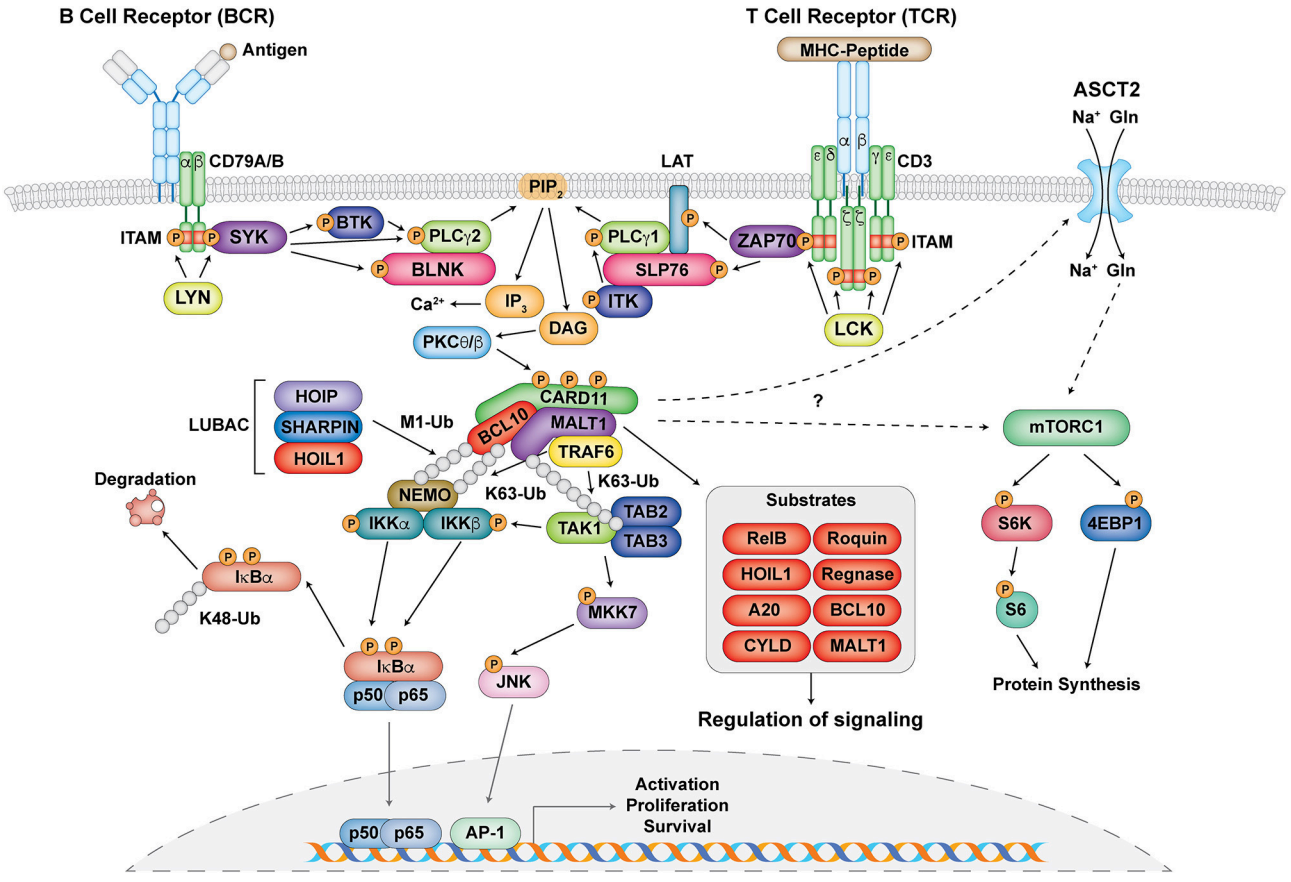

FIGURE 2 | The central role of the CBM complex in BCR- and TCR- signaling. Schematic representation of proximal antigen receptor signaling events in the BCR and TCR, activation and assembly of the CBM complex, and downstream targets and effects of CBM activation. Gray circles represent ubiquitin chains.

Signaling to NF-κB

Canonical NF-κB activation is mediated by the activation of the IκB kinase (IKK) complex, which consists of two catalytic subunits IKKα and IKKβ and a regulatory subunit NF-κB essential modulator (NEMO, also known as IKKγ) (5). After the assembly of the CBM complex, various ubiquitination events occur in order to facilitate the phosphorylation and activation of the IKK complex (35) (**Figure 2**). MALT1 contains binding motifs for the E3 ubiquitin ligase TRAF6 and acts as a scaffold to facilitate the oligomerization and activation of TRAF6 (44, 45). It is thought that TRAF6 and BCL10, as well as other factors such as the ubiquitin conjugating enzyme UBC13, mediate the K63-linked ubiquitination of various proteins including MALT1 and NEMO (35, 46–48). In addition to K63-linked ubiquitination, M1-linked linear ubiquitin chains are also ligated to NEMO and BCL10 through the linear ubiquitin chain assembly complex (LUBAC), which consists of heme-oxidized IRP2 ubiquitin ligase 1 (HOIL1), HOIL1-interacting protein (HOIP), and SHANK-associated RH domain interacting protein (SHARPIN) (49–51) (**Figure 2**). These two types of ubiquitination collectively mediate optimal recruitment and phosphorylation/activation of the IKK complex (5).

The phosphorylation of IKKα/β after antigen receptor ligation is thought to be principally mediated by TGFβ-activated kinase 1 (TAK1) and its associated adaptor proteins TAB2/3 (44, 52, 53). It is speculated that since both TAB2/3 and NEMO can specifically recognize K63-linked ubiquitination (47, 54), these two complexes are brought in close proximity to each other, thus facilitating optimal IKK complex activation (34). NF-κB inhibitor alpha (IκBα) in resting cells normally exists in a complex with the NF-κB subunits p50 and p65, which prevents them from becoming activated. The activated IKK complex can phosphorylate IκBα, which causes it to undergo K48-linked ubiquitination and degradation by the proteasome. This allows NF-κB to translocate into the nucleus to initiate target gene transcription (5) (**Figure 2**).

Signaling to JNK

Another arm of antigen receptor signaling that the CBM complex mediates is the c-Jun N-terminal kinase (JNK) pathway (**Figure 2**) [reviewed in (55)]. This process is usually activated by successive phosphorylation events mediated by mitogen-activated protein kinases (MAPKs) (56), with TAK1 also playing a critical role in JNK activation (57, 58). This highlights a cross-talk mechanism in NF-κB and JNK signaling. Although regulation of this process by the CBM complex is not as well understood as the NF-κB pathway, it is thought that TAK1 associates with CARD11-mediated BCL10 oligomers, MKK7 gets recruited, and the selective phosphorylation of JNK2 occurs (59) (**Figure 2**). This ultimately leads to the accumulation and phosphorylation of c-Jun, which regulates lymphocyte proliferation as part of the AP-1 transcription factor complex.

Signaling to mTORC1

The mechanistic target of rapamycin (mTOR) kinase is a PI3K-related kinase (PIKK) represented by two distinct catalytic protein complexes, mTOR Complex 1 (mTORC1) and 2 (mTORC2), which have different mechanisms of activation and signaling (60). In particular, mTORC1 can be activated by TCR and CD28 co-stimulation, environmental stimuli such as growth factors and stressors, and nutrients such as amino acids (61). It is critical for regulating T cell growth and proliferation (62) as well as T helper 1 (Th1) and Th17 differentiation (63). Recent studies have demonstrated that the CBM complex regulates TCR-mediated glutamine uptake and the subsequent activation of the mTOR pathway independent of NF-κB (32, 64, 65). Following TCR stimulation, CBM components associate with and mediate the upregulation of the alanine-serine-cysteine transporter 2 (ASCT2) glutamine transporter at the cell surface (32, 64) (**Figure 2**). MALT1 also has the ability to associate with mTOR, and its paracaspase activity mediates the phosphorylation of the ribosomal protein S6, a target of mTORC1, ultimately impacting metabolic programming (65) (**Figure 2**). However, the exact molecular mechanism by which the CBM complex links TCR signals to glutamine uptake and the activation of mTOR is unknown and requires further study.

THE CARD FAMILY

The CARMA/CARD protein family consists of CARD9, CARD10 (or CARMA3), CARD11 (or CARMA1), and CARD14 (or CARMA2) (66). These scaffold proteins are evolutionarily conserved, structurally homologous, mostly membrane-associated (with the exception of CARD9) and have varying patterns of expression in the body. Mutations in this family of proteins have been implicated in different pathological states, including CARD9 deficiency increasing susceptibility to fungal infections [reviewed in (67)] and CARD14 mutations being linked to increased susceptibility to psoriasis (68, 69) and the skin disease pityriasis rubra pilaris (70).

Each CARD protein participates in its own "CBM" complex with BCL10 and MALT1 in different cell types to facilitate downstream signaling events leading to NF-κB activation (66). CARD11 mediates the activation of lymphocytes by the antigen receptors BCR and TCR and facilitates natural killer (NK) cell activation downstream of ITAM-coupled receptors such as natural killer group 2, member D (NKG2D), NK1.1, Ly49D, and Ly49H (71, 72). CARD14 is expressed in the placenta and skin tissue (69) and can mediate NF-κB activation in keratinocytes possibly downstream of Dectin-1 (73). CARD10 is broadly expressed in non-hematopoietic cells and serves as a link between G-protein coupled receptors (GPCRs) and NF-κB (74). CARD9 is mostly expressed by myeloid cells (macrophages, dendritic cells, neutrophils) and transduces signals emanating from C-type lectin receptors (Dectin-1, Dectin-2, Mincle) and ITAM-associated receptors (FcRγ, DAP12) (67). Although CARD9 deficiency also causes immunodeficiency, this has been covered in detail very recently in the "CARMA Proteins: Playing a Hand of Four CARDs" *Research Topic* (67) and thus, we will be focusing on immune defects caused by mutations in *CARD11*.

CARD11

Role of CARD11 in Immunity

CARD11 is a ∼130 kDa protein originally discovered by bioinformatics screens (8, 75). It is primarily expressed in hematopoietic tissue and lymphocytes and is crucial for antigen receptor signaling (11, 76). CARD11 is a classic scaffold molecule comprised of various defined domains, including CARD, LATCH, coiled-coil (CC), inhibitory, postsynaptic density protein (PSD95), *Drosophila* disc large tumor suppressor (Dlg1), zonula occludens-1 protein (zo-1) (PDZ), SRC homology 3 (SH3), and guanylate kinase (GUK) domains (**Figure 1**). Initial insight into CARD11 function came from *in vitro* studies on leukemia cell lines, which demonstrated its essential role in NF-κB activation downstream of the TCR complex (77–79). Following this, various CARD11 mouse models were generated, including the *Card11*$^{-/-}$ mouse and CARD11 "unmodulated" (*Card11*$^{un/un}$) mouse (11–13, 80) (compared in **Table 1**).

Card11-deficient mice were found to be immunodeficient and displayed defective antigen receptor-induced NF-κB and JNK signaling, impaired B and T cell proliferation, and decreased expression of immune activation markers; however, ERK and p38 activation remained intact. Lymphocyte numbers were generally normal, but some abnormalities were present: decreased B1 and marginal zone (MZ) B cells, decreased Th2 and Th17 cells, and absent regulatory T cells (Tregs) (11, 12, 81–84). In addition, both immunoglobulin levels and antibody responses were impaired. These studies highlighted the essential role of CARD11 in mediating B cell development, Treg development, and antibody production.

The *Card11*$^{un/un}$ mouse, in contrast, possessed a single ENU mutagenesis-induced point mutation in the coiled-coil domain of *Card11*, which did not impact CARD11 protein expression but conveyed a hypomorphic effect on NF-κB and JNK signaling (13). Similar to the *Card11*$^{-/-}$ mice, *Card11*$^{un/un}$ lymphocytes displayed impaired proliferation and upregulation of activation markers after stimulation (13). Surprisingly, *Card11*$^{un/un}$ mice did not exhibit overt pathology but developed spontaneous atopy and dermatitis with age. Accordingly, despite some immunoglobulins being decreased, IgE was significantly elevated (13, 85) and this was paired with elevated Th2 cells, diminished Tregs, and unchanged Th1 and Th17 cells (85). These mice highlighted a possible role for CARD11 in the pathogenesis of allergic disease and tolerance. Indeed, a genome-wide association study identified *CARD11* as a susceptibility locus for atopic dermatitis (94) and it was found that CARD11 is important for both Th2 polarization and allergic airway disease (95, 96).

Of the three CBM components, *CARD11* mutations have been associated with the most diverse phenotypes. Human germline *CARD11* mutations cause a broad (and expanding) range of clinical phenotypes including SCID, CID and atopy, and BENTA—with more being characterized (summarized in **Tables 2**, **4**–**7**).

Biallelic Loss-of-Function *CARD11* Mutations Causing SCID

Germline homozygous loss-of-function (LOF) mutations in *CARD11* are associated with SCID (OMIM 615206) (17–19) (**Table 2**). To date, there have been three reported cases of complete CARD11 deficiency and they were discovered by whole exome sequencing (WES) or directed Sanger sequencing, with mutations localizing to either the CC (19) or GUK (17, 18) domains. Patients were of different ethnicities but all were born to consanguineous parents: a Palestinian girl with p.Phe902_Glu946del mutations/exon 21 deletion (17), a Central European girl with p.Gln945* mutations (18), and a Turkish boy with p.Cys150* mutations (19). The p.Cys150* homozygous boy also had an older sister with the same mutation, but she additionally had a second site somatic reversion (p.Cys150Leu), which led to Omenn syndrome (19).

Patients typically presented within the first year of life (3–15 months) with severe respiratory tract infections/pneumonia caused by *Pneumocystis jirovecii* (PJP) and abnormal serum immunoglobulin levels that progressed to panhypogammaglobulinemia (3/3 patients). Development was generally normal, and patients did not have any overt organ pathology. All patients generally had normal numbers of total B and T cells, κ-deleted receptor excision circle (KREC)/T cell receptor excision circle (TREC) values (where available), and recent thymic emigrants (**Table 2**). However, detailed immune profiling revealed a developmental block in B cells, with increased transitional B cells and decreased (class-switched) memory B cells (3/3 patients). All patients had severely diminished Tregs (3/3 patients) and a predominantly naïve T cell phenotype (2/2 patients). Functional evaluation of these patients revealed absent/severely diminished lymphocyte activation of NF-κB and decreased T cell proliferation in response to antigen receptor stimulation (3/3 patients).

Fuchs and colleagues described a Turkish girl homozygous for p.C150* who had a somatic second site reversion (p.C150L), which restored some CARD11 protein expression and function in her lymphocytes (19). Consequently, this young girl had a very different clinical course from the fully CARD11-deficient patients. She presented at the age of 5 months with features of Omenn syndrome, including severe eczema that progressed to generalized erythroderma, lymphadenopathy, and hepatosplenomegaly (**Table 2**). She experienced multiple bouts of sepsis caused by both bacteria and viruses (*Staphylococcus aureus*, *Enterococcus*, *Pseudomonas*) and eventually succumbed to viral pneumonia positive for human metapneumovirus, rhinovirus, and cytomegalovirus (CMV). Immune investigations revealed progressive T cell lymphoproliferation, massive infiltration of highly proliferative T cells in the skin, oligoclonal T cell expansion, and elevated IgE. Interestingly, the patient also had some features that overlapped with fully-deficient patients, including progressive panhypogammaglobulinemia and reduced T cell proliferation (**Table 2**). Surprisingly, this somatic reversion led to only a partial restoration of NF-κB activity without causing a gain-of-function (GOF) effect. It is thought that the somatic reversion occurred only in some founder T cells, giving them a proliferative advantage over the fully CARD11-deficient T cells. In the context of specific immune triggers such as viral infections, these T cell clones expanded, perturbing immune homeostasis in the absence of Tregs, and ultimately caused skin infiltration,

TABLE 1 | Overview of CBM-deficient mouse models.

Feature	*Card11*$^{-/-}$	*Card11*$^{un/un}$	*Bcl10*$^{-/-}$	*Malt1*$^{-/-}$	*Malt1*$^{PD/PD}$
B CELLS					
Populations					
Total	Normal	Normal	Normal	Normal	Normal
FO	Normal	Normal	↓	Normal	Normal
MZ	↓	Normal	↓	↓	↓
B1	↓	↓	↓	↓	↓
GC	ND	ND	ND	↓	↓
Proliferation					
IgM	↓	↓	↓	↓	Normal
CD40	↓	↓	↓	↓	ND
CD40L	ND	ND	ND	↓	↓
IgM+CD40	↓	ND	↓	ND	ND
LPS	↓	Normal	Normal	↓ or normal	↓ or normal
IgM+IL-4	ND	↓	ND	↓	↓
CD40+IL-4	ND	↓	ND	↓ or normal	Normal
Signaling					
IκBα/NF-κB	↓	↓	↓	↓ or normal	Normal
JNK	↓	↓	↓	↓ or normal	↓ or normal
ERK	Normal	Normal	Normal	Normal	Normal
Tyrosine	Normal	Normal	ND	Normal	ND
Calcium	Normal	Normal	Normal	ND	ND
T CELLS					
Populations					
Total	Normal	Normal	Normal	Normal	Normal
CD4	Normal	Normal	Normal	Normal	Normal
CD8	Normal	Normal	Normal	Normal	Normal
Treg	↓	↓	↓	↓	↓
Th1	↓	Normal	ND	↑ or normal	↑
Th2	↓	↑	ND	↑ or normal	↑
Th17	↓	Normal	ND	↓ or normal	↑
Tfh	ND	ND	ND	↓	↓
NKT	Normal	ND	Normal	ND	ND
DN3	↓	ND	ND	↓	ND
DN4	↑	ND	↑	↑	↑
DP	ND	ND	↓	Normal	Normal
Proliferation					
CD3	↓	Normal	↓	↓	↓
CD3+CD28	↓	↓	↓	↓	↓
P/I	↓	ND	↓	↓	ND
Signaling					
IκBα/NF-κB	↓	ND	↓	↓	Normal
JNK	↓	ND	ND	↓	↓ or normal
ERK	Normal	ND	Normal	Normal	Normal
Tyrosine	Normal	ND	Normal	Normal	ND
Calcium	Normal	ND	Normal	ND	ND
Activation Markers (α-CD3+CD28)					
CD25	↓	↓	↓	↓	Normal
CD69	↓	↓	↓	↓	ND
CD40L	ND	↓	ND	ND	ND
OX40	ND	↓	ND	ND	ND
ICOS	ND	↓	ND	ND	ND
CD44	↓	ND	↓	↓	ND
IMMUNOGLOBULINS					
Basal					
IgM	↓	↓	↓	↓	↓
IgG1	↓	Normal	↓	↓	↑
IgG2a	↓	ND	↓	↓	↓
IgG2b	↓	Normal	↓	↓	↓
IgG3	↓	↓	↓	↓	↓
IgA	↓	ND	↓	↓ or normal	Normal
IgE	ND	↑	ND	ND	↑
T-dependent					
IgM	↓	↓	↓	↓	↓
IgG1	↓	↓	↓	↓	↓
IgG2a	↓	ND	↓	ND	ND
IgG2b	ND	ND	↓	ND	ND
IgG3	ND	ND	↓	ND	ND
Other immune manifestations	None	Atopy and dermatitis with age	None	None	Spontaneous multi-organ inflammation
References	(11, 12, 81–84)	(13, 17, 85)	(14, 15, 86, 87)	(16, 88–90)	(89, 91–93)

Lymphocyte characteristics, immunoglobulin levels, and additional immune features are summarized and compared for Card11$^{-/-}$*, Card11*$^{un/un}$*, Bcl10*$^{-/-}$*, Malt1*$^{-/-}$*, Malt1*$^{PD/PD}$ *mice. ND, no data; ↑, increased levels relative to normal range; ↓, decreased levels relative to normal range; FO, follicular B cell; MZ, marginal zone B cell; GC, germinal center B cell; LPS, lipopolysaccharide; IL-4, interleukin 4; IκBα, NF-κB inhibitor alpha; NF-κB, nuclear factor kappa B; Treg, T regulatory cell; Th, T helper cell; Tfh, T follicular helper cell; NKT, natural killer T cell; DN, double negative; DP, double positive; P/I, phorbol 12-myristate 13-acetate (PMA) / ionomycin; JNK, c-Jun N-terminal kinase; ERK, extracellular signal-regulated kinase; ICOS, inducible T cell costimulatory.*

progressive eczema and erythroderma, lymphadenopathy, and hepatosplenomegaly. This case highlights the differential requirements for NF-κB signaling between T cell ontogeny and maintenance.

Diagnosis and Treatment of CARD11 Deficiency

The first cases of CARD11 deficiency were diagnosed by WES (17, 18), while the latter two were found by directed Sanger sequencing based on suspicion and similarity to the first two cases (19). CARD11 deficiency should be considered in patients who present in early life with respiratory tract infections most commonly caused by *Pneumocystis jirovecii* (PJP) (3/3 patients), impaired B cell development with increased transitional and decreased memory (3/3 patients), predominantly naïve T cells (2/2 patients), impaired T cell proliferation (3/3 patients), and panhypogammaglobulinemia (3/3 patients) (**Table 3**). Specific testing for NF-κB phosphorylation, IκBα degradation, and IL-2 secretion, while often only available in the research setting, will show decreased/absent response. In the appropriate clinical context, sequencing of the *CARD11* gene should help confirm the diagnosis, but depending on the nature of any genetic variants identified, functional tests of the CBM may be required to make a definitive diagnosis (97).

TABLE 2 | Clinical and laboratory phenotype of human CARD11 deficiency.

Mutation	**p.Gln945***	**p.Phe902_Glu946del Exon 21 del**	**p.Phe902_Glu946del Exon 21 del**	**p.Phe902_Glu946del Exon 21 del**	**p.Cys150***	**p.Cys150* + somatic p.Cys150Leu**
Age	6 months	9 months	3 months	6 months	Birth	6 months
Sex	F	F	F	M	M	F
Ethnicity	Central European	Palestinian	Palestinian	Palestinian	Turkish	Turkish
Consanguinity	+	+	+	+	+	+
Functional Impact	Loss	Loss	Loss	Loss	Loss	Loss then moderate restoration
Inheritance	AR	AR	AR	AR	AR	AR
Gene Expression	Normal	Truncated	Truncated	Truncated	↓	Normal
Protein Expression	Truncated	None	None	None	None	Restored
INFECTIONS						
Pulmonary	+	+	ND	+	+	+
Pneumocystis jirovecii	+	+	ND	ND	+	–
CMV	–	–	ND	ND	+	+
Human metapneumovirus	–	–	ND	ND	–	+
Rhinovirus	–	–	ND	ND	–	+
Blood	–	–	ND	ND	+	+
Staphylococcus aureus	–	–	ND	ND	–	+
Enterococcus	–	–	ND	ND	+	+
Pseudomonas	–	–	ND	ND	–	+
Klebsiella	–	–	ND	ND	+	–
Eyes (retina)	–	–	–	–	–	+
CMV	–	–	–	–	–	+
Meningitis	–	+	–	+	–	–
CLINICAL MANIFESTATIONS						
Failure to thrive	–	–	+	ND	–	–
Eczema	–	–	ND	ND	–	+
Erythroderma	–	–	ND	ND	–	+
Lymphadenopathy	–	–	ND	ND	–	+
Hepatosplenomegaly	–	–	ND	ND	–	+
Dyspnea	–	+	ND	ND	–	–
Tachypnea	+	–	ND	ND	–	–
Microcephaly	–	–	ND	ND	+	+
Developmental delay	–	–	ND	ND	+	+
Congestive heart failure	–	–	ND	ND	–	+
Seizures	–	–	ND	ND	+	–
THERAPY						
Transplantation	+	+	–	–	–	–
Successful	+	+	N/A	N/A	N/A	N/A
IVIG	–	+	ND	ND	+	+
Anti-microbial prophylaxis	+	+	ND	ND	ND	ND
TMP/SMX	+	+	ND	ND	ND	ND
IMMUNOSUPPRESSION						
Pre-transplantation	+	ND	–	–	–	–
Treosulfan	+	ND	–	–	–	–
Fludarabine	+	ND	–	–	–	–
Alemtuzumab	+	ND	–	–	–	–
Post-transplantation	+	ND	–	–	–	–
Cyclosporine	+	ND	–	–	–	–
Mycophenolate mofetil	+	ND	–	–	–	–
Outcome	Alive	Alive	Dead	Dead	Dead	Dead
Cause of death	N/A	N/A	Respiratory failure	Respiratory failure	Sepsis	Interstitial pneumonia

(Continued)

TABLE 2 | Continued

Mutation	p.Gln945*	p.Phe902_Glu946del Exon 21 del	p.Phe902_Glu946del Exon 21 del	p.Phe902_Glu946del Exon 21 del	p.Cys150*	p.Cys150* + somatic p.Cys150Leu
LYMPHOCYTES						
Total CD19 B cells	Normal	Normal	ND	ND	Normal	↓ then normal
Naive	↓	↑	ND	ND	ND	ND
Transitional	↑	↑	ND	ND	↑	ND
(Class-switched) memory	↓	↓	ND	ND	↓	ND
Total CD3 T cells	Normal	ND	ND	ND	↑	↓ then ↑↑↑
CD4	Normal	Normal	ND	ND	Normal	↓ then ↑↑↑
CD4 CD45RA	↑	Normal	ND	ND	Normal	Normal then ↓
CD8	Normal	Normal	ND	ND	↑	↓ then ↑↑↑
CD8 CD45RA	↑	Normal	ND	ND	ND	ND
Treg	↓	↓	ND	ND	↓	↓
PROLIFERATION						
PHA	↓	↓	ND	ND	↓	↓
ConA	↓	ND	ND	ND	ND	ND
PWM	Normal	ND	ND	ND	ND	ND
CD3	↓	ND	ND	ND	ND	ND
CD3+CD28	ND	↓	ND	ND	↓	↓
IMMUNOGLOBULINS						
IgG	↓	↓	ND	↓	↓	↓
IgA	↓	↓	ND	↓	↓	↓
IgM	↓	↓	ND	↓	↓	↓
IgE	ND	ND	ND	ND	Normal	↑
Specific antibodies						
Tetanus	ND	ND	ND	ND	Negative	Negative
Pertussis	ND	ND	ND	ND	Negative	Negative
Diphtheria	ND	ND	ND	ND	Negative	Negative
Haemophilus influenzae B	ND	ND	ND	ND	Negative	Negative
References	(18)	(17)	(17)	(17)	(19)	(19)

*Key molecular, immunological, infectious, and pathological findings for all patients with CARD11 deficiency described to date. ND, no data; ↑, increased levels relative to normal range; ↓, decreased levels relative to normal range; +, present; −, absent; *premature stop; AR, autosomal recessive; CMV, cytomegalovirus; IVIG, intravenous immunoglobulin; TMP/SMX, trimethoprim/sulfamethoxazole; PHA, phytohemagglutinin; ConA, concanavalin A; PWM, pokeweed mitogen.*

In addition, patients presenting with features of Omenn syndrome should also be evaluated for CARD11 deficiency (with possible somatic second site reversion) (19). Although there has only been a single patient described with this phenotype to date, suggestive clinical features include erythroderma, lymphadenopathy, hepatosplenomegaly, T cell lymphocytosis, diminished naïve T cells, eosinophilia, and elevated IgE. Analysis of TCR rearrangement would possibly detect oligoclonality. Sequencing *CARD11* in cells from different sites of the body may show different genotypes (LOF vs. LOF+somatic reversion).

In general, CARD11 deficiency is fatal within the first 2 years of life (3/5 died). Infection-related respiratory failure was the most common cause of death (2/5 patients) (17) and one died of sepsis (19). The two patients who survived (17, 18) received successful hematopoietic stem cell transplants. One survivor received bone marrow-derived stem cells from a human leukocyte antigen (HLA)-identical brother who was a heterozygous carrier of the *CARD11* mutation (17), emphasizing that *CARD11* haploinsufficiency is not pathological. The second survivor received peripheral blood hematopoietic stem cells from an HLA-matched unrelated donor (18). Overall, these results indicate that patients with confirmed CARD11 deficiency should be considered for curative hematopoietic stem cell transplantation as soon as possible following diagnosis. While awaiting transplant, CARD11-deficient patients should receive immunoglobulin replacement therapy and PJP prophylaxis.

Dominant Negative Loss-of-Function *CARD11* Mutations Causing CID, Atopy, and Novel Phenotypes

Germline heterozygous LOF mutations in *CARD11* are associated with severe atopic disease and CID with a susceptibility to infections (OMIM 617638) (31, 32). These LOF mutations dominantly interfere with wild-type (WT) *CARD11* and signaling to NF-κB and mTORC1, thus explaining the observed autosomal dominant inheritance pattern. To date, five distinct dominant negative (DN) LOF CARD11 mutations have been linked to disease in 12 patients (**Figure 1**). Although the cohort of known CARD11 DN patients and associated clinical phenotypes is expanding rapidly (98) (**Table 4**), the

TABLE 3 | "Red flags" suggestive of human CARD11 deficiency (LOF *CARD11* mutations).

Clinical features	Proportion	Penetrance (%)
Infections (bacterial/viral)		
P. jirovecii pneumonia	3/3	100
Bacterial sepsis (*Enterococcus* etc.)	1/3	33
Viral pneumonia (Rhinovirus etc.)	1/3	33
LABORATORY TESTS		
Cell populations		
Normal total lymphocyte numbers	3/3	100
↓ Treg	3/3	100
↑ Naïve ↓ Memory B cells	3/3	100
↑ Naïve ↓ Effector T cells	2/2	100
Response		
↓ T cell proliferation (PHA, α-CD3/CD28)	3/3	100
↓ NF-κB phosphorylation/IκBα degradation	3/3	100
↓ IL-2 secretion	3/3	100
Ig		
Panhypogammaglobulinemia	3/3	100

Tabulation of findings that may be diagnostic clues for CARD11 deficiency. Included are the proportion of patients where the data is available as well as the percentage of patients with the specific phenotype. ↑, increased levels relative to normal range; ↓, decreased levels relative to normal range.

TABLE 4 | "Red flags" suggestive of CADINS disease (DN LOF *CARD11* mutations).

Clinical features	Proportion	Penetrance (%)
Atopic disease	**39/44**	**89**
Atopic dermatitis	32/44	73
Asthma	24/44	55
Food allergies	14/44	32
Eosinophilic esophagitis	3/44	7
Cutaneous viral infections	**30/44**	**68**
Respiratory infections	**30/44**	**68**
Autoimmunity	9/44	20
Neutropenia	6/44	14
Oral ulcers	6/44	14
Lymphoma	3/44	7
LABORATORY TESTS		
Cell Populations		
↑ Total $CD4^+$ T cells	4/40	10
↓ Memory $CD4^+$ T cells	9/26	35
Normal total $CD8^+$ T cells	41/43	95
↓ Memory $CD8^+$ T cells	4/15	27
↓ Total B cells	8/43	19
↓ Class-switched/memory B cells	10/35	29
↓ NK cells	8/43	19
↓ Tregs	2/29	7
↑ Eosinophils	26/40	65
***In vitro* responses**		
↓ T cell proliferation	19/31	61
↓ NF-κB phosphorylation/IκBα degradation	11/12	92
Specific antibody response defect	20/41	49
Total antibody response defect	12/42	29
Ig		
Panhypogammaglobulinemia	5/44	11
↑ IgE	31/42	74

Summary of major clinical and immunological phenotypes associated with human germline DN LOF CARD11 mutations causing CARD11-associated Atopy with Dominant Interference of NF-κB Signaling (CADINS) disease. Proportion of patients and penetrance is calculated based on number of patients with available data. Clinical "red flags" for potential diagnosis of CADINS disease are marked in blue. ↑, increased levels relative to normal range; ↓, decreased levels relative to normal range.

cardinal feature noted in ∼90% of patients is severe atopic disease, encompassing symptoms of immediate hypersensitivity (allergic rhinitis, food allergy) and/or allergic inflammation (atopic dermatitis, eosinophilic esophagitis), specific allergens notwithstanding (99). Importantly, as discussed in the "Role of CARD11 in Immunity" section, similar atopic phenotypes were described in unmodulated ($Card11^{un/un}$) mice harboring a hypomorphic mutation in *Card11* (13, 85) and *CARD11* has previously been identified as a risk locus for atopic dermatitis in a Japanese genome-wide association study (94).

Heterozygous *CARD11* mutations were initially identified by WES in eight patients with severe atopic dermatitis (32). These mutations included three missense mutations encoding p.Glu57Asp, p.Leu194Pro, and p.Arg975Trp and one in-frame mutation encoding a 14-amino acid insertion (p.Met183_Lys196). These patients generally possessed features of recalcitrant atopic dermatitis with elevated serum IgE levels and eosinophilia, with severity waning with age in certain patients. Most patients also presented with respiratory distress associated with recurrent pulmonary infections and pneumonias, as well as viral skin infections (e.g., molluscum, eczema herpeticum). Four additional patients were subsequently described with missense mutations encoding p.Arg30Trp, leading to multiorgan atopy, autoimmunity, and a prominent susceptibility to infections (31).

These mutations affected several different domains of the CARD11 protein, with 2 in the CARD (p.Arg30Trp and p.Glu57Asp), 2 in the CC (p.Leu194Pro and p.Met183_Lys196), and 1 in the GUK (p.Arg975Trp) domain (31, 32). Patient T cells and mutant plasmid-transfected Jurkat T leukemia cell lines demonstrated that each variant impaired TCR-induced NF-κB activation by disrupting WT CARD11 signaling. Subsequent studies of an expanded patient cohort have identified at least 10 additional DN mutations primarily found in the CARD and CC domains, where they are most likely to impede CBM complex assembly by thwarting BCL10 and MALT1 binding and oligomerization (98). In addition to NF-κB blockade, many (but not all) of these mutations also reduced TCR-mediated mTORC1 activation, ostensibly by preventing optimal glutamine uptake through upregulation of the ASCT2 transporter (32). These TCR signaling defects not only resulted in impaired T cell proliferation and induction of cell surface activation markers, but also contributed to a Th2-skewed $CD4^+$ T cell phenotype, with enhanced secretion of IL-4 and IL-13 and decreased IFN-γ production. Intriguingly, *in vitro* culture of patient T cells with excess glutamine partially restored T cell proliferation and IFN-γ

TABLE 5 | "Red flags" suggestive of BENTA disease (GOF *CARD11* mutations).

Clinical features	Proportion	Penetrance (%)
Splenomegaly in childhood	**14/14**	**100**
INFECTIONS		
Otitis media/sinopulmonary	**21/21**	**100**
EBV	9/21	43
Molluscum contagiosium	8/22	36
LABORATORY TESTS		
Cell populations		
B cell lymphocytosis	**21/21**	**100**
↑ % Naïve mature B (IgM^+ IgD^+)	21/21	100
↑ % Immature/transitional B ($CD10^+$)	21/21	100
↓ % Class-switched and memory B	21/21	100
Normal T cells (abs #)	21/21	100
↑ % DN T cells	6/10	60
Autoantibodies	5/21	23
Autoimmune hemolytic anemia	4/21	19
***IN VITRO* RESPONSES**		
Naïve B cells		
Normal proliferation	7/7	100
↓ Plasma cell differentiation	7/7	100
↓ IgG secretion	7/7	100
T cells		
↓ Proliferation (α-CD3/CD28)	7/7	100
↓ IL-2 secretion (α-CD3/CD28, mitogens)	7/7	100

Summary of major clinical and immunological phenotypes associated with human germline GOF mutations in CARD11 causing B cell Expansion with NF-κB and T-cell Anergy (BENTA) disease. Proportion of patients and penetrance is calculated based on number of patients tested with available data. Clinical "red flags" for potential diagnosis of BENTA disease are marked in blue. GOF CARD11 mutations are bolded. ↑, increased levels relative to normal range; ↓, decreased levels relative to normal range.

secretion in the presence of cytokines that trigger NF-κB (e.g., IL-1/TNF) and signal transducer and activator of transcription (STAT3) (e.g., IL-6) activation independent to the TCR (32). These findings suggest that both NF-κB and mTORC1 signaling defects contribute to atopic predisposition and disease pathology, even though diagnostic readouts of impaired mTORC1 signaling (e.g., ribosomal protein S6 phosphorylation) can be variable and difficult to detect experimentally. In contrast to *Card11*$^{un/un}$ mice, the frequency and suppressive function of Tregs is normal in almost all CARD11 DN patients tested to date, suggesting important mechanistic discrepancies between mouse and human (31, 32).

Diagnosis and Treatment of Disease Caused by DN *CARD11* Mutations

The recent identification of many additional patients harboring CARD11 DN variants provides a clearer picture of the full phenotypic spectrum of disease (98) (**Table 4**). Clinically, patients with germline DN *CARD11* mutations most often present in early childhood with atopy, cutaneous viral infections, and recurrent respiratory infections. These signs and symptoms occur in an autosomal dominant manner with high penetrance and no gender bias. However, subsets of patients may also present with hypogammaglobulinemia and specific antibody deficiency (SAD), neutropenia, oral ulcers, autoimmunity (e.g., alopecia), or lymphoma. Diagnostic tests include: (i) assaying for a NF-κB signaling defect in response to TCR or PMA stimulation (reduced p65 phosphorylation, IκB degradation) and (ii) sequencing *CARD11* to identify rare/novel variants, with CARD and CC domain variants having the highest likelihood of being pathogenic. Ultimately, functional testing (e.g., Jurkat T cell transfections) is highly recommended to confirm DN LOF activity for any novel variants found.

Based on these collective clinical and experimental findings, we propose to classify this disorder as CARD11-associated Atopy with Dominant Interference of NF-κB Signaling (CADINS) disease. Although more work is required to mechanistically connect faulty CARD11 signaling to the various phenotypes of CADINS disease, defects in both T and B cell function explain CID in these patients and underscore the essential role of CARD11 in governing peripheral lymphocyte differentiation and effective humoral immune responses. Continued mechanistic studies will also inform future clinical management and therapeutic strategies for these patients. Although glutamine supplementation may offer the simplest intervention (see "Novel Therapeutic Insights Emerging From Our Understanding of Human CBM-opathies" section), newer biologics targeting Th2 cytokine signaling (e.g., dupilumab, mepolizumab) or IgE directly (omalizumab) may be useful in ameliorating atopic disease (100). In contrast to CARD11 deficiency, hematopoietic stem cell transplantation should only be considered in the most severe pediatric cases, since symptoms may improve with age.

Gain-Of-Function *CARD11* Mutations Causing BENTA

B cell Expansion with NF-κB and T-cell Anergy (BENTA) is a congenital lymphoproliferative and immunodeficiency disorder caused by heterozygous GOF *CARD11* mutations (OMIM 616452) (26). The first patient diagnosed with BENTA disease was initially reported in 1971, and presented with splenomegaly and persistent B cell lymphocytosis that worsened with splenectomy and resembled chronic lymphocytic leukemia (CLL) (101). This patient eventually developed monoclonal CLL around age 44 and received a curative hematopoietic stem cell transplant from his sister (26). His two daughters presented with frequent sinopulmonary and ear infections and were found to exhibit splenomegaly and marked B cell lymphocytosis in infancy (26). RNA-Seq analyses of this first patient and his two daughters revealed a novel heterozygous missense mutation (p.Glu134Gly), located in the N-terminal portion of the CC domain of CARD11. A fourth unrelated patient that presented with similar symptoms was simultaneously identified with unique heterozygous missense mutations located in the LATCH domain (p.Gly123Ser) (26). Since the initial description of BENTA disease in these four patients in 2012, GOF *CARD11* mutations associated with BENTA have been identified in >25 additional patients (27–30, 102–104) (**Figure 1**, **Table 5**).

The primary hallmark of BENTA disease is polyclonal B cell lymphocytosis in early childhood paired with splenomegaly and lymphadenopathy. Pediatric patients possess excessive accumulation of immature transitional ($CD10^+CD24^{hi}CD38^{hi}$) and mature naïve (IgM^+IgD^+) polyclonal B cells, with very low

TABLE 6 | Clinical and laboratory phenotype of human BCL10 deficiency (LOF *BCL10* mutations).

Mutation	**g.85741978C>T;IVS1+1G>A**
Age	6 months
Sex	M
Ethnicity	Amerindian
Consanguinity	+
Functional Impact	Loss
Inheritance	AR
Gene Expression	None
Protein Expression	None
INFECTIONS	
Pulmonary	+
Influenza A + B	+
RSV	+
Adenovirus	+
Gastrointestinal	+
Campylobacter jejuni	+
Clostridium difficile	+
Adenovirus	+
Oral	+
Candida albicans	+
CLINICAL MANIFESTATIONS	
Failure to thrive	–
Dysmorphic facies	–
Periodontal disease	–
Eczema	–
Enteropathy	+
Bronchiectasis	–
THERAPY	
Transplantation	–
Successful	N/A
IVIG	+
Anti-inflammatory	
Mesalazine	+
Antibiotics	+
Vancomycin	+
Metronidazole	+
Other	Levetiracetam
Outcome	Death
Cause of death	Respiratory failure
LYMPHOCYTES	
Total CD19 B cells	↑
Naive	↑
(Class-switched) memory	↓
Total CD3 T cells	↑
CD4	↑
CD4 Naïve	↑
CD4 CM	↓
CD4 EM	Normal
CD8	Normal
CD8 Naïve	↑
CD8 CM	↓
CD8 EM	Normal
Treg	↓
PROLIFERATION	
PHA	Normal
ConA	Normal
PWM	Normal
CD3+CD28	↓
IMMUNOGLOBULINS	
IgG	↓
IgA	↓
IgM	↓
IgE	Normal
Reference	(20)

Main clinical and immune findings of the single BCL10-deficient patient described to date. ↑, increased levels relative to normal range; ↓, decreased levels relative to normal range; +, present; –, absent; RSV, respiratory syncytial virus; CM, central memory; EM, effector memory.

percentages of circulating memory and class-switched B cells. Circulating naïve and transitional B cell counts typically decrease into adulthood, likely reflecting reduced output of immature B cells from the bone marrow. Conversely, patient T cell numbers are usually normal, unless chronic viral infection (e.g., EBV) is present. Histologic analyses of lymphoid tissues reveal follicular hyperplasia with an impressive expansion of naïve IgD^+ B cells in mantle zones, but normal numbers and distribution of $CD3^+$ T cells (26). Aside from selective B cell lymphocytosis, BENTA patients also exhibit features of primary immunodeficiency. All BENTA patients experienced frequent ear and sinus infections in early life, and opportunistic viral infections such as molluscum contagiosum and JC/BK virus are noted in some patients. Chronic EBV infection with moderate viremia is also found in ∼50% of BENTA patients (104).

Similar to specific antibody deficiency (SAD) (105), poor humoral immune responses are observed in most BENTA patients in response to T cell-independent vaccines such as pneumococcal and meningococcal polysaccharide vaccines, even with repeated boosts. Some patients also fail to mount lasting protective titers to T cell-dependent conjugate vaccines for pneumococcal bacteria (i.e., Prevnar), varicella-zoster virus (VZV), or measles. Low serum IgM and IgA levels are noted in some patients, with IgG being variable. *In vitro* studies of naïve patient B cells demonstrated impaired B cell differentiation into plasmablasts and long-lived plasma cells, consistent with poor IgG secretion in culture (106). These defects could be explained in part by a failed induction of specific factors required for plasma cell commitment, including BLIMP-1 and XBP-1. Conversely, in mice, ectopic expression of GOF *CARD11* variants in activated B cells promoted the transient expansion of self-reactive plasmablasts and autoantibody production (107). This discrepancy may be due to differences in mouse and human B cell differentiation requirements or may reflect the need for *in vivo* cytokines that were not provided *in vitro*. Nevertheless, profound apoptosis resistance was readily observed in both mouse and human B cells expressing GOF *CARD11* variants

TABLE 7 | Clinical and laboratory phenotype of human MALT1 deficiency (LOF *MALT1* mutations).

Mutation	**p.Trp580Ser**	**p.Ser89Ile**	**p.Ser89Ile**	**c.[1019-2A>G];[1060delC]**	**p.Asp184Tyr**	**p.Asp184Tyr**
Age	15yo	4yo	2.25yo	9–13 months	7yo	4yo
Sex	F	F	M	M	F	M
Ethnicity	Kurdish	Lebanese	Lebanese	American	ND	ND
Consanguinity	+	+	+	−	+	+
Functional Impact	Loss	Loss	Loss	Loss	Loss	Loss
Inheritance	AR	AR	AR	AD	AR	AR
Gene Expression	Normal	Normal	ND	Decreased/none	Normal	Normal
Protein Expression	↓↓↓	None	ND	None	None	None
INFECTIONS						
Pulmonary	+	+	+	+	+	+
Staphylococcus aureus	+	−	+	−	−	−
Streptococcus pneumoniae	+	+	−	−	+	−
Haemophilus influenzae	−	−	+	−	−	−
Klebsiella pneumoniae	−	−	+	−	−	−
Pneumocystis jirovecii	−	−	−	−	+	−
Pseudomonas	−	+	−	−	−	−
CMV	+	−	−	+	+	−
EBV	−	−	−	−	+	−
RSV	−	−	−	+	−	−
Adenovirus	−	−	−	−	+	+
Candida albicans	−	+	−	−	−	−
Gastrointestinal	−	+	+	+	+	+
Salmonella	−	−	−	−	+	+
Campylobacter jejuni	−	−	−	−	+	−
Clostridium difficile	−	−	−	+	−	−
CMV	−	−	−	−	+	−
EBV	−	−	−	−	+	−
Rotavirus	−	−	−	−	+	−
Adenovirus	−	−	−	−	+	−
Candida albicans	−	−	+	−	−	−
Skin	+	−	−	+	+	+
Staphylococcus aureus	+	−	−	+	−	−
Pseudomonas	−	−	−	−	−	+
HSV-1	+	−	−	−	+	+
VZV	+	−	−	−	−	−
Candida albicans	−	−	−	+	+	+
Blood	−	−	−	+	+	−
Staphylococcus aureus	−	−	−	−	+	−
Streptococcus pneumoniae	−	−	−	−	+	−
CMV	−	−	−	+	−	−
Urine	−	+	+	−	−	−
CMV	−	+	+	−	−	−
Meningitis	−	+	−	−	−	−
Haemophilus influenzae	−	+	−	−	−	−
Streptococcus pneumoniae	−	+	−	−	−	−
Keratitis	−	−	−	−	+	−
HSV-1	−	−	−	−	+	−
CLINICAL MANIFESTATIONS						
Failure to thrive	+	+	+	+	+	−
Dysmorphic facies	+	−	−	−	+	+
Periodontal disease	+	+	+	+	+	+
Eczema	+	−	−	+	+	+
Enteropathy	+	+	+	+	+	−
Bronchiectasis	+	+	+	−	+	−

(Continued)

TABLE 7 | Continued

Mutation	p.Trp580Ser	p.Ser89Ile	p.Ser89Ile	c.[1019-2A>G];[1060delC]	p.Asp184Tyr	p.Asp184Tyr
THERAPY						
Transplantation	+	−	−	+	+	+
Successful	+	N/A	N/A	+	+	+
IVIG	−	+	+	+	+	−
Anti-microbial prophylaxis	ND	ND	ND	+	+	+
Antibiotics	ND	ND	ND	+	+	+
TMP/SMX	ND	ND	ND	ND	+	+
ANTI-VIRAL						
Gancyclovir	−	−	−	+	−	−
Foscarnet	−	−	−	+	+	+
Acyclovir	−	−	−	−	+	+
IMMUNOSUPPRESSION						
Pre-transplantation	+	−	−	−	+	+
Treosulfan	−	−	−	−	−	−
Fludarabine	+	−	−	−	+	+
Busulfan	−	−	−	−	+	+
Alemtuzumab	+	−	−	−	+	+
Cyclophosphamide	−	−	−	+	−	−
Melphalan	−	−	−	+	−	−
R α-thymocyte globulin	−	−	−	+	−	−
Post-transplantation	+	−	−	+	+	+
Cyclosporine	+	−	−	+	+	+
Mycophenolate mofetil	+	−	−	−	+	+
Methylprednisone	+	−	−	−	−	−
Methotrexate	−	−	−	+	−	−
Tacrolimus	−	−	−	−	−	+
Outcome	Alive	Dead	Dead	Alive	Alive	Alive
Cause of death	N/A	Respiratory failure	Respiratory failure	N/A	N/A	N/A
LYMPHOCYTES						
Total CD19 B cells	↓	Normal	↓	Normal	Normal	Normal
Naive	↑	ND	ND	ND	ND	ND
(Class-switched) memory	↓	ND	ND	ND	ND	ND
MZ	↓	ND	ND	ND	ND	ND
Total CD3 T cells	↑	Normal	Normal	↑	↑	↑
CD4	↑	Normal	↑	↑	↑	↑
CD4 CD45RA	ND	Normal	Normal	Normal	Normal	↑
CD8	ND	↑	Normal	↑	Normal	↑
CD8 CD45RA	ND	ND	ND	↑	ND	ND
Treg	Normal	ND	ND	↓	↓	↓
PROLIFERATION						
PHA	↓	↓	↓	↓	↑	Normal
ConA	ND	↓	↓	↓	ND	ND
PWM	ND	↓	↓	Normal	ND	ND
CD3	ND	↓	↓	ND	ND	ND
CD3+CD28	ND	ND	ND	ND	↓	↓
Tetanus	ND	↓	↓	ND	ND	ND
Diphtheria	ND	↓	↓	ND	ND	ND
Candida	ND	↓	↓	ND	ND	ND
IMMUNOGLOBULINS						
IgG	Normal	Normal	Normal	↓	Normal	Normal
IgA	Normal	Normal	Normal	Normal	Normal	Normal
IgM	Normal	Normal	Normal	↓	↓	↓
IgE	↑	Normal	Normal	Normal	↑	↑

(Continued)

TABLE 7 | Continued

Mutation	p.Trp580Ser	p.Ser89Ile	p.Ser89Ile	c.[1019-2A>G];[1060delC]	p.Asp184Tyr	p.Asp184Tyr
Specific antibodies						
Tetanus	Positive	Negative	Negative	Negative	ND	ND
Pneumococcal	ND	Negative	Negative	Negative	ND	ND
Diphtheria	Positive	ND	ND	Negative	ND	ND
Isohemagglutinins	Positive	Negative	Negative	↓	ND	ND
Haemophilus influenzae B	ND	ND	ND	Negative	ND	ND
References	(22)	(21)	(21)	(23)	(24)	(24)

Summary of molecular, immunological, infectious, and pathological findings for all MALT1-deficient patients described to date. ND, no data; ↑, increased levels relative to normal range; ↓, decreased levels relative to normal range; +, present; −, absent; EBV, Epstein-Barr virus; HSV-1, herpes simplex encephalitis 1; VZV, varicella-zoster virus; R, rabbit.

and may be the most likely driver of B cell lymphocytosis in BENTA disease. Surprisingly, BENTA patient T cells are generally hyporesponsive in culture with poor proliferation and reduced IL-2 secretion (26). T cell function can largely be rescued by stronger stimulation or IL-2 supplementation *in vitro*, implying a mild state of anergy in BENTA T cells. Although autoantibodies are detected in a few patients, autoimmune disease symptoms are not common in BENTA patients, perhaps reflecting underlying B and T cell differentiation defects.

Most of the germline GOF *CARD11* mutations described in BENTA patients (p.Cys49Tyr, p.Gly123Ser, p.Gly123Asp, p.Phe130Ile, p.Glu134Gly) are also found as somatic GOF *CARD11* mutations in diffuse large B cell lymphoma (DLBCL) and other lymphoid malignancies (9, 108). In fact, knockdown of *CARD11* effectively kills DLBCL cell lines harboring GOF *CARD11* mutations, underscoring the connection between enhanced CBM signaling and B cell growth and survival. Remarkably, these single GOF mutations can disrupt the auto-inhibition of CARD11 conferred by several repressive elements within the inhibitory linker domain (109, 110). This allows CARD11 to adopt an open, active conformation and drive constitutive NF-κB activation via spontaneous aggregation, unimpeded recruitment of BCL10/MALT1, and IKKα/β phosphorylation, in the absence of antigen receptor engagement (26, 28, 109, 110). Indeed, spontaneous CARD11 aggregation and elevated NF-κB signaling is also observed in B and T cells from BENTA patients (26). In addition, the ectopic expression of BENTA-associated *CARD11* mutants in B and T cell lines results in the spontaneous assembly of large protein aggregates including CARD11, BCL10, MALT1, and phosphorylated IKKα/β, which induces constitutive NF-κB signaling independent of antigen receptor ligation (26, 28).

Despite highly congruent signaling pathways emanating from the TCR and BCR, constitutive activation of canonical NF-κB driven by GOF CARD11 mutations in BENTA disease leads to surprisingly distinct functional consequences in B and T cells. However, the mechanisms behind this dichotomy in B and T cell phenotypes remain unclear. Previous studies using conditional transgenic mice offer tantalizing parallels; while B cell-specific expression of constitutively active IKKβ (caIKKβ) promotes survival and proliferation even in the absence of B cell activating factor (BAFF) (111), restricted transgenic expression of caIKKβ renders murine T cells anergic and more susceptible to apoptosis, consistent with poor responses to bacterial infections (112). Collectively, studies of BENTA patients to date indicate that constitutive NF-κB can also lead to combined immunodeficiency, albeit less severe than patients harboring (DN) LOF CARD11 mutations. We therefore speculate that intrinsic B cell defects in BENTA disease most likely contribute to impaired humoral immunity and frequent infections with extracellular bacteria, while mildly anergic T cells could make BENTA patients more susceptible to certain viral infections.

Diagnosis and Treatment of BENTA

Patients presenting with splenomegaly, selective B cell lymphocytosis, and frequent sinopulmonary infections early in life should raise suspicion for BENTA disease. Sequencing of *CARD11* may find variants, particularly in the LATCH or CC domains. It is recommended that novel variants be confirmed experimentally (e.g., B or T cell line transfections to look for constitutive NF-κB activation) and cross-referenced to reported somatic mutations in lymphoma using Catalogue of Somatic Mutations in Cancer (COSMIC) (113) or related databases of oncogenic mutations.

At present, BENTA patients are clinically managed with supportive therapy, and minimal therapeutic interventions are available. Polyclonal B cell lymphocytosis in BENTA disease may predispose patients to B cell malignancies later in life. However, only two patients with confirmed malignancy have been reported to date: B cell CLL at ∼44 years in the original index patient (26), and another with Hodgkin's lymphoma at ∼50 years of age. Still, BENTA patients should be regularly monitored for B cell clonal outgrowth using flow cytometry and IgH heavy chain rearrangement analyses. The presence of EBV viremia may also heighten the risk of B cell lymphomagenesis.

Removal of the spleen is generally not recommended, given that circulating B cell counts rose dramatically in 3 patients after splenectomy, and splenectomy itself may put the patient at increased risk for certain bacterial infections (26, 28). One patient with a p.Gly123Asp mutation and an exceptionally high number of peripheral B cells after

splenectomy was treated with methotrexate for 4 years to restrain B cell counts and reduce the risk of stroke (28). Rituximab was effective in both this patient and another with respiratory distress and excessive lymphocytic nodules in her lungs. However, the utility of B cell depleting agents for BENTA should be evaluated on a case-by-case basis and may not be necessary as B cell lymphocytosis wanes over time. Intravenous or subcutaneous immunoglobulin therapy has also been administered in a few patients during childhood to control infections. Interestingly, MALT1 protease inhibitors, which specifically constrain CBM signaling output without completely blocking NF-κB activation, could be an attractive targeted treatment option for certain BENTA patients (see Novel Therapeutic Insights Emerging From Our Understanding of Human CBM-opathies section). These inhibitors are currently being explored for treating B cell lymphomas and autoimmune diseases (114–117).

BCL10

Role of BCL10 in Immunity

BCL10 was originally identified from a recurrent breakpoint (1p22) in mucosa-associated lymphoid tissue (MALT) B cell lymphomas possessing the t(1;14)(p22;q32) translocation, which caused BCL10 to be overexpressed (118). This observation, in combination with the finding that BCL10 could potently induce NF-κB activation (119, 120), highlighted its involvement in NF-κB signaling. BCL10 is a ∼27 kDa protein, which contains an N-terminal CARD domain and C-terminal serine/threonine rich region (**Figure 1**). Through CARD-CARD interactions, BCL10 can oligomerize with other CARD-containing proteins, including CARD9, CARD10, CARD11, and CARD14 (8, 75, 121–123) as well as MALT1 (7) to form various CBM complexes. These complexes collectively regulate both innate and adaptive immune processes in various cell types, although its lymphoid role is the main focus here. Like CARD11, BCL10 also undergoes various post-translational modifications that regulate CBM assembly and signaling and can form high order filamentous structures [reviewed in (124)]. The generation of *Bcl10*$^{-/-}$ mice defined key physiological roles for BCL10, particularly its essential role in antigen receptor signaling (**Table 1**) (14, 15, 86, 87).

Deletion of *Bcl10* in mice causes partial embryonic lethality (1/3 die) caused by issues with neural tube closure during development (14). Aside from this particular phenotype, *Bcl10*$^{-/-}$ mice were immunodeficient and generally resembled *Card11*$^{-/-}$ mice. They possessed normal total numbers of B and T cells, but decreased numbers of Tregs, natural killer T (NKT), B1, and MZ B cells (15, 86). Lymphocytes lacking Bcl10 failed to activate NF-κB, secrete pro-inflammatory cytokines, proliferate effectively in response to antigen receptor stimulation, and upregulate activation markers (14). Similar to CARD11-deficient mice, *Bcl10*$^{-/-}$ mice also had panhypogammaglobulinemia and impaired T-dependent humoral responses (15).

Interestingly, it was recently demonstrated that BCL10 also contributes to glutamine uptake via the ASCT2 transporter (as mentioned in the "Signaling to mTORC1" section), and together with CARD11 and MALT1, governs Th1 and Th17 polarization independent of the NF-κB pathway (64). However, another group found that BCL10 was dispensable in the phosphorylation of S6 (65). Thus, BCL10 contribution to this pathway is controversial and requires further investigation.

Loss-of-Function *BCL10* Mutations Causing Combined Immunodeficiency

A single case of BCL10 deficiency has been identified in a consanguineous Amerindian boy from Ecuador caused by homozygosity for a germline loss-of-function mutation (OMIM 616098) (20). The patient exhibited features of CID and immune dysregulation. WES discovered a homozygous splice site mutation (g.85741978C>T;IVS1+1G>A) affecting the invariant first nucleotide of intron 1 (donor site for splicing), which led to absent mRNA and protein expression. The patient had a complex clinical course, including respiratory infections positive for influenza A/B, adenovirus, respiratory syncytial virus, gastroenteritis, otitis, oral candidiasis and diaper dermatitis from *Candida albicans* superinfection, recurrent diarrhea positive for *Campylobacter jejuni*, adenovirus, and *Clostridium difficile* at different times, acute gastroenteritis positive for adenovirus, chronic colitis, and suspected encephalitis (**Table 6**). The patient eventually died due to respiratory failure.

Lymphocyte counts were generally normal, but B and T cells mostly displayed a naïve phenotype with an associated reduction in memory B and T cells and a profound absence of Tregs (**Table 6**). In keeping with the naïve phenotype, the patient also displayed hypogammaglobulinemia. Interestingly, in contrast to murine studies, patient myeloid cells responded normally to innate ligands (125–127), while fibroblasts displayed impaired NF-κB activation in response to Toll-like receptor (TLR)2/6, TLR4, and Dectin-1 stimulation as measured by NF-κB nuclear translocation and cytokine secretion (20). In addition, patient T cells displayed an impaired proliferative response to antigen receptor ligation (but not mitogen stimulation), and this was paired with a significant reduction in the expression of activation markers ICOS and CD25. Contrary to murine studies (14), CD69 expression was upregulated normally by T cells.

Diagnosis and Treatment of BCL10 Deficiency

BCL10 deficiency should be considered if a patient is found to have broad immune defects/CID affecting both innate (fibroblasts) and adaptive immunity (B and T cells), especially if a patient presents with severe inflammatory gastrointestinal (GI) and respiratory disease. Diagnostic clues include hypogammaglobulinemia, absent Tregs, and the presence of mostly naïve B and T cells with reduced memory compartments. Sequencing of BCL10 is likely to confirm a diagnosis, although functional assessment of novel BCL10 variants may be needed to definitively link the variant to the clinical phenotype. At this time, since only a single patient has been described and he died at the age of three from respiratory failure, validated treatment options remain unclear. However, based on our understanding of BCL10 biology, an allogeneic hematopoietic stem cell transplant would be anticipated to restore immune function by normalizing BCL10 protein expression and function in cells of hematopoietic origin.

MALT1

Role of MALT1 in Immunity

MALT1 paracaspase (also known as mucosa-associated lymphoid tissue lymphoma translocation protein 1) was first identified from MALT lymphomas possessing the chromosomal breakpoint t(11;18)(q21;q21) (128–131). This led to the formation of an oncogenic fusion protein of MALT1 with inhibitor of apoptosis (IAP2) called API2-MALT1. It was later found that API2-MALT1 was capable of interacting with BCL10 and potently inducing NF-κB activation (7).

MALT1 is a ∼92 kDa protein, which consists of an N-terminal death domain (DD), three immunoglobulin-like domains (Ig), and a caspase-like (paracaspase) domain (**Figure 1**). As mentioned in the BCL10 section, MALT1 exists in a complex with BCL10 (7), and together they associate with a variety of CARD proteins in response to stimulation to form the family of CBM complexes. This makes MALT1 an important regulator of both innate and adaptive immunity. Initially believed to act mostly as a scaffold for the recruitment of other NF-κB signaling proteins (e.g., TRAF6), MALT1 is now appreciated to also have important proteolytic activity (at mostly arginine residues), allowing it to cleave substrates involved in the regulation of NF-κB, JNK, mTORC1, and more [reviewed in (114, 132)] (**Figure 2**). There are currently a total of ten validated MALT1 paracaspase substrates: A20 (133), BCL10 (134), CYLD (135), RelB (136), Regnase-1 (137, 138), Roquin-1/2 (138), MALT1 (139), HOIL1 (140–142), NIK (143), and LIMA1α (144), with more likely to be discovered. By cleaving these substrates, MALT1 can positively regulate canonical NF-κB (A20), JNK (CYLD), DNA binding of RelA and c-Rel (RelB), and mRNA stability (Regnase-1 and Roquin-1/2). However, MALT1 protease activity may also negatively regulate NF-κB activity (HOIL1). How MALT1 paracaspase activity fine-tunes immune function in different cellular contexts is an area of intense research activity.

In order to better understand the physiological roles of MALT1, two important murine models have been generated: the *Malt1*$^{-/-}$ mouse and the MALT1 paracaspase dead/mutated mouse (*Malt1*$^{PD/PD}$) (**Table 1**). *Malt1*$^{-/-}$ mice share many features with *Card11*$^{-/-}$ and *Bcl10*$^{-/-}$ mice, including having generally normal total numbers of B and T cells, diminished innate B cells (MZ and B1), severely impaired Treg numbers, and panhypogammaglobulinemia paired with compromised T-dependent antibody responses (16, 88–91). In response to stimulation, both B and T cells proliferate poorly, with T cells being more profoundly impacted as measured by the activation of NF-κB, JNK, p38, and the upregulation of activation markers. In addition, *Malt1*$^{-/-}$ mice had absent germinal center B cells with an associated decrease in T follicular helper (Tfh) cells. Together, these studies confirmed that MALT1 is an essential regulator of T cell activation and Treg development. The contribution of MALT1 to B cell activation remains less clear.

Malt1$^{PD/PD}$ mice on the other hand, had intact MALT1 protein expression and scaffolding activity, but abrogated paracaspase function (89, 91–93). Surprisingly, these mice developed spontaneous multi-organ inflammation, including autoimmune gastritis, which was not seen in MALT1-deficient mice. Interestingly, immune findings between the two mouse models were quite similar, including decreased MZ, B1 cells, Tregs, and proliferation, although these phenotypes were less pronounced in *Malt1*$^{PD/PD}$ mice. In contrast to its scaffolding function, protease activity was mostly dispensable for NF-κB and JNK activation. Interestingly, *Malt1*$^{PD/PD}$ mice possessed expanded Th1, Th2, Th17 phenotypes, CD4^{+} and CD8^{+} effector T cells, and elevated IFN-γ, IgE, and IgG. These studies highlighted the unique contributions of MALT1 scaffolding and paracaspase functions in signaling and lymphocyte development; for example, IKK and JNK activation were dependent on the scaffolding role rather than protease activity. In particular, it seems proteolytic activity is important for the development of anti-inflammatory Tregs as well as controlling excessive IFN-γ secretion and accumulation of effector T cells (93). More studies are needed to understand the exact factors and cell populations mediating this inflammatory phenotype. It is possible that this inflammatory phenotype may be mediated in part by the lack of Tregs and the inability of MALT1 to cleave HOIL1 to turn off NF-κB activation (114).

Loss-of-Function MALT1 Mutations Causing Combined Immunodeficiency

Germline loss-of-function mutations in MALT1 cause CID (OMIM 615468). To date, six cases of MALT1 deficiency have been reported (21–24) (**Figure 1** and **Table 7**). This includes a 4-year-old girl and 2-year-old boy who were both homozygous for the p.Ser89Ile mutation (21), a 15-year-old Kurdish-Canadian girl homozygous for the p.Trp580Ser mutation (22), a 1-month-old boy who was compound heterozygous for c.[1019-2A>G];[1060delC] mutations (23), and a 4-year-old boy and 7-year-old girl who were both homozygous for the p.Asp184Tyr mutation (24). All patients were identified by next generation sequencing techniques; the majority were found by WES (5/6 patients) and one case was discovered by whole genome sequencing (21). Most patients were born to consanguineous parents (4/6 patients) and possessed homozygous mutations, while one patient possessed *de novo* compound heterozygous mutations (23). These mutations span the length of the MALT1 protein, including the DD (21), the first Ig-like domain (24), the paracaspase domain (23), and the third Ig-like domain (22) and generally caused no MALT1 protein to be expressed (**Figure 1**).

MALT1 deficiency is characterized by recurrent sinopulmonary infections, enteropathy, eczema, periodontal disease, and failure to thrive (6). Indeed, patients typically presented with recurrent bacterial, viral, and fungal infections affecting the lungs (6/6 patients), skin (3/6 patients), and GI tract (3/6 patients) (**Table 7**). However, some patients experienced bloodborne infections, including one patient who had *Staphylococcus aureus* and *Streptococcus pneumoniae* bacteremia (24) and another who had CMV viremia (23). One of the patients also had meningitis positive for *Streptococcus pneumoniae* and *Haemophilus influenzae* (21).

Periodontal disease (6/6 patients) was common to all patients, with many developing aphthous ulcers, cheilitis, gingivitis, and thrush (21–24, 145). In addition, both dermatitis (4/6 patients) and inflammatory GI disease (5/6 patients) were frequently

reported findings. Consequently, significant T cell infiltration in the skin and or the GI tract was found in biopsies (21–24). Developmentally, half of the patients had abnormal facial features (although these may be related to inflammatory changes affecting the oral cavity) (22, 24) and the majority had failure to thrive (5/6 patients).

Some patients had additional unique presentations of disease. The patient carrying the p.Trp580Ser was found to have very low bone density and suffered from fractures due to low-impact injuries (22). She also recurrently generated granulation tissue on her vocal cords, larynx, and external auditory canal. In addition, the two patients carrying the p.Ser89Ile mutation also developed mastoiditis (21).

Immunophenotyping of these MALT1-deficient patients found generally normal (21, 23, 24) or decreased (21, 22) B cell numbers. Interestingly, in contrast to other patients, the p.Trp580Ser mutation was associated with a developmental block in their B cell compartment characterized by absent MZ B cells, reduced transitional and class-switched memory B cells, and elevated naïve B cells (22). Despite relatively normal B cell populations, only the p.Ser89Ile siblings had normal serum immunoglobulin titers (21), while half of the patients possessed diminished IgM (23, 24) and elevated IgE (22, 24). On the other hand, $CD3^+$ and $CD4^+$ T cells were found to be expanded in most patients (4/6 patients) with the exception of the p.Ser89Ile siblings (21) who were within the normal range. $CD8^+$ T cells were mostly elevated (3/5 patients) or within the normal range. Similar to CARD11- and BCL10-deficient patients, these patients also generally had diminished Tregs (3/4 patients). All MALT1-deficient patient T cells showed impaired proliferation in response to PHA or α-CD3/CD28 stimulation. In line with impaired T cell responses, most patients also possessed poor vaccine antibody titers (3/4 patients) (21–23).

Biochemical characterization of patient cells demonstrated completely abrogated NF-κB phosphorylation and/or IκBα degradation, along with diminished IL-2 secretion (21–24). In addition, McKinnon et al. was also able to demonstrate impaired paracaspase activity as measured by BCL10 cleavage (22). Using these MALT1-deficient patient cells, the same group discovered the novel MALT1 substrate HOIL1 (140). This defined a novel negative regulatory role for MALT1 in NF-κB signaling, where, by cleaving HOIL1, linear ubiquitination-mediated signaling and inflammation is decreased/turned off. It is possible that in MALT1-deficient patients, the loss of MALT1 proteolytic activity on HOIL1 leads to an accumulation in linear ubiquitination, resulting in unrestricted NF-κB activation and chronic inflammation, thus contributing to the exaggerated skin and mucosal inflammation seen in MALT1-deficient patients (140).

TABLE 8 | "Red flags" suggestive of human MALT1 deficiency.

Clinical features	Proportion	Penetrance (%)
INFECTIONS (BACTERIAL/VIRAL/FUNGAL)		
Pulmonary	6/6	100
Skin	3/6	50
Gastrointestinal tract	3/6	50
ORGAN INVOLVEMENT		
Periodontal disease	6/6	100
Gastrointestinal inflammation	5/6	83
Dermatitis	4/6	67
DEVELOPMENT		
Failure to thrive	5/6	83
Abnormal Facies	3/6	50
LABORATORY TESTS		
Cell populations		
Normal lymphocytes numbers	3/4	75
↓ Treg	3/4	75
Normal B cells	4/6	67
↑ $CD3^+$, $CD4^+$ T cells	4/6	67
↑ $CD8^+$ T cells	3/5	60
Response		
↓ T cell proliferation (PHA, α-CD3/CD28)	6/6	100
↓ NF-κB phosphorylation/IκBα degradation	6/6	100
↓ IL-2 secretion	6/6	100
Ig		
↓ specific antibodies	3/4	75
↓ IgM	3/6	50
↑ IgE	3/6	50

Common features found in MALT1-deficient patients. Included are proportion of patients where data is available and the percentage of patients with that finding. ↑, increased levels relative to normal range; ↓, decreased levels relative to normal range.

Diagnosis and Treatment of MALT1 Deficiency

All cases of MALT1 deficiency described to date have been discovered by next generation sequencing. However, based on this small cohort of patients, there are some diagnostic clues that raise suspicion for MALT1 deficiency (**Table 8**). Specifically, MALT1 deficiency should be considered in patients who present with the majority of the following: (i) severe recurrent sinopulmonary infections positive for bacteria or viruses, (ii) severe inflammatory GI disease, (iii) eczematous rash, (iv) severe periodontal disease, and (v) failure to thrive. Diagnostic testing "red flags" include finding relatively normal lymphocyte and B cell numbers, expanded $CD3^+$ and $CD4^+$ T cell subsets, impaired T cell proliferation, and compromised NF-κB phosphorylation, IκBα degradation, and IL-2 secretion.

MALT1 deficiency can be cured by hematopoietic stem cell transplantation (4/6 patients received successful transplants) (23, 24, 146). Highlighting the value of curative transplantation, the siblings homozygous for the p.Ser89Ile were not transplanted and they continued to experience persistent infections until their eventual deaths due to respiratory failure at the ages of 7 and 13.5 years (21). Successful donor choices have included: bone marrow from an HLA-matched sibling (p.Trp580Ser patient) (146); peripheral stem cells from two unrelated 10/10 HLA-matched donors (p.Asp184Tyr siblings) (24); and peripheral stem cells from an unrelated 9/10 HLA-matched donor (c.[1019-2A>G];[1060delC] patient) (23). Despite successful engraftment being achieved in these patients, there were some noteworthy post-transplantation complications. The p.Trp580Ser patient

experienced a range of infections including CMV, Epstein-Barr virus (EBV), VZV, and herpes simplex virus-1 (HSV-1), adenovirus viremia, *Staphylococcus aureus* bacteremia, *Klebsiella pneumoniae* pneumonia, extended spectrum beta-lactamase positive *Streptococcus pneumoniae* and *Escherichia coli*, BK virus-associated hemorrhagic cystitis, and rotavirus-associated gastroenteritis (146). The c.[1019-2A>G];[1060delC] patient developed diarrhea and CMV viremia (23). The p.Asp184Tyr siblings developed transient CMV viremia and the younger brother developed an adenovirus infection as well as bacterial pneumonia (24).

CBM MUTATIONS IN RELATION TO OTHER PRIMARY ATOPIC TCR-MEDIATED DISORDERS

Germline MALT1 and CARD11 mutations can be considered primary atopic disorders in that they are associated with early-onset, severe atopic disease, amongst other comorbidities (99). Primary atopic disorders are often associated with primary immunodeficiency, most commonly caused by mutations in cytokine signaling or disruptions in TCR signaling or repertoire. Atopy is hypothesized to be caused by the propensity of naïve CD4 T cells to skew toward Th2 differentiation when relatively weak TCR signals are delivered (147). While CBM-associated mutations are the most directly linked to TCR signaling, other disruptions which can indirectly impact TCR signaling to cause atopic disease include actin cytoskeleton remodeling genes such as dedicator of cytokinesis 8 (DOCK8) deficiency (148), Wiskott-Aldrich Syndrome (WAS) protein interacting protein (WIP) deficiency (149), Wiskott-Aldrich Syndrome (150), actin related protein 2/3 (ARP2/3) complex mutations (151–153) and, potentially, ZAP70 deficiency (154, 155). The clinical presentation of DOCK8 deficiency is somewhat similar to CBM mutation-associated atopy, though infectious and neoplastic manifestations are more severe. WIP-, WAS- and ARP2/3-associated disease have more systemic manifestations including thrombocytopenia likely due to more broad protein expression patterns. In addition, the clearest TCR repertoire defect associated with atopic disease is Omenn syndrome, which is caused by hypomorphic mutations in most genes associated with SCID [including one CARD11-deficient case (19)], and results in an oligoclonal expansion of CD4 T cells. This, in turn, leads to severe dermatitis, elevated IgE, eosinophilia, and lymphoproliferation.

COMPARING AND CONTRASTING CBM-OPATHIES: UNANSWERED QUESTIONS

In adaptive immunity, the CBM complex functions in a highly synergistic manner. In line with this, CARD11-, BCL10-, and MALT1-deficient patients share many features, including having CID/SCID with normal total B and T cell numbers, aberrant B and T cell subsets, little-to-no Tregs, impaired T cell proliferation, and recurrent bacterial/viral infections (17–24). As a group, patients with these CBM-opathies have established that the CBM complex is a critical regulator of human Treg development and tolerance; however, the exact mechanisms by which this occurs are not completely understood. In murine models, it is thought that the ability of the CBM complex to modulate TCR signal strength and transduce signals downstream of the IL-2R contribute significantly to this process (33, 88, 89, 92, 93, 156).

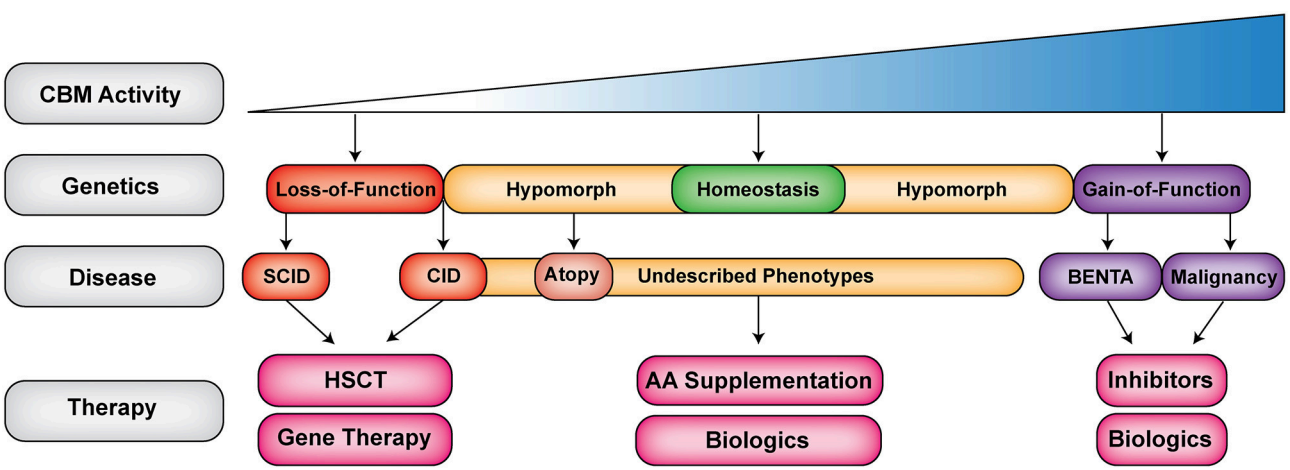

FIGURE 3 | The expanding clinical spectrum of CBM-opathies. Shown is a gradient of CBM activity caused by germline mutations. Activity ranges from absent to hyperactive CBM activity. Red indicates loss-of-function (LOF) mutations (CARD11, BCL10, and MALT1 deficiencies), yellow indicates hypomorphic mutations that do not completely abrogate signaling leading to combined immunodeficiency and atopy as well as novel emerging phenotypes (DN LOF *CARD11*), purple indicates gain-of-function (GOF) mutations that can lead to BENTA (GOF *CARD11*) or malignancy (somatic GOF in CBM). Biologics refer to antibodies, which target cells, cytokines or cell surface receptors. SCID, severe combined immunodeficiency; CID, combined immunodeficiency; AA, amino acid; HSCT, hematopoietic stem cell transplantation.

While CARD11 is mostly restricted to hematopoietic cells, BCL10 and MALT1 have much broader cellular expression and associate with other CARD proteins downstream of a diverse assortment of receptors (66). Thus, individual CBM-opathies each have their own unique features (**Figure 3**). For example, CARD11-deficient patients characteristically exhibit panhypogammaglobulinemia, which is not present in MALT1 or BCL10 deficiency. In contrast, all CBM-deficient mice have panhypogammaglobulinemia. This demonstrates both important differences between mouse models and human patients as well as an incomplete understanding of how the CBM complex regulates antibody production. Another clinical feature that varies between the CBM-opathies is susceptibility to *Pneumocystis jirovecii* pneumonia (PJP). PJP is a very common infection in CARD11 deficiency (reported in 75% of identified patients) but is not a reported pathogen in MALT1 and BCL10 deficiency. It is still not known why *Pneumocystis jirovecii* seems to preferentially infect CARD11-deficient patients.

Moving beyond infections, both MALT1- and BCL10-deficient patients presented simultaneously with immunodeficiency and immune dysregulation, where in addition to recurrent infections, they also developed inflammatory gastrointestinal disease (20–24). These features were not present in CARD11-deficient patients, nor were they found in *Card11*$^{-/-}$, *Malt1*$^{-/-}$, and *Bcl10*$^{-/-}$ mice. In fact, the pharmacological inhibition of MALT1 in dextran sulfate solution (DSS)-induced colitis was found to be protective through the inhibition of NF-κB and NLRP3 inflammasome activation in macrophages (157), and a T cell-dependent transfer model of autoimmune colitis found that *Malt1*$^{-/-}$ T cells were unable to induce colitis (92). However, it is important to note that *Malt1*$^{PD/PD}$ mice developed inflammatory gastrointestinal disease, and this was associated with an expansion of Th1, Th2, and Th17, with increased inflammatory cytokines and IgE, which was not present in the *Malt1*$^{-/-}$ mice (89, 91–93). It is tempting to speculate that the diminished Tregs, dysregulated tolerance, and lack of MALT1 paracaspase regulation collectively mediated the inflammatory phenotype in patients. In addition, both MALT1-deficient and BCL10-deficient patients displayed elevated CD3^{+} and CD4^{+} T cells, but it is not known whether there was any skewing in Th1 and Th2 responses (as is the case in *Malt1*$^{PD/PD}$ mice), which could be significant pro-inflammatory cytokine secretors, thus contributing to pathology. It should also be noted that MALT1 and BCL10 have wider expression than CARD11 and some non-hematopoietic cells in these patients could be contributing to the gastrointestinal pathology.

GOF and DN LOF *CARD11* mutations give rise to considerably different phenotypes from CBM-deficiencies, with GOF manifesting chiefly as selective B cell lymphocytosis and DN LOF leading to severe atopic disease. Deeper mechanistic studies are needed to address several outstanding questions, including (i) how GOF *CARD11* mutations dampen T cell responsiveness, (ii) whether GOF *CARD11* mutations enhance JNK and mTORC1 signaling, and how this contributes to differential T and B cell responses, (iii) if/how DN *CARD11* mutations ultimately skew Th2 responses via decreased NF-κB signaling and/or restricted CARD11-dependent glutamine uptake, and (iv) whether DN *CARD11* mutations affect B cell intrinsic signaling, including the fate of class-switched IgE^{+} B cells. Overall, shared phenotypes in BENTA and CADINS patients (e.g., poor antibody responses, increased respiratory and skin infections) emphasize the requirement for properly "tuned" CBM signaling to ensure proper B and T cell differentiation in response to antigens in order to maintain immune homeostasis.

NOVEL THERAPEUTIC INSIGHTS EMERGING FROM OUR UNDERSTANDING OF HUMAN CBM-OPATHIES

CBM-opathies have been invaluable in enhancing our understanding of how dysregulated CBM complex signaling contributes to the pathogenesis of various diseases including immunodeficiency, atopic disease (94), autoimmunity (158), and malignancies (159). Given the role of the CBM complex in a range of human pathologies, there is considerable interest in developing and studying therapeutics that can target/ameliorate these diseases. In the realm of cancer, targeting either the CBM complex or the catalytic function of MALT1 have been the methods of choice (160). In particular, MALT1 inhibitors have received a great deal of attention for their specificity and efficiency. These inhibitors may eventually be promising options for treating cancers and diseases that have a lymphoproliferative component, including BENTA (104). However, given the central position of the CBM complex in signaling, inhibition should be approached with caution. Here, LOF mutations in individual CBM components and the recent characterization of *Malt1*$^{PD/PD}$ mice have been uniquely informative in highlighting possible side effects that can arise from the therapeutic inhibition of the CBM complex, including decreasing Tregs and tolerance (114).

Currently, the treatment of complete CARD11, BCL10, and MALT1 deficiencies relies upon hematopoietic stem cell transplantation in order to functionally normalize immune function (with immunoglobulin replacement and prophylactic antimicrobials used as supportive therapy). Without transplantation, the survival rate is very low. Moving forward, autologous gene therapy may be an attractive therapeutic option, whereby patient hematopoietic stem cells could be "corrected" by genetic approaches (e.g., viral transduction or CRISPR/Cas9 editing) and re-infused to give rise to a normal immune system (161). In support of this approach, transplantation outcomes have been quite good for CBM deficiency patients (17, 146) and the artificial expression of WT genes in patient cells is able to rescue NF-κB activation (22). Further proof of concept studies in mice or patient stem cells will have to be done to determine efficacy and safety.

The initial description of *Card11*$^{un/un}$ mice (13) paired with the recent discovery of DN LOF mutations in CARD11 causing atopy and immunodeficiency (31, 32), implicated the CBM complex in the pathogenesis of allergic disease. Affected patients were found to have decreased upregulation of ASCT2 and impaired mTORC1 signaling, which is thought to contribute to Th2 skewing (32). Since it was previously shown that

impaired mTORC1 signaling and Th1 differentiation could be rescued by glutamine supplementation (64), Ma et al. tested whether glutamine supplementation could rescue the phenotype of patient cells. Interestingly, this was able to partially rescue signaling defects (32). This demonstrated that modulating immune metabolism through amino acid supplementation could be useful for therapy. Indeed, glutamine supplementation is currently being explored in low birth weight infants for the reduction of atopic dermatitis and has shown some success (162).

CONCLUDING REMARKS

The CBM complex is an essential molecular bridge linking cell surface antigen receptor signaling with downstream activation of NF-κB, JNK, and mTORC1. This makes it a critical regulator of lymphocyte activation, differentiation, proliferation, maintenance, and metabolism. Since the discovery of germline loss-of-function mutations in CARD11 causing SCID just 5 years ago (17), ∼48 patients with genetically confirmed CBM-opathies have been described. Germline mutations in this complex have led to an impressive spectrum of diseases, ranging from CID/SCID to CID with atopy to BENTA disease (**Figure 3**). The detailed study of these rare patients with CBM-opathies has provided unique insights into how the CBM complex regulates human immune reactivity and tolerance. Ultimately, the discovery and characterization of more CBM-opathies will not only benefit the affected patients but will broadly inform any future therapeutic targeting of these signaling pathways in cancer, autoimmunity, and allergic disease.

AUTHOR CONTRIBUTIONS

All authors listed have made a substantial, direct and intellectual contribution to the work, and approved it for publication.

FUNDING

This work was supported in part by the Canadian Institutes of Health Research (CIHR), Genome British Columbia (SIP007 to ST), the National Institutes of Health (NIH) (R21AI109187 to AS), the Canadian Allergy, Asthma and Immunology Foundation, and the BC Children's Hospital Foundation. ST also holds the Aubrey J. Tingle Professorship in Pediatric Immunology and is a clinical scholar of the Michael Smith Foundation for Health Research. HL is supported by the Shaughnessy Hospital Volunteer Society Fellowship in Healthcare, Theodore E Arnold Fellowship, and University of British Columbia Faculty of Medicine Graduate Award.

REFERENCES

1. Picard C, Bobby Gaspar H, Al-Herz W, Bousfiha A, Casanova JL, Chatila T, et al. International union of immunological societies: 2017 primary immunodeficiency diseases committee report on inborn errors of immunity. *J Clin Immunol*. (2018) 38:96–128. doi: 10.1007/s10875-017-0464-9
2. Tak PP, Firestein GS. NF-kappaB: a key role in inflammatory diseases. *J Clin Invest*. (2001) 107:7–11. doi: 10.1172/JCI11830
3. Karin M. NF-kappaB as a critical link between inflammation and cancer. *Cold Spring Harb Perspect Biol*. (2009) 1:a000141. doi: 10.1101/cshperspect.a000141
4. Sun SC, Chang JH, Jin J. Regulation of nuclear factor-kappaB in autoimmunity. *Trends Immunol*. (2013) 34:282–9. doi: 10.1016/j.it.2013.01.004
5. Zhang Q, Lenardo MJ, Baltimore D. 30 Years of NF-kappaB: A Blossoming of relevance to human pathobiology. *Cell* (2017) 168:37–57. doi: 10.1016/j.cell.2016.12.012
6. Turvey SE, Durandy A, Fischer A, Fung SY, Geha RS, Gewies A, et al. The CARD11-BCL10-MALT1 (CBM) signalosome complex: Stepping into the limelight of human primary immunodeficiency. *J Allergy Clin Immunol*. (2014) 134:276–84. doi: 10.1016/j.jaci.2014.06.015
7. Lucas PC, Yonezumi M, Inohara N, McAllister-Lucas LM, Abazeed ME, Chen FF, et al. Bcl10 and MALT1, independent targets of chromosomal translocation in malt lymphoma, cooperate in a novel NF-kappa B signaling pathway. *J Biol Chem*. (2001)276:19012–9. doi: 10.1074/jbc.M009984200
8. Gaide O, Martinon F, Micheau O, Bonnet D, Thome M, Tschopp J. Carma1, a CARD-containing binding partner of Bcl10, induces Bcl10 phosphorylation and NF-kappaB activation. *FEBS Lett*. (2001) 496:121–7. doi: 10.1016/S0014-5793(01)02414-0
9. Lenz G, Davis RE, Ngo VN, Lam L, George TC, Wright GW, et al. Oncogenic CARD11 mutations in human diffuse large B cell lymphoma. *Science*. (2008) 319:1676–9. doi: 10.1126/science.1153629
10. Davis RE, Ngo VN, Lenz G, Tolar P, Young RM, Romesser PB, et al. Chronic active B-cell-receptor signalling in diffuse large B-cell lymphoma. *Nature*. (2010) 463:88–92. doi: 10.1038/nature08638
11. Hara H, Wada T, Bakal C, Kozieradzki I, Suzuki S, Suzuki N, et al. The MAGUK family protein CARD11 is essential for lymphocyte activation. *Immunity*. (2003)18:763–75. doi: 10.1016/S1074-7613(03)00148-1
12. Egawa T, Albrecht B, Favier B, Sunshine MJ, Mirchandani K, O'Brien W, et al. Requirement for CARMA1 in antigen receptor-induced NF-kappa B activation and lymphocyte proliferation. *Curr Biol*. (2003) 13:1252–8. doi: 10.1016/S0960-9822(03)00491-3
13. Jun JE, Wilson LE, Vinuesa CG, Lesage S, Blery M, Miosge LA, et al. Identifying the MAGUK protein Carma-1 as a central regulator of humoral immune responses and atopy by genome-wide mouse mutagenesis. *Immunity*. (2003) 18:751–62. doi: 10.1016/S1074-7613(03)00141-9
14. Ruland J, Duncan GS, Elia A, del Barco Barrantes I, Nguyen L, Plyte S, et al. Bcl10 is a positive regulator of antigen receptor-induced activation of NF-kappaB and neural tube closure. *Cell*. (2001) 104:33–42. doi: 10.1016/S0092-8674(01)00189-1
15. Xue L, Morris SW, Orihuela C, Tuomanen E, Cui X, Wen R, et al. Defective development and function of Bcl10-deficient follicular, marginal zone and B1 B cells. *Nat Immunol*. (2003)4:857–65. doi: 10.1038/ni963
16. Ruefli-Brasse AA, French DM, Dixit VM. Regulation of NF-kappaB-dependent lymphocyte activation and development by paracaspase. *Science*. (2003) 302:1581–4. doi: 10.1126/science.1090769
17. Stepensky P, Keller B, Buchta M, Kienzler AK, Elpeleg O, Somech R, et al. Deficiency of caspase recruitment domain family, member 11 (CARD11), causes profound combined immunodeficiency in human subjects. *J Allergy Clin Immunol*. (2013) 131:477–85 e1. doi: 10.1016/j.jaci.2012.11.050.
18. Greil J, Rausch T, Giese T, Bandapalli OR, Daniel V, Bekeredjian-Ding I, et al. Whole-exome sequencing links caspase recruitment domain 11 (CARD11) inactivation to severe combined immunodeficiency. *J Allergy Clin Immunol*. (2013) 131:1376–83 e3. doi: 10.1016/j.jaci.2013.02.012
19. Fuchs S, Rensing-Ehl A, Pannicke U, Lorenz MR, Fisch P, Jeelall Y, et al. Omenn syndrome associated with a functional reversion due to a somatic second-site mutation in CARD11 deficiency. *Blood* (2015) 126:1658–69. doi: 10.1182/blood-2015-03-631374
20. Torres JM, Martinez-Barricarte R, Garcia-Gomez S, Mazariegos MS, Itan Y, Boisson B, et al. Inherited BCL10 deficiency impairs hematopoietic

and nonhematopoietic immunity. *J Clin Invest.* (2014) 124:5239–48. doi: 10.1172/JCI77493
21. Jabara HH, Ohsumi T, Chou J, Massaad MJ, Benson H, Megarbane A, et al. A homozygous mucosa-associated lymphoid tissue 1 (MALT1) mutation in a family with combined immunodeficiency. *J Allergy Clin Immunol.* (2013) 132:151–8. doi: 10.1016/j.jaci.2013.04.047
22. McKinnon ML, Rozmus J, Fung SY, Hirschfeld AF, Del Bel KL, Thomas L, et al. Combined immunodeficiency associated with homozygous MALT1 mutations. *J Allergy Clin Immunol.* (2014)133:1458–62, 62 e1-7. doi: 10.1016/j.jaci.2013.10.045
23. Punwani D, Wang H, Chan AY, Cowan MJ, Mallott J, Sunderam U, et al. Combined immunodeficiency due to MALT1 mutations, treated by hematopoietic cell transplantation. *J Clin Immunol.* (2015) 35:135–46. doi: 10.1007/s10875-014-0125-1
24. Charbit-Henrion F, Jeverica AK, Begue B, Markelj G, Parlato M, Avcin SL, et al. Deficiency in mucosa-associated lymphoid tissue lymphoma translocation 1: a novel cause of IPEX-Like Syndrome. *J Pediatr Gastroenterol Nutr.* (2017) 64:378–84. doi: 10.1097/MPG.0000000000001262
25. Biggs CM, Lu HY, Turvey SE. Monogenic immune disorders and severe atopic disease. *Nat Genet.* (2017) 49:1162–3. doi: 10.1038/ng.3925
26. Snow AL, Xiao W, Stinson JR, Lu W, Chaigne-Delalande B, Zheng L, et al. Congenital B cell lymphocytosis explained by novel germline CARD11 mutations. *J Exp Med.* (2012) 209:2247–61. doi: 10.1084/jem.20120831
27. Buchbinder D, Stinson JR, Nugent DJ, Heurtier L, Suarez F, Sukumar G, et al. Mild B-cell lymphocytosis in patients with a CARD11 C49Y mutation. *J Allergy Clin Immunol.* (2015) 136:819–21 e1. doi: 10.1016/j.jaci.2015.03.008
28. Brohl AS, Stinson JR, Su HC, Badgett T, Jennings CD, Sukumar G, et al. Germline CARD11 mutation in a patient with severe congenital B Cell Lymphocytosis. *J Clin Immunol.* (2015) 35:32–46. doi: 10.1007/s10875-014-0106-4
29. Gupta M, Aluri J, Desai M, Lokeshwar M, Taur P, Lenardo M, et al. Clinical, Immunological, and molecular findings in four cases of B Cell expansion with NF-κB and T Cell anergy disease for the first time from India. *Front Immunol.* (2018) 9:1049. doi: 10.3389/fimmu.2018.01049
30. Outinen T, Syrjanen J, Rounioja S, Saarela J, Kaustio M, Helminen M. Constant B cell lymphocytosis since early age in a patient with CARD11 mutation: a 20-year follow-up. *Clin Immunol.* (2016) 165:19–20. doi: 10.1016/j.clim.2016.02.002
31. Dadi H, Jones TA, Merico D, Sharfe N, Ovadia A, Schejter Y, et al. Combined immunodeficiency and atopy caused by a dominant negative mutation in caspase activation and recruitment domain family member 11 (CARD11). *J Allergy Clin Immunol.* (2018) 141:1818–30 e2. doi: 10.1016/j.jaci.2017.06.047
32. Ma CA, Stinson JR, Zhang Y, Abbott JK, Weinreich MA, Hauk PJ, et al. Germline hypomorphic CARD11 mutations in severe atopic disease. *Nat Genet.* (2017) 49:1192–201. doi: 10.1038/ng.3898
33. Roche MI, Ramadas RA, Medoff BD. The role of CARMA1 in T cells. *Crit Rev Immunol.* (2013) 33:219–43. doi: 10.1615/CritRevImmunol.2013007056
34. Meininger I, Krappmann D. Lymphocyte signaling and activation by the CARMA1-BCL10-MALT1 signalosome. *Biol Chem.* (2016) 397:1315–33. doi: 10.1515/hsz-2016-0216
35. Hu H, Sun SC. Ubiquitin signaling in immune responses. *Cell Res.* (2016) 26:457–83. doi: 10.1038/cr.2016.40
36. Bojarczuk K, Bobrowicz M, Dwojak M, Miazek N, Zapala P, Bunes A, et al. B-cell receptor signaling in the pathogenesis of lymphoid malignancies. *Blood Cells Mol Dis.* (2015) 55:255–65. doi: 10.1016/j.bcmd.2015.06.016
37. Woyach JA, Johnson AJ, Byrd JC. The B-cell receptor signaling pathway as a therapeutic target in CLL. *Blood* (2012) 120:1175–84. doi: 10.1182/blood-2012-02-362624
38. Huse M. The T-cell-receptor signaling network. *J Cell Sci.* (2009) 122:1269–73. doi: 10.1242/jcs.042762
39. Matsumoto R, Wang D, Blonska M, Li H, Kobayashi M, Pappu B, et al. Phosphorylation of CARMA1 plays a critical role in T Cell receptor-mediated NF-kappaB activation. *Immunity* (2005) 23:575–85. doi: 10.1016/j.immuni.2005.10.007
40. Sommer K, Guo B, Pomerantz JL, Bandaranayake AD, Moreno-Garcia ME, Ovechkina YL, et al. Phosphorylation of the CARMA1 linker controls NF-kappaB activation. *Immunity* (2005) 23:561–74. doi: 10.1016/j.immuni.2005.09.014
41. Qiao Q, Yang C, Zheng C, Fontan L, David L, Yu X, et al. Structural architecture of the CARMA1/Bcl10/MALT1 signalosome: nucleation-induced filamentous assembly. *Mol Cell* (2013) 51:766–79. doi: 10.1016/j.molcel.2013.08.032
42. David L, Li Y, Ma J, Garner E, Zhang X, Wu H. Assembly mechanism of the CARMA1-BCL10-MALT1-TRAF6 signalosome. *Proc Natl Acad Sci USA.* (2018) 115:1499–504. doi: 10.1073/pnas.1721967115
43. Che T, You Y, Wang D, Tanner MJ, Dixit VM, Lin X. MALT1/paracaspase is a signaling component downstream of CARMA1 and mediates T cell receptor-induced NF-kappaB activation. *J Biol Chem.* (2004) 279:15870–6. doi: 10.1074/jbc.M310599200
44. Sun L, Deng L, Ea CK, Xia ZP, Chen ZJ. The TRAF6 ubiquitin ligase and TAK1 kinase mediate IKK activation by BCL10 and MALT1 in T lymphocytes. *Mol Cell* (2004) 14:289–301. doi: 10.1016/S1097-2765(04)00236-9
45. Noels H, van Loo G, Hagens S, Broeckx V, Beyaert R, Marynen P, et al. A Novel TRAF6 binding site in MALT1 defines distinct mechanisms of NF-kappaB activation by API2middle dotMALT1 fusions. *J Biol Chem.* (2007) 282:10180–9. doi: 10.1074/jbc.M611038200
46. Zhou H, Wertz I, O'Rourke K, Ultsch M, Seshagiri S, Eby M, et al. Bcl10 activates the NF-kappaB pathway through ubiquitination of NEMO. *Nature* (2004) 427:167–71. doi: 10.1038/nature02273
47. Oeckinghaus A, Wegener E, Welteke V, Ferch U, Arslan SC, Ruland J, et al. Malt1 ubiquitination triggers NF-kappaB signaling upon T-cell activation. *EMBO J.* (2007) 26:4634–45. doi: 10.1038/sj.emboj.7601897
48. Shambharkar PB, Blonska M, Pappu BP, Li H, You Y, Sakurai H, et al. Phosphorylation and ubiquitination of the IkappaB kinase complex by two distinct signaling pathways. *EMBO J.* (2007) 26:1794–805. doi: 10.1038/sj.emboj.7601622
49. Yang Y, Schmitz R, Mitala J, Whiting A, Xiao W, Ceribelli M, et al. Essential role of the linear ubiquitin chain assembly complex in lymphoma revealed by rare germline polymorphisms. *Cancer Discov.* (2014) 4:480–93. doi: 10.1158/2159-8290.CD-13-0915
50. Dubois SM, Alexia C, Wu Y, Leclair HM, Leveau C, Schol E, et al. A catalytic-independent role for the LUBAC in NF-kappaB activation upon antigen receptor engagement and in lymphoma cells. *Blood* (2014) 123:2199–203. doi: 10.1182/blood-2013-05-504019
51. Satpathy S, Wagner SA, Beli P, Gupta R, Kristiansen TA, Malinova D, et al. Systems-wide analysis of BCR signalosomes and downstream phosphorylation and ubiquitylation. *Mol Syst Biol.* (2015) 11:810. doi: 10.15252/msb.20145880
52. Sato S, Sanjo H, Tsujimura T, Ninomiya-Tsuji J, Yamamoto M, Kawai T, et al. TAK1 is indispensable for development of T cells and prevention of colitis by the generation of regulatory T cells. *Int Immunol.* (2006) 18:1405–11. doi: 10.1093/intimm/dxl082
53. Schuman J, Chen Y, Podd A, Yu M, Liu HH, Wen R, et al. A critical role of TAK1 in B-cell receptor-mediated nuclear factor kappaB activation. *Blood* (2009) 113:4566–74. doi: 10.1182/blood-2008-08-176057
54. Wu CJ, Ashwell JD. NEMO recognition of ubiquitinated Bcl10 is required for T cell receptor-mediated NF-kappaB activation. *Proc Natl Acad Sci USA.* (2008) 105:3023–8. doi: 10.1073/pnas.0712313105
55. Blonska M, Lin X. CARMA1-mediated NF-kappaB and JNK activation in lymphocytes. *Immunol Rev.* (2009) 228:199–211. doi: 10.1111/j.1600-065X.2008.00749.x
56. Davis RJ. Signal transduction by the JNK group of MAP kinases. *Cell* (2000) 103:239–52. doi: 10.1016/S0092-8674(00)00116-1
57. Liu HH, Xie M, Schneider MD, Chen ZJ. Essential role of TAK1 in thymocyte development and activation. *Proc Natl Acad Sci USA.* (2006) 103:11677–82. doi: 10.1073/pnas.0603089103
58. Wan YY, Chi H, Xie M, Schneider MD, Flavell RA. The kinase TAK1 integrates antigen and cytokine receptor signaling for T cell development, survival and function. *Nat Immunol.* (2006) 7:851–8. doi: 10.1038/ni1355
59. Blonska M, Pappu BP, Matsumoto R, Li H, Su B, Wang D, et al. The CARMA1-Bcl10 signaling complex selectively regulates JNK2 kinase in the T cell receptor-signaling pathway. *Immunity* (2007) 26:55–66. doi: 10.1016/j.immuni.2006.11.008

60. Saxton RA, Sabatini DM. mTOR Signaling in growth, metabolism, and disease. *Cell* (2017) 169:361–71. doi: 10.1016/j.cell.2017.03.035
61. Pollizzi KN, Powell JD. Regulation of T cells by mTOR: the known knowns and the known unknowns. *Trends Immunol.* (2015) 36:13–20. doi: 10.1016/j.it.2014.11.005
62. Yang K, Chi H. mTOR and metabolic pathways in T cell quiescence and functional activation. *Semin Immunol.* (2012) 24:421–8. doi: 10.1016/j.smim.2012.12.004
63. Chi H. Regulation and function of mTOR signalling in T cell fate decisions. *Nat Rev Immunol.* (2012) 12:325–38. doi: 10.1038/nri3198
64. Nakaya M, Xiao Y, Zhou X, Chang JH, Chang M, Cheng X, et al. Inflammatory T cell responses rely on amino acid transporter ASCT2 facilitation of glutamine uptake and mTORC1 kinase activation. *Immunity* (2014) 40:692–705. doi: 10.1016/j.immuni.2014.04.007
65. Hamilton KS, Phong B, Corey C, Cheng J, Gorentla B, Zhong X, et al. T cell receptor-dependent activation of mTOR signaling in T cells is mediated by Carma1 and MALT1, but not Bcl10. *Sci Signal.* (2014) 7:ra55. doi: 10.1126/scisignal.2005169
66. Blonska M, Lin X. NF-kappaB signaling pathways regulated by CARMA family of scaffold proteins. *Cell Res.* (2011) 21:55–70. doi: 10.1038/cr.2010.182
67. Drummond RA, Franco LM, Lionakis MS. Human CARD9: a critical molecule of fungal immune surveillance. *Front Immunol.* (2018) 9:1836. doi: 10.3389/fimmu.2018.01836
68. Jordan CT, Cao L, Roberson ED, Duan S, Helms CA, Nair RP, et al. Rare and common variants in CARD14, encoding an epidermal regulator of NF-kappaB, in psoriasis. *Am J Hum Genet.* (2012) 90:796–808. doi: 10.1016/j.ajhg.2012.03.013
69. Jordan CT, Cao L, Roberson ED, Pierson KC, Yang CF, Joyce CE, et al. PSORS2 is due to mutations in CARD14. *Am J Hum Genet.* (2012) 90:784–95. doi: 10.1016/j.ajhg.2012.03.012
70. Fuchs-Telem D, Sarig O, van Steensel MA, Isakov O, Israeli S, Nousbeck J, et al. Familial pityriasis rubra pilaris is caused by mutations in CARD14. *Am J Hum Genet.* (2012) 91:163–70. doi: 10.1016/j.ajhg.2012.05.010
71. Malarkannan S, Regunathan J, Chu H, Kutlesa S, Chen Y, Zeng H, et al. Bcl10 plays a divergent role in NK cell-mediated cytotoxicity and cytokine generation. *J Immunol.* (2007) 179:3752–62. doi: 10.4049/jimmunol.179.6.3752
72. Gross O, Grupp C, Steinberg C, Zimmermann S, Strasser D, Hannesschlager N, et al. Multiple ITAM-coupled NK-cell receptors engage the Bcl10/Malt1 complex via Carma1 for NF-kappaB and MAPK activation to selectively control cytokine production. *Blood* (2008) 112:2421–8. doi: 10.1182/blood-2007-11-123513
73. Van Nuffel E, Schmitt A, Afonina IS, Schulze-Osthoff K, Beyaert R, Hailfinger S. CARD14-Mediated activation of paracaspase MALT1 in keratinocytes: implications for psoriasis. *J Invest Dermatol.* (2017) 137:569–75. doi: 10.1016/j.jid.2016.09.031
74. Sun J. CARMA3: A novel scaffold protein in regulation of NF-kappaB activation and diseases. *World J Biol Chem.* (2010) 1:353–61. doi: 10.4331/wjbc.v1.i12.353
75. Bertin J, Wang L, Guo Y, Jacobson MD, Poyet JL, Srinivasula SM, et al. CARD11 and CARD14 are novel caspase recruitment domain (CARD)/membrane-associated guanylate kinase (MAGUK) family members that interact with BCL10 and activate NF-kappa B. *J Biol Chem.* (2001) 276:11877–82. doi: 10.1074/jbc.M010512200
76. Rawlings DJ, Sommer K, Moreno-Garcia ME. The CARMA1 signalosome links the signalling machinery of adaptive and innate immunity in lymphocytes. *Nat Rev Immunol.* (2006) 6:799–812. doi: 10.1038/nri1944
77. Wang D, You Y, Case SM, McAllister-Lucas LM, Wang L, DiStefano PS, et al. A requirement for CARMA1 in TCR-induced NF-kappa B activation. *Nat Immunol.* (2002) 3:830–5. doi: 10.1038/ni824
78. Gaide O, Favier B, Legler DF, Bonnet D, Brissoni B, Valitutti S, et al. CARMA1 is a critical lipid raft-associated regulator of TCR-induced NF-kappa B activation. *Nat Immunol.* (2002) 3:836–43. doi: 10.1038/ni830
79. Pomerantz JL, Denny EM, Baltimore D. CARD11 mediates factor-specific activation of NF-kappaB by the T cell receptor complex. *EMBO J.* (2002) 21:5184–94. doi: 10.1093/emboj/cdf505
80. Newton K, Dixit VM. Mice lacking the CARD of CARMA1 exhibit defective B lymphocyte development and impaired proliferation of their B and T lymphocytes. *Curr Biol.* (2003) 13:1247–51. doi: 10.1016/S0960-9822(03)00458-5
81. Medoff BD, Sandall BP, Landry A, Nagahama K, Mizoguchi A, Luster AD, et al. Differential requirement for CARMA1 in agonist-selected T-cell development. *Eur J Immunol.* (2009) 39:78–84. doi: 10.1002/eji.200838734
82. Molinero LL, Cubre A, Mora-Solano C, Wang Y, Alegre ML. T cell receptor/CARMA1/NF-kappaB signaling controls T-helper (Th) 17 differentiation. *Proc Natl Acad Sci USA.* (2012) 109:18529–34. doi: 10.1073/pnas.1204557109
83. Blonska M, Joo D, Zweidler-McKay PA, Zhao Q, Lin X. CARMA1 controls Th2 cell-specific cytokine expression through regulating JunB and GATA3 transcription factors. *J Immunol.* (2012) 188:3160–8. doi: 10.4049/jimmunol.1102943
84. Pappu BP, Lin X. Potential role of CARMA1 in CD40-induced splenic B cell proliferation and marginal zone B cell maturation. *Eur J Immunol.* (2006) 36:3033–43. doi: 10.1002/eji.200535663
85. Altin JA, Tian L, Liston A, Bertram EM, Goodnow CC, Cook MC. Decreased T-cell receptor signaling through CARD11 differentially compromises forkhead box protein 3-positive regulatory versus T(H)2 effector cells to cause allergy. *J Allergy Clin Immunol.* (2011) 127:1277–85 e5. doi: 10.1016/j.jaci.2010.12.1081
86. Schmidt-Supprian M, Tian J, Grant EP, Pasparakis M, Maehr R, Ovaa H, et al. Differential dependence of CD4+CD25+ regulatory and natural killer-like T cells on signals leading to NF-kappaB activation. *Proc Natl Acad Sci USA.* (2004) 101:4566–71. doi: 10.1073/pnas.0400885101
87. Jost PJ, Weiss S, Ferch U, Gross O, Mak TW, Peschel C, et al. Bcl10/Malt1 signaling is essential for TCR-induced NF-kappaB activation in thymocytes but dispensable for positive or negative selection. *J Immunol.* (2007) 178:953–60. doi: 10.4049/jimmunol.178.2.953
88. Ruland J, Duncan GS, Wakeham A, Mak TW. Differential requirement for Malt1 in T and B cell antigen receptor signaling. *Immunity* (2003) 19:749–58. doi: 10.1016/S1074-7613(03)00293-0
89. Bornancin F, Renner F, Touil R, Sic H, Kolb Y, Touil-Allaoui I, et al. Deficiency of MALT1 paracaspase activity results in unbalanced regulatory and effector T and B cell responses leading to multiorgan inflammation. *J Immunol.* (2015) 194:3723–34. doi: 10.4049/jimmunol.1402254
90. Brustle A, Brenner D, Knobbe CB, Lang PA, Virtanen C, Hershenfield BM, et al. The NF-kappaB regulator MALT1 determines the encephalitogenic potential of Th17 cells. *J Clin Invest.* (2012) 122:4698–709. doi: 10.1172/JCI63528
91. Yu JW, Hoffman S, Beal AM, Dykon A, Ringenberg MA, Hughes AC, et al. MALT1 protease activity is required for innate and adaptive immune responses. *PLoS ONE* (2015) 10:e0127083. doi: 10.1371/journal.pone.0127083
92. Jaworski M, Marsland BJ, Gehrig J, Held W, Favre S, Luther SA, et al. Malt1 protease inactivation efficiently dampens immune responses but causes spontaneous autoimmunity. *EMBO J.* (2014) 33:2765–81. doi: 10.15252/embj.201488987
93. Gewies A, Gorka O, Bergmann H, Pechloff K, Petermann F, Jeltsch KM, et al. Uncoupling Malt1 threshold function from paracaspase activity results in destructive autoimmune inflammation. *Cell Rep.* (2014) 9:1292–305. doi: 10.1016/j.celrep.2014.10.044
94. Hirota T, Takahashi A, Kubo M, Tsunoda T, Tomita K, Sakashita M, et al. Genome-wide association study identifies eight new susceptibility loci for atopic dermatitis in the Japanese population. *Nat Genet.* (2012) 44:1222–6. doi: 10.1038/ng.2438
95. Medoff BD, Seed B, Jackobek R, Zora J, Yang Y, Luster AD, et al. CARMA1 is critical for the development of allergic airway inflammation in a murine model of asthma. *J Immunol.* (2006) 176:7272–7. doi: 10.4049/jimmunol.176.12.7272
96. Ramadas RA, Roche MI, Moon JJ, Ludwig T, Xavier RJ, Medoff BD. CARMA1 is necessary for optimal T cell responses in a

murine model of allergic asthma. *J Immunol*. (2011) 187:6197–207. doi: 10.4049/jimmunol.1101348
97. Lu HY, Sharma M, Biggs CM, Huang YH, Shopsowitz KE, Frosk P, et al. The importance of functional validation after next-generation sequencing: evaluation of a novel CARD11 variant. *Pediatr Allergy Immunol*. (2018) 29:663–8. doi: 10.1111/pai.12930
98. Dorjbal, B., Stinson, J. R., Ma, C. A., Weinreich, M. A., Miraghazadeh, B., Hartberger, J. M., et al. (in press). Hypomorphic *CARD11* mutations associated with diverse immunologic phenotypes with or without atopic disease. *J. Allergy Clin. Immunol.* doi: 10.1016/j.jaci.2018.08.013
99. Lyons JJ, Milner JD. Primary atopic disorders. *J Exp Med*. (2018) 215:1009–22. doi: 10.1084/jem.20172306
100. Manka LA, Wechsler ME. New biologics for allergic diseases. *Expert Rev Clin Immunol*. (2018) 14:285–96. doi: 10.1080/1744666X.2018.1459188
101. Darte JM, McClure PD, Saunders EF, Weber JL, Donohue WL. Congenital lymphoid hyperplasia with persistent hyperlymphocytosis. *N Engl J Med*. (1971) 284:431–2. doi: 10.1056/NEJM197102252840807
102. Arjunaraja S, Snow AL. Gain-of-function mutations and immunodeficiency: at a loss for proper tuning of lymphocyte signaling. *Curr Opin Allergy Clin Immunol*. (2015) 15:533–8. doi: 10.1097/ACI.0000000000000217
103. Buchbinder D, Sassoon A. A case of bad Carma! *Blood* (2017) 129:1737. doi: 10.1182/blood-2016-12-756007
104. Arjunaraja S, Angelus P, Su HC, Snow AL. Impaired control of epstein-barr virus infection in B-cell expansion with NF-kappaB and T-Cell anergy disease. *Front Immunol*. (2018) 9:198. doi: 10.3389/fimmu.2018.00198
105. Perez E, Bonilla FA, Orange JS, Ballow M. Specific antibody deficiency: controversies in diagnosis and management. *Front Immunol*. (2017) 8:586. doi: 10.3389/fimmu.2017.00586
106. Arjunaraja S, Nose BD, Sukumar G, Lott NM, Dalgard CL, Snow AL. Intrinsic plasma cell differentiation defects in B cell expansion with NF-kappaB and T Cell anergy patient B cells. *Front Immunol*. (2017) 8:913. doi: 10.3389/fimmu.2017.00913
107. Jeelall YS, Wang JQ, Law HD, Domaschenz H, Fung HK, Kallies A, et al. Human lymphoma mutations reveal CARD11 as the switch between self-antigen-induced B cell death or proliferation and autoantibody production. *J Exp Med*. (2012) 209:1907–17. doi: 10.1084/jem.20112744
108. Chan W, Schaffer TB, Pomerantz JL. A quantitative signaling screen identifies CARD11 mutations in the CARD and LATCH domains that induce Bcl10 ubiquitination and human lymphoma cell survival. *Mol Cell Biol*. (2013) 33:429–43. doi: 10.1128/MCB.00850-12
109. Jattani RP, Tritapoe JM, Pomerantz JL. Intramolecular interactions and regulation of cofactor binding by the four repressive elements in the caspase recruitment domain-containing protein 11 (CARD11) inhibitory domain. *J Biol Chem*. (2016) 291:8338–48. doi: 10.1074/jbc.M116.717322
110. Jattani RP, Tritapoe JM, Pomerantz JL. Cooperative control of caspase recruitment domain-containing protein 11 (CARD11) signaling by an unusual array of redundant repressive elements. *J Biol Chem*. (2016) 291:8324–36. doi: 10.1074/jbc.M115.683714
111. Sasaki Y, Derudder E, Hobeika E, Pelanda R, Reth M, Rajewsky K, et al. Canonical NF-kappaB activity, dispensable for B cell development, replaces BAFF-receptor signals and promotes B cell proliferation upon activation. *Immunity* (2006) 24:729–39. doi: 10.1016/j.immuni.2006.04.005
112. Krishna S, Xie D, Gorentla B, Shin J, Gao J, Zhong XP. Chronic activation of the kinase IKKbeta impairs T cell function and survival. *J Immunol*. (2012) 189:1209–19. doi: 10.4049/jimmunol.1102429
113. Forbes SA, Beare D, Boutselakis H, Bamford S, Bindal N, Tate J, et al. COSMIC: somatic cancer genetics at high-resolution. *Nucleic Acids Res*. (2017) 45:D777–83. doi: 10.1093/nar/gkw1121
114. Demeyer A, Staal J, Beyaert R. Targeting MALT1 Proteolytic activity in immunity, inflammation and disease: Good or Bad? *Trends Mol Med*. (2016) 22:135–50. doi: 10.1016/j.molmed.2015.12.004
115. Lee CH, Bae SJ, Kim M. Mucosa-associated lymphoid tissue lymphoma translocation 1 as a novel therapeutic target for rheumatoid arthritis. *Sci Rep*. (2017) 7:11889. doi: 10.1038/s41598-017-12349-9
116. Saba NS, Wong DH, Tanios G, Iyer JR, Lobelle-Rich P, Dadashian EL, et al. MALT1 inhibition is efficacious in both naive and ibrutinib-resistant chronic lymphocytic leukemia. *Cancer Res*. (2017) 77:7038–48. doi: 10.1158/0008-5472.CAN-17-2485
117. Bardet M, Unterreiner A, Malinverni C, Lafossas F, Vedrine C, Boesch D, et al. The T-cell fingerprint of MALT1 paracaspase revealed by selective inhibition. *Immunol Cell Biol*. (2018) 96:81–99. doi: 10.1111/imcb.1018
118. Willis TG, Jadayel DM, Du MQ, Peng H, Perry AR, Abdul-Rauf M, et al. Bcl10 is involved in t(1;14)(p22;q32) of MALT B cell lymphoma and mutated in multiple tumor types. *Cell* (1999) 96:35–45. doi: 10.1016/S0092-8674(00)80957-5
119. Costanzo A, Guiet C, Vito P. c-E10 is a caspase-recruiting domain-containing protein that interacts with components of death receptors signaling pathway and activates nuclear factor-kappaB. *J Biol Chem*. (1999) 274:20127–32. doi: 10.1074/jbc.274.29.20127
120. Koseki T, Inohara N, Chen S, Carrio R, Merino J, Hottiger MO, et al. CIPER, a novel NF kappaB-activating protein containing a caspase recruitment domain with homology to Herpesvirus-2 protein E10. *J Biol Chem*. (1999) 274:9955–61. doi: 10.1074/jbc.274.15.9955
121. Bertin J, Guo Y, Wang L, Srinivasula SM, Jacobson MD, Poyet JL, et al. CARD9 is a novel caspase recruitment domain-containing protein that interacts with BCL10/CLAP and activates NF-kappa B. *J Biol Chem*. (2000) 275:41082–6. doi: 10.1074/jbc.C000726200
122. Wang L, Guo Y, Huang WJ, Ke X, Poyet JL, Manji GA, et al. Card10 is a novel caspase recruitment domain/membrane-associated guanylate kinase family member that interacts with BCL10 and activates NF-kappa B. *J Biol Chem*. (2001) 276:21405–9. doi: 10.1074/jbc.M102488200
123. McAllister-Lucas LM, Inohara N, Lucas PC, Ruland J, Benito A, Li Q, et al. Bimp1, a MAGUK family member linking protein kinase C activation to Bcl10-mediated NF-kappaB induction. *J Biol Chem*. (2001) 276:30589–97. doi: 10.1074/jbc.M103824200
124. Gehring T, Seeholzer T, Krappmann D. BCL10 – Bridging CARDs to immune activation. *Front Immunol*. (2018) 9:1539. doi: 10.3389/fimmu.2018.01539
125. Liu Y, Dong W, Chen L, Xiang R, Xiao H, De G, et al. BCL10 mediates lipopolysaccharide/toll-like receptor-4 signaling through interaction with Pellino2. *J Biol Chem*. (2004) 279:37436–44. doi: 10.1074/jbc.M400241200
126. Gross O, Gewies A, Finger K, Schafer M, Sparwasser T, Peschel C, et al. Card9 controls a non-TLR signalling pathway for innate anti-fungal immunity. *Nature* (2006) 442:651–6. doi: 10.1038/nature04926
127. Gringhuis SI, Wevers BA, Kaptein TM, van Capel TM, Theelen B, Boekhout T, et al. Selective C-Rel activation via Malt1 controls anti-fungal T(H)-17 immunity by dectin-1 and dectin-2. *PLoS Pathog*. (2011) 7:e1001259. doi: 10.1371/journal.ppat.1001259
128. Dierlamm J, Baens M, Wlodarska I, Stefanova-Ouzounova M, Hernandez JM, Hossfeld DK, et al. The apoptosis inhibitor gene API2 and a novel 18q gene, MLT, are recurrently rearranged in the t(11;18)(q21;q21) associated with mucosa-associated lymphoid tissue lymphomas. *Blood* (1999) 93:3601–9.
129. Akagi T, Motegi M, Tamura A, Suzuki R, Hosokawa Y, Suzuki H, et al. A novel gene, MALT1 at 18q21, is involved in t(11;18) (q21;q21) found in low-grade B-cell lymphoma of mucosa-associated lymphoid tissue. *Oncogene* (1999) 18:5785–94. doi: 10.1038/sj.onc.1203018
130. Morgan JA, Yin Y, Borowsky AD, Kuo F, Nourmand N, Koontz JI, et al. Breakpoints of the t(11;18)(q21;q21) in mucosa-associated lymphoid tissue (MALT) lymphoma lie within or near the previously undescribed gene MALT1 in chromosome 18. *Cancer Res*. (1999) 59:6205–13.
131. Rosebeck S, Rehman AO, Lucas PC, McAllister-Lucas LM. From MALT lymphoma to the CBM signalosome: three decades of discovery. *Cell Cycle* (2011) 10:2485–96. doi: 10.4161/cc.10.15.16923
132. Afonina IS, Elton L, Carpentier I, Beyaert R. MALT1–a universal soldier: multiple strategies to ensure NF-kappaB activation and target gene expression. *FEBS J*. (2015) 282:3286–97. doi: 10.1111/febs.13325
133. Coornaert B, Baens M, Heyninck K, Bekaert T, Haegman M, Staal J, et al. T cell antigen receptor stimulation induces MALT1 paracaspase-mediated cleavage of the NF-kappaB inhibitor A20. *Nat Immunol*. (2008) 9:263–71. doi: 10.1038/ni1561
134. Rebeaud F, Hailfinger S, Posevitz-Fejfar A, Tapernoux M, Moser R, Rueda D, et al. The proteolytic activity of the paracaspase MALT1 is key in T cell activation. *Nat Immunol*. (2008) 9:272–81. doi: 10.1038/ni1568
135. Staal J, Driege Y, Bekaert T, Demeyer A, Muyllaert D, Van Damme P, et al. T-cell receptor-induced JNK activation requires proteolytic inactivation of CYLD by MALT1. *EMBO J*. (2011) 30:1742–52. doi: 10.1038/emboj.2011.85

136. Hailfinger S, Nogai H, Pelzer C, Jaworski M, Cabalzar K, Charton JE, et al. Malt1-dependent RelB cleavage promotes canonical NF-kappaB activation in lymphocytes and lymphoma cell lines. *Proc Natl Acad Sci USA*. (2011) 108:14596–601. doi: 10.1073/pnas.1105020108
137. Uehata T, Iwasaki H, Vandenbon A, Matsushita K, Hernandez-Cuellar E, Kuniyoshi K, et al. Malt1-induced cleavage of regnase-1 in CD4(+) helper T cells regulates immune activation. *Cell* (2013) 153:1036–49. doi: 10.1016/j.cell.2013.04.034
138. Jeltsch KM, Hu D, Brenner S, Zoller J, Heinz GA, Nagel D, et al. Cleavage of roquin and regnase-1 by the paracaspase MALT1 releases their cooperatively repressed targets to promote T(H)17 differentiation. *Nat Immunol*. (2014) 15:1079–89. doi: 10.1038/ni.3008
139. Baens M, Bonsignore L, Somers R, Vanderheydt C, Weeks SD, Gunnarsson J, et al. MALT1 auto-proteolysis is essential for NF-kappaB-dependent gene transcription in activated lymphocytes. *PLoS ONE* (2014) 9:e103774. doi: 10.1371/journal.pone.0103774
140. Klein T, Fung SY, Renner F, Blank MA, Dufour A, Kang S, et al. The paracaspase MALT1 cleaves HOIL1 reducing linear ubiquitination by LUBAC to dampen lymphocyte NF-kappaB signalling. *Nat Commun.* (2015) 6:8777. doi: 10.1038/ncomms9777
141. Douanne T, Gavard J, Bidere N. The paracaspase MALT1 cleaves the LUBAC subunit HOIL1 during antigen receptor signaling. *J Cell Sci*. (2016) 129:1775–80. doi: 10.1242/jcs.185025
142. Elton L, Carpentier I, Staal J, Driege Y, Haegman M, Beyaert R. MALT1 cleaves the E3 ubiquitin ligase HOIL-1 in activated T cells, generating a dominant negative inhibitor of LUBAC-induced NF-kappaB signaling. *FEBS J*. (2016) 283:403–12. doi: 10.1111/febs.13597
143. Rosebeck S, Madden L, Jin X, Gu S, Apel IJ, Appert A, et al. Cleavage of NIK by the API2-MALT1 fusion oncoprotein leads to noncanonical NF-kappaB activation. *Science* (2011) 331:468–72. doi: 10.1126/science.1198946
144. Nie Z, Du MQ, McAllister-Lucas LM, Lucas PC, Bailey NG, Hogaboam CM, et al. Conversion of the LIMA1 tumour suppressor into an oncogenic LMO-like protein by API2-MALT1 in MALT lymphoma. *Nat Commun*. (2015) 6:5908. doi: 10.1038/ncomms6908
145. Tsang P, Derkson G, Priddy R, Junker AK, Slots J, Larjava H. Severe periodontitis in a 5-year-old girl with hyperimmunoglobulin E syndrome. *Pediatr Dent*. (2005) 27:68–73.
146. Rozmus J, McDonald R, Fung SY, Del Bel KL, Roden J, Senger C, et al. Successful clinical treatment and functional immunological normalization of human MALT1 deficiency following hematopoietic stem cell transplantation. *Clin Immunol.* (2016) 168:1–5. doi: 10.1016/j.clim.2016.04.011
147. Milner JD. TCR Signaling abnormalities in human Th2-associated atopic disease. *Front Immunol.* (2018) 9:719. doi: 10.3389/fimmu.2018.00719
148. Zhang Q, Davis JC, Lamborn IT, Freeman AF, Jing H, Favreau AJ, et al. Combined immunodeficiency associated with DOCK8 mutations. *N Engl J Med*. (2009) 361:2046–55. doi: 10.1056/NEJMoa0905506
149. Lanzi G, Moratto D, Vairo D, Masneri S, Delmonte O, Paganini T, et al. A novel primary human immunodeficiency due to deficiency in the WASP-interacting protein WIP. *J Exp Med*. (2012) 209:29–34. doi: 10.1084/jem.20110896
150. Ochs HD. Mutations of the Wiskott-Aldrich Syndrome Protein affect protein expression and dictate the clinical phenotypes. *Immunol Res*. (2009) 44:84–8. doi: 10.1007/s12026-008-8084-3
151. Kuijpers TW, Tool ATJ, van der Bijl I, de Boer M, van Houdt M, de Cuyper IM, et al. Combined immunodeficiency with severe inflammation and allergy caused by ARPC1B deficiency. *J Allergy Clin Immunol.* (2017) 140:273–7 e10. doi: 10.1016/j.jaci.2016.09.061
152. Kahr WH, Pluthero FG, Elkadri A, Warner N, Drobac M, Chen CH, et al. Loss of the Arp2/3 complex component ARPC1B causes platelet abnormalities and predisposes to inflammatory disease. *Nat Commun*. (2017) 8:14816. doi: 10.1038/ncomms14816
153. Somech R, Lev A, Lee YN, Simon AJ, Barel O, Schiby G, et al. Disruption of Thrombocyte and T Lymphocyte Development by a Mutation in ARPC1B. *J Immunol*. (2017) 199:4036–45. doi: 10.4049/jimmunol.1700460
154. Turul T, Tezcan I, Artac H, de Bruin-Versteeg S, Barendregt BH, Reisli I, et al. Clinical heterogeneity can hamper the diagnosis of patients with ZAP70 deficiency. *Eur J Pediatr*. (2009) 168:87–93. doi: 10.1007/s00431-008-0718-x
155. Karaca E, Karakoc-Aydiner E, Bayrak OF, Keles S, Sevli S, Barlan IB, et al. Identification of a novel mutation in ZAP70 and prenatal diagnosis in a Turkish family with severe combined immunodeficiency disorder. *Gene.* (2013) 512:189–93. doi: 10.1016/j.gene.2012.10.062
156. Lee AJ, Wu X, Cheng H, Zhou X, Cheng X, Sun SC. CARMA1 regulation of regulatory T cell development involves modulation of interleukin-2 receptor signaling. *J Biol Chem*. (2010) 285:15696–703. doi: 10.1074/jbc.M109.095190
157. Liu W, Guo W, Hang N, Yang Y, Wu X, Shen Y, et al. MALT1 inhibitors prevent the development of DSS-induced experimental colitis in mice via inhibiting NF-kappaB and NLRP3 inflammasome activation. *Oncotarget* (2016) 7:30536–49. doi: 10.18632/oncotarget.8867
158. International Multiple Sclerosis Genetics C, Wellcome Trust Case Control C, Sawcer S, Hellenthal G, Pirinen M, Spencer CC, et al. Genetic risk and a primary role for cell-mediated immune mechanisms in multiple sclerosis. *Nature*. (2011) 476:214–9. doi: 10.1038/nature10251
159. Juilland M, Thome M. Role of the CARMA1/BCL10/MALT1 complex in lymphoid maliignancies. *Curr Opin Hematol*. (2016) 23:402–9. doi: 10.1097/MOH.0000000000000257
160. Yang C, David L, Qiao Q, Damko E, Wu H. The CBM signalosome: potential therapeutic target for aggressive lymphoma? *Cytokine Growth Factor Rev*. (2014) 25:175–83. doi: 10.1016/j.cytogfr.2013.12.008
161. Thrasher AJ, Williams DA. Evolving gene therapy in primary immunodeficiency. *Mol Ther*. (2017) 25:1132–41. doi: 10.1016/j.ymthe.2017.03.018
162. van Zwol A, Neu J, van Elburg RM. Long-term effects of neonatal glutamine-enriched nutrition in very-low-birth-weight infants. *Nutr Rev*. (2011) 69:2–8. doi: 10.1111/j.1753-4887.2010.00359.x

Conflict of Interest Statement: The authors declare that the research was conducted in the absence of any commercial or financial relationships that could be construed as a potential conflict of interest.

frontiers in Immunology

CASE REPORT
published: 12 December 2018
doi: 10.3389/fimmu.2018.02944

A Unique Heterozygous *CARD11* Mutation Combines Pathogenic Features of Both Gain- and Loss-of-Function Patients in a Four-Generation Family

Marylin Desjardins[1,2†], Swadhinya Arjunaraja[3†], Jeffrey R. Stinson[3], Batsukh Dorjbal[3], Janani Sundaresan[3], Julie Niemela[4], Mark Raffeld[5], Helen F. Matthews[6], Angela Wang[7,8], Pamela Angelus[7,8], Helen C. Su[7], Bruce D. Mazer[1,2†] and Andrew L. Snow[3†]*

[1] Division of Allergy and Immunology, Department of Paediatrics, McGill University Health Centre, Montreal, QC, Canada, [2] Meakins-Christie Laboratories of the Research Institute of the McGill University Health Centre, Montreal, QC, Canada, [3] Department of Pharmacology and Molecular Therapeutics, Uniformed Services University of Health Sciences, Bethesda, MD, United States, [4] Department of Laboratory Medicine, NIH Clinical Center, Bethesda, MD, United States, [5] Laboratory of Pathology, Center for Cancer Research, National Cancer Institute, National Institutes of Health, Bethesda, MD, United States, [6] Laboratory of Immune System Biology, National Institute of Allergy and Infectious Diseases, National Institutes of Health, Bethesda, MD, United States, [7] Laboratory of Clinical Immunology and Microbiology, National Institute of Allergy and Infectious Diseases, National Institutes of Health, Bethesda, MD, United States, [8] Clinical Research Directorate/Clinical Monitoring Research Program, Leidos Biomedical Research, Inc., National Cancer Institute at Frederick, Frederick, MD, United States

OPEN ACCESS

Edited by:
Menno C. van Zelm, Monash University, Australia

Reviewed by:
Ruben Martinez-Barricarte, Rockefeller University, United States
Michel J. Massaad, American University of Beirut Medical Center, Lebanon

***Correspondence:**
Andrew L. Snow
andrew.snow@usuhs.edu

[†] These authors have contributed equally to this work

Specialty section:
This article was submitted to Primary Immunodeficiencies, a section of the journal Frontiers in Immunology

Received: *15 July 2018*
Accepted: *30 November 2018*
Published: *12 December 2018*

Citation:
Desjardins M, Arjunaraja S, Stinson JR, Dorjbal B, Sundaresan J, Niemela J, Raffeld M, Matthews HF, Wang A, Angelus P, Su HC, Mazer BD and Snow AL (2018) A Unique Heterozygous CARD11 Mutation Combines Pathogenic Features of Both Gain- and Loss-of-Function Patients in a Four-Generation Family. Front. Immunol. 9:2944. doi: 10.3389/fimmu.2018.02944

CARD11 is a lymphocyte-specific scaffold molecule required for proper activation of B- and T-cells in response to antigen. Germline gain-of-function (GOF) mutations in the *CARD11* gene cause a unique B cell lymphoproliferative disorder known as B cell Expansion with NF-κB and T cell Anergy (BENTA). In contrast, patients carrying loss-of-function (LOF), dominant negative (DN) *CARD11* mutations present with severe atopic disease. Interestingly, both GOF and DN CARD11 variants cause primary immunodeficiency, with recurrent bacterial and viral infections, likely resulting from impaired adaptive immune responses. This report describes a unique four-generation family harboring a novel heterozygous germline indel mutation in *CARD11* (c.701-713delinsT), leading to one altered amino acid and a deletion of 4 others (p.His234_Lys238delinsLeu). Strikingly, affected members exhibit both moderate B cell lymphocytosis *and* atopic dermatitis/allergies. Ectopic expression of this *CARD11* variant stimulated constitutive NF-κB activity in T cell lines, similar to other BENTA patient mutations. However, unlike other GOF mutants, this variant significantly impeded the ability of wild-type CARD11 to induce NF-κB activation following antigen receptor ligation. Patient lymphocytes display marked intrinsic defects in B cell differentiation and reduced T cell responsiveness *in vitro*. Collectively, these data imply that a single heterozygous *CARD11* mutation can convey both GOF and DN signaling effects, manifesting in a blended BENTA phenotype with atopic features. Our findings further emphasize the importance of balanced CARD11 signaling for normal immune responses.

Keywords: CARD11, BENTA, Atopy, B cell lymphocytosis, primary immumunodeficiencies

INTRODUCTION

BENTA disease [B cell Expansion with nuclear factor kappa B (NF-κB) and T cell Anergy] is a rare immunodeficiency disorder that presents with splenomegaly and unusual peripheral blood lymphocytosis comprised of naïve and immature B cells (1, 2). BENTA is caused by germline, heterozygous GOF mutations in *CARD11*, which encodes a large multi-domain scaffold molecule best known for connecting antigen receptor (AgR) ligation to NF-κB activation in B and T lymphocytes. Similar to somatic GOF mutations typically found in the coiled-coil (CC) domain of CARD11 and associated with diffuse large B-cell lymphoma (3), BENTA CARD11 mutants spontaneously aggregate to form active signaling clusters with BCL-10 and MALT1 (CBM complex), resulting in constitutive NF-κB activation without requiring B or T cell receptor interaction (4). NF-κB drives the expression of pro-survival genes in transitional and naïve B-cells to confer enhanced survival, while paradoxically rendering T cells less responsive to TCR stimulation with reduced IL-2 production (5–7). Despite the striking expansion of polyclonal B cells, BENTA patients exhibit reduced B cell memory and poor antibody responses to specific vaccines, due in part to intrinsic B cell defects in plasma cell differentiation (8). Moreover, mildly anergic T cell responses may explain increased susceptibility to certain viral infections [e.g., molluscum contagiousum, Epstein-Barr virus (EBV)]. Together, these immune abnormalities increase patients' susceptibility to viral and bacterial infections, including chronic EBV infection, and may to contribute to a higher potential risk of B-cell malignancy (9).

More recently, heterozygous, hypomorphic CARD11 mutations were uncovered in patients with elevated circulating IgE, severe atopic dermatitis, and other allergic manifestations (e.g., rhinitis, asthma, food allergies) (10–12). Strikingly, these variants dominantly interfere with wild-type (WT) CARD11 signaling to both NF-κB and mTORC1, contributing to defective T cell responses that skew toward a T helper 2 (Th2) profile consistent with atopy. Most *CARD11* DN patients also share signs of immunodeficiency that overlap with those noted in BENTA patients, including frequent sinopulmonary bacterial infections and viral infections (e.g., molluscum), and fewer class-switched memory B cells. However, B cell lymphocytosis was not observed in this cohort. Furthermore, atopic disease has not been described to date in BENTA patients.

CASE PRESENTATION AND RESULTS

The index patient (IV.1) was referred to our dedicated immunology clinic (McGill University Health Centre-MUHC) at 18 months of age for evaluation of dermatitis and recurrent infections. He was treated with oral antibiotics at 5, 8, and 13 months of age for balanitis. He also suffered from chest X-ray-documented pneumonia and an acute otitis media, which occurred at 6 and 12 months of age, respectively. At 14 months, he was admitted to the hospital for febrile neutropenia with pneumonia and treated with intravenous antibiotics. The neutropenia resolved, but marked persistent lymphocytosis persisted. Small reactive lymphocytes were present on the peripheral blood smear. The physical examination revealed dry lichenified erythematous skin lesions with no palpable lymphadenopathy and no appreciable splenomegaly. Dermatology confirmed a diagnosis of pustular psoriasis, which was complicated by a superimposed recurrent *molluscum contagiosum* affecting his abdomen, back, perianal and leg areas as well as streptococcal perianal dermatitis.

Initial blood analyses performed at MUHC in 2012 showed a lymphocyte count of 20.4×10^9/L and composed predominantly of $CD19^+$ B-cells (12.4×10^9/L, 61.0%), with a decreased proportion of $CD3^+$ T-cells (6.7×10^9/L, 33.0%) and normal $CD16^+CD56^+$ NK-cells (0.6×10^9/L, 3.0%). An extended flow cytometry panel performed in 2015 (MUHC) revealed increased proportions of naïve $CD19^+sIgM^+$ B-cells (24.9×10^8/L, 72.0%) and $CD19^+CD5^+$ B-cells (20.0×10^8/L, 58.0%). The proportion of class-switched $CD19^+CD27^+IgD^-$memory B-cells (0.2×10^8/L, 0.6%) was decreased. IgH gene rearrangement analysis demonstrated a polyclonal B-cell lymphocytosis pattern (**Supplementary Figure 1**). The patient had mild hypogammaglobulinemia (IgG 3.1 g/L) associated with slightly decreased serum IgA levels (0.19 g/L), absent serum IgM (<0.25 g/L) and normal IgE levels (63 μg/L). IgE levels increased to 444 μg/L (normal 0–240 μg/L) later when the patient reached 4 years of age. Although, the patient received all recommended vaccines for age (including live attenuated vaccines against measles, mumps, rubella and varicella), he had no specific antibody responses against *Haemophilus influenzae type B* (IgG <0.1 μg/mL) and *Streptococcus pneumoniae* (0/14 IgG serotypes were above 1.3 μg/mL). The specific antibody responses were normal for tetanus (IgG above 4.0 IU/mL) and diphtheria toxoids (IgG above 3.0 IU/mL). Lymphocyte proliferation responses to phytohemagglutinin, concanavalin A, and anti-CD3 were also normal. Pokeweed mitogen proliferative response was decreased (stimulation index of 23.2 compared to 85.6 in healthy control). Mild splenomegaly (8.5 cm) was confirmed on abdominal ultrasound. The CT scan showed small bilateral cervical lymph nodes. Blood serology and PCR for EBV and cytomegalovirus (CMV) were negative. The patient was treated with weekly subcutaneous immunoglobulin (scIg) injection therapy (equivalent to 0.65 g/kg/month). At 5 years of age, he suffered from two consecutive pneumonias with the second episode associated with rhinovirus infection, which required hospitalization and oxygen supplementation. Among other relevant medical problems, he is known for mild bilateral conductive hearing loss and atopy IgE-mediated milk allergy (milk specific IgE: 9.95 IU/L and positive skin prick test to cow's milk extract at 2 years old) and allergic rhinitis to birch and cat.

The family reported that parents were not related and were of Caucasian origin (**Figure 1A**). The father (Patient III.1, 29 years old) was investigated as a child for splenomegaly, atopic dermatitis, mild intermittent asthma, molluscum contagiosum (on buttocks, legs, and arms from age 1–5 years old) and "high total B-cell number." No diagnosis was established at the time. Over the years, he developed recurrent warts and persistent finger onychomycosis (since age 4–5). He had chickenpox at 11 years old followed by shingles as a young adult. More recently, he was treated with intravenous antibiotic for recurrent knee

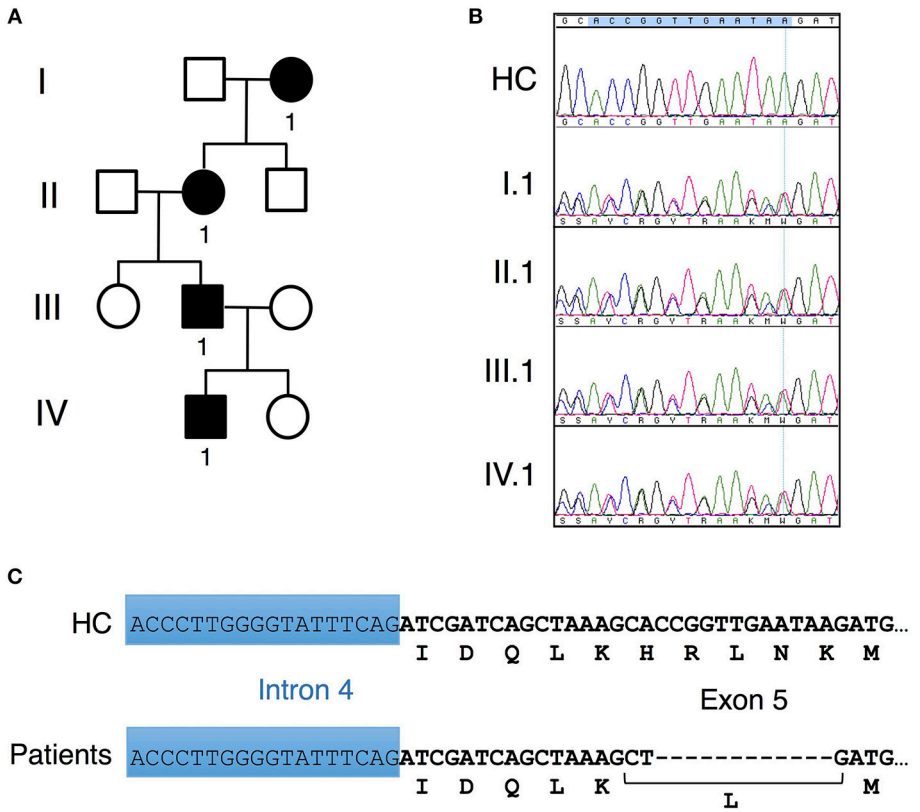

FIGURE 1 | Unique *CARD11* mutation in a four-generation family. **(A)** Pedigree of patients in a four-generation BENTA family. Squares and circles represent males and females, respectively, and black represents affected patients. **(B)** Sanger DNA sequencing showing a novel in-frame 12 bp deletion in genomic DNA derived from PBMC isolated from patients II.1, III.1 and IV.1 compared to healthy control (HC). **(C)** Schematic diagram showing the nucleotide and corresponding amino acid changes comprising the H234LΔ235-8 CARD11 variant found in patients vs. healthy control.

effusions and recurrent folliculitis of the forearms and thighs. *Staphylococcus aureus* was isolated on the initial bacterial culture. Further immunological investigations revealed a polyclonal B-cell lymphocytosis (absolute lymphocyte count of 3.4×10^9/L with 33.0% of circulating $CD19^+$ B-cells). B-cell subpopulation analysis also demonstrated an increased proportion of naïve $CD19^+sIgM^+$ B-cells (7.9×10^8/L, 74.0%) and $CD19^+CD5^+$ B-cells (5.3×10^8/L, 50.0%), while the proportion of class-switched $CD19^+CD27^+IgD^-$memory B-cells (0.1×10^8/L, 1.0%) was severely decreased. The father had a mild decrease in serum IgM level (0.48 g/L), but otherwise normal serum immunoglobulins (IgG 12.7 g/L, IgA 1.8 g/L, IgE 37–107 μg/L) and specific antibody responses against tetanus (0.9 IU/mL), diphtheria (0.6 IU/mL), and *Haemophilus influenzae type B* (HIB, 1.9 μg/mL) post vaccination. The specific humoral response against polysaccharide antigens was suboptimal with <50% of pneumococcal serotypes above 1.3 μg/mL despite Pneumovax booster. Numbers and proportions of peripheral blood T and NK cells populations were within normal range for age. Lymphocyte mitogen proliferation assays were also normal. The father was closely monitored for the occurrence of possible lymphoproliferative disorder; he had persistently positive EBV PCR (46 774 copies/mL, EBV VCA positive ≥1/4000, EBV EBNA <1/10) with enlarged axillary lymph nodes (up to 1.7 × 1.2 cm on the left size) and prominent fluorodeoxyglucose activity on PET-CT scan. His spleen size was at the upper limit of normal (13.3 cm). He was treated with frequent boosters of conjugated pneumococcal vaccines (e.g., Prevnar-13) and use of immunoglobulin replacement therapy was considered by the medical team.

The grandmother (II.1) reported frequent otitis externa and colds as a child. As an adult she had two pneumonias and two episodes of shingles, and was treated for Hodgkin's lymphoma (2A, mixed cellularity) at 33 years old. She has allergic rhinitis to dust and molds, frequent rhinosinusitis, persistent warts, and persistent onychomycosis. The great-grandmother (Patient I.1, 78 years old) suffered from recurrent warts, shingles and sinusitis over the years. A clinical evaluation was offered to the great grandmother at MUHC but never performed. The index patient, father and grandmother were subsequently evaluated at the NIH Clinical Center in 2015 and again in 2017. On physical exam, warts were noted on the index patient (one on toe) and father (multiple on hands). The most recent flow cytometric evaluation of PBMC confirmed expansion of naïve and immature B cells in the index patient, with few class-switched memory B cells detected (**Table 1**). The same pattern was evident in

TABLE 1 | Flow cytometric phenotyping of patient PBMC and serum Ig levels.

	II.1		III.1		IV.1		Normal range (adult)	
	%	#	%	#	%	#	%	#
Total B cells	20	612	32.5	1,066	43.3	1,602	3–19	59–329
Naïve CD19+IgD+	17.7	542	30.3	994	41.3	1,528	1.4–14.4	25–324
CD19+ CD10+	4	122	14.5	476	33.3	1,232	0.1–3.4	2–76
CD19+ CD27+	0.2	6	0.1	3	0	0	0.4–2.3	5–46
CD3+ T	71.3	2,182	61.2	2,007	53	1,961	60–83.7	714–2266
CD4+ T	35.1	1,074	405	1,328	34.9	1,291	31.9–62.2	359–1565
CD8+ T	31.7	970	16.3	535	13.7	507	11.2–34.8	178–853
NK cells	8.9	272	6.5	213	4.1	152	6.2–34.6	126–729
NKT cells	10	306	6	197	3.6	133	2.2–12.4	29–299

	II.1	III.1	IV.1
IgG	1135 (700–1600 mg/dL)	1129 (700–1600 mg/dL)	1204 (504–1465 mg/dL)
IgA	255 (70–400 mg/dL)	161 (70–400 mg/dL)	72(27–195 mg/dL)
IgM	37 (40–230 mg/dL)	39 (40–230 mg/dL)	14 (24–210 mg/dL)
IgE	16 (0–90 IU/mL)	37.5 (0–90 IU/mL)	136 (0–90 IU/mL)

Values in blue and red color indicate lower and higher levels, respectively, compared to normal healthy control ranges listed at right. Absolute counts indicated for each cell type are per μl. Normal Ig levels corresponding to patient age groups are indicated in parentheses.

the father and grandmother, although circulating B cell counts decreased inversely with age. PCR indicated moderate EBV viremia in both father and grandmother (3.13 and 4.45 Log10 IU/ml). Serum IgE levels were slightly elevated in the index patient; otherwise total immunoglobulin levels were normal for all subjects. For the father, random antibody titers against rubella, measles, and VZV were normal, but absent against mumps. The grandmother showed normal antibody titers to measles, rubella, mump, tetanus and HIB, with poor responses to Pneumovax (5/23 serotypes detected).

Affected patients displayed multiple clinical hallmarks of B cell Expansion with NF-κB and T cell Anergy (BENTA) disease, including (a) splenomegaly, (b) polyclonal B cell lymphocytosis, featuring elevated naïve/immature B cells with few class-switched memory B cells, (c) poor responses to pneumococcal vaccines, (d) bacterial/viral infections including pneumonias, molluscum contagiosium/warts, and moderate EBV viremia (2, 9). Because BENTA is caused by gain-of-function (GOF) variants in the lymphocyte scaffold molecule CARD11 (1, 4), we focused on *CARD11* as a potential candidate gene. Sanger sequencing was first performed on genomic DNA isolated from peripheral blood mononuclear cells (PBMC) from the index patient (IV.1) and his father (III.1). This analysis revealed a heterozygous four amino acid deletion and missense mutation within exon 5 of *CARD11* (NM_032415.3 c.701_713delinsT, p.His234_Lys238delinsLeu, hereafter referred to as H234LΔ235-8) (**Figures 1B,C**). The grandmother and great-grandmother were later confirmed to carry the same pathological mutation (**Figure 1B**). A CARD11 expression plasmid of this variant was constructed and expressed in a variant of the Jurkat human T cell line (JPM50.6) that lacks endogenous CARD11 expression and harbors an NF-κB-driven green fluorescent protein reporter (GFP) (13). Similar to a confirmed gain-of-function (GOF) CARD11 mutation (E134G) (4), H234LΔ235-8 induced constitutive NF-κB activation in unstimulated cells, increasing slightly upon TCR/CD28 crosslinking (**Figures 2A,B**). However, unlike E134G, co-expression of H234LΔ235-8 with WT CARD11 sharply reduced constitutive NF-κB activity. Strikingly, H234LΔ235-8 also significantly reduced WT CARD11-dependent NF-κB activation following TCR/CD28 stimulation (**Figure 2B**). Protein expression of WT, E134G and H234LΔ235-8 CARD11 were similar in transfected cells (**Figure 2C**). Co-immunoprecipitations in WT Jurkat transfectants revealed a substantial reduction of total CARD11 association with BCL10 and MALT1 following stimulation in the presence of H234LΔ235-8 but not WT or E134G CARD11 (**Figure 2D**). This decrease in CARD11-BCL10-MALT1 (CBM) complex formation was comparable, but slightly less pronounced, than that noted with a *bona fide* dominant negative (DN) CARD11 variant R47H (11). Moreover, FLAG-tagged CARD11 variants co-precipitated with WT GFP-tagged CARD11 when co-expressed in JPM50.6 cells, indicating WT CARD11 can directly associate with mutant CARD11 protein regardless of stimulation (**Figure 2E**). Taken together, these results suggest the H234LΔ235-8 CARD11 mutant can disrupt normal activation-induced CBM complex assembly and NF-κB signaling in T cells through DN interference. Similar to other patients harboring CARD11 DN variants, we also observed marked defects in NF-κB p65 phosphorylation and IκBα degradation in stimulated primary $CD4^+$ T cells from patients III.1 and IV.1 relative to healthy control subjects (**Figure 2F**).

At baseline, the patient (IV.1) and his father (III.1) showed marked B-cell lymphocytosis: 51.6% and 44.5%, respectively,

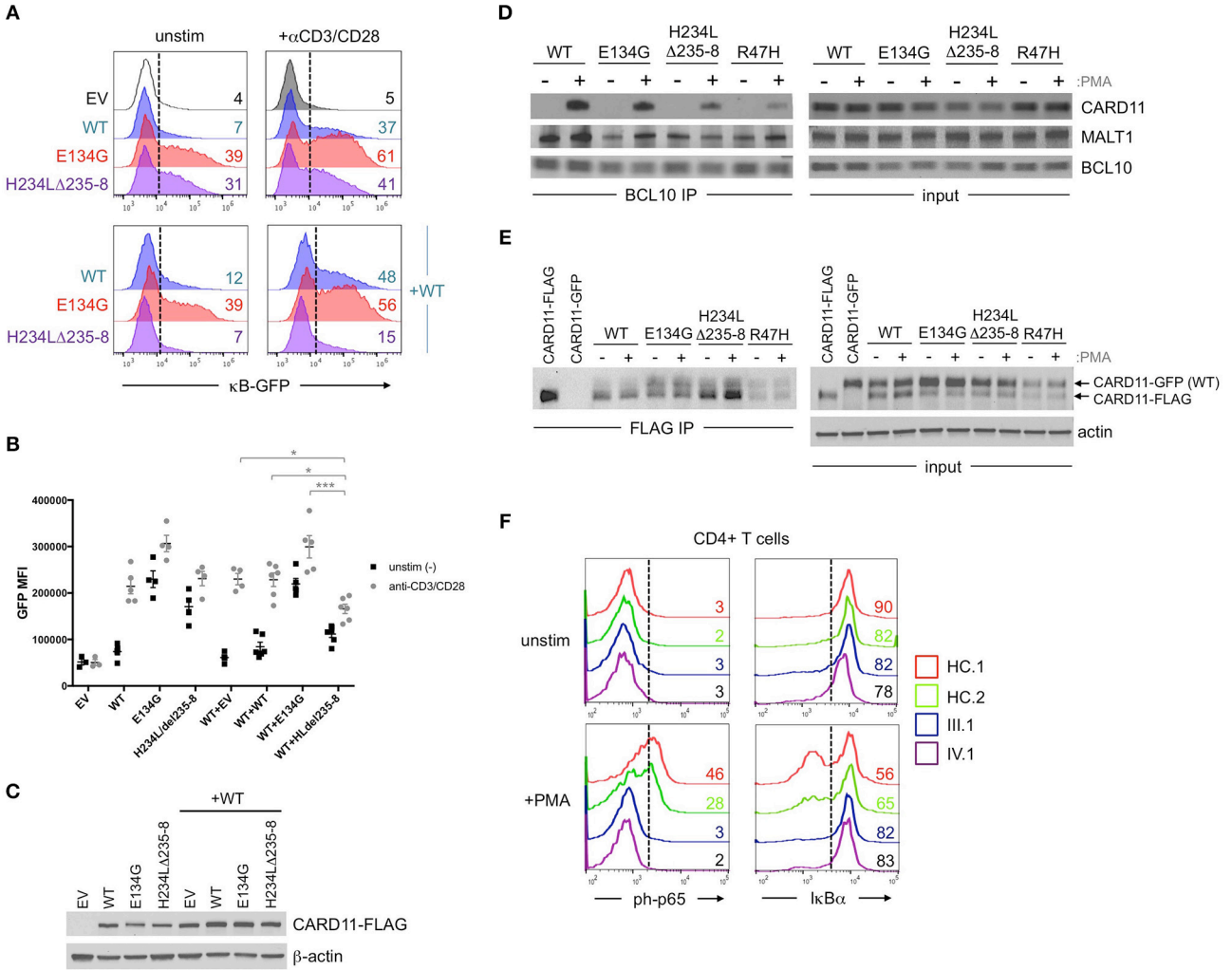

FIGURE 2 | Abnormal NF-κB activation induced by H234LΔ235-8 CARD11 *in vitro*. **(A)** JPM50.6 T cells were transfected with 5 μg of either empty vector (EV), WT, E134G (GOF mutant), or H234LΔ235-8 mutant CARD11-FLAG plasmids alone (top panel) or in the presence of 5 μg WT CARD11 plasmid (bottom panel) as previously described (14). After 24 h incubation in complete RPMI, transfected cells were stimulated with 1 μg/ml of anti-CD3 and anti-CD28 Abs or left unstimulated for an additional 24 h. GFP expression (reflecting relative NF-κB activity) was subsequently measured by flow cytometry; %GFP cells are labeled in each histogram. **(B)** Quantification of NF-κB driven GFP reporter expression in transfected JPM50.6 cells as described in (A). Data are mean ± SEM for mean fluorescence intensity of GFP^+ cells for 3 separate transfection experiments. Asterisks denote statistically significant differences (2-way ANOVA) between the stimulated groups indicated. **(C)** Immunoblots confirming the comparable expression of WT and mutant CARD1-FLAG proteins in cells from (A) at 24 h post-transfection. β-actin served as a loading control. Data are representative of 3 separate experiments. **(D)** WT Jurkat T cells were transfected with WT or mutant CARD11-FLAG plasmids as in (A). After 24 h, cells were stimulated with phorbol 12-myristate 13-acetate (PMA) for 20 min and lysed. Immunoprecipitations (IPs) using anti-BCL10 Ab were performed as previously described (12). BCL10 IPs and input lysates were separated by SDS-PAGE and immunoblotted Abs against CARD11, BCL10, and MALT1. **(E)** JPM50.6 cells were transfected with WT CARD11-GFP –/+ WT or mutant CARD11-FLAG plasmids as in (A). After 24 h, cells were stimulated with PMA for 20 min and lysed. FLAG IPs and input lysates were immunoblotted for total CARD11 protein; arrows indicate GFP- vs. FLAG-tagged CARD11. Actin served as a loading control for input lysates. IPs in (D,E) are representative of 2 separate experiments each. **(F)** PBMC from 2 healthy controls (HC) and patients III.1 and IV.1 were stimulated with PMA (20 ng/ml) plus monensin (2 μM) for 20 min. Cells were stained with FITC-conjugated mouse anti-human CD4 mAb, fixed in 1.5% paraformaldehyde and permeabilized in ice cold methanol before staining with AlexaFluor647-conjugated mouse anti-human phospho-p65 (Ser529) or AlexaFluor647-conjugated mouse anti-human IκBα. NF-κB activation was assessed in gated $CD4^+$ T cells by flow cytometry; numbers in each histogram denote % of phospho-$p65^+$ (left) or $IκBα^{hi}$ cells (right). Data are representative of 2 separate experiments.

of their PBMC were $CD19^+$ B-cells, compared to 13.8% for the patient's mother (healthy control, HC) and 10.2 ± 4.4% for a reference cohort. The majority were naive IgM^+IgD^+ B-cells (IV.1 74.9%, III.1 52.1%, HC 8.4%). To assess *in vitro* B-cell differentiation, PBMC (1×10^6/mL) were cultured for 7 days with anti-CD40 (1 μg/mL), IL-4 (200 U/mL), and IL-21 (50 ng/mL) at 1×10^6 PBMC/mL in complete medium [RPMI 1640 + 10% FBS, 2 mM glutamine, 1 mM sodium pyruvate, 15 mM HEPES buffer (pH 7.0), and 100 U/ml penicillin/streptomycin]. IL-21 promotes B-cell differentiation

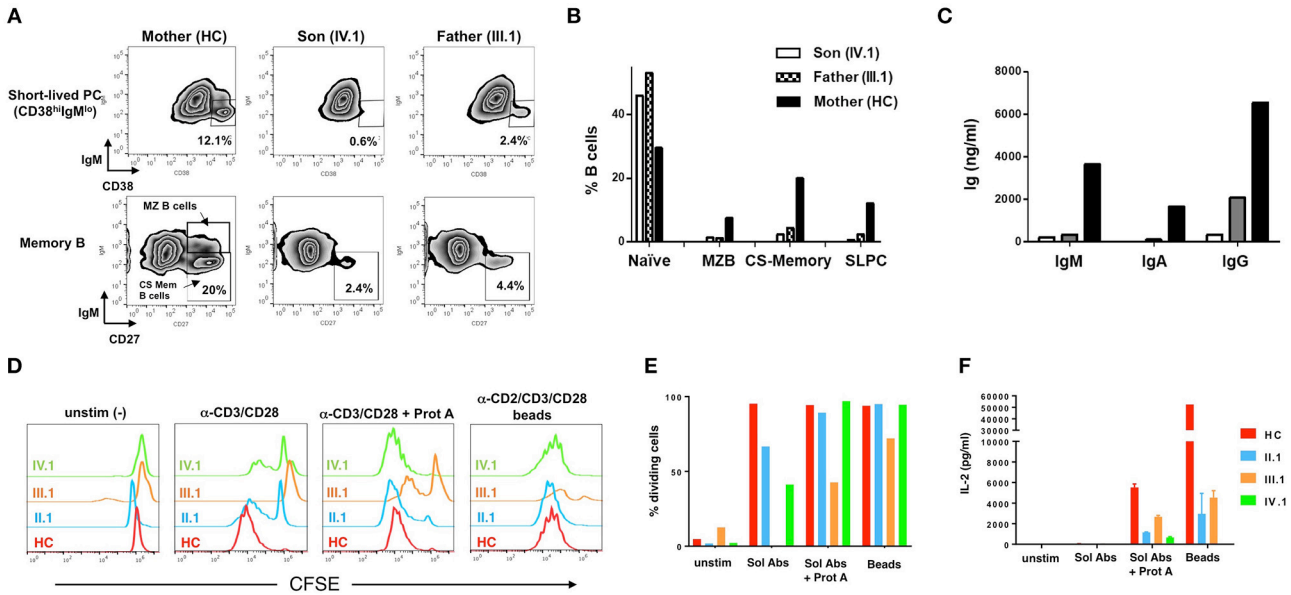

FIGURE 3 | Impaired patient B cell differentiation and T cell hyporesponsiveness to polyclonal stimuli *in vitro*. **(A)** PBMCs from mother (healthy control), III.1 and IV.1 were cultured in cRPMI media with anti-CD40 (1 μg/mL) + IL-4 (200 U/mL) + IL-21 (50 ng/mL) at 37°C and 5% CO_2 for 7 days as previously described (8, 15). B-cell subpopulations were analyzed by flow cytometry (Becton Dickinson LSRII, FlowJo Software) using Zombie aqua fixable viability dye and the following antibodies: PE-Cy7-conjugated mouse anti-human CD19, APC-conjugated mouse anti-human CD27, FITC-conjugated mouse anti-human CD38, PE-conjugated mouse anti-human IgM. Representative density plots are shown, with gates demarcating short-lived plasma cells (PC) (CD19+CD38+IgM–), class-switched (CS) memory B cells ($CD19^+CD27^+IgM^-$) and marginal zone B-cells ($CD19^+CD27^+IgM^+$). **(B)** Bar graph indicating the percentages of baseline naïve B cells ($CD19^+CD27^-IgM^+$) and marginal, CS memory B and short-lived PC after *in vitro* differentiation in healthy mother and patients. **(C)** Immunoglobulin production in cell supernatants after 7 days *in vitro* stimulation of healthy mother and patients' PBMC with anti-CD40+IL-4+IL-21, quantified by ELISA. Data in **(A–C)** are representative of three independent experiments. **(D)** Healthy control, II.1, III.1, and IV.1 patient CD4+ T cells were labeled with 1 μM CFSE and stimulated with 2 μg/ml of soluble anti-CD3 and CD28 Abs ± Protein A (2.5 μg/ml), or MACS iBead particles (1:1 bead:cell ratio) loaded with biotinylated anti-CD2, anti-CD3, and anti-CD28 Abs (Miltenyi Biotec) in cRPMI for 5–6 days. Histogram overlays display T cell proliferation based on CFSE dilution on day 5. **(E)** Bar graph denoting the percentage of dividing T cells in each group in response to various stimuli. **(F)** IL-2 levels in day 6 T cell culture supernatants were measured by ELISA as previously described (4, 13). Data in **(D–F)** are representative of two independent experiments.

into class-switched (CS) memory and antibody-secreting plasma cells in the presence of CD40 signaling (14), and IL-4 enhances these effects (15, 16). Cells from patient (IV.1) and father (III.1) not only displayed poor short-lived plasma cell differentiation (**Figure 3A**, top panel) compared to the healthy mother (IV.1 0.6%, III.1 2.4%, HC 12.1%), but also decreased $CD27^+$ memory B-cell differentiation including IgM^- $CD27^+$ CS memory B-cells (IV.1 2.4%, III.1 4.4%, HC 20%) (**Figure 3A**, bottom panel). B cell differentiation phenotypes were quantified in **Figure 3B**. These results were associated with marked decreases in production of IgM (IV.1 0.2 mg/L, III.1 0.4 mg/L, HC 3.7 mg/L), IgA (IV.1 0.0 mg/L, III.1 0.1 mg/L, HC 1.7 mg/L), and IgG (IV.1 0.4 mg/L, III.1 2.1 mg/L, HC 6.5 mg/L) (**Figure 3C**). Purified T cells from affected family members showed impaired proliferation in response to anti-CD3/CD28 Ab stimulation *in vitro*, which was largely rescued by more robust stimuli (Ab crosslinking or Ab-conjugated beads) (**Figures 3D,E**). Nevertheless, patient T cells secreted less IL-2 in response to all stimuli (**Figure 3F**, **Supplementary Figure 2**). These results are consistent with previous work demonstrating that BENTA patient B-cells exhibit intrinsic differentiation defects despite enhanced survival *in vitro* (8), whereas T cells from both BENTA (CARD11 GOF) and CARD11 DN patients are hyporesponsive *in vitro* (4, 12).

DISCUSSION

Here we describe a unique four-generation family harboring a novel germline heterozygous indel mutation (c.701–713delinsT) in exon 5 of *CARD11*, leading to one altered amino acid and a deletion of 3 others (p.His234_Lys238delinsLeu). Clinical and laboratory findings suggested a relatively mild presentation of BENTA disease, based on a modest selective expansion of naïve/immature B cells that inversely correlated with age. Lackluster pneumococcal vaccine responses and moderate EBV viremia were also noted. Also consistent with BENTA disease, our *in vitro* assays also revealed profound defects in B cell differentiation and Ab secretion, as well as T cell hyporesponsiveness. Interestingly, members of this family also exhibited mild atopic manifestations (e.g., eczema, food allergy, elevated IgE) that waned over time. Collectively, we posit that these effects may result from dual GOF and DN effects of this unique mutation on TCR-induced NF-κB activation (**Figure 2**). However, in contrast to the family described here, T cells from patients with potent DN mutations generally proliferate poorly even after robust stimulation and strongly skew toward a Th2 phenotype, reflecting more severe defects in TCR-induced NF-κB and

mTORC1 signaling (10–12). Although we suspect that the unique CARD11 variant described here is the major driver of shared phenotypes across four generations of affected family members, additional autosomal dominant gene variants may influence or modify disease presentation. Thus future whole exome sequencing (WES) analyses of this family could be informative.

Although CARD11 signaling is restrained by a complex set of redundant intramolecular interactions, single point mutations in the LATCH and CC domains can unlock an active signaling conformation without requiring AgR-dependent phosphorylation (17, 18). CARD11 must also oligomerize to signal (19), suggesting that both WT and mutant proteins should associate in shared CBM complexes (**Figures 2D–E**). For this unique variant, we speculate that the relative distribution of WT and mutant CARD11 molecules in these complexes may collectively allow for both constitutive NF-κB activation at steady state, *and* dominant interference of WT-dependent NF-κB signaling upon AgR engagement (**Figure 2F**). Nevertheless, the relative decline in disease severity observed with age (e.g., decreased B cell lymphocytosis, splenomegaly, and atopic symptoms) suggests the strongest phenotypic effects stemming from abnormal CARD11 signaling are ultimately overcome or somehow circumvented over time, as noted in both classic BENTA and CARD11 DN atopic patients.

The description of this family underscores some of the challenges in the clinical management of BENTA patients, including use of frequent boosters of conjugated vaccines, immunoglobulin replacement therapy, and increased likelihood of possible B cell malignancy (e.g., Hodgkin's lymphoma in II.1), particularly in the context of chronic EBV infection. Still, the family history described here suggests more aggressive clinical interventions to reduce the overall B cell burden (e.g., rituximab, immunosuppressants) are not warranted.

CONCLUDING REMARKS

This first report of a family with blended BENTA and atopic symptoms further expands the spectrum of disease phenotypes that can be ascribed to a novel heterozygous *CARD11* variant. The signaling effects ascribed to this unusual mutation highlight the CC domain as a crucial governor of complex intra- and intermolecular CARD11 protein interactions. Despite the many congruent pathways linked to AgR ligation, aberrant CARD11 signaling appears to affect the proliferation, survival and differentiation of B and T cells differently. Clinically, the longitudinal perspective afforded here by four affected generations further suggests that although careful surveillance of such patients is essential, disease symptoms often improve over time.

ETHICS STATEMENT

Patients' and biological parents' blood/tissue samples were obtained after informed consent through protocols established by the Lymphocyte Molecular Genetics Unit and approved by the Institutional Review Boards (IRB) of McGill University Health Centre and the National Institutes of Health (NIH). Experiments involving patient blood samples were performed at McGill University Health Center and Uniformed Services University conforming to IRB protocols.

AUTHOR CONTRIBUTIONS

MD and SA designed, executed and analyzed patient cell experiments, and wrote the manuscript. JRS, BD, and JS performed transfection experiments. BD performed biochemical and immunoprecipitation experiments. JRS and JN performed Sanger sequencing analysis. MR performed immunoglobulin heavy chain rearrangement analysis. AW, HM, and PA obtained consent and managed clinical care for patients at NIH. MD and BM provided clinical care at MUHC. HS provided clinical care at NIH. HS, BM, and AS supervised research studies and wrote and edited the manuscript.

FUNDING

This work was supported by the Intramural Research Program of the National Institute of Allergy and Infectious Diseases, NIH, the Meakins-Christie Laboratories of the Research Institute of McGill University Health Centre, AllerGen NCE, and grants from the National Institutes of Health (1R21AI109187 to AS), the Concern Foundation, and an intramural grant from USUHS. This project has also been funded in part with federal funds from the National Cancer Institute, National Institutes of Health, under Contract No. HHSN261200800001E. The content of this publication does not necessarily reflect the views or policies of the Department of Health and Human Services, nor does mention of trade names, commercial products, or organizations imply endorsement by the U.S. Government. MD and BM received funding support from Allergen NCE.

ACKNOWLEDGMENTS

We thank the family members for participating in this research; blood samples were obtained with written informed consent through protocols approved by the institutional review boards of the National Institutes of Allergy and Infectious Diseases (NIH), McGill University Health Centre, and Uniformed Services University. Patients also provided written informed consent allowing for publication of this manuscript. We also thank Dr. Sergio Rosenzweig and Dr. Thomas Fleisher (NIH Clinical Center) for supporting diagnostic flow cytometric analysis, and Dr. Zhaozhang Li and Dr. Kateryna Lund in the USUHS Bioinstrumentation Center for DNA primer synthesis, Sanger sequencing, and flow cytometry support. MD and BM received funding support from AllerGen NCE.

SUPPLEMENTARY MATERIAL

The Supplementary Material for this article can be found online at: https://www.frontiersin.org/articles/10.3389/fimmu.2018.02944/full#supplementary-material

REFERENCES

1. Arjunaraja S, Snow AL. Gain-of-function mutations and immunodeficiency: at a loss for proper tuning of lymphocyte signaling. *Curr Opin Allergy Clin Immunol*. (2015) 15:533–8. doi: 10.1097/ACI.0000000000000217
2. Lu HY, Bauman BM, Arjunaraja S, Dorjbal B, Milner JD, Snow AL, et al. The CBM-opathies-a rapidly expanding spectrum of human inborn errors of immunity caused by mutations in the CARD11-BCL10-MALT1 complex. *Front Immunol*. (2018) 9:2078. doi: 10.3389/fimmu.2018.02078
3. Lenz G, Davis RE, Ngo VN, Lam L, George TC, Wright GW, et al. Oncogenic CARD11 mutations in human diffuse large B cell lymphoma. *Science* (2008) 319:1676–9. doi: 10.1126/science.1153629
4. Snow AL, Xiao W, Stinson JR, Lu W, Chaigne-Delalande B, Zheng L, et al. Congenital B cell lymphocytosis explained by novel germline CARD11 mutations. *J Exp Med*. (2012) 209:2247–61. doi: 10.1084/jem.20120831
5. Turvey SE, Durandy A, Fischer A, Fung SY, Geha RS, Gewies A, et al. The CARD11-BCL10-MALT1 (CBM) signalosome complex: Stepping into the limelight of human primary immunodeficiency. *J Allergy Clin Immunol*. (2014) 134:276–84. doi: 10.1016/j.jaci.2014.06.015
6. Sasaki Y, Derudder E, Hobeika E, Pelanda R, Reth M, Rajewsky K, et al. Canonical NF-kappaB activity, dispensable for B cell development, replaces BAFF-receptor signals and promotes B cell proliferation upon activation. *Immunity* (2006) 24:729–39. doi: 10.1016/j.immuni.2006.04.005
7. Krishna S, Xie D, Gorentla B, Shin J, Gao J, Zhong XP. Chronic activation of the kinase IKKbeta impairs T cell function and survival. *J Immunol*. (2012) 189:1209–19. doi: 10.4049/jimmunol.1102429
8. Arjunaraja S, Nose BD, Sukumar G, Lott NM, Dalgard CL, Snow AL. Intrinsic plasma cell differentiation defects in B cell expansion with NF-kappaB and T cell anergy patient B cells. *Front Immunol*. (2017) 8:913. doi: 10.3389/fimmu.2017.00913
9. Arjunaraja S, Angelus P, Su HC, Snow AL. Impaired control of epstein–barr virus infection in B-cell expansion with NF-κB and T-cell anergy disease. *Front Immunol*. (2018) 9:198. doi: 10.3389/fimmu.2018.00198
10. Dadi H, Jones TA, Merico D, Sharfe N, Ovadia A, Schejter Y, et al. Combined immunodeficiency and atopy caused by a dominant negative mutation in caspase activation and recruitment domain family member 11 (CARD11). *J Allergy Clin Immunol*. (2017) 141:1818–30.e2. doi: 10.1016/j.jaci.2017.06.047
11. Dorjbal B, Stinson JR, Ma CA, Weinreich MA, Miraghazadeh B, Hartberger JM, et al. Hypomorphic caspase activation and recruitment domain 11 (CARD11) mutations associated with diverse immunologic phenotypes with or without atopic disease. *J Allergy Clin Immunol*. (2018). doi: 10.1016/j.jaci.2018.08.013. [Epub ahead of print].
12. Ma CA, Stinson JR, Zhang Y, Abbott JK, Weinreich MA, Hauk PJ, et al. Germline hypomorphic CARD11 mutations in severe atopic disease. *Nat Genet*. (2017) 49:1192–201. doi: 10.1038/ng.3898
13. Brohl AS, Stinson JR, Su HC, Badgett T, Jennings CD, Sukumar G, et al. Germline CARD11 mutation in a patient with severe congenital B cell lymphocytosis. *J Clin Immunol*. (2015) 35:32–46. doi: 10.1007/s10875-014-0106-4
14. Desjardins M, Mazer BD. B-cell memory and primary immune deficiencies: interleukin-21 related defects. *Curr Opin Allergy Clin Immunol*. (2013) 13:639–45. doi: 10.1097/ACI.0000000000000009
15. Desjardins M, Beland M, Dembele M, Lejtenyi D, Drolet JP, Lemire M, et al. Modulation of the interleukin-21 pathway with interleukin-4 distinguishes common variable immunodeficiency patients with more non-infectious clinical complications. *J Clin Immunol*. (2018) 38:45–55. doi: 10.1007/s10875-017-0452-0
16. Avery DT, Bryant VL, Ma CS, de Waal Malefyt R, Tangye SG. IL-21-induced isotype switching to IgG and IgA by human naive B cells is differentially regulated by IL-4. *J Immunol*. (2008) 181:1767–79. doi: 10.4049/jimmunol.181.3.1767
17. Jattani RP, Tritapoe JM, Pomerantz JL. Cooperative control of caspase recruitment domain-containing protein 11 (CARD11) signaling by an unusual array of redundant repressive elements. *J Biol Chem*. (2016) 291:8324–36. doi: 10.1074/jbc.M115.683714
18. Jattani RP, Tritapoe JM, Pomerantz JL. Intramolecular interactions and regulation of cofactor binding by the four repressive elements in the caspase recruitment domain-containing protein 11 (CARD11) inhibitory domain. *J Biol Chem*. (2016) 291:8338–48. doi: 10.1074/jbc.M116.717322
19. Tanner MJ, Hanel W, Gaffen SL, Lin X. CARMA1 coiled-coil domain is involved in the oligomerization and subcellular localization of CARMA1 and is required for T cell receptor-induced NF-kappaB activation. *J Biol Chem*. (2007) 282:17141–7. doi: 10.1074/jbc.M700169200

Conflict of Interest Statement: The authors declare that the research was conducted in the absence of any commercial or financial relationships that could be construed as a potential conflict of interest.

frontiers in Immunology

REVIEW
published: 26 September 2018
doi: 10.3389/fimmu.2018.02167

CARD14/CARMA2 Signaling and its Role in Inflammatory Skin Disorders

Tiziana Zotti[1,2], *Immacolata Polvere*[1,2], *Serena Voccola*[1,2], *Pasquale Vito*[1,2]* and *Romania Stilo*[1,2]

[1] Genus Biotechnology, Università degli Studi del Sannio, Benevento, Italy, [2] Dipartimento di Scienze e Tecnologie, Università degli Studi del Sannio, Benevento, Italy

CARMA proteins represent a family of scaffold molecules which play several crucial biological functions, including regulation of immune response and inflammation, tissue homeostasis, and modulation of G-Protein Coupled Receptor (GPCR) signaling. Among the CARMA proteins, CARD14/CARMA2 and its alternatively spliced isoforms are specifically expressed in epithelial cells and keratinocytes. Recent evidences have shown that CARD14/CARMA2 mediates induction of inflammatory response in keratinocytes, and that mutations in CARD14/CARMA2 gene segregate with familial transmission of chronic inflammatory disorders of the human skin. Similarly to CARD11/CARMA1 and CARD10/CARMA3, CARD14/CARMA2 signaling occurs trough formation of a trimeric complex which includes BCL10 and MALT1 proteins. However, it is becoming increasingly evident that in addition to the CBM complex components, a number of accessory molecules are able to finely modulate the signals conveyed on and amplified by CARD14/CARMA2. The study of these molecules is important both to understand the molecular mechanisms that underlie the role of CARMA2 in keratinocytes and because they represent potential therapeutic targets for the development of therapeutic strategies aiming at the treatment of inflammatory diseases of the human skin. In this review, we provide an overview on the molecular mechanisms mediating CARD14/CARMA2 signaling and its implication in our understanding of the pathogenesis of human inflammatory skin disorders.

Keywords: CARD14, CARMA2, NF-kappa B, psoriasis, Bcl10, Malt1, CBM complex

OPEN ACCESS

Edited by:
Andrew L. Snow,
Uniformed Services University of the Health Sciences, United States

Reviewed by:
Jolan Eszter Walter,
University of South Florida, United States
Levi Watkin,
Baylor College of Medicine, United States

***Correspondence:**
Pasquale Vito
vito@unisannio.it

Specialty section:
This article was submitted to Primary Immunodeficiencies, a section of the journal Frontiers in Immunology

Received: *06 June 2018*
Accepted: *03 September 2018*
Published: *26 September 2018*

Citation:
Zotti T, Polvere I, Voccola S, Vito P and Stilo R (2018) CARD14/CARMA2 Signaling and its Role in Inflammatory Skin Disorders. Front. Immunol. 9:2167. doi: 10.3389/fimmu.2018.02167

CARMA FAMILY: AN OVERVIEW

Caspase recruitment domain (CARD)-containing membrane-associated guanylate kinase (MAGUK) proteins constitute a family of three scaffold proteins, highly conserved in their amino acidic sequence, named CARD11/CARMA1 (CARMA1), CARD14/CARMA2 (CARMA2), and CARD10/CARMA3 (CARMA3) (1, 2). CARMA proteins were identified in 2001, while screening sequence databases and two-hybrid libraries for novel CARD-containing proteins, and were shown to be able to interact with the CARD domain of B-Cell Leukemia 10 (BCL10) (3–6). The human CARMA proteins are encoded by three conserved genes, respectively located on chromosomes 7, 17, and 22. Structurally, CARMA proteins are characterized by a typical modular organization, with the CARD domain at the N-terminus, followed by a Coiled-Coil region and a C-terminal MAGUK domain, consisting of PDZ, SH3, and GUK modules (**Figure 1A**). Despite the high degree of structural similarity, the expression pattern of each CARMA protein is restricted to distinct tissues, where they are involved in cell-specific signaling pathways that

control activation of NF-κB, a pleiotropic transcription factor that controls transcription of, among others, immunomodulatory and inflammatory genes and genes that generally promote cell proliferation and survival (7). Indeed, CARMA1 is mainly expressed in lymphoid cells and hematopoietic tissues, where it mediates NF-κB induction following antigen receptor engagement. Notably, CARMA1 deficient-mice show a severe defect in lymphocyte proliferation following T- and B-cell receptor stimulation, with impaired production and release of cytokines (8–10), due to defective NF-κB activation. Consistently with evidences from animal models, whereas loss-of-function mutations in human *CARMA1* gene cause severe forms of immunodeficiencies (11–13), gain-of-function mutations have been frequently described in patients affected by diverse lymphoid malignancies, such as T-cell lymphomas, gastric B-cell lymphomas, some non-Hodgkin's lymphomas and others (14).

Conversely, CARMA2 and CARMA3 are both expressed in non-lymphoid tissues, but in a non-overlapping manner. In fact, CARMA2 protein is preferentially expressed in epithelial cells of the skin and in mucosae, while CARMA3 has a broader non-hematopoietic expression pattern (2). In these districts, CARMA3 regulates NF-κB activation following stimulation of G-protein coupled receptors (GPCRs) with several ligands, such as angiotensin II, endothelin I, and lyso-phosphatidic acid (15, 16). In addition, CARMA3 has also been shown to be involved in NF-κB activation downstream of the epithelial growth factor receptor (17). Not surprisingly, CARMA3 over-expression has been shown to be implicated in the onset and progression of different cancers by several studies (18, 19).

Compared to CARMA1 and CARMA3, CARMA2 is less characterized. Only recent studies have shed light on the crucial role this scaffold protein plays in the human skin, where it regulates tissue homeostasis.

CARMA2: CLONING, SPLICE VARIANTS, EXPRESSION

CARMA2 was originally identified as a placenta-specific cytoplasmic 1,004 amino acids protein containing a CARD module and a MAGUK domain, and capable to activate the NF-κB-controlled expression of a luciferase reporter gene when transfected in cultured cell lines (3). Subsequent works have demonstrated that *CARMA2* mRNA undergoes alternate splicing processes (20) and that the deriving protein isoforms show a wider distribution profile, being expressed also in epidermal keratinocytes, dermal endothelial cells, mucosae and different cell lines (20, 21). In particular, three transcript variants of human *CARMA2* gene have been identified, named CARMA2*fl* (*full length*; 1,004 amino acids), the longest polypeptide containing all the typical CARMA domains and modules; CARMA2*sh* (*short*; 740 amino acids), the prominent isoform expressed in the human skin, lacking the SH3 and GuK modules and containing the CARD, coiled coil and PDZ domains; and CARMA2*cl* (*cardless*; 434 amino acids), containing only a portion of the coiled coil domain, the linker region and a shorter PDZ module (**Figure 1B**). Due to the absence of a complete MAGUK domain, CARMA2*cl* and CARMA2*sh* variants may not be exclusively associated to the cell membrane, but rather distributed in the cytosol where they possibly transduce intracellular signals (20).

As assessed by NF-κB-luciferase reporter assays, while CARMA2*fl* and especially CARMA2*sh* are strong inducers of NF-κB, CARMA2*cl* is unable to promote activity of this transcription factor (20), confirming the CARD region as an essential domain for NF-κB signaling regulated by CARD-containing proteins. Indeed, similarly to CARMA1 and CARMA3, CARMA2*fl*, and CARMA2*sh*, but not CARMA2*cl*, interact with BCL10 via an homotypic CARD-CARD association and, together with the paracaspase Mucosa Associated lymphoid tissue Lymphoma Translocation protein 1 (MALT1), are able to form a CARMA-BCL10-MALT1 (CBM) complex (**Figure 1C**). Assembly of the CBM complex is crucial for the recruitment of downstream signaling components that lead to NF-κB activation (20, 22, 23). Differently from the longest CARMA2 isoforms, CARMA2*cl* has a very limited expression profile in non-epidermal tissue, and in transfection experiments it may function as a natural dominant-negative regulator of CARMA2*sh* signaling in the skin (Scudiero and Vito, unpublished results). Overall, the identification of alternative transcripts for *CARMA2* is intriguing for several reasons: first, their expression pattern is not totally overlapping, suggesting that they could play diverse functions in different cell types; second, even within the same cell type, *CARMA2* transcript variants could regulate different stimuli, starting both from the cell membrane and intracellular organules, or regulate signals from the same stimulus at several levels.

CARMA2 IN KERATINOCYTES AND SKIN DISORDERS

Psoriasis is an inflammatory disorder of the human skin, characterized by well-demarcated oval-shaped erythematous plaques on the skin due to abnormal keratinization and proliferation of superficial keratinocytes, and persistence of nucleated cells in the corneus layer (24). The onset of psoriasis depends on both genetic and environmental factors and is characterized by the disruption of the epithelial barrier function and tissue homeostasis due to stressing or traumatic events within the epidermis, and a dysregulated immune response. Epidemiologic studies based on data collected on psoriatic patients from 20 different countries show that psoriasis is a complex genetic-based immune-mediated disease with a prevalence ranging from 0 to 1.37% in children and from 0.51 to 11.43% in adults, with at least 100 million individuals affected worldwide (25). Indeed, in the human genome multiple susceptibility loci, collectively called *PSORS*s, have been associated to the familial transmission of the psoriatic tract, with the identification of about 40 genes involved in antigen presentation, interleukin and cytokine signaling, antiviral response, NF-κB signaling and, more generally, in the adaptive and innate immunity (24). Nevertheless, although a genetic base underlies psoriasis and psoriasis-related diseases, <20% of

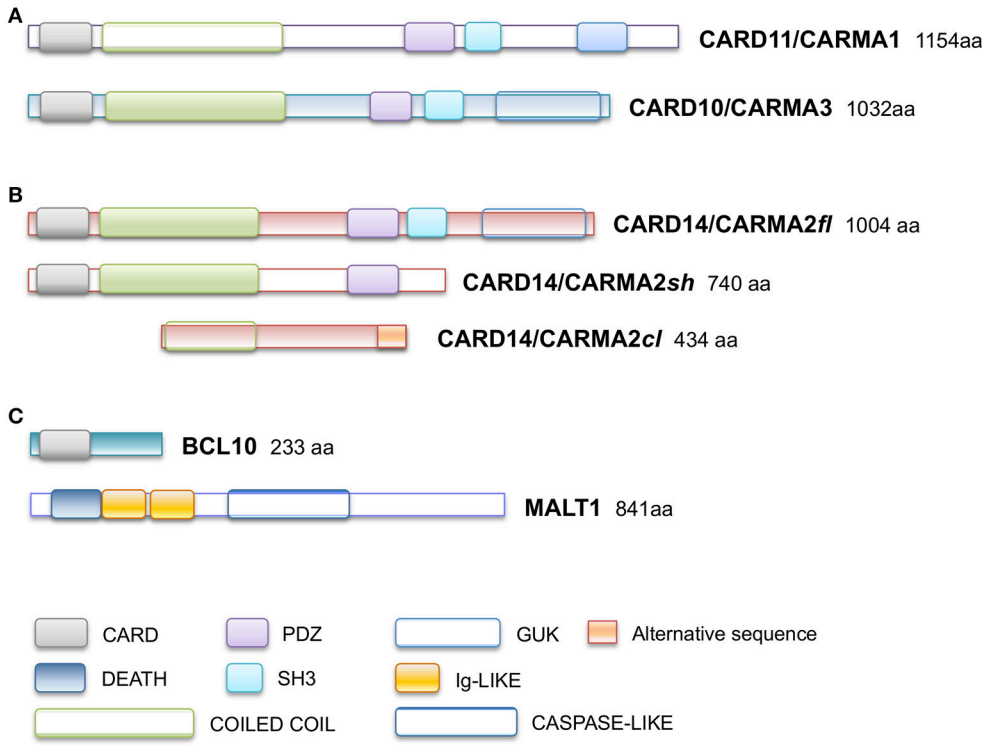

FIGURE 1 | Schematic representation of domain organization of **(A)** CARD11/CARMA1 (UniProt Entry: Q9BXL7) and CARD10/CARMA3 (UniProt Entry: Q9BWT7) proteins, **(B)** CARD14/CARMA2 isoforms (UniProt Entry: Q9BXL6) **(C)** BCL10 (UniProt Entry: O95999) and MALT1 proteins (UniProt Entry: Q9UDY8). Aminoacid numbering and domains are referred to human proteins. CARD, CAspase-Recruitment Domain; PDZ, post-synaptic density protein (PSD95), Drosophila disc large tumor suppressor (Dlg1), and Zonula occludens-1 protein (Zo-1) domain; GuK, guanylate kinase-like; DEATH, death domain; SH3, Src homology 3; Ig-LIKE, immunoglobulin-like domain; COILED COIL, coiled coil region; CASPASE-LIKE, Cysteine-ASpartic ProteASEs-like domain.

disease variance is explained by mutations in the aforementioned genes, suggesting the existence of additional mechanisms which could trigger these skin inflammatory pathologies (26).

In 2012, Jordan et al. established that *PSORS2* was due to gain-of-function mutations in the *CARD14* gene, as assessed by exome capture and next generation sequencing over genomic DNA from both familial and sporadic cases of psoriasis and psoriatic arthritis (27, 28). Most of the psoriasis-linked mutations harbored in CARMA2*sh* produced an enhanced activity of NF-κB transcription factor in luciferase assays, with a consequent up-regulation of NF-κB-induced inflammatory transcripts in keratinocytes, such as CXCL8, CCL20, IL8, and IL6, confirming the crucial role played by this transcription factor in epithelial homeostasis (27, 28). In addition to genetic psoriasis, mutations in *CARMA2* were also found in familial cases of pityriasis rubra pilaris, a papulosquamous disorder phenotypically related to psoriasis (29).

Subsequently, plenty of sequence variations and mutations in the *CARD14* gene have been mapped and associated to psoriasis, pityriasis and other skin disorders phenotipically related to them. **Table 1** reports all known CARMA2*sh* variants associated to skin inflammatory illnesses that have been identified so far, updating a list already provided by Van Nuffel et al. (50). **Figure 2** show that base mutations preferentially involve codons in exon 4, resulting in amino acidic substitutions within the CARD and Coiled-Coil domains.

Although many of the *CARMA2* mutations found in a variety of inflammatory disorders of the human skin point to an aberrant activation of NF-κB, it is worth noting that some patients carry mutations in CARMA2*sh* (such as Arg38Cys; Arg69Trp; Arg151Trp; His171Asn; Ser200Asn; Ala216Thr; Thr420Ala) that, at least in luciferase-based *in vitro* assays, do not determine a remarkably stronger activation of NF-κB (28, 30, 50), suggesting that CARMA2*sh* could participate to additional intracellular mechanisms regulating skin homeostasis. In fact, other studies have demonstrated that several CARMA2*sh* variant, including Arg820Trp, could significatively affect the response to anti-TNFα treatment in psoriasis patients, with interesting implications for optimal therapy settings (51, 52).

CARMA2 SIGNALING

Given its involvement in the pathogenesis of psoriasis, many efforts have focused on the understanding of the molecular mechanisms through which CARMA2*sh* regulates signaling cascades in human keratinocytes (**Figure 3**). Experimental data indicate that CARMA2*sh* signaling requires assembly of a molecular complex that, in addition to CARMA2*sh*, also includes

TABLE 1 | List of CARMA2 variants associated to psoriasis or psoriasiform inflammatory diesases.

Mutation	Disease	References
R38C	Psoriasis vulgaris	(27)
R62Q	Psoriasis vulgaris	(27, 30)
R69W	Psoriasis vulgaris	(30)
G117S	Psoriasis vulgaris; Pityriasis rubra pilaris	(27, 28, 30–33)
c.349 + 5G > A	Psoriasis vulgaris	(27, 28)
c.349 + 5G > C	Psoriasis; Pityriasis rubra pilaris	(34)
c.349 + 1G > A	Pityriasis rubra pilaris; Generalized pustular psoriasis	(29, 35)
M119R	Pityriasis rubra pilaris	(36)
M119T	Psoriasis; Pityriasis rubra pilaris	(34)
M119V	Generalized pustular psoriasis	(37)
L124P	Pityriasis rubra pilaris	(38)
C127S	Pityriasis rubra pilaris	(33)
Q136L	Pityriasis rubra pilaris	(33)
E138A	Generalized pustular psoriasis	(27, 28)
E138K	Pityriasis rubra pilaris	(39, 40)
E138del	Pityriasis rubra pilaris	(29)
E142K	Psoriasis vulgaris	(27, 28)
E142G	Psoriasis vulgaris	(27, 28)
L150R	Psoriasis vulgaris	(27, 30)
R151W	Psoriasis vulgaris	(30)
R151Q	Psoriasis vulgaris	(30)
L156P	Pityriasis rubra pilaris	(29)
Q157P	Psoriasis; Pityriasis rubra pilaris	(34)
R166H	Generalized pustular psoriasis	(37)
H171N	Psoriasis vulgaris	(27)
D176H	Psoriasis vulgaris; Generalized pustular psoriasis; Pityriasis rubra pilaris	(27, 41–45)
R179H	Psoriasis vulgaris; Pityriasis rubra pilaris	(27, 43)
V191L	Psoriasis vulgaris	(27)
E197K	Psoriasis vulgaris; Pityriasis rubra pilaris; Psoriatic arthritis	(30, 43)
S200N	Psoriasis vulgaris; Generalized pustular psoriasis; Pityriasis rubra pilaris	(27, 30, 31, 43)
L209P	Psoriasis vulgaris	(30)
A216T	Psoriasis vulgaris	(30, 37, 44)
D285G	Psoriasis vulgaris	(27)
M338V	Psoriasis vulgaris	(30)
T420A	Psoriasis vulgaris	(30)
R430W	Acute generalized exanthematous pustulosis	(46)
c.1356 + 5G > A	Psoriasis vulgaris	(30)
T591M	Psoriasis vulgaris	(37)
I593N	Psoriasis vulgaris	(27)
S602L	Psoriasis vulgaris; Generalized pustular psoriasis; Pityriasis rubra pilaris	(30)
R682W	Psoriasis vulgaris; Generalized pustular psoriasis	(27, 37)
G714S	Psoriasis vulgaris	(27)
R820W	Psoriasis vulgaris; Psoriatic arthritis	(27, 47–49)
D973E	Psoriasis vulgaris	(27)

the adapter protein BCL10 and the protease MALT1, as demonstrated by experiments conducted using short interfering RNAs, genome editing methods and chemical inhibitors (20, 22, 53). Most of the details that control assembly of the CBM complex and its activation derive from data obtained with CARMA1 in lymphocytes. In un-stimulated cells, CARMA1 is held in check by the inhibitory linker region, located between the coiled-coil domain and the PDZ domain. Following cell stimulation, such auto-inhibition is removed through PKCs-mediated phosphorylation of serine residues in the linker region,

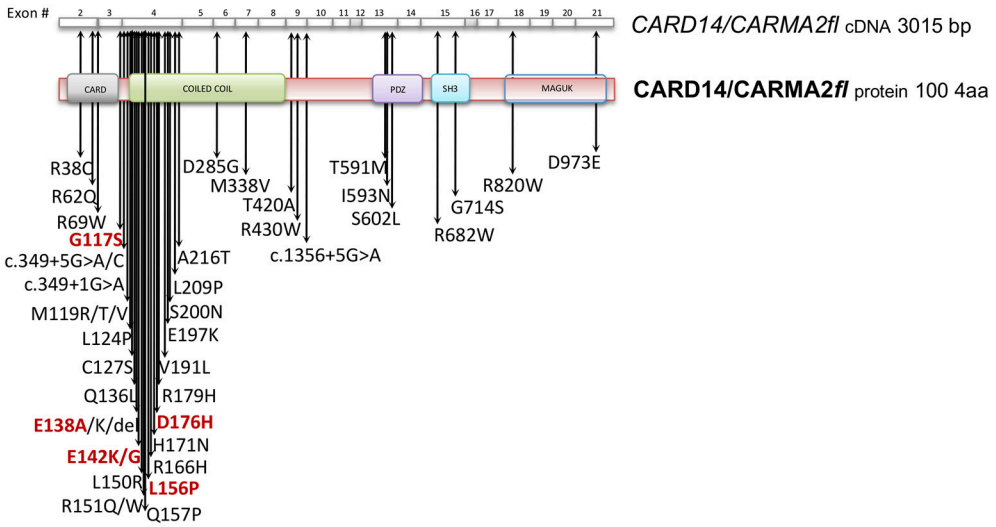

FIGURE 2 | CARD14/CARMA2 variants associated to skin inflammatory diseases (see also **Table 1**). Arrows indicate mutated base positions within CARD14/CARMA2 exons and corresponding aminoacid substitution identified in psoriasiform patients. In red, missense mutations having a reported positive effect on NF-κB activation.

thereby facilitating BCL10 and MALT1 binding to the CARMA1 (54, 55). The assembly of the CBM complex eventually results in the recruitment of the IKK complex and the consequent NF-κB activation (23). The similarity of the mechanisms of activation of the different CARMA proteins is also suggested by the fact that ectopic expression of the deubiquitinase A20 inhibits activation of NF-κB mediated by each of the CARMA proteins (20, 22, 56). Consistently with the model that considers assembly of the CBM complex as a crucial point for activation of the NF-κB pathway, two highly penetrant psoriasis-linked CARMA2*sh* point mutations, Gly117Ser, and Glu138Ala, abrogate CARMA2 auto-inhibition and stimulate MALT1 protease activity, causing constitutive activation of the CBM complex and aberrant NF-κB-dependent induction of downstream inflammatory genes (22, 53). Interestingly, MALT1 deficiency or chemical inhibition of its catalytic activity can block hyperactivation of the inflammatory signaling program (including the induction of TNFα, IL17C, CXCL8, and HBD2 genes), triggered by pathogenic psoriasis-related CARMA2*sh* mutants or by cell stimulation with the fungal cell wall component zymosan or with *Staphilococcus aureus,* pointing to MALT1 as a potential target for therapeutic treatment of skin disorders caused by aberrant CARMA2*sh* signaling (22, 50, 53, 57). In addition to the component of the CBM complex, the NF-κB-inducing activity of CARMA2*sh* also requires the adapter molecule TRAF2 (20), although this evidence comes from experiments carried out in non-keratinocytic cell lines. In these cells, CARMA2*sh* expression protects cells from apoptosis induced by different stimuli, including ER stress (20).

The psoriasis-associated CARMA2*sh* mutants Glu138Ala and Glu142Gly also escape the negative regulation exerted by two novel CARMA2*sh* interactors identified by two-hybrid screening in yeast, namely the serine/threonine kinase Unc-51 Like Autophagy Activating Kinase 2 (ULK2) and the E3 ubiquitin ligase Ring Finger protein 7 (RNF7) (57–59). Both ULK2 and RNF7 are indeed able to repress CARMA2*sh*-induced NF-κB activation, although through different mechanisms. In particular, ULK2 phosphorylates CARMA2*sh* and promotes lysosomal degradation of BCL10, whereas RNF7 alters the ubiquitination state of MALT1 and NEMO (58, 59). Intriguingly, a protein similar to RNF7, named RNF181, has been identified as an interactor of CARMA1 and functions as an E3 ubiquitin ligase to inhibit antigen receptor signaling to NF-κB downstream of CARMA1 (60). Conversely, the ability of CARMA2*sh* to activate NF-κB is positively regulated by the DEP domain-containing protein DEPDC7, which may be required to specifically convey on the CBM complex signals coming from activated G protein-coupled receptors (61).

Recent evidence indicates that CARMA2*sh* and MALT1 play a role in the signal transduction pathway that connects pathogen-associated molecular patterns recognition to NF-κB activation (57, 58). Microorganisms, such as bacterial and fungi cells display in fact pathogen-associated molecular patterns (PAMPs), which are molecules associated with groups of pathogens, and activate NF-κB upon agonistic binding to Pattern Recognition Receptors, including members of the Toll-like receptors (TLR) family expressed on human keratinocytes. Indeed, depletion of each of the components of the CBM complex significantly impairs expression of NF-κB target genes in human epithelia keratinocytes exposed to heat-killed *Escherichia coli*, *Sthaphylococcus aureus* or *Candida valida* (58). Altogether, these findings strengthen the existence of a causal link between microbial infections and the onset of psoriasis and encourage more efforts in further clarifying how exposure to PAMPs could determine disruption of skin homeostasis, inflammation and hyperproliferation in susceptible keratinocytes.

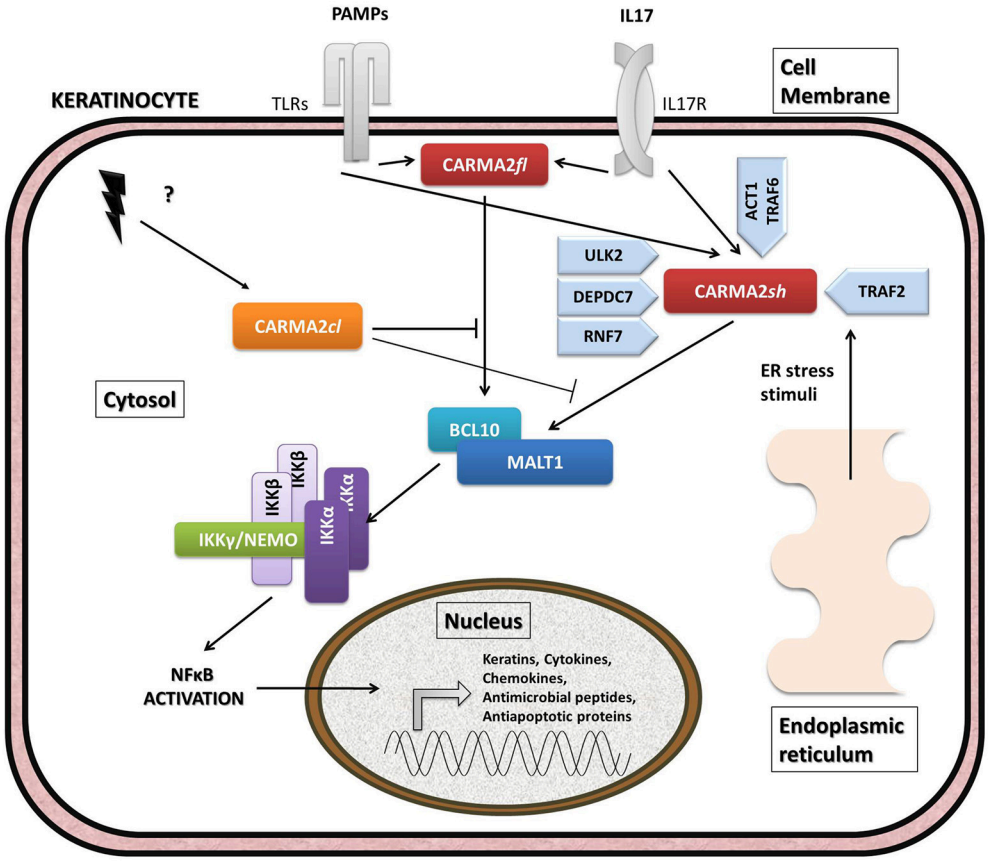

FIGURE 3 | Schematic overview of intracellular pathways involving CARD14/CARMA2 variants in keratinocytes. In the skin, CARMA2-mediated signals are prompted by intracellular organelles, such as endoplasmic reticulum, and by surface receptors, such as Toll-Like Receptors (TLRs) and IL17-Receptor (IL17R) in response to Pathogen Associated Membrane Patterns (PAMPs) and IL17, respectively. While CARMA2cl would act as a natural negative regulator, CARMA2sh and CARMA2fl variants interact with BCL10 and MALT1, thereby forming CBM complex. In turn, CBM triggers a canonical NEMO-dependent NF-κB-activation pathway, mediated by the IκB Kinase complex (IKK complex), which leads to expression of target genes in the nucleus, such as keratins, antimicrobial compounds and inflammatory mediators. Negative and positive regulators of CARMA2sh identified so far are also reported in the figure.

ANIMAL MODELS

Many interesting information can be inferred from the very recent generation of murine strains genetically modified in the *CARMA2* locus. Tanaka and colleagues generated CARMA2-deficient mice, which appear viable and healthy at birth and after, with normal epidermal and dermal tissue architecture (62). Interestingly, CARMA2$^{-/-}$ mice are resistant to psoriasis provoked by intraperitoneal injection of recombinant IL-23 or treatment with imiquimod (IMQ) cream, an agonist of TLR7/TLR9. From these data, the authors suggest that CARMA2 is relevant for IL-23 receptor signaling in a population of IL-17- and IL-22-producing γδ T cells (62). The data, however, does not exclude the possibility that CARMA2 also controls the signaling cascade strarting from TLR7/TLR9.

In another study carried out by Mellet et al. (63), the psoriasic phenotype spontaneously develops in C57BL/6J mice harboring a CARMA2 mutation consisting in the deletion of a key glutamic acid residue at position 138 (CARMA2Δ138). Interestingly, while mice homozygous for E138 deletion show developmental abnormalities and die perinatally, heterozygous animals are viable, and a single copy of the gain-of-function mutation is sufficient to trigger psoriatic pathogenesis *in vivo*. Indeed, *CARD14*$^{\Delta E138/+}$ mice display all clinical and immunological features of chronic plaque-type psoriatic disease, with diffuse skin lesions characterized by epidermis thickening, persistence of hyperproliferating nucleated keratinocytes and immune cell infiltration in upper epidermal layers. In addition, affected skin from *CARD14*$^{\Delta E138/+}$ mice shows a transcriptome profile resembling the typical gene expression signature observed in human psoriatic plaques, including upregulation of hyperproliferative keratins, cytokines, chemokines and antimicrobial peptide-encoding genes. Consistently with previous findings, the pathologic skin phenotype displayed by this murine model is driven by the activation of IL23/IL17 axis, that promotes Th17 cell polarization via IL23, as confirmed by the fact that neutralization of IL23p19 with an antagonist antibody ameliorates disease symptoms, by reducing skin lesions

and expression of inflammatory and anti-microbial genes (63). Similarly, the *CARD14*$^{E138A/+}$ and *CARD14*$^{\Delta Q136/+}$ murine strains generated by Wang et al. also spontaneously develop psoriasis-like skin inflammation, which resulted from enhanced activation of the IL23/IL17 cytokine axis (64). Interestingly, these authors also show that CARMA2 associates with the ACT1-TRAF6 signaling complex, thereby mediating IL-17-induced NF-κB and MAPK signaling pathway activation, eventually responsible for expression of pro-inflammatory molecules.

CONCLUSIONS

After establishing that *PSORS2* is due to NF-κB-activating mutations in *CARMA2*, current scientific advances are shedding some light on the molecular mechanisms that link these mutations to the development of human inflammatory skin diseases. Indeed, although for a long time CARMA2 was the most unknown of CARMA proteins, its clear involvement in the incipit and progression of inflammatory human skin disorders has acted as a strong propeller to clarify the biological and molecular processes in which this protein is involved. In many ways, CARMA2 acts just like the similar CARMA1 and CARMA3 proteins, with the CBM complex representing the molecular motor driving the signals transmission. However, some aspects of the signal tranduction pathways controlled by CARMA2 remain elusive. For example, it is not yet clear exactly what types of stimuli are channeled through CARMA2 to trigger NF-κB activation. Data generated in cell lines implicate CARMA2 in the signal transduction pathways starting from intracellular organelles, such as the endoplasmic reticulum, and from TLR receptors. In these contexts, CARMA2 activity seems to be controlled by TRAFs proteins and by molecules involved in autophagic processes, such as ULK2. Furthermore, ubiquitination mechanisms in which RNF and DEPDC7 proteins are involved seem to play a role in the capacity of CARMA2 to regulate the activity of NF-κB transcription factor.

The recent generation of murine strains harboring genetic modifications in the *CARMA2* locus is undoubtedly another important tool that will offer great opportunities to study in a complex biological system the role CARMA2 plays in the physiology and pathology of keratinocytes. Psoriasis is a typically human disease, and probably the lack of animal models that spontaneously develop the same disease has certainly represented a limit to our knowledge of this disease. Taking into account the obvious differences existing between human skin and murine skin, the fact that *CARMA2*-modified mouse strains develop inflammatory disorders with features largely overlapping to human psoriasis represents a real breaktrough. The phenotypic analyzes conducted on these mice indicate that the main alteration resides in the signal transduction along the IL23/IL17 cytokine axis, that would be ultimately responsible for the development of the psoriatic phenotype.

The coming years will undoubtedly be decisive in placing all the knowledge we have acquired so far on CARMA2 in a clearer and more coherent picture.

AUTHOR CONTRIBUTIONS

TZ, IP, SV, RS, and PV reviewed the literature and wrote the manuscript.

REFERENCES

1. Blonska M, Lin X. NF-κB signaling pathways regulated by CARMA family of scaffold proteins. *Cell Res.* (2011) 21:55–70. doi: 10.1038/cr.2010.182
2. Scudiero I, Vito P, Stilo R. The three CARMA sisters: so different, so similar: a portrait of the three CARMA proteins and their involvement in human disorders. *J Cell Physiol.* (2014) 229:990–7. doi: 10.1002/jcp.24543
3. Bertin J, Wang L, Guo YJ, Poyet J, Srinivasula S, Merriam S, et al. CARD11 and CARD14 are novel caspase recruitment domain (CARD)/membrane-associated guanylate kinase (MAGUK) family members that interact with BCL10 and activate NF-kappa B. *J Biol Chem*. (2001) 276:11877–82. doi: 10.1074/jbc.M010512200
4. Wang L, Guo Y, Huang WJ, Ke X, Poyet JL, Manji GA, et al. Card10 is a novel caspase recruitment domain/membrane-associated guanylate kinase family member that interacts with BCL10 and activates NF-kappa B. *J Biol Chem.* (2001) 276:21405–9. doi: 10.1074/jbc.M102488200
5. Gaide O, Martinon F, Micheau O, Bonnet D, Thome M, Tschopp J. Carma1, a CARD-containing binding partner of Bcl10, induces Bcl10 phosphorylation and NF-kappaB activation. *FEBS Lett*. (2001) 496:121–7. doi: 10.1016/S0014-5793(01)02414-0
6. McAllister-Lucas LM, Inohara N, Lucas PC, Ruland J, Benito A, Li Q, et al. Bimp1, a MAGUK family member linking protein kinase C activation to Bcl10-mediated NF-kappaB induction. *J Biol Chem*. (2001) 276:30589–97. doi: 10.1074/jbc.M103824200
7. Jiang C, Lin X. Regulation of NF-κB by the CARD proteins. *Immunol Rev.* (2012) 246:141–53. doi: 10.1111/j.1600-065X.2012.01110.x
8. Hara H, Wada T, Bakal C, Kozieradzki I, Suzuki S, Suzuki N, et al. The MAGUK family protein CARD11 is essential for lymphocyte activation. *Immunity* (2003) 18:763–75. doi: 10.1016/S1074-7613(03)00148-1
9. Egawa T, Albrecht B, Favier B, Sunshine MJ, Mirchandani K, O'Brien W, et al. Requirement for CARMA1 in antigen receptor-induced NF-kappa B activation and lymphocyte proliferation. *Curr Biol.* (2003) 13:1252–8. doi: 10.1016/S0960-9822(03)00491-3
10. Newton K, Dixit V. Mice lacking the CARD of CARMA1 exhibit defective B lymphocyte development and impaired proliferation of their B and T lymphocytes. *Curr Biol.* (2003) 13:1247–51. doi: 10.1016/S0960-9822(03)00458-5
11. Greil J, Rausch T, Giese T, Bandapalli OR, Daniel V, Bekeredjian-Ding I, et al. Whole-exome sequencing links caspase recruitment domain 11 (CARD11) inactivation to severe combined immunodeficiency. *J Allergy Clin Immunol.* (2013) 131:1376–83. doi: 10.1016/j.jaci.2013.02.012
12. Stepensky P, Keller B, Buchta M, Kienzler AK, Elpeleg O, Somech R, et al. Deficiency of caspase recruitment domain family, member 11 (CARD11), causes profound combined immunodeficiency in human subjects. *J Allergy Clin Immunol.* (2013) 131:477–85. doi: 10.1016/j.jaci.2012.11.050
13. Dadi H, Jones TA, Merico D, Sharfe N, Ovadia A, Schejter Y, et al. Combined immunodeficiency and atopy caused by a dominant negative mutation in caspase activation and recruitment domain family member 11 (CARD11). *J Allergy Clin Immunol.* (2018) 141:1818–30.e2. doi: 10.1016/j.jaci.2017.06.047
14. Juilland M, Thome M. Role of the CARMA1/BCL10/MALT1 complex in lymphoid malignancies. *Curr Opin Hematol.* (2016) 23:402–9. doi: 10.1097/MOH.0000000000000257

15. Grabiner B, Blonska M, Lin P, You Y, Wang D, Sun J, et al. CARMA3 deficiency abrogates G protein-coupled receptor-induced NF-{kappa}B activation. *Genes Dev.* (2007) 21:984–96. doi: 10.1101/gad.1502507
16. McAllister-Lucas L, Ruland J, Siu K, Jin X, Gu S, Kim DS, et al. CARMA3/Bcl10/MALT1-dependent NF-kappaB activation mediates angiotensin II-responsive inflammatory signaling in nonimmune cells. *Proc Natl Acad Sci USA*. (2007) 104:139–44. doi: 10.1073/pnas.0601947103
17. Jiang T, Grabiner B, Zhu Y, Jiang C, Li H, You Y, et al. CARMA3 is crucial for EGFR-Induced activation of NF-κB and tumor progression. *Cancer Res.* (2011) 71:2183–92. doi: 10.1158/0008-5472.CAN-10-3626
18. Li Z, Qu L, Dong Q, Huang B, Li H, Tang Z, et al. Overexpression of CARMA3 in non-small-cell lung cancer is linked for tumor progression. *PLoS ONE* (2012) 7:e36903. doi: 10.1371/journal.pone.0036903
19. Xia ZX, Li ZX, Zhang M, Sun LM, Zhang QF, Qiu XS, et al. CARMA3 regulates the invasion, migration, and apoptosis of non-small cell lung cancer cells by activating NF-κB and suppressing the P38 MAPK signaling pathway. *Exp Mol Pathol*. (2016) 100:353–60. doi: 10.1016/j.yexmp.2015.10.004
20. Scudiero I, Zotti T, Ferravante A, Vessichelli M, Vito P, Stilo R. Alternative splicing of CARMA2/CARD14 transcripts generates protein variants with differential effect on NF-κB activation and endoplasmic reticulum stress-induced cell death. *J Cell Physiol*. (2011) 226:3121–31. doi: 10.1002/jcp.22667
21. Harden J, Lewis S, Pierson K, Suárez-Fariñas M, Lentini T, Ortenzio FS, et al. CARD14 expression in dermal endothelial cells in psoriasis. *PLoS ONE* (2014) 9:e111255. doi: 10.1371/journal.pone.0111255
22. Afonina IS, Van Nuffel E, Baudelet G, Driege Y, Kreike M, Staal J, et al. The paracaspase MALT1 mediates CARD14-induced signaling in keratinocytes. *EMBO Rep*. (2016) 17:914–27. doi: 10.15252/embr.201642109
23. Stilo R, Liguoro D, Di Jeso B, Formisano S, Consiglio E, Leonardi A, et al. Physical and functional interaction of CARMA1 and CARMA3 with Ikappa kinase gamma-NFkappaB essential modulator. *J Biol Chem.* (2004) 279:34323–31. doi: 10.1074/jbc.M402244200
24. Xu X, Zhang H. The immunogenetics of psoriasis and implications for drug repositioning. *Int J Mol Sci.* (2017) 18:E2650. doi: 10.3390/ijms18122650
25. Michalek IM, Loring B, John SM. A systematic review of worldwide epidemiology of psoriasis. *J Eur Acad Dermatol Venereol*. (2017) 31:205–12. doi: 10.1111/jdv.13854
26. Chen H, Poon A, Yeung C, Helms C, Pons J, Bowcock AM, et al. A genetic risk score combining ten psoriasis risk loci improves disease prediction. *PLoS ONE* (2011) 6:e19454. doi: 10.1371/journal.pone.0019454
27. Jordan CT, Cao L, Roberson ED, Pierson KC, Yang CF, Joyce CE, et al. PSORS2 is due to mutations in CARD14. *Am J Hum Genet*. (2012) 90:784–95. doi: 10.1016/j.ajhg.2012.03.012
28. Jordan C, Cao L, Roberson E, Duan S, Helms C, Nair R, et al. Rare and common variants in CARD14, encoding an epidermal regulator of NF-kappaB, in psoriasis. *Am J Hum Genet.* (2012a) 90:796–808. doi: 10.1016/j.ajhg.2012.03.013
29. Fuchs-Telem D, Sarig O, van Steensel M, Isakov O, Israeli S, Nousbeck J, et al. Familial pityriasis rubra pilaris is caused by mutations in CARD14. *Am J Hum Genet*. (2012) 91:163–70. doi: 10.1016/j.ajhg.2012.05.010
30. Ammar M, Jordan C, Cao L, Lim E, Bouchlaka Souissi C, Jrad A, et al. CARD14 alterations in Tunisian patients with psoriasis and further characterization in European cohorts. *Br J Dermatol*. (2016) 174:330–7. doi: 10.1111/bjd.14158
31. Körber A, Mössner R, Renner R, Sticht H, Wilsmann-Theis D, Schulz P, et al. Mutations in IL36RN in patients with generalized pustular psoriasis. *J Invest Dermatol.* (2013) 133:2634–7. doi: 10.1038/jid.2013.214
32. Eskin-Schwartz M, Basel-Vanagaite L, David M, Lagovsky I, Ben-Amitai D, Smirin-Yosef P, et al. Intra-familial variation in clinical phenotype of CARD14-related psoriasis. *Acta Derm Venereol.* (2016) 96:885–7. doi: 10.2340/00015555-2405
33. Takeichi T, Sugiura K, Nomura T, Sakamoto T, Ogawa Y, Oiso N, et al. Pityriasis rubra pilaris type V as an autoinflammatory disease by CARD14 mutations. *JAMA Dermatol.* (2017) 153:66–70. doi: 10.1001/jamadermatol.2016.3601
34. Craiglow B, Boyden L, Hu R, Virtanen M, Su J, Rodriguez G, et al. CARD14-associated papulosquamous eruption: a spectrum including features of psoriasis and pityriasis rubra pilaris. *J Am Acad Dermatol.* (2018) 79:487–94. doi: 10.1016/j.jaad.2018.02.034
35. Takeichi T, Kobayashi A, Ogawa E, Okuno Y, Kataoka S, Kono M, et al. Autosomal dominant familial generalized pustular psoriasis caused by a CARD14 mutation. *Br J Dermatol*. (2017) 177:e133–5. doi: 10.1111/bjd.15442
36. Lwin S, Hsu CK, Liu L, Huang, HY, Levell NJ, McGrath JA. Beneficial effect of ustekinumab in familial pityriasis rubra pilaris with a new missense mutation in CARD14. *Br J Dermatol*. (2018) 178:969–72. 10.1111/bjd.15462
37. Qin P, Zhang Q, Chen M, Fu X, Wang C, Wang Z, et al. Variant analysis of CARD14 in a Chinese Han population with psoriasis vulgaris and generalized pustular psoriasis. *J Invest Dermatol*. (2014) 134:2994–6. doi: 10.1038/jid.2014.269
38. Eytan O, Sarig O, Sprecher E, van Steensel M. Clinical response to ustekinumab in familial pityriasis rubra pilaris caused by a novel mutation in CARD14. *Br J Dermatol*. (2014) 171:420–2. doi: 10.1111/bjd.12952
39. Has C, Schwieger-Briel A, Schlipf N, Hausser I, Chmel N, Rösler B, et al. Target-sequence capture and high throughput sequencing identify a de novo CARD14 mutation in an infant with erythrodermic pityriasis rubra pilaris. *Acta Derm Venereol.* (2016) 96:989–90. doi: 10.2340/00015555-2446
40. Inoue N, Dainichi T, Fujisawa A, Nakano H, Sawamura D, Kabashima K. CARD14 Glu138 mutation in familial pityriasis rubra pilaris does not warrant differentiation from familial psoriasis. *J Dermatol.* (2016) 43:187–9. doi: 10.1111/1346-8138.13008
41. Sugiura K, Muto M, Akiyama M. CARD14 c.526G>C (p.Asp176His) is a significant risk factor for generalized pustular psoriasis with psoriasis vulgaris in the Japanese cohort. *J Invest Dermatol*. (2014) 134:1755–7. doi: 10.1038/jid.2014.46
42. Berki DM, Liu L, Choon SE, David Burden A, Griffiths CEM, Navarini AA, et al. Activating CARD14 mutations are associated with generalized pustular psoriasis but rarely account for familial recurrence in psoriasis vulgaris. *J Invest Dermatol.* (2015) 135:2964–70. doi: 10.1038/jid.2015.288
43. Mössner R, Frambach Y, Wilsmann-Theis D, Löhr S, Jacobi A, Weyergraf A, et al. Palmoplantar pustular psoriasis is associated with missense variants in CARD14, but not with loss-of-function mutations in IL36RN in European patients. *J Invest Dermatol.* (2015) 135:2538–41. doi: 10.1038/jid.2015.186
44. Zhu K, Shi G, Liu H, Zhu C, Fan Y. Variants of CARD14 gene and psoriasis vulgaris in southern Chinese cohort. *An Bras Dermatol.* (2016) 91:45–8. doi: 10.1590/abd1806-4841.20164016
45. Lau BW, Lim DZ, Capon F, Barker JN, Choon SE. Juvenile generalized pustular psoriasis is a chronic recalcitrant disease: an analysis of 27 patients seen in a tertiary hospital in Johor, Malaysia. *Int J Dermatol.* (2017) 56:392–9. doi: 10.1111/ijd.13489
46. Podlipnik S, Castellanos-Moreira R, Florez-Enrich H, Arostegui JI, Mascaró JM Jr. Acute generalized exanthematous pustulosis and polyarthritis associated with a novel CARD14 mutation. *Australas J Dermatol.* (2018) 59:e70–3. doi: 10.1111/ajd.12669
47. González-Lara L, Coto-Segura P, Penedo A, Eiris N, Díaz M, Santos-Juanes J, et al. SNP rs11652075 in the CARD14 gene as a risk factor for psoriasis (PSORS2) in a Spanish cohort. *DNA Cell Biol.* (2013) 32:601–4. doi: 10.1089/dna.2013.2109
48. Sugiura K, Kitoh T, Watanabe D, Muto M, Akiyama M. Childhood-onset PsA in Down syndrome with psoriasis susceptibility variant CARD14 rs11652075. *Rheumatology* (2015) 54:197–9. doi: 10.1093/rheumatology/keu419
49. Feng C, Wang T, Li SJ, Fan YM, Shi G, Zhu KJ. CARD14 gene polymorphism c.C2458T (p.Arg820Trp) is associated with clinical features of psoriasis vulgaris in a Chinese cohort. *J Dermatol*. (2016) 43:294–7. doi: 10.1111/1346-8138.13065
50. Van Nuffel E, Schmitt A, Afonina IS, Schulze-Osthoff K, Beyaert R, Hailfinger S. CARD14-mediated activation of paracaspase MALT1 in keratinocytes: implications for psoriasis. *J Invest Dermatol.* (2017) 137:569–75. doi: 10.1016/j.jid.2016.09.031
51. Coto-Segura P, González-Fernández D, Batalla A, Gómez J, González-Lara L, Queiro R, et al. Common and rare CARD14 gene variants affect the antitumour necrosis factor response among patients with psoriasis. *Br J Dermatol.* (2016) 175:134–41. doi: 10.1111/bjd.14461
52. Wu K, Reynolds N. CARD14 mutations may predict response to antitumour necrosis factor-α therapy in psoriasis: a potential further step towards personalized medicine. *Br J Dermatol.* (2016) 175:17–8. doi: 10.1111/bjd.14795

53. Howes A, O'Sullivan P, Breyer F, Ghose A, Cao L, Krappmann D, et al. Psoriasis mutations disrupt CARD14 autoinhibition promoting BCL10-MALT1-dependent NF-κB activation. *Biochem J*. (2016) 473:1759–68. doi: 10.1042/BCJ20160270
54. Sommer K, Guo B, Pomerantz JL, Bandaranayake AD, Moreno-García ME, Ovechkina YL, et al. Phosphorylation of the CARMA1 linker controls NF-kappaB activation. *Immunity* (2005) 23:561–74. doi: 10.1016/j.immuni.2005.09.014
55. Matsumoto R, Wang D, Blonska M, Li H, Kobayashi M, Pappu B, et al. Phosphorylation of CARMA1 plays a critical role in T Cell receptor-mediated NF-kappaB activation. *Immunity* (2005) 23:575–85. doi: 10.1016/j.immuni.2005.10.007
56. Stilo R, Varricchio E, Liguoro D, Leonardi A, Vito P. A20 is a negative regulator of BCL10- and CARMA3-mediated activation of NF-kappaB. *J Cell Sci.* (2008) 121:1165–71. doi: 10.1242/jcs.021105.
57. Schmitt A, Grondona P, Maier T, Brändle, M, Schönfeld C, Jäger G, et al. MALT1 protease activity controls the expression of inflammatory genes in keratinocytes upon zymosan stimulation. *J Invest Dermatol.* (2016) 136:788–97. doi: 10.1016/j.jid.2015.12.027
58. Scudiero I, Mazzone P, D'Andrea L, Ferravante A, Zotti T, Telesio G, et al. CARMA2sh and ULK2 control pathogen-associated molecular patterns recognition in human keratinocytes: psoriasis-linked CARMA2sh mutants escape ULK2 censorship. *Cell Death Dis*. (2017) 8:e2627. doi: 10.1038/cddis.2017.51
59. Telesio G, Scudiero I, Pizzulo M, Mazzone P, Zotti T, Voccola S, et al. The E3 ubiquitin ligase RNF7 negatively regulates CARD14/CARMA2sh signaling. *Int J Mol Sci.* (2017) 18:E2581. doi: 10.3390/ijms18122581
60. Pedersen SM, Chan W, Jattani RP, Mackie DS, Pomerantz JL. Negative regulation of CARD11 signaling and lymphoma cell survival by the E3 ubiquitin ligase RNF181. *Mol Cell Biol*. (2015) 36:794–808. doi: 10.1128/MCB.00876-15
61. D'Andrea EL, Ferravante A, Scudiero I, Zotti T, Reale C, Pizzulo M, et al. The dishevelled, EGL-10 and pleckstrin (DEP) domain-containing protein DEPDC7 binds to CARMA2 and CARMA3 proteins, and regulates NF-κB activation. *PLoS ONE* (2014) 9:e116062. doi: 10.1371/journal.pone.0116062
62. Tanaka M, Kobiyama K, Honda T, Uchio-Yamada K, Natsume-Kitatani Y, Mizuguchi K, et al. Essential role of CARD14 in murine experimental psoriasis. *J Immunol*. (2018) 200:71–81. doi: 10.4049/jimmunol.1700995
63. Mellett M, Meier B, Mohanan D, Schairer R, Cheng P, Satoh TK, et al. CARD14 gain-of-function mutation alone is sufficient to drive IL-23/IL-17-mediated psoriasiform skin inflammation *in vivo*. *J Invest Dermatol.* (2018) 138:2010–23. doi: 10.1016/j.jid.2018.03.1525
64. Wang M, Zhang S, Zheng G, Huang J, Songyang Z, Zhao X, et al. Gain-of-function mutation of card14 leads to spontaneous psoriasis-like skin inflammation through enhanced keratinocyte response to IL-17A. *Immunity* (2018) 49:66–79.e5. doi: 10.1016/j.immuni.2018.05.012

Conflict of Interest Statement: The authors declare that the research was conducted in the absence of any commercial or financial relationships that could be construed as a potential conflict of interest.

frontiers in Immunology

REVIEW
published: 16 October 2018
doi: 10.3389/fimmu.2018.02239

Clinical and Genetic Heterogeneity of *CARD14* Mutations in Psoriatic Skin Disease

Laura Israel[1]* *and Mark Mellett*[2]*

[1] Novartis Institutes for BioMedical Research, Novartis Campus, Basel, Switzerland, [2] Department of Dermatology, University Hospital Zürich, Zürich, Switzerland

The CARD: BCL10: MALT1 (CBM) complex is an essential signaling node for maintaining both innate and adaptive immune responses. CBM complex components have gained considerable interest due to the dramatic effects of associated mutations in causing severe lymphomas, immunodeficiencies, carcinomas and inflammatory disease. While MALT1 and BCL10 are ubiquitous proteins, the CARD-containing proteins differ in their tissue expression. CARD14 is primarily expressed in keratinocytes. The CARD14-BCL10-MALT1 complex is activated by upstream pathogen-associated molecular pattern-recognition *in vitro*, highlighting a potentially crucial role in innate immune defense at the epidermal barrier. Recent findings have demonstrated how CARD14 orchestrates activation of the NF-κB and MAPK signaling pathways *via* recruitment of BCL10 and MALT1, leading to the upregulation of pro-inflammatory genes encoding IL-36γ, IL-8, Ccl20 and anti-microbial peptides. Following the identification of CARD14 gain-of function mutations as responsible for the psoriasis susceptibility locus *PSORS2*, the past years have witnessed a large volume of case reports and association studies describing CARD14 variants as causal or predisposing to a wide range of inflammatory skin disorders. Recent publications of mouse models also helped to better understand the physiological contribution of CARD14 to psoriasis pathogenesis. In this review, we summarize the clinical, genetic and functional aspects of human and murine CARD14 mutations and their contribution to psoriatic disease pathogenesis.

Keywords: CARD14 (CARMA2), gain-of-function (GoF) mutation, keratinocytes, skin inflammation, psoriasis, pityriasis rubra pilaris

OPEN ACCESS

Edited by:
Andrew L. Snow, Uniformed Services University of the Health Sciences, United States

Reviewed by:
Masashi Akiyama, Nagoya University, Japan
Anne Bowcock, Icahn School of Medicine at Mount Sinai, United States

***Correspondence:**
Laura Israel
laura.israel@novartis.com
Mark Mellett
mark.mellett@usz.ch

Specialty section:
This article was submitted to Molecular Innate Immunity, a section of the journal Frontiers in Immunology

Received: *28 May 2018*
Accepted: *10 September 2018*
Published: *16 October 2018*

Citation:
Israel L and Mellett M (2018) Clinical and Genetic Heterogeneity of CARD14 Mutations in Psoriatic Skin Disease. Front. Immunol. 9:2239. doi: 10.3389/fimmu.2018.02239

INTRODUCTION

Caspase Recruitment Domain-containing protein 14 (CARD14) (also called CARMA2 or BIMP2) is the second member of the CARMA family that consists of CARD11 (CARMA1), CARD10 (CARMA3) and related molecule CARD9 (1). Like its family members, CARD14 recruits interacting partners BCL10 and MALT1 (2–4) to form the so-called CBM complex and thus initiate NF-κB and MAPK signaling pathways. Therefore, the CARMA proteins trigger a shared downstream pathway and are, with the exception of CARD9, highly similar in sequence and structure (1, 3). BCL10 and MALT1 are ubiquitously expressed proteins whereas the CARD molecule gives cell specificity to the complex, with CARD11 localizing to lymphoid cells and tissue, CARD9 being restricted to myeloid cells, CARD14 in skin and mucosal tissues, whereas CARD10

displays a broader expression in epithelial and endothelial tissue (1, 5, 6). Mutations associated with the CARMA family proteins therefore result in very different human maladies (7, 8).

CARD14 was originally identified in placental tissue (3) but microarray data later revealed that the molecule is highly expressed in adipose tissue, esophagus and mucosal tissues (1). In 2012, first reports from the Bowcock group described autosomal dominant CARD14 gain-of-function (GoF) mutations in a young patient presenting with a severe form of pustular psoriasis and in two multiplex families with plaque psoriasis (9, 10). Additionally, CARD14 was discovered to be highly expressed in keratinocytes and was identified as the causative gene at the *Psoriasis Susceptibility* (*PSORS*) *2* locus, which had previously been identified as one of the principle risk loci for psoriasis (11). Furthermore, a report from the Sprecher group broadened the occurrence of CARD14 mutations to pityriasis rubra pilaris (PRP), a rarer form of psoriatic skin disease (12). These studies were the first to reveal a pathogenic role for CARD14 and also highlighted the physiological variation and scope of the CARMA protein family's influence to human health and disease.

Since these inaugural discoveries, further studies have revealed CARD14 variants associated with various entities in the psoriasis disease spectrum. Of particular note is the considerable clinical heterogeneity associated with CARD14 mutations in terms of phenotype and severity, even within a single disease entity. In this review, we discuss the subtypes of the psoriatic disease spectrum, which have been described to be associated with CARD14 mutations and seek to differentiate between causal and predisposing variants.

INFLAMMATORY SKIN DISORDERS ASSOCIATED WITH CARD14 VARIANTS

Psoriasis

Clinical Features

Psoriasis is a common chronic inflammatory skin disease with a complex genetic background affecting approximately 2% of the global population (13) though this varies depending on ethnicity, demographics and latitude (14). It is now well established that psoriasis is a multigenic disease that arises in genetically susceptible individuals in response to an environmental trigger, such as skin trauma or infection (15). Immunopathogenesis is orchestrated by a complex interplay between keratinocytes, skin resident immune cells and infiltrating leukocytes, including neutrophils, macrophages, conventional and plasmacytoid dendritic cells. Infiltrating type 1 and type 17 helper T cells (Th1/Th17) cells maintain the chronic inflammation associated with established disease (16). The term "psoriasis" envelopes various forms, which are typically classified by morphology, distribution and anatomical localisation (17). Major distinctions include plaque and pustular forms, which contrast in appearance and with the immune cell infiltrate involved.

Plaque psoriasis [or psoriasis vulgaris (PsV)] is the most common form of psoriasis, accounting for approximately 80–90% of psoriatic cases (18), it is characterized by raised demarcated erythematous circular plaques on the skin of sufferers, due to hyperproliferation of keratinocytes (15), leading to thickening of the skin (acanthosis). Plaque psoriasis is also associated with dilation and increased number of blood vessels, facilitating the immune cell infiltration and maintaining chronicity.

Comorbidities including cardiovascular disease, Crohn's disease, obesity and metabolic syndrome have been linked with PsV (19–21). Additionally, 25% of cases are associated with psoriatic arthritis, though this can also precede the skin condition in some patients (22). These comorbidities emphasize the systemic nature of psoriasis with effects spreading beyond the skin. The link with comorbidities is not well understood, though it has been proposed that elevated levels of circulating pro-inflammatory cytokines found in the serum of patients, in particular IL-17A, foster these systemic abnormalities in secondary organs (23–25).

Pustular psoriasis is characterized by skin eruptions of white pustules and surrounding red erythematous skin and can take both localized and generalized forms. Infiltrating neutrophils and monocytes to skin tissue is a hallmark of the disease entity. Skin flares in generalized pustular psoriasis (GPP) can be accompanied by high fever, fatigue and muscle and joint pain and secondary effects include acute respiratory disease, uveitis, osteoarthritis and cholangitis of the bile ducts, which is mediated by neutrophilic activation (26). Patients with GPP carrying loss-of-function (LoF) mutations in *IL36RN* (encoding IL-36 receptor antagonist) or heterozygous mutations in *AP1S3* (resulting in increased IL-36α expression) were described, suggesting a pivotal role of IL-36 cytokine activity in driving pustular psoriasis (27–31).

Genetics

Genome-wide linkage analysis studies identified nine "Psoriasis Susceptibility" regions or loci (*PSORS1-9*) (11), however only *PSORS1*, *-2* and *-4* findings were replicated in independent studies (32). In 1994, the psoriasis susceptibility locus (*PSORS2* ([MIM 602723]) was mapped at the distal end of human chromosome 17q in a large Caucasian kindred with several affected generation members presenting with plaque type psoriasis (33) and this was confirmed by other studies, in particular in a five-generation Taiwanese family with psoriasis (34, 35). Extensive analysis of these two families by Jordan et al., led to the identification of *CARD14* as being the responsible gene for the underlying association of the *PSORS2* locus with psoriasis (9). In the family of European descent, a heterozygous missense mutation (p.G117S) was identified, whereas in the Taiwanese kindred an intronic mutation (c.349 + 5G>A) was found. Both these variants created a cryptic splice site resulting in a 22 amino acid insertion between exons 3 and 4. In addition, Jordan et al. identified a *de novo* mutation (p.E138A) in a young patient, originating from Haiti, presenting with early-onset GPP (**Table 1** and **Figure 1**). By screening seven psoriasis cohorts with varying ancestries (over 6,000 cases and 4,000 controls), Jordan and colleagues also identified 15 additional rare and common

TABLE 1 | CARD14 Gain-of-function mutants associated with psoriatic skin disease.

Protein	mRNA	SNP	MAF in ExAC	Disease	Penetrance	Inheritance	Zygosity	Co factor	References
G117S	c.349G>A	rs281875215	not found	PsV	complete	AD	Het	no HLA-Cw(06:02)	(9)
				PsV			Het		(10)
				PsV	Incomplete (1 healthy carrier)	AD	Het		(36)
				PsV					(37)
				PsV and GPP	Incomplete (1 healthy carrier)	AD	cpd Het	other CARD14 variants HLA-Cw(06:02)	(40)
				GPP			Het	IL36RN Het mutation (S113L)	(76)
				PRP type V	Incomplete (1 healthy carrier)	AD	Het		(56)
				CAPE	complete	AD	Hom		(39)
splice	c.349 + 1G>A	rs886041402	not found	familial PRP	incomplete	AD	Het		(12)
				GPP familial	Incomplete (2 healthy carriers)	AD	Het		(45)
splice	c.349+5G>A	rs587777763	not found	PsV	complete	AD	Het	no HLA-Cw(06:02)	(9)
				CAPE		AD	Het		(39)
E138K	c.412G>A		not found	erythro PRP		*de novo*	Het		(58)
				PRP type V sporadic		*de novo*	Het		(59)
				CAPE		*de novo*	Het		(39)
E138A	c.413A>C	rs281875214	not found	GPP		*de novo*	Het	no IL36RN/no HLA-Cw(06:02)	(9)
				PsV			Het		(10)
E138del	c.412_414delGAG		not found	familial PRP	incomplete	AD	Het		(12)
E142K	c.424G>A	rs281875212	not found	PsV			Het		(10)
E142G	c.425A>G	rs281875213	not found	PsV			Het		(10)
L156P	c.467T>C	rs387907240	not found	familial PRP	complete	AD	Het		(12)
				CAPE	complete	AD	Het		(39)
H171N	c.511C>A	rs281875216	not found	PsV			Het		(10)
D176H	c.526G>C	rs144475004	0.00495	PsV			Het		(10)
				GPP with PsV			Het	no IL36RN/no HLA-Cw(06:02)	(44)
				PsV	found in controls				(49)
				GPP			Het		(38)
				PPP			Het	no HLA-Cw(06:02)	(41)
				PsV			Het		(51)
				PPP			Het		(76)
				PRP type I and IV			Het		(56)

CARD14 mutations that were described as GoF based on in vitro functional studies.

AD, autosomal dominant; CAPE, CARD14-associated papulosquamous; CC, coiled-coil; GPP, generalized pustular psoriasis; Het, heterozygous; Hom, homozygous; PPP. Palmoplantar pustular psoriasis; PRP, pityriasis rubra pilaris; PsV, psoriasis vulgaris; Cpd, compound.

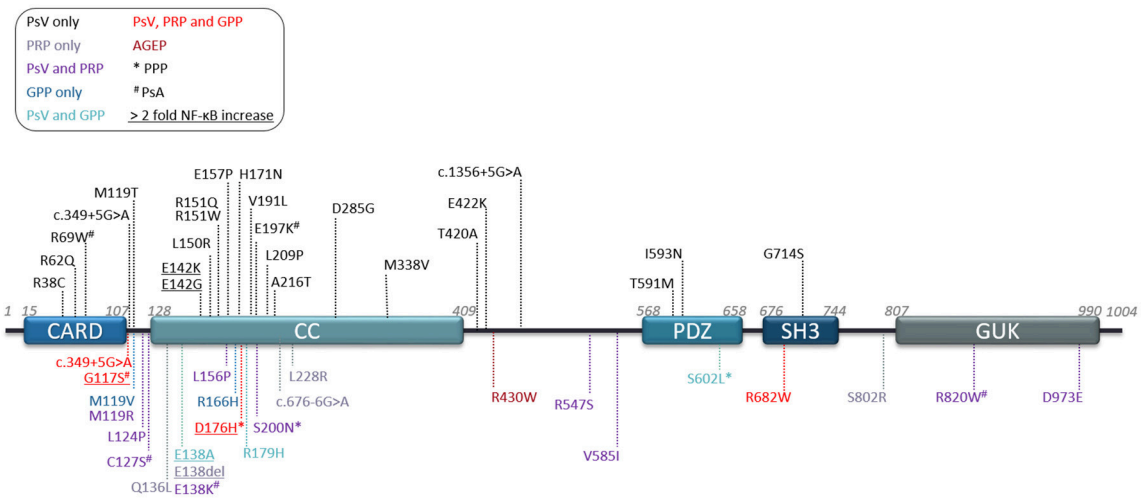

FIGURE 1 | Human CARD14 protein domains and reported variants. Schematic depicting protein domains of the human CARD14 protein and location of all variants reported to date. Legend key shows disease association by color and reports of associated palmoplantar pustular psoriasis (*PPP) or psoriatic arthritis (#PsA). Underlined variants are mutants studied in terms of NF-κB activation in overexpression studies and showing at least 2 fold more induction than CARD14-WT. AGEP, Acute generalized exanthematous pustulosis; GPP, generalized pustular psoriasis; PRP, pityriasis rubra pilaris; PsV, psoriasis vulgaris.

CARD14 variants that were enriched in cases over controls (10) (**Tables 1**, **2**).

Following these initial studies, CARD14 variants were reported by several groups as causal or predisposing factors for psoriasis with or without psoriatic arthritis or palmoplantar pustular psoriasis (PPP) (36–51). Together, these studies indicate a diverse range of disease symptoms associated with CARD14 mutations. However, dissecting whether CARD14 variants function as causal mutations or predisposing factors has become difficult to interpret.

The majority of CARD14 variants were found in the heterozygous state. However, a few patients were described with compound heterozygous (40, 42, 52) or homozygous variants (39, 43) nevertheless, these were not associated with a more severe phenotype. CARD14 variants are reported in exons 2, 3, 4, 6, 7, 9, 13, 15, 18, and 21, but exon 3 and 4 (encoding partly for the CARD and Coiled-coil (CC) domains) represent a clear hotspot with 63% of published variants (**Figure 1**). Some of these mutations are synonymous with CARD11 mutants, which have been described to affect the autoinhibitory conformation that impedes recruitment of BCL10 (53). These mutations result in spontaneous or sustained activation of downstream NF-κB and MAPK pathways.

Treatments

Psoriasis runs a chronic course and current treatments alleviate symptoms rather than treat causative drivers at the root of disease pathogenesis. Traditionally treatments include methotrexate, corticosteroids, UV phototherapy for mild cases, Acitretin a second-generation retinoid, Vitamin D analogs and also coal tar (54). Recently, biologic therapy has expanded beyond TNFα inhibitors to IL-12/IL-23p40-, IL-17A-, IL-17RA-, and IL-23p19-targeting antibodies, which have demonstrated increased efficacy in clinical trials compared to TNF blockade [reviewed elsewhere (55)]. It remains of interest to determine whether targeting the IL-23/Th17 axis will also be beneficial in alleviating associated comorbidities.

To assess whether CARD14 variants could be associated with better responses in psoriasis patients to anti-TNF therapy, Coto-Segura and colleagues tested the presence of such variants in 116 patients who underwent anti-TNF treatment (48). These patients were all previous non-responders to classical psoriasis treatments (phototherapy, methotrexate, acitretin or cyclosporine). A higher frequency of CARD14 variants, in particular the common p.R820W polymorphism, were found among responders to TNFα-targeted blockade, suggesting that CARD14-associated psoriasis could benefit from anti-TNF treatment. Takeichi et al. also reported beneficial treatment with anti-TNF therapy in CARD14-associated familial GPP (56). Additionally, Craiglow et al. described a beneficial outcome upon treatment with ustekinumab (anti-IL-12/IL-23p40) in CARD14-associated psoriasis in individual patients (39).

Pityriasis Rubra Pilaris (PRP)

Clinical Features

CARD14 variants were also found to be associated with another inflammatory skin disorder related to psoriasis, called pityriasis rubra pilaris (PRP) (12, 52, 56–61). PRP is an extremely rare inflammatory skin disease with an estimated prevalence of 1/400,000 individuals (62). It is characterized by scaly salmon-colored ("rubra") plaques on the skin of affected individuals and though a separate entity to psoriasis the two diseases share overlapping clinical features, which makes ambiguous cases of PRP challenging to diagnose. Typically, clinical and histological features enable correct identification of PRP; these include

TABLE 2 | CARD14 variants associated with psoriatic skin disease.

Prot.	mRNA	SNP	MAF in ExAC	Disease	Origin	Cohort size case/ctr	MAF CASE	MAF CTR	Cofactors		Treatment/Response	References
									Other CARD14	HLA-Cw0602		
R38C	c.112C>T	rs281875217	not found	PsV	Caucasian/Asian	6000/4000	0.00019	0				(10)
R62Q	c.185G>A	rs115582620	0.002606	PsV	Caucasian/Asian	6000/4000	0.0014	0.00084				(10)
				PsV	Tunisian	282/192	0.0053	0				(37)
R69W	c.205C>T	rs375624435	0.0001945	PsV	Tunisian	282/192	0.008865	0				(37)
M119 R	c.356T>G		not found	CAPE		15 kindreds	1 patient				etanercept/partial	(39)
				familial PRP		case report (2 Pts)					ustekinumab/comple te	(61)
M119T	c.356T>C		not found	CAPE		15 kindreds	2 patients					(39)
M119V	c.355A>G		not found	GPP	Han Chinese	174 PsV,62 GPP/365 C	0.002 (GPP)	0				(49)
				CAPE		15 kindreds	1 patient				ustekinumab/complete	(39)
L124P	c.371T>C		not found	familial PRP		case report (1 kindred)					ustekinumab/complete	(57)
				familial PRP, Psv		case report (1 kindred)			yes	yes		(42)
C127S	c.380G>C		not found	CAPE		15 kindreds	1 kindred				MTX and etanercept/partial	(39)
				PRP type V.		22/100	0.0227	0				(56)
Q136L	c.407A>T		not found	PRP type V		22/100	0.0227	0				(56)
L150R	c.449T>G	rs146214639	0.001859	PsV	Caucasian/Asian	6000/4000	0.0025	0.0016				(10)
				PsV	Tunisian	282/192	0.001773	0				(37)
R151Q	c.452G>A	rs200731780	0.0003399	PsV	Tunisian	282/192	0.001773	0				(37)
R151W	c.451C>T	rs777305616	4.217E-05	PsV	European							(37)
Q157P	c.470A>C		not found	CAPE		15 kindreds	1 patient				MTX/partial	(39)
R166H	c.497G>A		not found	GPP	Han Chinese	174 PsV,62 GPP/365 C	0.002 (GPP)	0				(49)
R179H	c.536G>A	rs199517469	0.0002708	PsV	Caucasian/Asian	6000/4000	0.00025	0.00027				(10)
				GPP		51 patients						(76)
V191L	c.571G>T	rs281875218	not found	PsV	Caucasian/Asian	6000/4000	0.00014	0.00027				(10)
E197K	c.589G>A	rs200790561	0.000776	PsV	Tunisian	282/192	0.01241	0.002604				(37)
S200N	c.599G>A	rs114688446	0.01096	PRP		48 patients	0.03125					(60)
				PsV	Caucasian/Asian	6000/4000	0.011	0.0084				(10)
				PsV	Tunisian	282/192	0.003546	0				(37)
				PPP		251/1054	0.01195	0.00332		no		(41)

(Continued)

TABLE 2 | Continued

Prot.	mRNA	SNP	MAF in ExAC	Disease	Origin	Cohort size case/ctr	MAF CASE	MAF CTR	Cofactors		Treatment/Response	References
									Other CARD14	HLA-Cw0602		
L209P	c.626T>C		not found	PsV	European							(37)
A216T	c.646G>A	rs574982768	5.798E-05	PsV	Han Chinese	174 PsV,62 GPP/ 365 C	0.002 (PsV)	0				(49)
				PsV	European							(37)
				PsV	Han Chinese	131/207	0.0076	0				(51)
splice	c.676-6G>A	rs28674001	0.3481	sporadic PRP	Hungarian	case report			yes			(81)
L228R	c.683T>G	rs142246283	9.359E-05	PRP		48 patients	0.01042					(60)
D285G	c.854A>G	rs281875219	not found	PsV	Caucasian/Asian	6000/4000	0.00019	0				(10)
M338V	c.1012A>G	rs200132496	9.074E-05	PsV	Tunisian	282/192	0.003546	0				(37)
T420A	c.1258A>G	rs762364495	not found	PsV	Tunisian	282/192	0.001773	0				(37)
E422K	c.1264G>A	rs61751629	not found	PsV, anti TNF response		116 patients (79 resp,37 non resp)	0.04 (resp)	0 (non resp)			anti TNF/positive	(48)
R430W	c.1288C>T		6.673E-05	AGEP	Spanish	case report (1 Pt)						(90)
splice	c.1356+5G>A	rs376524884	0.0001012	PsV	Tunisian	282/192	0.001773	0				(37)
R547S	c.1641G>C	rs2066964	0.3772	PsV	Yemenite Ashkenazi	case report (1 kindred)			yes	yes		(40)
				PsV	Han Chinese	174 PsV,62 GPP/ 365 C	0.441	0.46				(49)
				sporadic PRP	Taiwanese	case reports (8 patients)			yes			(52)
				familial PRP, Psv		case report (1 kindred)			yes	yes		(42)
				sporadic PRP	Hungarian	case report			yes			(81)
V585I	c.1753G>A	rs34367357	0.08418	PsV	Yemenite Ashkenazi	case report (1 kindred)			yes	yes		(40)
				PsV	Han Chinese	174 PsV,62 GPP/365 C	0.074	0.056				(49)
				familial PRP, Psv		case report (1 kindred)			yes	yes		(42)
T591M	c.1772C>T	rs200102454	0.0003674	PsV	Han Chinese	174 PsV,62 GPP/ 365 C	0.002 (PV)	0				(49)
I593N	c.1778T>A		not found	PsV	Caucasian/Asian	6000/4000	0.00024	0.00048				(10)
S602L	c.1805C>T	rs201285077	0.0002346	GPP	European							(37)

(Continued)

TABLE 2 | Continued

Prot.	mRNA	SNP	MAF in ExAC	Disease	Origin	Cohort size case/ctr	MAF CASE	MAF CTR	Cofactors		Treatment/Response	References
									Other CARD14	HLA-Cw0602		
R682W	c.2044C>T	rs117918077	0.01103	PsV	Caucasian/Asian	6000/4000	0.013	0.012				(10)
				GPP	Han Chinese	174 PsV,62 GPP/ 365 C	0.002 (GPP)	0				(49)
				PsV, anti TNF response		116 patients (79 resp,37 non resp)	0.01 (resp)	0 (non resp)			anti TNF/positive	(48)
				PRP		48 patients	0.01042					(60)
				sporadic PRP	Hungarian	case report			yes			(81)
G714S	c.2140G>A	rs151150961	0.000423	PsV	Caucasian/Asian	6,000/4,000	0.0021	0.0014				(10)
S802R	c.2406C>A		not found	PRP		48 patients	0.01042					(60)
R820W	c.2458C>T	rs11652075	0.4244	PsV and PRP	Caucasian/Asian	6,000/4,000	common variant			yes		(10)
				PsV and PA	Spanish	400/420	0.4375	0.5214				(47)
				PsV	Han Chinese	174 PsV,62 GPP/365 C	0.443	0.482				(49)
				PsA	Japanese	case report (1 Pt)						(43)
				PsV, anti TNF response		116 patients (79 resp,37 non resp)	0.55 (in resp)	0.38 (non resp)			anti TNF/positive	(48)
				PsV	Caucasian/Asian	32,807/45,458						(50)
				PsV	Yemenite Ashkenazi	case report (1 kindred)			yes	yes		(40)
				sporadic PRP	Taiwanese	case reports (8 Pt)			yes			(52)
				familial PRP, Psv		case report (1 kindred)			yes	yes		(42)
				sporadic PRP	Hungarian	case report			yes			(81)
D973E	c.2919C>G	rs144285237	0.003435	PsV and PRP	Caucasian/Asian	6,000/4,000	0.0024	0.0015				(10)

*Reported variants described in CARD14 excluding pathogenic mutants (**Table 1**). CARD14 variants here have not been studied functionally or did not appear GoF in vitro.*

AGEP, Acute generalized exanthematous pustulosis eruption; CAPE, CARD14-associated papulosquamous; GPP, generalized pustular psoriasis; PRP, pityriasis rubra pilaris; PsV, psoriasis vulgaris; Pts, patients; Resp, responder; Non resp, non-responder; MTX, methotrexate.

the presence of "sparing-islands" of uninvolved skin, and the presence of distinctive alternating ortho- and parakeratosis (63).

PRP has a bimodal age-of-onset distribution and is subclassified into 6 types. The most common type (type I, approximately 50% of cases) initially affects both men and women in their late fifties and sixties, while other forms may have a juvenile or neonatal onset. The latter cases are particularly associated with familial PRP (type V) and present with a deleterious form that runs a chronic course and is refractory to conventional psoriasis treatments (12, 62, 64). Familial cases have been associated with *CARD14* GoF mutations and *CARD14* mutant variants have also been described in other sporadic forms (52, 56).

Besides *CARD14* mutations, other causal factors of PRP remain elusive. Interestingly, cases have been reported to be preceded by bacterial or viral infections (65–67) and indeed HIV-associated PRP has been classified as a distinct type of PRP (type VI) (68, 69).

Like psoriasis, PRP also presents with associated comorbidities including hypothyroidism, dyslipidaemia and the most common form, classical adult onset (type I) has been associated with underlying malignancies (62, 69, 70).

Genetics

Several groups reported CARD14 mutations in patients with both familial and sporadic PRP (12, 42, 52, 56–59, 61) (**Tables 1**, **2**). Indeed, PRP type V is considered a PRP subtype caused by CARD14 mutations (56). Interestingly, Craiglow et al. recently described 15 patients with CARD14 mutations that present with both psoriasis and PRP symptoms, and grouped these skin inflammatory phenotypes under the appellation *CARD14-associated papulosquamous eruption* (CAPE) (39). CAPE is characterized by distinctive facial plaques on the cheeks, chin and upper lip with absence below the lower lip. Erythema of the ears, trunk and extremity involvement and palmoplantar keratoderma are also present.

As with psoriasis, most CARD14 variants associated with PRP are heterozygous, with very few compound heterozygous patients having being described (42, 52). CARD14 variants associated with PRP, like psoriasis, are spread throughout the protein domains (**Figure 1**) but also concentrate in exons 3 and 4. To date, no correlation has been made between variant localisation and disease severity or age of onset. However, mutations in this area affect the ability of the molecule to maintain its autoinhibitory state (2, 71–73).

Treatments

First-line treatments of PRP include oral retinoids and methotrexate, followed by topical corticosteroids or emollients. Difficult cases prove refractory to conventional psoriasis treatments and UV-light therapy can trigger or aggravate symptoms (70). The use of biologic therapy targeting TNFα (infliximab) or IL-12/IL-23p40 (ustekinumab) has proven effective in individual cases (61, 74, 75). Other groups also described beneficial effect upon treatment with ustekinumab in CARD14-associated familial PRP (57, 61).

GENETIC HETEROGENEITY ASSOCIATED WITH CARD14 VARIANTS

In addition to the association of CARD14 variants with different disease entities, it is also noteworthy that several CARD14 variants have been associated with more than one type of skin disease. For example, p.D176H (**Table 1**), which was initially described in patients with PsV only (10, 51) or PsV with PPP (41, 76), was subsequently also described as associated with GPP but not with PsV in Asian populations (38, 44) and Takeichi et al. also found the p.D176H variant in patients with PRP type V (56). This reflects the broad heterogeneity found in patients with CARD14 mutations. It might also suggest that these particular variants are predisposing factors and require cofactors or environmental triggers that then determine progression of different disease entities. This is supported by the fact that most of CARD14 variants display incomplete penetrance, where healthy carriers may carry protective factors or lack susceptibility genetic cofactors or exposure to environmental stimuli.

PSORS1 is the locus shown to confer the greatest risk for psoriasis, accounting for 35–50% of heritability (77) and in 2000, *HLA-Cw*0602* was described as the psoriasis risk allele mapping to this locus (78, 79). Some studies revealed increased evidence for association of CARD14 p.R820W with psoriasis when the study was conditioned on *HLA-Cw*0602 (10)* and one kindred with familial psoriasis associated with CARD14 mutations were shown to be also positive for the *HLA-Cw*0602* allele (40). On the other hand, patients harboring CARD14 variants were found negative for this allele in other studies (9, 44) or no association was found between CARD14 variants and the *HLA* locus (44). Unfortunately, this locus was not systematically assessed in patients with CARD14-associated psoriasis and further investigation are required to better understand if these loci might act as cofactors in triggering pathology.

In other studies, genetic association between psoriasis and CARD14 is also not clear. Berki et al. analyzed a cohort of 416 PsV patients and were unable to identify any CARD14 variant (38). Suguira and colleagues described a Down syndrome patient with PsA homozygous for the p.R820W CARD14 variant. However, both parents were also homozygous for this variant and at date of publication, had not developed any psoriatic phenotype, supporting the fact that p.R820W is a common variant found in healthy individuals (MAF = 0.4244 in ExAc), which might only predispose to psoriatic skin diseases (43). Finally, Eskin-Schwartz et al., described an interesting kindred with CARD14-related psoriasis with extreme clinical variability (from mild plaque-type to GPP) (40). Affected members were heterozygous for the p.G117S pathogenic CARD14 allele, but most severely affected members were also carrying three additional CARD14 variants (p.R547S, p.V585I, and p.R820W) as well as the *HLA-Cw*0602* allele. However, one family member is also a healthy carrier of the p.G117S, suggesting incomplete penetrance, also supported by Ammar et al. reporting one healthy carrier for p.G117S (36). This healthy carrier from the Eskin-Schwartz report is negative for the three additional CARD14 variants and for the 06:02 allele at the HLA-C locus, suggesting that genetic cofactors as well as

environmental triggers might be required for CARD14-induced psoriasis.

Altogether, these studies indicate that the assessment of linkage to psoriasis susceptibility loci should be made cautiously as a number of factors complicate the analyses, including genetic cofactors, statistical limitations due to studies with narrow sample size, incomplete penetrance, environmental factors, and misdiagnosis.

HETEROGENEOUS IMPACT OF CARD14 MUTATIONS AT THE MOLECULAR LEVEL

Immunohistochemistry staining and mRNA assessment revealed that CARD14 localizes to the basal cell layer of the epidermis in healthy skin whereas it is found in suprabasal layers in psoriatic tissue (1, 9, 12).

Several CARD14 mutants were studied at the molecular level in terms of their ability to activate NF-κB (**Table 3**). In reporter gene assays, when compared to WT-CARD14, NF-κB luciferase activity was found strongly increased upon over expression of p.E138A (7–9 fold), p.E138del (2–3 fold), p.E142K/G (4–5 fold), p.G117S (3–4 fold), and p.D176H (2–3 fold); and moderately increased for p.R179H, p.E197K, p.L150R, and p.L228R (1.4–1.7 fold) (**Table 3**). However, NF-κB activity was found unaffected upon overexpression of p.R68Q, p.V191L, p.D285G, p.M338V, p.I593N, p.S602L, p.R682W, and p.G714S and reduced for variants p.R38C, p.R69W, p.R151Q, p.S200N, p.L209P, p.H171N, p.T420A (0.1–0.7 fold) (9, 10, 37, 60). Other variants were not assessed in terms of NF- κB luciferase activity.

Seventeen CARD14 variants were tested for mRNA induction upon overexpression in the keratinocyte cell-line, HEK001 cells, by microarray or quantitative RT-PCR (9, 10) (**Table 3**). Four of these (p.E138A, p.G117S, p.E142K, p.E142G) displayed a pathogenic signature with strong induction of 13 genes including genes encoding CXCL8, IL-8, CSF2, SOD2, and TNFα, suggesting a role in skin inflammation. Additionally, CXCL8, CCL20, SOD2, and IL36γ transcripts were found increased in psoriatic skin from a GPP patient carrying the E138A mutation who also displayed an increased number of CARD14-positive keratinocytes by immunostaining. However, the other 13 variants (p.G714S, p.S200N, p.D176H, p.R179H, p.R38C, p.R62Q, p.I593N, p.H171N, p.R682W, p.L150R, p.V191L, p.D285G, p.R547S) failed to induce this pathogenic signature.

The CC domain of CARD11 is known to mediate its oligomerization upon activation (80). GoF mutations in the CC domain of CARD11 have been shown to trigger spontaneous protein aggregation and constitutive activation of NF-κB signaling leading to lymphoma (53). Berki et al. showed spontaneous CARD14 oligomerization for three variants located in the CC domain (p.E138A, p.D176H, and p.L156P), which did not occur in CARD14 WT or in the p.G117S variant, where the mutation is located outside the CC domain (38). Variants p.E138A, p.G117S, pE142K, and p.H171N were further characterized and show enhanced interaction with BCL10 and MALT1, thus resulting in increased NF-κB, ERK, and p38 MAPK activation (2, 71). This hyperactivity is reduced upon MALT1 protease inhibition with mepazine, thus suggesting that MALT1 treatment could benefit patients with CARD14-associated psoriasis.

Harden et al., showed CARD14 overexpression in dermal endothelial cells in psoriatic skin from patients harboring p.E138A and p.G117S mutations (5). This also correlated with enhanced NF-κB activity and proinflammatory gene induction, suggesting that CARD14 GoF in endothelial cells might also contribute to psoriasis pathogenesis. Intriguingly, the expression of CARD14 in aortic endothelial cells was also determined and warrants further investigation into the association of CARD14 mutation and associated cardiovascular defects in some psoriasis patients.

Recently, Danis et al showed that isolated primary keratinocytes from a patient with PRP type V, harboring three heterozygous variants (p.R547S, pR682W, p. R820W) and carrying a homozygous splice site variant (c.676-6G/A), displayed increased NF-κB activity compared to keratinocytes from healthy control (81). In this case, the analysis *ex vivo* of patient's cells carrying four variants do not allow to conclude about pathogenicity for each variant. However, it is interesting to note that at least two of these variants (p.R547S and pR682W) failed to induce increased NF-κB activity *in vitro* independently suggesting that *in vitro* assays might not be adequate to predict pathogenicity or that there is a cumulative effect occurring *in vivo*.

To conclude, there is strong evidence to consider p.E138A, p.E138del, p.G117S, p.E142K, p.E142G, and p.D176H as GoF variants based on their ability to trigger NF-κB activity and an inflammatory gene signature. p.E138A, p.E138del, p.D176H, and p.L156P could also be considered GoF due to their ability to trigger spontaneous CARD14 oligomerization and p.H171N based on its increased interaction with BCL10 (**Table 1**). It is however surprising that p.L156P and p.H171N trigger an increased CBM complex formation without increased NF-κB activation (38). This might be due to a sensitivity limitation of the assay used. Finally, p.E138A, p.E138K, p.E138del, p.G117S, p.E142K, p.E142G, p.L156P, and p.H171N could be considered as pathogenic since they are not found in healthy individuals according to public databases. Regarding other reported variants, more systematic functional studies and *ex vivo* studies from patient material are required to better understand how they could contribute to pathogenesis but they might be considered as variants associated with increased susceptibility to psoriasis rather than causal mutations.

PHYSIOLOGICAL ROLE OF CARD14 IN MOUSE PSORIASIS MODELS

Findings in mouse models have further illuminated the physiological role of CARD14 in driving psoriatic skin disease. Heterozygous mice harboring a GoF mutation in the *Card14* gene at the glutamic acid residue E138 (*Card14*Δ*E138*) spontaneously develop a chronic psoriatic skin disease at 5 days-old (72). Deletion of this glutamic acid is synonymous to a human variant described in familial PRP family (12) and mutation of this

TABLE 3 | Functional characterization of CARD14 variants.

Protein Change	CARD14 domain	NF-κB reporter	Pathogenic signature upon O/E	Other functional testing
R38C	CARD	0.11	no	
R62Q	CARD	1.06	no	
R69W	CARD	0.144	nd	
G117S	Between CARD-CC	3.71	yes	- over expressed in EC in psoriatic skin - no spontaneous oligomerization - increased interaction with MALT1 and BCL10, increased ERK/p38 activation
M119R	Between CARD-CC	nd	nd	
M119T	Between	nd	nd	
	CARD-CC			
M119V	Between	nd	nd	
	CARD-CC			
L124P	Between CARD-CC	nd	nd	
C127S	Between CARD-CC	nd	nd	
Q136L	CC	nd	nd	
E138K	CC	nd	nd	
E138A	CC	8.95	yes	- increased CARD14 staining and proinfl. gene expression in lesional skin - over expressed in EC in psoriatic skin - spontaneous CARD14 oligomerization - increased interaction with MALT1 and BCL10, increased ERK/p38 activation
E138del	CC	≈2.5	yes (mouse)	- spontaneous CARD14 oligomerization - increased interaction with BCL10
E142G	CC	5	yes	
E142K	CC	4.03	yes	- increased interaction with MALT1 and BCL10, increased ERK/p38 activation
L150R	CC	1.79	no	
R151Q	CC	0.576	nd	
R151W	CC	1.766	nd	
L156P	CC	≈1.2	nd	- spontaneous CARD14 oligomerization
Q157P	CC	nd	nd	
R166H	CC	nd	nd	
H171N	CC	0.68	no	- increased interaction with MALT1 and BCL10, increased ERK/p38 activation
D176H	CC	2.78	no	- spontaneous CARD14 oligomerization
R179H	CC	1.38	no	
V191L	CC	1.02	no	
E197K	CC	1.667	nd	
S200N	CC	0.67	no	
L209P	CC	0.575	nd	
A216T	CC	nd	nd	
L228R	CC	1.5	nd	
D285G	CC	1.14	no	
M338V	CC	0.914	nd	
T420A	linker	0.663	nd	
E422K	linker	nd	nd	
R430W	linker	nd	nd	
R547S	linker	1	no	
V585I	linker	nd	nd	
T591M	PDZ	nd	nd	
I593N	PDZ	1.3	no	
S602L	PDZ	1.1	nd	
R682W	SH3	0.95	no	
G714S	SH3	1.02	no	
S802R	none	nd	nd	
R820W	GUK	nd	nd	
D973E	none	nd	nd	

Summary of functional studies performed on CARD14 variants depicting ability to activate NF-κB and interaction with binding partners, BCL10 and MALT1.
CC, coiled-coil; GuK, guanylate-kinase domain; PDZ, PSD-95, discs-large, zona occludens-1 domain; SH3, Src homology 3 domain; O/E, overexpression.

residue has also been associated with the severe case of *de novo* GPP reported by Jordan and two sporadic cases of PRP with neonatal onset (58, 59). Like human disease the phenotype runs a chronic course in *Card14*Δ*E138*$^{+/-}$ mice yet is mostly restricted to ear and tail tissue. Wang et al. subsequently generated *Card14E138A*$^{+/-}$ and *Card14*Δ*Q136*$^{+/-}$ mouse models and reported similar phenotypes to the *Card14*Δ*E138*$^{+/-}$ mouse (82). Interestingly, the *Card14E138A*$^{+/-}$ mouse had impaired survival rates compared to *Card14*Δ*Q136*$^{+/-}$ mice, probably due to a more severe phenotype, in line with the enhanced potency of the human p.E138A mutation in *in vitro* studies. Though serendipitous incorrect editing by the CRISPR/Cas9 system generated the Card14ΔQ136 mutation, a similar human variant, p.Q136L, has been previously found in PRP type V (56). Histological analysis of *Card14* GoF mutant mice revealed typical hallmark features of human psoriatic skin disease with keratinocyte hyperproliferation, epidermal thickening and areas of parakeratosis and orthokeratosis, and with enlarged and increased number of blood vessels in the dermal compartment (72, 82). Other interesting features described in *Card14*Δ*E138*$^{+/-}$ mutant mice include mild spongiosis within the epidermis, keratotic follicular plugging, which is a key feature of human PRP and the presence of neutrophil-rich microabscesses in the epidermis. Immune cell infiltration in *Card14* GoF mice consists of innate and adaptive immune arms, with significant high numbers of neutrophils, myeloid cells, as well as γδ- and αβ-T cells (72, 82).

Transcriptomic analysis of psoriatic tissue from *Card14*Δ*E138*$^{+/-}$ ear pinnae revealed over 500 differentially expressed genes compared to wild-type littermates. These included genes encoding proinflammatory molecules of the adaptive (IL-17F, IL-20, IL-22, IL-23) and innate (IL-1 and IL-36 family cytokines, IL-19, IL-17C,) immune compartments. Neutrophil and Th17-chemoattractants, CXCL2 and CCL20 were also highly expressed as well as β-defensins and S100 proteins, which mirrors human psoriatic tissue. Indeed, antimicrobial peptides have a key role in driving human psoriatic skin disease and an increased copy number of β-defensins was previously associated with susceptibility to psoriasis (83). IL-17-responsive genes including small proline-rich proteins (SPRRs) and lipocalin-2 were also highly upregulated. Interestingly, and demonstrating the autoinflammatory and autoimmunity networks evident in this mouse model, genes encoding NOD2, Caspase-1, Caspase-4 and NLRP3 are also upregulated. This echoes the bimodal immune activation of psoriasis pathogenesis proposed by Christophers, showing innate neutrophils and macrophages orchestrating pathology alongside infiltrating Th17 cells, which maintain the chronic form of the disease (16). Interestingly, IL-38, an endogenous antagonist of IL-36 signaling was downregulated in psoriatic tissue from *Card14*Δ*E138* heterozygous mice, further suggesting a role for IL-36 signaling in this model. Enrichment analysis of the *Card14*Δ*E138*$^{+/-}$ transcriptome compared to two published human datasets revealed high correlation of the murine phenotype with human plaque psoriasis.

Wang and colleagues demonstrated that the phenotype of *Card14*Δ*Q136*$^{+/-}$ mice was ameliorated when crossed with *Il17a*- or *Rag1*-deficient animals, demonstrating an important contribution of T cells, in particular IL-17A-positive $\alpha\beta$ T cells to the phenotype (82). Interestingly, *Card14*-deficient keratinocytes showed impaired responses to IL-17A and it was demonstrated that CARD14 interacts with the IL-17 receptor adaptor molecule, ACT1, suggesting that CARD14 is activated downstream of IL-17A in keratinocytes.

While CARD14 GoF is enough to drive full-blown psoriatic phenotype in mice, Tanaka and colleagues reported a requirement of CARD14 for psoriasiform disease development in other mouse models (84). The imiquimod mouse model is the most widely-used psoriasiform model for studying psoriatic skin disease due to the capability of TLR7 agonist imiquimod to activate plasmacytoid dendritic cells (pDCs), which are also implicated in mediating early events in human psoriasis pathogenesis (85, 86), *Card14*$^{-/-}$ mice did not display thickening of the epidermis or immune cell infiltration of IL-17- and IL-22-secreting γδ T cells, characteristic of the imiquimod model. Therefore, CARD14-deficient mice were protected against developing psoriasiform disease in response to imiquimod compared to wild-type controls (84). These findings were corroborated by Wang and colleagues (82). Additionally, acanthosis caused by intradermal administration of IL-23 in wild-type mice mouse ears was diminished in CARD14-deficient animals and migration of IL-17- and IL-22-producing γδ T cells were significantly impaired in response to IL-23 in mice lacking functional CARD14 (84). This could be due to breaking of the chronic amplification loop in this model due to diminished CARD14-signaling within keratinocytes. However, the authors established bone-marrow chimeras and reported that *Card14*$^{-/-}$ mice receiving a bone-marrow transplant from wild-type mice showed partial response to imiquimod, while conversely, irradiated WT recipient mice receiving bone-marrow from *Card14*$^{-/-}$ donors showed decreased ear swelling in response to imiquimod compared to wild-type: wild-type chimeras. Tanaka's results suggest that CARD14 expression on radio-sensitive hematopoietic cells also contributes to psoriasiform disease in mice. Conversely, in the *Card14* GoF model, it was shown, using bone marrow chimeras, that transferring hematopoietic cells from *Card14*Δ*Q136*$^{+/-}$ mice could not induce a psoriasiform phenotype in recipient WT mice, suggesting non-hematopoietic cells expressing mutant CARD14 are the drivers of disease pathogenesis in this model (82).Taken together these studies demonstrate a pivotal role for CARD14 in murine psoriasiform disease. Interestingly, while Tanaka and colleagues report that CARD14 is required for IL-23-induced disease and Wang demonstrated a role for CARD14 downstream of IL-17A in keratinocytes, the *Card14* GoF models show that CARD14 GoF mutation drives the pathogenic IL-23/IL-17 axis, suggesting that CARD14 is central to maintaining the chronic inflammatory cycle in murine psoriasiform disease. Furthermore, neutralization of IL-23p19 in Card14Δ*E138*$^{+/-}$ mice significantly alleviated psoriatic skin, which mirrors the impact of targeting this cytokine subunit in clinical trials for human plaque psoriasis (87–89). These findings from murine psoriasis models would suggest that the CARD14 pathway is an important mediator of pro-inflammatory effects in human

psoriatic skin disease also in patients lacking CARD14 GoF mutations.

DISCUSSION

Since the initial identification of GoF mutations of CARD14 as being responsible for psoriasis in two large kindreds and in a sporadic case of severe GPP, 44 missense, 4 splice site variants and 1 in frame deletion have been described in CARD14 in patients with several psoriatic skin disorders. One of the main complications is to understand how these variants contribute to disease progression. Among 49 variants reported as associated with psoriatic skin disease, 21 of them have never been tested functionally and eight others where only tested for NF-κB induction in overexpression systems. Interestingly, among the 28 variants tested for the ability to activate NF-κB, only six of these triggered increased NF-κB reporter activity more than two fold compared to overexpressed WT CARD14 (21%) (p.E138A, p.E138del, p.G117S, p.E142K, p.E142G, and p.D176H) (**Table 3**). Two other variants (p.L156P and p.H171N) did not show increased NF-κB induction but p.L156P displayed spontaneous CARD14 oligomerization (38). It remains to be clarified how this variant can contribute to psoriasis pathogenesis. Regarding the CARD14 variants that failed to induce enhanced NF-κB activity compared to WT CARD14, it is difficult to consider them as GoF and it remains to be elucidated by which mechanism they could be pathogenic. In this review, we have classified CARD14 reported variants as causal (**Table 1**) and associated (**Table 2**) based on the functional studies available but a better understanding of their mechanism of pathogenicity would help to classify pathogenic and non-pathogenic variants to comprehend the genetic contribution of CARD14 in psoriatic disorders. To date, the only common feature found between all pathogenic variants (with the exception of p.G117S) is their localization within the CARD14 coiled-coil domain, and they likely affect the autoinhibitory state of the protein. This might suggest that patients with variants in other regions of the CARD14 protein should undergo further genetic screening for potential cofactors.

Existence of cofactors have been reported in some studies, therefore it is possible that some CARD14 mutations only confer an increased risk of developing disease and other mutations are needed to develop psoriasis. Interestingly, in addition to *HLA-Cw*0602*, Spoerri and colleagues reported a kindred in which family members presented with PRP or psoriasis (42). While all family members had CARD14 mutations, the PRP sufferers had an additional frame-shift mutation in *DTX1*, a regulator of regulatory T cells, while the psoriasis-affected individual harbored a mutation in *NLRC5*, a molecule that activates NF-κB but also regulates MHC-I transcription (42). This kindred highlights how genetic cofactors may dictate how CARD14 mutations might contribute to diverse psoriatic entities.

Recently, another type of pustular skin type was also shown to be associated with CARD14. Acute exanthematous generalized pustular eruption (AGEP) is a rare generalized pustular skin rash that is triggered by an adverse reaction to drug administration (usually antibiotics but occasionally also anti-fungal or anti-malarial drugs), though sometimes in response to bacterial or viral infection (90, 91). The underlying disease mechanism of AGEP currently remains unknown but recent identification of *IL36RN* mutations being a causative factor in patients suggests a genetic and mechanistic connection between pustular psoriasis and AGEP (26, 92). Podlipnik et al. describe a 47-year old male patient presenting with AGEP and polyarthritis induced by dipyrone, a known AGEP culprit drug. It was discovered that the patient carried a heterozygous mutation (p.R430W) in the linker region of CARD14 (90). The authors predict that the variant is pathogenic based on bioinformatic analysis and its low frequency in healthy individuals from public database information (90).

The CARMA family have emerged as major mediators of both adaptive and innate immune responses and CARD14 was recently shown to have an important role in innate immune defense in keratinocytes in response to stimulation of the fungal Pattern Recognition Receptor, Dectin-1 and in response to bacterial ligands (73, 93). These *in vitro* data suggest that CARD14 plays a crucial role in modulating host defense at the skin barrier. However, this requires further clarification beyond *in vitro* studies. Utilizing CARD14-deficient mice in skin infection or barrier disruption models will lead to a greater understanding of how this molecule is activated and mounts an innate immune response to infection.

Interestingly, another CARMA molecule, CARD10, has recently turned out to be important in keratinocyte-induced immune responses. CARD10 was shown to be highly expressed in proliferating keratinocytes, whereas CARD14 was shown to be expressed at low levels in proliferating keratinocytes but induced upon their differentiation (6). This balance between CARD10 and CARD14 might be important in the context of psoriasis where keratinocyte differentiation processes are known to be dysregulated. Additionally, CARD10 was shown to regulate NF-κB in endothelial cells, for example in response to angiotensin (94) and potentially GoF mutation in CARD14 might destabilize a potential CARD10/CARD14 balance, and thus could contribute to cardiovascular comorbidities.

Beyond keratinocytes and endothelial cells, expression of CARD14 was also described in bone marrow-derived hematopoietic cells in mice. It will be of interest to determine the contribution of these cell types, harboring CARD14 mutations, to human psoriasis pathogenesis. To date, CARD14 GoF mutation studies have been limited to overexpression systems, primarily in cell-lines. It can be anticipated that CRISPR/Cas9 technology will aid in further elucidating the function of CARD14 GoF mutations in different cell types from *in vivo* models and in keratinocyte cell-lines. Little is known, also about the function of CARD14 in other tissue types.

CARD14 has previously been shown as a strong inducer of IL-36γ in primary keratinocytes highlighting a link between *CARD14* GoF mutations and the IL-36 cytokines responsible for GPP pathogenesis. Interestingly, plaque and pustular forms of psoriasis can present concurrently (16, 95) and Christophers and colleagues propose a bimodal model of immune activation within psoriasis with alternate activation of autoinflammatory and autoimmune networks (16). Due to the shared characteristics

of psoriasis entities caused by *CARD14* and *IL-36RN* mutation Akiyama and colleagues propose that these disease subtypes should be grouped together as autoinflammatory keratinization diseases (AIKDs) (96, 97). The main defining factors of AIKDs is that the primary inflammatory sites occur at the epidermis and upper dermis resulting in hyperkeratosis with mixed autoinflammatory and autoimmunity circuits driving pathogenesis. Therefore, *IL-36RN*-associated GPP, and CARD14-mediated pustular psoriasis, PRP type V and familial keratosis lichenoides chronica (KLC) caused by *NLRP1* mutation, can be considered AIKDs.

In *Card14*Δ*E138*$^{+/-}$ mice both autoinflammatory and autoimmune networks were upregulated at the transcript level suggesting that CARD14 GoF mutation drives both adaptive and innate immune networks, which might explain why mutant variants of CARD14 have been associated with both plaque and pustular forms of psoriasis. Disruption of the adaptive immune response by TNF and IL-12/IL-23 blockade has proven successful in case reports of patients harboring CARD14 GoF mutations and findings from mouse models suggest that targeting the IL-23/IL-17 axis would also be beneficial for patients. Utilising an NF-κB inhibitor was also favorable in Card14 GoF mice (82) and specific inhibition of MALT1 or CARD14, itself, might also be attractive therapeutic options in the future.

AUTHOR CONTRIBUTIONS

All authors listed have made a substantial, direct and intellectual contribution to the work, and approved it for publication.

FUNDING

MM is supported by grants from CRPP radiz—Rare Disease Initiative Zurich, University of Zurich and the Monique Dornonville de la Cour Foundation.

REFERENCES

1. Blonska M, Lin X. NF-κB signaling pathways regulated by CARMA family of scaffold proteins. *Cell Res*. (2011) 21:55–70. doi: 10.1038/cr.2010.182
2. Afonina IS, Van Nuffel E, Baudelet G, Driege Y, Kreike M, Staal J, et al. The paracaspase MALT1 mediates CARD14-induced signaling in keratinocytes. *EMBO Rep*. (2016) 17:914–27. doi: 10.15252/embr.201642109
3. Bertin J, Wang L, Guo Y, M.Jacobson D, J.Poyet L, S.Srinivasula M, et al. CARD11 and CARD14 are novel caspase recruitment domain (CARD)/membrane-associated guanylate kinase (MAGUK) family members that interact with BCL10 and activate NF-κB. *J Biol Chem*. (2001) 276:11877–82. doi: 10.1074/jbc.M010512200
4. Scudiero I, Zotti T, Ferravante A, Vessichelli M, Vito P, Stilo R. Alternative splicing of CARMA2/CARD14 transcripts generates protein variants with differential effect on NF-kappaB activation and endoplasmic reticulum stress-induced cell death. *J Cell Physiol*. (2011) 226:3121–31. doi: 10.1002/jcp.22667
5. Harden JL, Lewis SM, Pierson KC, Suarez-Farinas M, Lentini T, Ortenzio FS, et al. CARD14 expression in dermal endothelial cells in psoriasis. *PLoS ONE* (2014) 9:e111255. doi: 10.1371/journal.pone.0111255
6. Israel L, Bardet M, Huppertz A, Mercado N, Ginster S, Unterreiner A, et al. A CARD10-dependent tonic signalosome activates MALT1 paracaspase and regulates IL-17/TNF-alpha driven keratinocyte inflammation. *J Invest Dermatol*. (2018) 138:2075–79. doi: 10.1016/j.jid.2018.03.1503
7. Scudiero I, Vito P, Stilo R. The three CARMA sisters: so different, so similar: a portrait of the three CARMA proteins and their involvement in human disorders. *J Cell Physiol*. (2014) 229:990–7. doi: 10.1002/jcp.24543
8. Perez de Diego R, Sanchez-Ramon S, Lopez-Collazo E, Martinez-Barricarte R, Cubillos-Zapata C, Ferreira Cerdan A, et al. Genetic errors of the human caspase recruitment domain-B-cell lymphoma 10-mucosa-associated lymphoid tissue lymphoma-translocation gene 1 (CBM) complex: molecular, immunologic, and clinical heterogeneity. *J Allergy Clin Immunol*. (2015) 136:1139–49. doi: 10.1016/j.jaci.2015.06.031
9. Jordan CT, Cao L, Roberson ED, Pierson KC, Yang CF, Joyce CE, et al. PSORS2 is due to mutations in CARD14. *Am J Hum Genet*. (2012) 90:784–95. doi: 10.1016/j.ajhg.2012.03.012
10. Jordan CT, Cao L, E.Roberson D, Duan S, Helms CA, Nair RP, et al. Rare and common variants in CARD14, encoding an epidermal regulator of NF-κB, in psoriasis. *Am J Hum Genet*. (2012) 90:796–808. doi: 10.1016/j.ajhg.2012.03.013
11. International Psoriasis Genetics C. The International Psoriasis Genetics Study: assessing linkage to 14 candidate susceptibility loci in a cohort of 942 affected sib pairs. *Am J Hum Genet*. (2003) 73:430–7. doi: 10.1086/377159
12. Fuchs-Telem D, Sarig O, van Steensel MA, Isakov O, Israeli S, Nousbeck J, et al. Familial pityriasis rubra pilaris is caused by mutations in CARD14. *Am J Hum Genet*. (2012) 91:163–70. doi: 10.1016/j.ajhg.2012.05.010
13. Christophers E. Psoriasis–epidemiology and clinical spectrum. *Clin Exp Dermatol*. (2001) 26:314–20. doi: 10.1046/j.1365-2230.2001.00832.x
14. Chandran V, Raychaudhuri SP. Geoepidemiology and environmental factors of psoriasis and psoriatic arthritis. *J Autoimmun*. (2010) 34:J314–21. doi: 10.1016/j.jaut.2009.12.001
15. Nestle FO, Kaplan DH, Barker J. Psoriasis. *N Engl J Med*. (2009) 361:496–509. doi: 10.1056/NEJMra0804595
16. Christophers E, Metzler G, Rocken M. Bimodal immune activation in psoriasis. *Br J Dermatol*. (2014) 170:59–65. doi: 10.1111/bjd.12631
17. Griffiths CE, Christophers E, Barker JN, Chalmers RJ, Chimenti S, Krueger GG, et al. A classification of psoriasis vulgaris according to phenotype. *Br J Dermatol*. (2007) 156:258–62. doi: 10.1111/j.1365-2133.2006.07675.x
18. Griffiths CE, Barker JN. Pathogenesis and clinical features of psoriasis. *Lancet* (2007) 370: 263–71. doi: 10.1016/S0140-6736(07)61128-3.
19. Henseler T, Christophers E. Disease concomitance in psoriasis. *J Am Acad Dermatol*. (1995) 32:982–6. doi: 10.1016/0190-9622(95)91336-X
20. Neimann AL, Shin DB, Wang X, Margolis DJ, Troxel AB, Gelfand JM. Prevalence of cardiovascular risk factors in patients with psoriasis. *J Am Acad Dermatol*. (2006) 55:829–35. doi: 10.1016/j.jaad.2006.08.040
21. Sommer DM, Jenisch S, Suchan M, Christophers E, Weichenthal M. Increased prevalence of the metabolic syndrome in patients with moderate to severe psoriasis. *Arch Dermatol Res*. (2006) 298:321–8. doi: 10.1007/s00403-006-0703-z
22. Mease PJ, Gladman DD, Papp KA, Khraishi MM, Thaci D, Behrens F, et al. Prevalence of rheumatologist-diagnosed psoriatic arthritis in patients with psoriasis in European/North American dermatology clinics. *J Am Acad Dermatol*. (2013) 69:729–35. doi: 10.1016/j.jaad.2013.07.023
23. Krueger JG, Brunner PM. Interleukin-17 alters the biology of many cell types involved in the genesis of psoriasis, systemic inflammation and associated comorbidities. *Exp Dermatol*. (2018) 27:115–123. doi: 10.1111/exd.13467
24. Suarez-Farinas M, Li K, Fuentes-Duculan J, Hayden K, Brodmerkel C, Krueger JG. Expanding the psoriasis disease profile: interrogation of the skin and serum of patients with moderate-to-severe psoriasis. *J Invest Dermatol*. (2012) 132:2552–64. doi: 10.1038/jid.2012.184
25. Arican O, Aral M, Sasmaz S, Ciragil P. Serum levels of TNF-alpha IFN-gamma IL-6, IL-8, IL-12, IL-17, and IL-18 in patients with active psoriasis and correlation with disease severity. *Mediators Inflamm*. (2005) 2005:273–9. doi: 10.1155/MI.2005.273
26. Bachelez H. Pustular psoriasis and related pustular skin diseases. *Br J Dermatol*. (2018) 178:614–618. doi: 10.1111/bjd.16232

27. Marrakchi S, Guigue P, Renshaw BR, Puel A, Pei XY, Fraitag S, et al. Interleukin-36-receptor antagonist deficiency and generalized pustular psoriasis. *N Engl J Med*. (2011) 365:620–8. doi: 10.1056/NEJMoa1013068
28. Onoufriadis A, Simpson MA, Pink AE, Di Meglio P, Smith CH, Pullabhatla V, et al. Mutations in IL36RN/IL1F5 are associated with the severe episodic inflammatory skin disease known as generalized pustular psoriasis. *Am J Hum Genet*. (2011) 89:432–7. doi: 10.1016/j.ajhg.2011.07.022
29. Sugiura K, Takemoto A, Yamaguchi M, Takahashi H, Shoda Y, Mitsuma T, et al. The majority of generalized pustular psoriasis without psoriasis vulgaris is caused by deficiency of interleukin-36 receptor antagonist. *J Invest Dermatol*. (2013) 133:2514–21. doi: 10.1038/jid.2013.230
30. Setta-Kaffetzi N, Simpson MA, Navarini AA, Patel VM, Lu HC, Allen MH, et al. AP1S3 mutations are associated with pustular psoriasis and impaired Toll-like receptor 3 trafficking. *Am J Hum Genet*. (2014) 94:790–7. doi: 10.1016/j.ajhg.2014.04.005
31. Mahil SK, Twelves S, Farkas K, Setta-Kaffetzi N, Burden AD, Gach JE, et al. AP1S3 Mutations cause skin autoinflammation by disrupting keratinocyte autophagy and Up-Regulating IL-36 production. *J Invest Dermatol*. (2016) 136:2251–9. doi: 10.1016/j.jid.2016.06.618
32. Capon F. The genetic basis of psoriasis. *Int J Mol Sci*. (2017) 18:E2526. doi: 10.3390/ijms18122526
33. Tomfohrde J, Silverman A, Barnes R, Fernandez-Vina MA, Young M, Lory D, et al. Gene for familial psoriasis susceptibility mapped to the distal end of human chromosome 17q. *Science* (1994) 264:1141–5. doi: 10.1126/science.8178173
34. Hwu WL, Yang CF, Fann CS, Chen CL, Tsai TF, Chien YH, et al. Mapping of psoriasis to 17q terminus. *J Med Genet*. (2005) 42:152–8. doi: 10.1136/jmg.2004.018564
35. Nair RP, Henseler T, Jenisch S, Stuart P, Bichakjian CK, Lenk W, et al. Evidence for two psoriasis susceptibility loci (HLA and 17q) and two novel candidate regions (16q and 20p) by genome-wide scan. *Hum Mol Genet*. (1997) 6:1349–56. doi: 10.1093/hmg/6.8.1349
36. Ammar M, Bouchlaka-Souissi C, Helms CA, Zaraa I, Jordan CT, Anbunathan H, et al. Genome-wide linkage scan for psoriasis susceptibility loci in multiplex Tunisian families. *Br J Dermatol*. (2013) 168:583–7. doi: 10.1111/bjd.12050
37. Ammar M, Jordan CT, Cao L, Lim E, Bouchlaka Souissi C, Jrad A, et al. CARD14 alterations in Tunisian patients with psoriasis and further characterization in European cohorts. *Br J Dermatol*. (2016) 174:330–7. doi: 10.1111/bjd.14158
38. Berki DM, Liu L, Choon SE, David Burden A, Griffiths CEM, Navarini AA, et al. Activating CARD14 mutations are associated with generalized pustular psoriasis but rarely account for familial recurrence in psoriasis vulgaris. *J Invest Dermatol*. (2015) 135:2964–70. doi: 10.1038/jid.2015.288
39. Craiglow BG, L.Boyden M, Hu R, Virtanen M, Su J, Rodriguez G, et al. CARD14-associated papulosquamous eruption: a spectrum including features of psoriasis and pityriasis rubra pilaris. *J Am Acad Dermatol*. (2018) 79:487–94. doi: 10.1016/j.jaad.2018.02.034
40. Eskin-Schwartz M, Basel-Vanagaite L, David M, Lagovsky I, Ben-Amitai D, Smirin-Yosef P, et al. Intra-familial variation in clinical phenotype of CARD14-related Psoriasis. *Acta Derm Venereol*. (2016) 96:885–7. doi: 10.2340/00015555-2405
41. Mossner R, Frambach Y, Wilsmann-Theis D, Lohr S, Jacobi A, Weyergraf A, et al. Palmoplantar pustular psoriasis is associated with missense variants in CARD14, but not with loss-of-function mutations in IL36RN in European patients. *J Invest Dermatol*. (2015) 135:2538–41. doi: 10.1038/jid.2015.186
42. Spoerri I, Herms S, Eytan O, Sarig O, Heinimann K, Sprecher E, et al. Immune-regulatory genes as possible modifiers of familial pityriasis rubra pilaris-Lessons from a family with PRP and psoriasis. *J Eur Acad Dermatol Venereol*. (2018). doi: 10.1111/jdv.15029
43. Sugiura K, Kitoh T, Watanabe D, Muto M, Akiyama M. Childhood-onset PsA in Down syndrome with psoriasis susceptibility variant CARD14 rs11652075. *Rheumatology (Oxford)* (2015) 54:197–9. doi: 10.1093/rheumatology/keu419
44. Sugiura K, Muto M, Akiyama M. CARD14 c.526G>C (p.Asp176His) is a significant risk factor for generalized pustular psoriasis with psoriasis vulgaris in the Japanese cohort. *J Invest Dermatol*. (2014) 134:1755–7. doi: 10.1038/jid.2014.46
45. Takeichi T, Kobayashi A, Ogawa E, Okuno Y, Kataoka S, Kono M. et al. Autosomal dominant familial generalized pustular psoriasis caused by a CARD14 mutation. *Br J Dermatol*. (2017) 177:e133–5. doi: 10.1111/bjd.15442
46. Feng C, Wang T, Li SJ, Fan YM, Shi G, Zhu KJ. CARD14 gene polymorphism c.C2458T (p.Arg820Trp) is associated with clinical features of psoriasis vulgaris in a Chinese cohort. *J Dermatol*. (2016) 43:294–7. doi: 10.1111/1346-8138.13065
47. Gonzalez-Lara L, Coto-Segura P, Penedo A, Eiris N, Diaz M, Santos-Juanes J, et al. SNP rs11652075 in the CARD14 gene as a risk factor for psoriasis (PSORS2) in a Spanish cohort. *DNA Cell Biol*. (2013) 32:601–4. doi: 10.1089/dna.2013.2109
48. Coto-Segura P, Gonzalez-Fernandez D, Batalla A, Gomez J, Gonzalez-Lara L, Queiro R, et al. Common and rare CARD14 gene variants affect the antitumour necrosis factor response among patients with psoriasis. *Br J Dermatol*. (2016) 175:134–41. doi: 10.1111/bjd.14461
49. Qin P, Zhang Q, Chen M, Fu X, Wang C, Wang Z, et al. Variant analysis of CARD14 in a Chinese Han population with psoriasis vulgaris and generalized pustular psoriasis. *J Invest Dermatol*. (2014) 134:2994–6. doi: 10.1038/jid.2014.269
50. Shi G, Li SJ, Wang TT, Cheng CM, Fan YM, Zhu KJ. The common CARD14 gene missense polymorphism rs11652075 (c.C2458T/p.Arg820Trp) is associated with psoriasis: a meta-analysis. *Genet Mol Res*. (2016) 15. doi: 10.4238/gmr.15038357
51. Zhu K, Shi G, Liu H, Zhu C, Fan Y. Variants of CARD14 gene and psoriasis vulgaris in southern Chinese cohort. *An Bras Dermatol*. (2016) 91:45–8. doi: 10.1590/abd1806-4841.20164016
52. Hong JB, P.Chen L, Chen YT, Tsai TF. Genetic analysis of CARD14 in non-familial pityriasis rubra pilaris: a case series. *Acta Derm Venereol*. (2014) 94:587–8. doi: 10.2340/00015555-1814
53. Lamason RL, McCully RR, Lew SM, Pomerantz JL. Oncogenic CARD11 mutations induce hyperactive signaling by disrupting autoinhibition by the PKC-responsive inhibitory domain. *Biochemistry* (2010) 49:8240–50. doi: 10.1021/bi101052d
54. van de Kerkhof PC. An update on topical therapies for mild-moderate psoriasis. *Dermatol Clin*. (2015) 33:73–7. doi: 10.1016/j.det.2014.09.006
55. Tsai YC, Tsai TF. Anti-interleukin and interleukin therapies for psoriasis: current evidence and clinical usefulness. *Ther Adv Musculoskelet Dis*. (2017) 9:277–94. doi: 10.1177/1759720X17735756
56. Takeichi T, Sugiura K, Nomura T, Sakamoto T, Ogawa Y, Oiso N, et al. Pityriasis Rubra Pilaris Type V as an Autoinflammatory Disease by CARD14 Mutations. *JAMA Dermatol*. (2017) 153:66–70. doi: 10.1001/jamadermatol.2016.3601
57. Eytan O, Qiaoli L, Nousbeck J, van Steensel MA, Burger B, Hohl D, et al. Increased epidermal expression and absence of mutations in CARD14 in a series of patients with sporadic pityriasis rubra pilaris. *Br J Dermatol*. (2014) 170:1196–8. doi: 10.1111/bjd.12799
58. Has C, Schwieger-Briel A, Schlipf N, Hausser I, Chmel N, Rosler B, et al. Target-sequence Capture and High Throughput Sequencing Identify a *De novo* CARD14 Mutation in an Infant with Erythrodermic Pityriasis Rubra Pilaris. *Acta Derm Venereol*. (2016) 96:989–90. doi: 10.2340/00015555-2446
59. Inoue N, Dainichi T, Fujisawa A, Nakano H, Sawamura D, Kabashima K. CARD14 Glu138 mutation in familial pityriasis rubra pilaris does not warrant differentiation from familial psoriasis. *J Dermatol*. (2016) 43:187–9. doi: 10.1111/1346-8138.13008
60. Li Q, Jin Chung H, Ross N, Keller M, Andrews J, Kingman J, et al. Analysis of CARD14 Polymorphisms in pityriasis rubra pilaris: activation of NF-κB. *J Invest Dermatol*. (2015) 135:1905–8. doi: 10.1038/jid.2015.65
61. Lwin SM, Hsu CK, Liu L, Huang HY, Levell NJ, McGrath JA. Beneficial effect of ustekinumab in familial pityriasis rubra pilaris with a new missense mutation in CARD14. *Br J Dermatol*. (2018) 178:969–72. doi: 10.1111/bjd.15462
62. Griffiths WA. Pityriasis rubra pilaris. *Clin Exp Dermatol*. (1980) 5:105–12.
63. Soeprono FF. Histologic criteria for the diagnosis of pityriasis rubra pilaris. *Am J Dermatopathol*. (1986) 8:277–83.
64. Vasher M, Smithberger E, Lien MH, Fenske NA. Familial pityriasis rubra pilaris: report of a family and therapeutic response to etanercept. *J Drugs Dermatol*. (2010) 9:844–50.

65. Betto P, Vassilopoulou A, Colombari R, Veller-Fornasa C. Acute juvenile pityriasis rubra pilaris: a case report after mononucleosis infection. *G Ital Dermatol Venereol*. (2008) 143:271–3.
66. Mohrenschlager M, Abeck D. Further clinical evidence for involvement of bacterial superantigens in juvenile pityriasis rubra pilaris (PRP): report of two new cases. *Pediatr Dermatol*. (2002) 19:569. doi: 10.1046/j.1525-1470.2002.00236_5.x
67. Kawara S, Miyake M, Oiso N, Kawada A. Pityriasis rubra pilaris with preceding cytomegalovirus infection. *Dermatology* (2009) 219:350–2. doi: 10.1159/000240018
68. Miralles ES, Nunez M, De Las Heras ME, Perez B, Moreno R, Ledo A. Pityriasis rubra pilaris and human immunodeficiency virus infection. *Br J Dermatol*. (1995) 133:990–3. doi: 10.1111/j.1365-2133.1995.tb06939.x
69. Auffret N, Quint L, Domart P, Dubertret L, Lecam JY, Binet O. Pityriasis rubra pilaris in a patient with human immunodeficiency virus infection. *J Am Acad Dermatol*. (1992) 27(2 Pt 1): 260–1. doi: 10.1016/S0190-9622(08)80734-7
70. Ross NA, Chung HJ, Li Q, Andrews JP, Keller MS, Uitto J. Epidemiologic clinicopathologic diagnostic, and management challenges of pityriasis rubra pilaris: a case series of 100 patients. *JAMA Dermatol*. (2016) 152:670–5. doi: 10.1001/jamadermatol.2016.0091
71. Howes A, O'Sullivan PA, Breyer F, Ghose A, Cao L, Krappmann D, et al. Psoriasis mutations disrupt CARD14 autoinhibition promoting BCL10-MALT1-dependent NF-κB activation. *Biochem J*. (2016) 473:1759–68. doi: 10.1042/BCJ20160270
72. Mellett M, Meier B, Mohanan D, Schairer R, Cheng P, T.Satoh K, et al. CARD14 gain-of-function mutation alone is sufficient to drive IL-23/IL-17-mediated psoriasiform skin inflammation *in vivo*. *J Invest Dermatol*. (2018) 138:2010–23. doi: 10.1016/j.jid.2018.03.1525
73. Scudiero I, Mazzone P, D'Andrea LE, Ferravante A, Zotti T, Telesio G, et al. CARMA2sh and ULK2 control pathogen-associated molecular patterns recognition in human keratinocytes: psoriasis-linked CARMA2sh mutants escape ULK2 censorship. *Cell Death Dis*. (2017) 8:e2627. doi: 10.1038/cddis.2017.51
74. Wohlrab J, Kreft B. Treatment of pityriasis rubra pilaris with ustekinumab. *Br J Dermatol*. (2010) 163:655–6. doi: 10.1111/j.1365-2133.2010.09855.x
75. Muller H, Gattringer C, Zelger B, Hopfl R, Eisendle K. Infliximab monotherapy as first-line treatment for adult-onset pityriasis rubra pilaris: case report and review of the literature on biologic therapy. *J Am Acad Dermatol*. (2008) 59(5 Suppl.): S65–70. doi: 10.1016/j.jaad.2008.05.037
76. Mossner R, Wilsmann-Theis D, Oji V, Gkogkolou P, Lohr S, Schulz P, et al. The genetic basis for most patients with pustular skin disease remains elusive. *Br J Dermatol*. (2018) 178:740–8. doi: 10.1111/bjd.15867
77. Mahil SK, Capon F, Barker JN. Genetics of psoriasis. *Dermatol Clin*. (2015) 33:1–11. doi: 10.1016/j.det.2014.09.001
78. Nair RP, Stuart P, Henseler T, Jenisch S, N.Chia V, Westphal E, et al. Localization of psoriasis-susceptibility locus PSORS1 to a 60-kb interval telomeric to HLA-C. *Am J Hum Genet*. (2000) 66:1833–44. doi: 10.1086/302932
79. Mallon E, Bunce M, Savoie H, Rowe A, Newson R, Gotch F, et al. HLA-C and guttate psoriasis. *Br J Dermatol*. (2000) 143:1177–82. doi: 10.1046/j.1365-2133.2000.03885.x
80. Qiao Q, Yang C, Zheng C, Fontan L, David L, Yu X, et al. Structural architecture of the CARMA1/Bcl10/MALT1 signalosome: nucleation-induced filamentous assembly. *Mol Cell*. (2013) 51:766–79. doi: 10.1016/j.molcel.2013.08.032
81. Danis J, Goblos A, Gal B, Sulak A, Farkas K, Torok D, et al. Nuclear factor κB activation in a Type V pityriasis rubra pilaris patient harboring multiple CARD14 variants. *Front Immunol*. (2018) 9:1564. doi: 10.3389/fimmu.2018.01564
82. Wang M, Zhang S, Zheng G, Huang J, Songyang Z, Zhao X, et al. Gain-of-function mutation of Card14 leads to spontaneous psoriasis-like skin inflammation through enhanced keratinocyte response to IL-17A. *Immunity* (2018) 49:66–79 e5. doi: 10.1016/j.immuni.2018.05.012
83. Hollox EJ, Huffmeier U, Zeeuwen PL, Palla R, Lascorz J, Rodijk-Olthuis D, et al. Psoriasis is associated with increased beta-defensin genomic copy number. *Nat Genet*. (2008) 40:23–5. doi: 10.1038/ng.2007.48
84. Tanaka M, Kobiyama K, Honda T, Uchio-Yamada K, Natsume-Kitatani Y, Mizuguchi K, et al. Essential role of CARD14 in murine experimental psoriasis. *J Immunol*. (2018) 200:71–81. doi: 10.4049/jimmunol.1700995
85. van der Fits L, Mourits S, Voerman JS, Kant M, Boon L, Laman JD, et al. Imiquimod-induced psoriasis-like skin inflammation in mice is mediated via the IL-23/IL-17 axis. *J Immunol*. (2009) 182:5836–45. doi: 10.4049/jimmunol.0802999
86. Nestle FO, Conrad C, Tun-Kyi A, Homey B, Gombert M, Boyman O, et al. Plasmacytoid predendritic cells initiate psoriasis through interferon-alpha production. *J Exp Med*. (2005) 202:135–43. doi: 10.1084/jem.20050500
87. Nakamura M, Lee K, Jeon C, Sekhon S, Afifi L, Yan D, et al. Guselkumab for the Treatment of psoriasis: a review of phase III trials. *Dermatol Ther (Heidelb)*. (2017) 7:281–92. doi: 10.1007/s13555-017-0187-0
88. Papp K, Kimball AB, Tyring S, Sinclair R, Metha A, Cichanowitz N, et al. Maintenance of treatment response in chronic plaque psoriasis patients continuing treatment or discontinuing treatment with tildrakizumab in a 64-week, randomized controlled, phase 3 trial. *J Am Acad Dermatol*. (2017) 76:Ab164. doi: 10.1016/j.jaad.2017.04.637
89. Reich K, Papp KA, Blauvelt A, Tyring SK, Sinclair R, Thaci D, et al. Tildrakizumab versus placebo or etanercept for chronic plaque psoriasis (reSURFACE 1 and reSURFACE 2): results from two randomised controlled, phase 3 trials. *Lancet* (2017) 390:276–88. doi: 10.1016/S0140-6736(17)31279-5
90. Podlipnik S, Castellanos-Moreira R, Florez-Enrich H, Arostegui JI, Mascaro JM Jr. Acute generalized exanthematous pustulosis and polyarthritis associated with a novel CARD14 mutation. *Australas J Dermatol*. (2017) 59:e70–3. doi: 10.1111/ajd.12669
91. Szatkowski J, Schwartz RA. Acute generalized exanthematous pustulosis (AGEP): a review and update. *J Am Acad Dermatol*. (2015) 73:843–8. doi: 10.1016/j.jaad.2015.07.017
92. Navarini AA, Valeyrie-Allanore L, Setta-Kaffetzi N, J.Barker N, Capon F, Creamer D, et al. Rare variations in IL36RN in severe adverse drug reactions manifesting as acute generalized exanthematous pustulosis. *J Invest Dermatol*. (2013) 133:1904–7. doi: 10.1038/jid.2013.44
93. Schmitt A, Grondona P, Maier T, Brandle M, Schonfeld C, Jager G, et al. MALT1 protease activity controls the expression of inflammatory genes in keratinocytes upon zymosan stimulation. *J Invest Dermatol*. (2016) 136:788–97. doi: 10.1016/j.jid.2015.12.027
94. McAllister-Lucas LM, Jin X, Gu S, Siu K, McDonnell S, Ruland J, et al. The CARMA3-Bcl10-MALT1 signalosome promotes angiotensin II-dependent vascular inflammation and atherogenesis. *J Biol Chem*. (2010) 285:25880–4. doi: 10.1074/jbc.C110.109421
95. Navarini AA, Burden AD, Capon F, Mrowietz U, Puig L, Koks S, et al. European consensus statement on phenotypes of pustular psoriasis. *J Eur Acad Dermatol Venereol*. (2017) 31:1792–9. doi: 10.1111/jdv.14386
96. Akiyama M, Takeichi T, McGrath JA, Sugiura K. Autoinflammatory keratinization diseases. *J Allergy Clin Immunol*. (2017) 140:1545–7. doi: 10.1016/j.jaci.2017.05.019
97. Akiyama M, Takeichi T, McGrath JA, Sugiura K. Autoinflammatory keratinization diseases: an emerging concept encompassing various inflammatory keratinization disorders of the skin. *J Dermatol Sci*. (2018) 90:105–111. doi: 10.1016/j.jdermsci.2018.01.012

Conflict of Interest Statement: The authors declare that the research was conducted in the absence of any commercial or financial relationships that could be construed as a potential conflict of interest.

Advantages of publishing in Frontiers

OPEN ACCESS
Articles are free to read for greatest visibility and readership

FAST PUBLICATION
Around 90 days from submission to decision

HIGH QUALITY PEER-REVIEW
Rigorous, collaborative, and constructive peer-review

TRANSPARENT PEER-REVIEW
Editors and reviewers acknowledged by name on published articles

Frontiers
Avenue du Tribunal-Fédéral 34
1005 Lausanne | Switzerland

Visit us: www.frontiersin.org
Contact us: info@frontiersin.org | +41 21 510 17 00

REPRODUCIBILITY OF RESEARCH
Support open data and methods to enhance research reproducibility

DIGITAL PUBLISHING
Articles designed for optimal readership across devices

FOLLOW US
@frontiersin

IMPACT METRICS
Advanced article metrics track visibility across digital media

EXTENSIVE PROMOTION
Marketing and promotion of impactful research

LOOP RESEARCH NETWORK
Our network increases your article's readership